DEVELOPMENT OF AQUEOUS PHASE HYDROXYL RADICAL REACTION RATE CONSTANTS PREDICTORS FOR ADVANCED OXIDATION PROCESSES

A Dissertation
Presented to
The Academic Faculty

by

Daisuke Minakata

In Partial Fulfillment
of the Requirements for the Degree
of Engineering in the
School of Civil and Environmental Engineering

Georgia Institute of Technology
December, 2010

COPYRIGHT 2010 BY DAISUKE MINAKATA

DEVELOPMENT OF AQUEOUS PHASE HYDROXYL RADICAL REACTION RATE CONSTANTS PREDICTORS FOR ADVANCED OXIDATION PROCESSES

Approved by:

Dr. John C. Crittenden, Advisor
School of Civil and Environmental Engineering
Georgia Institute of Technology

Dr. Jae-Hong Kim
School of Civil and Environmental Engineering
Georgia Institute of Technology

Dr. Ching-Hua Huang
School of Civil and Environmental Engineering
Georgia Institute of Technology

Dr. James Mulholland
School of Civil and Environmental Engineering
Georgia Institute of Technology

Dr. David Sherrill
School of Chemistry and Biochemistry
Georgia Institute of Technology

Date Approved: July 16th, 2010

To my mother and deceased father

ACKNOWLEDGEMENTS

First of all, I would like to thank my adviser, Dr. John Crittenden, very much for his tremendous supports and advices to me. He has been my coach over the course of my doctorate study years who told me to be a super-athlete. Though I may not be a super-athlete just yet, I could not have made any progresses without his support. I would also like to thank other committee members at Georgia Tech: Dr. Jae-Hong Kim for his continuous encouragement, Dr. David Sherrill for his technical advices in quantum mechanical calculations, Dr. Ching Hua-Huang and Dr. James Mulhold for their constructive advices.

My appreciation extends to my former committee members at Arizona State University: Dr. Ke Li who is now at the University of Georgia for his mentor and advisement in research as well as in carrier, and Dr. Paul Westerhoff from ASU for his technical advices and collaborations in research.

I would like to include following names in appreciation for providing high performance computing resources: Drs. Karsten Schwan, Mattew Wolf and Chad Huneycutt from College of Computing at Georgia Tech; Drs. Ron Huchinsons and Neil Bright from Georgia Tech Office of Information Technology; Drs. Dan Stantione and Doug Fuller from ASU HPC. I also appreciate the IT support from CEE IT services from Georgia Tech: James Martino and Mike Anderson.

Following individuals helped me with experiments: Ryan Ravenelle from Georgia Tech for his technical advices and support, and his friendship; Dr. Weihua Song from University of California, Irvine for his tremendous assistance for arranging experiments and overcoming experimental difficulties; Ryan Lisk from Environmental Health Service

at Georgia Tech for shipment of hazardous chemical materials. Thank you so much, folks.

I also appreciate others in research group at Georgia Tech as well as at ASU.

Faculty and Staff at Brook Bayer Institute for Sustainable Systems encouraged me and helped me with business prospect: Dr. Michael Chang, Dr. Ming Xu, Martha Lindsay, Christy Shannon, and Brent Verrill. Thank you.

I would like to acknowledge the following foundations, institutes and assistantships for their funding supports: National Science Foundation; Brook Bayer Institute for Sustainable Systems; High Tower Chair and Georgia Research Alliance at Georgia Tech; University of Notre Dame Radiation Center and Department of Energy; Richard Snell Chair at ASU.

My deepest gratitude goes to my family; my mother, sister, brother, uncle, aunt, and grandparents. My mother, Chiaki, always supports my decision and encourages me to move forward. Reminiscence of my deceased father still influences me in many ways to live everyday strong as well. Finally, I appreciate the continuous support with tremendous love from my favorite person, Ayako.

TABLE OF CONTENTS

Page

ACKNOWLEDGEMENTS iv

LIST OF TABLES ix

LIST OF FIGURES xi

SUMMARY xiv

CHAPTER 1 1

INTRODUCTION

1.1 SIGNIFICANCE AND OBJECTIVES 1
1.2 STRUCTURE OF THIS DISSERTATION 10
1.3 LITERATURE CITED 11

CHAPTER 2 16

DEVELOPMENT OF A GROUP CONTRIBUTION METHOD TO PREDICT AQUEOUS PHASE HYDROXYL RADICAL REACTION RATE CONSTANTS

2.1 ABSTRACT 17
2.2 INTRODUCTION 18
2.3 DEVELOPMENT OF THE GROUP CONTRIBUTION METHOD 22
2.3.1 Hydrogen-atom Abstraction 23
2.3.2 HO• Addition to Alkenes 26
2.3.3 HO• Addition to Aromatic Compounds 29
2.3.4 HO• Interactions with Sulfur-, Nitrogen-, or Phosphorus-atom-containing Compounds 31
2.4 RESULTS AND DISCUSSION 32
2.4.1 Calibration and Prediction 32
2.4.2 Overall Results 40
2.4.3 Hydrogen-Atom Abstraction from Saturated Aliphatic Compounds 43
2.4.3.1 Group Rate Constants for H-atom Abstraction 44
2.4.3.2 Group Contribution Factors for H-atom Abstraction 46
2.4.4 HO• Addition to Alkenes 50
2.4.4.1 Group Rate Constants and Group Contribution Factors for HO• Addition to Alkenes. 50
2.4.5 HO• Addition to Aromatic Compounds 52
2.4.5.1 Group Rate Constants for HO• Addition to Aromatic Compounds 55

2.4.5.2 Group Contribution Factors for HO• Addition to Aromatic Compounds. 58
2.4.6 HO• Interactions with Sulfur-, Nitrogen-, or Phosphorus-containing-compounds 59
2.4.6.1 Group Rate Constants for HO• Interaction 60
2.4.6.2 S-, N-, or P-atom-Containing Group Contribution Factors 62
2.4.7 Predictabilities of GCM and Future Studies 64
2.5 ACKNOWLEDGEMENT 68
2.6 APPENDICES 68
2.7 LITERATURE CITED 68

CHAPETER 3 74

LINEAR FREE ENERGY RELATIONSHIPS BETWEEN AQUEOUS PHASE HYDROXYL RADICAL REACTION RATE CONSTANTS AND FREE ENERGY OF ACTIVATION

3.1 ABSTRACT 75
3.2 INTRODUCTION 75
3.3 LINEAR FREE ENERGY RELATIONSHIPS 87
3.4 COMPUTATIONAL METHODS 89
3.5 RESULTS AND DISCUSSION 92
3.5.1 A Comparison of *Ab* initio Quantum Mechanical Methods for HO• + CH4 in the Gaseous Phase 92
3.5.2 Verifications of *Ab* initio Quantum Mechanical Methods for the Gaseous Phase HO• Reactions 96
3.5.3 A Comparison of Implicit Solvation Models 98
3.5.4 Linear Free Energy Relationships between Aqueous Phase Free Energy of Activation and Logarithm of HO• Reaction Rate Constant 101
3.6 ACKNOWLEDGEMENT 113
3.7 APPENDICES 113
3.8 LITERATURE CITED 113

CHAPTER 4 126

QUANTITATIVE UNDERSTANDING OF AQUEOUS PHASE HYDROXYL RADICAL REACTIONS WITH HALOACETATE IONS:

EXPERIMENTAL AND THEORETICAL STUDIES

4.1 ABSTRACT 127
4.2 INTRODUCTION 128
4.3 METHODS 133
4.3.1 Experimental 133
4.3.1.1 Linear Accelerator (LINAC) 133
4.3.1.2 Flow Cell 135
4.3.1.3 Radiolysis of Water 136
4.3.1.4 Competition Kinetics 138
4.3.1.5 Procedures 139
4.3.1.6 Thermochemical Properties 140
4.3.2 Group Contribution Method 142

4.3.3 Theoretical Basis 143
4.3.4 Linear Free Energy Relationships 145
4.4 RESULTS AND DISCUSSION 147
4.4.1 Experimental Section 147
4.4.1.1 Hydroxyl Radical Reaction Rate Constants 147
4.4.1.2 Arrhenius Parameters 150
4.4.1.3 Thermochemical Properties of Reactions 152
4.4.2 Update of Group Contribution Method 154
4.4.3 THEORETICAL 156
4.4.3.1 *Ab* initio Quantum Mechanical Approach 156
4.4.3.2 Optimized Structure of Stationary, Pre-reactive Complex and Transition States 161
4.4.3.3 Linear Free Energy Relationships 164
4.4.3.4 Entropy Contribution 165
4.4.3.5 Charge Distribution and Reaction Mechanisms 170
4.4.3.6 Addition of Explicit Water Molecules 175
4.5 CONCLUSIONS 179
4.6 ACKNOWLEDGEMENT 180
4.7 APPENDICES 180
4.8 LITERATURE CITED 180
CHAPTER 5 188
IMPLICATIONS AND FUTURE STUDIES
APPENDIX A 196
APPENDIX B 203
APPENDIX C 242
APPENDIX D 254
APPENDIX E 260
APPENDIX F 316
APPENDIX G 344
VITA 379

LIST OF TABLES

Table 2.1: Calculated HO• reaction rate constants (Normal: calculated, *Italic*: predicted, **Bold**: error is out of the EG) as compared to literature-reported experimental values….34

Table 2.2: Summary of experimental data and statistical results for calibration……..42

Table 2.3: Summary of experimental data and statistical results for prediction……43

Table 2.4: Group rate constants and group contribution factors for H-atom abstraction..48

Table 2.5: Summary of the structural configurations in equation (2.13) based on the experimental rate constants……50

Table 2.6: Group rate constants and group contribution factors for HO• addition to alkenes……52

Table 2.7: Summary of structural configurations in equation (2.17) based on the experimental rate constants with aromatic compounds……54

Table 2.8: Group rate constants and group contribution factors for HO• addition to aromatic compounds that include benzene rings……...56

Table 2.9: Group rate constants and group contribution factors for HO• addition to aromatic compounds that include pyridine……57

Table 2.10: Group rate constants and group contribution factors for HO• addition to aromatic compounds that include furan……57

Table 2.11: Group rate constants and group contribution factors for HO• addition to aromatic compounds that include imidazole……..58

Table 2.12: Group rate constants and group contribution factors for HO• addition to aromatic compounds that include triazine……59

Table 2.13: Group rate constants and group contribution factors for S, N, and P-atom containing compounds……...61

Table 2.14: Predicted HO• reaction rate constants for emerging contaminants……67

Table 3.1: Number of available experimental rate constants in the aqueous phase AOPs on the basis of the extensive literature review……...77

Table 3.2: Summary of theoretical studies of gaseous phase HO• reactions……81

Table 3.3: A comparison of *Ab* initio quantum mechanical methods for the gaseous phase reaction of HO• with CH_4……..93

Table 3.4: Calculated energy barrier for the gaseous phase reactions of HO• with CH_3OH, CH_3CHO, CH_3OCH_3, CH_3COCH_3, CH_3COOH, CH_3F, CH_3Cl and CH_3Br, and the literature-reported values……...97

Table 3.5: Calculated $\Delta G^{\neq}_{rxn,aq}$, tunneling factor and literature reported HO• reaction rate constants for the H-atom……..…102

Table 3.6: Calculated $\Delta G^{\neq}_{rxn,aq}$, tunneling factor and literature reported HO• reaction rate constants for the HO• addition to alkenes……103

Table 3.7: Calculated diffusion coefficients, radius of molecule and diffusion rate constants……...109

Table 4.1: Experimentally obtained temperature-dependent HO• rate constants and thermochemical properties, and theoretically calculated free energies of activation…..148

Table 4.2: Calibrated group rate constants and group contribution factors…….155

Table 4.3: Molecules and rate constants that were used for the calibration……156

Table 4.4: Calculated gaseous and aqueous phase barrier height and free energy of activation……..160

Table 4.5: Geometry of HO• and H_2O……162

Table 4.6: Geometry of acetate and halogenated acetate……162

Table 4.7: Geometry of transition states for the reaction of HO• with halogenated acetate……..163

Table 4.8: Calculated cavitation entropy of activation, change in cavity volume, nonelectrostatic energy of activation and experimentally obtained entropy of activation……..167

LIST OF FIGURES

Figure 1.1: Skeleton of the modules and placement of this study……...4

Figure 1.2: General reaction mechanisms that is induced by HO•……..5

Figure 1.3: Comparison of Henry's constant, log K_{OW} , and HO• rate constants for 87 organic compounds: □: the magnitude of $k_{HO\bullet}$ is 10^{7th} order, ○:10^{8th} order Δ: 1.0~5.0×10^9, ▲: ~5.0×10^9 and ×: unknown rate constants calculated by the group contribution method……..7

Figure 2.1: Comparison of the aqueous and gaseous phase HO• reaction rate constants. The unit of the gaseous phase rate constant was converted from 1/molecule/cm^3/s to 1/M/s……..21

Figure 2.2: The experimental HO• reaction rate constants as a function of the number of –CH_2- alkyl functional group for some functional groups. The chemical formula is expressed as CH_3-$(CH_2)_n$-R, where R is –CH_3, -OH, -COOH, -NH_2, -CN, -CHO, -Cl, and –Br, for alkane, alcohol, carboxylic, amine, cyano, aldehyde, chlorine, and bromine, respectively, and *n* is the number of –CH_2- alkyl functional groups. *There are only two rate constants available for –Cl……..26

Figure 2.3: Total of 434 HO• reaction rate constants from calibrations and predictions versus experimental rate constants for four reaction mechanisms. Error bars represent the range of experimentally reported values……43

Figure 2.4: Comparison of the group contribution factors for H-atom abstraction with the Taft constant, σ*[60]. Group contribution factors include ●: alkyl, oxygenated, and halogenated functional groups, ▲: S-, N-, or P-atom containing functional groups……49

Figure 2.5: Comparison of the group contribution factors for HO• addition to aromatic compounds with electrophilic substituent parameter, σ+, (Karelson, 2000) (right). Figure includes the group contribution factors for benzene (■), pyridine (●), and furan compounds (▲). The σ* of [-$CHCl_2$], [-CO], [-COO, COOH], [–S-, -SS- -HS-], [-NH_2, -NH-, -N<] is an average of [CH_2Cl, CH_2Br, $CHCl_2$, $CHBr_2$], [$COCH_3$, COC_2H_5, $COC(CH_3)_3$, COC_6H_5, COF, COCl], [COOH, $COOC_2H_5$], [SCH_3, SC_2H_5, $SCH(CH_3)_2$], and [$NHCH_3$, $NH(CH_2)_3CH_3$, $N(C_2H_5)_2$], respectively. The σ* of [-SO] and [-N-CO-] refer to [$S(O)CH_3$] and [$NHCOC_6H_5$], respectively……..59

Figure 3.1: Relationship between the logarithm of aqueous phase $k_{HO\bullet}$ and calculated energy gap of HOMO-SOMO for 477 compounds……...86

Figure 3.2: A comparison of calculated barrier height for the CH_4 + HO•……...94

Figure 3.3: A plot of calculated free energy of solvation against experimental free energy of salvation……99

Figure 3.4: Log k_I – log k_R versus ΔG^{act}_I - ΔG^{act}_R for the H-atom abstraction from the C-H bond by HO•. The error bar represents the range of the literature-reported experimental rate constants……105

Figure 3.5: Log k_I – log k_R versus ΔG^{act}_I - ΔG^{act}_R HO• addition to alkenes. The error bar represents the range of the literature-reported experimental rate constants……106

Figure 3.6: Plot of the ratio, $R(=k_{exp}/k_D)$, versus calculated free energy of activation…108

Figure 3.7: Plot of predicted HO• rate constants against the literature-reported experimental rate constants. The error bar represents the range of the literature-reported experimental rate constants……..110

Figure 4.1: Schematic picture of waters distributed in the cavity, first solvation shell and bulk phase for transition state for the reaction of HO• with acetate. Dotted line represents the hydrogen bond……..131

Figure 4.2: Overall system of Linear Electron Accelerator (LINAC)……134

Figure 4.3: Kinetics of $(SCN)_2^{\bullet-}$ formation at 472 nm for N_2O saturated 3.00×10^{-4} M KSCN solution containing 0 (∇), 1.56 (◊), 2.41(▼), 3.48(Δ), and 5.01 (○) mM $ClCH_2COO^-$……149

Figure 4.4: Competition kinetics plots for hydroxyl radical reaction with chloroacetate, dichloroacetate and trichloroacetate, respectively, using SCN^- as a standard. The error bar represents 95% of confidential values……...149

Figure 4.5: Plot of logarithm of k versus inverse of temperature……151

Figure 4.6: LFERs obtained from experiments, calculations at G4 and the SMD solvation model, and calculations that include two explicit water molecules. 1: formate; 2: propionate; 3: malonate; 4: succinate; 5: chloroacetate; 6: difluoroacetate; 7: dibromoacetate; 8: pyruvate; 9: dichloroacetate; 10: acetate; 11: glyoxylate; 12: trichloroacetate; 13: tribromoacetate; 14: iodoacetate; 15: lactate (note that the compound # is consistent for other Figures though this chapter)……..153

Figure 4.7: Isokinetic relation between the experimentally obtained enthalpy and entropy of activation……154

Figure 4.8: Comparison of calculated and experimental free energy of solvation for ionized compounds……..158

Figure 4.9: Schematic picture of acetate with R functional group……..162

Figure 4.10: Schematic picture of pre-reactive complex between HO• with acetate, R is functional group……...163

Figure 4.11: Schematic picture of transition state between HO• with acetate, R is functional group……...163

Figure 4.12: Experimentally obtained free energies of entropies versus theoretically calculated change in cavity, ΔV_{cav}, $Å^3$, and non-electrostatic energy of activation at G4 with the SMD model for series of acetate……169

Figure 4.13: Charge distributions of reactants, transition states and products for the gaseous and aqueous phases HO• reactions with acetate……....171

Figure 4.14: Charge distributions of reactants, transition states and products for the aqueous phases HO• reactions with halogenated acetate……173

Figure 4.15: Comparison of observed barrier height for the reactions of HO• with a series of halogenated acetates in the absence of presence of explicit water molecule(s). Note that the transition state of the reaction of HO• with $CHCl_2COO^-$ could not be located..174

Figure 4.16: Optimized transition state for the reaction of HO• with chloroacetate in the presence of explicit water molecule(s)……177

Figure 4.17: Charge distributions of reactants, transition states and products for the aqueous phases HO• reactions with chloroacetate in the absence and presence of explicit water molecule(s). The transition state in the presence of one explicit water molecule shows three conformations……..179

Figure 5.1: Aqueous phase free energy change profiles for the reactions that are initiated by HO•……....190

Figure 5.2: Aqueous phase free energy change profiles for 1,2-H shift reaction of oxyl radical in the absence or presence of a water molecule……...191

Figure 5.3: Aqueous phase free energy change profiles for hydrolysis reaction of formaldehyde with one and two water molecules assisted……..191

SUMMARY

Emerging contaminants are defined as synthetic or naturally occurring chemicals or microorganisms that are not currently regulated but have the potential to enter the environment and cause adverse ecological and/or human health effects. With recent development in analytical techniques, emerging contaminants have been detected in wastewater, source water, and finished drinking water. These environmental occurrence data have raised public concern about the fate and ecological impacts of such compounds. Concerns regarding emerging contaminants and the many chemicals that are in use or production necessitate a task to assess their potential health effects and removal efficiency during water treatment.

Advanced oxidation processes (AOPs) are attractive and promising technologies for emerging contaminant control due to its capability of mineralizing organic compound via reactions with highly active hydroxyl radicals. However, the nonselective reactivity of hydroxyl radicals and the radical chain reactions make AOPs mechanistically complex processes. In addition, the diversity and complexity of the structure of a large number of emerging contaminants make it difficult and expensive to study the degradation pathways of each contaminant and the fate of the intermediates and byproducts. The intermediates and byproducts that are produced may pose potential effects to human and aquatic ecosystems. Consequently, there is a need to develop first-principle based mechanistic models that can enumerate reaction pathway, calculate concentrations of the byproducts, and estimate their human effects for both water treatment and reuse practices.

This dissertation develops methods to predict reaction rate constants for elementary reactions that are identified by a previously developed computer-based

reaction pathway generator. Many intermediates and byproducts that are experimentally identified for HO• induced reactions with emerging contaminants include common lower molecular weight organic compounds on the basis of several carbons. These lower carbon intermediates and byproducts also react with HO• at relatively smaller reaction rate constants (i.e., $k < 10^9$ $M^{-1}s^{-1}$) and may significantly affect overall performance of AOPs. In addition, the structures of emerging contaminants with various functional groups are too complicated to model. As a consequence, the rate constant predictors are established based on the conventional organic compounds as an initial approch.

A group contribution method (GCM) predicts the aqueous phase hydroxyl radical reaction rate constants for compounds with a wide range of functional groups. The GCM is a first comprehensive tool to predict aqueous phase hydroxyl radical reaction rate constants for reactions that include hydrogen-atom abstraction from a C-H bond and/or a O-H bond by hydroxyl radical, hydroxyl radical addition to a C=C unsaturated bond in alkenes and aromatic compounds, and hydroxyl radical interaction with sulfur-, nitrogen-, or phosphorus-atom-containing compounds. The GCM shows predictability; factor of difference of 2 from literature-reported experimental values. The GCM successfully predicts the hydroxyl radical reaction rate constants for a limited number of emerging contaminants.

Linear free energy relationships (LFERs) bridge a kinetic property with a thermochemical property. The LFERs is a new proof-of-concept approach for *Ab initio* reaction rate constants predictors. The kinetic property represents literature-reported and our experimentally obtained hydroxyl radical reaction rate constants for neutral and ionized compounds. The thermochemical property represents quantum mechanically

calculated aqueous phase free energy of activation. Various *Ab initio* quantum mechanical methods and solvation models are explored to calculate the aqueous phase free energy of activation of reactantas and transition states. The quantum mechanically calculcated aqueous phase free energies of activation are within the acceptable range when compared to those that are obtained from the experiments. These approaches may be applied to other reaction mechanisms to establish a library of rate constant predictions for the mechanistic modeling of AOPs. The predicted kinetic information enables one to identify important pathways of AOP mechanisms that are initiated by hydroxyl radical, and can be used to calculate concentration profiles of parent compounds, intermediates and byproducts. The mechanistic model guides the design of experiments that are used to examine the reaction mechanisms of important intermediates and byproducts and the application of AOPs to real fields.

CHAPTER 1

INTRODUCTION

1.1 Significance and Objectives

Emerging contaminants are defined as synthetic or naturally occurring chemicals or microorganisms that are not currently regulated but have the potential to enter the environment and cause adverse ecological and/or human health effects. With recent improvements in analytical techniques (Richardson, 2009; 2004; 2003; 2001; Richardson and Ternes, 2005; Pertović et al., 2003; Koester et al., 2003; Vanderford et al., 2003), emerging contaminants have been detected in wastewater, source waters, and finished drinking water (Benotti et al., 2009; Pedersen et al., 2005; Kolpin et al., 2002). Several surveys on emerging contaminants found relatively high residual levels in the environment presumably due to runoff and discharge of municipal and industrial wastewater effluents (Phillips et al., 2010; USGS, 2009; Benotti et al., 2008; Conn, et al., 2006; Kolpin et al., 2002; Snyder et al., 2001; Halling-Sorensen et al., 1998). These environmental occurrence data have raised public concern about the fate and ecological impacts of such compounds (Bruce et al., 2010; Hayes et al., 2010; Snyder, 2008; Snyder et al., 2007; RNRF, 2006; Schwarzenbach et al., 2006; NRC, 1999). As a result of their ubiquity and persistence in the environment, it is an urgent task to assess their potential health effects and removal efficiency during water treatment.

Chemical oxidation and reduction processes have been used for many years to treat potable water, wastewater, contaminated groundwater, and various industrial wastewater streams. Several technologies that have shown promise to destroy many of the emerging organic contaminants in water are the so-called advanced oxidation

processes (AOPs) (e.g., hydrogen peroxide with ultraviolet photolysis (UV/H_2O_2), ozone with hydrogen peroxide (O_3/H_2O_2), titanium dioxide with ultraviolet photolysis (TiO_2/UV)), which produce highly reactive hydroxyl radical (HO•) at room temperature and atmospheric pressure (Hoigné, 1998; Glaze and Kang, 1989; Glaze et al., 1987). The HO• is an electrophile that reacts rapidly and non-selectively with most electron-rich organic compounds, and is capable of mineralizing organic compound via radical chain reactions. The reported second-order HO• reaction rate constants for most organic contaminants in water are on the order of 10^7-10^9 $Lmol^{-1}s^{-1}$ (Buxton et al., 1988; Farhataziz and Ross, 1977), which are approximately three or four orders of magnitude higher than those of conventional oxidants employed in water treatment (Ikehata and Gamal El-Din, 2005a,b; von Gunten, 2003a; Deborde and von Gunten, 2008; Lee et al., 2008) .

AOPs are attractive technologies that may be used to control the emerging contaminants; however, the nonselective reactivity of HO• and the radical chain reactions make AOPs mechanistically complex processes. In addition, the diversity and complexity of structure of a large number of emerging contaminants make AOPs difficult and expensive to study the degradation pathways of each contaminant and the fate of the intermediates and byproducts. For example, trichloroethylene (TCE) (Li et al., 2007; 2004), acetone (Stefan and Bolton, 1999), *para*-dioxane (*p*-dioxane) (Stefan and Bolton, 1998), and methyl *tert*-butyl ether (M*t*BE) (Stefan et al., 2000) destruction using UV/H_2O_2 and M*t*BE destruction using O_3/ H_2O_2 (Kang et al., 1999; Liang, et al., 1998) have been examined in detail. These studies shed light on the detailed elementary reactions and the radical pathways in AOPs but are limited to only these contaminants.

The intermediates and byproducts that are produced may pose potential effects to human and aquatic ecosystems (Dodd et al., 2009). As a consequence, there is a need to develop a first-principle based mechanistic model that can enumerate reaction pathway, calculate concentrations of intermediates and byproducts, and estimate intermediates and byproducts and their human health effects for both water treatment and reuse practices. The increasing concerns about emerging contaminants make this requirement more urgent.

Figure 1.1 displays a basic flow diagram of the overall methodology for this work. The reaction pathway generator will enumerate all reaction possibilities that are based on the known reaction rules (see below for these). Either rate constant calculation or toxic screening modules will simplify the pathways by selecting reactions that have smaller reaction rates and intermediates that have high toxicity. Algorithms that can predict the reaction rate constants assign rate constants to the selected pathways. An algorithm will solve the ordinary differential equations (ODEs). The DGEAR algorithm (Hindmarsh and Gear, 1974) was successfully used to solve the ODEs for the UV/H_2O_2 kinetic models (Li et al., 2008; 2007; 2004; Crittenden et al., 1999). Solving these ODEs will simulate the concentration profiles of the parent compound, the selected intermediates, and final byproducts. Although detailed procedures vary for each module, Phaendtner and Broadbelt (2008a) demonstrated mechanistic modeling of the degradation of lubricating oils during the process of condensed-phase hydrocarbon autoxidation based on the automated mechanisms generation and structure-reactivity relationships (Phaendtner and Broadbelt, 2008b; 2007).

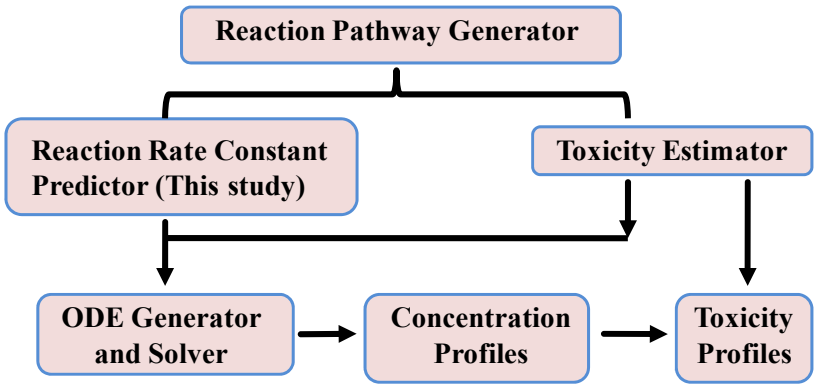

Figure 1.1: Skeleton of the modules and placement of this study

In previous research, a computerized pathway generator that predicts the degradation pathways by the HO• initiated chain reactions in AOPs was developed (Li and Crittenden, 2009). The model was based on the general reaction rules that were discovered during past experimental research (Stefan et al., 2000; Stefan and Bolton, 1998; 2000; Bolton and Carter, 1994) as shown in Figure 1.2. Accordingly, the pathway generator enumerates possible intermediates and their associated reactions that are not able to be detected in the experiments. For example, the generated pathway for ethane contains 137 intermediates (molecules and radicals) and 3367 reactions. Some organic intermediate compounds (e.g. carboxylic acids) have lower reaction rate constants with HO• (i.e. 10^6-10^7 $Lmol^{-1}s^{-1}$) than the parent compounds. These intermediates require longer retention times and might impose potential risks to human health (e.g., haloacetic acids). In order to calculate the concentration profile, it is critical to utilize the reaction rate constants and the toxicity of intermediates that are predicted by the rate constant predictor and toxicity estimator, respectively, to include only important pathways.

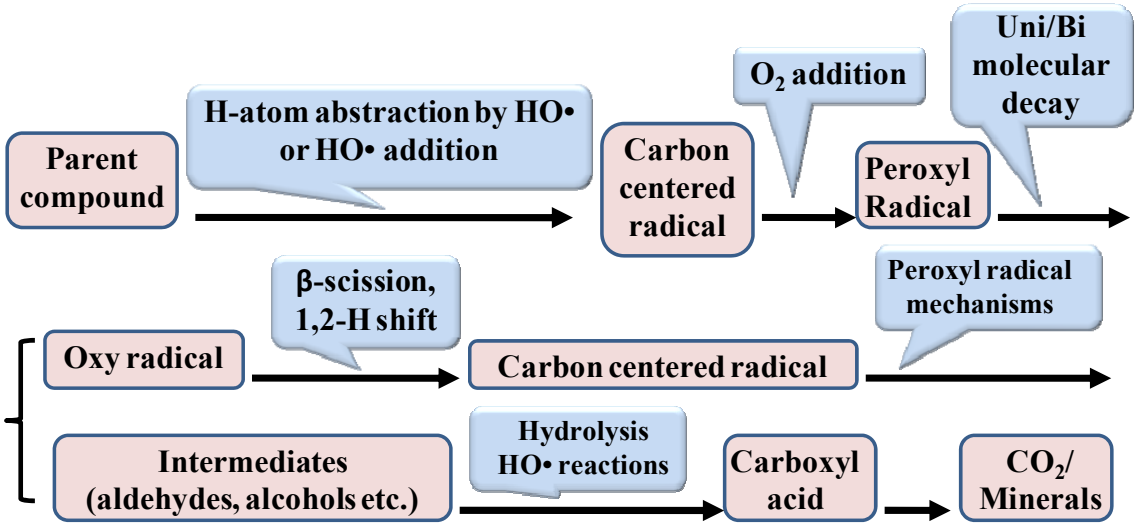

Figure 1.2: General reaction mechanisms that is induced by HO•

The complexity of the pathway requires an algorithm that can calculate the rate constant to establish a library of reaction rate constant predictors for mechanistic modeling. Practically, although HO• reaction rate constants for many compounds have been measured experimentally and compiled in the critical review (Buxton et al., 1988), measuring the reaction rate constants for exited chemical compounds and many intermediates in different reaction mechanisms is far from complete. Greater than 50 million chemical compounds have been registered in chemical abstract services (CAS, 2010) and more than 40 million chemicals are commercially available (CAS, 2010), and concerns about emerging contaminants makes the task even more challenging if not impossible. In addition, no apparent consistent relations are observed between the rate constants and general physical chemical properties (e.g., Kow, Henry's constant). For example, Figure 1.3 plots Henry's constant and log Kow of 87 Contaminant Candidate List 3 organic compounds associated with literature-reported experimental HO• reaction

rate constants. Adding to the difficulty of estimating the reaction rate constants, a compound generally reacts with HO• via several elementary reactions. The measured reaction rate constants are overall rate constants instead of the rate constants for specific elementary reactions that are generated by the pathway generator. It should be noted that many intermediates and byproducts that are experimentally identified for reactions of HO• with emerging contaminants include common lower molecular weight organic compounds on the basis of several carbons (Cooper et al., 2009; Stefan et al., 2000; Stefan and Bolton, 1998; 2000). Considering that these lower carbon intermediates and byproducts also react with HO• at relatively smaller reaction rate constants (i.e., $k < 10^9$ $M^{-1}s^{-1}$) and may significantly affect overall performance of AOP, the rate constant predictor should be established based on the conventional organic compounds as an initial approch.

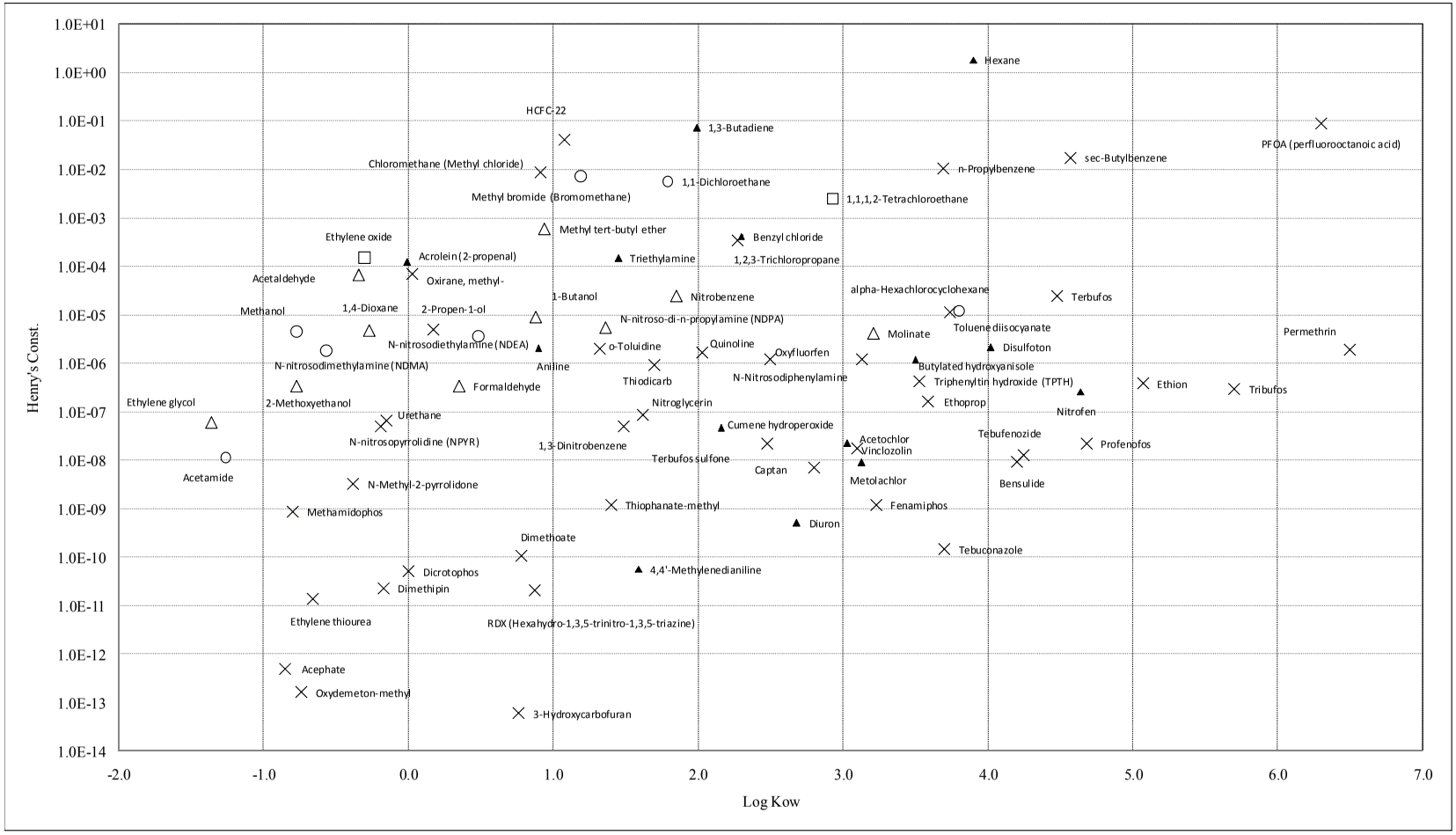

Figure 1.3: Comparison of Henry's constant, log K_{OW} , and HO• rate constants for 87 organic compounds: □: the magnitude of $k_{HO\bullet}$ is 10^{7th} order, ○:10^{8th} order Δ: 1.0~5.0×10^{9}, ▲: ~5.0×10^{9} and ×: unknown rate constants calculated by the group contribution method

Several robust tools have been developed to predict radical reaction rate constants for gaseous phase reactions, including: (1) a group contribution method (GCM) (Atkinson, 1986; 1987; Kwok and Atkinson, 1995), (2) quantitative structure-activity relationships (QSARs) (Wang et al., 2009; Gramatica et al., 2004), (3) bond dissociation energies (BDEs) (Heicklen, 1981), (4) computational molecular orbital OH radical (MOOH) methods (Klamt, 1996; Böhnhardt et al., 2008), (5) extrapolation of transition state theory (Cohen, 1982), and (6) neural networks (Bakken and Jurs, 1999). In addition, with use of quantum mechanical methods, it has become possible to calculate the reaction rate constants for various gas phase radical reactions. However, for aqueous phase, only a few studies have developed empirical models for HO• reaction rate constants, including the GCM (Monod et al., 2005), correlations of bond dissociation energies (BDEs) with Arrhenius activation energy (Herrmann, 2003; Gligorovski and Herrmann, 2004) and neural networks (Dutot et al., 2003). There are only a few theoretical studies that have focused on predicting HO• reaction rate constants and other radical reactions in AOPs (Dematteo et al., 2005; Nicolaescu et al., 2005; Pramod et al., 2006; McKee, 2003; Bhat et al., 2004). These studies shed light on detailed reactivity trends for relatively larger molecules but they may not be applicable to a comprehensive model to predict rate constants for the reactions that take place in AOPs.

This study will explore methods to predict the reaction rate constants for the predicted reaction pathways in the aqueous phase AOPs. First, we will develop a GCM for the aqueous phase HO• reaction rate constants. Data base of literature-reported experimental HO• reaction rate constants will be compiled for the GCM. Second, we

will develop linear free energy relationships (LFERs) to relate the logarithm of aqueous phase HO• reaction rate constants with free energies of activation for neutral compounds. The aqueous phase free energy of activation will be calculated using *Ab initio* quantum mechanical methods for the gaseous phase and a solvation method to consider the impact of water. Several solvation methods will be compared using implicit solvation models and statistical solvation model. The quantum mechanically calculated free energy of activation in the aqueous phase will be compared to those that are estimated from the experimentally obtained Arrhenius activation energy and frequency factor. Third, we will examine temperature dependent-reaction rate constants for ionized compounds (i.e., a series of haloacetate ions). The thermochemical properties that are obtained from experiments will be compared to the theoretical calculations. We will also develop the LFERs for the ionized compounds. Once the LFERs are validated with the experimentally obtained values, these LFERs will predict the reaction rate constants for compounds that have not been examined experimentally. The uses of the rate constants predictors are two fold: they enable kinetic modeling, and they indicate the relative importance of pathways.

This study will help engineers and researchers gain a quantitative insight of HO• induced reactions. Predicting reaction rate constant is important for quantifying the efficacy of AOPs as alternative treatment processes and in developing criteria such as reaction time, dose or residual requirements for AOPs optimization. The predicted overall HO• reaction rate constants can also be used as a screening tool associated with apparent removal efficiency for a newly identified contaminant during water treatment processes where HO• is involved. For engineering design, it will free engineers from

complex chemistry details and identify the pitfalls of AOP's technology. Understanding and developing algorithms that can predict the reaction rate constants will help researchers explore chemical kinetics and the practical design of AOPs. Sophisticated quantum mechanical theories help engineers understanding the chemical disciplines and fundamental scientific knowledge. The theoretical studies will give a benchmark to the experimental investigation and engineering design, and improve in understanding AOPs.

1.2 Structure of This Dissertation

This dissertation consists of the introductory part, three main chapters, future studies, and appendices. After this introductory chapter, Chapter 2 discusses development of a group contribution method to predict the aqueous phase HO• reaction rate constants. The work from this chapter has been published and presented in Minakata et al., (2009; 2008). In Chapter 3, linear free energy relationships are developed for neutral compounds. A part of the work from this chapter has been submitted and will be presented in Minakata and Crittenden (2010a,b). Chapter 4 addresses measurement of temperature-dependent HO• reaction rate constants for ionic compounds and development of LFERs. This Chapter includes an update of the GCM. The work from this chapter will be presented and plans to be submitted in Minakata and Crittenden (2010c) and Minakata et al., (2010), respectively. Implications and future studies will be addressed lastly. Appendices cover the detailed computational codes, data, procedures of calculations, and optimized molecular structure of each compound that is determined in this study.

1.3 Literature Cited

Benotti, M. J.; Trenholm, R. A.; Vanderford, B. J.; Holady, J. C.; Stanford, B. D.; Snyder, S. A. Pharmaceuticals and endocrine disrupting compounds in US drinking water. *Environ. Sci. Technol*. 2008, *43*(3), 597-603.

Bolton, J. R.; Carter, S. R. Homogeneous photodegradation pf pollutants in contaminated water: An introduction, Chap. 33, in G. R. Helz, R. G. Zepp, and D. G. Crosby (eds), *Aquatic and Surface Photochemistry*, CRC Press, Boca Raton, FL.

Bruce, G.M.; Pleus, R.C.; Snydere, S.A. Toxicological relevance of pharmaceuticals in drinking water. *Environ. Sci. Technol*. 2010. ASAP.

Buxton, V. B.; Greenstock, C. L.; Helman, W. P.; Ross, A. B. Critical review of rate constants for reactions of hydrated electrons, hydrogen atoms and hydroxyl radicals (•OH/•O^-) in aqueous solution. *J. Phys. Chem. Ref. Data*. 1988, *17* (2) 513-795.

Chemical Abstract Services (CAS). A division of the American Chemical Society. http://www.cas.org/ (accessed September 30, 2009).

Conn, K.E.; Barber, L.B.; Brown, G.K.; Siegrist, R.L. Occurrence and fate of organic contaminants during onsite wastewater treatment. *Environ. Sci. Technol*. 2006, *40*, 7358-7366.

Cooper, W.J.; Cramer, C.J.; Martin, N.H.; Mezyk, S.P.; O'Shea, K.E.; von Sonntag, C. Free radical mechanisms for the treatment of methyl tert-butyl ether (MTBE) via advanced oxidation/reduction processes in aqueous solutions. *Chem. Rev*. 2009, *109*(3), 1302-1345.

Deborde, M.; von Gunten, U. Reactions of chlorine with inorganic and organic compounds during water treatment-kinetics and mechanisms: A critical review. *Wat.Res*.2008, *42*, 13-51.

Dodd, M.C.; Kohler, H-P.E.; von Gunten, U. Oxidation of antibacterial compounds by ozone and hydroxyl radical: Elimination of biological activity during aqueous ozonation processes. *Environ. Sci. Technol*. 2009, *43*, 2498-2504.

Farhataziz; Ross, A.B. Selected specific rates of reactions of transients from water in aqueous solution. III. Hydroxyl radical and perhydroxyl radical and their radical ions. *NSRDS-NBS* 59. 1977, 1-113.

Glaze, W. H.; Kang, J-W.; Chapin, H. D. The chemistry of water treatment processes involving ozone, hydrogen peroxide and ultraviolet radiation. *Ozone. Sci. Eng*. 1987, *9*, 335-352.

Glaze. W. H.; Kang, J-W. Advaced oxidation processes. Test of a kinetic model for the oxidation of organic compounds with ozone and hydrogen peroxide in a semibatch reactor. *Ind. Eng. Chem. Res*. 1989, *28*, 1580-1587.

Halling-Sorensen, B.; Nielsen, S.N.; Lanzky, P.F.; Ingerslev, F.; Holten Lützhoft, H.C.; Jøgensen, S.E. Occurrence, fate and effects of pharmaceutical substances in the environment – a review. *Chemosphere*. 1998, *36*(2), 357-393.

Hayes, T.B.; Khoury, V.; Narayan, A.; Nazir, M.; Park, A.; Brown, T.; Adame, L.; Chan, E.; Buchholz, D.; Stueve, T.; Gallipeau, S. Atrazine induces complete feminization and chemical castration in male African cawed frogs. *PNAS*, 2010, *107*(10), 4612-4617.

Hindmarsh, A.C.; Gear, C.W. Ordinary differential equation system solver. UCID-30001 Rev. 3 Lawrence Livermore Laboratory, Livermore, Ca. 1974.

Hoigné, J. Chemistry of aqueous ozone, and transformation of pollutants by ozonation and advanced oxidation processes. In: J. Hubrec, editor. The handbook of environmental chemistry quality and treatment of drinking water. Berlin: Springer, 1998.

Ikehata, K.; Gamal El-Din, M. Aqueous pesticide degradation by ozonation and ozone-based advanced oxidation processes: A review (part I). *Ozone Sci and Eng*. 2005, *27*, 83-114.

Ikehata, K.; Gamal El-Din, M. Aqueous pesticide degradation by ozonation and ozone-based advanced oxidation processes: A review (part II). *Ozone Sci and Eng*. 2005, *27*, 173-202.

Kang, J-W.; Angelalin, H-M.; Hoffmann, M. Sonolytic destruction of methyl *tert*-butyl ether by ultrasonic irradiation: The role of O_3, H_2O_2, frequency and power density. *Environ. Sci. Technol*. 1999, *33*, 3199-3205.

Kang, J-W.; Angelalin, H-M.; Hoffmann, M. Sonolytic destruction of methyl *tert*-butyl ether by ultrasonic irradiation: The role of O_3, H_2O_2, frequency and power density. *Environ. Sci. Technol*. 1999, *33*, 3199-3205.

Koester, C.J.; Simonich, S.L.; Esser, B.K. Environmental analysis. *Anal. Chem*. 2003, *75*, 2813-2829.

Kolpin, D.W.; Furlong, E.T.; Meyer, M.T.; Thurman, E.M.; Zaugg, S.D.; Barber, L. B.; Buxton, H.T. Pharmaceuticals, hormones, and other organic wastewater contaminants in U.S. streams, 1999-2000: A national reconnaissance. *Envrion. Sci. Technol*. 2002, *36*, 1202-1211.

Lee, Y.; Escher, B.I.; von Gunten, U. Efficient removal of estrogenic activity during oxidative treatment of waters containing steroid estrogens. *Environ. Sci. & Technol*. 2008, 42(17), 6333-6339.

Li, K.; Crittenden, J.C. Computerized pathway elucidation for hydroxyl radical-induced chain reaction mechanisms in aqueous phase advanced oxidation processes. *Environ. Sci. & Technol*. 2009, *43(8)*, 2831-2837.

Li, K.; Hokanson, D.R.; Crittenden, J.C.; Trussell, R.R.; Minakata, D. Evaluating UV/H_2O_2 processes for methyl tert-butyl ether and tertiary butyl alcohol removal. *Wat. Res*. 2008, *42*(20), 5045-5053.

Li, K.; Stefan, M.I.; Crittenden, J.C. Trichloroethene degradation by UV/H_2O_2 advanced oxidation process: product study and kinetic modeling. *Environ. Sci. Technol*. 2007, *41*, 1696-1703.

Li, K.; Stefan, M.I.; Crittenden, J.C. UV photolysis of trichloroethylene: Product study and kinetic modeling. *Environ. Sci. Technol*. 2004, *38*, 6685-6693.

Liang, J.; Palencia, S. L.; Yates, S. R.; Davis, K. M.; Wolfe, L. R. Oxidation of methyl tertiary-butyl ether (MTBE) by ozone and peroxone processes. *J. AWWA*, 1998, *91* (6), 104-114.

Minakata, D.; Li, K.; Westerhoff, P.; Crittenden, J. Development of a group contribution method to predict aqueous phase hydroxyl radical (HO•) reaction rate constants. *Environ. Sci. & Technol*. 2009, *43*, 6220-6227.

Minakata, D.; Li, K.; Crittenden, J.; Westerhoff, P. Development of Group Contribution Method (GCM) for Hydroxyl Radical (HO•) Reaction Rate Constant in the Aqueous Phase. The 14th International Conference on Advanced Oxidation Technologies for Treatment of Water, Air and Soil (AOTs-14). Town & Country Resort, San Diego, California, USA. September 22-25, 2008.

Minakata, D.; Crittenden, J. Quantitative Understanding of Advanced Oxidation Processes for the Treatment of Emerging Contaminants**.** IWA World Water Congress & Exhibition. Montreal, Canada, September 19-24, 2010a.

Minakata, D.; Crittenden, J. Linear Free Energy Relationships between the Aqueous Phase Hydroxyl Radical (HO•) Reaction Rate Constants and the Free Energy of Activation. *Environ. Sci. & Technol*. 2010b. Submitted.

Minakata, D.; Crittenden, J. Linear Free Energy Relationship (LFER) for the Aqueous Phase Hydroxyl Radical (HO•) Reactions with Ionized Species: Experimental and Theoretical Studies. 240th American Chemical Society (ACS) National Meeting & Exposition, Boston, Massachusetts. August 22-26, 2010c.

Minakata, D.; Song, W.; Crittenden, J. Temperature-dependent aqueous phase hydroxyl radical reaction rate constants with ionized compounds: Experimental and theoretical studies. *Environ. Sci. & Technol*. 2010. In preparation.

NRC, 1999, Hormonally Active Agents in the Environment, NAP, Washington, D.C.

NRC, 1999, Identifying Future Drinking Water Contaminants, NAP, Washington, D.C.

Pedersen, J.A.; Soliman, M.; Suffet, I.H. Human pharmaceuticals, hormones, and personal care product ingredients in runoff from agricultural fields irrigated with treated wastewater. *J. Agric. Food Chem*. 2005, *53*, 1625-1632.

Pertović, M.; Gonzalez, S.; Barceló, D. Analysis and removal of emerging contaminants in wastewater and drinking water. *Trends in Analytical Chemistry*, 2003, *22*(10), 685-696.

Pfaendtner, J.; Broadbelt, L. J. Mechanistic modeling of lubricant degradation. 2. The autoxidation of decane and octane. *Ind. Eng. Chem. Res.* 2008a, *47*, 2897-2904.

Pfaendtner, J.; Broadbelt, L. J. Mechanistic modeling of lubricant. 1. Structure-reactivity relationships for free-radical oxidation. *Ind. Eng. Chem. Res.* 2008b, *47*, 2886-2896.

Pfaendtner, J.; Broadbelt, L.J. Elucidation of structure-reactivity relationships in hindered phenols via quantum chemistry and transition state theory. *Chem. Eng. Sci*. 2007, *62*, 5232-5239.

Phillips, P.J.; Smith, S.G.; Kolpin, D.W.; Zaugg, S.D.; Buxton, H.T.; Furlong, E.T.; Esposito, K.; Stinson, B. Pharmaceutical formulation facilities as sources of opioids and other pharmaceuticals to wastewater treatment plant effluents. *Environ. Sci. Technol*. 2010, *44*, 4910-4916.

Renewable Natural Resources Foundations. Environmental Impacts of Emerging Contaminants. *Renewable Resource Journal*. 2006, *24*(1), 1-36.

Richardson, S.D. Water analysis: Emerging contaminants and current issues. *Anal. Chem*. 2009, *81*, 4645-4677.

Richardson, S.D. Environmental mass spectrometry: Emerging contaminants and current issues. *Anal. Chem*. 2004, *76*, 3337-3364.

Richardson, S.D. Mass spectrometry in environmental sciences. *Chem. Rev*. 2001, *101*, 211-254.

Richardson, S.D. Water analysis: Emerging contaminants and current issues. *Anal. Chem*. 2003, 2831-2857.

Richardson, S.D.; Ternes, T.A. Water analysis: Emerging contaminants and current issues. *Anal. Chem*. 2005, *77*, 3807-3838.

Schwarzenbach, R.P.; Escher, B.I.; Fenner, K.; Hofstetter, T.B.; Johnson, C.A.; von Gunten, U.; Wehrli, B. The challenge of micropollutants in aquatic systems. *Science*. 2006, *313*, 1072-1077.

Snyder, S. A.; Wert, E. C.; Hongxia, L.; Westerhoff, P.; Yoon, Y. Removal of EDCs and Pharmaceuticals in Drinking and Reuse Treatment Processes. AWWARF Project, 2007.

Snyder, S.A.; Villeneuve, D.L.; Snyder, E.M.; Giesy, J.P. Identification and quantification of estrogen receptor agonists in wastewater effluents. *Environ. Sci. & Technol*. 2001, *35*, 3620-3625.

Snyder, S.A. Occurrence, treatment, and toxicological relevance of EDCs and pharmaceuticals in water. *Ozone. Sci. Eng*. 2008, *30*, 65-69.

Stefan, M. I.; Bolton, J. R. Mechanism of the degradation of 1, 4-Dioxane in dilute aqueous solution using the UV/hydrogen peroxide process. *Environ. Sci.& Technol*. 1998, *32*, 1588-1595.

Stefan, M. I.; Bolton, J. R. Reinvestigation of the acetone degradation mechanisms in dilute aqueous solution by the UV/H_2O_2 process. *Environ. Sci. & Technol*. 1999, *33*, 870-873.

Stefan, M. I.; Mack, J.; Bolton, J. R. Degradation pathways during the treatment of methyl *tert*-butyl ether by the UV/H_2O_2 process. *Environ. Sci. & Technol*. 2000, *34*, 650-658.

Hopple, J.A.; Delzer, G.C.; Kingsbury, J.A. Anthropogenic organic compounds in source water of selected community water systems that use groundwater, 2002-05. Scientific Investigations Report 2009-5200. U.S.Department of the Interior and U.S. Geological Survey 2009.

Vanderford, B.J.; Pearson, R.A.; Rexing, D.J.; Snyder, S.A. Analysis of endocrine disruptors, pharmaceuticals, and personal care products in water using liquid chromatography/tandem mass spectrometry. *Anal Chem*. 2003, 75(*22*):6265-74.

von Gunten, U. Ozonation of drinking water: Part I. Oxidation kinetics and products formation. *Wat. Res.* 2003a, *37*, 1443-1467.

CHAPTER 2

Development of a Group Contribution Method to Predict Aqueous Phase Hydroxyl Radical Reaction Rate Constants

†*work from this chapter has been published and presented in the following citation:*
Minakata, D.; Li, K.; Westerhoff, P.; Crittenden, J. Development of a group contribution method to predict aqueous phase hydroxyl radical (HO•) reaction rate constants. *Environ. Sci. & Technol*. 2009, *43*, 6220-6227.

Minakata, D.; Li, K.; Crittenden, J.C. Rational Design of Advanced Oxidation Processes using Computational Chemistry. The 16th International Conference on Advanced Oxidation Technologies for Treatment of Water, Air and Soil (AOTs-16). Novermber 15-18, 2010. San Diego, California, USA.

Minakata, D.; Li, K.; Crittenden, J.; Westerhoff, P. Development of Group Contribution Method (GCM) for Hydroxyl Radical (HO•) Reaction Rate Constant in the Aqueous Phase. The 14th International Conference on Advanced Oxidation Technologies for Treatment of Water, Air and Soil (AOTs-14). September 22-25, 2008. Town & Country Resort, San Diego, California, USA.

2.1 Abstract

Hydroxyl radical (HO•) is a strong oxidant that reacts with electron-rich sites of organic compounds and initiates complex chain mechanisms. In order to help understand the reaction mechanisms, a rule-based model was previously developed to predict the reaction pathways. For a kinetic model, there is a need to develop a rate constant estimator that predicts the rate constants for a variety of organic compounds. In this study, a group contribution method (GCM) is developed to predict the aqueous phase HO• reaction rate constants for the following reaction mechanisms: (1) H-atom abstraction, (2) HO• addition to alkenes, (3) HO• addition to aromatic compounds, and (4) HO• interaction with sulfur (S)-, nitrogen (N)- or phosphorus (P)-atom-containing compounds. The GCM hypothesizes that an observed experimental rate constant for a given organic compound is the combined rate of all elementary reactions involving HO•, which can be estimated using the Arrhenius activation energy, E_a, and temperature. Each E_a for those elementary reactions can be comprised of two parts: (1) a base part that includes a reactive bond in each reaction mechanism and (2) contributions from its neighboring functional groups.

The GCM includes 66 group rate constants and 80 group contribution factors, which characterize each HO• reaction mechanism with steric effects of the chemical structure groups and impacts of the neighboring functional groups, respectively. Literature-reported experimental HO• rate constants for 310 and 124 compounds were used for calibration and prediction, respectively. The genetic algorithms were used to determine the group rate constants and group contribution factors. The group contribution factors for H-atom abstraction and HO• addition to the aromatic compounds were found to linearly correlate with the Taft constants, σ*, and electrophilic substituent

parameters, σ^+, respectively. The best calibrations for 83% (257 rate constants) and predictions for 62% (77 rate constants) of the rate constants were within 0.5 to 2 times the experimental values. This accuracy may be acceptable for model predictions of the advanced oxidation processes (AOPs) performance depending on how sensitive the model is to the rate constants.

2.2 Introduction

The hydroxyl radical (HO•) is a reactive electrophile that reacts rapidly and nonselectively with most electron-rich sites of organic contaminants. It is the active species that potentially leads to complete mineralization of emerging contaminants in advanced oxidation processes (AOPs) (e.g., O_3/H_2O_2, UV/H_2O_2, UV/TiO_2) and natural waters (Westerhoff, et al., 2005; Huber et al., 2003; Rosenfeldt and Linden, 2004). Because of the concerns of emerging contaminants and the large number of chemicals that are in use or being produced (CAS, 2009), there is a need for kinetic models that can quickly assess their removal by AOPs. The three critical components for building a kinetic model to predict AOPs performance are (1) numerical methods that solve ordinary differential equations (ODEs), (2) algorithms that can predict reaction pathways, and (3) algorithms that can predict reaction rate constants. Many kinetic models have been built for known reaction pathways (Li et al., 2008; 2007; Stefan et al., 1996; Crittenden et al., 1999). Recently, a model that can generate reaction pathways for the aqueous phase AOPs has been developed (Li and Crittenden, 2009). Yet the capability of generating rate constants for the aqueous phase radical reactions is still limited because of the complexity of radical chemistry.

A number of studies have been conducted to predict the HO• reaction rate constants in the gaseous phase, including 1) a group contribution method (GCM) (King et al., 1999; Atkinson, 1987; Kwok and Atkinson, 1995), 2) quantitative structure-activity relationships (QSARs) (Wang et al., 2009; Öberg, 2005; Gramatica et al., 2004; Medven et al., 1996), 3) bond dissociation energies (BDEs) (Heicklen, 1981), 4) computational molecular orbital OH radical (MOOH) methods (Klamt, 1996; Böhnhardt et al., 2008), 5) extrapolation of transition state theory (Cohen, 1982), 6) correlation with ionization potential (IP) (Percival et al., 1995; Grosjean and Williams, 1992) and 7) neural networks (NNs) (Bakken and Jurs, 1999). When the experimental rate constants for compounds with different functional groups were available, the GCM was proven to be robust for the prediction of gas phase rate constants for compounds with a wide range of functional groups. Atkinson's GCM is one of the most widely accepted methods and is implemented in the U.S. Environmental Protection Agency software, AOPWIN (US EPA, 2000). In their method, the HO• rate constant was determined by the reaction mechanism and effect of neighboring functional group of compound of interest. For each reaction mechanism such as H-atom abstraction, HO• addition, and interactions of HO• with S-, N-, or P-atom-containing compounds, there were "group rate constants" that represented the reaction mechanism and "substitutent factors" that represented the effects of neighboring and next-nearest neighboring functional groups. Using this GCM, the gaseous-phase rate constants at 298 K of ~90% of approximately 485 organic compounds were predicted within a difference of a factor of 2 from the experimental values (Kwok and Atkinson, 1995).

Although the GCM is successful in the gaseous phase, applying it to the aqueous phase requires carefully discerning the mechanistic differences between aqueous and gaseous phase reactions. It is reported that for the H-atom abstraction involving C-H bonds, relative solvent effects are usually much smaller as compared to other reaction mechanisms (e.g., β-scission) (Avila et al., 1993) (which is why the gaseous phase C-H bond strengths in BDE can be used to rationalize reactions in solution). For the aqueous phase, uncertainties still remain associated with long/short range interactions between solvent and solute in the first solvation shell and on its boundary. Figure 2.1 compares the HO• reaction rate constants in the gaseous and aqueous phases for a total of 92 organic compounds. A rough linear correlation was found for the HO• rate constants between two phases. The linearity for alkanes is better than that for oxygenated aliphatic compounds (e.g. alcohol, ether, ester). In general, these polar compounds form hydrogen bond in the aqueous phase, which makes the adjacent C-H bonds vulnerable and the aqueous phase reactions distinctive from the gaseous phase ones. In addition, there are significant mechanistic differences of the formation of the transition state in two phases. Solvent cage (Persico and Granucci, 2007) during the solvation process affects the free energy of activation of reactions (Cramer, 2004) and, thus, changes the rate constant. The impact varies significantly for different radicals and functional groups.

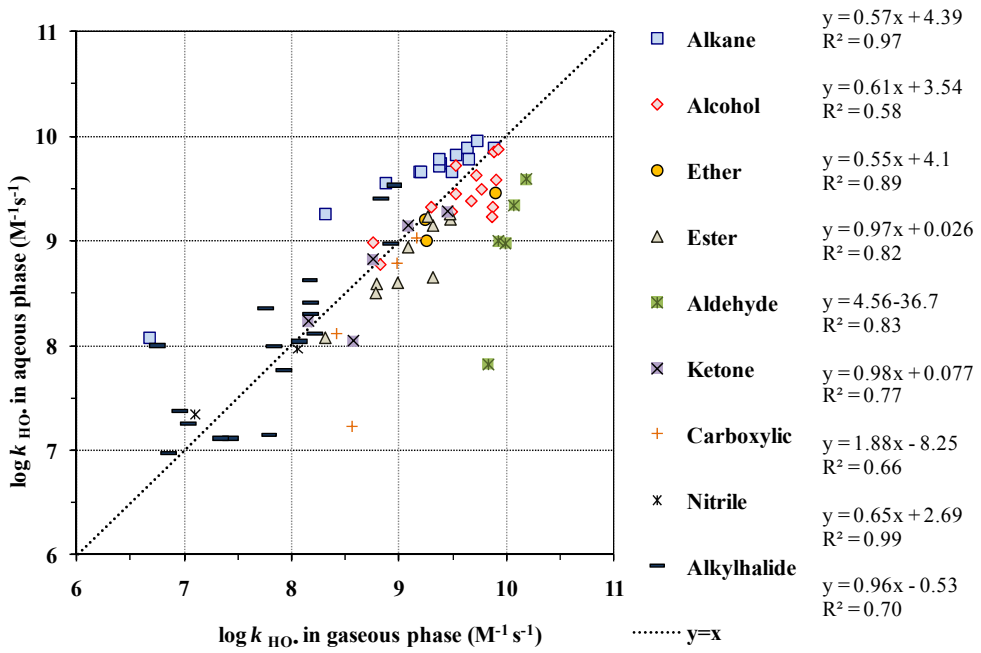

Figure 2.1: Comparison of the aqueous and gaseous phase HO• reaction rate constants. The unit of the gaseous phase rate constant was converted from 1/molecule/cm^3/s to 1/M/s

There are only a few studies concerned with the prediction of aqueous phase reaction rate constants in AOPs. Monod et al. (2005) applied the GCM to estimate the aqueous phase HO• rate constants for the oxygenated aliphatic compounds. They reported that 84% of their 128 calculated data were within a difference of a factor of 5 from the experimental values. However, the parameters that represented the property of functional groups in their GCM did not follow trends that would be expected on the basis of the reaction mechanisms. For example, their "substituent factors at 298K" of $–CH_3$ and $–CH_2–$ groups were different in magnitude of an order (i.e., 1.00 and 11.13, respectively), while –OH group has 6.76 of "substituent factor at 298K". Herrmann (2003) used the correlation between BDE (uncertainty of ± 8.4 kJ/mol) of the weakest C-

H bond broken and Arrhenius activation energy, E_a, and obtained the Evans and Polanyi relationship for 16 oxygenated compounds with a 0.75 correlation coefficient. Dutot et al. (2003) used an artificial neural network and multilayer perception (MLP) to estimate HO• rate constants, and 87% of the MLP predictions were within a factor of 2 from the experimental data.

In this study, a GCM is developed to predict the aqueous phase HO• rate constants that integrate the reaction mechanisms in the aqueous phase and the essential features of Atkinson's GCM. The potential errors and limitations of the GCM will be discussed herein.

2.3 Development of the Group Contribution Method

The GCM is based on Benson's thermochemical group additivity (Benson, 1976). It hypothesizes that an observed experimental rate constant for a given organic compound is the combined rate of all elementary reactions involving HO•, which can be estimated using E_a. For each reaction mechanism, there is a base activation energy, E_a^0, and a functional group contribution of activation energy, $E_a^{R_i}$, due to the neighboring (i.e., α-position) and/or the next nearest neighboring (i.e., β-position) functional group (i.e., R_i). These contributions to the rate constant can be parameterized and determined empirically when sufficient rate constant data are available.

The GCM considers four reaction mechanisms that HO• initiates in the aqueous phase, which include (1) H-atom abstraction, (2) HO• addition to alkenes, (3) HO• addition to aromatic compounds, (4) HO• interaction with sulfur (S)-, nitrogen (N)-, or phosphorus (P)-atom-containing compounds. Accordingly, an overall reaction rate constant, $k_{overall}$, may be given in equation (2.1).

$$k_{\text{overall}} = k_{\text{abs}} + k_{\text{add-alkene}} + k_{\text{add-aromatic}} + k_{\text{int}} \tag{2.1}$$

where, k_{abs}, $k_{\text{add-alkene}}$, $k_{\text{add-aromatic}}$, and k_{int} are the rate constants for the aforementioned reaction mechanisms 1 – 4, respectively. The manner in which these rate constants are determined is discussed in the following section.

2.3.1 Hydrogen-atom Abstraction

For H-atom abstraction, the active bond is a C-H bond. According to the functional groups on the C atom, there are primary, secondary, and tertiary C-H bond(s) except in the special case of methane. Therefore, the fragments of a molecule are CH_3R_1, $CH_2R_1R_2$, and $CHR_1R_2R_3$, where R_i is a functional group (i = 1-3). Each of the fragments corresponds to a partial rate constant $k_{\text{CH}_3\text{R}_1}$, $k_{\text{CH}_2\text{R}_1\text{R}_2}$, and $k_{\text{CHR}_1\text{R}_2\text{R}_3}$, respectively. The E_a for the reaction of HO• is affected by the C-H bond itself and adjacent functional group(s). The contribution that results from the C-H bond to the E_a is defined as base activation energy, E_a^0, while the contribution of the functional groups is defined as a group contribution parameter, $E_{a,\text{abs}}^{\text{R}_i}$, due to the functional group R_i for H-atom abstraction. For example, the base activation energy for H-atom abstraction from one of the primary C-H bonds is $E_{a,\text{prim}}^0$. The $E_{a,\text{abs}}^{\text{R}_i}$ indicates the electron-donating and -withdrawing ability of the functional group. An electron-donating functional group decreases the E_a^0 and, hence, increases the overall reaction rate constant and vice versa. Accordingly, the partial rate constant for the fragmented part, CH_3R_1, can be written as below

$$k_{\text{CH}_3\text{R}_1} = 3A_{\text{prim}}\, e^{-\frac{E_{a,\text{prim}}^0 + E_{a,\text{abs}}^{\text{R}_1}}{RT}} \tag{2.2}$$

where 3 is the amount of primary C-H bonds, A_{prim} denotes the Arrhenius frequency factor for the reaction of HO• with CH_3R_1, R is the universal gas constant, and T denotes absolute temperature.

Similarly, the partial rate constants for other fragmented parts CH_2R_2 and $CHR_1R_2R_3$ are expressed in equations (2.3) and (2.4) using the corresponding frequency factors, A_{sec} and A_{tert}, and group contribution parameters, $E_{a,\text{abs}}^{\text{R}_2}$ and $E_{a,\text{abs}}^{\text{R}_3}$, respectively.

$$k_{\text{CH}_2\text{R}_1\text{R}_2} = 2A_{\text{sec}} e^{-\frac{E_{a,\text{sec}}^0 + E_{a,\text{abs}}^{\text{R}1} + E_{a,\text{abs}}^{\text{R}2}}{RT}} \tag{2.3}$$

$$k_{\text{CHR}_1\text{R}_2\text{R}_3} = A_{\text{tert}}\, e^{-\frac{E_{a,\text{tert}}^0 + E_{a,\text{abs}}^{\text{R}1} + E_{a,\text{abs}}^{\text{R}2} + E_{a,\text{abs}}^{\text{R}3}}{RT}} \tag{2.4}$$

However, for equations (2.2) – (2.4), the functional group contribution is ignored for cases where the neighboring functional groups have no effect on the H-atom abstraction (i.e., $E_{a,\text{abs}}^{\text{-H}}$ is zero, where a valence bond of the H-atom is expressed as a line before H).

The group rate constants that represent H-atom abstraction from the primary, secondary, and tertiary C-H bond are defined as k_{prim}^0, k_{sec}^0, and k_{tert}^0 and are expressed in equations (2.5)-(2.7).

$$k_{\text{prim}}^0 = A_{\text{prim}}^0 e^{-\frac{E_{a,\text{prim}}^0}{RT}} \tag{2.5}$$

$$k_{\text{sec}}^0 = A_{\text{sec}}^0 e^{-\frac{E_{a,\text{sec}}^0}{RT}} \tag{2.6}$$

$$k_{\text{tert}}^0 = A_{\text{tert}}^0 e^{-\frac{E_{a,\text{tert}}^0}{RT}} \tag{2.7}$$

In addition, the group rate constant k_{R_4} is defined for the HO• interaction with the functional group R_4 (e.g., -OH and -COOH). The detailed discussions for R_4 will be

given in the following sections. The group contribution factor, X_{R_i}, that represents the influence of functional group R_i is defined in equation (2.8).

$$X_{\mathrm{R}_i} = e^{-\frac{E_{a,\mathrm{abs}}^{\mathrm{R}_i}}{RT}} \tag{2.8}$$

Because each reaction is independent of one another, the rate constant for H-atom abstraction, k_{abs}, may be written as the sum of the partial rate constants

$$k_{\mathrm{abs}} = 3\sum_{0}^{I} k_{\mathrm{prim}}^{0}\, X_{\mathrm{R}_1} + 2\sum_{0}^{J} k_{\mathrm{sec}}^{0} X_{\mathrm{R}_1} X_{\mathrm{R}_2} + \sum_{0}^{K} k_{\mathrm{tert}}^{0}\, X_{\mathrm{R}_1} X_{\mathrm{R}_2} X_{\mathrm{R}_3} + k_{\mathrm{R}_4} \tag{2.9}$$

where, I, J, and K denote the number of the fragments CH_3R_1, CH_2R_2, and $CHR_1R_2R_3$, respectively. Equation (2.10) shows an example of the rate constant calculation for 1,2-dichloro-3-bromopropane (CH_2Cl-$CHCl$-CH_2Br). The detailed definitions of the functional groups will be given in the Results and Discussions.

$$k_{\mathrm{overall}} = 2k_{\mathrm{sec}}^{0} X_{\text{-Cl}} X_{\text{-CHCl-}} + k_{\mathrm{tert}}^{0} X_{\text{-Cl}} X_{\text{-CH}_2\text{Cl}} X_{\text{-CH}_2\text{Br}} + 2k_{\mathrm{sec}}^{0} X_{\text{-Br}} X_{\text{-CHCl-}} \tag{2.10}$$

Rate constant additivity can be an important concern. To investigate this, the experimental rate constants for the linear and longer chain compounds with some functional groups were compared with the number of -CH_2- alkyl functional group as shown in Figure 2.2. The linear relationship was observed, and it verified the rate constant additivity. For nonlinear compounds, nonadditive effects arise from different contributions to entropy of activation (Cohen and Benson, 1987) and hence affect A. Generally, A can be assumed to be constant for the same reaction mechanism because intrinsic entropy due to translation and rotation can be assumed to be constant. Strictly speaking, however, moments of inertia of primary, secondary, and tertiary C-H bond would be different and thus affect entropy (Cohen, 1991). Although this difference is insignificant when compared to other factors such as the impacts of neighboring

functional groups (Cohen and Benson, 1987), the GCM considers different A_{prim}, A_{sec}, and A_{tert}. Therefore, this should be sufficient to treat nonlinear compounds.

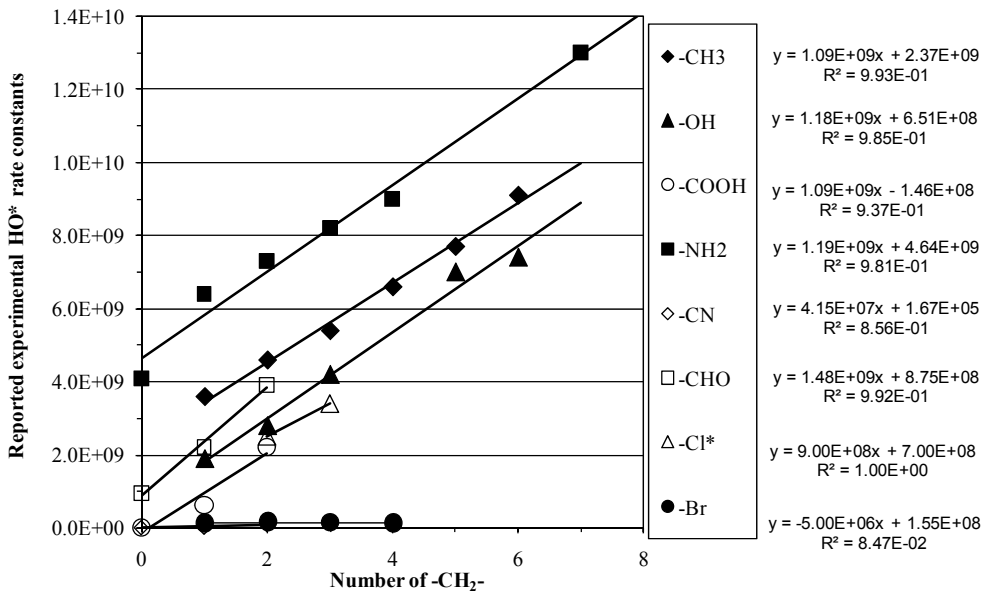

Figure 2.2: The experimental HO• reaction rate constants as a function of the number of –CH_2- alkyl functional group for some functional groups. The chemical formula is expressed as CH_3-$(CH_2)_n$-R, where R is –CH_3, -OH, -COOH, -NH_2, -CN, -CHO, -Cl, and –Br, for alkane, alcohol, carboxylic, amine, cyano, aldehyde, chlorine, and bromine, respectively, and *n* is the number of –CH_2- alkyl functional groups. *There are only two rate constants available for –Cl.

2.3.2 HO• Addition to Alkenes

Detailed mechanisms of HO• addition to alkene in the aqueous phase have not been elucidated yet. It is expected that molecular solvation affects the E_a and water molecules interact with the HO• approaching the carbon double bonds. Nevertheless, it can be a reasonable assumption that there is little difference in the major reaction mechanisms between the aqueous and gaseous phases (Singleton and Cvetanović, 1976; Davey et al., 2004; Getoff, 1991). As postulated by Cvetanović (1976), the reactions

between HO• and alkene proceeds via a π complex which is initiated to loose association of HO• to the π-electron cloud spanning the double bond. Recent observation by infrared spectroscopy suggests a T-shaped reactant complex between HO• and acetylene (the hydrogen of HO• pointing toward the alkene) (Davey et al., 2004). Several quantum calculations on HO• addition to alkene in the gaseous phase supports the general mechanisms of the HO• addition on π bonds (Greenwald et al., 2005). The initial transition reaction of HO• with alkene is via a barrier-less association reaction followed by an addition on the double bond through a transition state slightly above the π-complex energy (Peeters et al., 2007). Villà et al. (1997) found that there is a correlation between activation energy and energy at a saddle point of entrance channel relative to reactants. The negative energy on the saddle point indicates that there is a second transition state in some energy range near the reaction threshold. On the first saddle point (i.e. inner transition state), the bottleneck at the high energies is dominant, whereas on the second saddle point (i.e. outer transition state), the bottleneck at the low energies is dominant. At the first transition state, the rate of HO• addition can be significantly affected by the polar effect of the functional group. If the functional group at the neighboring carbon atom is electron-donating group (e.g. $-CH_3$), the addition reaction of HO• is enhanced and the vise-versa in case of the electron-withdrawing group.

$$HO\bullet + H_2C{=}CH\text{-}R \rightarrow \left[\overset{\delta-}{HO} \cdots CH_2 \overset{\cdots\cdots}{=} \overset{\delta+}{CH} - R \right]^{\neq} \rightarrow HOCH_2\text{-}\dot{C}HR \qquad (2.11)$$

Although there are many explanations in terms of the differences in stabilities of the newly formed radical centered, it is not convincing because the stabilities of the radicals formed play only a minor role in determining the rate of HO• addition to alkenes in case that the alkene functional groups are varied. Consequently, the functional groups

exert polar effects of similar magnitude reflecting to a first approximation only the difference in the steric effects of the functional groups. In addition, the functional groups at a carbon atom undergoing attack in the α-position have the different effects to the HO• addition than those at the neighboring carbon atom in the β-position.

Considering a basic C=C double bond structure (i.e., one σ-bond and one π-bond, >C=C<), HO• has two places to add. The probability of HO• addition to either of the carbons depends on the functional groups bonded to the unsaturated carbons. Except in the special case of ethylene, six basic structures associated with the number of H-atoms and their positions are considered, including *cis* and *trans* conformations (i.e., >C=C<, H>C=C<, H_2C=C<, H>C=C<H(cis), H>C=C<H(trans), and H_2C=C<H). If the base structure is symmetrically associated with the number and position of hydrogen atom(s), the probability of HO• addition to two unsaturated carbons is assumed to be identical, whereas it is different for the asymmetrical base structure. This treatment reflects the differences in the *A* resulting from regioselectivity. Accordingly, the group rate constant, $k^0_{(\text{structure})-h}$, and group contribution factor, Y_{R_l}, for HO• addition to one of the base structures may be written using Arrhenius frequency factor, $A^0_{(\text{structure})-h}$, and group contribution parameter, $E^{\text{R}_l}_{a,\text{add-alkene}}$, of functional group R_l (*l* denotes the number of functional groups, *l* = 1-4), respectively.

$$k^0_{(\text{structure})-h} = A^0_{(\text{structure})\text{-}h} e^{-\frac{E^0_{\text{a}\,,(\text{structure})}}{RT}} \tag{2.12}$$

$$Y_{\text{R}_l} = e^{-\frac{E^{\text{R}_l}_{a,\text{add-alkene}}}{RT}} \tag{2.13}$$

where (structure) represents six base structures that are addressed above, $E^0_{a,(\text{structure})}$ denotes a base part of E_a for (structure), and h denotes a position for HO• to add (i.e., 1 and 2 for the addition to the left and right carbon, respectively). The rate constant for HO• addition to alkene, $k_{\text{add-alkene}}$, may be written in equation (2.14).

$$k_{\text{add-alkene}} = \sum g\, k^0_{(\text{structure})\text{-}h}\, Y_{\text{R}_l} \tag{2.14}$$

where g indicates 1 or 2 that represents asymmetrical and symmetrical addition, respectively. Equation (2.15) shows an example for tetrachloroethylene ($Cl_2C{=}CCl_2$).

$$k = 2k^0_{>\text{C=C}<}\, Y_{\text{-Cl}} Y_{\text{-Cl}} Y_{\text{-Cl}} Y_{\text{-Cl}} \tag{2.15}$$

2.3.3 HO• Addition to Aromatic Compounds

It has been proposed that HO• fixation at a given carbon may be via a short-lived π-complex for the aqueous phase reactions of HO• with aromatic compounds (Ashton et al., 1995). The formation of the π-complex is a reversible reaction on one hand. On the other hand, HO-adduct radical by the fixation of HO• to the π-bond is irreversibly produced to form σ bond. High regioselectivity of HO• addition occurs at the transition state from the π- to the σ- complex.

$$\text{Ar} + \text{HO}\bullet \rightarrow [\text{HO}\cdots\text{Ar}]^{\bullet}_{\pi} \tag{2.16}$$

$$[\text{HO}\cdots\text{Ar}]^{\bullet}_{\pi} \rightarrow \text{Ar} + \text{HO}\bullet \tag{2.17}$$

$$[\text{HO}\cdots\text{Ar}]^{\bullet}_{\pi} \rightarrow [\text{HO}\cdots\text{Ar}]^{\bullet}_{\sigma} \tag{2.18}$$

Reaction (2.16) is diffusion-controlled and Reactions (2.17) and (2.18) are activation-controlled. According to Ashton et al. (1995), the rearrangement of the π- to the σ- complex requires little or no activation energy, whereas the dissociation of the σ-complex requires approximately 20 kJ/mol.

Although the HO• preferentially adds to the aromatic ring at the close to diffusion-controlled rates, the HO• addition to the aromatic ring can be expected to be highly regioselective due to the electrophilic HO•. Therefore, the electron-donating and -withdrawing functional groups on the aromatic ring can significantly affect the rate constants and the ratio of *ortho*-, *meta*-, *para*-, and *ipso*-positions.

For the HO• addition to aromatic compounds, the following points are considered. (1) Probability for the symmetrical HO• addition to the benzene ring is identical. (2) Addition to the *ipso*-position is negligible due to the significant steric effect (Mvula et al., 2001; Raghavan and Steenken, 1980; Merga et al., 1996). Although some studies report the possibility for the addition to the *ipso*-position (Razavi et al., 2009), it is quite negligible for the aromatic compounds with single functional groups, which are used for the calibration (e.g., <8% for phenol (Mvula et al., 2001; Raghavab and Steenken, 1980) and <1% for chloro benzene (Merga et al., 1996)). Therefore, only when all positions on the aromatic ring are filled with the functional groups, HO• adds to the *ipso*-position with the identical probability on all available positions. The reaction rate constant for the HO• addition to aromatic compounds is formulated in the following manner. The E_a is a sum of two parts: (i) a base part, E_a^0, resulting from the HO• addition to the aromatic ring depending on the number(s) and position(s) of the functional group and (ii) group contribution parameter(s), $E_{a,\text{add-aromatic}}^{\text{R}_m}$, due to the functional group, R_m (where m is the number of functional group(s), m = 1-6), on the aromatic ring. We assume that A differs not by the types of the functional group to reduce the number of group contribution factors to calibrate but by the number and position of the functional groups. Accordingly,

the group rate constant, $k^0_{(i-\text{name})-j}$, and the group contribution factor, Z_{R_m}, may be expressed as below

$$k^0_{(i-\text{name})-j} = A^0_{(i-\text{name})-j} e^{-\frac{E^0_{a,(i-\text{name})}}{RT}} \tag{2.19}$$

$$Z_{\text{R}_m} = e^{-\frac{E^{\text{R}_m}_{a,\text{add-aromatic}}}{RT}} \tag{2.20}$$

where, $A^0_{(i-\text{name})-j}$ denotes the Arrhenius frequency factor; $E^0_{a,(i-\text{name})}$ denotes a base part of E_a; the name, benz, pyr, fur, imid, or triaz denotes a compound that has a base structure of benzene, pyridine, furan, imidazole, or triazine, respectively; *i* denotes position(s) of the functional group, and *j* denotes position(s) for HO• to add. The rate constant for the HO• addition to aromatic compounds may be expressed as shown in equation (2.21)

$$k_{\text{add-aromatic}} = \sum n k^0_{(i\text{-name})\text{-}j} Z_{\text{R}_m} \tag{2.21}$$

where *n* denotes the number of available position(s) to add. Equation (2.22) shows an example for 1,4-*tert*-butylphenol [$(CH_3)_3C\text{-}C_6H_4\text{-}OH$].

$$k = \left\{ 2k^0_{(1,4-\text{benz})-2,6} + 2k^0_{(1,4-\text{benz})-3,5} \right\} Z_{\text{-OH}} Z_{\text{-Alkane}} + 3 \times 3 \times k^0_{\text{prim}} X_{>\text{C}<} + k_{\text{-OH}} \tag{2.22}$$

2.3.4 HO• Interactions with Sulfur-, Nitrogen-, or Phosphorus-atom Containing Compounds

When a molecule has S-, N-, or P-atom-containing functional groups, HO• interacts with the S-, N-, or P-atom in the aqueous phase forming a 2σ/1σ* two-center–three-electron (2c-3e) adduct (Asmus and Bonifačič, 1999). These functional groups also affect the H-atom abstraction reaction by donating or withdrawing electrons on the C-H bond. The group rate constant, k_{R_4}, in equation (2.9) represents the HO• interaction with S-, N-, or P-containing compounds. Because almost all of the functional groups in the

neighboring positions were alkyl functional groups, and therefore, we assume that the effect of the functional groups might be uniform, the influence of neighboring functional groups was not considered for the interaction reactions. Equation (2.23) shows an example for iminodiacetic acid (HOOC-CH_2-NH-CH_2-COOH).

$$k = 2 \times 2k_{\text{sec}}^{0} X_{\text{-COOH}} X_{\text{-NH-}} + k_{\text{-NH-}} + 2k_{\text{-COOH}} \tag{2.23}$$

2.4 Results and Discussion

2.4.1 Calibration and Prediction

The group rate constants and group contribution factors for each reaction mechanism were calibrated with literature-reported experimental rate constants. The objective function (OF) was minimized using the genetic algorithms (Goldberg, 1989; Charbonneau and Knapp, 1995). Appendix A includes the source code of genetic algorithms.

$$\text{OF} = \sqrt{\frac{1}{N-1}\sum_{i=1}^{N}\left[(k_{\text{exp},i} - k_{\text{cal},i})/k_{\text{exp},i}\right]^2} \tag{2.24}$$

where, $k_{\text{exp},i}$ and $k_{\text{cal},i}$ are the experimental and calculated reaction rate constant of compound i, respectively, and N is the number of the rate constants. First, group rate constants, k^0, and group contribution factors for the H-atom abstraction, X_{R_i}, were calibrated. Then, these group rate constants and group contribution factors were used when aliphatic side chains were present in the alkene and aromatic compounds upon the calibrations of the group rate constants and group contribution factors for alkenes and aromatic compounds (i.e., Y_{R_i} for alkene and Z_{R_i} for aromatic compounds, respectively). For the HO• interaction, the group rate constant, k_{R_4}, in equation (2.9), and group contribution factors for S-, N-, or P-atom-containing functional groups were calibrated.

We critically evaluated the literature reported experimental rate constants before the calibrations. When several rate constants were reported for the same compound, an average value was used or the most reasonable rate constant was selected by comparing the value to those for compounds with similar structures (Hermann, 2003; Buxton et al., 1988; U of Notre Dame RCDC, 2009). The rate constants that we used for the calibration are at standard conditions (i.e., 25ºC and 1 mol/L) in the aqueous phase. When the experimental conditions were not reported in the literature, we used those reported values. Our objective is to calibrate the group rate constants and group contribution factors with the experimental data and predict rate constants within a factor of 0.5 to 2.0 of the experimental value, which we refer to as our error goal (EG). This EG would be in the range of general experimental errors (Buxton et al., 1988; U of Notre Dame RCDC, 2009) and sufficient for decision-making that has been used for the physical-chemical property estimators (e.g., within an order of magnitude) (US EPA, 2007). For calibration, rate constants for single-functional group compounds were used to avoid the interference of different functional groups. For prediction, we used the calibrated group rate constants and group contribution factors to predict the rate constants for multifunctional group compounds. Sample deviation (SD) that was calculated from equation (2.24) was also used to evaluate the rate constants from calibrations and predictions. All observed overall HO• rate constants for the 434 compounds were summarized in Table 2.1. Appendix B includes up-to-date literature-reported experimental HO• rate constants.

Table 2.1: Calculated HO• reaction rate constants (Normal: calculated, *Italic*: predicted, **Bold**: error is out of the EG) as compared to literature-reported experimental values

group		formula	compound	*k* exp	*k* cal	((*k* exp-*k* cal)/*k* exp)2	*k* cal/*k* exp
Alkane	**1**	**CH3-CH3**	**ethane**	**1.80E+09**	**7.90E+08**	**0.31476**	**0.44**
	2	CH3-CH2-CH3	propane	3.60E+09	2.11E+09	0.17127	0.59
	3	CH3-CH(CH3)-CH3	2-methylpropane	4.60E+09	4.04E+09	0.01490	0.88
	4	CH3-(CH2)2-CH3	butane	4.60E+09	3.52E+09	0.05556	0.76
	5	CH3-(CH2)3-CH3	pentane	5.40E+09	4.92E+09	0.00776	0.91
	6	CH3-(CH2)4-CH3	hexane	6.60E+09	6.33E+09	0.00164	0.96
	7	CH3-(CH2)5-CH3	heptane	7.70E+09	7.74E+09	0.00003	1.01
	8	CH3-(CH2)6-CH3	octane	9.10E+09	9.15E+09	0.00003	1.01
	9	CH3-CH(CH3)-CH3	2-methylpropane	4.60E+09	4.04E+09	0.01490	0.88
	10	CH3-CH2-CH(CH3)-CH3	2-methylbutane	5.20E+09	5.10E+09	0.00035	0.98
	11	CH3-CH2-CH(CH2-CH3)-CH2-CH3	3-ethylpentane	5.90E+09	8.49E+09	0.19332	1.44
	12	CH3-C(CH3)2-CH2-CH(CH3)-CH3	2,2,4-Trimethylpentane	6.10E+09	6.41E+09	0.00259	1.05
Alcohol	**13**	**CH3-OH**	**methanol**	**9.70E+08**	**3.04E+08**	**0.47157**	**0.31**
	14	CH3-CH2-OH	ethanol	2.10E+09	1.18E+09	0.19372	0.56
	15	CH3-(CH2)2-OH	1-propanol	3.20E+09	2.55E+09	0.04109	0.80
	16	CH3-(CH2)3-OH	1-butanol	4.20E+09	3.96E+09	0.00327	0.94
	17	(CH3)3-C-OH	tert-butanol	7.00E+08	8.21E+08	0.02972	1.17
	18	CH3-(CH2)5-OH	1-hexyanol	7.00E+09	6.78E+09	0.00102	0.97
	19	CH3-(CH2)6-OH	1-heptanol	7.40E+09	8.19E+09	0.01127	1.11
	20	CH3-CH(OH)-CH3	2-propanol	1.90E+09	2.37E+09	0.06154	1.25
	21	CH3-CH(CH3)-CH2-OH	2-methyl-1-propanol	3.30E+09	4.55E+09	0.14411	1.38
	22	CH3-CH2-C(CH3)(OH)-CH3	2-methyl-2-butanol	1.90E+09	2.34E+09	0.05322	1.23
	23	**CH3-C(CH3)2-CH2-OH**	**2,2-dimethyl-1-propanol**	**5.20E+09**	**2.04E+09**	**0.37026**	**0.39**
	24	CH3-CH2-CH(CH3)-CH2-OH	3-methyl-1-butanol	3.80E+09	6.04E+09	0.34681	1.59
	25	CH3-CH(OH)-CH2-CH3	2-butanol	3.50E+09	3.78E+09	0.00662	1.08
	26	CH3-C(CH3)(OH)-CH2-CH3	tert-amyl alcohol	1.90E+09	1.77E+09	0.00439	0.93
Diol	***27***	***HO-CH2-OH***	***dihydroxymethane***	***1.30E+09***	***5.41E+08***	***0.34047***	***0.42***
	28	*HO-CH2-CH2-OH*	*ethyleneglycol*	*2.40E+09*	*1.59E+09*	*0.11475*	*0.66*
	29	*CH3-CH(OH)2*	*1,1-ethanediol*	*1.20E+09*	*1.36E+09*	*0.01753*	*1.13*
	30	*CH3-CH(OH)-CH2-OH*	*1,2-propanediol*	*1.70E+09*	*2.82E+09*	*0.43429*	*1.66*
	31	*HO-(CH2)3-OH*	*1,3-propanediol*	*2.50E+09*	*3.00E+09*	*0.03929*	*1.20*
	32	*CH3-CH(OH)-CH2-CH2-OH*	*1,3-butanediol*	*2.20E+09*	*4.23E+09*	*0.85046*	*1.92*
	33	*HO-(CH2)4-OH*	*1,4-butanediol*	*3.20E+09*	*4.40E+09*	*0.14158*	*1.38*
	34	***CH3-CH(OH)-CH(OH)-CH3***	***2,3-butanediol***	***1.30E+09***	***4.05E+09***	***4.48664***	***3.12***
	35	*HO-(CH2)5-OH*	*1,5-pentanediol*	*3.60E+09*	*5.81E+09*	*0.37775*	*1.61*
	36	***CH3-CH(OH)-CH2-CH(OH)-CH3***	***2,4-pentanediol***	***2.30E+09***	***5.46E+09***	***1.89022***	***2.37***
	37	*HO-(CH2)6-OH*	*1,6-hexyanediol*	*4.70E+09*	*7.22E+09*	*0.28774*	*1.54*
	38	*HO-CH2-CH(OH)-CH2-OH*	*glycerol*	*2.00E+09*	*3.17E+09*	*0.34377*	*1.59*
Ether	39	CH3CH(OCH3)2	1,1-dimethoxyethane	2.20E+09	1.48E+09	0.10720	0.67
	40	**CH3-O-CH3**	**dimethylether**	**1.00E+09**	**3.89E+08**	**0.37364**	**0.39**
	41	***CH3-O-CH2-O-CH3***	***methylene glycol diethyl ether***	***3.20E+08***	***6.99E+08***	***1.40301***	***2.18***
	42	CH3-CH2-O-CH2-CH3	diethylether	2.90E+09	2.09E+09	0.07809	0.72
	43	(CH3)2HC-O-CH(CH3)2	diisopropyl ether	2.49E+09	4.41E+09	0.59325	1.77
	44	(CH3)3-C-O-CH2-CH3	tert-butyl-ethyl-ether	1.80E+09	1.77E+09	0.00037	0.98
	45	$C_2H_5C(CH_3)_2OCH_3$	tert-amyl methyl ether	2.37E+09	1.87E+09	0.04479	0.79
	46	*CH3CH2-O-CH2CH2-CH2CH2-O-CH2CH3*	*diethylene glycol diethyl ether*	*3.20E+09*	*6.23E+09*	*0.89594*	*1.95*
	47	*CH3CH2-O-CH2CH2-O-CH2CH3*	*ethylene glycol diethyl ether*	*2.30E+09*	*3.41E+09*	*0.23369*	*1.48*
	48	*CH3-O-CH2-CH2-O-CH3*	*ethylene glycol dimethyl ether*	*1.60E+09*	*1.71E+09*	*0.00481*	*1.07*
	49	CH2(OC2H5)2	diethoxymethane	1.60E+09	2.40E+09	0.24995	1.50
	50	CH2(OCH3)2	dimethoxymethane	1.20E+09	6.99E+08	0.17428	0.58
	51	***CH3-C(CH3)(OCH3)CH2-OH***	***2-methyl-2-methoxy propanol***	***8.40E+08***	***1.82E+09***	***1.35033***	***2.16***
	52	*CH3-O-CH2-CH2-OH*	*2-methoxyethanol*	*1.30E+09*	*1.65E+09*	*0.07206*	*1.27*
	53	*C2H5-O-CH2-CH2-OH*	*2-ethoxyethanol*	*1.70E+09*	*2.50E+09*	*0.22113*	*1.47*
	54	*HO-CH2-CH2-O-CH2-CH2-OH*	*diethylene glycol*	*2.10E+09*	*2.91E+09*	*0.14849*	*1.39*
Ketone	***55***	***CH3-CO-CO-CH3***	***2,3-butanedion***	***2.80E+08***	***1.09E+08***	***0.37456***	***0.39***
	56	CH3-CH2-CO-CH3	2-butanone	8.10E+08	6.45E+08	0.04165	0.80
	57	CH3-CO-CH3	acetone	1.10E+08	1.09E+08	0.00015	0.99
	58	CH3-CH2-CH2-CO-CH3	2-pentanone	1.90E+09	2.00E+09	0.00260	1.05
	59	CH3-CH2-CO-CH2-CH3	3-pentanone	1.40E+09	1.18E+09	0.02453	0.84
	60	***CH3-CO-CH(OH)-CH3***	***3-hydro-2-butanone***	***2.90E+09***	***7.67E+08***	***0.54106***	***0.26***
	61	(CH3)2-CH-CH2-CO-CH3	methyl-iso-butyl ketone	2.10E+09	4.00E+09	0.81715	1.90
	62	*CH3-CO-CH2CH2-CO-CH3*	*acetonyl acetone*	*7.60E+08*	*4.78E+08*	*0.13754*	*0.63*

Table 2.1: Calculated HO• reaction rate constants (Normal: calculated, *Italic*: predicted, **Bold**: error is out of the EG) as compared to literature-reported experimental values (Continued)

Aldehyde	63	CH3-CHO	acetaldehyde	9.50E+08	1.01E+09	0.00464	1.07
	64	CH3-CH2-CHO	propionaldehyde	2.20E+09	1.94E+09	0.01355	0.88
	65	CH3-CH2-CH2-CHO	butyraldehyde	3.90E+09	3.32E+09	0.02205	0.85
	66	(CH3)2-CH-CHO	isobutyl aldehyde	2.90E+09	3.17E+09	0.00876	1.09
	67	***CH3-C(CH3)(OCH3)-CHO***	***2-methyl-2-methoxy-propanal***	***3.99E+09***	***1.52E+09***	***0.38446***	***0.38***
	68	*HO-C(CH3)2-CHO*	*hydroxy-iso-butylaldehyde*	*3.00E+09*	*1.77E+09*	*0.16826*	*0.59*
	69	***CH3-CO-CHO***	***methyl glyoxal***	***5.30E+08***	***1.65E+08***	***0.47519***	***0.31***
	70	***CHOCOOH***	***glyoxalic acid***	***5.90E+08***	***3.15E+07***	***0.89604***	***0.05***
	71	***CH3-COCHO***	***pyruvic aldehyde***	***6.49E+08***	***8.51E+07***	***0.75487***	***0.13***
Ester	**72**	**CH3-COO-CH3**	**methyl acetate**	**1.20E+08**	**1.52E+07**	**0.76318**	**0.13**
	73	CH3-COO-CH2-CH3	ethyl acetate	4.00E+08	4.29E+08	0.00536	1.07
	74	CH3-COO-CH2-CH2-CH3	propyl acetate	1.40E+09	1.77E+09	0.07099	1.27
	75	CH3-CH2-COO-CH3	methyl propionate	4.50E+08	4.63E+08	0.00088	1.03
	76	CH3-CH2-COO-CH2-CH3	ethyl propionate	8.70E+08	8.77E+08	0.00007	1.01
	77	*CH3-COO-CH2CH2OH*	*2-hydroxyethyl acetate*	*9.10E+08*	*8.09E+08*	*0.01240*	0.89
	78	CH3COOCH(CH3)2	isopropyl acetate	4.50E+08	8.43E+08	0.76430	1.87
	79	CH3-COO-(CH2)3-CH3	n-butylacetate	1.80E+09	3.18E+09	0.58911	1.77
Carboxyl	80	CH3-CH2-COOH	propionic acid	3.20E+08	4.64E+08	0.20261	1.45
	81	CH3-(CH2)2-COOH	butyric acid	2.20E+09	1.81E+09	0.03140	0.82
	82	**(CH3)2CHCH2COOH**	**3-methylbutyric acid**	**1.40E+09**	**3.81E+09**	**2.96711**	**2.72**
	83	(CH3)3-C-COOH	tri-methyl-acetic acid	6.50E+08	7.21E+08	0.01206	1.11
	84	*CH3-C(CH3)(OCH3)-COOH*	*2-methyl-2-methoxy-propanoic acid*	*7.73E+08*	*6.76E+08*	*0.01590*	*0.87*
	85	***HOCH2COOH***	***glycolic acid***	***5.40E+08***	***1.26E+08***	***0.58749***	***0.23***
	86	*CH3-CH(OH)-COOH*	*lactic acid*	*4.30E+08*	*5.70E+08*	*0.10634*	*1.33*
	87	*CH3CH2CH(OH)COOH*	*2-hydroxybutyric acid*	*1.30E+09*	*1.92E+09*	*0.22499*	*1.47*
	88	***HO-CH2-(CHOH)4-COOH***	***glucuronic acid***	***1.30E+09***	***6.01E+09***	***13.12216***	***4.62***
	89	CH3COOH	acetic acid	1.70E+07	1.59E+07	0.00443	0.93
Dicarboxylic	***90***	***HOOC-CH2-COOH***	***malonic acid***	***1.60E+07***	***3.29E+06***	***0.63098***	***0.21***
	91	*HOOC-(CH2)2-COOH*	*succinic acid*	*1.10E+08*	*1.05E+08*	*0.00243*	*0.95*
	92	*HOOC-(CH2)3-COOH*	*glutaric acid*	*8.30E+08*	*1.51E+09*	*0.67739*	*1.82*
	93	*HOOC-(CH2)4-COOH*	*adipic acid*	*2.00E+09*	*2.92E+09*	*0.21236*	*1.46*
	94	*HOOC-(CH2)6-COOH*	*saberic acid*	*4.80E+09*	*5.74E+09*	*0.03825*	*1.20*
	95	*HOOC-(CH2)7-COOH*	*azelaic acid*	*5.40E+09*	*7.15E+09*	*0.10470*	*1.32*
	96	*HOOC-(CH2)8-COOH*	*sabacic acid*	*6.40E+09*	*8.56E+09*	*0.11347*	*1.34*
	97	***HOOC-CH(OH)-CH(OH)-COOH***	***tartaric acid***	***7.00E+08***	***3.18E+08***	***0.29850***	***0.45***
	98	***HOOC-CH2-C(COOH)(OH)-CH2-COOH***	***citric acid***	***5.00E+07***	***1.62E+08***	***5.01353***	***3.24***
	99	*HOOC-CH(OH)-COOH*	*tartoronic acid*	*1.70E+08*	*1.04E+08*	*0.15289*	*0.61*
	100	***HOOC-CH2-CH(OH)-COOH***	***malic acid***	***8.20E+08***	***2.11E+08***	***0.55146***	***0.26***
Halogenated	***101***	***Cl-CH2-COOH***	***chloroacetic acid***	***4.30E+07***	***9.63E+06***	***0.60227***	***0.22***
	102	Cl2-CH2	dichloromethane	5.80E+07	4.22E+07	0.07428	0.73
	103	Br2-CH2	dibromomethane	9.90E+07	1.45E+08	0.21590	1.46
	104	**BrCl2CH**	**bromodichloromethane**	**7.10E+07**	**3.10E+07**	**0.31816**	**0.44**
	105	Cl3C-CHCl2	pentachlrooethane	1.00E+07	9.22E+06	0.00603	0.92
	106	CHBr2Cl	chlorodibromomethane	8.30E+07	5.74E+07	0.09528	0.69
	107	CHBr3	tribromomethane	1.50E+08	1.06E+08	0.08460	0.71
	108	BrCH2-CH2Br	1,2-dibromoethane	2.60E+08	2.83E+08	0.00756	1.09
	109	CH3-CHCl2	1,1-dichloroethane	1.30E+08	2.22E+08	0.49556	1.70
	110	CH2Cl-CH2Cl	1,2-dichloroethane	2.00E+08	1.52E+08	0.05653	0.76
	111	Cl2CH-CCl3	pentachloroethane	1.00E+07	9.22E+06	0.00603	0.92
	112	Br2CH-CHBr2	1,1,2,2-tetrabromoethane	2.20E+08	2.07E+08	0.00332	0.94
	113	Cl3C-CH2Cl	1,1,1-2-tetrachloroethane	1.80E+07	2.33E+07	0.08698	1.29
	114	ClCH2-CHCl2	1,1.-2-trichloroethane	1.10E+08	1.06E+08	0.00108	0.97
	115	**CCl3-CH3**	**1,1,1-trichloroethane**	**1.00E+08**	**3.96E+07**	**0.36488**	**0.40**
	116	**CH3CH2CH2-Cl**	**1-chloropropane**	**2.50E+09**	**1.08E+09**	**0.32351**	**0.43**
	117	**CH2Cl-CHCl-CH2Br**	**1,2-dichloro-3-bromopropane**	**7.30E+08**	**2.72E+08**	**0.39359**	**0.37**
	118	**CH2Br-CH2-CH2Br**	**1,3-dibromopropane**	**4.10E+09**	**1.04E+09**	**0.55646**	**0.25**
	119	CH2Cl-CHCl-CH3	1,2-dichloropropane	4.00E+08	3.72E+08	0.00491	0.93
	120	CH3-(CH2)3-Cl	1-chlorobutane	3.40E+09	2.44E+09	0.07938	0.72
	121	***Br-CH2-CH2-OH***	***2-bromoethanol***	***3.50E+08***	***7.69E+08***	***1.43156***	***2.20***
	122	*Cl-CH2-CH2-OH*	*2-chloroethanol*	*9.50E+08*	*5.61E+08*	*0.16800*	*0.59*
	123	***CCl3-CH2-OH***	***2,2,2-trichloroethanol***	***4.20E+08***	***1.66E+08***	***0.36485***	***0.40***
	124	*CF3-CH2-OH*	*2,2,2-trifluoroethanol*	*2.30E+08*	*1.60E+08*	*0.09227*	*0.70*
	125	***CCl3-CH(OH)2***	***chloral hydrate***	***3.10E+09***	***2.75E+08***	***0.83066***	***0.09***
	126	CF3-CHClBr	Halothane	1.30E+07	1.55E+07	0.03719	1.19
	127	CHCl3	chloroform	1.40E+07	1.67E+07	0.03709	1.19
	128	CF3-CHCl2	2,2-dichloro-1,1,1-trifluoroethane	1.30E+07	8.36E+06	0.12712	0.64
	129	*CHF2-O-CHCl-CF3*	*Isoflurane*	*2.40E+07*	*2.27E+07*	*0.00300*	*0.95*

Table 2.1: Calculated HO• reaction rate constants (Normal: calculated, *Italic*: predicted, **Bold**: error is out of the EG) as compared to literature-reported experimental values (Continued)

Sulfide, Disulfide	***130***	***H3C-S-CH3***	***dimethyl sulfide***	***1.90E+10***	***4.05E+09***	***0.61940***	***0.21***
	131	***H3C-S-S-CH3***	***di-methyl-di-sulfides***	***1.70E+10***	***5.36E+09***	***0.46893***	***0.32***
	132	*H3C-CH2-S-CH2-CH3*	*di-ethyl-sulfides*	*1.40E+10*	*8.66E+09*	*0.14554*	*0.62*
	133	*H3C-CH2-S-S-CH2-CH3*	*di-ethyl-di-sulfides*	*1.40E+10*	*9.97E+09*	*0.08282*	*0.71*
	134	(CH3)2-CH-S-S-CH-(CH3)2	di-ethyl-methyl-di-sulfides	2.00E+10	1.73E+10	0.01876	0.86
	135	CH3-S-CH2-CH2-OH	2-methylthio-ethanol	7.90E+09	6.86E+09	0.01719	0.87
	136	H3C-S-CH2-CH2-CHO	methional	8.20E+09	7.63E+09	0.00477	0.93
	137	***HO-CH2-CH2-S-CH2-CH2-OH***	***2,2'-thiodiethanol***	***2.00E+10***	***9.68E+09***	***0.26617***	***0.48***
	138	*HO-CH2CH2CH2-S-CH2CH2CH2-OH*	*3,3'-thiodiethanol*	*1.40E+10*	*7.67E+09*	*0.20451*	*0.55*
	139	**HOOC-CH2-S-CH2-COOH**	**thiodiacetic acid**	**6.00E+09**	**2.57E+09**	**0.32636**	**0.43**
Sulfoxide	***140***	***CH3-SO-CH3***	***di-methyl-sulfoxide***	***6.50E+09***	***2.23E+09***	***0.43088***	***0.34***
	141	*CH3-CH2-SO-CH2-CH3*	*di-ethyl-sulfoxide*	*6.50E+09*	*3.77E+09*	*0.17692*	*0.58*
	142	*CH3-CH2-CH2-SO-CH2-CH2-CH3*	*di-propyl-sulfoxide*	*6.30E+09*	*6.50E+09*	*0.00103*	*1.03*
	143	*(CH3)2CH-SO-CH(CH3)2*	*di(1-methyl-ethyl)sulfoxide*	*6.80E+09*	*5.80E+09*	*0.02176*	*0.85*
	144	(CH3-CH2-CH2-CH2)2-SO	di-butyl-sulfoxide	8.00E+09	9.32E+09	0.02721	1.16
	145	CH3-SO-CH2-S-CH3	methyl methyl thiomethyl sulfoxide	4.80E+09	6.37E+09	0.10649	1.33
	146	HO-CH2CH2-SO-CH2CH2-OH	di(2-hydroxyethyl) sulfoxide	5.30E+09	4.57E+09	0.01877	0.86
	147	(CH3)2-CH-SO-CH-(CH3)2	diisopropyl sulfoxide	6.80E+09	5.80E+09	0.02176	0.85
Thiol	148	HS-CH2-CH2-OH	mercaptoethanol	6.80E+09	4.65E+09	0.09962	0.68
	149	HS-CH2-COOH	mercaptoacetic acid	1.20E+09	1.10E+09	0.00707	0.92
	150	**HS-CH2-COOCH3**	**methyl thioglycolate**	**2.10E+10**	**1.10E+09**	**0.89813**	**0.05**
	151	HS-CH2-CH(OH)-CH(OH)-CH2-SH	dithiothreitol	1.50E+10	1.11E+10	0.06789	0.74
Nitrile	**152**	**CH3-CN**	**acetonitrile**	**2.20E+07**	**6.46E+06**	**0.49898**	**0.29**
	153	CN-CN	cyanogen	1.00E+07	1.09E+07	0.00877	1.09
	154	**CH3-CH2-CN**	**propionitrile**	**9.30E+07**	**6.58E+06**	**0.86352**	**0.07**
	155	**NC-CH2-CH2-CN**	**succino nitrile**	**3.80E+07**	**1.11E+07**	**0.50119**	**0.29**
Nitro	**156**	**CH3-CH2-CH2-NO2**	**1-nitropropane**	**2.50E+08**	**1.89E+09**	**43.05812**	**7.56**
	157	**(CH3)2-CH-NO2**	**2-nitropropane**	**8.00E+07**	**9.61E+08**	**121.23321**	**12.01**
	158	*CH2ClNO2*	*chloronitromethane*	*1.94E+08*	*1.33E+08*	*0.10015*	*0.68*
	159	***CHCl2NO2***	***dichloronitromethane***	***5.12E+08***	***1.33E+08***	***0.54908***	***0.26***
	160	*CH2BrNO2*	*bromonitromethane*	*8.36E+07*	*1.33E+08*	*0.34364*	*1.59*
	161	***CHBr2NO2***	***dibromonitromethane***	***4.75E+08***	***1.33E+08***	***0.51959***	***0.28***
	162	***CHBrClNO2***	***bromochloronitromethane***	***4.20E+08***	***1.33E+08***	***0.46822***	***0.32***
Amide	163	CH3-CO-NH2	acetamide	1.90E+08	1.54E+08	0.03564	0.81
	164	**HO-CH2-CO-NH2**	**glycolamide**	**1.10E+09**	**2.91E+08**	**0.54119**	**0.26**
	165	**HO-CH(CH3)-CO-NH2**	**2-hydroxypropionamide**	**1.30E+09**	**4.53E+08**	**0.42496**	**0.35**
	166	**(CH3)2-CH-CO-NH2**	**2-methylpropionamide**	**1.60E+09**	**5.93E+08**	**0.39619**	**0.37**
	167	**C2H5-CO-NH2**	**propionamide**	**7.00E+08**	**3.30E+08**	**0.27881**	**0.47**
	168	(CH3)3-C-CO-NH2	trimethylacetamide	1.50E+09	1.34E+09	0.01107	0.89
	169	**(CH3)2-CH-CO-NH2**	**isobutyramide**	**1.60E+09**	**5.93E+08**	**0.39619**	**0.37**
	170	CH3-CO-NH-C-(CH3)3	N-tert-butyl-acetamide	1.10E+09	1.80E+09	0.40164	1.63
	171	CH3-CO-NH-CH3	N-methylacetamide	1.60E+09	1.68E+09	0.00241	1.05
	172	(CH3)2-CH-CO-NH-CH3	N-butylformamide	1.90E+09	2.84E+09	0.24314	1.49
	173	(CH3)3-C-CO-NH-CH3	N-methyl-pivalamide	2.40E+09	2.87E+09	0.03779	1.19
	174	CH3-CH2-CO-NH-CH3	N-methyl-propionamide	1.40E+09	1.85E+09	0.10551	1.32
	175	(CH3)2-CH-CO-NH-CH3	N-methylisobutyramide	1.90E+09	2.12E+09	0.01308	1.11
	176	CH3-CO-N-(CH3)2	N,N-dimethyl acetamide	3.50E+09	3.30E+09	0.00326	0.94
	177	(CH3)3-C-CO-N-(CH3)2	N,N-dimethyl pivalamide	3.90E+09	3.41E+09	0.01585	0.87
Amine	178	H2N-CH2-CO-NH2	2-aminoacetamide	2.80E+09	4.35E+09	0.30821	1.56
	179	CH3-NH2	methyl amine	5.70E+09	4.57E+09	0.03910	0.80
	180	CH3-CH2-NH2	ethyl amine	6.40E+09	6.28E+09	0.00037	0.98
	181	CH3-(CH2)3-NH2	N-butyl amine	8.20E+09	9.12E+09	0.01255	1.11
	182	CH3-CH2-CH2-NH2	propyl amine	7.30E+09	7.71E+09	0.00316	1.06
	183	**H2N-CH2-CH2-NH2**	**ethylenediamine**	**5.50E+09**	**1.19E+10**	**1.35598**	**2.16**
	184	(CH3)3-C-NH2	tert-butyl amine	6.00E+09	5.24E+09	0.01601	0.87
	185	CH3-(CH2)4-NH2	N-amyl amine	7.00E+09	1.05E+10	0.25390	1.50
	186	CH3-(CH2)5-NH2	Hexylamine	1.30E+10	1.19E+10	0.00670	0.92
	187	CH3-(CH2)7-NH2	N-octylamine	1.46E+10	1.48E+10	0.00011	1.01
	188	(CH3)2-CH-NH2	iso-propyl amine	1.30E+10	8.89E+09	0.09983	0.68
	189	**CH3-O-NH2**	**O-methyl hydroxy amine**	**1.40E+10**	**4.19E+09**	**0.49073**	**0.30**
	190	**CH3-NH-CH3**	**dimethylamine**	**8.90E+09**	**1.25E+09**	**0.73888**	**0.14**
	191	CH3-(CH2)3-NH-(CH2)3-CH3	dibutyl amine	1.80E+10	1.03E+10	0.18103	0.57
	192	***HOOC-CH2-NH-CH2-COOH***	***Iminodiacetic acid***	***4.90E+07***	***2.45E+08***	***16.05732***	***5.01***
	193	***(C2H5)2-N-OH***	***N,N-diethyl hydroxyl amine***	***1.30E+09***	***8.09E+09***	***27.27052***	***6.22***
	194	(CH3(CH2)3)3-N	tributyl amine	1.70E+10	1.89E+10	0.01240	1.11
	195	(C2H5)3-N	triethyl amine	1.00E+10	1.04E+10	0.00135	1.04
	196	**(CH3)3-N**	**trimethyl amine**	**1.30E+10**	**5.26E+09**	**0.35486**	**0.40**
	197	(HO-CH2-CH2)3-N	triethanolamine	8.00E+09	1.18E+10	0.22263	1.47
	198	(CH2COOH)3-N	Nitrilotriacetic acid	2.10E+09	3.75E+09	0.61681	1.79
	199	(HOCH2CH2)3-N	Nitrilotriethanol	8.00E+09	1.18E+10	0.22263	1.47
	200	(CH3)2-N-NH2	1,1-dimethyl hydrazine	1.60E+10	8.68E+09	0.20932	0.54
	201	***(HO-CH2)3C-NH2***	***2-amino-2-propane-1,3-diol***	***1.50E+09***	***1.02E+10***	***33.33204***	***6.77***

Table 2.1: Calculated HO• reaction rate constants (Normal: calculated, *Italic*: predicted, **Bold**: error is out of the EG) as compared to literature-reported experimental values (Continued)

Nitroso, Nitramine	**202**	**(CH3)2-N-NO**	**N-nitrosodimethylamine**	**4.30E+08**	**7.44E+06**	**0.96571**	**0.02**
	203	**CH3-CH2-N(CH3)-N=O**	**methylethylnitrosamine**	**4.95E+08**	**1.00E+09**	**1.04348**	**2.02**
	204	CH3-CH2-N(N=O)-CH2-CH3	diethylnitrosamine	6.99E+08	8.52E+08	0.04814	1.22
	205	**(CH3)2-N-NO2**	**dimethylnitramine**	**5.44E+08**	**1.25E+08**	**0.59463**	**0.23**
	206	(CH3-CH2)2-N-NO2	diethyl nitramine	8.67E+08	1.23E+09	0.17748	1.42
	207	(CH3)(CH3CH2)-N-NO2	methyl ethyl nitramine	7.60E+08	6.78E+08	0.01153	0.89
	208	(CH3-CH2-CH2)2-N-NO	N-nitrosodipropylamine	2.30E+09	3.52E+09	0.27939	1.53
	209	(CH3-CH2-CH2-CH2)2-N-NO	N-nitrosodibutylamine	4.71E+09	6.33E+09	0.11871	1.34
	210	(CH3-CH2-CH2-CH2)(CH3-CH2)-N-NO	N-nitrosoethylbutylamine	3.10E+09	3.58E+09	0.02403	1.16
	211		N-nitrosopyrrolidine	1.75E+09	2.42E+09	0.14783	1.38
	212		N-nitrosopiperidine	2.98E+09	4.23E+09	0.17472	1.42
	213		N-nitrosohexamethyleneimine	4.35E+09	5.63E+09	0.08715	1.30
Phosphorus	214	**(CH3)(CH3-O-)2-P=O**	**dimethyl methylphosphonate (DMMP)**	**2.00E+08**	**9.83E+07**	**0.25837**	**0.49**
	215	(CH3)(CH3CH2)(CH3CH2O)-PO	Diethyl methylphosphonate (DEMP)	6.00E+08	9.72E+08	0.38393	1.62
	216	PO4-(CH3)3	trimethyl phosphate	1.20E+08	1.34E+08	0.01274	1.11
	217	PO4-(CH2-CH3)3	triethyl phosphate	2.90E+09	1.47E+09	0.24189	0.51
	218	PO4-(CH2-CH2-CH3)3	tributyl phosphate	1.00E+10	9.74E+09	0.00069	0.97
Cyclo	219		cycloheptane	7.70E+09	9.86E+09	0.07867	1.28
	220		***cycloheptanol***	***1.70E+09***	***1.01E+10***	***24.63004***	***5.96***
	221		cyclohexane	6.10E+09	8.45E+09	0.14857	1.39
	222		cyclopentane	4.50E+09	6.06E+09	0.11974	1.35
	223		***tetrahydrofuran***	***4.00E+09***	***1.14E+09***	***0.51223***	***0.28***
	224		*1,4-dioxane*	*3.10E+09*	*2.64E+09*	*0.02160*	*0.85*
	225		*1,4-dithiane*	*1.80E+10*	*1.55E+10*	*0.01891*	*0.86*
	226		1,3,5-trioxane	1.50E+09	1.60E+09	0.00413	1.06
	227		*tetramethylene sulfoxide*	*7.00E+09*	*4.94E+09*	*0.08670*	*0.71*
	228		**2-methyl-1,3-dioxalane**	**3.50E+09**	**1.61E+09**	**0.29277**	**0.46**
	229		**1,3-dioxolane**	**4.00E+09**	**1.59E+09**	**0.36155**	**0.40**
	230		ethylene oxide	6.80E+07	6.87E+07	0.00012	1.01
	231		***1,2-epoxybutane***	***7.80E+08***	***1.87E+09***	***1.95576***	***2.40***
	232		***1,2-epoxypropane***	***2.50E+08***	***5.23E+08***	***1.19651***	***2.09***
	233		*2,3-epoxypropanol*	*4.70E+08*	*9.06E+08*	*0.86236*	*1.93*
alkene	234	H2C=CHCH2OH	allyl alcohol	5.90E+09	4.62E+09	0.04712	0.78
	235	H2C=CHCH2CH3	1-butene	7.00E+09	5.49E+09	0.04670	0.78
	236	**H2C=CHCH3**	**propylene**	**7.00E+09**	**2.08E+09**	**0.49370**	**0.30**
	237	(CH3)2C=CH2	isobutylene	5.40E+09	3.67E+09	0.10322	0.68
	238		1,4-cyclohexadiene	7.70E+09	7.75E+09	0.00004	1.01
	239		cyclopentene	7.00E+09	6.13E+09	0.01558	0.88
	240		cyclohexene	8.80E+09	8.07E+09	0.00693	0.92
	241	H2C=CHCOCH3	1-butene-3-one	8.50E+09	6.11E+09	0.07895	0.72
	242	H2C=CHCONH2	acrylamide	5.90E+09	6.20E+09	0.00251	1.05
	243	H2C=C(CH3)-CO-NH2	methyl acrylamide	1.30E+10	1.05E+10	0.03674	0.81
	244	-CO, -CO	1,4-benzoquinone	1.20E+09	1.62E+09	0.11969	1.35
	245	H2C=CH-OH	vinyl alcohol	1.50E+08	1.00E+08	0.11111	0.67
	246	H2C=CHCHO	acrolein	7.00E+09	6.77E+09	0.00104	0.97
	247	CH3CH=CHCHO	crotonaldehyde	5.80E+09	7.25E+09	0.06251	1.25
	248	H2C=CHCOOH	acrylic acid	1.50E+09	2.37E+09	0.33583	1.58
	249	**Cis HOOC-CH=CH-COOH**	**maleic acid**	**6.00E+09**	**2.66E+09**	**0.31067**	**0.44**
	250	**HOOC-CH=CH-COOH (trans)**	**fumaric acid**	**6.00E+09**	**1.15E+09**	**0.65287**	**0.19**
	251	**H2C=CHCOOCH2CH2OH**	**2-hydroxyethyl acrylate**	**1.10E+10**	**3.16E+09**	**0.50771**	**0.29**
	252	**H2C=C(CH3)COOCH3**	**methyl methacrylate**	**1.10E+10**	**4.41E+09**	**0.35916**	**0.40**
	253	**H2C=CHCl**	**vinyl chloride**	**1.20E+10**	**2.12E+09**	**0.67771**	**0.18**
	254	H2C=CCl2	vinylidine chloride	6.80E+09	4.46E+09	0.11884	0.66
	255	ClCH=CHCl (cis)	dichloroethylene	3.80E+09	2.66E+09	0.09068	0.70
	256	ClCH=CHCl (trans)	dichloroethylene	4.40E+09	5.01E+09	0.01935	1.14
	257	Cl2C=CCl2	tetrachloroethylene	2.00E+09	2.03E+09	0.00017	1.01
	258	-F, -F, -F, -F	fluoranil	3.90E+09	3.91E+09	0.00001	1.00
	259	H2C=CHCH2CN	allyl cyanide	6.90E+09	3.94E+09	0.18459	0.57
	260	H2C=CHCN	acrilonitrile	5.30E+09	5.20E+09	0.00032	0.98
	261	H2C=C(CH3)CN	methacylonitrile	1.20E+10	9.26E+09	0.05215	0.77

Table 2.1: Calculated HO• reaction rate constants (Normal: calculated, *Italic*: predicted, **Bold**: error is out of the EG) as compared to literature-reported experimental values (Continued)

Benzene	262	C6H5-CH2CH3	ethylbenzene	7.50E+09	7.11E+09	0.00268	0.95
	263	C6H5-OH	phenol	6.60E+09	7.14E+09	0.00674	1.08
	264	C6H5-F	fluorobenzene	5.70E+09	5.40E+09	0.00283	0.95
	265	C6H5Cl	chlorobenzene	4.30E+09	5.43E+09	0.06870	1.26
	266	C6H5-Br	bromobenezene	5.20E+09	4.87E+09	0.00393	0.94
	267	C6H5-I	iodobenzene	5.30E+09	4.56E+09	0.01972	0.86
	268	C6H5-CN	benzonitrile	3.90E+09	2.28E+09	0.17232	0.58
	269	C6H5-NO2	nitrobenzene	3.90E+09	2.25E+09	0.17940	0.58
	270	C6H5-CHO	benzaldehyde	4.40E+09	4.44E+09	0.00010	1.01
	271	C6H5-COOH	benzoic acid	4.30E+09	3.77E+09	0.01509	0.88
	272	C6H5-COCH3	acetophenone	6.40E+09	5.50E+09	0.01982	0.86
	273	C6H5-CONH2	benzamide	4.60E+09	4.81E+09	0.00210	1.05
	274	C6H5-SOCH3	methyl phenyl sulfoxide	9.70E+09	4.89E+09	0.24564	0.50
	275	C6H5-CH2OH	benzylalcohol	8.40E+09	6.24E+09	0.06591	0.74
	276	C6H5-NH-CO-CH3	acetanilide	5.20E+09	4.80E+09	0.00592	0.92
	277	C6H5-SO3H	benzenesulfonic acid	2.10E+09	2.07E+09	0.00019	0.99
	278	**C6H5-NH-OH**	**phenyl hydroxylamine**	**1.50E+10**	**6.23E+09**	**0.34155**	**0.42**
	279	C6H5-CH2CH2-C(CH3)2-OH	2-methyl-4-phenyl-2-butanol	5.90E+09	9.09E+09	0.29222	1.54
	280	C6H5-CHOHCH(CH3)2	2-methyl-1-phenyl-1-propanol	9.50E+09	1.07E+10	0.01498	1.12
	281	C6H5-CHOHCH3	phenylethanol	1.10E+10	7.42E+09	0.10607	0.67
	282	C6H5-CH(OH)(CH2-CH3)	1-phenyl-1-propanol	1.00E+10	8.76E+09	0.01534	0.88
	283	**C6H5-CH2-CH2--OH**	**1-phenyl-2-propanol**	**2.10E+10**	**7.55E+09**	**0.41045**	**0.36**
	284	C6H5-O-CH3	anisol	5.40E+09	5.93E+09	0.00974	1.10
	285	(C6H5)2-CO	benzophenone	9.00E+09	1.09E+10	0.04407	1.21
	286	(C6H5)2-NH	diphenylamine	1.00E+10	1.23E+10	0.05141	1.23
	287	(C6H5)2-SO	diphenyl sulfoxide	6.30E+09	7.28E+09	0.02418	1.16
	288	C6H5-CH(OH)-CH3	1-phenyl-1-propanol	1.00E+10	7.36E+09	0.06994	0.74
	289	*HO-C6H4-CH3*	*o-cresol*	*1.10E+10*	*6.77E+09*	*0.14786*	*0.62*
	290	*HO-C6H4-CH3*	*p-cresol*	*1.20E+10*	*7.14E+09*	*0.16394*	*0.60*
	291	C6H4-Cl2	1,2-dichlorobenzene	4.00E+09	4.76E+09	0.03595	1.19
	292	C6H4-Cl2	1,3-dichlorobenzene	5.70E+09	6.02E+09	0.00308	1.06
	293	C6H4-Cl2	1,4-dichlorobenzene	5.40E+09	5.04E+09	0.00450	0.93
	294	*C6H4-(OH)2*	*1,2-benzenediol*	*1.10E+10*	*8.21E+09*	*0.06425*	*0.75*
	295	*1,3-C6H4-(OH)2*	*resorcinol*	*1.20E+10*	*8.68E+09*	*0.07644*	*0.72*
	296	*HO-C6H4-Cl*	*2-chlorophenol*	*1.20E+10*	*6.27E+09*	*0.22766*	*0.52*
	297	*HO-C6H4-Cl*	*3-chlorophenol*	*7.20E+09*	*7.91E+09*	*0.00963*	*1.10*
	298	*HO-C6H4-Cl*	*4-chlorophenol*	*9.30E+09*	*6.64E+09*	*0.08199*	*0.71*
	299	***HO-C6H4-O-CH3***	***2-methoxyphenol***	***2.00E+10***	***6.82E+09***	***0.43408***	***0.34***
	300	***HO-C6H4-O-CH3***	***3-methoxyphenol***	***3.20E+10***	***8.55E+09***	***0.53706***	***0.27***
	301	***HO-C6H4-O-CH3***	***4-methoxyphenol***	***2.60E+10***	***7.21E+09***	***0.52247***	***0.28***
	302	*HO-C6H4-NO2*	*4-nitrophenol*	*3.80E+09*	*2.94E+09*	*0.05180*	*0.77*
	303	***4-CH3-C6H4-CN***	***4-tolunitrile***	***1.20E+10***	***3.11E+09***	***0.54935***	***0.26***
	304	1,4-C6H4(CN)2	1,4-dicyanobenzene	7.80E+08	8.90E+08	0.01989	1.14
	305	*4-F-C6H4-CN*	*p-fluorobenzonitrile*	*3.50E+09*	*1.78E+09*	*0.24221*	*0.51*
	306	**(CH3)3-C-C6H4-OH**	**tert-butylphenol**	**1.90E+10**	**6.69E+09**	**0.41986**	**0.35**
	307	C6H4-F2	o-difluorobenzene	7.50E+09	4.71E+09	0.13884	0.63
	308	**C6H4-F2**	**p-difluorobenzene**	**1.00E+10**	**4.98E+09**	**0.25182**	**0.50**
	309	C6H4-(OCH3)2	1,2-dimethoxybenzene	5.20E+09	5.71E+09	0.00958	1.10
	310	C6H4-(OCH3)2	1,3-dimethoxybenzene	7.20E+09	7.12E+09	0.00014	0.99
	311	C6H4-(OCH3)2	1,4-dimethoxybenzene	7.00E+09	6.02E+09	0.01954	0.86
	312	**4-O2N-C6H4-NH2**	**p-nitroaniline**	**1.40E+10**	**3.16E+09**	**0.59950**	**0.23**
	313	***CH3-C6H4-CN***	***p-tolunitrile***	***1.20E+10***	***2.52E+09***	***0.62419***	***0.21***
	314	4-Cl-C6H4NO2	1-chloro-4-nitrobenzene	1.30E+09	2.09E+09	0.36644	1.61
	315	4-O2N-C6H4-COCH3	4-nitroacetophenone	3.30E+09	2.15E+09	0.12185	0.65
	316	*(HO)2-C6H3-Cl*	*1,2,4--chlorocatecohol*	*7.00E+09*	*6.87E+09*	*0.00034*	*0.98*
	317	C6H3-(OH)3	phloroglucinol	1.00E+10	1.06E+10	0.00336	1.06
	318	*3,4-(HO)2-C6H3-CHO*	*dihydroxybenzaldehyde*	*8.30E+09*	*5.50E+09*	*0.11400*	*0.66*
	319	***(HO)2-C6H3-COCH3***	***2,4-dihydroxyacetophenone***	***3.00E+10***	***6.95E+09***	***0.59054***	***0.23***
	320	*(HO)2-C6H3-COCH3*	*2,5-dihydroxyacetophenone*	*8.00E+09*	*9.64E+09*	*0.04201*	*1.20*
	321	*(HO)2-C6H3-COCH3*	*3,4-dihydroxyacetophenone*	*1.00E+10*	*8.20E+09*	*0.03232*	*0.82*
	322	***(NO2)2-C6H3-OCH3***	***3,5-dinitroanisole***	***5.20E+09***	***1.05E+09***	***0.63751***	***0.20***
	323	C6H3-(OCH3)3	1,2,3-trimethoxybenzene	7.00E+09	7.15E+09	0.00047	1.02
	324	C6H3-(OCH3)3	1,2,4-trimethoxybenzene	6.20E+09	5.27E+09	0.02267	0.85
	325	C6H3-(OCH3)3	1,3,5-trimethoxybenzene	8.10E+09	6.15E+09	0.05822	0.76
	326	***HO-C6H3-CH3O***	***2,3-dimethoxyphenol***	***2.00E+10***	***8.55E+09***	***0.32778***	***0.43***
	327	***HO-C6H3-CH3O***	***2,4-dimethoxyphenol***	***2.60E+10***	***6.24E+09***	***0.57783***	***0.24***
	328	***HO-C6H3-CH3O***	***3,5-dimethoxyphenol***	***2.00E+10***	***7.31E+09***	***0.40229***	***0.37***

Table 2.1: Calculated HO• reaction rate constants (Normal: calculated, *Italic*: predicted, **Bold**: error is out of the EG) as compared to literature-reported experimental values (Continued)

	329	C6H5-CH3	toluene	5.10E+09	5.91E+09	0.02495	1.16
	330	C6H5-NH2	aniline	1.70E+10	2.05E+10	0.04239	1.21
	331	H3C-C6H4-CH3	o-xylene	6.70E+09	5.69E+09	0.02286	0.85
	332	H3C-C6H4-CH3	m-xylene	7.50E+09	7.00E+09	0.00437	0.93
	333	H3C-C6H4-CH3	p-xylene	7.00E+09	5.98E+09	0.02125	0.85
	334	-CH3, -CH3, -CH3	1,2,3-trimethyl benzene	7.00E+09	7.01E+09	0.00000	1.00
	335	-CH3, -CH3, -CH3	1,2,4-trimethyl benzene	6.20E+09	5.30E+09	0.02100	0.86
	336	-CH3, -CH3, -CH3	1,3,5-trimethyl benzene (mesitylene)	6.40E+09	6.10E+09	0.00222	0.95
	337	F, F, F, F,F	hexafluorobenzene	1.40E+09	1.58E+09	0.01714	1.13
	338	-CH3, -CH3, -CH3, -CH3, -CH3	hexamethylbenzene	7.20E+09	4.00E+09	0.19813	0.55
	339	F,F,F,F,F,F	pentafluorobenzene	7.00E+09	6.15E+09	0.01478	0.88
	340	-CH3 (6)	pentamethylbenzene	7.50E+09	8.85E+09	0.03263	1.18
	341	F, F,F,F,F,I	pentafluoroiodobenzene	1.20E+09	1.34E+09	0.01295	1.11
	342	-CH3, -CH3, -CH3, -CH3	1,2,3,4-tetramethylbenzene	7.20E+09	8.80E+09	0.04952	1.22
	343	F, F, F, F	1,2,3,4-tetrafluorobenzene	8.00E+09	6.59E+09	0.03086	0.82
	344	-CH3, -CH3, -CH3, -CH3	1,2,3,5-tetramethylbenzene	7.10E+09	7.04E+09	0.00008	0.99
	345	-CH3, -CH3, -CH3, -CH3	1,2,4,5-tetramethylbenzene	7.00E+09	8.48E+09	0.04498	1.21
	346	-OCH3 (4)	1,2,4,5-tetramethoxybenzene	7.00E+09	8.85E+09	0.06951	1.26
	347	**-Cl, -Cl, -Cl, -OH**	**2,4,5-trichlorophenol**	**1.20E+10**	**4.29E+09**	**0.41309**	**0.36**
	348	*-Cl, -Cl, -O-COOH*	*2,4-dichlorophenoxyacetic acid*	*6.60E+09*	*4.19E+09*	*0.13339*	*0.63*
	349	*-O-COOH*	*phenoxyacetic acid*	*1.00E+10*	*5.74E+09*	*0.18155*	*0.57*
	350	-Cl, -Cl, -OH	2,4-dichlrophenol	7.10E+09	5.24E+09	0.06860	0.74
	351	-OH, -OH, -OH	1,2,4-trihydroxybenzene	8.60E+09	8.95E+09	0.00170	1.04
	352	-OH, -OH, -C(CH3)3	tert-butyl hydroquinone	6.30E+09	8.27E+09	0.09748	1.31
	353	**1,2,4,5-Cl, OH, OH, Cl**	**2,5-dichlorohydroquinone**	**2.10E+10**	**5.63E+09**	**0.53545**	**0.27**
	354	-F, -F, -F, -F, -OH, -OH	tetrafluorohydroquinone	3.10E+09	2.90E+09	0.00434	0.93
	355	*-F, -F, -F*	*1,3,5-trifluorobenzene*	*4.10E+09*	*4.63E+09*	*0.01651*	*1.13*
	356	*-F, -F, -F*	*1,2,3-trifluorobenzene*	*3.70E+09*	*5.46E+09*	*0.22722*	*1.48*
	357	*-F, -F, -F*	*1,2,4-trifluorobenzene*	*3.90E+09*	*3.90E+09*	*0.00000*	*1.00*
	358	*F, F, F, F,F, -COCH3*	*pentafluoroacetophenone (PFA)*	*1.50E+09*	*1.65E+09*	*0.01023*	*1.10*
	359	*F, F, F, F, F, CHO*	*pentafluorobenzaldehyde*	*2.00E+09*	*1.81E+09*	*0.00902*	*0.91*
	360	*F, F, F, F, F, -COOH*	*pentafluorobenzoic acid*	*1.10E+09*	*1.11E+09*	*0.00004*	*1.01*
	361	***F, F, F, F,F -NH2***	***pentafluoroaniline***	***9.60E+09***	***2.41E+09***	***0.56079***	***0.25***
	362	***F,F,F,F,F, -OH***	***pentafluorophenol***	***9.50E+09***	***2.17E+09***	***0.59599***	***0.23***
pyridine	363	-CH3	2-methyl pyridine	2.50E+09	2.82E+09	0.01641	1.13
	364	-CH3	3-methyl pyridine	2.40E+09	2.40E+09	0.00000	1.00
	365	-NH2	2-pyridine amine	8.40E+09	4.48E+09	0.21746	0.53
	366	-NH2	4-pyridine amine	5.00E+09	5.87E+09	0.03020	1.17
	367	-Br	2-bromopyridine	2.40E+09	1.55E+09	0.12596	0.65
	368	-Br	3-bromopyridine	1.10E+09	1.28E+09	0.02769	1.17
	369	-Cl	2-chloropyridine	1.80E+09	2.08E+09	0.02478	1.16
	370	-Cl	4-chloropyridine	3.10E+09	1.61E+09	0.23171	0.52
	371	-CN	3-cyanopyridine	7.50E+08	7.07E+08	0.00322	0.94
	372	-OH	2-pyridone	6.50E+09	5.16E+09	0.04247	0.79
	373	-OH	3-pyridinol	5.40E+09	4.29E+09	0.04197	0.80
	374	-OH	4-pyridinol	1.10E+10	6.73E+09	0.15102	0.61
	375	-COOH	2-pyridine carboxylic acid	2.60E+07	2.84E+07	0.00822	1.09
	376	-COOH	3-pyridinecarboxylic acid	2.20E+07	2.36E+07	0.00542	1.07
	377	-COOH	4-pyridinecarboxylic acid	6.00E+07	3.69E+07	0.14812	0.62
	378	-pyr	4,4'-bipyridine	5.30E+09	6.72E+09	0.07154	1.27
	379	-pry	2,2'-bipyridine	6.20E+09	5.13E+09	0.02972	0.83
	380	-CONH2	4-pyridinecarboxyamide	1.60E+09	1.67E+09	0.00214	1.05
	381	-CONH2	3-pyridinecarboxyamide	1.40E+09	1.06E+09	0.05910	0.76
	382		2,6-dimethyl pyridine	3.00E+09	3.28E+09	0.00869	1.09
	383		3,5-dimethyl pyridine	8.00E+09	8.30E+09	0.00139	1.04
	384		2,4,6-trimethylpyridine	2.50E+09	2.41E+09	0.00122	0.97
Furan	385	-CH3	2-methylfuran	1.90E+10	1.29E+10	0.10188	0.68
	386	-CH2-OH	furfuryl alcohol	1.50E+10	1.33E+10	0.01325	0.88
	387	-CHO	furaldehyde	7.80E+09	7.29E+09	0.00434	0.93
	388	-CH3	5-methylfurfural	7.20E+09	1.02E+10	0.17522	1.42
	389	-O-CH3	5-hydroxymethylfurfuryl	5.80E+09	8.46E+09	0.20982	1.46
	390	-NO2	5-nitro-2-furaldehyde	5.50E+09	6.46E+09	0.03066	1.18
Urea	391	H2N-CO-NH2	urea	7.90E+05	8.18E+05	0.00123	1.04
	392	H2N-CS-NH2	thiourea	1.20E+10	8.00E+09	0.11129	0.67
	393	(CH3)2N-CS-N(CH3)2	tetramethyl thiourea	8.00E+09	9.36E+09	0.02902	1.17
	394	CH3-NH-CS-NH-CH3	1,3-dimethyl thiourea	1.20E+09	1.35E+09	0.01574	1.13
	395	CH3-NH-CO-NH-CH3	1,3-dimethylurea	2.60E+09	2.25E+09	0.01830	0.86
	396	CH3-NH-CO-NH2	methylurea	2.00E+09	1.12E+09	0.19160	0.56
	397	(CH3)2-N-CO-N-(CH3)2	tetramethyl urea	5.20E+09	4.50E+09	0.01836	0.86

Table 2.1: Calculated HO• reaction rate constants (Normal: calculated, *Italic*: predicted, **Bold**: error is out of the EG) as compared to literature-reported experimental values (Continued)

Imidazole	398		xanthine	5.20E+09	4.68E+09	0.00994	0.90
	399		theophilline	6.30E+09	6.93E+09	0.00997	1.10
	400		isoguanine	1.20E+10	7.47E+09	0.14259	0.62
	401		guanine	9.20E+09	5.31E+09	0.17865	0.58
	402		imidazole	3.90E+09	4.49E+09	0.02312	1.15
	403		1-methyl imidazole	8.10E+09	4.85E+09	0.16141	0.60
	404		theobromine	5.80E+09	6.78E+09	0.02843	1.17
	405		caffeine	6.90E+09	7.90E+09	0.02107	1.15
	406		*5-nitrofuroic acid*	*5.30E+09*	*6.18E+09*	*0.02730*	*1.17*
	407		nifuroxime	1.00E+10	1.44E+10	0.18964	1.44
	408		2-acetyl furan	4.50E+09	4.18E+09	0.00505	0.93
	409		2-furancarboxamide	5.50E+09	6.34E+09	0.02307	1.15
	410		2-phenylfuran	1.60E+10	1.51E+10	0.00297	0.95
	411		5-bromofurfural	3.90E+09	5.49E+09	0.16641	1.41
	412		**5-nitrofuroic acid**	**5.30E+09**	**1.32E+10**	**2.23704**	**2.50**
	413		***5-phenylfurfural***	***5.90E+09***	***1.51E+10***	***2.44642***	***2.56***
	414		furoin	1.30E+10	1.69E+10	0.08935	1.30
triazine	415		**2,4,6-trimethoxy-1,3,5-triazine**	**2.06E+08**	**5.83E+08**	**3.35339**	**2.83**
	416		**2-chloro-4,6-diamino-s-triazine**	**5.00E+07**	**3.03E+08**	**25.52272**	**6.05**
	417		simazine	2.10E+09	3.12E+09	0.23397	1.48
	418		**atrazine**	**2.00E+09**	**4.88E+09**	**2.07497**	**2.44**
	419		**propazine**	**1.20E+09**	**6.65E+09**	**20.59739**	**5.54**
	420		simetone	4.70E+09	3.90E+09	0.02866	0.83
	421		terbutazine	2.80E+09	2.80E+09	0.00000	1.00
	422		**simetryne**	**2.60E+10**	**6.48E+09**	**0.56350**	**0.25**
	423		**ametryne**	**2.60E+10**	**8.25E+09**	**0.46618**	**0.32**
	424		*cycloserine*	*9.00E+09*	*5.47E+09*	*0.15376*	*0.61*
	425		*Linuron*	*6.50E+09*	*4.78E+09*	*0.06980*	*0.74*
	426		*diuron*	*7.50E+09*	*5.71E+09*	*0.05683*	*0.76*
	427		*isoproturon*	*5.70E+09*	*1.01E+10*	*0.59055*	*1.77*
	428		*chlortoluron*	*7.50E+09*	*6.15E+09*	*0.03263*	*0.82*
	429		*acetaminophen*	*9.80E+09*	*5.87E+09*	*0.16076*	*0.60*
	430		*Diazepam*	*7.20E+09*	*1.14E+10*	*0.34270*	*1.59*
	431		*Diclofenac*	*7.50E+09*	*1.18E+10*	*0.33286*	*1.58*
	432		*Ibuprofen*	*7.40E+09*	*1.06E+10*	*0.18241*	*1.43*
	433		*2,4-D (2,4-dichlorophenoxy)-acetic acid*	*6.60E+09*	*4.28E+09*	*0.12396*	*0.65*
	434		*clofibric acid*	*4.70E+09*	*5.81E+09*	*0.05559*	*1.24*

2.4.2 Overall Results

Tables 2.2 and 2.3 summarize experimental data and statistical results for calibrations and predictions, respectively. The total degrees of freedom (DF) were 164. The best calibration for 83% (257 rate constants) of the rate constants and the prediction for 62% (76 rate constants) of the rate constants were within the EG. The SD was 0.92 from the calibration, which indicated that the calibrated data were distributed within the range from 1.65σ (90%) to 1.96σ (95%) from the experimental values under the assumption of a normal distribution. Figure 2.3 plots 434 rate constants from calibrations and predictions against the experimental rate constants for four reaction mechanisms. The least-squares fit is $y = 0.65x$ and has a correlation coefficient, r, of 0.58 (note that the

OF in equation (2.24) weighs all data points equally, so that the lowest data point would not significantly change the overall correlation even though it is eliminated). The correlation coefficient is comparable to the literature-reported values (e.g., 0.56 with the recalculated MOOH method (Böhnhardt et al., 2008) and 0.59 with Atkinson's GCM (Kwok and Atkinson, 1995), respectively, from 805 gaseous phase HO• rate constants).

Table 2.2: Summary of experimental data and statistical results for calibration

Group rate constant and functional group		# of group rate constant	# of group contribution factor	# of experimental data	# of data within EG (%)	S.D.
Overall		**66**	**80**	**310**	**257 (83%)**	**0.92**
H-atom abstraction						
Overall for H-atom abstraction		**5**	**18**	**84**	**71 (85%)**	**0.42**
alkyl	k_0^{prim}, k_0^{sec}, k_0^{tert} -CH_3, (-CH_2- ≈ -CH< ≈ >C<)	3	2	12	11 (90%)	0.27
alkyl halides	Cl, Br, -CF_3, -CCl_3, -CH_n(halogen)$_m$	-	5	22	17 (77%)	0.40
cycloalkanes	RS3, RS5, -O-(2nd)	-	3	7	5 (71%)	0.41
alcohol	k_{OH}, -OH	1	1	14	12 (86%)	0.37
ether	-O-	-	1	8	7 (88%)	0.48
carbonyl	-CO-	-	1	5	5 (100%)	0.47
aldehyde	-CHO	-	1	4	4 (100%)	0.13
ester	-OCOR	-	1	7	6 (86%)	0.60
carboxylic	k_{COOH}, (-COOH ≈ -COOR)	1	2	12	10 (83%)	0.70
HO• addition to alkene						
Overall for HO• addition		**7**	**7**	**28**	**22 (79%)**	**0.40**
alkyl	-CH3 ≈ -CH2-	-	1	7	6 (86%)	0.34
carbonyl	-CO	-	1	4	4 (100%)	0.28
aldehyde	-CHO	-	1	2	2 (100%)	0.25
carboxylic	-COOH ≈ COO	-	1	5	1 (20%)	0.74
alkyl halides	-F, -Cl	-	2	6	5 (83%)	0.43
cyanide	-CN	-	1	3	3 (100%)	0.34
HO• addition to aromatic compounds						
Overall for HO• addition to aromactic compounds		**40**	**45**	**120**	**106 (88%)**	**0.73**
Overall for benzene		**21**	**18**	**68**	**61 (90%)**	**0.30**
alkyl	-CH_3 ≈ -CH_2- ≈ -CH< ≈ >C<	-	1	22	21 (95%)	0.30
alkyl halides	-F, -Cl, -Br, -I	-	4	17	14 (82%)	0.32
oxygenated	-OH, -CHO, -COOH, -CO, -O-	-	5	20	18 (90%)	0.27
S-containing	-SO, -SO3H	-	2	3	3 (100%)	0.30
N-containing	-CONH2, -CN, -NO2, -NH-CO-, -NH-, -NH2	-	6	7	7 (100%)	0.36
Overall for pyridine		**12**	**8**	**22**	**22 (100%)**	**0.24**
alkyl	-CH3	-	1	5	5 (100%)	0.083
oxygenated	-OH, -COOH	-	2	6	6 (100%)	0.28
alkyl halides	-Cl, -Br	-	2	4	4 (100%)	0.37
N-containing	-CONH2, -CN, -NH2	-	3	5	5 (100%)	0.28
Overall for furan		**4**	**10**	**13**	**13 (100%)**	**0.52**
alkyl	-CH3 ≈ -CH2	-	1	3	3 (100%)	0.38
oxygenated	-O-, -CHO, -CO, -COOH	-	4	5	5 (100%)	0.80
alkyl halides	-Br	-	1	1	1 (100%)	N.A.
N-containing	-NO2, -CONH2-, -CHCN-	-	3	4	4 (100%)	0.91
aromatic	-C6H5	-	1	1	1 (100%)	N.A.
Overall for imidazole		**2**	**4**	**8**	**8 (100%)**	**0.29**
alkyl	-CH3 ≈ >C<	-	1	2	2 (100%)	0.55
carbonyl	-CO	-	1	5	5 (100%)	0.25
N-containing	-NH, -N<	-	2	6	6 (100%)	0.28
Overall for triazine		**1**	**5**	**9**	**3 (33%)**	**2.57**
ether	-O-	-	1	1	0 (0%)	N.A.
alkyl halides	-Cl	-	1	5	2 (40%)	3.48
S-containing	-S-	-	1	2	0 (0%)	1.01
N-containing	-NH2, -NH-	-	2	8	3 (38%)	2.66
HO• Interaction with S, N, or P-atom containing compounds						
Overall for HO• interaction		**14**	**10**	**78**	**58 (74%)**	**1.5**
Overall for S-containing		**4**	**2**	**12**	**10 (83%)**	**0.38**
sulfide, thiol	-S- ≈ -S-S- ≈ -HS	3	1	8	6 (75%)	0.45
sulfoxide	-SO-	1	1	4	4 (100%)	0.24
Overall for N-containing		**8**	**6**	**54**	**37 (69%)**	**1.8**
nitriles	-CN	1	1	4	3 (25%)	0.79
nitro	-NO2	1	1	2	0 (0%)	13
amide	-N-CO-	3	1	15	10 (67%)	0.46
amine	-NH2 ≈ -NH- ≈ -N<	3	1	21	17 (81%)	0.47
nitroso and nitramine	-N-NO, -N-NO2	0	2	12	9 (75%)	0.58
urea	$k_{-N-CO-N-}$	1	0	7	7 (100%)	0.25
phosphorus	->P=O, -O-P<-	1	2	5	5 (100%)	0.47

Table 2.3: Summary of experimental data and statistical results for prediction

Reaction mechanism	Number of experimental data	Number of data within EG (%)	S.D.
Overall	**124**	**76 (62%)**	**1.2**
H-atom abstraction	60	35 (58%)	1.1
HO• addition to aromatic compounds	46	33 (72%)	0.53
HO• Interaction with S, N, or P-atom containing compounds	18	8 (44%)	2.2

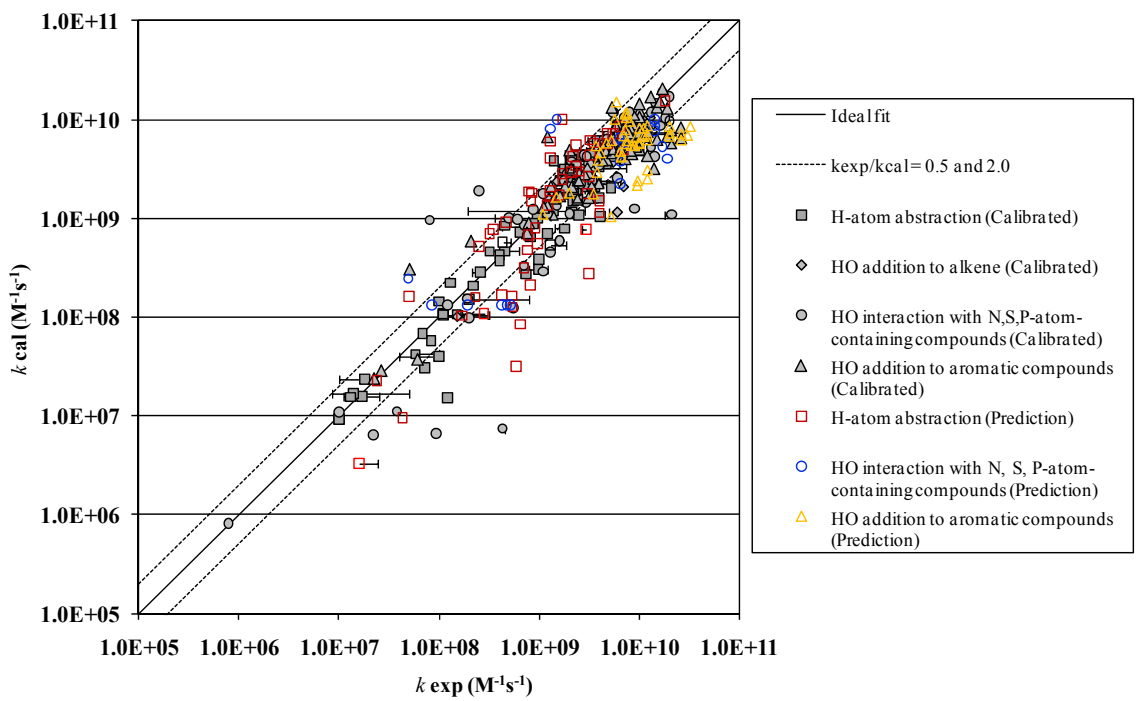

Figure 2.3: Total of 434 HO• reaction rate constants from calibrations and predictions versus experimental rate constants for four reaction mechanisms. Error bars represent the range of experimentally reported values.

2.4.3 Hydrogen-Atom Abstraction from Saturated Aliphatic Compounds

The group rate constants of primary, secondary, and tertiary C-H bonds, k^0_{prim}, k^0_{sec}, and k^0_{tert}, respectively, and group contribution factors, X_{R_i}, of alkyl and halogenated

functional groups were calibrated first. Then, other group contribution factors were subsequently calibrated using these group rate constants and alkyl group contribution factors. For the calibration, the multifunctional group compounds (e.g., glycol, poly-carboxylic) were not used except for the alkyl halides (e.g., CH_2ClBr). As shown in Table 2.2, for the overall H-atom abstraction, the DF were 61. 85% of the calibrated data was within the EG. The S.D. was 0.42.

Once the group rate constants and group contribution factors were calibrated, 60 of the rate constants for the multifunctional group compounds were used to predict rate constants and were compared with experimental values. Table 2.3 summarizes the results from the prediction. A total of 58% of the predicted data were within the EG. The SD was 1.1.

2.4.3.1 Group Rate Constants for H-atom Abstraction

Group rate constants of $k^0_{\text{prim}}, k^0_{\text{sec}}$, and, k^0_{tert} are 1.18×10^8, 5.11×10^8, and 1.99×10^9 $M^{-1}s^{-1}$, respectively. The trend $k^0_{\text{prim}} < k^0_{\text{sec}} < k^0_{\text{tert}}$ is consistent with the radical stability of primary, secondary, and tertiary carbon-centered radicals due to the hyperconjugation. The approximate magnitude of the group rate constants can be verified from the experimentally obtained E_a (Monod et al., 2005; Elliot and McCracken, 1989) and A (Monod et al., 2005; Asmus et al., 1973). For instance, $E^0_{\text{prim}} + E^{-\text{OH}}_{a,\text{abs}}$ and $E^0_{\text{prim}} + E^{-\text{CO}}_{a,\text{abs}}$ are equivalent to 4.8 kJ/mol of methane and 11.6 kJ/mol of acetone, respectively. Due to their electron withdrawing-ability (i.e., $E^{-\text{OH}}_{a,\text{abs}}$ and $E^{-\text{CO}}_{a,\text{abs}}$ are greater than 0), E^0_{prim} should be less than 4.8 kJ/mol. Assuming the typical Arrhenius frequency factor, A, as 10^{10} $M^{-1}s^{-1}$ for the H-atom abstraction by HO• (e.g., 7.2×10^9 for methanol; 1.6×10^{10} for acetone), the

approximate magnitude of k^0_{prim} can range from 10^8 to10^9, which is in agreement with our estimated k^0_{prim}.

When aqueous-phase group rate constants are compared with gaseous-phase ones, the aqueous-phase group rate constants are more variable than the gaseous-phase ones (i.e., $k^0_{\text{tert}} / k^0_{\text{prim}}$ = 16.9 and $k^0_{\text{sec}} / k^0_{\text{prim}}$ = 4.3 versus $k^0_{\text{tert(gas)}} / k^0_{\text{prim(gas)}}$ = 4.3 and $k^0_{\text{sec(gas)}} / k^0_{\text{prim(gas)}}$ = 1.0). This is probably due to both the cage effect and the effect of solvation (Benson, 1982). In the aqueous phase, HO• and solute molecules significantly interfere with water molecules that form a first solvation cage surrounding a targeted molecule. As a result of restriction of their molecular rotation and translation in the solvent cage, the solutes suffer a significant decrease in entropy. According to the following equation (2.25) (Brezonik, 2002) that relates the activation of entropy in the aqueous phase, $\Delta S^{\neq}$, with the Arrhenius frequency factor A,

$$A = e\kappa T / h \exp\left(\Delta S^{\neq} / R\right) \tag{2.25}$$

the A in the aqueous phase generally becomes smaller than the gaseous phase one. In addition, it may be more difficult for HO• to attack tertiary C-H bond due to three other functional groups than to the secondary and primary C-H bonds. As a result, the following trend is observed: $A_{\text{tert}}/A_{\text{prim}} > A_{\text{tert(gas)}}/A_{\text{prim(gas)}}$. One can also understand the effect of water molecules to the E_a from free energy of solvation as shown in the following equation

$$\Delta G^{\neq} = E_{\text{a}} - RT - T\Delta S^{\neq} \tag{2.26}$$

where $\Delta G^{\neq}$ is free energy of activation in solution, and for the aqueous phase (Brezonik, 2002)

$$E_{\text{a}} = \Delta H^{\neq} + RT \tag{2.27}$$

As a consequence, in general, larger rate constants are observed in the aqueous phase than in the gaseous phase, although this depends on the polarizability of solute molecules. For non-polarized molecules (e.g., alkanes), positive solvation energy is observed. Theoretically calculated solvation energy (i.e., G_{sov} ($CHCl_3$) < G_{sov} (CH_2Cl) < G_{sov} (CH_3Cl)) (Vassilev and Baerends, 2005) also verifies our obtained trend $k_{tert}>k_{sec}>k_{prim}$.

In the aqueous phase, the H-atom abstraction reaction from a C-H bond preferentially occurs before an O-H bond due to the smaller BDEs of C-H bond. In addition, the polarity of oxygen makes the molecule extensively soluble in the aqueous phase because of the formation of hydrogen bonds, which prevent attacks to the O-H bond by HO•. Nonetheless, several experimental studies reported approximately 10% of H-atom abstraction from the O-H bond (Asmus et al., 1973). Therefore, a term k_{R_4} accounted for the group rate constants $k_{\text{-OH}}$ and $k_{\text{-COOH}}$, respectively, as shown in equation (2.9). The $k_{\text{-OH}}$ is 1.00×10^8 $M^{-1}s^{-1}$, which represents 33, 8.5, and <5% of the H-atom abstraction from the O-H bond in methanol, ethanol, and other alcohol compounds, respectively. These percentages are comparable with the experimental observations (Asmus et al., 1973). The k_{COOH} is 7.0×10^5 $M^{-1}s^{-1}$. The magnitude of the k_{COOH} is consistent with the rate constant for oxalic acid (Getoff et al., 1971).

2.4.3.2 Group Contribution Factors for H-atom Abstraction.

A total of 18 group contribution factors for H-atom abstraction (i.e., X_{R_i}) are summarized in Table 2.4. The group contribution factors of $X_{\text{-CH}_2\text{-}}$, $X_{\text{>CH-}}$, and $X_{\text{>C<}}$ were assumed to be identical because of the following reasons: (1) limited data availability for the >C< functional group and (2) identical BDEs affected by the corresponding functional group (i.e., 400.8 kJ/mol for CH_3CH_2C-**H**$(CH_3)_2$, 399.2 kJ/mole for

$(CH_3)_2CHC$-**H**$(CH_3)_2$, and 400.4 kJ/mol for $(CH_3)_3C$-**H**, respectively) (Luo, 2002). When the alkyl functional groups had the ether functional groups at both sides of the α-positions, another group contribution factor $X_{\text{-O-(second)}}$ was considered. Group contribution factors for carboxylic and ester functional groups, -COOH and –COOR, were assumed to be identical due to their similar electron-withdrawing ability. Because of their strong electron-withdrawing ability, the influence of the β-position that resulted from the halogen functional groups was considered. This represented $X_{\text{-CH}_n\text{(halogen)}_m}$ where (n,m) = (1,1), (1,2), or (2,1) for Cl or Br atom, (i.e., $X_{\text{-CH}_2\text{Cl}} \approx X_{\text{-CHCl}_2} \approx X_{\text{-CHCl-}} \approx X_{\text{-CH}_2\text{Br}} \approx X_{\text{-CHBr}_2} \approx X_{\text{-CHBr-}}$), respectively, which was assumed to be identical for the purpose of reducing the number of group contribution factors. The values of $X_{\text{-F}}$, $X_{\text{-I}}$, and $X_{\text{-CF}_2\text{-}}$ were not available because no experimental data were available for these functional groups. Ring structures were expected to increase E_a because of the extra energy to form the ring structure; consequently, group contribution factors for the 3-ring, X_{RS_3} , and the 5-ring, X_{RS_5} , for saturated cyclic compounds were considered, respectively.

Table 2.4: Group rate constants and group contribution factors for H-atom abstraction

Group rate constant ($\times 10^{-8}$ $M^{-1}s^{-1}$)	
k^0_{prim}	1.18
k^0_{sec}	5.11
k^0_{tert}	19.9
k_{OH}	1.00
k_{COOH}	0.00700
Group contribution factor, *X*	
$-CH_3$	1.12
$-CH_2$, >CH-, >C<	1.17
->C-(oxygenated)-	0.681
-OH	0.578
-O-	0.551
-CO-	0.154
-CHO	0.602
=O	0.360
-COO, -COOH	0.0430
-O-second	0.945
-OCOR	0.000
-RS5 (5 ring strain)	0.860
-RS3 (3 ring strain)	0.0520
-Cl	0.203
-Br	0.377
$-CF_3$	0.102
$-CCl_3$	0.112
$-CH_2Cl$, $-CHCl_2$, -CHCl-, $-CH_2Br$, $-CHBr_2$, -CHBr-	0.367

The group contribution factors for the H-atom abstraction linearly correlate with the Taft constant, σ* (Karelson, 2000), as shown in Figure 2.4. Because the alkyl functional groups contribute to weakening the C-H bond with release of the steric compression as the alkyl functional group moves apart to form a planar radical, they

increase in the HO• reactivity in the H-atom abstraction reactions. Therefore, $X_{\text{-CH}_3}$ and $X_{\text{-CH}_2\text{-}} \approx X_{\text{>CH-}} \approx X_{\text{>C<}}$ values are greater than 1.0, which correspond to negative values of the Taft constant. All of the group contribution factors for the oxygenated and the halogenated functional groups show smaller than 1.0, which indicate the electron-withdrawing ability of the functional groups.

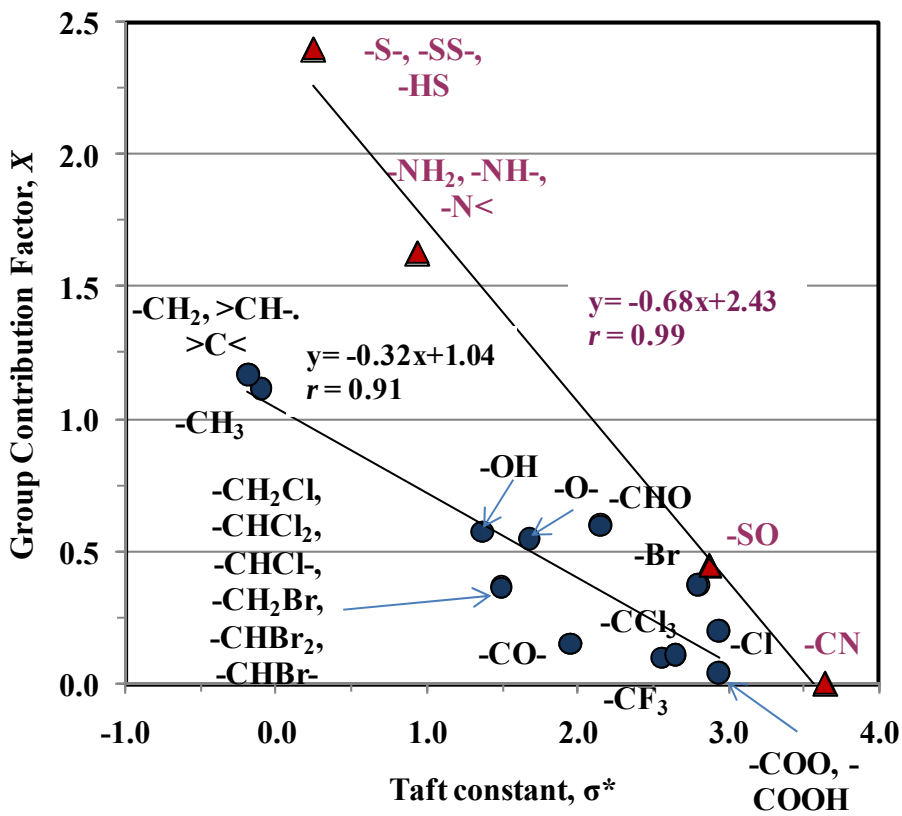

Figure 2.4: Comparison of the group contribution factors for H-atom abstraction with the Taft constant, σ*[60]. Group contribution factors include ●: alkyl, oxygenated, and halogenated functional groups, ▲: S-, N-, or P-atom containing functional groups.

2.4.4 HO• Addition to Alkenes

Twenty-eight alkenes were categorized based on the base C=C double-bond structures and position(s) of hydrogen atom(s) adjacent to those base structures. Table 2.5 summarizes the structural configurations for equation (2.13) based on the basis of the compounds that are available in the literature. There were few rate constants reported for the conjugated and unconjugated dienes. Therefore, these compounds were excluded from calibration. As shown in Table 2.2, the total DF were 14. A total of 79% of the calibrated data was within the EG. The SD was 0.4.

Table 2.5: Summary of the structural configurations in equation (2.13) based on the experimental rate constants

structure	*l*	*g*	*h*
>C=C<	4	2	-
H>C=C<	3	1	$\frac{1}{2}$
HH>C=C<	2	1	$\frac{1}{2}$
H>C=C<H(cis)	2	2	-
H>C=C<H(trans)	2	2	-
HH>C=C<H	1	1	$\frac{1}{2}$

2.4.4.1 Group Rate Constants and Group Contribution Factors for HO• Addition to Alkenes.

Group rate constants and group contribution factors are summarized in Table 2.6. It was found that the group contribution factors did not linearly correlate with the Taft

constant (data not shown). Two reasons can be considered. First, the functional group contribution to the E_a does not follow the general inductive effect (i.e., Taft constant). For example, the group contribution factor for alkane does not indicate the electron-donating value (i.e., $Y_{\text{-alkane}} = 0.171$). Because of the limited data availability and gaseous phase reaction mechanisms (Greenwald et al., 2005; Alvarez-Idaboy et al., 2000), the rate constant expression as shown in equation (2.13) did not consider the different effects of functional groups to two unsaturated carbons (one being attacked and the neighboring one). For example, the effects of three chlorine functional groups for 1,1,2-trichloroethylene were treated identical in association with the two unsaturated carbons in the >C=CH- base structure. Although Peeters et al. (2007) successfully applied the GCM to the gaseous phase HO• rate constants with nonconjugated and conjugated (poly) alkenes on the basis of the number of functional groups on the neighboring carbon, their approach was limited to nonpolar functional groups, and it was not clear if it was applicable to the heteroatom functional groups and aqueous phase reactions. Second, the experimental rate constants do not seem to follow the inductive effect (e.g., vinyl chloride > ethylene > vinyl alcohol) because of the experimental errors or the existence of unknown reaction mechanisms. We suggest more experimental studies be conducted for alkenes to confirm this.

Table 2.6: Group rate constants and group contribution factors for HO• addition to alkenes

Group rate constant ($\times 10^{-9}$)	
$k^{0}_{(HH>C=C<H)-1}$	10.0
$k^{0}_{(HH>C=C<H)-2}$	0.10
$k^{0}_{(HH>C=C<)-1}$	97.9
$k^{0}_{(HH>C=C<)-2}$	3.16
$k^{0}_{(H>C=C<H)(cis)}$	30.1
$k^{0}_{(H>C=C<H)(trans)}$	52.1
$k^{0}_{>C=C<}$	514
Group contribution factor, *Y*	
-Alkane	0.171
-CO-	0.600
-CHO	0.600
-COOH, -COOR	0.234
-F	0.000
-Cl	0.210
-CN	0.171

Despite the observation of the nonlinear correlation between the group contribution factors and the Taft constant, 79% of the calibrated rate constants were within the EG, and this might be acceptable for a rate constant estimator. It should be addressed that more quantitative investigations are required to examine the effect of the functional groups in the aqueous phase.

2.4.5 HO• Addition to Aromatic Compounds

Table 2.7 summarizes the structural configurations for equation (2.17) based on the basis of the compounds that were available in the literature. As shown in Table 2.2, for the overall HO• addition to aromatic compounds, the total DF were 35. 88% of the

rate constants from the calibration was within the EG. The SD was 0.73. Once the group rate constants and group contribution factors were calibrated, the rate constants for 46 compounds were predicted as shown in Table 2.3. A total of 64% of the rate constants from the prediction was within the EG. The SD was 0.53.

Table 2.7: Summary of structural configurations in equation (2.17) based on the experimental rate constants with aromatic compounds

name		*m*	*i*	*n*	*j*
benz	mono-	1	1	2	2,6
				1	4
				2	3,5
	di-	2	1,2	2	3,6
				2	4,5
			1,3	1	2
				2	4,6
				1	5
			1,4	2	2,6
				2	3,5
	tri-	3	1,2,3	2	4,6
				1	5
			1,2,4	1	3
				1	5
				1	6
			1,3,5	3	2,4,6
	tetra-	4	1,2,3,4	2	5,6
			1,2,3,5	2	4,6
			1,2,4,5	2	3,6
	penta-	5	1,2,3,4,5	1	6
	hexa-	6	1,2,3,4,5,6	6	1,2,3,4,5,6
pyr	mono-	1	2	2	3,6
				2	4,5
			3	1	2
				2	4,6
				1	5
			4	2	2,6
				2	3,5
	di-	2	2,6	2	3,5
				1	4
			3,5	2	2,6
				1	4
	tri-	3	2,4,6	2	3,5
fur	mono-	1	2	1	3
				1	4
				1	5
	di-	2	2,5	2	3,4
imid	di-	2	3,4	1	1
				2	3,4
triaz	tri-	3	1,3,5	3	2,4,6

2.4.5.1 Group Rate Constants for HO• Addition to Aromatic Compounds.

Tables 2.8-2.12 summarize the group rate constants for aromatic compounds that include benzene, pyridine, furan, imidazole and triazine compounds, respectively. The approximate magnitude of the group rate constants can be compared with theoretical studies because there is no experimental data for E_a. According to Ashton et al. (1995), E_a between 13 and 21 kJ/mol of the net reaction was observed for various aromatic compounds. From their conclusion that the electron-withdrawing functional groups increased the E_a by approximately 2.1-8.4 kJ/mol, the magnitude of group rate constants fell in the range of 10^9 orders. This is consistent with the group rate constants from the calibration.

Because the group rate constants for pyridine, furan, imidazole, and triazine compounds include the hetero atoms (e.g., N, NH, and O) that affect the HO• addition to aromatic ring, the calibrated group rate constants vary in magnitude of order from 10^6 to 10^9 $M^{-1}s^{-1}$. For example, the group rate constant, $k^0_{(2\text{-pyr})\text{-}3,6}$, that represents one functional group on 2-position and the addition of HO• to either the 3- or 6-position is 9.9×10^8 $M^{-1}s^{-1}$. This value and other group rate constants for pyridine are smaller than those of benzene compounds because of the lower reactivity and lower electrophilic nature of the pyridine nucleus toward the HO• (Solar et al., 1993). For triazine compounds, the group rate constant $k^0_{(1,3,5\text{-triaz})\text{-}2,4,6}$ (i.e., functional groups located on the 1,3,5-positions and HO• interacts with each N-atom located on the 2,4,6-positions) represents the reactivity of HO• with the triazine base structure other than the functional groups. However, this single group rate constant does not seem to represent the reaction mechanisms well.

Additional group rate constants may be required and can be calibrated when more experimental data are available.

Table 2.8: Group rate constants and group contribution factors for HO• addition to aromatic compounds that include benzene rings

Group rate constant ($\times 10^{-9}$ $M^{-1}s^{-1}$) (benzene)		Group contribution factor, Z (functional group on benzene ring)	
$k^{0}_{(1\text{-benz})\text{-}2,6}$	1.02	-Alkane	1.00
$k^{0}_{(1\text{-benz})\text{-}3,5}$	1.29	-OH	1.27
$k^{0}_{(1\text{-benz})\text{-}4}$	0.914	-O-	1.03
$k^{0}_{(1,2\text{-benz})\text{-}3,6}$	1.78	-CHO	0.672
$k^{0}_{(1,2\text{-benz})\text{-}4,5}$	0.706	-COOH	0.680
$k^{0}_{(1,3\text{-benz})\text{-}2}$	0.989	-CO-	0.981
$k^{0}_{(1,3\text{-benz})\text{-}4,6}$	1.70	$-CONH_2$	0.842
$k^{0}_{(1,3\text{-benz})\text{-}5}$	1.91	-F	0.973
$k^{0}_{(1,4\text{-benz})\text{-}2,6}$	0.713	-Cl	0.978
$k^{0}_{(1,4\text{-benz})\text{-}3,5}$	1.92	-Br	0.878
$k^{0}_{(1,2,3\text{-benz})\text{-}4,6}$	2.15	-I	0.821
$k^{0}_{(1,2,3\text{-benz})\text{-}5}$	1.64	-NH-	1.11
$k^{0}_{(1,2,4\text{-benz})\text{-}3}$	2.80	-NH-CO-	0.855
$k^{0}_{(1,2,4\text{-benz})\text{-}5}$	0.307	$-NH_2$	1.48
$k^{0}_{(1,2,4\text{-benz})\text{-}6}$	1.13	-CN	0.411
$k^{0}_{(1,3,5\text{-benz})\text{-}2,4,6}$	1.68	$-NO_2$	0.405
$k^{0}_{(1,2,3,4\text{-benz})\text{-}5,6}$	3.68	$-SO_3H$	0.373
$k^{0}_{(1,2,3,5\text{-benz})\text{-}4,6}$	2.80	-SO	0.656
$k^{0}_{(1,2,4,5\text{-benz})\text{-}3,6}$	3.53		
$k^{0}_{(1,2,3,4,5\text{-benz})\text{-}6}$	7.06		
$k^{0}_{(1,2,3,4,5,6\text{-benz})\text{-}1,2,3,4,5,6}$	0.312		

Table 2.9: Group rate constants and group contribution factors for HO• addition to aromatic compounds that include pyridine

Group rate constant ($\times 10^{-9}$ $M^{-1}s^{-1}$) (pyridine)		Group contribution factor (functional group on pyridine)	
$k^{0}_{(2\text{-pyr})\text{-}3,6}$	0.990	-Alkane (Pyr)	0.962
$k^{0}_{(2\text{-pyr})\text{-}4,5}$	0.293	-OH (Pyr)	1.97
$k^{0}_{(3\text{-pyr})\text{-}2}$	0.456	-COOH (Pyr)	0.011
$k^{0}_{(3\text{-pyr})\text{-}4,6}$	0.823	-$CONH_2$ (Pyr)	0.498
$k^{0}_{(3\text{-pyr})\text{-}5}$	0.025	-Cl (Pyr)	0.812
$k^{0}_{(4\text{-pyr})\text{-}2,6}$	0.791	-Br (Pyr)	0.603
$k^{0}_{(4\text{-pyr})\text{-}3,5}$	0.889	-CN (Pyr)	0.333
$k^{0}_{(2,6\text{-pyr})\text{-}3,5}$	1.03	-NH_2 (Pyr)	1.75
$k^{0}_{(2,6\text{-pyr})\text{-}4}$	0.732		
$k^{0}_{(3,5\text{-pyr})\text{-}2,6}$	3.71		
$k^{0}_{(3,5\text{-pyr})\text{-}4}$	0.793		
$k^{0}_{(2,4,6\text{-pyr})\text{-}3,5}$	0.761		

Table 2.10: Group rate constants and group contribution factors for HO• addition to aromatic compounds that include furan

Group rate constant ($\times 10^{-9}$ $M^{-1}s^{-1}$) (furan)		Group contribution factor (functional group on furan)	
$k^{0}_{(2\text{-fur})\text{-}3}$	3.92	-Alkane (fur)	1.24
$k^{0}_{(2\text{-fur})\text{-}4}$	4.81	-O- (fur)	1.02
$k^{0}_{(2\text{-fur})\text{-}5}$	1.42	-CHO (fur)	0.647
$k^{0}_{(2,5\text{-fur})\text{-}3,4}$	5.71	-CO- (fur)	0.406
		-COOH (fur)	0.600
		-$CONH_2$-(fur)	0.610
		-Br (fur)	0.647
		-NO_2 (fur)	0.778
		-CH-CN-(fur)	0.903
		-C_6H_5 (fur)	0.943

Table 2.11: Group rate constants and group contribution factors for HO• addition to aromatic compounds that include imidazole

Group rate constant ($\times 10^{-9}$ $M^{-1}s^{-1}$) (imidazole)		Group contribution factor (functional group on imidazole)	
$k^{0}_{(3,4\text{-imid})\text{-}1}$	1.71	-Alkane (imid)	1.17
$k^{0}_{(3,4\text{-imid})\text{-}3,4}$	1.08	-CO (imid)	0.731
		-NH (imid)	1.43
		-N< (imid)	1.61

Table 2.12: Group rate constants and group contribution factors for HO• addition to aromatic compounds that include triazine

Group rate constant ($\times 10^{-6}$ $M^{-1}s^{-1}$) (triazine)		Group contribution factor (funtional group on triazine)	
$k^{0}_{(1,3,5\text{-triaz})\text{-}2,4,6}$	4.13	-O- (triaz)	0.214
		-Cl (triaz)	1.00
		$-NH_2$ (triaz)	4.95
		-NH- (triaz)	0.0416
		-S- (triaz)	1.83

2.4.5.2 Group Contribution Factors for HO• Addition to Aromatic Compounds.

Tables 2.9-2.12 summarize the group contribution factors for the HO• addition to aromatic compounds. Figure 2.5 plots those values against electrophilic substituent constants, σ^{+} (Karelson, 2000), for benzene (r= 0.89), pyridine (r= 0.93), and furan (r= 0.65) compounds. Because only one σ^{+} for imidazole functional groups is available, Figure 2.5 does not include the plot for imidazole. These observations validate that the group contribution factors that are empirically derived from the experimental rate constants linearly correlate with the general electron-donating and -withdrawing property. For furan compounds, the weak correlation may be due to insufficient number of data.

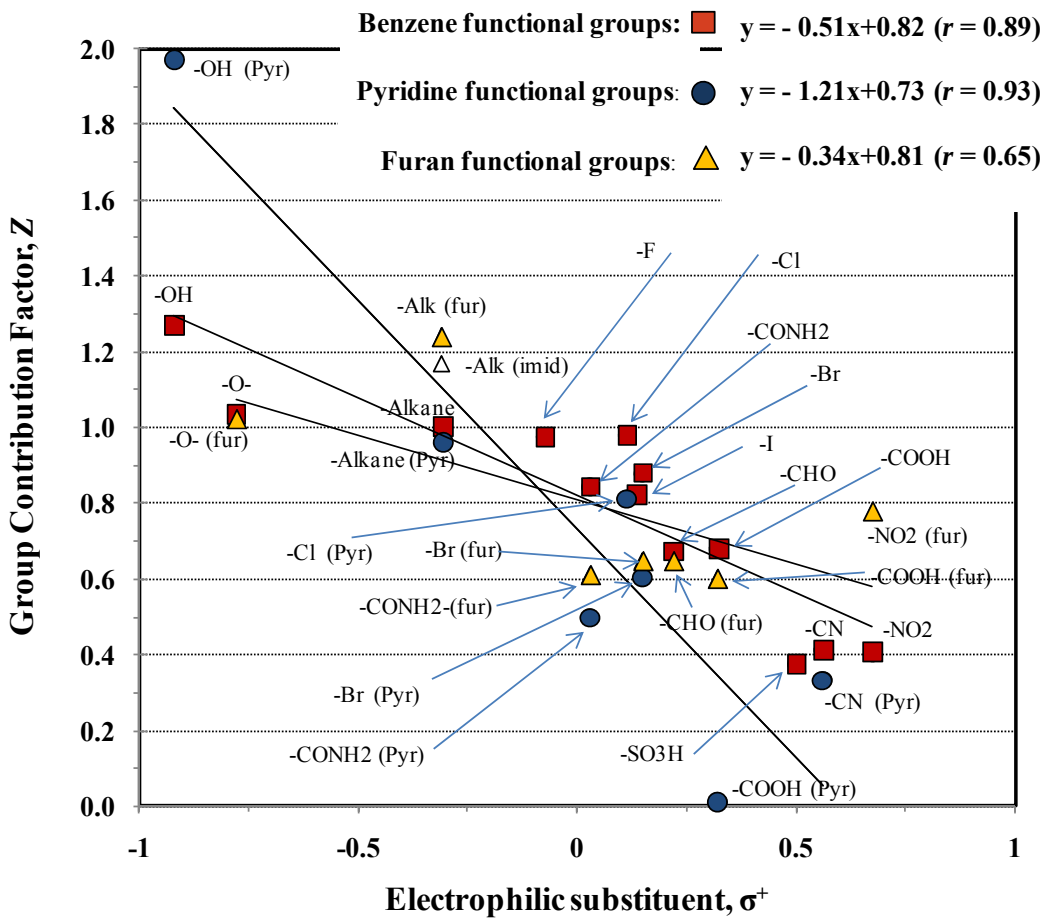

Figure 2.5: Comparison of the group contribution factors for HO• addition to aromatic compounds with electrophilic substituent parameter, σ+, (Karelson, 2000) (right). Figure includes the group contribution factors for benzene (■), pyridine (●), and furan compounds (▲). The σ* of [-$CHCl_2$], [-CO], [-COO, COOH], [–S-, -SS- -HS-], [-NH_2, -NH-, -N<] is an average of [CH_2Cl, CH_2Br, $CHCl_2$, $CHBr_2$], [$COCH_3$, COC_2H_5, $COC(CH_3)_3$, COC_6H_5, COF, COCl], [COOH, $COOC_2H_5$], [SCH_3, SC_2H_5, $SCH(CH_3)_2$], and [$NHCH_3$, $NH(CH_2)_3CH_3$, $N(C_2H_5)_2$], respectively. The σ* of [-SO] and [-N-CO-] refer to [$S(O)CH_3$] and [$NHCOC_6H_5$], respectively.

2.4.6 HO• Interactions with Sulfur-, Nitrogen-, or Phosphorus-containing-Compounds

As shown in Table 2.2, the DF were 54. 74% of the calibrated data was within the EG. The SD was 1.5. Once the group rate constants and group contribution factors were determined, 18 of the rate constants were predicted and compared with the

experimental rate constants as shown in Table 2.3. A total of 44% of the rate constants was within the EG. The SD was 2.2.

2.4.6.1 Group Rate Constants for HO• Interaction

The group rate constants and group contribution factors were summarized in Table 2.13. Because no direct interactions were experimentally observed (Mezyk et al., 2006; 2004), the group rate constants, $k_{\text{-N-NO}}$ and $k_{\text{-N-NO}_2}$ were not considered. The group rate constants $k_{\text{-CN}}$ and $k_{\text{-NH2}}$ can be compared with the rate constants for compounds that react with HO• via only interaction such as cyanogen and thiourea, respectively. The rate constant for thiourea is approximately twice of $k_{\text{-NH2}}$ because the electron positive -CS- functional group does not significantly affect the electron density of the N-atom. The reaction of HO• with urea may be different because two amine functional groups in urea bond to the electron-negative functional group, -CO-. As a result, another group rate constant $k_{\text{-N-CO-N-}}$ was considered for methylurea, tetramethyl urea, and 1,3-dimethylurea.

The magnitude of most group rate constants for the S-containing compounds was in the same order as for the amine-related compounds but approximately 1 order of magnitude larger than those for the amide-related compounds. This is probably because of the electronegative –CO- functional group that is a part of amide functional groups.

Table 2.13: Group rate constants and group contribution factors for S, N, and P-atom containing compounds

Group rate constant ($\times 10^{-8}$ $M^{-1}s^{-1}$)	
$k_{\text{-S-}}$	23.6
$k_{\text{-S-S-}}$	36.7
$k_{\text{-SO}}$	19.2
$k_{\text{-HS-}}$	9.93
$k_{\text{-CN}}$	0.0555
$k_{\text{-NO2}}$	1.33
$k_{\text{-CO-NH2}}$	0.998
$k_{\text{-CO-NH-}}$	5.00
$k_{\text{-CO-N<}}$	9.98
$k_{\text{-NH2}}$	40.0
$k_{\text{-NH-}}$	1.00
$k_{\text{-N<}}$	35.3
$k_{\text{-N-CO-N-}}$	0.00409
$k_{\text{-P}\equiv}$	0.258
Group contribution factor, *X*	
-S-, -SS-, -HS-	2.40
-SO	0.445
-CN	0.00292
$-NO_2$	0.00
$-NH_2$, -NH-, -N<	1.63
-N-CO-	3.19
-N-NO	0.0105
$-N-NO_2$	0.176
->P=O	0.103
-O-P<-	0.00004

2.4.6.2 S-, N-, or P-atom-Containing Group Contribution Factors

The S-, N-, or P-atom-containing group contribution factors apparently play the same role as the functional groups for H-atom abstraction, i.e., $X_{\mathrm{R}_i} = e^{-\frac{E_{a,\mathrm{abs}}^{\mathrm{R}_i}}{RT}}$. However, it is anticipated that S-, N-, or P-atom-containing functional groups may have different effects on H-atom abstraction. The group contribution factors for -S, -S-S- and -SH, and $–NH_2$, -NH- and -N<, respectively, were assumed to be identical due to the following reasons: (1) limited data availability for single functional group compounds, (2) similar electron inductive ability, and (3) application for the gaseous phase. One might consider additional rate constants (e.g., amino acids) to overcome the limited data availability. However, the single-functional group compounds were used to calibrate the group contribution factors to avoid the interference of different functional groups. In addition, the same data sets for the S- and N-atom containing-compounds were used to calibrate the group rate constants, $k_{\text{-S-}}$, $k_{\text{-S-S-}}$ and $k_{\text{-SH}}$, and $k_{\text{-NH2}}$, $k_{\text{-NH-}}$ and $k_{\text{-N<}}$, respectively. These group rate constants were not assumed to be identical because the interaction of HO• with each functional group might be more significant than the electron donating effects that result from these functional groups. Therefore, within the limited data availability, our assumption should be acceptable. For similar electron inductive ability, the Taft constant indicates similar values among these S- and N-atom-containing functional groups. For example, the Taft constants for SCH_3, SC_2H_5, and SH are 1.66, 1.44, and 1.52, respectively (Karelson, 2000), and those for NH_2, $NHCH_3$, $N(CH_3)_2$, $NH(CH_2)_3CH_3$, and $N(C_2H_5)_2$ are 0.62, 0.94, 1.02, 1.08, and 1.00, respectively (Karelson, 2000). These values are well distinguished from 3.61 of NH_3^+, 4.66 of NO_2, 4.16 of $N+(CH_3)_3$, and 3.64 of CN. Finally, Atkinson (Atkinson, 1986; 1987; Kwok and Atkinson, 1995)

assumed that the "substituent factors" for -S-, -S-S-, and –SH, and for $–NH_2$, -NH-, -N<, -NNO, and $–NNO_2$ were identical and successfully predicted the gaseous phase HO• rate constants. Although the reaction mechanisms for the interaction in the gaseous phase may be different from the aqueous phase, the manner in which S- and N-atom-containing functional groups affect the neighboring C-H bond could be very similar between two phases. The –SO and –N-CO- functional groups were treated separately because of the electronegative oxygen atom. In contrast, the $X_{\text{-CO-N-}}$ was treated as identical to $X_{\text{-CO-}}$. It is observed that the amide nitrogen is much more effective in activating the methyl group that undergoes the H-atom abstraction than ester oxygen (Hayon et al., 1970). This is consistent with the group contribution factors (i.e., $X_{\text{-COO}} = 0.04$, $X_{\text{-N-CO}} = 3.19$).

Figure 2.4 compares the group contribution factors of S-, N-, or P-atom-containing functional groups with the Taft constant, σ* (Karelson, 2000). A linear correlation between these group contribution factors and σ* was observed ($r = 0.99$). As compared with X_{R_i} for the alkyl, oxygenated, and halogenated functional groups, those for S-, N-, or P-atom-containing functional groups are greater. This implies that S, N, or P-atom-containing functional groups donate more electrons toward the neighboring C-H bond(s), hence, enhancing the H-atom abstraction by HO•. It should be noted that insufficient experimental data resulted in poor calibration for nitrile and nitro compounds. As it turns out, we may have to consider the electron-negative effect of these compounds in the β-position because of their strong electron-withdrawing ability. However, this will have to wait until more data become available.

2.4.7 Predictabilities of GCM and Future Studies

Because the GCM is based on the group additivity of the rate constants, it is not able to predict the rate constants for the reactions that are close to the diffusion-control limit. The rate constant expression may not thoroughly reflect the reaction mechanisms in the aqueous phase due to the unknown reaction mechanisms (e.g., HO• addition to alkenes). In addition, there are insufficient experimental data sets (e.g., nitriles and nitros, furan, and triazine compounds) and suspect data (e.g., alkenes). As a result, nonlinear correlation was observed between the group contribution factors with the electron-donating and -withdrawing ability, i.e., the Taft constant or electrophilic substitutent parameter. The observed inconsistencies of the experimental data may have resulted from the difference in experimental protocols such as the differences of analytical approach or HO• production methods (e.g., pulse radiolysis, UV/H_2O_2, O_3/H_2O_2). For these groups, additional experimental studies are needed to obtain better calibration.

Solvation effects can be expected to affect the reactions for polar- and nonpolar functional groups differently due to the absence or presence of the hydrogen bonds. These might cause over or under prediction for the oxygenated multifunctional group compounds (i.e., poly alcohols, poly carboxylic compounds, and benzenes with di- and trifunctional groups) because of the invalid thermochemical additivity. A more sophisticated approach (e.g., quantum mechanical calculation) may be required to investigate these effects, and this is an undergoing project.

Steric hindrance that results from the halogenated and carboxylic functional groups may also cause over and under prediction. While alcohols with –CF_3 or –CCl_3 functional groups undergo the solvation effect, steric hindrance might be more significant (i.e.,

steric constants, E_s, for $–CF_3$ and $–CCl_3$ are -2.40 and -3.30, respectively, as compared to -1.24 for $–CH_3$ and -0.46 for –Cl (Karelson, 2000)). We are also currently investigating the steric hindrance for specific functional groups. Although the GCM uses only experimentally reported rate constants based on the thermochemical additivity of the E_a, the group contribution factors linearly correlate with the general inductive constants for most cases. In addition, the rate constants for the multifunctional group compounds were predicted and compared with the experimental rate constants. It turns out that the GCM can predict most of the rate constants within the 0.5 to 2 times the experimental values. Therefore, the GCM can be used to predict the rate constants for many compounds with any kinds of functional groups that we have sufficient data to calibrate group rate constants and group contribution factors within the EG, and this may be acceptable for the design of AOPs, depending on how sensitive the model is to the rate constants.

As an extra trial, the GCM predicted the rate constants for 11 emerging aromatic compounds and compared them with the experimental rate constants as shown in Table 2.1. It was found that all of the predicted values were within the EG. In addition, the GCM predicted the rate constants for 68 emerging compounds that include the EPA's Contaminate Candidate List 2 (CCL2) and 3 (CCL3) compounds as shown in Table 2.14. Table 2.14 includes calculated half-lives for HO• concentrations of 10^{-9}, 10^{-10}, and 10^{-11} mole/L based on equations (2.28) and (2.29):

$$\frac{dC_R}{dt} = -k_{HO}.C_{HO}.C_R \tag{2.28}$$

$$t_{1/2} = \frac{\ln(2)}{k_{HO}.C_{HO}.} \tag{2.29}$$

It is clear that as the HO• concentration decreases to 10^{-11} mole/L due to HO• scavengers (e.g., natural organic matters, carbonate and bicarbonate, iron and manganese) in water, longer retention time in AOPs will be required. Although the HO• rate contants for these compounds have not been experimentally obtained, our calculcated half-life of these emergning contaminants can be used as a screening tool to examine the initial fate of these emerging contaminants during AOPs.

Table 2.14: Predicted HO• reaction rate constants for emerging contaminants

	CAS	Note	*k* cal	Half-life, min		
				[HO•] = 10^{-9} mole/L	[HO•] = 10^{-10} mole/L	[HO•] = 10^{-11} mole/L
1,1-dichloropropane	78-99-9	CCL2	9.31E+08	0.745	7.45	74.5
1,2-diphenylhydrazine	122-66-7	CCL2	1.23E+10	0.057	0.565	5.65
1,3-dichloropropane	142-28-9	CCL2	6.25E+08	1.11	11.1	111
cis-1,3-dichloropropene	10061-01-5	CCL2	5.13E+09	0.135	1.35	13.5
trans-1,3-dichloropropene	10061-02-6	CCL2	8.72E+09	0.079	0.795	7.95
2,2-dichloropropane	594-20-7	CCL2	7.92E+07	8.75	87.5	875
2,4-dichlorophenol	120-83-2	CCL2	5.24E+09	0.132	1.32	13.2
2,4-Dinitrophenol	51-28-5	CCL2	1.14E+09	0.610	6.10	61.0
2,4-dinitrotoluene	121-14-2	CCL2	9.50E+08	0.730	7.30	73.0
2,6-dinitrotoluene	606-20-2	CCL2	1.23E+09	0.564	5.64	56.4
2-methylphenol	95-48-7	CCL2	6.32E+09	0.110	1.10	11.0
Acetochlor	34256-82-1	CCL2	1.14E+10	0.061	0.610	6.10
Aldrin	309-00-2	CCL2	2.58E+10	0.027	0.268	2.68
DDE (dichlorodiphenyl dichloroethylene)	72-55-9	CCL2	5.57E+10	0.012	0.125	1.25
Diazinon	333-41-5	CCL2	9.90E+09	0.070	0.700	7.00
Dieldrin	60-57-1	CCL2	1.53E+10	0.045	0.452	4.52
Disulfoton	298-04-4	CCL3	6.63E+09	0.104	1.04	10.4
EPTC	759-94-4	CCL2	2.08E+10	0.033	0.334	3.34
Fonofos	944-22-9	CCL2	4.61E+09	0.151	1.51	15.1
Cymene, isopropyltoluene	99-87-6		8.95E+09	0.077	0.774	7.74
Methylbromide	74-83-9	CCL3	1.33E+08	5.22	52.2	522
Metolachlor	51218-45-2		1.22E+10	0.057	0.568	5.68
Metribuzin	21087-64-9		4.72E+09	0.147	1.47	14.7
Molinate	2212-67-1		1.89E+10	0.037	0.367	3.67
Cyclonite	121-82-4		1.03E+08	6.75	67.5	675
Alachlor	15972-60-8		1.06E+10	0.066	0.655	6.55
Carbofuran	1563-66-2		7.73E+09	0.090	0.896	8.96
Dalapon	75-99-0		4.15E+08	1.67	16.7	167
Endothall	145-73-3		5.39E+09	0.129	1.29	12.9
Epichlohydrin	106-89-8		3.03E+08	2.29	22.9	229
Glyphosate	1071-83-6		7.45E+08	0.930	9.30	93.0
Lindane (alpha-Hexachlorocyclohexane)	58-89-9	CCL3	3.27E+08	2.12	21.2	212
Methyoxychlor	72-43-5		6.06E+09	0.114	1.14	11.4
Oxamyl	23135-22-0		6.97E+09	0.099	0.995	9.95
TCEP tri(2-chloroethyl)phosphate	115-96-8		8.68E+08	0.799	7.99	79.9
Meprobamate	57-53-4		3.86E+09	0.180	1.80	18.0
DEET (N,N-diethyl-3-methyl-benzamide)	134-62-3		1.44E+10	0.048	0.483	4.83
Gemfibrozil	25812-30-0		9.40E+09	0.074	0.738	7.38
Dilantin	57-41-0		5.55E+09	0.125	1.25	12.5
Triclosan	3380-34-5		9.72E+09	0.071	0.713	7.13
Benzafibrate	41859-37-0		1.60E+10	0.043	0.433	4.33
Clofibric acid	882-09-7		5.81E+09	0.119	1.19	11.93
Cyclophosphamide	50-18-0		4.07E+09	0.170	1.70	17.01
Aspirin	50-78-2		3.51E+09	0.197	1.97	19.74
Decabromobipheyl ether (DBDE)	1163-19-5		2.02E+09	0.343	3.43	34.3
Hexabromobiphyl	36355-01-8		9.56E+09	0.073	0.725	7.25
Hexabromocyclodecane (HBCD)	3194-55-6		7.03E+09	0.099	0.987	9.87
Octabromobiphenyl ether (OBDE)	67889-00-3		8.41E+09	0.082	0.824	8.24
Pentabromodiphenyl ether (penta BDE)	32534-81-9		8.32E+09	0.083	0.833	8.33
Tetrabromobisphenol A (TBBPA)	79-94-7		1.20E+10	0.058	0.577	5.77
1,2-bis(2,4,6-tribromophenoxy)ethane (TBE)	37853-59-1		9.18E+09	0.075	0.755	7.55
2,3,4,5,6-pentabromoethylbenzene (PEB)	85-22-3		2.54E+09	0.273	2.73	27.3
1,2,3-Trichloropropane	96-18-4	CCL3	1.04E+09	0.663	6.63	66.3
1,3-Dinitrobenzene	99-65-0	CCL3	1.03E+09	0.671	6.71	67.1
2-Propen-1-ol	107-18-6	CCL3	4.62E+09	0.150	1.50	15.0
Benzylchloride	100-44-7	CCL3	6.57E+09	0.105	1.05	10.5
Cumen hydroperoxide	80-15-9	CCL3	6.48E+09	0.107	1.07	10.7
Hydrazine	302-01-2	CCL3	8.00E+09	0.087	0.867	8.67
n-Propylbenzene	103-65-1	CCL3	8.51E+09	0.081	0.814	8.14
o-Toluidine	95-53-4	CCL3	1.17E+10	0.059	0.591	5.91
Oxirane, methyl-	75-56-9	CCL3	5.23E+08	1.32	13.2	132
Oxydemeton-methyl	301-12-2	CCL3	6.63E+09	0.105	1.05	10.5
Profenofos	41198-08-7	CCL3	1.18E+10	0.059	0.587	5.87
RDX (Hexahydro-1,3,5-trinitro-1,3,5-triazine)	121-82-4	CCL3	9.55E+07	7.26	72.6	726
sec-Butylbenzene	135-98-8	CCL3	1.03E+10	0.067	0.670	6.70
Triethylamine	121-44-8	CCL3	1.04E+10	0.067	0.669	6.69
Tribufos	78-48-8	CCL3	1.81E+10	0.038	0.382	3.82
Urethane	51-79-6	CCL3	4.14E+08	1.67	16.7	167

2.5 Acknowledgement

This work was supported by National Science Foundation Award 0607332 award from the National Science Foundation. Any opinions, findings, conclusions, or recommendations expressed in this publication are those of the authors and do not necessarily reflect the view of the supporting organizations. Authors also appreciate support from the Snell Research Assistantship at Arizona State University and the Hightower Chair and Georgia Research Alliance at Georgia Institute of Technology. We gratefully acknowledge the contributions of Jessica Brosilo for her editorial assistance.

2.6 Appendices

An executed program is provided along with an input text file for the calculations of the HO• reaction rate constants. In addition, a Microsoft Excel spread sheet is also given for this purpose. Appendix A contains the source of genetic algorithm. Appendix B includes up-to-date experimental HO• radical rate constants. Appendix C includes a GCM identifier.F90 program source code.

2.7 Literature Cited

A division of the American Chemical Society. CAS (Chemical Abstract Service). http://www.cas.org/expertise/cascontent/index.html (accessed June 12, 2009).

Alvarez-Idaboy, J.R.; Mora-Diez, N.; Vivier-Bunge, A. A quantum chemical and classical transition state theory explanation of negative activation energies in OH addition to substituted ethenes. *J. Am. Chem. Soc*. 2000, *122*, 3715-3720.

Ashton, L.; Buxton, G.V.; Stuart, C.R. Temperature dependence of the rate of reaction of OH with some aromatic compounds in aqueous solution. Evidence for the formation of a π complex intermediate? *J. Chem. Soc. Faraday. Trans*. 1995, *91*(11), 1631-1633.

Asmus, K.-D.; Bonifačič, M. In Sulfur-Centered Reactive Intermediates as Studied by Radiation Chemical and Complementary Techniques; Chapter 5. 141-191. Alfassi, Z. B. Eds. The Chemistry of Free Radicals S-Centered Radicals. 1999. Chichester, U.K.

Asmus, K.-D.; Möckel, H.; Henglein, A. Pulse radiolytic study of the site of OH• radical attack on aliphatic alcohols in aqueous solution. *J. Phy. Chem.* 1973, *77*(10), 1218-1221.

Atkinson, R. A structure-activity relationship for the estimation of rate constants for the gas-phase reactions of OH radicals with organic compounds. *Int. J. Chem. Kinet*. 1987, 19, 799-828.

Atkinson, R. Kinetics and mechanisms of the gas-phase reactions of the hydroxyl radical with organic compounds under atmospheric condition. *Chem. Rev*. 1986, *86*, 69-201.

Avila, D.V.; Brown, C.E.; Ingold, K.U.; Lusztyk, J. Solvent effects on the competitive β-scission and hydrogen atom abstraction reactions of the cumyloxyl radical. Resolution of a long-standing problem. *J. Am. Chem. Soc*. 1993, *115*, 466-470.

Bakken, G.; Jurs, P.C. Prediction of hydroxyl radical rate constants from molecular structure. *J. Chem. Inf. Comput. Sci*. 1999, *39*, 1064-1075.

Benson, S.W. "Thermochemical Kinetics", 2nd ed. Wiley, Interscience, New York, 1976.

Benson, S.W. The Foundations of Chemical Kinetics Robert E. Krieger, Malabar, Florida, 1982.

Böhnhardt, A.; Kühne, R.; Ebert, R-U.; Schüürmann, G. Indirect photolysis of organic compounds: Prediction of OH reaction rate constants through molecular orbital calculations. *J. Phys. Chem*. 2008, *112*, 11391-11399.

Brezonik, P.L. Chemical kinetics and process dynamics in aquatic systems. Lewis Publishers. CRC Press. Boca Raton, 2002.

Buxton, V. B.; Greenstock, C. L.; Helman, W. P.; Ross, A. B. Critical review of rate constants for reactions of hydrated electrons, hydrogen atoms and hydroxyl radicals (•OH/•O^-) in aqueous solution. *J. Phys. Chem. Ref. Data*. 1988, *17* (2) 513-795.

Charbonneau, P.; Knapp, B. 1995, A User's guide to PIKAIA 1.0, *NCAR Technical Note 418+IA*, National Center for Atmospheric Research, Boulder.

Cohen, N. Are reaction rate coefficients additive? Revised transition state theory calculations for OH + alkane reaction. *Int. J. Chem. Kinet*. 1991, *23*, 397-417.

Cohen, N. The use of transition-state theory to extrapolate rate coefficients for reactions of OH with alkanes. *Int. J. Chem. Kint*. 1982, *14*, 1339-1362.

Cohen, N.; Benson, S.W. Empirical correlations for rate coefficients for reactions of OH with haloalkanes. *J. Phys. Chem*. 1987, *91*, 171-175.

Cramer, C.J. Essential of computational chemistry 2nd ed. John Wiley & Sons. Ltd. England, 2004; Chapter 11.

Crittenden, J.C.; Hu, S.; Hand, D.W.; Green, S.A. A kinetic model for H_2O_2/UV process in a completely mixed batch reactor. *Wat. Res*. 1999, *33*(10), 2315-2328.

Davey, J.B.; Greenslade, M.E.; Marshall, M.D.; Lester, M.I.; Wheeler, M.D. Infrared spectrum and stability of a π-type hydrogen-bonded complex between the OH and C_2H_2 reactants. *J.Chem.Phys*. 2004, *121*(7), 3009-3018.

Dutot, A-L.; Rude, J.; Aumont, B. Neural network method to estimate the aqueous rate constants for the OH reactions with organic compounds. *Atmos. Environ*. 2003, *37*, 269-276.

Elliot, A.J.; McCracken, D.R. Effect of temperature on O^- reactions and equilibria: a pulse radiolysis study. *Radiat. Phys. Chem*. 1989, *33*, 69-74.

Getoff, N. Radiation and photoinduced degradation of pollutants in water. A comparative study. *Radiat. Phys. Chem*. 1991, *37*(5/6), 673-680.

Getoff, N.; Schwörer, F.; Markovic, V.M.; Sehested, K.; Nielsen, S.O. Pulse radiolysis of oxalic acid and oxalates. *J. Phys. Chem*., 1971, 75(*6*), 749-755.

Goldberg, D.E. Genetic algorithms in search, optimization, and machine learning. Addison-Wesley Publishing Company, INC. Massachusetts, U.S.A. 1989.

Gramatica, P.; Pilutti, P.; Papa, E. Validated QSAR prediction of OH tropospheric degradation of VOCs: Splitting into training – test sets and consensus modeling. *J. Chem. Inf. Comput. Sci*. 2004, *44*, 1794-1802.

Greenwald, E.E.; North, S.W.; Georgievskii, Y.; Klippenstein, S.J. A two transition state model for radical-molecule reactions: a case study of the addition of OH to C_2H_4. *J. Phy. Chem. A*. 2005, *109*, 6031-6044.

Greenwald, E.E.; North, S.W.; Georgievskii, Y.; Klippenstein, S.J. A two transition state model for radical-molecule reactions: a case study of the addition of OH to C_2H_4. *J. Phy. Chem. A*. 2005, *109*, 6031-6044.

Grosjean, D.; Williams II, E.L. Environmental persistence of organic compounds estimated from structure-reactivity and linear free-energy relationships. Unsaturated aliphatics. *Atmos. Environ*. 1992, 26A(*8*), 1395-1405.

Hayon, E.; Ibata, T.; Lichtin, N.N.; Simic, M. Sites of attack of hydroxyl radicals on amides in aqueous solution. *J. Am. Chem. Soc*. 1970, *92*(13), 3898-3903.

Heicklen, J. The correlation of rate coefficients for H-atom abstraction by HO radicals with C-H bond dissociation enthalpies. *Int. J. Chem. Kint*. 1981, *13*, 651-665.

Herrmann, H. Kinetics of aqueous phase reactions relevant for atmospheric chemistry. *Chem. Rev*. 2003, *103*, 4691-4716.

Huber, M.M.; Canonica, S.; Park, G-Y.; Von Gunten, U. Oxidation of pharmaceuticals during ozonation and advanced oxidation processes. *Environ. Sci. Technol*. 2003, *37*, 1016-1024.

Karelson, M. Molecular Descriptors in QSAR/QSPR. John Wiley & Sons, INC. New York, 2000.

King, M.D.; Canosa-Mas, C.E.; Wayne, R.P. A structure-activity relationship (SAR) for predicting rate constants for the reaction of NO_3, OH and O_3 with monoalkenes and conjugated dienes. *Phys. Chem. Chem. Phys*., 1999, *1*, 2239-2246.

Klamt, A. Estimation of gas-phase hydroxyl radical rate constants of oxygenated compounds based on molecular orbital calculations. *Chemosphere*. 1996, *32*(4), 717-726.

Kwok, E.S.C.; Atkinson, R. Estimation of hydroxyl radical reaction rate constants for gas-phase organic compounds using a structure-reactivity relationship: An update. *Atmos. Environ*. 1995, *29*(14), 1685-1695.

Li, K.; Crittenden, J.C. Computerized pathway elucidation for hydroxyl radical-induced chain reaction mechanisms in aqueous phase Advanced Oxidation Processes. *Environ. Sci. Technol*. 2009, *43*, 2831-2837.

Li, K.; Hokanson, D.R.; Crittenden, J.C.; Trussell, R.R.; Minakata, D. Evaluating UV/H_2O_2 processes for methyl tert-butyl ether and tertiary butyl alcohol removal. *Wat. Res*. 2008, *42*(20), 5045-5053.

Li, K.; Stefan, M.I.; Crittenden, J.C. Trichloroethene degradation by UV/H_2O_2 advanced oxidation process: product study and kinetic modeling. *Environ. Sci. Technol*. 2007, *41*, 1696-1703.

Luo, Y-R. "Handbook of Bond Dissociation Energies in Organic Compounds", CRC Press, 2002.

Medven, Ž.; Güsten, H.; Sabljić, A. Comparative QSAR study on hydroxyl radical reactivity with unsaturated hydrocarbons: PLS versus MLR. *J. Chemometrics*. 1996, *10*, 135-147.

Merga, G.; Schuchmann, H.-P.; Madhava Rao, B.S.; von Sonntag, C. •OH radical-induced oxidation of chlorobenzene in aqueous solution in the absence and presence of oxygen. *J. Chem. Soc., Perkin Trans. 2*, 1996, 1097-1103.

Mezyk, S.P.; Cooper, W.J.; Madden, K.P.; Bartels, D.M. Free radical destruction of N-nitrosodimethylamine in water. *Environ. Sci. Technol*. 2004, *38*, 3161-3167.

Mezyk, S.P.; Ewing, D.B.; Kiddle, J.J.; Madden, K.P. Kinetics and mechanisms of the reactions of hydroxyl radicals and hydrated electrons with nitrosamines and nitramines in water. *J. Phy. Chem.* A. 2006, *110*, 4732-4737.

Monod, A.; Poulain, L.; Grubert, S.; Voisin, D.; Wortham, H. Kinetics of OH-initiated oxidation of oxygenated organic compounds in the aqueous phase: new rate constants, structure-activity relationships and atmospheric implications. *Atmos. Environ*. 2005, *39*, 7667-7688.

Mvula, E.; Schuchmann, M.N.; von Sonntag, C. Reaction of phenol-OH-adduct radicals. Phenoxyl radical formation by water elimination vs. oxidation by dioxygen. *J. Chem. Soc., Perkin Trans. 2*, 2001, 264-268.

Öberg, T. A QSAR for the hydroxyl radical reaction rate constant: validation, domain of application, and prediction. *Atmos. Environ*. 2005, *39*, 2189-2200.

Peeters, J.; Boullart, W.; Pultau, V.; Vandenberk, S.; Vereecken, L. Structure-activity relationship for the addition of OH to (poly)alkenes: site-specific and total rate constants. *J. Phy. Chem. A*. 2007, *111*, 1618-1631.

Percival, C.J.; Marston, G.; Wayne, R.P. Correlations between rate parameters and calculated molecular properties in the reactions of the hydroxyl radical with hydrofluorocarbons. *Atmos. Environ*. 1995, *29*(3), 305-311.

Persico, M.; Granucci, G. Photochemistry in condensed phase. In "Continuum Solvation Models in Chemical Physics." Mennucci, B.; Cammi, R. 2007, John Wiley & Sons. Ltd. England.

Raghavan, N.V.; Steenken, S. Electrophilic reaction of the OH radical with phenol. Determination of the distribution of isomeric dihydroxycyclohexadienyl radicals. *J. Am. Chem. Soc*. 1980, *102*(10), 3495-3499.

Razavi, B.; Song, W.; Cooper, W.J.; Greaves, J.; Jeong, J. Free-radical-induced oxidative and reductive degradation of fibrate pharmaceuticals: Kinetic studies and degradation mechanisms. *J. Phys. Chem. A*. 2009, *113*, 1287-1294.

Rosenfeldt, E.J.; Linden, K.G. Degradation of endocrine disrupting chemicals bisphenol A, ethinyl estradiol, and estradiol during UV photolysis and advanced oxidation processes. *Environ. Sci. Technol*. 2004, *38*, 5476-5483.

Schuchmann H-P.; von Sonntag, C. Photolysis at 185 nm of dimethyl ether in aqueous solution: involvement of the hydroxymethyl radical. *J. Photochem*. 1981, *16*, 289-295.

Singleton, D.L.; Cvetanović, R.J. Temperature dependence of the reactions oxygen atoms with olefins. *J.Am.Chem.Soc*. 1976, *98*, 6812-6819.

Solar, S.; Getoff, N.; Sehested, K.; Holcman, J. Pulse radiolysis of pyridine and methylphyridines in aqueous solutions. *Radiat. Phys. Chem*. 1993, *41*(6), 825-834.

Stefan, M.I.; Hoy, A.R.; Bolton, J.R. Kinetics and mechanisms of the degradation and mineralization of acetone in dilute aqueous solution sensitized by the UV photolysis of hydrogen peroxide. *Environ. Sic. Technol*. 1996, *30*, 2382-2390.

U.S. Environmental Protection Agency. AOPWIN. v1.91, 2000.

U.S. EPA. Office of the Administrator Science Advisory Board. Science Advisory Board (SAB) Review of the Estimation Programs Interface Suite (EPI Suite^{TM}), 20460, 2007.

University of Notre Dame, The Radiation Chemistry Data Center (RCDC), http://www.rad.nd.edu/rcdc/index.html (accessed June 12, 2009).

Vassilev, P.L., M.J.; Baerends, E.J., Hydroxyl radical and hydroxide ion in liquid water: A comparative electron density functional theory study. *J. Phys. Chem. B*. 2005. *109*, 23605-23610.

Villá, J.; González-Lafont, A.; Lluch, J.M.; Corchado, J.C.; Espinosa-García, J. Understanding the activation energy trends for the $C_2H_4 + OH \rightarrow C_2H_4OH$ reaction by using canonical variational transition state theory. *J.Chem.Phys*. 1997, 107(*18*), 7266-7274.

Wang, Y-n.; Chen, J.; Li, X.; Wang, B.; Cai, X.; Huang, L. Predicting rate constants of hydroxyl radical reactions with organic pollutants: Algorithm, validation, applicability domain, and mechanistic interpretation. *Atmos. Environ*. 2009, *43*, 1131-1135.

Westerhoff, P.; Yoon, Y.; Snyder, S.; Wert, E. Fate of endocrine-disruptor, pharmaceutical, and personal care product chemicals during simulated drinking water treatment processes. *Environ. Sci. Technol*. 2005, *39*, 6649-6663.

CHAPETER 3

Linear Free Energy Relationships between Aqueous Phase Hydroxyl Radical Reaction Rate Constants and Free Energy of Activation

†*work from this chapter will be presented and plan to be published in the following citation:*

Minakata, D.; Crittenden, J. Quantitative Understanding of Advanced Oxidation Processes for the Treatment of Emerging Contaminants**.** IWA World Water Congress & Exhibition. Montreal, Canada, September 19-24, 2010.

Minakata, D.; Li, K.; Crittenden, J.C. Rational Design of Advanced Oxidation Processes using Computational Chemistry. The 16th International Conference on Advanced Oxidation Technologies for Treatment of Water, Air and Soil (AOTs-16). Novermber 15-18, 2010. San Diego, California.

Minakata, D.; Crittenden, J. Linear Free Energy Relationships between the Aqueous Phase Hydroxyl Radical (HO•) Reaction Rate Constants and the Free Energy of Activation. *Environ. Sci. & Technol*. Submitted.

3.1 Abstract

Hydroxyl radical (HO•) is a strong oxidant that reacts with electron-rich sites on organic compounds and initiates complex radical chain reactions in aqueous phase advanced oxidation processes (AOPs). For mechanistic modeling, we need to develop a method that can predict reaction rate constants. Previously, we reported a reaction pathway generator that can enumerate the most important elementary reactions. In this study, we develop linear free energy relationships (LFERs) between aqueous phase literature-reported HO• reaction rate constants and theoretically calculated free energies of activation. The theoretical method uses *Ab initio* quantum mechanical calculations for gas phase reactions and solvation methods to estimate the impact of water. The aim of this study is to develop LFERs for H-atom abstraction from a C-H bond and HO• addition to alkenes. This approach may be applied to other reaction mechanisms to establish a library of rate constant predictions for mechanistic modeling of AOPs.

3.2 Introduction

The hydroxyl radical (HO•) is a reactive electrophile that reacts rapidly and nonselectively with most electron-rich sites on organic contaminants. It is the active species that potentially leads to complete mineralization of emerging contaminants in advanced oxidation processes (AOPs) (e.g., O_3/H_2O_2, UV/H_2O_2, UV/TiO_2) and natural waters (Westerhoff et al., 2005; Huber et al., 2003; Rosenfeldt and Linden, 2004). Concerns regarding emerging contaminants (Richardson, 2009) and the many chemicals that are in use or production (CAS, 2009) necessitate mechanistic modeling (Pfaendtner and Broadbelt, 2008) that can quickly assess their removal by AOPs.

A mechanistic model to evaluate performance in AOPs includes three critical components: (1) numerical methods that solve ordinary differential equations (ODEs), (2)

algorithms that can predict reaction pathways, and (3) algorithms that can predict reaction rate constants. The DGEAR algorithm (Hindmarsh and Gear, 1974) was successfully used to solve the ODEs for UV/H_2O_2 kinetic models (Li et al., 2008; 2007; 2004; Crittenden et al., 1999). A model that generates reaction pathways for aqueous phase AOPs has also been developed (Li and Crittenden, 2009). A group contribution method (GCM) recently has been developed (Minakata et al., 2009) to predict aqueous phase HO• reaction rate constants for compounds with a wide range of functional groups. The GCM calibrated 55 group rate constants and 80 group contribution factors with 310 compounds and predicted 124 compounds. It showed that 83% (257 rate constants) and 62% (77 rate constants) of the rate constants from calibrations and predictions were within 0.5 to 2.0 times the experimental values.

The GCM was shown to predict the rate constants for compounds with a wide range of functional groups. Nevertheless, certain assumptions and factors limit the use of the GCM. Essentially, the GCM can only deal with molecules for which all required group rate constants and group contribution factors have been calibrated before. As a result, for more minor functional groups and compounds with limited experimental rate constants, the GCM suffers from the parameters that do not represent comprehensive abiliy of functional groups. Table 3.1 summarizes number of literature-reported experimental rate constants for the reactions that are appeared in AOPs.

Table 3.1: Number of available experimental rate constants in the aqueous phase AOPs on the basis of the extensive literature review

Reaction mechanisms	Genetic representations of reaction mechanisms	Compound groups	Experimental k	Exp. Free energy of solvation of compounds	Arrehenius parameters, E_a and A
H-atom abstraction	$CHR_3 + HO\bullet \rightarrow \bullet CR_3 + H_2O$	Hydrocarbons (alkanes)	12	10	0
		Oxygenated compounds (Alcohols, Diol, Ether, Ester, Aldehyde, Ketone, Carboxylic)	122	15	39
		Alkyl halides	52	7	0
HO• addition to alkenes	$R_2C{=}CR'_2 + HO\bullet \rightarrow R_2(HO)C\text{-}\bullet CR'_2$	Unsaturated alkenes	21	n.a.	0
O_2 addition	$\bullet CR_3 + O_2 \rightarrow \bullet OOCR_3$	Alkyl carbon centered radicals (Aliphatic)	34	n.a.	1
β-scission and 1,2-H shift	$R\text{-}C(O)O\bullet \rightarrow R\bullet + CO_2$ $CR_3CR'_2O\bullet \rightarrow \bullet CR_3 + R'_2C{=}O$ $HR_2CO\bullet \rightarrow \bullet C(OH)R_2 + R_2C{=}O$	Alkyl oxyl radicals (Aliphatics)	<5	n.a.	-
Formation of tetroxide	$R_3COO\bullet + \bullet OOCR'_3 \rightarrow R_3COOOOCR'_3$	Alkyl peroxyl radical (Aliphatics)	10	n.a.	-
Peroxyl radical reaction mechanisms	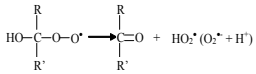	Uni-molecular decay (Elimination of $HO_2\bullet$-/$O_2\bullet$-)	12	n.a.	5
	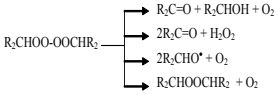	Bi-molecular	-	n.a.	-
Hydrolysis (aldehyde)	$R\text{-}CHO \rightarrow R\text{-}CH(OH)_2 \rightarrow RC\bullet(OH)_2 \rightarrow R\text{-}(OH)_2C\text{-}OO\bullet \rightarrow R\text{-}COOH$	Aliphatic compounds	a.v.	a.v.	-

*R, R'=alkyl or H; n.a. = not available; "-" = not clear; a.v.=available

According to Table 3.1, there are only limited number of rate constants that are available for the reaction mechanisms other than the HO• involving reaction mechanisms. In addition, because the GCM assumes that a functional group has approximately the same interaction properties under a given molecule, it disregards the changes of the functional group properties that can arise from the intramolecular environment by electronic push-pull effects, or by intramolecular hydrogen bond formation, or by steric effects. It is expected that these intramolecular electron-interactions might be very different between the gaseous and aqueous phases and, therefore, solvation effect that results from the surrounding water molecules should be considered for the aqueous phase reactions. Accordingly, there is a need to develop more robust approaches to consider the effect of

both intramolecular electron interactions and solvation for the aqueous phase (Klamt, 2005; Cohen, 1991).

Quantum mechanics is very attractive for investigation of electronic behavior for different functional groups. Quantum mechanical methods have proven to reliably reproduce molecular structures (Chen et al., 1993; Montogomery, 1999; Parkinson et al., 1999; Papasavva et al., 1996; DeFrees et al., 1982), vibrational spectroscopy (Pople et al., 1993; Wong, 1996), heats of reaction (Zhong and Bozzelli, 1997; Andzelm and Wimmer, 1992), activation energies (Jursic, 2000; Saeys et al., 2003) and kinetic rate data (Zhang et al., 2000; Zhu et al., 1999; Sheng et al., 2002; Fontana et al., 2001; Maity et al., 1999; Chandra et al., 2000; Gonzalez-Lafont et al., 2001; Masgrau et al., 2001; Louis et al., 2000; Melissas and Truhlar, 1993; Truong and Truhular, 1993; Urata et al., 2003). Due to the increased computational abilities as computers and software tools have improved, quantum chemical approaches have become attractive for examining larger and more complicated chemical systems.

A procedure to calculate the thermochemical properties in the gaseous phase using quantum mechanics has been well-established. Standard statistical mechanical calculations are applied following either Ochterski (2000) or Irikura (1998). The selection of a reasonable computational method and basis set combination is an important factor in quantum mechanical calculations. There is a tradeoff between the computational cost and the accuracy. To our best knowledge, there are little comprehensive studies that explore the computational methods and basis sets on the calculations of thermochemical properties for the reactions in AOPs. For example, the density functional theory (DFT) has been widely accepted to optimize structures of

molecules and radicals for both ground-state and transition state and recognized as the most cost-effective accurate method in quantum calculations. However, Izgorodina et al. (2007) found that all of the DFT methods they examined failed to provide an accurate description of the energetics of the radical reactions as compared with benchmark G3(MP2)-RAD values. While molecular structures are predicted well at lower levels of theories, reaction barriers are often underpredicted with the standard small basis sets like 6-31G(d). To eliminate these errors, high level single point calculations, or a series of them (i.e., multi-point energy calculations), are often done with much larger basis sets or more expensive and accurate methods.

A number of studies in calculating thermochemical properties in the gaseous phase have proved an improvement for calculated energies using multi-point energy calculations (e.g. Gaussian-*n*- series (Pople et al., 1989; Curtiss, 1991; Curtiss et al., 1998) and completely basis set (CBS) (Nyden and Perterson, 1981; Ochterski and Peterson, 1996; Montgomery and Frisch, 1999; 2000) over the expensive coupled-cluster method (e.g. CCST(T)). Table 3.2 summarizes the theoretical studies to examine the thermochemical properties for the gaseous phase reactions of HO• at the transition state. Among these, some studies applied transition state theory (TST) (Eyring et al., 1935; Eyring, 1938) and variational transition state theory (VTST) (Truhlar and Garrett, 1980) to estimate temperature-dependent reaction rate constants. In addition to the HO• induced mechanisms, the cyclization/fission mechanism for the 1,2-H shift in the gaseous phase (George et al., 2000), the gaseous phase beta-scission reactions of peptide-backbone alkoxyl radicals (Wood et al., 2006; 2005), neopentyl radical (Zheng et al., 2005), *n*-butyl radical (Zheng and Blowers, 2007), propyl radical (Zheng and Blowers,

2006), alkoxyl radicals (Rauk et al., 2003; Headlam and Davies, 2002; Fittschen et al., 2000) and peroxyl radical self-reaction [e.g., ethyl peroxyl radical (Sun et al., 2007; Zheng et al., 2005; Boyd et al., 1990)] have been theoretically studied.

Table 3.2: Summary of theoretical studies about the gaseous phase reactions of HO•

Compounds	Methods*	References
CH4, C2H6, 2-C3H8, 3-C4H10	G2, G2(MP2)	Aliagas and Gronert, 1998
CH4, CH3F, CH2F2, CHF3	B3LYP/6-311G(2d,2p)//B3LYP/6-311G(2d,2p)	Jursic 1996
CH4	CBS-Q	Jursic 2000
CH4	QCISD/cc-pVTZ//MP2/adj-cc-pVTZ	Melissas and Truhlar, 1993
Hydrocarbons C1 to C10	CBS-QB3, MPW1K/6-31G(d)	Saeys et al., 2003
H2COO•	CCSD(T)/aug-cc-pVTZ//B3LYP/6-311+G(2df,2p)	Mansergas and Anglada, 2006
	CCSD(T)/aug-cc-pVTZ//QCISD/6-311+G(d,p)	
	CASPT2(17,14)/6-311+G(2df,2p)//CASSCF(11,10)/6-311+G(2df,2p)	
CH3F	QCISD(T)/6-311+G(d,p)//MP2/6-31+G(d,p)	Lien et al 2001
	QCISD(T)/6-311+G(d,p)//MP2/6-311+G(d,p)	
	CCSD(T)/aug-cc-pVTZ//MP2/6-31G(d,p)	
	QCISD(T)/6-311++G(3df,3pd)//MP2/6-311+G(d,p)	
CF3CH2CH3	mPW1B95-41.0/6-31+G(d,p)	González-Lafont et al., 2008
CHF3	mPW1PW91X/6-31+G(d,p), B1B95X/6-31+G(d,p), mPW1B95X/6-31+G(d,p)	Abu and Swaminathan 2007
CH2F2	QCISD(T)/6-311++G(2df,p)//QCISD/6-311G(d,p)	Gonzalez-Lafont et al., 2001
CH3CH2F, CH2FCH3	G2, G2(MP2)	Sekuăk et al., 1996
CH3F, CH3Cl, CH3Br	PMP4(SDTQ)/6-311G(3df,2p)//UMP2/6-311G(2d,2p)	Louis et al., 2000
CH2F2, CH2FCl, CH2ClBr, CH2Br2	PMP4(SDTQ)/6-311++G(3df,3pd)//UMP2/6-311G(2d,2p)	
CHF3, CHF2Cl, CHF2Br, CHFCl2		
CH3CHF2	MPWB1K/6-31+G(d,p), MPW1K/6-31+G(d,p), MPWB95/6-31+G(d,p)	Taghikhani et al 2005
	MP2/6-311G(d,p), MPWB1K/MG3S//MPWB1K/6-31+G(d,p)	
	MP4SDTQ/aug-cc-pVTZ//MPWB1K/6-31+G(d,p)	
CF3OH	MP2/6-31G(d)//MP2/6-31G(d), MP2/6-311G(d,p)//MP2/6-31G(d)	Brudnik et al., 2001
	MP4/6-31G(d)//MP2/6-31G(d), MP4/6-311G(d,p)//MP2/6-31G(d)	
	QCISD/6-311G(d,p)//MP2/6-31G(d), QCISD(T)/6-311G(d,p)//MP2/6-31G(d)	
	G2MP2, G2	
CF3CH2OH	MC-QCISD//B3LYP/6-311G(d,p)	Wang et al., 2007
	B3LYP/6-311G(d,p)//B3LYP/6-311G(d,p)	
	G3(MP2)//B3LYP/6-311G(d,p)	
CF2HCF2CFH2	G3(MP2)//BB1K/6-31+G(d,p)	Gao et al., 2008
CF3CHFOCH3	G3(MP2)//MP2/6-311G(d,p)	Sun et al., 2009
CHF2CHFOCF3	MC-QCISD//B3LYP/6-311G(d,p)	Yang et al., 2008
CHF2CH2OCF3	MC-QCISD//BB1K/6-31+G(d,p)	
CF3CH2OCHF2	G3(MP2)	Yang et al., 2007
CH3Cl	MP(full)/6-311G(2df,2p)//MP(full)/6-311G(d,p)	Chandra and Uchimaru, 2000
	QCISD(T)/6-311G(2df,2p)//MP(full)/6-311G(d,p)	
CH2CCl2	G3(MP2)	Yamada et al., 2001
CH2CCl2	CBS-Q	
CH3CHFCH3	MC-QCISD-3//B3LYP/6-311G(d,p)	Wang et al., 2007
CH3Br	CCSD(T,full)/cc-pVTZ//MP2(full)cc-pVTZ	Tzima et al 2006
C2H5Br	CCSD(T)/6-311++G(2df,2p)//MP2/6-31G(d)	Martinez-Avilés et al., 2007
	CCSD(T)/6-311G(2d,2p)//MP2/6-31G(d)	
	MP2/6-31G(d)//MP2/6-31G(d)	
CH2Br2	PMP4(SDTQ)/6-311++G(3df,3pd)//UMP2/6-311G(2d,2p)	Louis et al., 2000
BrCH2CH2CH3	CCSD(T)/6-311++G(2df,2p)/MP2/6-31G(d)	Murtinez-Aviles et al., 2008
CH3CH2I	UHF/AM1	Maity and Mohan 2001
CH3CHO, CCl3CHO, CF3CHO		
CF3CHO, CH2ClCHO, CHCl2CHO	MNDO, AM1, PM3	Rayez et al., 1993
CH3OH	QCISD(T)/CBS//B3LYP/6-311++G(d,p)	Jasper et al., 2007
CH3OH	G2	Jodkowski et al., 1999
CH3OH	CCSD(T)/6-311+G(d,p)//B3LYP/6-311G(d,p)	Zhang et al., 2002
CH3OH, C2H5OH	CCSD(T)/6-311+G(3df,2p)//MP2/6-311+G(3df,2p)	Xu and Lin, 2007
CH3OH, C2H5OH	MP4SDQ/6-311G(d,p)	Pardo et al., 1999
HCHO	MP4(SDTQ)/6-311++G(3df,3pd)//MP2/6-311++G(d,p)	
CH3OCHO	MP2/6-31G(d)//MP2/6-31G(d)	Good et al., 1999
HCOOH	PMP2/6-311++G(2d,2p)//MP2/6-311++G(2d,1p)	Galano et al.,
HCOOH	CCSD(T)/aug-cc-pVTZ//QCISD/6-311+G(2df,2p)	Anglada
	CCSD(T)/aug-cc-pVTZ//QCISD/6-311+G(2df,2p)	
HCOOH, CH3COOH	CBS-QB3	
CH3COOH	G2M(CC,MP2)//B3LYP/6-311++G(2df,2pd)	Vimal and Stevens, 2006
CH3COOH	B3LYP/6-31G(d5d,p)//MP2/6-311++G(2df,2pd)	Smedt et al., 2005
	B3LYP/6-311++G(2df,2pd)MP2/6-311++G(2df,2pd)	
	CCSD(T)/aug-cc-pVDZ//MP2/6-311++G(2df,2pd)	
	G2M(CC,MP2)//MP2/6-311++G(2df,2pd)	
C4H9COOH	CBS-QB3, QCISD/6-311++G(d,p)	Sun et al., 2009
CH3C(O)OCH3	MC-QCISD//MP2/6-311G(d,p)	Yang et al., 2008
(CH3)3COCH3	MP2/6-31G(d,p)//MP2/6-31G(d,p), PMP2/6-31G(d,p)//MP2/6-31G(d,p)	Atadinc et al 2002
CH3OCH3	MP2/6-31G(d,p)//MP2/6-31(d,p), PMP2/6-31G(d,p)//MP2/6-31G(d,p)	
	MP4/6-311G(3df,2p)//MP2/6-31G(d,p), PMP4/6-311G(3df,2p)//MP2/6-31G(d,p)	
	CCSD(T)/6-311++G(d,p)//MP2/6-31G(d,p)	
CH3C(O)CH3	B3LYP++(2d,2p)	Davis et al 2005
CH3COCHO	G3X	Baeza-Romero et al 2007
HOCH2C(O)CH3	CCSD(T)/6-311++G(d,p)//BHandHLYP/6-311++G(d,p)	Galano 2006
CH3SH, C2H5SH, n-C3H7SH	CCSD(T)/6-311++G(d,p)//BHandHLYP/6-311++G(2d,2p)	Cruz-Torres and Galano, 2007
(CH3)2SO	mPW1PW91/6-311G(d,p)//PMP2/6-311G(d,p) or B3LYP/6-311G(d,p)	
	mPW1PW91/6-311G(df,p), mPW1PW91/6-311++G(d,p), mPW1PW91/6-311++G(df,p)	
	BHandHLYP/6-311G(d,p), BHandHLYP/6-311G(df,p)	
	BHandHLYP/6-311++G(d,p), BHandHLYP/6-311++G(df,p)	
(CH3)2S	MP2/6-311++G(3df,3pd)	Aloisio 2006
CH3SCH2CH3	MP4(SDTQ)/6-311+G(3df,2p)//MP2/6-31+G(2d,p)	
	QCISD(T)/6-311+G(3df,2p)//MP2/6-31+G(2d,p)	
	CCSD(T)/6-311+G(3df,2p)//MP2/6-31+G(2d,p)	
CH3-S-CH3	MP2/6-311++G(3df,3dp)	
CH3NHC(O)OCH3	BMC-CCSD//MP2/6-311+G(d,p)	Zhang et al., 2008
	MC-QCISD/3//MP2/6-311+G(d,p)	
	G3MP2//MP2/6-311+G(d,p)	
	QCISD(T)/6-311+G(2df,2p)//MP2/6-311+G(d,p)	
HCN, CH3CN	CCSD(T)/6-311++G(2d,2p)//BHandHLYP/6-311++G(2d,2p)	Galano 2007
toluene	CCSD(T)/6-311++G(d,p)//BHandHLYP/6-311++G(d,p)	Uc et al 2006
m-xylene	B3LYP/6-31G(d,p)//B3LYP/6-31G(d,p)	Fan and Zhang, 2008
Toluene 1,2-epoxide/2-methyloxepin	B3LYP/6-31G(d,p), B3LYP/6-311G(2df,2p), BHandHLYP/6-31G(d,p)	Cartas-Rosado and Castro, 2007

** method for energy calculation/basisset for energy calculation//method for geometry optimization/basis set for geometry optimization*

Although many studies focused on individual compounds, few studies explored comprehensive relationships between computationally obtained molecular or reaction energies and observed reaction rate constants for the prediction. A William Green's group developed new group additivity values (GAV) for transition-state-specific moieties for H-abstraction from alkanes by H and CH_3 radicals on the basis of the quantum mechanically calculated heats of formation, entropies, and heat of capacity values (Sumathi et al., 2001a). In their series of papers, they developed procedures for H-abstraction from alkenes, alkyl, alcohols, aldehydes, and acids by H-atoms, HO• addition, and isomerization reactions (Sumathi et al., 2001b). In addition, they presented the qualitative justification for partitioning the energy of the transition structure into contributions from unreactive and reactive moieties using atoms in molecule (AIM) analysis (Sumathi et al., 2002). Méreau et al (2000) built predictive structure-activity relationships (QSARs) on the basis of the kinetic and thermodynamic parameters obtained by using computational chemistry and transition state theory for the decomposition reactions of alkoxyl radicals and extrapolated to larger alkoxyl radicals. A Thanh Truong's group has developed a reaction class transition state theory hypothesizing that the reactions in the same class share similarities in the shape of the potential energy surfaces along the reaction path (Truong et al., 1999). Their method has been extended to H-atom abstraction by $\bullet CH_3$ with alkane (Kungwan and Truong, 2005), reaction of •CHO with alkane (Huynh and Truong, 2007), H-atom abstraction by H• with alkane (Truong, 2000) and by HO• with alkane (Huynh et al., 2006) and addition of HO• to alkene (Huynh et al., 2008). Pfaendtner and Broadbelt (2008) established a library of kinetic correlations that are suitable for the computer-based mechanistic modeling of

condensed-phase autoxidation of hydrocarbons. The Evans-Polanyi relationship related experimentally obtained Arrhenius activation energy (E_a) with quantum mechanically calculated enthalpies of reactions ($\Delta H^{\neq}$). They successfully captured the different reactivity trends for 17 different reaction families. However, the rate constants that result from the kinetics depend not only enthalpies but also entropic contribution, in particular for the solution phase. The significant contribution of the entropy that arises from the vibrational origin has been discovered for H-atom abstraction and proton-coupled electron-transfer (Mader et al., 2007). As a consequence, the free energy of activation ($\Delta G^{\neq}$) should be considered for the thermodynamic parameters.

In contrast to the gaseous phase reactions, only a few studies have been conducted theoretically for the aqueous phase reactions due to the complexities and difficulties in the solvation contribution to quantum mechanics. There are two major ways to model reactions in the aqueous phase, including an explicit model or using an implicit model. The explicit representation of the aqueous phase involves a large number of degrees of freedom, thereby having a high dimensionality (Ayala and Schlegel, 1997). As a result, a solute molecule must be treated averagely over these degrees of freedom. Monte Carlo (MC) simulation or Molecular Dynamics (MD) can be used to average energies over a sufficiently long time frame or to choose configurations of the system randomly with the averaged thermodynamic properties, respectively. The MC and MD approaches would be appropriate when dealing with a larger molecule in the aqueous phase, e.g., protein (Eisenberg and McLachlan, 1986). However there are uncertainties to represent solvent molecules (Marenich et al., 2008).

In the implicit model, the solvent is implicitly expressed as a continuum solvent. The implicit model has two main advantages over the explicit model: 1) it reduces the degrees of freedom by assuming the aqueous phase as a continuum medium and 2) it provides an accurate way to deal with electrostatic forces such as electronic polarization that dominates most solvation processes (Cramer and Truhlar, 1999). As a result of the continuum medium, computational demand is significantly reduced because the size of the electronic structure problem is essentially the same as in the gaseous phase (Cramer and Truhlar, 2008). For example, phenol (Bonin et al., 2007), benzene (DeMatteo et al., 2005), quinoline (Nicolaescu et al., 2005), azacytosines (Pramod et al., 2006) and amino acid (Štefanić et al., 2009) have been examined using the polarizable continuum model (PCM). There are few studies examined computationally for other reaction mechanisms such as beta-fragmentation of aminyl radial from amino acids (Bonifačić et al., 2000). However, these studies were limited to examining the potential energy differences of the reactions and products and few studies accounted the activation energy at the transition state. Ashcraft et al (2007) addressed the use of computational chemistry calculations for the estimation of physical properties and constants in solution by connecting between the pseudochemcial potential of Ben-Naim (Ben-Naim, 1987; 2006) and the traditional standard state-based thermochemistry. This work seems to be the most sophisticated application of computational chemistry to the solution phase up to date. However, for the reaction phases, there are almost no studies concerned with the AOP related reactions in the aqueous phase.

The electron densities on frontier orbitals of atoms provide useful means for the characterization of electron donor/acceptor interactions between molecules. According to

the frontier electron reactivity theory (Fukui et al., 1952), the majority of chemical reactions take place at the position and in the direction where the overlapping of the highest occupied molecular orbital (HOMO) and lowest unoccupied molecular orbital (LUMO) of the respective reactants is at maximum. While the HOMO energy characterizes the susceptibility of the molecule toward the attack by electrophiles, the LUMO energy features the susceptibility of the molecule toward the attack by nucleophiles. It has been anticipated that the energy gap between HOMO and LUMO could be related to the chemical stability of compounds. Larger HOMO-LUMO gaps are considered to be indicators of higher stability of compounds toward chemical reactions. For the H-atom abstraction reaction by HO•, a strong correlation between HOMO energy and the logarithms of the HO• rate constants in the gaseous phase was observed (Pfrang et al., 2006a, b; King et al., 1999; Bartolorri and Edney, 1994; Cooper et al., 1992). Yet, in the aqueous phase, only a few papers have examined the correlation of the HOMO-LUMO with the reaction rate constants in water treatment applications (e.g., O_3 reactions, Hu et al., 2000).

Figure 3.1 represents the correlations between the logarithm of a total of 477 aqueous phase HO• rate constants and the energy gap between HOMO and singly occupied molecular orbital (SOMO) of HO• (i.e., -1.83 eV, Schuiz et al., 1982). It is noted that the SOMO is used to represent the HO• reactivity of electrophile in stead of LUMO. The energies were calculated using the semi-empirical AM1 method (Dewar et al., 1985) with the HyperChem software. As a result, it is found that there is little clear correlation except for the H-atom abstraction from alkanes by HO•. Although the distribution of energy gap is close to each other for the same functional group, this

correlation is not quantitative enough to be useful for predicting the reaction rate constants for unknown compounds. In addition, the correlation of this energy gap neglects the electronic reorganization of the transition state, and therefore, may lead to quantitatively incorrect results. As a result, orbital energy that has been used for a number of organic compounds cannot be used for the aqueous phase HO• radical rate constant estimation. Appendix D includes all calculated data.

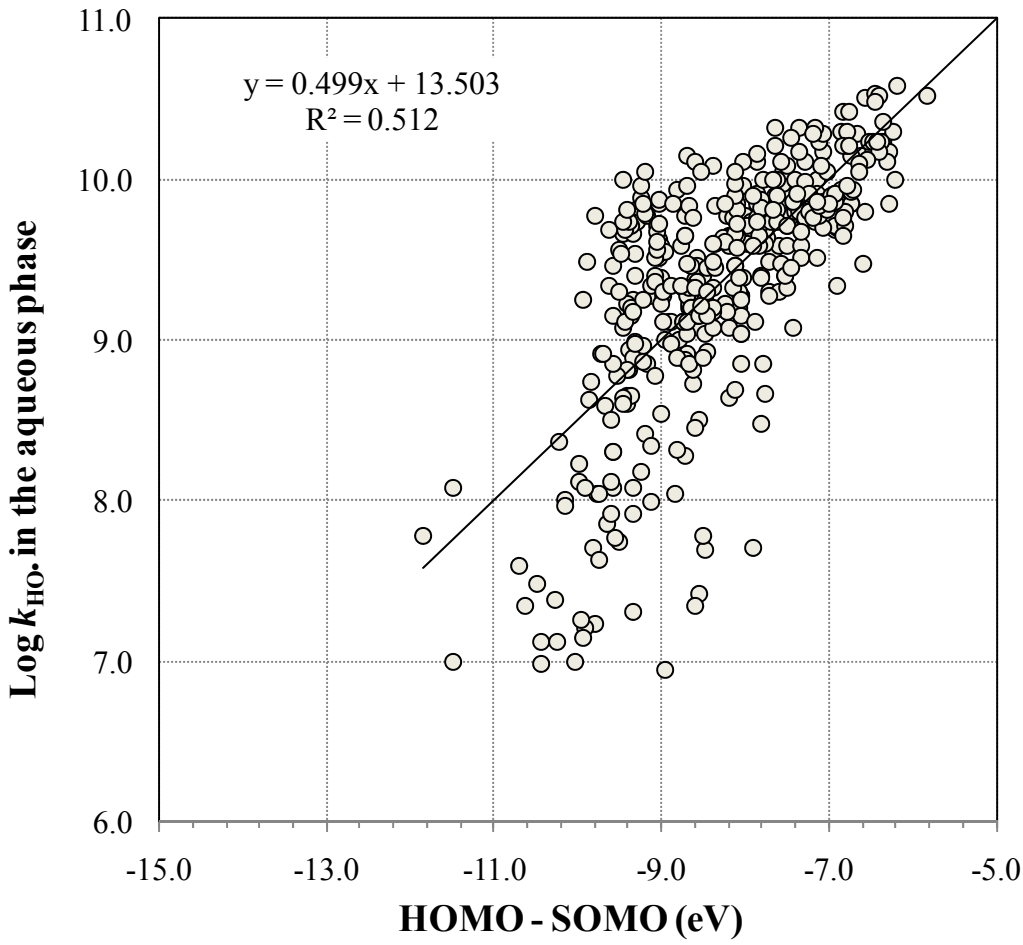

Figure 3.1: Relationship between the logarithm of aqueous phase $k_{HO\bullet}$ and calculated energy gap of HOMO-SOMO for 477 compounds.

In this study, we will develop linear free energy relationships (LFERs) that relate literature-reported experimental HO• reaction rate constants with theoretically calculated aqueous phase free energies of activation for two reaction mechanisms: H-atom abstraction from a C-H bond by HO•, and HO• addition to alkenes. We will compare the free energies of activation to estimates from literature-reported experimental values. Quantum mechanical approaches for calculating the free energy of activation will be explored herein.

3.3 Linear Free Energy Relationships

In this section, we will establish LFERs that bridge kinetics and thermochemical properties. The kinetic information is literature-reported experimental HO• reaction rate constants, while the thermochemical properties are theoretically calculated free energies of activation. The next section describes the theoretical methods in detail.

According to the LFERs, the log of the rate constant and the log of the equilibrium constant should be linearly related (Brezonik, 2002). Transition state theory (TST) (Eyring et al., 1935) states that the log of the rate constant and the free energy of activation are linearly related. For the same reaction mechanisms, the free energies of activation and the rate constants for an arbitrary and a reference reaction are related by equation (3.1):

$$\log_{10} k_{\mathrm{I}} - \log_{10} k_{\mathrm{R}} = -\rho\left(\Delta G^{\mathrm{act}}_{\mathrm{rxn,I}} - \Delta G^{\mathrm{act}}_{\mathrm{rxn,R}}\right) + \sigma \tag{3.1}$$

where k_{I} and k_{R} are the reaction rate constants, $\mathrm{M^{-1}s^{-1}}$, for an arbitrary reaction, I, and a reference reaction, R, respectively; ρ denotes coefficients for the difference in the free energy of activation; σ is a constant; and $\Delta G^{\mathrm{act}}_{\mathrm{rxn,I}}$ and $\Delta G^{\mathrm{act}}_{\mathrm{rxn,R}}$ are the free energies of activation, kcal/mol, (Pu et al., 2006) for reactions I and R, respectively. Figure 3.2 plots

the logarithms of literature-reported HO• rate constants versus $\Delta G^{\text{act}}_{\text{rxn}}$. The reaction of HO• with CH_4 was selected as the reference. $\Delta G^{\text{act}}_{\text{rxn}}$ was estimated from the experimentally obtained E_a values and frequency factors provided in the literature (Ervens, et al., 2003; Elliot and McCracken, 1989; Monod et al., 2005; Chin and Wine, 1994; Gligorovski and Herrmann, 2004; Herrmann, 2003).

The theoretically calculated free energy of activation in the aqueous phase, $\Delta G^{\neq}_{\text{rxn,aq}}$, which is defined as a quasithermodynamic molar free energy of activation (Pu et al., 2006) at a given temperature *T,* is given by

$$\Delta G^{\neq}_{\text{rxn,aq}} = G^{\neq}_{\text{aq}} - G_{\text{reactants,aq}} \tag{3.2}$$

where $G^{\neq}_{\text{aq}}$ is a quasithermodynamic quantity, kcal/mol, that indicates the free energy of the transition state, and $G_{\text{reactants,aq}}$ is the molar free energy of reactants, kcal/mol. $\Delta G^{\text{act}}_{\text{rxn}}$ can be related to $\Delta G^{\neq}_{\text{rxn,aq}}$ using the extrathermodynamic contribution to the free energy of activation (Pu et al., 2006), ΔG_{extra}, kcal/mol, as shown in equation (3.3):

$$\Delta G^{\text{act}}_{\text{rxn}} = \Delta G^{\neq}_{\text{rxn,aq}} + \Delta G_{\text{extra}} \tag{3.3}$$

where

$$\Delta G_{\text{extra}} = -RT \ln\gamma(T) \tag{3.4}$$

$\gamma(T)$ is a transmission coefficient that represents the effect of tunneling at temperature *T*. When a hydrogen atom is involved in a reaction, nuclear quantum effects, in particular quantized vibrations and tunneling, become important. Tunneling occurs when some systems pass through the transition state with less than the quantized energy. Because the transition state is a metastable state, it does not have quantized energy levels. To a good approximation, however, all bound modes of a potential energy surface can be assumed to have a quantized energy requirement (Wigner, 1932), and this is validated by accurate

quantum dynamics (Chartfield et al., 1992).

The solvated energy term should consider the interactions of the aqueous phase reactions. Essentially, the free energy of activation in the aqueous phase for a reaction, $\Delta G^{\neq}_{\text{rxn,aq}}$, is the sum of the free energy of solvation (Cramer, 2004), $\Delta\Delta G^{\neq}_{\text{rxn,solvation}}$, and the gaseous phase free energy of activation, $\Delta G^{\neq}_{\text{rxn,gas}}$, as shown below:

$$\Delta G^{\neq}_{\text{rxn,aq}} = \Delta G^{\neq}_{\text{rxn,gas}} + \Delta\Delta G^{\neq}_{\text{rxn,solvation}} \tag{3.5}$$

where $$\Delta\Delta G^{\neq}_{\text{rxn,solvation}} = \left(G^{\neq}_{\text{solvation}} - G^{\neq,0}_{\text{solvation}}\right) - \left(G_{\text{reactants,solvation}} - G^{0}_{\text{reactants,solvation}}\right) \tag{3.6}$$

$\Delta\Delta G^{\neq}_{\text{rxn, solvation}}$ is free energy of solvation, kcal/mol, for a reaction measured with respect to a system composed of the pure, unperturbed aqueous phase at equilibrium and the solute molecule(s) in a separate phase considered to be an ideal gas; $G^{\neq,0}_{\text{solvation}}$ and $G^{0}_{\text{reactants,solvation}}$ are the standard state free energies of solvation for the transition state and reactants, respectively, and $G^{\neq}_{\text{solvation}}$ and $G_{\text{reactants,solvation}}$ are the free energies of solvation that are computed in solution for the transition state and reactants, respectively (Tomasi et al., 2005). The detailed modifications associaed with the change of state are given in the Results and Discussion.

3.4 Computational Methods

For the gaseous phase, *Ab initio* molecular orbital and density functional theory (DFT) calculations were performed using Gaussian03 (Frisch et al., 2003). The Berny geometry optimization algorithm (Schlegel, 1982) optimized the geometry of reactants, complex compounds, and products with a key word of "Opt=Tight." The transition states were found as first-order saddle points on the potential energy surface (PES) using the quadratic synchronous transit method (QST) (Peng and Schlegel, 1993; Peng et al.,

1996). All transition states were verified by a single negative frequency, and some of them were confirmed by obtaining the true reactant(s)/product(s) using the intrinsic reaction coordinate (IRC) (Fukui et al., 1952). Using the optimized geometry and frequencies obtained from a Hessian calculation, the total microcanonical partition function was calculated for each molecule and radical within the rigid-rotor harmonic oscillator assumption. The zero-point vibrational energy (ZPVE) was included in each thermochemical property. A quadratically convergent self-consistent field (SCF) procedure (Bacskay, 1981), SCF=QC, was used for linear searches when far from convergence, and Newton-Raphson steps when close. The harmonic oscillator approximation is known to incorrectly treat low-frequency torsional modes due to internal rotation (Pitzer and Gwinn, 1942). However, the internal rotation correction had a very minor effect on the activation energy, even for molecules with many dihedrals (Pfaendtner and Broadbelt, 2007; Van Cauter et al., 2006). Furthermore, low-frequency vibrational modes contributed little to the vibrational contribution to the internal energy. Therefore, the contribution of anharmonicity from hindered rotors was not included in this study. Basis set superposition error (BSSE) was not considered because 1) the BSSE may not be too large as compared to the accuracy of the transition state calculations, 2) methods for BSSE correction are still controversial, and 3) BSSE corrections by the counterpoise method require additional expensive calculations. The effect of tunneling was included using Wigner's equation (Wigner, 1932).

To calculate the free energy of solvation, three implicit solvation models were used, namely: 1) the conductor-like polarizable continuum model (CPCM) (Cossi et al., 2003; Barone and Cossi, 1998) implemented in Gaussian03 (Frisch et al., 2003), 2) the

solvent model (SM8) (Zhu et al., 1998; Cramer and Truhlar, 1996; Still et all., 1990) implemented in GAMESSPLUS-v2009 (Higashi et al., 1993), and 3) the conductor-like screening model for real solvation (COSMO-RS) (Klamt, 1996, Klamt et al., 1998) implemented in COSMOtherm (Eckert and Klamt, 2006). CPCM defined the cavity using a United Atom Hartree-Fock (UAHF) model (Barone et al., 1997). SM8 used the van der Waals radii in the solvent-accessible surface area (SASA) (Hermann, 1972; Mennucci and Tomashi, 1997) calculation (Marenich et al., 2008). The COSMO approach defines the molecular cavity as the union of all those points that have a smaller relative distance to an atom of the molecule under consideration than to other molecules. The relative distance is defined as the ratio of the distance and the vdW radius of the entire atom. We compared these three solvation models for molecules at the ground state and determined which to use to establish the LFERs. In particular, we decided to use the COSMO-RS model to calculate $\Delta\Delta G^{\neq}_{\text{rxn, solvation}}$. In this process, the gaseous phase geometry was first optimized using DFT and MP2 (Moller and Plesset, 1934) with various basis sets. Because our investigations of the structures of reactants and transition states using the CPCM model showed few structural differences between the gaseous and aqueous phases, the optimized gaseous phase structures were used to calculate $\Delta\Delta G^{\neq}_{\text{rxn, solvation}}$. Second, the cosmo/ccf files that represent the charge distributions of the optimized structures were generated with the single point calculation using RI-DFT with BP-functional and def-TZVP basis set that are implemented in the TURBOMOLE (Ahlrichs et al., 1989) 'calculate' function. Lastly, the cosmo/ccf files were transmitted to COSMOtherm to calculate the chemical potential and partial pressure of a compound in the aqueous phase.

3.5 Results and Discussion

3.5.1 A Comparison of *Ab* initio Quantum Mechanical Methods for HO• + CH4 in the Gaseous Phase

It is important to compare various quantum mechanical methods and basis sets for transition state structure optimization and thermochemical property calculation for H-atom abstraction by HO•. We optimized the transition state structures of CH_4 and HO• using various DFT and MP2 methods and calculated the gaseous phase barrier height using both single point energy calculations and hybrid methods. The barrier height and energy of reaction for each method have been tabulated and compared to the literature-reported values, as shown in Table 3.3 and Figure 3.2.

Table 3.3: A comparison of *Ab initio* quantum mechanical methods for the gaseous phase reaction of HO• with CH_4.

Reaction CH_4 + HO• → •CH_3 + H_2O							
Method and basis set	Barrier height, kcal/mol	ZPE	$\langle S^2 \rangle$	Imaginary frequency	r(C-H), Å	r(O-H), Å	<(HOH)
mp2/6-311++G(3d,3p)//mp2/6-311++G(3d,3p)	6.95	0.051725	0.779599	-1792.6293			
mp2/6-311+G(3df,2p)//MP2(Full)/6-31G(d)	7.29	0.052417	0.785448	-2314.8722	1.22594	1.26893	99.45222
mp2/aug-cc-pVTZ//MP2(Full)/6-31G(d)	6.41	0.052174	0.785466	-2296.2110	1.22594	1.26893	99.45222
B3LYP/6-31++G(d,p)//B3LYP/6-31++G(d,p)	0.48				1.21724	1.32403	100.31456
B3LYP/6-311++G(3df,3pd)//B3LYP/6-31++G(d,p)	0.24						
BHandHLYP/6-31+G(d,p)	8.12	0.052359	0.765306	-1851.8709			
MPWB1K/6-31+G(d,p)	7.12	0.055848	0.752871	-64.7369	1.22086	1.27783	99.90577
M05 2X/6-31+G(d,p)	4.26	0.052074	0.759078	-1183.3195	1.21871	1.30625	100.99250
CBS-QB3	3.76	0.050051	0.756548	-1109.0212	1.23306	1.28573	99.17334
G1	5.65	0.048208	0.784800		1.22597	1.26888	99.45768
G2	6.25	0.048208	0.784807		1.22597	1.26888	99.45768
G2MP2	5.48	0.048208	0.784804		1.22594	1.26893	99.45217
G3	5.45	0.048208	0.761336		1.22594	1.26893	99.45217
G3MP2	6.01	0.048208	0.784807		1.22597	1.26888	99.45770
G3B3	4.43	0.048492	0.757109	-1447.5378	1.27386	1.23835	100.19049
G3MP2B3	4.95	0.050467	0.757115	-1444.3300	1.27326	1.23889	100.15053
QCISD(T)/6-311+G(d,p)//MP2(Full)/6-31G(d)	6.31	0.051093	0.787455	-1618.2755			
CCSD/6-31+G(d,p)//MP2(Full)/6-31G(d)	7.73	0.052108	0.786781	-1781.8067			
CCSD/6-31++G(d,p)//MP2(Full)/6-31G(d)	7.60	0.052014	0.786817	-1778.8191	1.22594	1.26893	99.45222
CCSD/6-311++G(d,p)//MP2(Full)/6-31G(d)	6.66	0.051625	0.787459	-1734.7900			
CCSD(T)/6-31+G(d,p)//MP2(Full)/6-31G(d)	7.82	0.051666	0.786781	-1658.9361			
CCSD(T)/6-311+G(d,p)//MP2(Full)/6-31G(d)	6.52	0.051162	0.787455	-1622.9927			
MCG3/3†	6.35						
MC3BB†	6.11						
MC3MPW†	6.15						
W1‡	6.22						
Exp.*	6.70						

†: *Ellingson et al., 2009;* ‡: *Boese and Martin, 2004;* **Lynch and Truhlar, 2001*

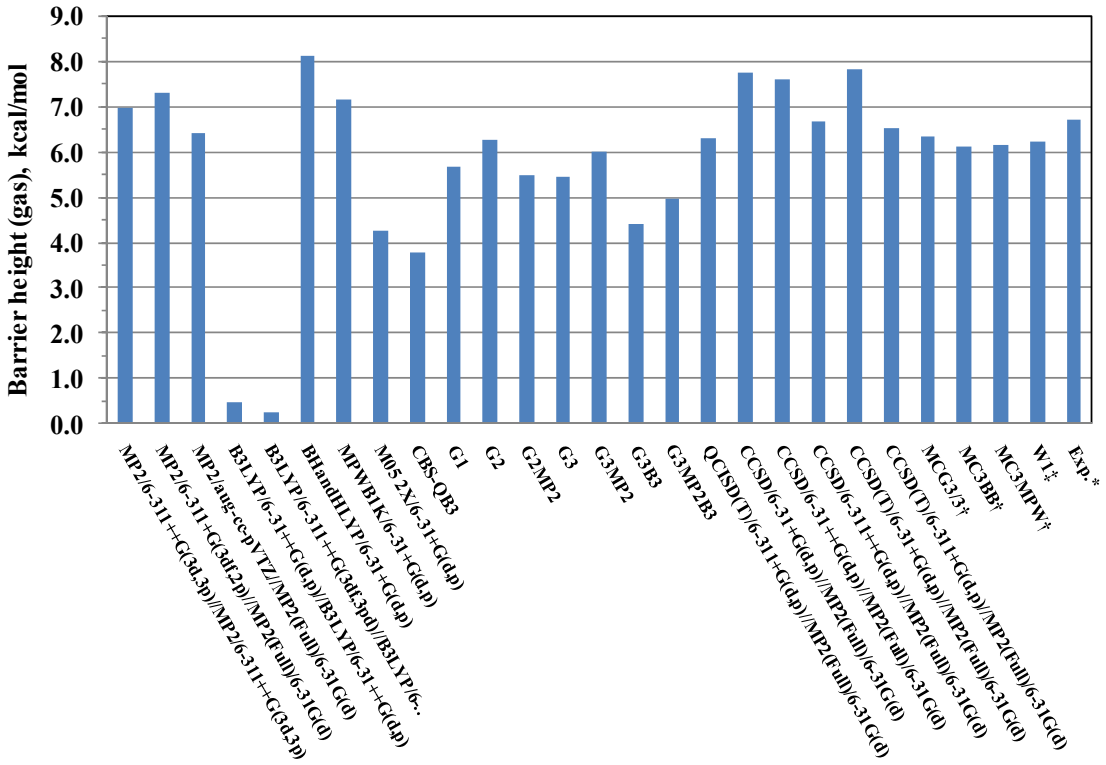

Figure 3.2: A comparison of calculated barrier height for the CH_4 + HO•

The various methods yielded only small differences in the optimized geometry of the transition states. DFT gives a larger angle for H-O-H. The addition of the diffuse function does not change the optimized geometry significantly. Overall, no significant spin contamination was observed. The MP2 methods provide similar barrier heights when different basis sets are used. The augmented correlation-consistent polarized valence triple-ζ sets (Dunning, 1989) are known to give more flexibility when considering electron-electron correlations. As compared to the 6-311+G(3df,2p) basis set, aug-cc-pVTZ provides a smaller barrier height. All values calculated by DFT with the B3LYP basis set (Becke, 1993; Lee et al., 1988) underestimate the barrier height significantly when compared to the values obtained by other methods. This is consistent

with the observation by Izgorodina et al. (2007). In addition, no improvement in the calculated energy was observed when the larger basis set, i.e., 6-311++G(3df,3pd), was used. The barrier heights calculated using the hybrid DFT methods varied based on the type of density functional used. In both of these functionals, the percentage of HF exchange has been parameterized for the calculation of accurate kinetics data (in particular barrier heights and energies of reaction). Nevertheless, for our tested system all hybrid-DFT methods slightly overestimate the barrier height as compared to the literature-reported values (e.g., W1 or the best estimated from the experiment) by approximately 1.0 kcal/mol. A composite method [i.e., CBS-QB3 (Montgomery et al., 1999; 2000); G1 (Pople et al., 1989; Curtiss and Jones, 1990); G2 (Curtiss, 1991) and G3 (Curtiss et al., 1998)] that includes several thermochemical property calculations with higher order corrections slightly underestimates the barrier height when compared to the literature-reported values. The coupled cluster (CC) (Čížek, 1966) with various basis sets gives higher energy values than the literature, but the largest basis set (i.e., 6-311++G(d,p)) provides a similar value to that in the literature. It should be mentioned that the Weizmann theory (Martin and Oliveira, 1999; Parthiban and Martin, 2001) and the CC method (e.g., CCSD(T)) (Purvis and Bartlett, 1982) that is typically used for the high level thermochemical property calculations may not be relevant in our case due to the expensive computational demand. Because we calculate the $\Delta G^{\neq}_{gas}$ using a high level *Ab initio* method for many compounds, the Gaussian-*n*-series should be sufficient.

3.5.2 Verifications of *Ab* initio Quantum Mechanical Methods for the Gaseous Phase HO• Reactions

To verify the Gaussian-*n*-series hybrid methods for different functional groups and atoms, we calculated the barrier heights for representative compounds from different functional groups (i.e., CH_3OH, CH_3CHO, CH_3OCH_3, CH_3COCH_3, CH_3COOH, CH_3F, CH_3Cl and CH_3Br) and compared them with literature-reported values. Table 3.4 summarizes the overall results for these calculations. Most of the calculated barrier heights are within ±2 kcal/mol of the results that are obtained by CCSD(T) and QCISD(T). The G3 hybrid methods underestimate the barrier height. Little difference is observed between the G1 and G2 hybrid methods. However, the G2 method estimates most of the calculated energies lower than does the G1 hybrid method. According to a general performance evaluation of the G2 and G3 methods, the mean absolute deviations (MADs) of the 147 enthalpies of formation calculated in the experiment were 1.56 kcal/mol and 0.94 kcal/mol (Curtiss et al., 1998), respectively. From these verifications, it can be concluded that the G1, G2 and G3 methods should be sufficient to provide highly accurate thermochemical properties within the acceptable computational errors for the gaseous phase reaction of HO• with aliphatic alkanes as well as with oxygenated and halogenated compounds.

Table 3.4: Calculated energy barrier for the gaseous phase reactions of HO• with CH_3OH, CH_3CHO, CH_3OCH_3, CH_3COCH_3, CH_3COOH, CH_3F, CH_3Cl and CH_3Br, and the literature-reported values.

	CH_3OH	CH_3CHO	CH_3OCH_3	CH_3COCH_3	CH_3COOH	CH_3F	CH_3Cl	CH_3Br
G3	0.41	2.84	3.01	2.20	3.76	3.90	3.12	
G3MP2	1.12	3.56	3.70	2.94	2.88	4.57	3.79	
G3B3	1.72	3.22	1.65	2.63	3.78	3.61	0.15	
G3MP2B3	2.68	0.05	2.26	0.15	4.53	4.32	0.17	
G2	2.14	1.02	1.25	0.40	1.97	2.06	1.33	1.77
G1	0.51	3.03	3.09	2.32	3.69	4.14	3.25	3.58
CBS-QB3	0.65	1.34	-0.61	1.40	2.61	2.84	-0.24	
MP2/aug-cc-pVTZ//MP2(Full)/6-31G(d)	2.89	3.96	2.47	3.36	5.16	5.39	4.61	4.50
CCSD(T)/6-311+G(d,p)//MP2(full)/6-31G(d)	1.75	4.54	0.45			5.26	4.08	
QCISD(T)						4.37[e]	4.38[g]	
CCSD(T)	1.0[a]		2.55[b]	3.99[d]		5.1[f]		3.39[h]
best estimate ‡			2.72[c]			2.80-3.06[e]		

a: CCSD(T)/6-311+G(3df,2p)//MP2/6-311+G(3df,2p). Xu and Lin, 2007
b: CCSD(T)/6-311++G(d,p)//MP2/6-31G(d,p). Atadinc et al., 2002
c: Kasai and Meyers, 1959
d: CCSD(T)/6-311G(d,p)//MP2/6-31G(d,p). Henon et al., 2003
e: QCISD(T)/6-311++G(3df,3pd)//MP2/6-311+G(d,p). Lien et al., 2001
f: CCSD(T)/aug-pVTZ//MP2/6-31G(d,p) Espinosa-García et al., 1998
g: QCISD(T)/6-311G(2df,2p)//MP2(full)/6-311G(d,p). Chandra and Uchimaru, 2000
h: CCSD(T,full)/cc-pVTZ//MP2(full)/cc-pVTZ. Tzima et al., 2006
‡: values obtained by fitting to experimental values

3.5.3 A Comparison of Implicit Solvation Models

To compare the performances of implicit solvation models, the free energies of solvation for alkanes as well as oxygenated and halogenated compounds were calculated using three implicit solvation models: 1) CPCM (Cossi et al., 2003; Barone and Cossi, 1998), 2) SM8 (Zhu et al., 1998; Cramer and Truhlar, 1996; Still et all., 1990), and 3) COSMO-RS (Klamt, 1996, Klamt et al., 1998)). The oxygenated compounds included alcohols, ethers, esters, aldehydes, and carbonyl and carboxylic compounds. The calculated free energies of solvation were compared with the literature-reported experimental values (Marenich et al., 2009). In the COSMO-RS approach, the free energy of solvation for a compound, i, $\Delta G^{i}_{\text{solvation, calc}}$, was calculated as corresponding to the partial vapor pressure of each compound (i.e., pure compound vapor pressure times the activity coefficient):

$$\Delta G^{i}_{\text{solvation, calc}} = RT \ln(10) \times [\log_{10} P - \log_{10}(1000)] \tag{3.7}$$

where P is the partial pressure, mbar. If the reference state is 1 bar, the $\log_{10}(1000)$ is the decadic logarithm of 1000 mbar pressure. This procedure was verified by comparing it to the COSMO-RS default method, as shown in equation (3.8):

$$\Delta G^{i}_{\text{solvation, default}} = (\mu^{i}_{\text{gas}} - \mu^{i}_{\text{aq}}) - \text{RT} \ln (\rho_{\text{s}} V^{i}_{\text{gas}} / MW_{\text{aq}}) \tag{3.8}$$

where μ^{i}_{gas} and μ^{i}_{aq} are the chemical potentials of the compound, i, in the ideal gas and aqueous phases, respectively; ρ_{s} is the density of water; V^{i}_{gas} is the molar volume of the ideal gas; and the MW_{aq} is the molecular weight of water. The $\Delta G^{i}_{\text{solvation, calc}}$ was converted into the state at 1 atm of ideal gas and 1 mol of liquid solvent. CPCM calculates the energy values at the ideal gas state, and therefore, a correction factor (Liptak and Shields, 2001) of 1.89 kcal/mol (i.e., $RT \ln(24.47)$) was included to account for a state change from 1 mol/24.47 L (gaseous phase at 298 K) to 1 mol/L (aqueous

phase). SM8 calculates the free energy of solvation at the standard state of 1 atm and 1 mol/L. Figure 3.3 plots the calculated free energies of solvation against the literature-reported experimental values. The sample deviation (SD) calculated in equation (3.9) is 0.79 (N=40) by COSMO-RS, 1.6 (N=38) by CPCM with G3B3 and UAHF radii, and 1.8 (N=39) by SM8 with M06-2X/6-31+G(d,p) and Bondi radii:

$$\mathrm{SD}=\sqrt{\frac{1}{N-1}\sum_{i=1}^{N}\left(\frac{\Delta G^{i}_{\mathrm{solvation,exp}}-\Delta G^{i}_{\mathrm{solvation,calc}}}{\Delta G^{i}_{\mathrm{solvation,exp}}}\right)^{2}} \tag{3.9}$$

where N is the total number of samples, and $G^{i}_{\mathrm{solvation,exp}}$ and $G^{i}_{\mathrm{solvation,calc}}$ are experimental and calculated free energies of solvation for molecule i.

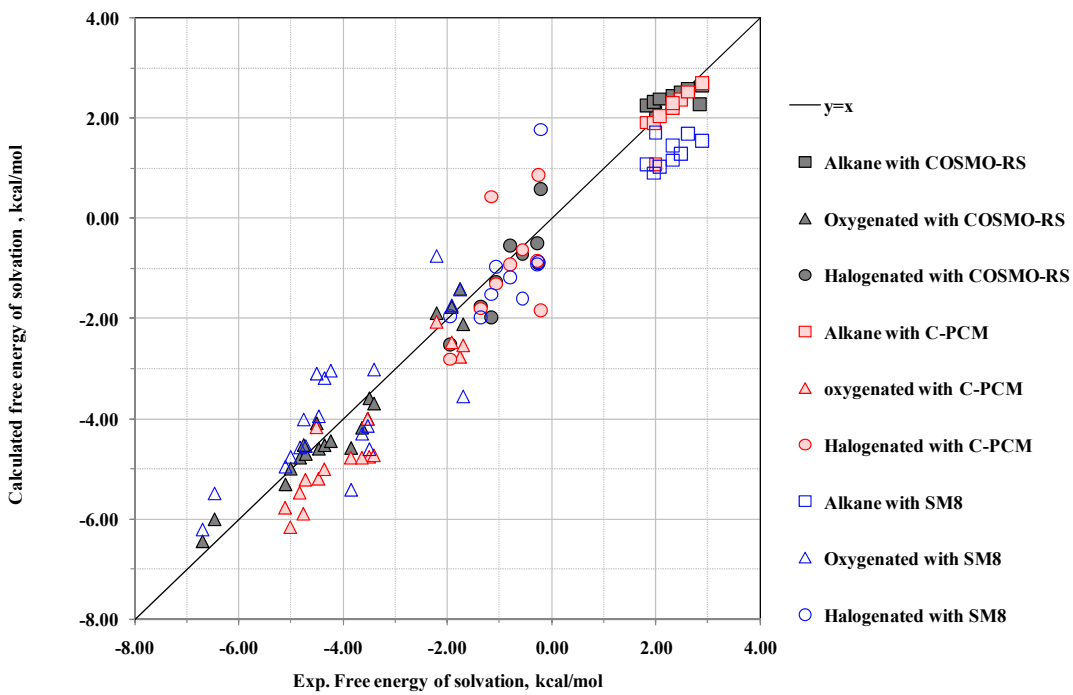

Figure 3.3: A plot of calculated free energy of solvation versus experimental free energy of solvation

COSMO-RS performs slightly better than CPCM and SM8. All solvation methods indicate larger errors as compared to the literature-reported experimental values (Marenich et al., 2009) for the following compounds: CHF_3, CCl_3CH_3 and $CH_3CH_2CH_2Cl$ than the rest of the compounds. For example, the calculated free energy of solvation for CHF_3 is 0.583, -1.840 and 1.768 kcal/mol with COSMO-RS, CPCM and SM8, respectively, as compared to the experimental value, -0.200 kcal/mol (Marenich et al., 2009). For CCl_3CH_3 and $CH_3CH_2CH_2Cl$, we observed a similar inconsistency. Therefore, calculation of the free energy of solvation for halogenated compounds is still limited. If these three compounds were eliminated, the SD values for COSMO-RS, CPCM and SM8 would be 0.19, 0.40 and 0.48, respectively.

In addition to its better performance, COSMO-RS has two major advantages over CPCM and SM8: 1) construction of potential energy operator and 2) the contribution of free energy of solvation. CPCM and SM8 model the surrounding solvent as a homogeneous medium characterized by a bulk permittivity (i.e., $\varepsilon = 78.4$ for water) and electrostatic solute-solvent interactions are treated linearly depending on the solute wave function. COSMO-RS does not assume either homogeneous behavior of the solvent or a linear response of the electrostatic interactions. Whereas CPCM and SM8 consider no change in the association free energy in the solution phase, COSMO-RS includes a temperature-dependent entropic term as well as an enthalpic contribution. Accordingly, the COSMO-RS theory was selected for establishing the LFERs.

3.5.4 Linear Free Energy Relationships between Aqueous Phase Free Energy of Activation and Logarithm of HO• Reaction Rate Constant

In this section, we establish the LFERs between the calculated aqueous phase $\Delta G^{\neq}_{rxn,aq}$ and the literature-reported experimental HO• reaction rate constants that were compiled in a previous study (Minakata et al., 2009). The gaseous phase free energy of activation, $\Delta G^{\neq}_{rxn,gas}$, was calculated using the G1, G2 and G3 methods, and $\Delta\Delta G^{\neq}_{rxn,solvation}$ was calculated using the COSMO-RS theory. $\Delta G^{\neq}_{rxn,gas}$ includes the zero point energy and the chemical potential, $\Delta\mu$, to consider the dissolution contribution of molecule. Among the different possible transition states and conformations of compounds, the lowest energy point was selected for the LFERs. The HO• reactions with methane and ethylene were selected for the reference reactions of H-atom abstraction and HO• addition to alkenes, respectively. Tables 3.5 and 3.6 summarize the calculated $\Delta G^{\neq}_{rxn,aq}$ and ΔG_{extra} values. Appendix E includes the optimized structures and their z-matrices of coordinates.

Table 3.5: Calculated $\Delta G^{\neq}_{rxn\,aq}$, tunneling factor and literature reported HO• reaction rate constants for the H-atom

Molecules * Italic-underline used for prediction	Chemical formula. **H indicates the targetted H-atom for abstraction	$\Delta G^{\neq}_{aq}$					Tunneling			Rate constant		
		G3 with COSMO-RS	G2 with COSMO-RS	G1 with COSMO-RS	Experimental	Estimated from TST	imaginary freq¶, $\nu^{\ddagger}$, cm^{-1} ¶uMP2(full)/6-31G(d)	γ [=1+1/24($h\nu^{\ddagger}$/k BT)^2]	ΔG_{extra} [=-RTln(γ)], kcal/mol	$k_{HO\bullet\,aq}$ exp	log $k_{HO\bullet\,aq}$	Reference of reaction rate constants
CH4	**H**-CH3	4.83	5.63	5.03		7.49	-2277.3876	6.0445	-1.06	1.20E+08	8.08	Getoff 1989
C2H6	**H**-CH2CH3	1.32	-0.42	1.64		5.78	-2037.8351	5.0391	-0.96	1.80E+09	9.26	Hickel, 1975
C3H8	**H**-CH2CH2CH3	2.51	0.75	2.82			-2032.7101	5.0188	-0.95			
	CH3CH-**H**-CH3 (Eclipse)	-0.10	-1.83	0.19		5.23	-1756.9491	4.0024	-0.82	3.60E+09	9.56	Rudakov 1981
	CH3CH-**H**-CH3 (Staggered)	0.20	-1.54	0.50			-1783.7622	4.0947	-0.83			
C4H10	**H**-CH2(CH2)2CH3 (Anti Staggered)	2.78	-4.63	2.67			-2028.0281	5.0003	-0.95			
	CH2CH-**H**-CH2CH3 (Anti Staggered)	1.51	-0.58	1.43		5.08	-1741.0187	3.9482	-0.81	4.60E+09	9.66	Rudakov 1981
C5H12	**H**-CH2(CH2)3CH3 (Anti Staggered)							1.0000	0.00			
	CH3CH-**H**-(CH2)2CH3 (Anti Staggered)	1.05	-0.63	1.34		4.98	-1738.1336	3.9384	-0.81	5.40E+09	9.73	Rudakov 1981
	CH3CH2CH-**H**-CH2CH3 (Anti Staggered)	1.59	-0.03	1.97			-1689.3046	3.7756	-0.79			
CH3CH(CH3)CH3	CH3C-**H**-(CH3)CH3	-1.84	-3.45	-1.78		4.93	-1467.7308	3.0953	-0.67	4.60E+09	9.66	Rudakov 1981
CH3Cl	**H**-CH2Cl	7.08	5.29	7.21		8.02	-2451.4575	6.8451	-1.14	5.50E+07	7.74	Milosavljevic et al., 2005
CHCB	**H-CCB**	**4.36**	**2.19**	**4.35**		**8.08**	**-2557.0942**	**7.3597**	**-1.18**	**5.40E+07**	**7.73**	**Haag and Yao, 1992**
CH2Cl2	**H**-CHCl2	4.11	2.11	4.02		7.76	-2519.5418	7.1743	-1.17	9.00E+07	7.95	Getoff, 1991
CH3CHCl2	CH3C-**H**-Cl2	3.41	1.46	3.48		7.49	-2394.2912	6.5757	-1.11	1.30E+08	8.11	Lat et al, 1988
	H-CH2CHCl2	8.87	7.19	8.99				1.0000	0.00			Milosavljevic et al., 2005
CH3CCl3	**H**-CH2CCl3	8.26	6.55	8.20		7.66	-2417.6716	6.6851	-1.12	1.00E+08	8.00	Getoff 1989
CH2ClCH2Cl	**H**-CHClCH2Cl (trans)	5.31	3.44	5.37		7.17	-2380.9542	6.5137	-1.11	2.20E+08	8.34	Milosavljevic et al., 2005
	H-CHClCH2Cl (cis)	8.21	6.38	8.22		7.17	-2361.6846	6.4248	-1.10	2.20E+08	8.34	
CH2ClCHCl2	**H**-CHClCHCl2	5.63	5.07	6.84			-2480.7342	6.9855	-1.15			
	CH2Cl-**H**-CCl2	5.00	4.35	6.34		7.01	-2429.2225	6.7395	-1.13	3.00E+08	8.48	Milosavljevic et al., 2005
CH3OH	**H**-CH2OH	3.92	2.13	4.03	5.25[a], 5.04[b]	6.15	-2052.4804	5.0973	-0.96	9.70E+08	8.99	Buxton 1988
CH3CH2OH	**H**-CH2CH2OH	2.45	0.73	2.35			-2289.3343	6.0976	-1.07			
	CH3CH-**H**-OH	1.70	-0.13	1.81	4.78 ± 2.87[a], 3.41[c]	5.65	-1837.2812	4.2832	-0.86	1.90E+09	9.28	Buxton 1988
CH3CH(OH)CH3	CH3C-**H**-(OH)CH3	1.85	0.02	1.85	4.54[a]	5.70	-1936.8323	4.6486	-0.91	1.90E+09	9.28	Buxton 1988
	H-CH2CH(OH)CH3	5.78	5.04	6.79			-2312.7695	6.2024	-1.08			
CH3CH2CH2OH	CH2-**H**-(CH2)2OH	5.47	3.78	5.83			-2013.2164	4.9421	-0.95			
	CH3CH-**H**-CH2OH	3.53	1.79	3.41			-2106.9496	5.3177	-0.99			
	CH3CH2CH-**H**-OH	1.09	-0.68	1.21	4.78 ± 4.06[a]	5.38	-1747.6682	3.9707	-0.82	2.80E+09	9.45	Buxton 1988
CH3OCH3	**H**-CH2OCH3	4.74	1.13	3.04		6.10	-1974.9769	4.7937	-0.93	1.00E+09	9.00	Eibenberger 1980
	H-CH2OCH3	5.87	4.48	5.62			-1974.9300	4.7936	-0.93			
CH3COCH3	**H**-CH2COCH3	9.98	8.18	6.50	6.21 ± 4.78[a], 6.30[c]	7.61	-2435.5382	6.7694	-1.13	1.10E+08	8.04	Buxton et al., 1988
HCOOH	**H**-COOH	10.80	4.84	6.68	6.45[a], 6.09[d]	7.73	-2598.6814	7.5682	-1.20	1.00E+08	8.00	Buxton 1988
CH3COOH	**H**-CH2COOH	10.68	8.90	10.61	7.64[a], 6.94[d]	8.70	-2395.7644	6.5825	-1.12	1.70E+07	7.23	Chin and Wine 1994
CH3CH2COOH	**H**-CH2CH2COOH	5.18	3.52	5.48	5.73 ± 3.1[a]	6.91	-2293.2677	6.1151	-1.07	3.20E+08	8.51	Ervens et al., 2002
	CH3-**H**-CHCOOH	8.11	6.45	8.42				1.0000	0.00			
CH3COOCH3	**H**-CH2COOCH3	9.37	7.32	9.18		7.53	-2380.4542	6.5114	-1.11	1.20E+08	8.08	Adams 1965
	CH3COOCH2-**H**	11.37	9.89	11.59			-2449.6606	6.8365	-1.14			
HCOOCH2CH3	HCOO-**H**-CHCH3	4.35	2.51	4.39		6.88	-2257.5596	5.9570	-1.06	3.30E+08	8.52	Gligorovski and Herrmann, 2004
	HCOOCH2CH2-**H**	3.58	6.04	7.82			-2257.5580	5.9570	-1.06			
HCHO	**H**-CHO	0.56	-1.38	0.49	6.45[a]	6.19	-2180.6953	5.6252	-1.02	1.00E+09	9.00	
CH3CHO	**H**-CH2CHO	9.28	7.45	9.46	6.20 ± 4.78[a]		-2463.6179	6.9032	-1.14			
	CH3CO-**H**	1.26	-0.66	1.18		5.28	-1853.6834	4.3421	-0.87	3.60E+09	9.56	Schuchmann and von Sonntag, 1988
(CH3)3COH	**H**-CH2(CH2)2COH	7.57	5.91	7.93	5.49 ± 1.91[a]	6.43	-2040.1477	5.0482	-0.96	6.00E+08	8.78	Buxton 1988
HOCH2OH	HOCH-**H**-OH	10.57	8.68	10.53	5.62[d]	6.11	-1697.9395	3.8041	-0.79	7.80E+08	8.89	Chin and Wine 1994
CH3CHOHOH	CH3C-**H**-(OH)2	6.70	4.71	6.83		6.01	-1511.9899	3.2235	-0.69	7.80E+08	8.89	Shuchmann 1988
	CH2-**H**-CH(OH)2	8.79	7.69	13.31			-2312.2171	6.2000	-1.08			
HO(CH2)2OH	HOCH2CH-**H**-OH	1.07	-0.66	0.71		5.76	-1933.4386	4.6358	-0.91	1.70E+09	9.23	Willson et al., 1971
CH3COCHO	**H**-CH2COCHO (Eclipsed)	11.07	9.17	11.25				1.0000	0.00			
	H-CH2COCHO (Staggered)	10.58	8.71	10.69			-2376.8010	6.4945	-1.11			
	H-COCOCH3 (Staggered)	0.03	-2.17	-0.22			-2508.4647	7.1201	-1.16			
	H-COCOCH3 (Eclipsed)	0.58	-1.54	0.35	5.02 ± 2.87[a]	6.53	-2368.5761	6.4565	-1.10	6.49E+08	8.81	Ervens et al., 2003
CH3COCOOH	**H**-CH2COCOOH (eclised)	11.05	8.24	10.18	6.69 ± 1.91[a]	7.55	-2427.1805	6.7299	-1.13	1.20E+08	8.08	Ervens et al., 2003
	H-CH2COCOOH (staggered)	11.28	9.00	10.96			-2401.7424	6.6104	-1.12			
CHOCOOH	**H**-COCOOH (cis)	18.16	9.59	11.23			-1900.4419	4.5128	-0.89			
	H-COCOOH (trans, staggered)	7.44	5.29	7.12	5.73 ± 2.87[a]	6.64	-2498.0206	7.0693	-1.16	5.90E+08	8.77	Ervens et al., 2003
	H-COCOOH (trans, eclipsed)	7.64	5.44	7.32			-2591.0319	7.5296	-1.19			
CH3COCOCH3	**H**-CH2COCOCH3	10.17	8.39	10.24	7.32[e]	7.32	-2360.4423	6.4191	-1.10	1.70E+08	8.23	Lilie 1968
HOOCCH2COOH	HOOC-**H**-CHCOOH	11.38	9.52	11.10		8.50	-2421.8843	6.7049	-1.13	2.40E+07	7.38	Scholes and Willson, 1967
CH2ClCOOH	CH-**H**-ClCOOH	7.88	5.96	7.72		8.16	-2437.5873	6.7791	-1.13	4.30E+07	7.63	Adams 1965
HOCH2COOH	HO-**H**-CHCOOH (cis)	6.98	5.24	6.77			-2122.5227	5.3818	-1.00			
	HO-**H**-CHCOOH (trans1)	4.03	2.26	3.91		6.49	-2183.4529	5.6369	-1.02	6.00E+08	8.78	Buxton et al., 1988
	HO-**H**-CHCOOH (trans2)	5.39	3.55	5.32			-2085.2222	5.2291	-0.98			
ClCH2CH2OH	ClCH-**H**-CH2OH	5.60	3.64	5.34			-2378.1241	6.5006	-1.11			
	ClCH2CH-**H**-OH	0.80	-0.90	0.85		6.16	-2056.4137	5.1131	-0.97	9.50E+08	8.98	Anbar and Neta, 1967
Cl3CH2OH	Cl3CH-**H**-OH	7.39	5.36	6.89		6.73	-2228.3268	5.8295	-1.04	4.20E+08	8.62	Walling et al., 1974
F3CH2OH	F3CH-**H**-OH	5.09	3.28	5.11		7.11	-2283.0368	6.0695	-1.07	2.30E+08	8.36	Walling et al., 1974
F3CCHCl2	F3CC-**H**-Cl2	8.48	6.49	8.50		8.91	-2537.7303	7.2637	-1.17	1.30E+07	7.11	Lal 1988

[a] *Ervens et al., 2003*
[b] *Elliot and McCracken, 1989*
[c] *Monod et al., 2005*
[d] *Chin and Wine 1994*
[e] *Gligorovski and Herrmann, 2004*

Table 3.6: Calculated $\Delta G^{\neq}_{rxn,aq}$, tunneling factor and literature reported HO• reaction rate constants for the HO• addition to alkenes.

Molecules	Chemical formula. **HO indicates the added HO radical	$\Delta G^{\neq}_{aq}$				Tunneling			Rate constant		
		G3 with COSMO-RS	G2 with COSMO-RS	G1 with COSMO-RS	Estimated from TST	Imaginary freq, $\nu^{\dagger}$, cm^{-1} ¶uMP2(full)/6-31G(d)	γ [$=1+1/24(h\nu^{\dagger}/kBT)^2$]	ΔG_{tunn} [$=-RT\ln(\gamma)$], kcal/mol	$k_{HO\bullet aq}$ exp	$\log k_{HO\bullet aq}$	Reference
H2C=CH2	H2C(**OH**)=CH2	-1.63	-3.32	-1.44	4.29		1.00	0.00	4.40E+09	9.64	Thomas 1967
H2C=CHCH3	H2C(**OH**)=CHCH3	-1.74	-3.41	-1.42	4.02	-540.5534	1.28	-0.15	7.00E+09	9.85	Thomas 1967
	H2C=C(**OH**)HCH3	-0.31	-2.06	-0.08		-535.1928	1.28	-0.15			
H2C=C(CH3)2	H2C(**OH**)=C(CH3)2	-4.10	-5.25	-3.36	4.17		1.00	0.00	5.40E+09	9.73	Thomas 1967
	H2C=C(**OH**)(CH3)2	-1.23	-2.47	-0.52			1.00	0.00			
H2C=CHCH2CH3	H2C(**OH**)=CHCH2CH3	-1.77	-3.35	-1.39	4.02	-503.9755	1.25	-0.13	7.00E+09	9.85	Thomas 1967
	H2C=C(**OH**)HCH2CH3	1.05	-0.58	1.33			1.00	0.00			
H2C=CHCH2OH	H2C(**OH**)=CHCH2OH	1.88	0.24	2.04	4.11	-599.8342	1.35	-0.18	6.00E+09	9.78	Maruthamuthu 1980
	H2C=C(**OH**)HCH2OH	0.49	-1.23	0.78		-521.0079	1.26	-0.14			
H2C=CHCOCH3	H2C(**OH**)=CHCOCH3	6.16	4.51	6.49	5.26	-537.4719	1.28	-0.15	8.50E+08	8.93	Kumar et al., 1990
	H2C=C(**OH**)HCOCH3	7.25	5.44	7.40		-519.9402	1.26	-0.14			
H2C=CHCOOH	H2C(**OH**)=CHCOOH	5.01	3.28	5.02	4.93	-531.1804	1.27	-0.14	1.50E+09	9.18	Walling et al., 1973
H2C=CHCl	H2C(**OH**)=CHCl	0.60	-1.18	0.67	3.70	-576.1003	1.32	-0.17	1.20E+10	10.08	Koester 1971
	H2C=C(**OH**)HCl	3.82	1.99	3.79		-658.1480	1.42	-0.21			
H2C=CHCl2	H2C(**OH**)=CCl2	0.34	-1.60	0.10	4.03	-572.6321	1.32	-0.16	6.80E+09	9.83	Koester 1971
	H2C=C(**OH**)Cl2	6.15	4.14	5.90		-759.3241	1.56	-0.26			
ClHC=CHCl	ClHC(**OH**)=CCHCl(cis)	3.20	1.54	3.19		-692.0306	1.47	-0.23			Koester and Asmus, 1971
	ClHC(**OH**)=CCHCl(trans)	2.19	0.20	2.02	4.22	-670.9326	1.44	-0.21	5.00E+09	9.70	Koester and Asmus, 1971
HClC=CCl2	CHCl=C(**OH**)Cl2	6.23	4.14	5.91		-766.6955	1.57	-0.27			
	ClHC(**OH**)=CCl2	3.42	1.42	2.83	4.46	-674.3879	1.44	-0.22	3.30E+09	9.52	Koester and Asmus, 1971
Cl2C=CCl2	Cl2C(**OH**)=CCl2	5.30	3.94	5.30	4.76		1.00	0.00	2.00E+09	9.30	Koester and Asmus, 1971

We observed linear correlations between log k_I – log k_R and $\Delta G^{act}_I - \Delta G^{act}_R$ for H-atom abstraction by HO• and HO• addition to alkenes, respectively (Figures 3.4 and 3.5). The compounds used include alkanes as well as oxygenated and halogenated compounds with a single functional group. With the exception of three chlorinated compounds (trichloromethane, dichloromethane and 1,1-dichloroethane), the least squares fit for H-atom abstraction calculated with COSMO-RS obtains linear correlations as: log k_I – log k_R = -0.176 (ΔG^{act}_I - ΔG^{act}_R) + 0.615 (N=26, r^2=0.851) by G3, log k_I – log k_R = -0.188 (ΔG^{act}_I - ΔG^{act}_R) + 1.138 (N=26, r^2=0.871) by G2, and log k_I – log k_R = -0.199 (ΔG^{act}_I - ΔG^{act}_R) + 0.498 (N=26, r^2=0.871) by G1. Underestimation of $\Delta G^{\neq}_{rxn,aq}$ of the three chlorinated compounds can be attributed to a relatively small activation barrier and a complex formed in the entrance channel of potential energy surface (Louis et al., 2000). In addition, the literature-reported experimental values for trichloromethane are in a relatively wider range (0.74 – 5.4 × 10^7 $M^{-1}s^{-1}$) (Buxton et al., 1988), and almost all data were obtained in the 1960s without reporting the precise experimental conditions (e.g., temperature, pH). For these reasons, we did not include these three compounds in the correlation.

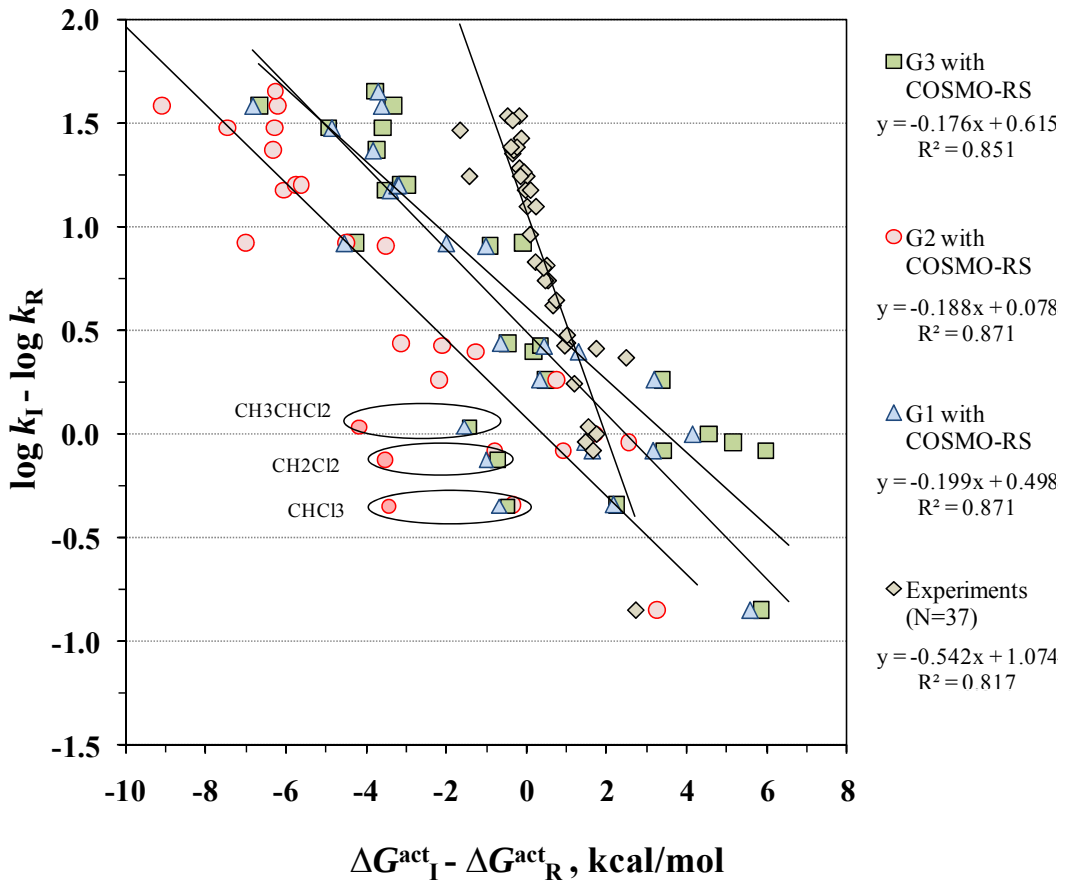

Figure 3.4: Log k_I – logk_R versus $\Delta G^{act}_I - \Delta G^{act}_R$ for H-atom abstraction from the C-H bond by HO•

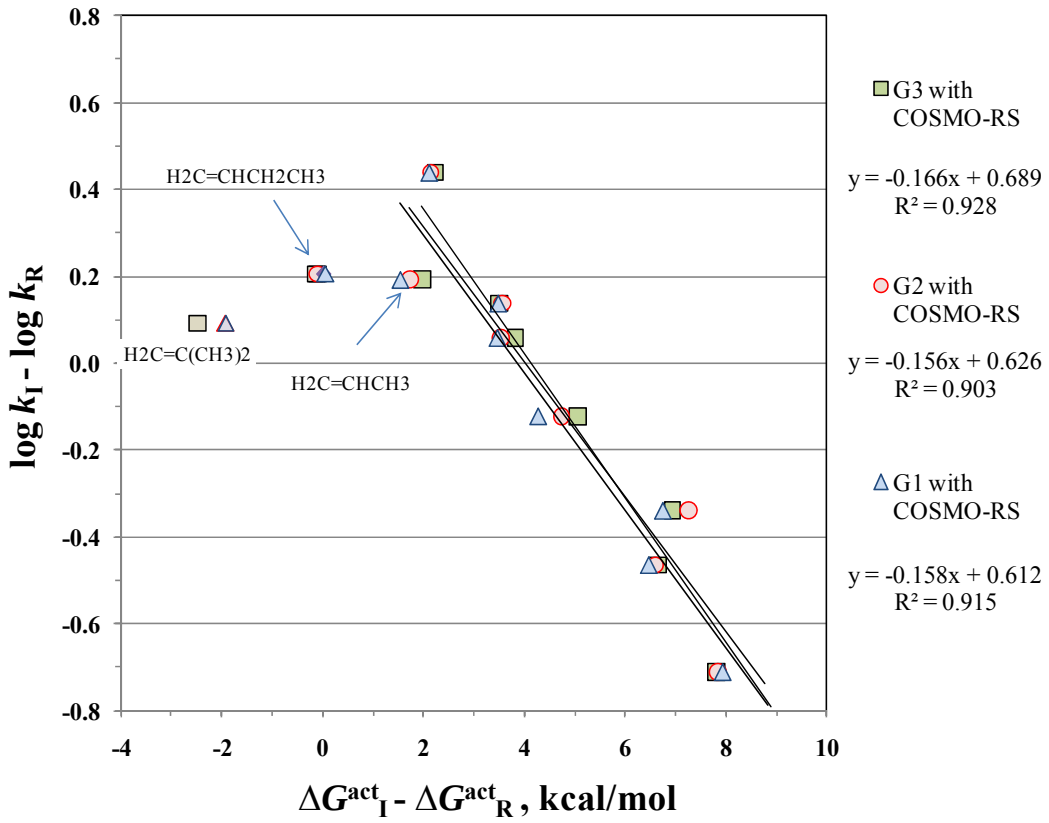

Figure 3.5: Log k_I – logk_R versus ΔG^{act}_I - ΔG^{act}_R for HO• addition to an alkene

For the HO• addition calculated with COSMO-RS, the obtained linear correlations are log k_I – log k_R = -0.166 (ΔG^{act}_I - ΔG^{act}_R) + 0.689 (N=10, r^2=0.928) by G3, log k_I – log k_R = -0.156 (ΔG^{act}_I - ΔG^{act}_R) + 0.626 (N=10, r^2=0.903) by G2, and log k_I – log k_R = -0.158 (ΔG^{act}_I - ΔG^{act}_R) + 0.612 (N=10, r^2=0.915) by G1. Regardless of the calculated $\Delta G^{\neq}_{rxn,aq}$, the logarithms of the experimental rate constants for propylene, isobutylene and 1-butene are identical. This is probably because the reactions involved in HO• addition to these compounds are close to the diffusion limit. To investigate the diffusion rate constant, we calculated the diffusion coefficient and the diffusion reaction

rate constant for each molecule using the Hayduk-Laudie correlation (Hayduk and Laudie, 1974).

The diffusion-encounter rate constant is based on diffusion toward the surface of a sphere around the reacting molecule and leads to values of k_D that are about half those based on the frequency factor given by the Smoluchowski equation (Adamson, 1979):

$$k_D = 4\times\pi\times D_l\times r\times N_0/1000 \tag{3.10}$$

where k_D is the diffusion-encounter rate constant, $M^{-1}s^{-1}$; D_l is the diffusion coefficient; r is the radius of the molecule; and N_0 is Avogadro's number. The diffusivities of small, uncharged molecules in water can be calculated using the Hayduk-Laudie correlation (Hayduk and Laudie, 1974), which is derived from the Wilke-Chang correlation.

$$D_l = \frac{13.26\times10^{-5}}{(\mu_\omega)^{1.14}(V_b)^{0.589}} \tag{3.11}$$

where D_l = liquid-phase diffusion coefficient of solute, cm^2/s; μ_ω = viscosity of water, cP (1 kg/m•s = 1000 cP); and V_b = molar volume of solute at normal boiling point, cm^3/mole. First, we calculated the V_b of a water molecule with B3LYP/6-311++G(3df,3pd) and compared it to the value obtained from LeBas (LeBas, 1915) to validate our methodology. This calculated value, 16.83 cm^3/mole, is close to the 18.8 cm^3/mol from LeBas. Then, we calculated the D_l of water as 2.51×10^{-6} cm^2/s, which is close to the literature-reported experimental value at 25ºC, 2.40×10^{-6} cm^2/s (Ferrell and Himmelblau, 1967). Using B3LYP/6-311++G(3df,3pd), we obtained 2.6×10^{-6} cm^2/s for the D_l of HO•.

Table 3.7 summarizes the calculated k_D for the HO• reactions that were investigated in the previous sections and provides a comparison with the chemical reaction rate $k_{HO\bullet}$. Figure 3.6 plots the ratio, R (=k_{exp}/k_D), against the calculated free

energy of activation in the aqueous phase, $\Delta G^{\neq}_{aq}$. The reactions considered here are all chemical rather than diffusion-limited reactions. As the calculated free energy of activation decreases (and molecular volume increases), the reaction approaches the diffusion rate reaction (i.e., R approaches 1.0).

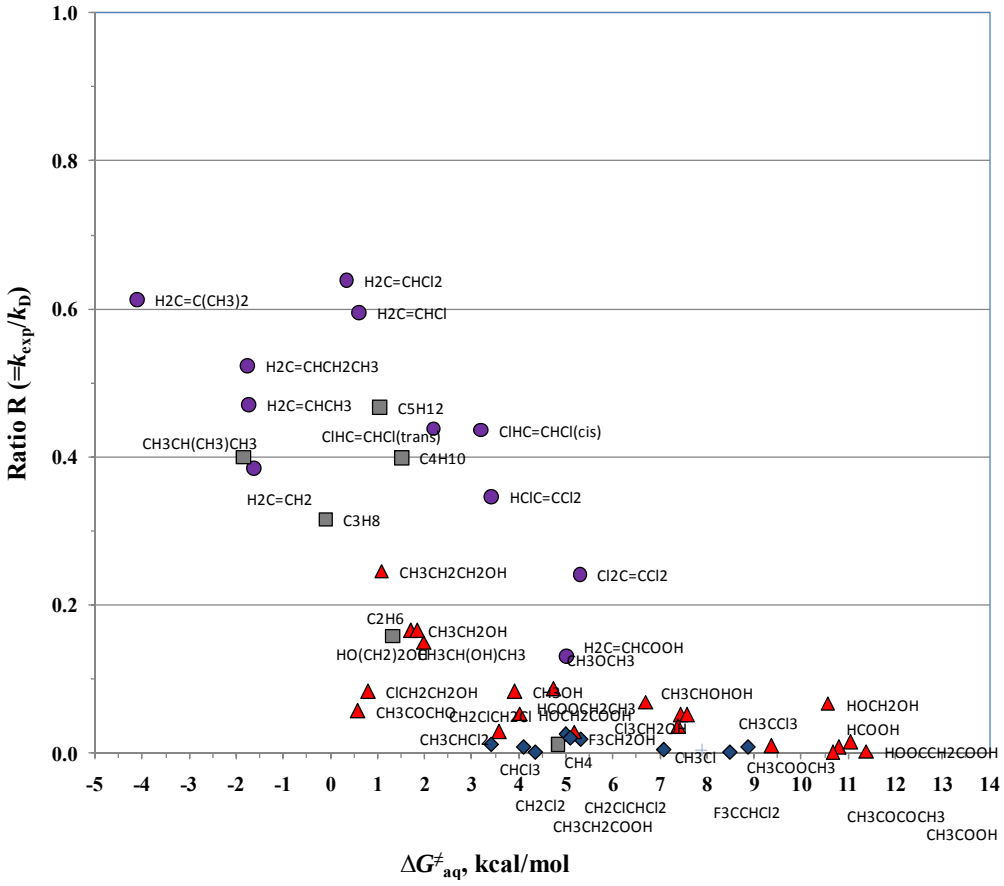

Figure 3.6: Plot of the ratio, $R(=k_{exp}/k_D)$, versus calculated free energy of activation.

Table 3.7: Calculated diffusion coefficients, molecular radii, and diffusion rate constants

Molecule A	Volume of molecule A*, cm^3/mole	Diffusion coefficient, D_A, cm2/sec	radius of molecule A, Å	D ($D_A + D_{HO\bullet}$†), cm^2/sec	λ ($\lambda_A + \lambda_{HO\bullet}$‡), cm	k_D, $M^{-1}s^{-1}$	k_{exp}, $M^{-1}s^{-1}$	R (=k_{exp}/k_D)
CH4	27.31	1.89E-05	1.87	4.49E-05	2.97E-08	1.0071E+10	1.20E+08	0.012
C2H6	43.33	1.44E-05	2.18	4.04E-05	3.74E-08	1.1418E+10	1.80E+09	0.158
C3H8	53.56	1.27E-05	2.34	3.87E-05	3.90E-08	1.1406E+10	3.60E+09	0.316
C4H10	79.77	1.01E-05	2.67	3.60E-05	4.23E-08	1.1526E+10	4.60E+09	0.399
C5H12	84.21	9.74E-06	2.72	3.57E-05	4.28E-08	1.1556E+10	5.40E+09	0.467
CH3CH(CH3)CH3	77.45	1.02E-05	2.64	3.62E-05	4.21E-08	1.1511E+10	4.60E+09	0.400
CH3Cl	45.74	1.40E-05	2.22	3.99E-05	3.78E-08	1.1410E+10	5.50E+07	0.005
CHCl3	76.90	1.03E-05	2.64	3.62E-05	4.20E-08	1.1508E+10	1.40E+07	0.001
CH2Cl2	59.64	1.19E-05	2.42	3.79E-05	3.98E-08	1.1420E+10	9.00E+07	0.008
CH3CHCl2	84.84	9.70E-06	2.73	3.57E-05	4.29E-08	1.1561E+10	1.30E+08	0.011
CH3CCl3	85.06	9.68E-06	2.73	3.56E-05	4.29E-08	1.1562E+10	1.00E+08	0.009
CH3Br	50.23	1.32E-05	2.29	3.92E-05	3.85E-08	1.1404E+10	2.20E+08	0.019
CH2ClCH2Cl	67.98	1.10E-05	2.53	3.70E-05	4.09E-08	1.1456E+10	2.20E+08	0.019
CH2ClCHCl2	69.01	1.10E-05	2.54	3.69E-05	4.11E-08	1.1461E+10	3.00E+08	0.026
CH3OH	28.90	1.83E-05	1.90	4.42E-05	3.46E-08	1.1595E+10	9.70E+08	0.084
CH3CH2OH	36.12	1.60E-05	2.05	4.20E-05	3.61E-08	1.1471E+10	1.90E+09	0.166
CH3CH(OH)CH3	65.84	1.13E-05	2.50	3.72E-05	4.07E-08	1.1445E+10	1.90E+09	0.166
CH3CH2CH2OH	48.25	1.35E-05	2.26	3.95E-05	3.82E-08	1.1405E+10	2.80E+09	0.246
CH3OCH3	41.46	1.48E-05	2.15	4.07E-05	3.71E-08	1.1427E+10	1.00E+09	0.088
CH3COCH3	49.99	1.32E-05	2.29	3.92E-05	3.85E-08	1.1404E+10	1.10E+08	0.010
HCOOH	35.31	1.62E-05	2.04	4.22E-05	3.60E-08	1.1481E+10	1.00E+08	0.009
CH3COOH	38.39	1.55E-05	2.09	4.14E-05	3.65E-08	1.1449E+10	1.70E+07	0.001
CH3CH2COOH	53.27	1.28E-05	2.33	3.87E-05	3.90E-08	1.1406E+10	3.20E+08	0.028
CH3COOCH3	64.32	1.14E-05	2.49	3.74E-05	4.05E-08	1.1439E+10	1.20E+08	0.010
HCOOCH2CH3	67.33	1.11E-05	2.52	3.71E-05	4.08E-08	1.1453E+10	3.30E+08	0.029
HCHO	31.42	1.74E-05	1.96	4.34E-05	3.52E-08	1.1541E+10	1.00E+09	0.087
CH3CHO	34.76	1.64E-05	2.02	4.24E-05	3.59E-08	1.1488E+10	3.60E+09	0.313
(CH3)3COH	68.14	1.10E-05	2.53	3.70E-05	4.10E-08	1.1457E+10	6.00E+08	0.052
HOCH2OH	45.38	1.40E-05	2.21	4.00E-05	3.77E-08	1.1410E+10	7.60E+08	0.067
CH3CHOHOH	44.76	1.41E-05	2.20	4.01E-05	3.76E-08	1.1412E+10	7.80E+08	0.068
HO(CH2)2OH	43.43	1.44E-05	2.18	4.03E-05	3.74E-08	1.1417E+10	1.70E+09	0.149
CH3COCHO	48.04	1.36E-05	2.26	3.95E-05	3.82E-08	1.1405E+10	6.49E+08	0.057
CH3COCOCH3	66.82	1.12E-05	2.52	3.71E-05	4.08E-08	1.1450E+10	1.70E+08	0.015
CHOCOOH	54.33	1.26E-05	2.35	3.86E-05	3.91E-08	1.1407E+10	5.90E+08	0.052
CH3COCOCH3	55.33	1.25E-05	2.36	3.84E-05	3.93E-08	1.1409E+10	1.70E+08	0.015
HOOCCH2COOH	68.66	1.10E-05	2.54	3.69E-05	4.10E-08	1.1460E+10	2.40E+07	0.002
CH2ClCOOH	56.75	1.23E-05	2.38	3.82E-05	3.95E-08	1.1412E+10	4.30E+07	0.004
HOCH2COOH	57.75	1.22E-05	2.40	3.81E-05	3.96E-08	1.1415E+10	6.00E+08	0.053
ClCH2CH2OH	58.75	1.20E-05	2.41	3.80E-05	3.97E-08	1.1418E+10	9.50E+08	0.083
Cl3CH2OH	59.75	1.19E-05	2.43	3.79E-05	3.99E-08	1.1421E+10	4.20E+08	0.037
F3CH2OH	60.75	1.18E-05	2.44	3.78E-05	4.00E-08	1.1424E+10	2.30E+08	0.020
F3CCHCl2	61.75	1.17E-05	2.45	3.76E-05	4.01E-08	1.1428E+10	1.30E+07	0.001
H2C=CH2	39.19	1.53E-05	2.11	4.12E-05	3.67E-08	1.1442E+10	4.40E+09	0.385
H2C=CHCH3	36.66	1.59E-05	2.06	4.19E-05	3.62E-08	1.1465E+10	5.40E+09	0.471
H2C=C(CH3)2	60.42	1.18E-05	2.43	3.78E-05	4.00E-08	1.1423E+10	7.00E+09	0.613
H2C=CHCH2CH3	68.55	1.10E-05	2.54	3.69E-05	4.10E-08	1.1459E+10	6.00E+09	0.524
H2C=CHCH2OH	48.88	1.34E-05	2.27	3.94E-05	3.83E-08	1.1404E+10	8.50E+08	0.075
H2C=CHCOCH3	48.23	1.35E-05	2.26	3.95E-05	3.82E-08	1.1405E+10	7.00E+09	0.614
H2C=CHCl	41.73	1.47E-05	2.15	4.07E-05	3.71E-08	1.1425E+10	6.80E+09	0.595
H2C=CHCl2	61.95	1.17E-05	2.45	3.76E-05	4.02E-08	1.1429E+10	7.30E+09	0.639
ClHC=CHCl(cis)	68.95	1.10E-05	2.54	3.69E-05	4.11E-08	1.1461E+10	5.00E+09	0.436
ClHC=CHCl(trans)	50.59	1.31E-05	2.29	3.91E-05	3.86E-08	1.1404E+10	5.00E+09	0.438
HCl2C=CCl2	82.06	9.89E-06	2.70	3.58E-05	4.26E-08	1.1542E+10	4.00E+09	0.347
Cl2C=CCl2	88.58	9.45E-06	2.77	3.54E-05	4.33E-08	1.1588E+10	2.80E+09	0.242
H2C=CHCOOH	67.21	1.11E-05	2.52	3.71E-05	4.08E-08	1.1452E+10	1.50E+09	0.131

** obtained by B3LYP/6-311++(3df,3pd)*

† $D_{HO\bullet} = 2.60 \times 10^{-6}$ cm^2/s

‡ $\lambda_{HO\bullet} = 1.56 \times 10^{-8}$ cm

Once the LFERs were established, we predicted the reaction rate constants of H-atom abstraction for 14 compounds with multiple functional groups (i.e., oxygenated and halogenated compounds). Figure 3.7 compares the predicted HO• rate constants with the literature-reported experimental values. Of the 14 predicted rate constants, 4 (29% of

predicted rate constants) and 13 (93% of predicted rate constants) are within 0.5 < k_{pred}/k_{exp} < 2.0 and 0.2 < k_{pred}/k_{exp} < 5.0, respectively. 1,1-dichloro-2,2,2-fluoroethane is the only compound outside the range of difference of factor of 5. If this compound is eliminated, the SD values would be 1.38, 1.45 and 1.45 by G3, G2 and G1 with COSMO-RS, respectively.

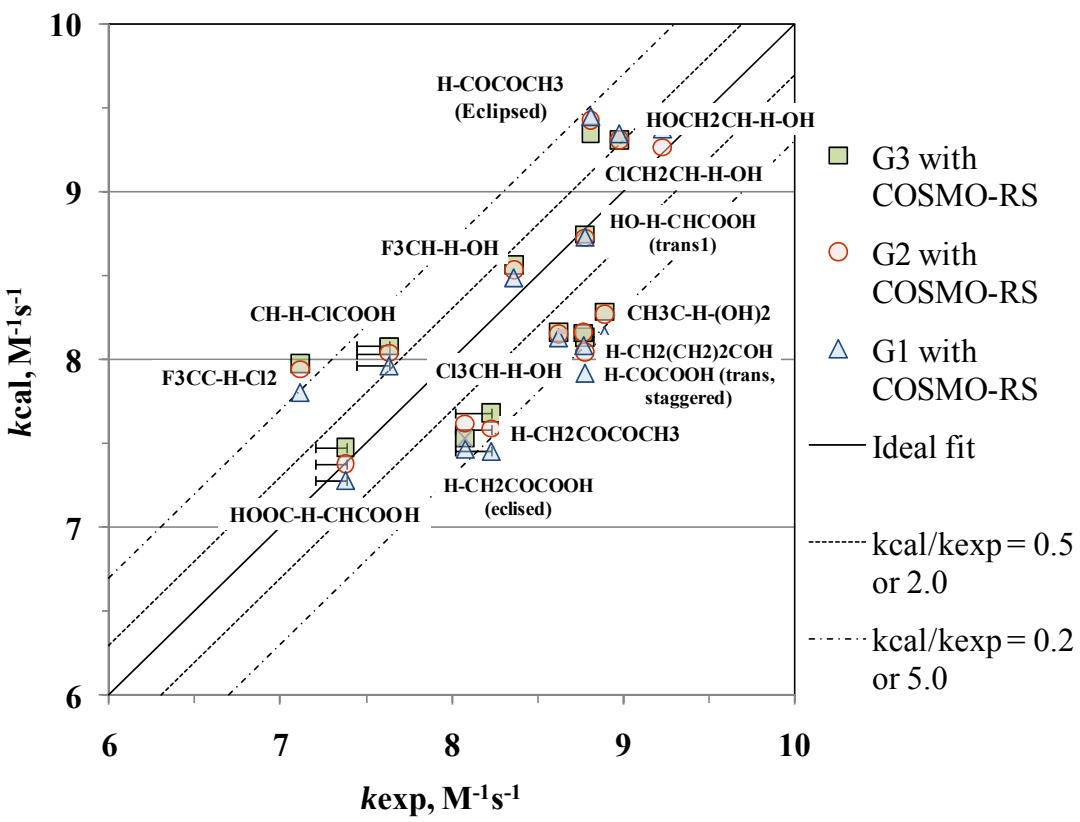

Figure 3.7: Plot of predicted HO• rate constants versus the literature-reported experimental rate constants. The error bar represents the range of the latter.

A limited number (37) of literature-reported experimental ΔG_{rxn}^{act} values have been estimated for oxygenated compounds from Arrehnius activation energy and frequency factor (Figure 3.4) by assuming the equilibrium at transition state. When these values are

compared with the theoretically calculated values for compounds with both single- and multiple-functional groups, the calculated $\Delta G^{\neq}_{\mathrm{rxn,aq}}$ are within ±4 kcal/mol. These errors should be within the errors derived from the quantum mechanical calculations and experiments. Typical errors (i.e., range of 95% of confidence value) in calculating aqueous phase free energy of activation based on experiments are reported in the range from 2 kcal/mol to 4 kcal/mol. For example, Ervens et al. (2003) experimentally obtained 5.25 kcal/mol, 4.78 ± 2.87 kcal/mol, 6.21 ± 4.78 kcal/mol and 5.73 ± 3.10 kcal/mol for the reaction of HO• with methanol, ethanol, acetone and propionic acid. Although great uncertainty remains particularly in calculating the aqueous phase free energy at transition state, typical errors that are caused by calculating gaseous phase free energy and free energy of solvation is approximately ±2.0 kcal/mol and ±1.0 kcal/mol, respectively. For example, the errors for the gaseous phase molecular atomization energies calculated by G3, G2 and G1 are reported within 2.0 kcal/mol (Pople et al., 1989; Curtiss, 1991; Curtiss et al., 1998). Although there is ongoing discussion regarding the free energy of solvation, the observed error for the aqueous phase free energy of solvation is within 1.0 kcal/mol (Klamt et al., 2009; Cramer and Truhlar, 2009). The SD for 17 calculated aqueous phase free energy of activation of compounds with both single- and multiple-functional groups are 0.61, 0.71 and 0.55, respectively, for G3, G2, and G1 with COSMO-RS. Notably, 1 kcal/mol of difference in $\Delta G^{\neq}_{\mathrm{rxn,aq}}$ causes 5.4 times difference in the rate constant according to the TST equation (3.12):

$$\Delta G^{\mathrm{act,TST}}_{\mathrm{rxn}} = -RT \ln\left(k_{\mathrm{exp}} \frac{h}{\gamma T} \right) \tag{3.12}$$

Although absolute prediction of reaction rate constants is not feasible, the LFERs that areestablished based on our theoretical calculations follow a trend in reactivity consistent with the experimental values, as shown in Figure 3.4.

Another validation for our theoretically calculated values is to compare them with the estimated $\Delta G_{\text{rxn}}^{\text{act, TST}}$ derived from TST (Eyring, 1938), as shown in equation (3.12). When compared to this $\Delta G_{\text{rxn}}^{\text{act, TST}}$, our theoretically calculated $\Delta G^{\neq}_{\text{rxn,aq}}$ gives SD of 0.33, 0.61 and 0.32 by G3, G2 and G1 with COSMO-RS, respectively (N=40). Although the TST does not thoroughly represent the aqueous phase reaction mechanisms (Kraut, 1988), this comparison proves the validity of our theoretically calculated $\Delta G^{\neq}_{\text{rxn,aq}}$. For the 1,1-dichloro-2,2,2-fluoroethane, the $\Delta G^{\neq}_{\text{rxn,aq}}$ is 8.48 kcal/mol, 6.49 kcal/mol and 8.50 kcal/mol by the G3, G2 and G1 with the COSMO-RS, respectively, and is close to the 8.91 kcal/mol of the $\Delta G^{\text{act,tst}}$. Because the reported rate constant is extremely low, 1.3×10^{7} $M^{-1}s^{-1}$ (Lal et al., 1988), which is close to the lower limit in the pulse radiolysis approach, the reported rate constant might have been significantly underestimated.

Despite the overall errors from the calculations, the theoretically calculated free energy of activation in the aqueous phase is within the errors derived from the gaseous phase quantum mechanical and free energy of solvation calculations. In addition, if uncertainty in the literature-reported experimental errors is accounted for, the LFERs should be acceptable for predicting the reaction rate constants of unknown compounds that have not been experimentally examined. Consequently, this approach may be applicable to other reaction mechanisms to establish a library of reaction rate constant predictors for mechanistic modeling.

3.6 Acknowledgement

This work was supported by the National Science Foundation Award 0854416 from the National Science Foundation. Any opinions, findings, conclusions, or recommendations expressed in this publication are those of the authors and do not necessarily reflect the view of the supporting organizations. Authors appreciate the support from the Hightower Chair and the Georgia Research Alliance at the Georgia Institute of Technology. Authors also appreciate Dr. Matthew Wolf at the College of Computing in Georgia Tech for the high performance and clustered computing resources. We gratefully acknowledge the contribution of Linly Hall and Mary Kate Varnau for her editorial assistance.

3.7 Appendices

Appendix D includes all calculated data for HOMO and SOMO energy gap. Appendix E includes the optimized structures and their z-matrices of coordinates.

3.8 Literature Cited

A division of the American Chemical Society. CAS (Chemical Abstract Service). http://www.cas.org/expertise/cascontent/index.html (accessed June 12, 2009).

Adamson, A.W. A Textbook of Physical Chemistry, 2nd edition., Academic Press, New York. 1979.

Ahlrichs, R; M. Bär, M.; Häse, M.; Horn, H.; Kölmel, C. Electronic structure calculations on workstation computers: The program system TURBOMOLE. *Chem. Physcs. Lett*. 1989, *162*(3), 165-169.

Andzelm, J.; Wimmer, E. Density functional gaussian-type-orbital approach to molecular geometries, vibrations, and reaction energies, *J. Phys. Chem*., 1992, 96, 1280-1303.

Ashcraft, R.W.; Raman, S.; Green, W.H. Ab initio aqueous thermochemistry: Application to the oxidation of hydroxylamine in nitric acid solution. *J. Phys. Chem. B*. 2007, *111*, 11968-11983.

Atadinc, F.; Selcuki, C.; Sari, L.; Aviyente, V. Theoretical study of hydrogen abstraction from dimethyl ether and methyl tert-butyl ether by hydroxyl radical. *Phys. Chem. Chem*.

Ayala, P.Y.; Schlegel, H.B. A combined method for determining reaction paths, minima, and transition state geometries. *J.Chem.Phys*. 1997, *107*(2), 375-384.

Bacskay, G.B. A Quadratically Convergent Hartree-Fock (QC-SCF) Method. Application to Closed Systems. *Chem. Phys. 1981*, 61, 385-404.

Barone, V.; Cossi, M. Quantum calculation of molecular energies and energy gradients in solution by a conductor solvent model. *J.Phys. Chem. A*, 1998, *102*, 1995-2001.

Barone, V.; Cossi, M.; Tomasi, J. A new definition of cavities for the computation of solvation free energies by the polarizable continuum model. *J.Chem.Phys*. 1997, *107*(8), 3210-3221.

Becke, A.D. Density-functional thermochemistry. III. The role of exact exchange. *J. Chem. Phys*. 1993, *98*, 5648-5652.

Ben-Naim, A. Molecular Theory of Solutions; Oxford University Press Inc.: New York, 2006.

Ben-Naim, A. Solvation Thermodynamics; Plenum Press: New York, 1987.

Boese, A.D.; Martin, J. M.L. Development of density functional for thermochemical kinetics. *J. Chem. Phys*. 2004, *121*(8), 3405-3416.

Bonifačić, M.; Möckel, H.; Bahnemann, D.; Asmus, K-D. Formation of positive ions and other primary species in the oxidation of sulphides by hydroxyl radicals. *J. Chem. Soc. Perkin I*. 1975, 675-685.

Brezonik, P.L. Chemical kinetics and process dynamics in aqueous systems. Lewis Publishers. 2002.

Buxton, V. B.; Greenstock, C. L.; Helman, W. P.; Ross, A. B. Critical review of rate constants for reactions of hydrated electrons, hydrogen atoms and hydroxyl radicals (•OH/•O^-) in aqueous solution. *J. Phys. Chem. Ref. Data*. 1988, *17* (2) 513-795.

Chandra, A. K.; Uchimaru, T.; Sugie, M., Kinetics of hydrogen abstraction reactions of 1,1- and 1,2-difluoroethane with hydroxyl radical: an ab initio study*, J. Comp. Chem*., 2000, *21*, 1305-1318.

Chandra, A.K.; Uchimaru, T. Kinetics of hydrogen abstraction from chloromethanes by the hydroxyl radical: A computational study.

Chartfield, D.C.; Friedman, R.S.; Schwenke, D.W.; Truhlar, D.G. Control of chemical reactivity by quantized transition states. *J. Phys. Chem*. 1992, *96*, 2414-2421.

Chen, H., M. Krasowski, and G. Fitzgerald, Density functional pseudo potential studies of molecular geometries, vibrations, and binding energies, *J. Chem. Phys*., 1993, *98*, 8710-8717.

Čížek, J. On the correlation problem in atomic and molecular systems. Calculation of wavefunction components in ursell-type expansion using quantum-field theoretical methods. *J. Chem. Phys*. 1966, *45*(11), 4256-4266.

Cohen, N. Are reaction rate coefficients additive? Revised transition state theory calculations for OH + alkane reaction. *Int. J. Chem. Kinet*. 1991, *23*, 397-417.

Cossi, M.; Rega, N.; Scalmani, G.; Barone, V. Energies, structures, and electronic properties of molecules in solution with the C-PCM solvation model. *J. Comp. Chem*. 2003, 24(6), 669-681.

Cramer, C.J. Essential of computational chemistry 2nd ed. John Wiley & Sons. Ltd. England, 2004; Chapter 11.

Cramer, C.J.; Truhlar, D.G. A universal approach to solvation modeling. *Acc. Chem. Res*. 2008, *41*(6), 760-768.

Cramer, C.J.; Truhlar, D.G. Commentary. On the performance of continuum solvation methods. Reply to comment on "A universal approaches to solvation modeling". *Acc. Chem. Res*. 2009, *42*(4), 493-497.

Cramer, C.J.; Truhlar, D.G. In Solvent Effects and Chemical Reactivity; Tapia, O., Bertrán, J., Eds.; Kluwer: Dordrecht, 1996; p1.

Crittenden, J.C.; Hu, S.; Hand, D.W.; Green, S.A. A kinetic model for H_2O_2/UV process in a completely mixed batch reactor. *Wat. Res*. 1999, *33*(10), 2315-2328.

Curtiss, L.A. Gaussian-2 theory for molecular energies of first- and second-row compounds, *J. Chem. Phys.* 1991, *94*(11), 7221-7230.

Curtiss, L.A.; Jones, C. Gaussian-1 theory of molecular energies for second-row compounds. *J. Chem. Phys.* 1990, *93*(4), 2537-2545.

Curtiss, L.A.; Redfern, P.C.; Rassolov, V.; Pople, J.A. Gaussian-3(G3) theory for molecules containing first and second-row atoms, *J. Chem. Phys.* 1998, *109*(18), 7764-7776.

DeFrees, D. J., Raghavachari, K.; Schlegel, H. B.; Pople, J. A., Effect of electron correlation on theoretical equilibrium geometries. 2. Comparison of third-order

perturbation and configuration interaction results with Experiment, *J. Am. Chem. Soc*., 1982, *104*, 5576-5580.

DeMatteo, M.P.; Poole, J.S.; Shi, X.; Sachdeva, R.; Hatcher, P.G.; Hadad, C.M.; Platz, M.S. On the electrophicility of hydroxyl radical: A laser flash photolysis and computational study. *JACS*. 2005, *147*, 7094-7109.

Dunning, Jr. T.H. Gaussian basis sets for use in correlated molecular calculations. I. The atoms boron through neon and hydrogen. *J. Chem. Phys*. 1989, *90*(2), 1007-1023.

Eckert, F and Klamt, A. COSMO*therm*, Version C2.1, Release 01.08; COSMO*logic* GmbH & Co. KG, Leverkusen, Germany, 2006.

Eisenberg, D.; McLachlan, A.D. Solvation energy in protein folding and binding. *Nature*, 1986, *319*, 199-203.

Ellingson, B.A.; Pu, J.; Lin, H.; Zhao, Y.; Truhlar, D.G. Multicoefficient Gaussian-3 calculation of the rate constant for the OH+CH4 reaction and its 12C/13C kinetic isotope effect with emphasis on the effects of coordinate system and torsional treatment. *J. Phys. Chem. A*., 2007, *111*, 11706-11717.

Elliot, A.J.; Geertsen, S.; Buxton, G.V. J. Oxidation of thiocyanate and iodide ions by hydrogen atoms in acid solutions. *Chem. Soc. Faraday Trans*. 1988, 1, *84*, 1101-1112.

Ervens, B.; Gligorovski, S.; Herrmann, H. Teperature-dependent rate constants for hydroxyl radical reactions with organic compounds in aqueous solution. *Phys. Chem. Chem. Phys*., 2003, *5*, 1811-1824.

Espinosa-García, J.; Coitino, E.L.; González-Lafont, A.; Lluch, J.M. Reaction-path and dual-level dynamics calculations of the CH3F + OH reaction. *J.Phys.Chem.A*. 1998, *102*, 10715-10722.

Eyring, H. The calculation of activation energies. *Reaction Kinetics*. 1938. 3-11.

Eyring, H.; Cershinowitz, H.; Sun, C.E. The absolute rate of homogeneous atomic reactions. *J. Chem. Phys.* 1935, *3*, 786-796.

Eyring, H.; Gershinowitz, H.; Sun, C.E. The absolute rate of homogeneous atomic reactions. *J. Chem. Phys*. 1935, *3*, 786-796.

Fittschen, C.; Hippler,H.; Viskolcz, B. The β C-C bond scission in alkoxy radicals: thermal unimolecular decomposition of *t*-butoxy radicals. *Phys.Chem.Chem.Phys*. 2000, *2*, 1677-1683.

Fontana, G.; Causa, M; Gianotti, V.; Marchionni, G., Computational studies of the reaction of the hydroxyl radical with hydroflurocarbons (HFCs) and hydrofluoroethers (HFEs), *J. Fluorine Chem*., 2001, *109*, 113-121.

Foreman, J.B.; Frisch, E. Exploring chemistry with electronic structure methods. 2nd ed. Gaussian, Inc. Pittsburgh, PA.

Frisch, M. J.; Trucks, G. W.; Schlegel, H. B.; Scuseria, G. E.; Robb, M. A.; Cheeseman, J. R.; Montgomery, J. A., Jr.; Vreven, T.; Kudin, K. N.; Burant, J. C.; Millam, J. M.; Iyengar, S. S.; Tomasi, J.; Barone, V.; Mennucci, B.; Cossi, M.; Scalmani, G.; Rega, N.; Petersson, G. A.; Nakatsuji, H.; Hada, M.; Ehara, M.; Toyota, K.; Fukuda, R.; Hasegawa, J.; Ishida, M.; Nakajima, T.; Honda, Y.; Kitao, O.; Nakai, H.; Klene, M.; Li, X.; Knox, J. E.; Hratchian, H. P.; Cross, J. B.; Bakken, V.; Adamo, C.; Jaramillo, J.; Gomperts, R.; Stratmann, R. E.; Yazyev, O.; Austin, A. J.; Cammi, R.; Pomelli, C.; Ochterski, J. W.; Ayala, P. Y.; Morokuma, K.; Voth, G. A.; Salvador, P.; Dannenberg, J. J.; Zakrzewski, V. G.; Dapprich, S.; Daniels, A. D.; Strain, M. C.; Farkas, O.; Malick, D. K.; Rabuck, A. D.; Raghavachari, K.; Foresman, J. B.; Ortiz, J. V.; Cui, Q.; Baboul, A. G.; Clifford, S.; Cioslowski, J.; Stefanov, B. B.; Liu, G.; Liashenko, A.; Piskorz, P.; Komaromi, I.; Martin, R. L.; Fox, D. J.; Keith, T.; Al-Laham, M. A.; Peng, C. Y.; Nanayakkara, A.; Challacombe, M.; Gill, P. M. W.; Johnson, B.; Chen, W.; Wong, M. W.; Gonzalez, C.; Pople, J. A. *Gaussian 03*, revision E. 01; Gaussian, Inc.: Wallingford, CT, 2003.

Fukui, K.; Yonezawa, Y.; Shingu, H. A molecular orbital theory of reactivity in aromatic hydrocarbons. *J.Chem.Phys*. 1952, *20*(4), 722-725.

Gonzalez-Lafont, A.; Lluch, J. M., Espinosa-Garcia, J., Variational transition state calculations of the CH2F2 + OH hydrogen abstraction reaction*, J. Phys. Chem. A*, 2001, *105*, 10553-10561.

Hayduk, W.; Laudie, H. Prediction of diffusion coefficients for non-electrolytes in dilute aqueous solutions. *AIChEJ*., 1974, *20*(3), 611-615.

Headlam, H.A.; Davies, M.J. Beta-scission of side-chain alkoxyl radicals on peptides and proteins results in the loss of side-chains as aldehydes and ketones. *Free Radical Biol & Med*. 2002, *32*(11), 1171-1184.

Henon, E.; Canneaux, S.; Bohr, F.; Dobe, S. Features of the potential energy surface for the reaction of OH radical with acetone. *Phys. Chem. Chem. Phys*. 2003, *5*, 333-341.

Hermann, R.B. Theory of hydrophobic bonding. II. The correlation of hydrocarbon solubility in water s with solvent cavity surface area*. J. Phys. Chem*. 1972, *76*, 2754.

Higashi, M.; Marenich, A. V.; Olson, R. M.; Chamberlin, A. C.; Pu, J.; Kelly, C. P.; Thompson, J. D.; Xidos, J. D.; Li, J.; Zhu, T.; Hawkins, G. D.; Chuang, Y.-Y.; Fast, P. L.; Lynch, B. J.; Liotard, D. A.; Rinaldi, D.; Gao, J.; Cramer, C. J.; Truhlar, D. G. GAMESSPLUS – version 2008–2*,* University of Minnesota, Minneapolis, 2008, based on

the General Atomic and Molecular Electronic Structure System (GAMESS) as described in Schmidt, M. W.; Baldridge, K. K.; Boatz, J. A.; Elbert, S. T.; Gordon, M. S.; Jensen, J. H.; Koseki, S.; Matsunaga, N.; Nguyen, K. A.; Su, S. J.; Windus, T. L.; Dupuis, M.; Montgomery J. A. *J. Comput. Chem*. 1993, *14*, 1347.

Hindmarsh, A.C.; Gear, C.W. Ordinary differential equation system solver. UCID-30001 Rev. 3 Lawrence Livermore Laboratory, Livermore, Ca. 1974.

Hohenberg, P.; Kohn, W. Inhomogeneous electron gas. *Phys.Rev*. 1964, *136*, B864-871.

Huber, M.M.; Canonica, S.; Park, G-Y.; Von Gunten, U. Oxidation of pharmaceuticals during ozonation and advanced oxidation processes. *Environ. Sci. Technol*. 2003, *37*, 1016-1024.

Huynh, L.K.; Ratkiewicz, A.; Truong, T.N. Kinetics of the hydrogen abstraction OH + alkane → H2O + alkyl reaction class: An application of the reaction class transition state theory. *J. Phys. Chem. A*. 2006, *110*, 473-484.

Huynh, L.K.; Truong, T.N. Kinetics of the hydrogen abstraction CHO + alkane → HCH alkyl reaction class: An application of the reaction class transition state theory. *Theor. Chem. Acc*. 2007

Huynh, L.K.; Zhang, S.; Truong, T.N. Kinetics of hydrogen abstraction O(3P) + alkane → OH + alkyl reaction class: An application of the reaction class transition state theory. *Combustion and Flame*, 2008, 152, 177-185.

Irikura, K. K., Fruruip, D. J., Computational thermochemistry: Prediction and estimation of molecular thermodynamics, 1998, American Chemical Society.

Izgorodina, E.I.; Brittain, D.R.B.; Hodgson, J.L.; Krenske, E.H.; Lin, C.Y.; Namazian, M.; Coote, M.L. Should contemporary density functional theory methods be used to study the thermodynamics of radical reactions? *J.Phys.Chem. A*. 2007, *111*, 10754-10768.

Izgorodina, E.I.; Brittain, D.R.B.; Hodgson, J.L.; Krenske, E.H.; Lin, C.Y.; Namazian, M.; Coote, M.L. Should contemporary density functional theory methods be used to study the thermodynamics of radical reactions? *J.Phys.Chem. A*. 2007, *111*, 10754-10768.

Jursic, B.S. Computing transition state structure and estimating reaction barriers with complete basis set ab initio method. *J. Mol. Structure (Theochem)*, 2000, *499*, 223-231.

Kasai, P.H.; Meyers, R.J. J. Chem. Phys. 1959, 30, 1096

Klamt, A. COSMO-RS from Quantum Chemistry to Fluid Phase Thermodynamics and Drug Design. 2005 Elservier. Amsterdam.

Klamt, A. Estimation of gas-phase hydroxyl radical rate constants of oxygenated compounds based on molecular orbital calculations. *Chemosphere*. 1996, *32*(4), 717-726.

Klamt, A.; Jonas, V.; Bürger, T.; Lohrenz, J.C.W. Refinement and parametrization of COSMO-RS. *J.Phys.Chem. A*. 1998, *102*, 5074-5085.

Klamt, A.; Mennucci, B.; Tomasi, J.; Barone, V.; Curutchet, C.; Orozco, M.; Luque, F.J. Commentary. On the performance of continuum solvation methods. A comment on "Universal approaches to solvation modeling". *Acc. Chem. Res*. 2009, *42*(4), 489-492.

Kohn, W.; Sham, L.J. Self-consistent equations including exchange and correlation effects. *Phys. Rev*. 1965, *140*, A1133-1138.

Kraut, J. How do enzymes work? *Science.* 1988, *242*, 533-540.

Kungwan, N.; Truong, T.N. Kinetics of the hydrogen abstraction •CH3 + alkane → CH4 + alkyl reaction class: An application of the reaction class transition state theory? *J. Phys. Chem. A*. 2005, *109*, 7742-4450.

Lal, M.; Schoeneich, C.; Moenig, J.; Asmus, K.-D. Rate constants for the reaction of halogenated organic radicals. *Int. J. Radiat. Biol*. 1988, *54*, 773-785.

LeBas The Molecular Volumes of Liquid Chemical Compounds. 1915, Longmans, London.Ferrell and Himmelblau 1967 Diffusion coefficients of nitrogen and oxygen in water. *J. Chem. Eng. Data*, *12*, 111-115.

Lee, C.; Yang, W.; Parr, R.G. Development of the colle-salvetti correlation-energy formula into a functional of the electron density. *Phys. Rev. B*., 1988, *37*, 785-789.

Li, K.; Crittenden, J.C. Computerized pathway elucidation for hydroxyl radical-induced chain reaction mechanisms in aqueous phase Advanced Oxidation Processes. *Environ. Sci. Technol*. 2009, *43*, 2831-2837.

Li, K.; Hokanson, D.R.; Crittenden, J.C.; Trussell, R.R.; Minakata, D. Evaluating UV/H_2O_2 processes for methyl tert-butyl ether and tertiary butyl alcohol removal. *Wat. Res*. 2008, *42*(20), 5045-5053.

Li, K.; Stefan, M.I.; Crittenden, J.C. Trichloroethene degradation by UV/H_2O_2 advanced oxidation process: product study and kinetic modeling. *Environ. Sci. Technol*. 2007, *41*, 1696-1703.

Li, K.; Stefan, M.I.; Crittenden, J.C. UV photolysis of trichloroethylene: Product study and kinetic modeling. *Environ. Sci. Technol*. 2004, *38*, 6685-6693.

Lien, P-Y.; You, R-M.; Hu, W-P. Theoretical modeling of the hydrogen abstraction reaction of fluoromethane by the hydroxyl radical. *J.Phys.Chem.A*, 2001, *105*, 2391-2400.

Liptak, M. D.; Shields, G. C. Accurate p*K*a Calculations for Carboxylic Acids Using Complete Basis Set and Gaussian-n Models Combined with CPCM Continuum Solvation Methods. *J. Am. Chem. Soc.* 2001, *123*, 7314-7319.

Louis, F.; Gonzalez, C.A.; Huie, R.E.; Kurylo, M.J. An ab initio study of the kinetics of the reactions of halomethanes with the hydroxyl radical. 2. A comparison between theoretical and experimental values of the kinetic parameters for 12 partially halogenated methanes. *J. Phys. Chem. A*. 2000, *104*, 8773-8778.

Louis, F.; Gonzalez, C.A.; Huie, R.E.; Kurylo, M.J. An ab initio study of the kinetics of the reactions of halomethanes with the hydroxyl radical. 2. A comparison between theoretical and experimental values of the kinetic parameters for 12 partially halogenated methanes. *J. Phys. Chem. A*. 2000, *104*, 8773-8778.

Lynch, B.J.; Truhlar, D. G. How well can hybrid density functional methods predict transition state geometries and barrier heights? *J. Phys. Chem. A*. 2001, *105*, 2936-2941.

Mader, E.A.; Davidson, E.R.; Mayer, J.M. Large ground-state entropy changes for hydrogen atom transfer reactions of iron complexes. *J.A.C.S.* 2007, *129*, 5153-5166.

Maity, D.K.; Duncan, W.T.; Truong, T.N. Direct ab inito dynamics studies of the hydrogen abstractions of hydrogen atom with fluoromethanes. *J. Phys. Chem. A*. 1999, 103, 2152-2159.

Marenich, A. V.; Kelly, C. P.; Thompson, J. D.; Hawkins, G. D.; Chambers, C. C.; Giesen, D. J.; Winget, P.; Cramer, C. J.; Truhlar, D. G. *Minnesota Solvation Database – version 2009*, University of Minnesota, Minneapolis, 2009.

Marenich, A.V.; Cramer, C.J.; Truhlar, D.G. Perspective on foundations of solvation modeling: The electrostatic contribution to the free energy of solvation. *J. Chem. Theory Comput*. 2008, *4*, 877-887.

Martin, J. M. L.; Oliveira, G. Towards standard methods for benchmark quality ab initio thermochemistry – W1 and W2 theory. *J. Chem. Phys.* 1999, 1843-1856.

Masgrau, L., Gonzalez-Lafont, A.; Lluch, J. M., The reactions CHnD4-n + OH -? P and CH4 + OD -> CH3 + HOD as a test of current dynamics computational methods to determine variational transition-state rate constants, *J. Chem. Phys*., 2001, *114*, 5, 2154-2165.

Melissas, V. S., Truhlar, D. G., Interpolated variational transition state theory and tunneling calculations of the rate constant of the reaction OH + CH4 at 223-2400 K, *J. Chem. Phys*, 1993, 99, 2, 1013-1027.

Mennucci, B.; Tomasi, J. Continuum solvation models: A new approach to the problem of solute's charge distribution and cavity boundaries. *J. Chem. Phys.* 1997, *106*, 5151-5158.

Méreau, R.; Rayez, M-T.; Caralp, F.; Rayez, J-C. Theoretical study of alkoxyl radical decomposition reactions: structure-activity relationship. *Phys. Chem. Chem. Phys*. 2000, *2*, 3765-3772.

Minakata, D.; Li, K.; Westerhoff, P.; Crittenden, J. Development of a group contribution method to predict aqueous phase hydroxyl radical (HO•) reaction rate constants. *Environ. Sci. & Technol*. 2009, *43*, 6220-6227.

Møller, C.; Plesset, M.S. Note on an approximation treatment for many-electron systems. *Phys. Rev*. 1934, *46*, 618-622.

Montgomery, J.A.; Frisch, M.J. A complete basis set model chemistry. VI. Use of density functional geometries and frequencies. *J. Chem. Phys.* 1999, *110*(6), 2822-2827.

Montgomery, J.A.; Frisch, M.J.; Ochterski, J.W. A complete basis set model chemistry. VII. Use of the minimum population localization method. *J. Chem. Phys.* 2000, *112*(15), 6532-6542.

Nicolaescu, A.R.; Wiest, O.; Kamat, P. Mechanistic pathways of the hydroxyl radical reactions of quinoline. 2. Computational analysis of hydroxyl radical attack at C atoms. *J. Phys. Chem. A*. 2005, *109*, 2829-2835.

Nyden, M.R.; Perterson, G.A. Complete basis set correlation energies. I. The asymptotic convergence of pair natural orbital expansions. *J. Chem. Phys.* 1981, *75*(*4*), 1843- 1862.

Ochterski J.W.; Peterson, G.A. A complete basis set model chemistry. V. Extensions to six or more heavy atoms. *J. Chem. Phys.* 1996*, 104*(7), 2598-2619.

Ochterski, J. W., Thermochemistry in Gaussian, Gaussian, Inc., 2000.
on workstation computers: The program system Turbomole. *Chem. Phys. Lett*., 1989, *162*(3), 165-169

Papasavva, S.; Illinger, K. H.; Kenny, J. E., Ab initio calculations on fluoroethanes: Geometries, dipole moments, vibrational frequencies, and infrared intensities, *J. Phys. Chem*., 1996, *100*, 10100-10110.

Parkinson, C. J., P. M. Mayer, and L. Radom, An assessment of theoretical procedures for the calculation of reliable radical stabilization energies, *J. Chem. Soc., Perkin Trans. 2*, 1999, 2305-2313.

Parthiban, S.; Martin, J. M. L. Assessment of W1 and W2 theories for the computation of electron affinities, ionization potentials, heats of formation, and proton affinities. *J. Chem. Phys*. 2001, *114*(14), 6014-6029.

Peng, C.; Ayala, P.Y.; Schlegel, H.B.; Frisch, M.J. Using redundant internal coordinates to optimize equilibrium geometries and transition states. *J. Comp. Chem. 1996, 17, 49-86.*

Peng, C.; Schlegel, H.B. Combining Synchronous Transit and Quasi-Newton Methods for Finding Transition States. *Israel J. Chem*. 1993, *33,* 449-54.

Pfaendtner, J.; Broadbelt, L. J. Elucidation of structure-reactivity relationships in hindered phenols via quantum chemistry and transition state theory. *Chem. Eng. Sci.* 2007, *62*, 5232-5239.

Pfaendtner, J.; Broadbelt, L. J. Mechanistic modeling of lubricant degradation. 2. The autooxidation of decane and octane. *Ind. Eng. Chem. Res*. 2008, *47*, 2897-2904.

Pfaendtner, J.; Broadbelt, L. J. Mechanistic modeling of lubricant degradation. 1. Structure-reactivity relationships for free-radical oxidation. *Ind. Eng. Chem. Res*. 2008, *47*, 2886-2896.

Pitzer, K.S.; Gwinn, W. Energy levels and thermodynamic functions for molecules with internal rotation. *J. Chem. Phys*. 1942, *10*, 428-440.

Pople, J. A.; Scott, A.P.; Wong, M.W.; Radom, L., Scaling factors for obtaining fundamental vibrational frequencies and zero-point energies from HF/6-31g* and MP2/6-31g* harmonic frequencies, *Is. J. Chem*., 1993, *33*, 345-350.

Pople, J.A.; Gordon, M.H.; Fox, D.J. Gaussian-1 theory: A general procedure for prediction of molecular energies. *J. Chem. Phys.* 1989, *90*(10), 5622-2629.

Pramod, G.; Prasanthkumar, K.P.; Mohan, H.; Manoj, V.M.; Manoj, P.; Suresh, C.H.; Aravindakumar, C.T. Reaction of hydroxyl radicals with azacytosines: A pulse radiolysis and theoretical study. *J. Phys. Chem. A*. 2006, *110*, 11517-11526.

Pu, J.; Gao, J.; Truhlar, D.G. Multidimensional tunneling, recrossing, and the transmission coefficient for enzymatic reactions. *Chem. Rev*. 2006, *106*, 3140-3169.

Purvis III, G.D.; Bartlett, R.J. A full coupled-cluster singles and doubles model: The inclusion of disconnected triples. *J. Chem. Phys*. 1982, *76*(4), 1910-1918.

Rauk,A.; Boyd, R.J.; Boyd, S.L.; Henry, D.J.; Radom, L. Alkoxy radicals in the gaseous phase: β-scission reactions and formation by radical addition to carbonyl compounds. *Can.J.Chem*. 2003, *81*, 431-442.

Richardson, S. D. Water Analysis: Emerging contaminants and current issues. *Anal. Chem*., 2009, *81*, 4645-4677.

Rosenfeldt, E.J.; Linden, K.G. Degradation of endocrine disrupting chemicals bisphenol A, ethinyl estradiol, and estradiol during UV photolysis and advanced oxidation processes. *Environ. Sci. Technol*. 2004, *38*, 5476-5483.

Saeys, M.; Reyniers, M-F.; Marin, G.B.; Speybroeck, V.V.; Waroquier, M. Ab initio calculations for hydrocarbons: Enthalpy of formation, transition state geometry, and activation energy for radical reactions. *J. Phys. Chem. A*. 2003, *107*, 9147-9159.

Schlegel, H.B. Optimization of equilibrium geometries and transition structures. *J. Comp. Chem.* 1982, *3*(2), 214-218.

Sheng, L.; Li, Z.-S.; Xiao, J.-F.; Liu, J.-Y.; Huang, X.-R.; Sun, C.-C., Direct ab initio dynamics studies on hydrogen-abstraction reactions of 1,1,1-trifluoroethane with hydroxyl radical, *Chem. Phys.,* 2002, *282*, 1-8.

Štefanić, I.; Ljubić, M.; Bonifačić, M.; Sabljić, A.; Asmus, K.-D. A surprisingly complex aqueous chemistry of the simplest amino acid. A pulse radiolysis and theoretical study on H/D kinetic isotope effects in the reaction of glycine anions with hydroxyl radicals. *Phys. Chem. Chem. Phys*. 2009, *11*, 2256-2267.

Still, W.C.; Tempczyk, A.T.; Hawley, R.C.; Hendrickson, T. Semianalytical treatment of solvation for molecular mechanics and dynamics. *J. Am. Chem. Soc*., 1990, *112*(16), 6127-6129.

Sumathi, R.; Carstensen, H.-H.; Green, Jr. W.H. Reaction rate prediction via group additivity part 1: H abstraction from alkanes by H and CH3. *J. Phys. Chem. A*. 2001, *105*, 6910-6925.

Sumathi, R.; Carstensen, H.-H.; Green, Jr. W.H. Reaction rate prediction via group additivity part 2: H abstraction from alkanes, alkynes, alcohols, aldehydes, and acid by H atoms. *J. Phys. Chem. A*. 2001, *105*, 8969-8984.

Sumathi, R.; Carstensen, H.-H.; Green, Jr. W.H. Reaction rate prediction via group additivity part 3: Effect of substituents with CH2 as the mediator. *J. Phys. Chem. A*. 2002, *106,* 5474-5489.

Sun, W.; Saeys, M. First principles study of the reaction of formic and acetic acids with hydroxyl radicals. *J. Phys. Chem. A*. 2008, *112*, 6918-6928.

Tomasi, J.; Mennucci, B.; Cammi, R. Quantum mechanical continuum solvation models. *Chem. Rev*. 2005, *105*, 2999-3093.

Truhlar, D.; Garrett, B.C. Variational transition-state theory. *Acc.Chem.Res*. 1980, *13*, 440-448.

Truong, T. N., Truhlar, D. G., Ab initio transition-state theory calculations of the reaction-rate for OH + CH4 -> H2O + CH3, *J. Chem. Phys*., 1990, *93*, 3, 1761-1769.

Truong, T.N. Reaction class transition state theory: Hydrogen abstraction reactions by hydrogen atoms as test cases. *J. Chem. Phys*. 2000, *113*(12), 4957-4964.

Truong, T.N.; Duncan, W.T.; Tirtowidjojo, M. A reaction class approach for modeling gas phase reaction rates. *Phys, Chem. Chem. Phys*., 1999, *1*, 1061-1065.

Tzima, T.D.; Papavasoleiou, K.D.; Papayannis, D.K.; Melissas, V.S. Theoretical kinetic study of the CH3Br + OH atmospheric system. *Chem. Phys*. 2006, *324*, 591-599.

Urata, S., Takada, A.; Uchimaru, T.; Chandra, A. K., Rate constants estimation for the reaction of hydrofluorocarbons and hydrofluoroethers with OH radicals, *Chem. Phys. Lett*., 2003, *368*, 215-223.

Van Cauter, K.; Van Speybroeck, V.; Vansteenkiste, P.; Reyniers, M. F.; Waroquier, M. Ab initio study of free-radical polymerization: Polyethylene propagation kinetics. *Chem. Phys. Chem* 2006, *7*, 131-140.

Westerhoff, P.; Yoon, Y.; Snyder, S.; Wert, E. Fate of endocrine-disruptor, pharmaceutical, and personal care product chemicals during simulated drinking water treatment processes. *Environ. Sci. Technol*. 2005, *39*, 6649-6663.

Wigner, E. Z. *f. physic. Chemie* B19, 203, 1932.

Wilke, C.R.; Chang, P.C. Correlation of diffusion coefficients in dilute solutions. *AIChEJ*., 1955, *1*, 264-270.

Wong, M. W., Vibrational frequency prediction using density functional theory, *Chem. Phys*. *Lett*., 1996, 256, 391-399.

Wood, G.P.F.; Easton, C.J.; Rauk, A.; Davies, M.; Radom, L. Effect of side chains on competing pathways for β-scission reactions of peptide-backbone alkoxyl radicals. *J.Phys.Chem. A*. 2006, *110*, 10316-10323.

Wood, G.P.F.; Rauk, A.; Radom,L. Modeling β-scission reactions of peptide backbone alkoxy radicals: Backbone C-C bond fission. *J.Chem.Theory Comput*. 2005, *1*, 889-899.

Xu, S.; Lin, M.C. Theoretical study on the kinetics for OH reactions with CH3OH and C2H5OH. *Proceedings of the combusion institute*. 2007, *31*, 159-166.

Zhang, X..-H. Ding, Z.-S. Li, X.-R. Huang, and C.-C. Sun, Accurate ab initio calculations on the rate constants of the direct hydrogen abstraction reaction C2H + H2-> C2H2 + H, *J. Phys. Chem. A*, 2000, *104*, 8375-8391.

Zheng, X.; and Blowers, P., The application of composite energy methods to n-butyl radical β-scission reaction kinetic estimations, *Theor. Chem. Acc*., 2007, *117*, 207-212.

Zheng, X.; Blowers, P. A first principle kinetic modeling of the 1-chloroethyl unimolecular decomposition reaction, *Industrial & Engineering Chemistry Research*, 2006, *45*, 2981-2985.

Zheng, X.; Blowers, P. The investigation of hydrocarbon cracking reaction energetics with composite energy methods, *Molecular Simulation*, 2005, *31*(14-15), 979-986.

Zhong, X. and J. W. Bozzelli, Thermochemical and kinetic analysis on the addition reactions of H, O, OH, and HO2 with 1,3-cyclopentadiene, *Int. J. Chem. Kinet*., 1997, 29, 893-913.

Zhu, L., J. W. Bozzelli, and W.-P. Ho, Reaction of OH radical with C2H3Cl: rate constant and reaction pathway analysis, *J. Phys. Chem. A,* 1999, *103*, 7800-7810.

Zhu, T.; Li, J.; Hawkins, G.D.; Cramer, C.J.; Truhlar, D.G. Density functional solvation model based on CM2 atomic charges. *J. Chem. Phys*. 1998, *109*(20), 9117-9133.

CHAPTER 4

Quantitative Understanding of Aqueous Phase Hydroxyl Radical Reactions with Haloacetate Ions: Experimental and Theoretical Studies

†*work from this chapter will be presented and plan to be published in the following citation:*

Minakata, D.; Crittenden, J. Linear Free Energy Relationship (LFER) for the Aqueous Phase Hydroxyl Radical (HO•) Reactions with Ionized Species: Experimental and Theoretical Studies. 240th American Chemical Society (ACS) National Meeting & Exposition, Boston, Massachusetts. August 22-26, 2010.

Minakata, D.; Li, K.; Crittenden, J.C. Rational Design of Advanced Oxidation Processes using Computational Chemistry. The 16th International Conference on Advanced Oxidation Technologies for Treatment of Water, Air and Soil (AOTs-16). Novermber 15-18, 2010. San Diego, California.

Minakata, D.; Song, W.; Crittenden, J.C. Temperature-dependent aqueous phase hydroxyl radical reaction rate constants with ionized compounds: Experimental and theoretical studies. *Environ. Sci.Technol.* 2010. In preparation.

Minakata, D.; Song, W.; Crittenden, J.C. Group Contribution Method for Aqueous Phase Hydroxyl Radical Reaction Rate Constant Prediction: Update and Experimental Verification. *Environ. Sci.Technol.* 2010. In preparation.

4.1 Abstract

Hydroxyl radical (HO•) is a highly reactive electrophile that potentially leads to complete mineralization of emerging contaminants in aqueous phase advanced oxidation processes (AOPs). Widespread usage and adverse human and ecological effect of halogenated and carboxylic compounds are of great concern. These compounds are major intermediates and byproducts from the reactions of HO• with many organic contaminants and indicate lower reactivity with HO• in aqueous phase AOPs. As a consequence, quantitative understanding in their reactions is necessary. In addition, considering deprotonated ionized state of these carboxylic compounds at around neutral pH, we need to verify if our previously established linear free energy relationships for neutral compounds can be applied to ionized compounds for our ultimate goal of establishing a mechanistic model.

We measured temperature-dependent aqueous phase HO• reaction rate constants for a series of halogenated acetates using electron-pulse radiolysis technique and calculated thermochemical properties from Arrhenius activation energies and frequency factors. We developed linear free energy relationships from logarithms of the HO• reaction rate constants and free energies of activation that were obtained at several temperatures. The free energy of activation was compared to quantum mechanically calculated values that were obtained by *Ab initio* quantum mechanical calculations using G4 with the SMD solvation model. Theoretical investigations based on quantum mechanical methods provide quantitative understandings of effects that result from halogenated functional groups and hydrogen bonding in the process of solvation. We found that quantum mechanical calculations can predict the aqueous phase free energies

of activation accurately and this may allow us to predict reaction rate constants for unknown compounds that have not been examined experimentally.

4.2 Introduction

The hydroxyl radical (HO•) is a highly reactive electrophile that reacts rapidly and nonselectively with most electron-rich sites on organic contaminants. The HO• potentially leads to complete mineralization of emerging contaminants in advanced oxidation processes (AOPs) (e.g., O_3/H_2O_2, UV/H_2O_2, UV/TiO_2) and natural waters (Westerhoff et al., 2005; Huber et al., 2003; Rosenfeldt and Linden, 2004). Among emerging contaminants, halogenated compounds are of serious concern (Eljarrat and Barceló, 2003; Woo et al., 2002; Eisenberg and Mckone, 1998) due to the widespread usage in industries and unknown adverse human and ecological effects. In particular, halogenated acetates are one of the major intermediates and byproducts that are appeared in AOPs at around neutral pH because of their lower reactivity with active radical species. However, due to the lack of understandings in detailed reactivity of these compounds with HO• (Fliount et al., 1997) and almost no experimental studies in examining Arrhenius kinetic parameters, there is no tool to predict the intermediates and products, and assess their human health effects based on thermochemical property and reaction kinetics. Accordingly, there is a need to investigate the detailed reactivity and develop a mechanistic model (Pfaendtner and Broadbelt, 2008) that can quickly assess their removal efficacy by AOPs.

A mechanistic model to evaluate the performance in AOPs includes the three critical components: (1) numerical methods that solve ordinary differential equations (ODEs), (2) algorithms that can predict reaction pathways, and (3) algorithms that can

predict reaction rate constants. The DGEAR algorithm (Hindmarsh and Gear, 1974) successfully solved the ODEs for the UV/H_2O_2 kinetic models (Li et al., 2008; 2007; 2004; Crittenden et al., 1999). A reaction pathway generator for the aqueous phase AOPs was developed (Li and Crittenden, 2009). A group contribution method (GCM) has been recently developed (Minakata et al., 2009) to predict the aqueous phase HO• reaction rate constants for compounds with a wide range of functional groups in the datasets.

Because the GCM assumes that a functional group has approximately the same interaction properties under a given molecule, it disregards the changes of the functional group properties that can arise from the intramolecular environment by electronic push-pull effects, or by intramolecular hydrogen bond formation, or by steric effects. It is expected that these intramolecular electron-interactions might be very different between the gaseous and aqueous phases, and therefore, solvation effect that results from the surrounding water molecules should be considered for the aqueous phase reactions. Accordingly, it is customary to seek a linear relation between a reaction energy accounting solvation and the logarithm of the rate constant for reaction (Partington, 1951; Beckwith et al., 1992; Wold and Sjöström, 1978). We have developed linear free energy relationships (LFERs) between logarithms of the literature-reported HO• reaction rate constants and quantum mechanically calculated aqueous phase free energies of activation for neutral compounds for H-atom abstraction by HO• from a C-H bond and HO• addition to unsaturated C=C double bond (Minakata and Crittenden, 2010). The calculated free energies of activation in the aqueous phase were within ±4.0 kcal/mol of those that were estimated from experimentally obtained Arrhenius activation energy and frequency factors.

When it comes to ionized compounds for aqueous phase molecular modeling, one must notice that the magnitudes of solvation free energies are much larger than those for the neutral compounds (Liu et al., 2010; Marenich et al., 2009; Kelly et al., 2006). The majority of the free energy of solvation is dominated by large electrostatic contributions (Marenich et al., 2009). In particular, the polarizability that results from the charge distribution at the transition state significantly changes the dipole moment and affects the process of solvation as compared to the viscosity or internal pressure (Tanko and Suleman, 1996). The large electrostatic contribution includes short-range and nonbulk electrostatics, as well as cavitation, exchange repulsion, dispersion, and disruption or formation of the nearby solvent structure (Marenich et al., 2009). Accordingly, entropy changes that arise from the solvent structure effect may be significant (Warren and Mayer, 2010; Mader et al., 2007). Because a pure dielectric continuum model (Cossi et al., 2003; Tomasi and Persico, 1994) includes only long range solute-solvent interaction in the bulk phase (Marenich et al., 2009) but the short-range and nonbulk electrostatics, the dielectric continuum model do not treat satisfactorily with the solvation process for ionized compounds.

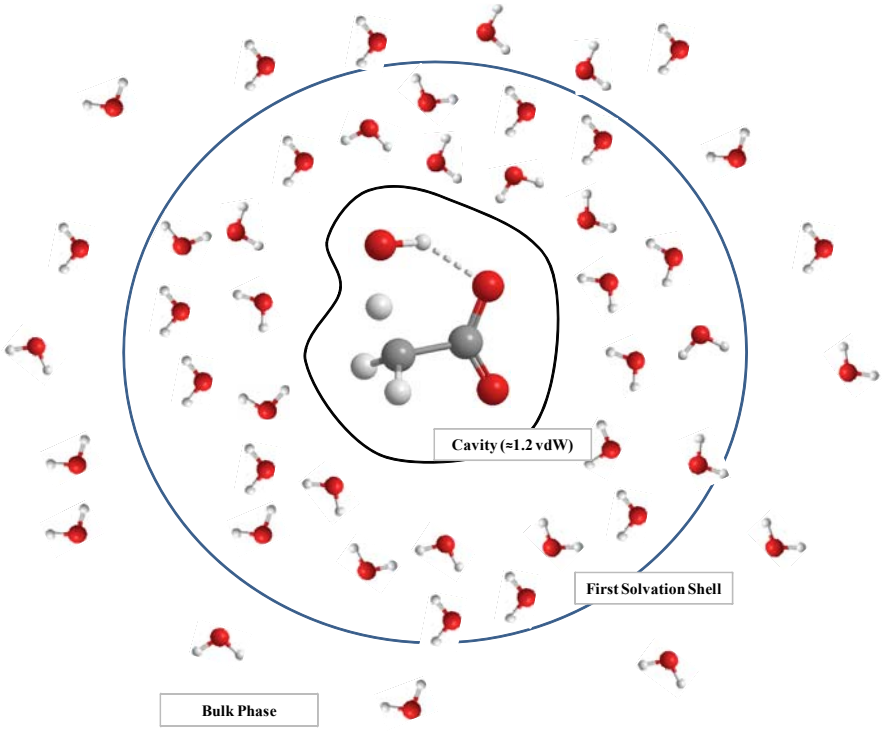

Figure 4.1: Schematic picture of waters distributed in the cavity, first solvation shell and bulk phase for transition state for the reaction of HO• with acetate. Dotted line represents the hydrogen bond.

In addition to the difficulties in molecular modeling for the ionized compounds, the effects of functional groups (e.g., halogen atoms and deprotonated carboxylate) are not thoroughly elucidated yet (Aquino et al., 2002). For example, because of their strong electron-withdrawing ability and larger atom size of halogen atoms, there is a qualitative agreement that the halogenated functional groups decrease the overall reactivity of HO• in particular for the H-atom abstraction from a C-H bond (Minakata et al., 2009; Lal et al., 1988; Neta et al., 1969). For the carboxylic functional groups in the aqueous phase, formation of H-bond (i.e., short-range intermolecular interactions between water molecules and carboxylate functional group) can be expected to affect the overall reactivity significantly.

Not many experimental efforts have investigated the effect of solvation associated with the reaction energy and validate the quantum mechanically calculated thermochemical properties. Hermann's group and Monod et al. (2005) have reported the temperature-dependent aqueous phase HO• rate constants and thermochemical properties for various oxygenated compounds (Gligorovski, et al., 2009; Gligorovski and Herrmann, 2004; Herrmann et al., 2003, Ervens et al., 2005). Their data compilation is for atmospheric chemistry, and therefore, there is a significant lack of data for the aqueous phase contaminants (e.g., halogenated compounds, and ionized compounds). Fliout et al (1997) experimentally investigated the fate of halogenated acetate radicals (•CBr_2COO- and •CCl_2COO-) and reactivity with other carbon centered radicals. They did not examine the thermochemical properties for these reactions. It is noted that the Arrhenius activation energy is obtained by the slope of logarithm of the reaction rate constant as a function of an inverse of temperature. Accordingly, obtaining the accurate thermochemical properties based on the Arrhenius parameters requires one careful investigation in the temperature using reliable methodology. It is commonly observed that the literature-reported E_a and A are scarce due to the diversity of the methodologies (Buxton et al., 1988).

In this study, temperature-dependent HO• reaction rate constants in the aqueous phase will be measured to obtain thermochemical properties for a series of halogenated acetates. Theoretical studies based on quantum mechanical methods will be conducted to reveal the function of halogenated functional groups toward the HO• reactivity and hydrogen bonding in the combination of explicit and implicit solvation model. The

experimentally obtained thermochemical properties will be compared with those that will be calculated based on the *Ab initio* quantum mechanical approaches.

4.3 Methods

4.3.1 Experimental

It is known that electron-pulse radiolysis coupled with standard time-resolved detection method is able to deliver reproducibility a short burst of energy as a function of nano- to micro-seconds that induces ionization and excitation among fast-kinetic studies in chemistry (von Sonntag and Schuchmann, 1997). In the past several decades, electron-pulse radiolysis has been used for measuring the uni-/bi-molecular reaction rate constants for various reactions that are induced by radical compounds (Buxton et al., 1988; Bielski and Cabelli, 1991). Followings are descriptions about the linear accelerator for the electron-pulse radiolysis, setup and experimental procedure.

4.3.1.1 Linear Accelerator (LINAC)

The linear accelerator (LINAC) electron pulse radiolysis system at the Radiation Laboratory, University of Notre Dame (NDRL) (Whitman et al., 1995) was used for determining all HO• reaction rate constants. Figure 4.2 represents the overall system of the LINAC that is comprised of electron accelerator, light source, sample flow cell, sample solution and data acquisition computer.

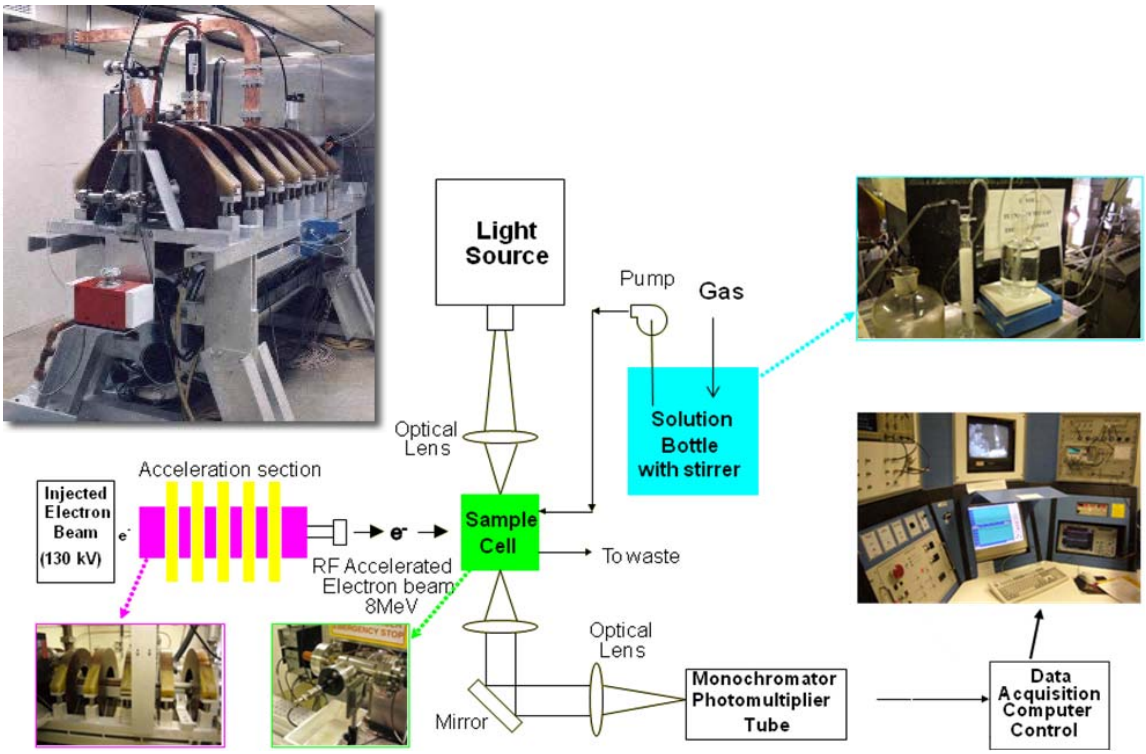

Figure 4.2: Overall system of Linear Electron Accelerator (LINAC)

This system has the following features (Whitman et al., 1995): (1) the system is designed to have very repeatable shot with low pre and post pulse radiation and give reproducible data, (2) the system has a ceramic envelope that is capable of withstanding 150 kV DC in air, stainless steel electrodes and vacuum parts, (3) the injector gun is followed by a high vacuum tee with ion pump, and isolation vacuum valve and a fast beam current monitor, (4) the accelerator is a 2 pi/3 mode, temperature stabilized guide with a tapered velocity buncher, (5) in order to maintain dose repeatability with ±1% between single pulse taken up to 30 minutes apart, the electron gun HV and control voltages and the PFN firing level are stabilized prior to triggering the pulse, (6) a water cooling system is employed to maintain the beam centerline components at 40±4°C. This system is also able to remove the heat from the klystron, modulator, and magnetic. The specification of the system is

2586 mHz of frequency and 18 mW maximum of input power. For the steady state operation, the system has 1.5 second of beam pulse width, 2 A of peak beam current and 6 MeV of energy. For the stored energy operation, the system ranges from 2 ns to 10 ns of beam pulse width, 4 A of beam current, 8 MeV of energy, less than 10 pC of dark current, ±100 pS of pulse jitter and ±1% of dose stability (i.e., pulse to pulse) (Hug et al., 1999; Asmus 1984; von Sonntag and Schuchmann 1997). The accuracy of an individual radiation chemical experiment is generally considered to be about plus and minus 10%. Numerical values for a specific yield or rate constant are always obtained for at least three different scavenger concentrations. Error margins for the mean of such a serides of single measurements never exceed 3% (von Sonntag, 1987).

4.3.1.2 Flow Cell

The 10 mm of quartz flow cell is located at the center of electron beam. The flow rate can be adjusted from 1 mL/min to 10 mL/min. Through the experiments the setup of the flow rate was 3 mL/min. Each pulse radiation was 2 ns and the spectra were recorded up to 100 μs. The flux of the solution was 3 cm/min. The solution moved 5×10^{-6} cm in 100 μs. When comparing to the electron irradiation diameter (i.e., 0.5 cm), we assumed that the solution was not replaced during the 100 μs of pulse radiation. All experimental data were taken by averaging 15 replicate pulses. The interval time of every pulse was 1.0 min, and therefore, the degradation products should be removed at the 3 ml/min of flow rate.

4.3.1.3 Radiolysis of Water

When water is irradiated by a fast electron injected from an accelerator, water is ionized immediately at approximately 10^{-16} seconds followed by the subsequent reactions (Buxton et al., 1988; Spinks and Woods, 1964; Schwarz, 1962):

$$H_2O \xrightarrow[\text{radiation}]{\text{ionization}} H_2O\bullet^{\oplus} + e^{-} \tag{4.1}$$

$$H_2O\bullet^{\oplus} \rightarrow HO\bullet + H^{\oplus} \tag{4.2}$$

$$e^{-} \xrightarrow{H_2O} e^{-}_{aq} \tag{4.3}$$

$$H_2O^{*} \rightarrow H\bullet + HO\bullet \tag{4.4}$$

$$H\bullet + H\bullet \rightarrow H_2 \tag{4.5}$$

$$e^{-}_{aq} + e^{-}_{aq} \rightarrow H_2 + 2HO^{-} \tag{4.6}$$

$$HO\bullet + HO\bullet \rightarrow H_2O_2 \tag{4.7}$$

$$e^{-}_{aq} + O_2 \rightarrow O_2\bullet^{-} \tag{4.8}$$

$$H\bullet + O_2 \rightarrow HO_2\bullet \tag{4.9}$$

Initial radiolysis products are produced via spur expansion and reactions. With expansions of spur via diffusion, a fraction of the compounds reacts together. In water, 10^{-7} second is the lifetime of a radical reacting at the diffusion-controlled state when the concentration of the solute is 10^{-3} mole/L. The overall stoichiometry (Buxton et al., 1988; Spinks and Woods, 1964) at 10^{-5} second (for the pH range from 3 to 11) is shown in equation.

$$H_2O \xrightarrow[\text{radiation}]{\text{ionization}} 0.27\, e^{-}_{aq} + 0.06\, H^{\oplus} + 0.28\, HO\bullet + 0.05\, H_2 + 0.07\, H_2O_2 + 0.27 H_3O^{\oplus} \tag{4.10}$$

The numbers are the *G* values for species production and the *G* is defined in μmol/J. Total radical concentrations that are produced by the pulse radiolysis are typically 2-4

μM. To exclude the other radical species but HO• at near neutral pH, all solutions are saturated with gaseous N_2O (~ 24.5 mM) to quantitatively convert the hydrated electrons and hydrogen atoms that are formed into this radical (Buxton et al., 1988):

$$e^-_{(aq)} + N_2O + H_2O \rightarrow N_2 + OH^- + HO\bullet \quad (4.11)$$

$$H\bullet + N_2O \rightarrow HO\bullet + N_2 \quad (4.12)$$

Reaction rate constants for reactions (4.11) and (4.12) are 9.1×10^9 $M^{-1}s^{-1}$ and 2.1×10^6 $M^{-1}s^{-1}$, respectively (Buxton et al., 1988). At around neutral pH, the reaction (4.12) is several magnitude of order slower than other reactions, and therefore, is not complete on typical measurement timescales. Furthermore, hydrogen atom also reacts with the added SCN^- ($k = 2.3 \times 10^8$ $M^{-1}s^{-1}$, $t_{1/2} \approx 90$ μs, Mezyk and Bartels, 2005) to produce $H(SCN)_2^{-\bullet}$ (Elliot et al., 1988) following by CN• at around neutral pH and $(SCN)_2^{\bullet-}$ (Martin et al., 2008). However, while these reactions occur, the reaction (4.12) (i.e., N_2O pathway) is dominant and constant fraction (8-10%, Martin et al., 2008) of the initially produced hydrogen atoms are ensured to be converted to HO•. Accordingly, these side reactions should not affect main reactions for competition kinetics (see below) significantly.

The advantage of radiolysis method over other methods results in the fact that there is proportional relationship between the amount of energy absorbed by any component of the system and its electron fraction. As a result, in the dilute aqueous solution, all the energy is absorbed by the water and the yields of the primary radicals are always confirmed.

4.3.1.4 Competition Kinetics

Competition kinetics was used in pulse radiolysis when neither the primary radical nor the reaction product can be obtained directly. In two separate solutions, HO• reacts with each solution producing its product:

$$\mathrm{HO}\bullet + \mathrm{S}_1 \xrightarrow{k_1} \mathrm{P}_1 \tag{4.13}$$

$$\mathrm{HO}\bullet + \mathrm{S}_2 \xrightarrow{k_2} \mathrm{P}_2 \tag{4.14}$$

From each reaction, the decay of the solution S_1 and S_2 can be expressed as below:

$$-\frac{d[\mathrm{S}_1]}{dt} = k_1[\mathrm{S}_1][\mathrm{HO}\bullet] \tag{4.15}$$

$$-\frac{d[\mathrm{S}_2]}{dt} = k_2[\mathrm{S}_2][\mathrm{HO}\bullet] \tag{4.16}$$

Integration of equations (4.15) and (4.16) from time 0 to time *t* yields:

$$\int_0^t \frac{d[\mathrm{S}_1]}{[\mathrm{S}_1]} = \int_0^t \frac{k_1}{k_2}\frac{d[\mathrm{S}_2]}{[\mathrm{S}_2]} \tag{4.17}$$

$$\Leftrightarrow \ln\left(\frac{[\mathrm{S}_1]_0}{[\mathrm{S}_1]_t}\right) = \frac{k_1}{k_2}\ln\left(\frac{[\mathrm{S}_2]_0}{[\mathrm{S}_2]_t}\right) \tag{4.18}$$

When the HO• reaction rate constant with S_2, k_2, is known, k_1 will be obtained by plotting the decay of both S_1 and S_2 concentration.

In practical manner, if there is no significant transient absorbance over the range from 250 – 800 nm, competition kinetics with use of thiocyanate ion (SCN^-) is effective. SCN^- ion reacts with HO• forming radical ion $(SCN)_2^{\bullet-}$. The reactions that are involved in the competition kinetics are as below:

$$\mathrm{HO}\bullet + \mathrm{X} \rightarrow \text{products} \tag{4.19}$$

$$\mathrm{HO}\bullet + \mathrm{SCN}^- \rightarrow (\mathrm{HOSCN})^{\bullet-} \tag{4.20}$$

$$(HOSCN)^{\bullet-} \rightarrow \bullet SCN + OH^- \quad (4.21)$$

$$\bullet SCN + SCN^- \rightarrow (SCN)_2^{\bullet-} \quad (4.22)$$

$(SCN)_2^{\bullet-}$ indicates the strong absorbance at wavelength of 472 nm (Milosavljevic et al., 2005). The second order reaction rate constant of hydroxyl radical with $(SCN)_2^{\bullet-}$ is known as 1.05×10^{10} $M^{-1}s^{-1}$ (Buxton et al., 1988). We can obtain the following relations from the reaction rates:

$$[HO\bullet + SCN^-] : [HO\bullet + X] = k_2 [SCN^-] : k_1 [X] = A_{[SCN^-]+[X]} : (A_{[SCN^-]} - A_{[SCN^-]+[X]}) \quad (4.23)$$

$$\frac{1}{A_{[SCN^-]+[X]}} = \frac{1}{A_{[SCN^-]}} + \frac{k_1[X]}{A_{[SCN^-]}k_2[SCN^-]}$$
$$\Leftrightarrow \frac{A_{[SCN^-]}}{A_{[SCN^-]+[X]}} = 1 + \frac{k_1[X]}{k_2[SCN^-]} \quad (4.24)$$

Therefore, the following relationship can be obtained:

$$\frac{\left[(SCN)_2^{\bullet-}\right]_0}{\left[(SCN)_2^{\bullet-}\right]} = 1 + \frac{k_1[X]}{k_2[SCN^-]} \quad (4.25)$$

where $\left[(SCN)_2^{\bullet-}\right]_0$ is the absorbance of blank solution. $\left[(SCN)_2^{\bullet-}\right]$ is the absorbance obtained in the presence of compound *X*. The [X] is the concentration of compound *X*. $[SCN^-]$ is the concentration of thiocyanate ion.

4.3.1.5 Procedures

All chemicals that were used for the reaction rate constant measurements were of the highest purity available (>99%) and used as received. Solutions of these chemicals were made by a Millipore Milli-Q system. All solutions were continuously sparged with high-purity N_2O gas to remove dissolved oxygen. The SCN^- solution that was used for all experiments was 0.3 mM with 20 mM of buffer solution at pH = 6.9-7.0. The

temperature of solution was severely controlled using water baths that have the heating unit, and both solution and water bath temperatures were continuously monitored with the thermostat during the experiments. The measurements were repeated 15 times to obtain each absorbance at each dose. At each concentration, the 15 times measurement at the same dose was repeated 4 times to obtain average value.

4.3.1.6 Thermochemical Properties

According to the transition state theory (TST) (Eyring, 1935), the reaction rate constant can be expressed in equation (4.24) using thermochemical properties at the transition state (i.e., free energy, entropy, and enthalpy of activation, respectively).

$$k = \frac{\kappa T}{h} \exp\left(\frac{-\Delta G_{\text{rxn}}^{\text{act}}}{RT}\right) = \frac{\kappa T}{h} \exp\left(\frac{-\Delta S_{\text{rxn}}^{\text{act}}}{R}\right) \exp\left(\frac{-\Delta H_{\text{rxn}}^{\text{act}}}{RT}\right) \tag{4.26}$$

where k is reaction rate constant, $M^{-1}s^{-1}$, κ is Boltzman constant, T is absolute temperature, h is plank constant, R is universal gas constant, and $\Delta G_{\text{rxn}}^{\text{act}}$, $\Delta S_{\text{rxn}}^{\text{act}}$ and $\Delta H_{\text{rxn}}^{\text{act}}$ are free energy, entropy and enthalpy of activation (Pu et al., 2006) that are obtained from the experiments, respectively. The equation (4.26) above represents the difference in the respective thermodynamic properties between the transition state and the reactants, when all are in their standard states (i.e., at unit concentration). It should be noted that the thermodynamic properties associated with the transition state are more numerous and complicated. Putting logarithm of both side of equation (4.26) yields the equation (4.27), and the left side of this equation equals to E_a/RT from the Arrhenius equation.

$$\ln k = \ln \frac{\kappa}{h} + \ln T + \ln K^{\neq} \tag{4.27}$$

According to the Clapeyron equation shown in the equation (4.28), the experimental Arrhenius activation energy, E_a, relates to the internal energy of activation ΔE^{act} and enthalpy of activation ΔH^{act}

$$\frac{d \ln k}{dT} = \frac{1}{T} + \frac{d \ln K^{\neq}}{dT} \tag{4.28}$$

$$E_a = \Delta E^{act} + RT \tag{4.29}$$

Because the internal energy, ΔE, is expressed in equation (4.30), the internal energy of activation can be approximately equal to the enthalpy of activation assuming that the volume of activation, ΔV^{act}, is nearly zero in solution.

$$\Delta E = \Delta H - P\Delta V = \Delta H - \Delta nRT \tag{4.30}$$

As a consequent, experimental Arrhenius activation energy can be expressed in equation (4.31):

$$E_a = \Delta H_{rxn}^{act} + RT \tag{4.31}$$

From the equation (4.31) and Arrhenius expression, the Arrhenius frequency factor can be expressed in the following equation (4.32):

$$A = \frac{e\kappa T}{h} \exp\left(\frac{-\Delta S_{rxn}^{act}}{R}\right) \tag{4.32}$$

where $e = 2.72$

The ΔG_{rxn}^{act}, can be calculated as below:

$$\Delta G_{rxn}^{act} = \Delta H_{rxn}^{act} - T\Delta S_{rxn}^{act} \tag{4.33}$$

4.3.2 Group Contribution Method

The detailed descriptions of group contribution method (GCM) can be found in our previously published paper (Minakata et al., 2009). In short, according to the GCM, the rate constant for H-atom abstraction, k_{abs}, can be written in equation (4.34)

$$k_{\text{abs}} = 3\sum_{0}^{I} k_{\text{prim}}^{0}\ X_{\text{R}_1} + 2\sum_{0}^{J} k_{\text{sec}}^{0} X_{\text{R}_1} X_{\text{R}_2} + \sum_{0}^{K} k_{\text{tert}}^{0}\ X_{\text{R}_1} X_{\text{R}_2} X_{\text{R}_3} + k_{\text{R}_4} \tag{4.34}$$

where, I, J, and K denote the number of the fragments CH_3R_1, CH_2R_2, and $CHR_1R_2R_3$, respectively, k_{prim}^{0}, k_{sec}^{0}, and k_{tert}^{0} are the group rate constants that represent H-atom abstraction from the primary, secondary, and tertiary C-H bond as expressed in equations (4.35)-(4.37).

$$k_{\text{prim}}^{0} = A_{\text{prim}}^{0} e^{-\frac{E_{a,\text{prim}}^{0}}{RT}} \tag{4.35}$$

$$k_{\text{sec}}^{0} = A_{\text{sec}}^{0} e^{-\frac{E_{a,\text{sec}}^{0}}{RT}} \tag{4.36}$$

$$k_{\text{tert}}^{0} = A_{\text{tert}}^{0} e^{-\frac{E_{a,\text{tert}}^{0}}{RT}} \tag{4.37}$$

k_{R_4} is defined for the HO• interaction with the functional group R_4 (e.g., -OH and -COOH). The group contribution factor, X_{R_i}, that represents the influence of functional group R_i is defined in equation (4.38).

$$X_{\text{R}_i} = e^{-\frac{E_{a,\text{abs}}^{\text{R}_i}}{RT}} \tag{4.38}$$

and $E_{a,\text{abs}}^{\text{R}_i}$ is the contribution of the functional groups and is defined as a group contribution parameter due to the functional group R_i for H-atom abstraction. In this study, we will calibrate new group rate constants (k_{Br}, k_{I}, $k_{\text{CH3COO-}}$) and group contribution factors ($X_{\text{-COO-}}$, $X_{\text{-F}}$, $X_{\text{-I}}$, $X_{\text{-CF2-}}$) that were not determined due to the lack of literature-

reported experimental rate constants. The objective function (OF) in equation (4.39) was minimized using the genetic algorithms (Goldberg, 1989; Charbonneau and Knapp, 1995).

$$\mathrm{OF} = \sqrt{\frac{1}{N-1}\sum_{i=1}^{N}\left[(k_{\mathrm{exp},i} - k_{\mathrm{cal},i})/k_{\mathrm{exp},i}\right]^2} \tag{4.39}$$

Here $k_{\mathrm{exp},i}$ and $k_{\mathrm{cal},i}$ are the experimental and calculated reaction rate constant of compound i, respectively, and N is the number of the rate constants.

4.3.3 Theoretical Basis

The *Ab initio* molecular orbital and density functional theory (DFT) based on quantum mechcanical calculations were performed using Gaussian09 (Frisch et al., 2009). The Berny geometry optimization algorithm (Schlegel, 1982) using GEDIIS (Li and Frisch, 2006) in redundant internal coordinate optimized the geometry of reactants, complex compounds and products. Transition states were found as first-order saddle points on the potential energy surface (PES). The quadratic synchronous transit method (QST) (Peng and Schlegel, 1993; Peng et al., 1996) was used to locate many of the transition states. All transition states were verified by a single negative frequency. It is known that the harmonic oscillator approximation incorrectly treats low-frequency torsional modes due to the internal rotation (Pitzer and Gwinn, 1942). However, it has recently been shown that the internal rotation correction has a very minor effect on the activation energy, even for molecules with many dihedrals (Pfaendtner and Broadbelt, 2007; Cauter et al., 2006). Additionally, low-frequency vibrational modes contribute little to the vibrational contribution to the internal energy. Therefore, the contribution of anhamonicity from hindered rotors can be neglected for studies in which the free energy

of activation is the only property desired (Pfaendtner and Broadbelt, 2008). Basis set superposition error (BSSE) was not considered because of the following reasons: 1) the BSSE may not be too large as compared to the transition state calculations, 2) methods for the BSSE correction are still controversial, and 3) the BSSE corrections by the counterpoise require the additional expensive calculations. The effect of tunneling was included using the Wigner's equation (Wigner, 1932).

For the aqueous phase, universal solvation model, SMD (Marenich et al., 2009), was used for calculating the aqueous phase free energy of activation. SMD includes two components: 1) the bulk electrostatic contribution that results from a self-consistent reaction field treatment that involves the solution of the nonhomogeneous Poisson equation for electrostatics associated with the integral equation-formalism polarizable continuum model (IEF-PCM) and 2) the contribution that arises from short-range interactions between the solute and solvent molecules in the first solvation shell. The atomic radii used the SMD-Coulomb for the polarizable continuum model calculations, which is called the intrinsic Coulomb radii. The van der Waals surface was used for the cavity formation using the GePol algorithms (Pascual-Ahuir and Silla, 1990). The default settings were used for the GePol algorithms.

Three High Performance and Cluster Computing Resources were used: (1) IBM BladeCenter H (16 blades × 2 sockets × Core2 Quad) with Red Hat Enterprise Linux 5 of Operation System; (2) Dell PowerEdge 1850 (2×3.2 GHz Pentium4 Xenon EMT64) with Red Hat Enterprise Linux 5 of Operation System and (3) 6 Core-AMD Opteron 8431 processors Atlus 2704 (24×2.34 GHz) with Red Hat Enterprise Linux 5. First two systems are maintained by College of Computing at Georgia Institute of Technology and

third system is by Office of Information Technology at Georgia Tech. In addition to these computing resources, we used a user-based workstation: Intel Core i7-960 3.2GHz Quad-Core with Red Hat Enterprise Linux 5 of OS.

4.3.4 Linear Free Energy Relationships

LFERs bridge kinetics and thermochemical properties. The kinetic information is the experimentally obtained or literature-reported HO• reaction rate constants, while the thermochemical properties are quantum mechanically calculated free energies of activation. According to LFERs, log of the rate constant and log of the equilibrium constant should be linearly related (Brezonik, 2002). Transition state theory (TST) (Eyring et al., 1935) states that log of rate constant and free energy of activation are linearly related. For the same reaction mechanisms, free energies of activation and rate constants for an arbitrary and a reference reaction are related by equation (4.40):

$$\log_{10} k_{\mathrm{I}} - \log_{10} k_{\mathrm{R}} = -\rho\left(\Delta G^{\mathrm{act}}_{\mathrm{rxn,I}} - \Delta G^{\mathrm{act}}_{\mathrm{rxn,R}}\right) + \sigma \tag{4.40}$$

where k_{I} and k_{R} are the reaction rate constants, $\mathrm{M^{-1}s^{-1}}$, for an arbitrary reaction, I, and a reference reaction, R, respectively; ρ denotes coefficients for the difference in the free energy of activation; σ is a constant; and $\Delta G^{\mathrm{act}}_{\mathrm{rxn,I}}$ and $\Delta G^{\mathrm{act}}_{\mathrm{rxn,R}}$ are the free energies of activation, kcal/mol, (Pu et al., 2006) for reactions I and R, respectively.

The quantum mechanically calculated free energy of activation in the aqueous phase, $\Delta G^{\neq}_{\mathrm{rxn,aq}}$, which is defined as a quasithermodynamic molar free energy of activation (Pu et al., 2006) at a given temperature *T,* is given by

$$\Delta G^{\neq}_{\mathrm{rxn,aq}} = G^{\neq}_{\mathrm{aq}} - G_{\mathrm{reactants,aq}} \tag{4.41}$$

where $G^{\neq}_{\mathrm{aq}}$ is a quasithermodynamic quantity, kcal/mol, that indicates the free energy of

the transition state, and $G_{\text{reactants,aq}}$ is the molar free energy of reactants, kcal/mol. $\Delta G^{\text{act}}_{\text{rxn}}$ can be related to $\Delta G^{\neq}_{\text{rxn,aq}}$ using the extrathermodynamic contribution to the free energy of activation (Pu et al., 2006), ΔG_{extra}, kcal/mol, as shown in equation (4.42):

$$\Delta G^{\text{act}}_{\text{rxn}} = \Delta G^{\neq}_{\text{rxn,aq}} + \Delta G_{\text{extra}} \tag{4.42}$$

where

$$\Delta G_{\text{extra}} = -RT \ln\gamma(T) \tag{4.43}$$

$\gamma(T)$ is a transmission coefficient that represents the effect of tunneling at temperature T. When a hydrogen atom is involved in a reaction, nuclear quantum effects, in particular quantized vibrations and tunneling, become important. Tunneling takes place when some systems pass through the transition state with less than the quantized energy. It should be noted that because the transition state is a metastable, it does not have quantized energy levels. To a good approximation, however, all bound modes of a potential energy surface can be assumed to have a quantized energy requirement (Wigner, 1932), and this is validated by accurate quantum dynamics (Chartfield et al., 1992). The free energy change associated with moving from a gaseous phase of 1 atm to an aqueous phase concentration of 1 M (i.e., 1.89 kcl/mol (Liptak and Shields, 2001)) was included. The solvent cage effects were included according to the corrections that were proposed by Okuno (1997), taking into account the free volume (FV) theory (Benson, 1982). These corrections are in good agreement with those independently obtained by Ardura et al (2005) and have been successfully used by other authors. The $\Delta G^{\neq}_{\text{rxn,aq}}$ decreases by 2.96 kcal/mol for a bimolecular reaction at 298K, with respect to the gaseous phase free energy of activation. This lowering is expected because the cage effects of the solvent reduce the entropy loss associated with any addition reaction or transition state formation

in reactions with molecularity equal to or greater than 2. Therefore, if the translational degrees of freedom in solution are treated as they are in the gaseous phase, the cost associated with their loss when two or more molecules from a complex system in solution is overestimated in case of the implicit continuum solvation model, and consequently, these processes are kinetically overpenalized in solution, leading to rate constants that are artificially underestimated. The Gaussian-4 theory (G4) (Curtiss et al., 2007) using the SMD solvation model (Marenich et al., 2009) was used for calculating $\Delta G^{\neq}_{rxn,aq}$ and ΔG_{extra}. The G4 theory includes the geometry optimization at the B3LYP/6-31G(2df,p), 0.9854 of a scaled factor for the zero-point energy (ZPE) frequency calculations, and several combinations of high level complementary single-point energy calculations.

4.4 Results and Discussion

4.4.1 Experimental Section

4.4.1.1 Hydroxyl Radical Reaction Rate Constants

The rate constants, Arrhenius parameters, and calculated thermochemical properties are summarized in Table 4.1. Typical kinetic data for chloroacetate that were obtained at 475 nm of wavelength and room temperature (22°C) are shown in Figure 4.3. An increased in the maximum $(SCN)_2^{\bullet-}$ absorption intensity was observed when chloroacetate was diluted by the SCN^- solution. The transformed plot shown in Figure 4.3 gives a weighted linear fit corresponding to a reaction rate constant of $k = (1.61 \pm 0.07) \times 10^8\ M^{-1}s^{-1}$. Figure 4.4 compares the kinetic data of chloroacetate, dichloroacetate, and trichloroacetate. The observed errors are within ±10%, which arises from the measurement precision (e.g., electron beam stability from the LINAC) and the chemical solution (e.g., purity, dilution).

Table 4.1: Experimentally obtained temperature-dependent HO• rate constants and thermochemical properties, and theoretically calculated free energies of activation

	temp, °C	k, $M^{-1}s^{-1}$	referece	E_a, kJ/mol (kcal/mol)	A, $M^{-1}s^{-1}$	ΔS^{act}_{rxn}, J/(mol·K) [cal/(mol·K)]	ΔH^{act}_{rxn}, kJ/mol (kcal/mol)	ΔG^{act}_{rxn}, kJ/mol (kcal/mol)	$\Delta G^{\neq}_{rxn,\ aq}$ kJ/mol (kcal/mol)
$ClCH_2COO^-$	23.0	$(1.61\pm0.07)\times10^8$	this study	14.1±0.2 (3.37±0.05)	$(5.20\pm0.26)\times10^{10}$	-48.1±0.40 (-11.5±0.10)	11.6±0.20 (2.77±0.05)	25.9±0.08 (6.19±0.02)	31.0 (7.4)
	30.0	$(2.07\pm0.03)\times10^8$							
	40.0	$(2.36\pm0.06)\times10^8$							
	50.0	$(2.66\pm0.08)\times10^8$							
Cl_2HCCOO^-	22.5	$(1.33\pm0.08)\times10^8$	this study	20.1±0.4 (4.80±0.10)	$(4.98\pm0.39)\times10^{11}$	-29.3±0.64 (-7.00±0.15)	17.6±0.35 (4.20±0.08)	26.3±0.16 (6.28±0.04)	n.a.
	30.0	$(1.91\pm0.08)\times10^8$							
	40.0	$(2.13\pm0.20)\times10^8$							
	50.0	$(2.82\pm0.08)\times10^8$							
Cl_3CCOO^-	22.5	$(5.50\pm0.03)\times10^7$	this study	33.3±0.1 (7.95±0.02)	$(4.84\pm0.21)\times10^{13}$	8.76±0.34 (2.09±0.08)	30.8±0.07 (7.36±0.02)	28.2±0.04 (6.73±0.01)	97.1 (23.2)
	30.0	$(1.09\pm0.03)\times10^8$							
	40.0	$(1.27\pm0.03)\times10^8$							
	50.0	$(1.94\pm0.02)\times10^8$							
Br_2HCCOO^-	23.0	$(1.85\pm0.06)\times10^8$	this study	23.6±0.03 (5.64±0.01)	$(2.87\pm0.15)\times10^{12}$	-14.7±0.41 (-3.51±0.10)	21.1±0.03 (5.04±0.01)	25.5±0.1 (6.09±0.02)	22.6 (5.4)
	30.6	$(2.66\pm0.10)\times10^8$							
	40.0	$(3.35\pm0.20)\times10^8$							
	51.0	$(4.34\pm0.12)\times10^8$							
Br_3CCOO^-	23.0	$(1.48\pm0.06)\times10^8$	this study	22.7±0.33 (5.42±0.08)	$(1.63\pm0.14)\times10^{12}$	-19.4±0.70 (-4.63±0.17)	20.2±0.33 (4.82±0.08)	26.0±0.12 (6.21±0.03)	53.2 (12.7)
	30.6	$(2.31\pm0.10)\times10^8$							
	40.0	$(2.70\pm0.10)\times10^8$							
	50.0	$(3.35\pm0.10)\times10^8$							
F_2HCCOO^-	23.0	$(2.89\pm0.50)\times10^7$	this study	53.3±2.61 (12.7±0.62)	$(8.38\pm4.95)\times10^{16}$	70.7±3.86 (16.9±0.92)	50.9±2.61 (12.2±0.62)	30.0±1.45 (7.11±0.35)	36.8 (8.8)
	30.0	$(6.30\pm1.10)\times10^7$							
	40.0	$(9.63\pm1.06)\times10^7$							
ICH_2COO^-	22.5	$(4.11\pm0.10)\times10^9$	this study	29.5±0.59 (7.05±0.14)	$(6.52\pm1.86)\times10^{14}$	30.4±2.09 (7.26±0.50)	27.0±0.59 (6.45±0.14)	18.0±0.03 (4.30±0.01)	-
	30.0	$(5.11\pm0.02)\times10^9$							
	40.0	$(7.03\pm0.10)\times10^9$							
	50.0	$(1.16\pm0.05)\times10^{10}$							
HCOO-	25.0	$(2.4\pm0.4)\times10^9$	Ervens et al., 2003	9±5 (2.15±1.19)	$(7.9\pm0.7)\times10^{10}$	-45±4 (-10.7±0.96)	7±4 (1.67±0.96)	20±13 (4.8±3.1)	10.8 (2.57)
		3.1×10^9	Chin and Wine, 1994	10 (2.39)	2.0×10^{11}	-37 (-8.84)	7.5 (1.79)	18.5 (4.4)	
		4.3×10^9	Elliot et al., 1990	4 (0.96)	2.2×10^{10}	-55 (-13.1)	1.5 (0.48)	18.0 (4.3)	
		3.8×10^9	Elliot and Simsons, 1994	8.5 (2.03)	1.3×10^{11}	-40 (-9.55)	6 (1.43)	18.1 (4.3)	
CH3COO-	25.0	7.0×10^7	Chin and Wine, 1984	15 (3.58)	2.8×10^{10}	-53 (-12.7)	13 (3.10)	28 (6.7)	31.1 (7.44)
CH3CH2COO-	25.0	$(7.2\pm0.4)\times10^8$	Ervens et al., 2003	15±4 (3.58±0.96)	$(3.2\pm0.2)\times10^{11}$	-33±2 (-7.88±0.48)	13±3 (3.10±0.72)	22±7 (5.3±1.7)	13.0 (3.11)
HOOCCH2COO-	25.0	$(6\pm1)\times10^7$	Ervens et al., 2003	11±5 (2.93±1.19)	$(3.2\pm0.4)\times10^9$	-72±9 (-17.2±2.15)	9±4 (2.15±0.96)	30±17 (7.2±4.1)	25.7 (6.15)
-OOC(CH2)2COO-	25.0	$(5.0\pm0.5)\times10^8$	Ervens et al., 2003	11±5 (2.93±1.19)	$(5.0\pm0.4)\times10^{10}$	-48±4 (-11.5±0.96)	9±4 (2.15±0.96)	23±12 (5.5±2.9)	15.1 (3.60)
CHOCOO-	25.0	$(2.6\pm0.9)\times10^9$	Ervens et al., 2003	36±8 (8.60±1.91)	$(6.0\pm0.4)\times10^{15}$	-48±3 (-11.5±0.72)	34±7 (8.12±1.67)	19±5 (4.5±1.2)	n.a.
CH3COCOO-	25.0	$(7\pm2)\times10^8$	Ervens et al., 2003	19±4 (4.54±0.96)	$(1.3\pm0.1)\times10^{12}$	-21±2 (-5.02±0.48)	17±3 (4.06±0.72)	23±7 (5.5±1.7)	28.2 (6.73)
CH3CH(OH)COO-	22.2	$(7.77\pm0.50)\times10^8$	Martin et al., 2008	10.8±0.35 (2.57±0.08)	6.1×10^{10}	-46.8 (-11.2)	8.28 (1.98)	22.2 (5.31)	

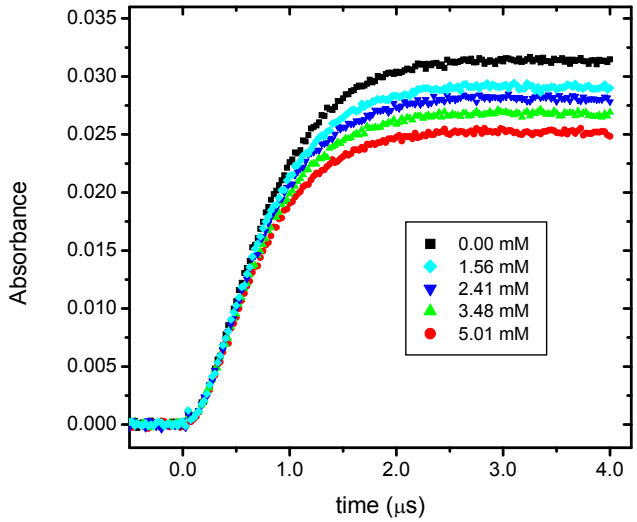

Figure 4.3: Kinetics of $(SCN)_2^{\bullet-}$ formation at 472 nm for N_2O saturated 3.00×10^{-4} M KSCN solution containing 0 (■), 1.56 (◊), 2.41(▼), 3.48(Δ), and 5.01 (○) mM $ClCH_2COO^-$

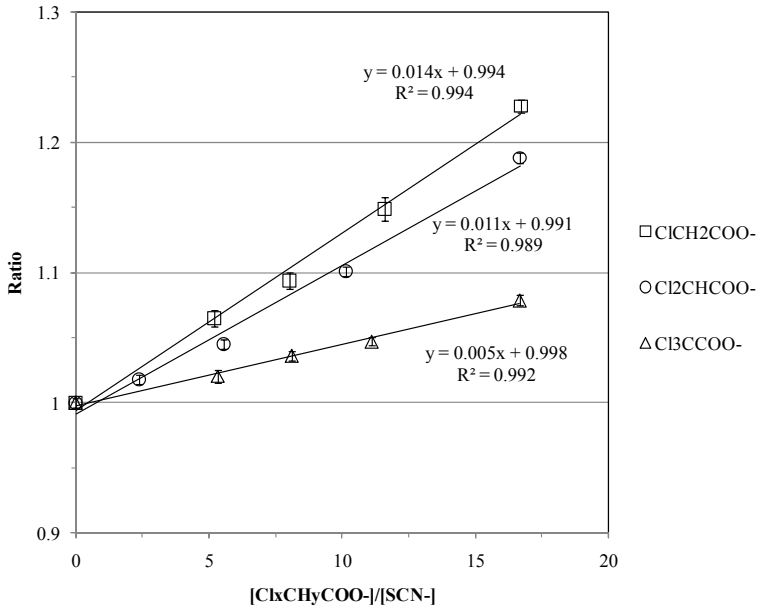

Figure 4.4: Competition kinetics plots for hydroxyl radical reaction with chloroacetate, dichloroacetate and trichloroacetate, respectively, using SCN^- as a standard. The error bar represents 95% of confidential values

4.4.1.2 Arrhenius Parameters

Figure 4.5 plots logarithms of k versus inverse of temperature for each compound. For all compounds that were investigated in this study, linear increases of the logarithms of reaction rate constants with the increase of inverse of the temperature were observed. The Arrhenius parameters, A and E_a, are obtained from the values on the y-axis and the slope of these linear relationships, respectively, and summarized in Table 4.1.

The experimentally obtained Arrhenius parameters are consistent with the general electron withdrawing ability of halogenated functional groups. For example, the experimentally obtained E_a for mono-, di- and tri-chloroacetate were 14.1±0.2, 20.1±0.4 and 33.3±0.1 kJ/mol, respectively. As the increase of chlorine atoms, the E_a increases due to the stronger influence of electron-withdrawing ability that is derived from the chlorine functional group, and hence the rate constant decreases. When comparing E_a of di-fluoro, di-chloro and di-bromo acetate, the experimentally obtained E_a were 53.3±2.61, 20.1±0.4 and 23.6±0.03 kJ/mol, respectively. Although the obtained temperature-dependent reaction rate constants were consistent with the trend of electron-withdrawing ability (i.e., $k_{F2HCCOO-} < k_{Cl2HCCOO-} < k_{Br2HCCOO-}$), the trend of E_a is not consistent with the Taft constants (i.e., $\sigma^* = 3.19$, 2.94 and 2.80 for fluorine, chlorine and bromine, respectively (Karelson, 2000)) that represent the electron-withdrawing ability of functional group. This inconsistency probably results from the underestimation of the E_a for di-chloroacetate. If the impact of single chlorine atom to reduce the overall E_a is proportional to number of chlorine atoms, the E_a for di-chloroacetate would be approximately 24 kcal/mol. Accordingly, this would lead to the consistent relation with the E_a for di-fluoro and di-bromo acetates.

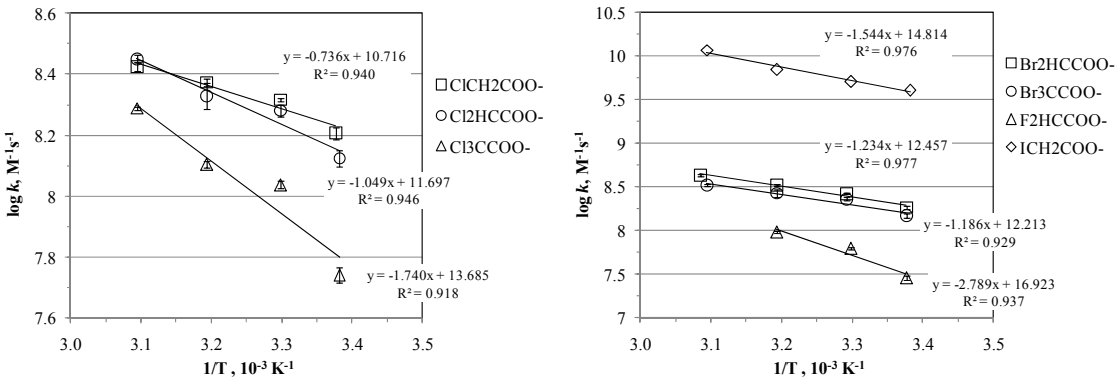

Figure 4.5: Plot of logarithm of *k* versus inverse of temperature

A comparison of obtained *A* values gives an insight of reaction mechanisms. Under the same reaction mechanism, it is typical that the *A* is within the close range of magnitude. We obtained the *A* for mono-chloro, di-chloro, di-bromo and tri-bromo acetate in the range from 10^{10} to 10^{12} $M^{-1}s^{-1}$, while the *A* for tri-chloro and iodo-acetate ions is several orders of magnitude larger than this. This is probably because the former is H-atom abstraction reaction and the latter is electron transfer reaction mechanisms. Evans et al (2003) examined the *A* in the range of magnitude from 10^{10} to 10^{12} for H-atom abstraction from a C-H bond of the linear aliphatic oxygenated compounds. They excluded compounds that had 10^{14}-10^{15} of *A* because of electron-transfer reactions. The detailed discussions on the reaction mechanisms will be given in the later section.

4.4.1.3 Thermochemical Properties of Reactions

Table 4.1 includes the ΔG^{act}_{rxn}, ΔH^{act}_{rxn} and ΔS^{act}_{rxn} for those reactions that are calculated based on the experimentally obtained E_a and A. Thermochemical properties that are obtained from the experiments give interesting insights. A linear relation is observed between the logarithms of the obtained reaction rate constants and the free energies of activation, ΔG^{act}_{rxn}, for ionized compounds (Figure 4.6) as we previously observed for the neutral compounds (Minakata and Crittenden, 2010). A least-square fit provides the LFER: $\log k_I - \log k_R = -0.741\ (\Delta G^{act}_I - \Delta G^{act}_R) + 0.0001$ (N=13, r^2=0.978), whereas the LFER for neutral compounds was $\log k_I - \log k_R = -0.542\ (\Delta G^{act}_I - \Delta G^{act}_R) + 1.074$ (N=37, r^2=0.817) (Minakata and Crittenden, 2010). The reference reaction for the LFER of ionized compounds was the reaction of HO• with acetate.

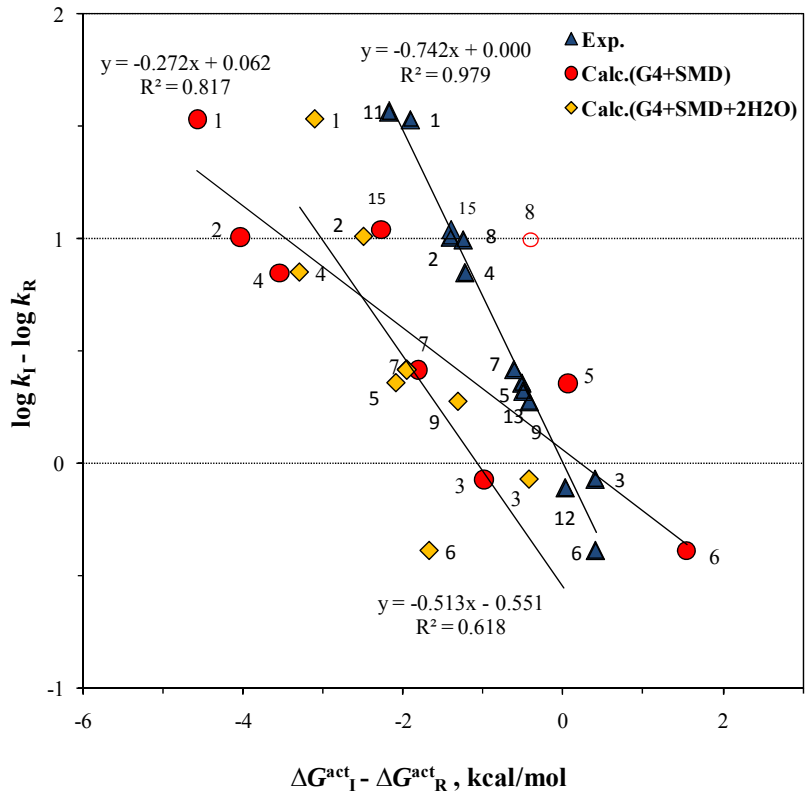

Figure 4.6: LFERs obtained from experiments, calculations at G4 and the SMD solvation model, and calculations that include two explicit water molecules. 1: formate; 2: propionate; 3: malonate; 4: succinate; 5: chloroacetate; 6: difluoroacetate; 7: dibromoacetate; 8: pyruvate; 9: dichloroacetate; 10: acetate; 11: glyoxylate; 12: trichloroacetate; 13: tribromoacetate; 14: iodoacetate; 15: lactate (note that the compound # is consistent for other Figures though this chapter).

The enthalpy of activation, ΔH^{act}_{rxn}, for halogenated acetates are in the range from 2.8 kcal/mol to 12.2 kcal/mol, which is relatively larger than those that are obtained from the literature-reported experimental values for the various acetates. This is probably because the halogenated functional groups that represent strong electron-withdrawing effect raises the barrier height. It is commonly assumed that for the same reaction group, the change of entropy is little so that the enthalpies are often used as thermodynamic properties that relate to Arrhenius activation energy (Pfaendtner and Broadbelt, 2008) using the Evans-Polanyí relation (Evans and Polanyí, 1938). However, when the entropy

contribution is significant (see isokinetic relation in Figure 2) due to the solvent effect and for the reactions that are involved in ionized compounds causing tighter binding of nearby solvent molecules, and polar molecules that results from the electrostatic contribution and loss of entropy, free energy change should be considered. This is verified for H-atom abstraction reactions of iron complexes (Mader et al., 2007). Detailed examination of the source of entropic contribution will be given in the theoretical section.

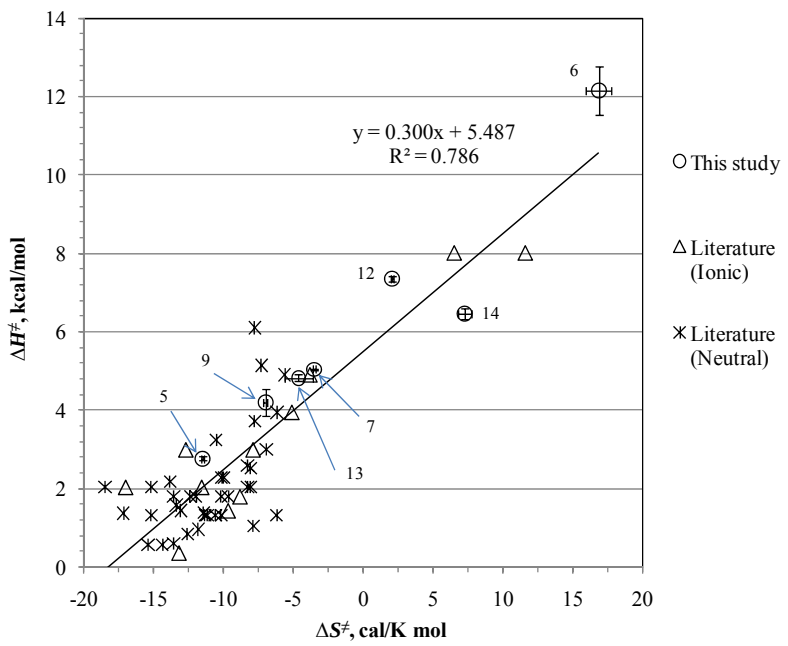

Figure 4.7: Isokinetic relation between the experimentally obtained enthalpy and entropy of activation.

4.4.2 Update of Group Contribution Method

The experimentally obtained reaction rate constants in this study are used to recalibrate the group rate constants and group contribution factors that were not determined in the previous study (Minakata et al., 2009). New group rate constants and

group contribution factors are calibrated and summarized in Table 4.2. The molecules that were used for the calibration are summarized along with the experimental and calculated rate constants in Table 4.3. All calibrated rate constants except propionate are within the $0.5 \leq k_{cal}/k_{exp} \leq 2.0$. When compared to the group rate constant for the carboxylic functional group (i.e., k_{COOH}), the k_{COO-} is two magnitude of order larger. The magnitude of k_{COO-} can be verified with the rate constant of oxalate ion di-anion (k=1.6×10^{8} M^{-1}s^{-1} (Ervens et al., 2003)) and mono-anion (k=1.9×10^{8} M^{-1}s^{-1} (Ervens et al., 2003)). The calibrated group rate constants are consistent with the general electron-donating and withdrawing ability (i.e., Taft constant).

Once group rate constants and group contribution factors are calibrated, they are used to predict the rate constants that are obtained in this study. Table 4.3 includes the predicted rate constants for halogenated acetates and acetate ions. The SD is 0.318. A total of three compounds such as CHOCOO^{-}, CH_3COCOO^{-} and $CHCl_2COO^{-}$ are out of our error goal (i.e., $0.5 \leq k_{cal}/k_{exp} \leq 2.0$).

Table 4.2: Calibrated group rate constants and group contribution factors

Group rate constant (×10^{-7} M^{-1}s^{-1})	
k_{I}	360
k_{COO-}	3.97
k_{Br}	0.362
Group contribution factor, X	
-COO-(ion)	0.184
-F	0.119
-I	0.166
-CF_2-	0.00003

Table 4.3: Molecules and rate constants that were used for the calibration

group		formula	compound	kexp	kcal	((*k* exp-*k* cal)/*k* exp)2	*k* cal/*k* exp
halogenated acetate	435	I2-CH2	diiodomethane	6.30E+09	7.23E+09	0.02170	-0.15
	436	I-CH2-COO-	iodoacetate	4.11E+09	3.67E+09	0.01142	0.11
	437	ICH2Cl	chloroiodomethane	4.00E+09	3.63E+09	0.00838	0.09
	438	CH3COO-	acetate	7.30E+07	1.05E+08	0.18640	-0.43
	439	**CH3CH2COO-**	**propionate**	**7.20E+08**	**3.15E+08**	**0.31651**	**0.56**
	440	F-CH2-COO-	fluoroacetate	2.89E+07	2.24E+07	0.05104	0.23
	441	Cl3CCOO-	trichloroacetate	5.50E+07	3.97E+07	0.07768	0.28
	442	CF3-CHClBr	Halothane	1.30E+07	1.49E+07	0.02070	-0.14
	443	CHF2-O-CF2-CHClF	Enflurane	9.50E+06	1.01E+07	0.00442	-0.07
	444	CF3-CHCl-O-CHF2	Isoflurane	2.40E+07	2.44E+07	0.00031	-0.02
	445	H3C-O-CF2-CHCl2	Methoxyflurane	8.30E+07	1.35E+08	0.38627	-0.62
	446	Br3CCOO-	tribromoacetate	1.48E+08	1.48E+08	0.00001	0.00

4.4.3 Theoretical

4.4.3.1 *Ab initio* Quantum Mechanical Approach

There is a tradeoff between computational accuracy and demand. To seek reasonable approach, we compared a limited number of methods and basis sets for HO• reactions in both gaseous and aqueous phases. Table 4.4 summarizes quantum mechanically calculated gaseous and aqueous phase barrier height and free energy of activation for reaction of HO• with acetate. The observed gaseous phase reactions are exergonic (i.e., $\Delta G^{\neq}_{rxn,gas} < 0$). This is consistent with the results from the reaction energies of HO• with glycine anions (Štefanić et al., 2009). The agreement among G4, CCSD(T)/6-31++G(d,p) and QCIST(T)/6-31++G(d,p) for the gaseous phase reactions is encouraging. The G4 theory significantly reduces the computational cost with the similar accuracy to the coupled cluster and configuration interaction methods in calculating the thermochemical properties.

Aqueous phase reactions are found to be exergonic (i.e., $\Delta G^{\neq}_{rxn,gas} > 0$). G4 and M05-2X/6-31+G(d,p) give similar values to the experimentally obtained literature-reported value (Chin and Wine, 1994). It was found that our previously established approach (i.e., G3 with COSMO-RS) (Klamt, 1996 and Klamt et al., 1998) significantly overestimates the aqueous phase free energy of activation. To confirm this, we calculated ground state free energy of solvation for ionized compounds and compared with the literature values (Marenich et al., 2009). The free energies of solvation of ionized compounds that are calculated by COSMO-RS are far from the experimental values (Figure 4.8). For the example, we obtained -94.5 kcal/mol, -74.0 kcal/mol, 65.8 kcal/mol and -57.6 kcal/mol of free energy of solvation for CH_3COO-, ClH_2CCOO-, Cl_2HCCOO- and F_3CCOO-, respectively, as compared to the experimental values -77.6 kcal/mol, -69.70 kcal/mol, -62.30 kcal/mol and -59.3 kcal/mol (Marenich et al., 2009). It is anticipated that the free energy of solvation for transition state may be overestimated by COSMO-RS.

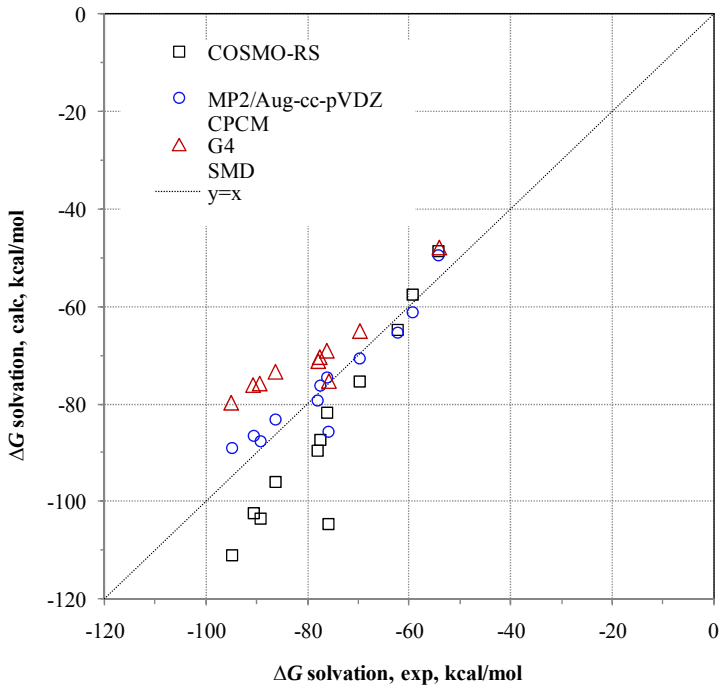

Figure 4.8: Comparison of calculated and experimental free energy of solvation for ionized compounds

SMD includes nonelectrostatic interactions (e.g., short range interaction) in addition to long range solute-solvent interaction in bulk phase, whereas CPCM does not include nonelectrostatic term. In addition, SMD is based on the polarized continuous quantum mechanical charge density of the solute (Marenich et al., 2009) and seems to be reasonable to represent the large electrostatic interactions that arise from ionized compounds and water molecules. As a consequent, SMD was chosen to calculate the aqueous phase free energy of activation. It is noted that G4 optimizes the geometry of molecules at B3LYP/6-31G(2df,p) that does not include diffuse functions. Although the inclusion of diffuse function for the ionized compounds is recommended (Cramer, 2004), it is speculated that the use of diffuse functions often decreases accuracy due to outlying

charge in the SMD model (Liu et al., 2010). Therefore, we use the default method for G4 upon the geometry optimization.

Table 4.4: Calculated gaseous and aqueous phase barrier height and free energy of activation

		G4	G3	CCSD(T)/6-31++G(d,p)// mp2(full)/6-31G(d)	QCISD(T)/6-31++G(d,p)// mp2(full)/6-31G(d)	MP2/cc-pVTZ// MP2/aug-cc-pVDZ *scale=0.9561
Vacuo	$\Delta E^{\neq}_{rxn,gas}$	-11.8	-11.1	-9.91	-9.78	-10.1
	$\Delta G^{\neq}_{rxn,gas}$	-1.76	-3.87	-1.02	-1.18	-0.80

		MP2/Aug-cc-pVDZ CPCM *scale=0.9615	MP2/6-311+G(3d,p) CPCM //MP2/aug-cc-pVDZ CPCM *scale=0.9570	MP2(full)/6-311++G(d,p) CPCM //MP2/aug-cc-pVDZ CPCM	G3 (gas) + COSMO-RS	MP2/Aug-cc-pVDZ CPCM *scale=0.9615	MP2/Aug-cc-pVDZ SMD *scale=0.9615	MP2/Aug-cc-pVTZ SMD //MP2/Aug-cc-pVDZ SMD *scale=0.9598	G09 M05-2X/ 6-31+(d,p) SMD	G4 SMD	G4 (gas) + COSMO-RS	Exp. [Chin and Wine, 1994]
Water	$\Delta E^{\neq}_{rxn,aq}$	6.87	7.33	8.33		9.20	3.62	3.56		0.99		
	$\Delta G^{\neq}_{rxn,aq} + \Delta G_{extra}$	12.3	13.6	14.6	21.2	14.4	9.7	9.6	6.6	7.4	26.3	6.7

4.4.3.2 Optimized Structure of Stationary, Pre-reactive Complex and Transition States

Tables 4.5-4.7 and Figures 4.9-4.11 summarize aqueous phase optimized stationary structures of HO•, H_2O and a series of halogenated acetates as well as pre-reactive complexes and transition state structures. Several gaseous phase optimized structures are given as a comparison. When the gaseous phase optimized structures are compared to the aqueous phase ones, it is found that there are a few structural differences associated with the length of bonds, angle and dihedral. For the stationary equilibrium structures of halogenated acetates, pre-reactive complexes and transition state, the effects of halogen atoms to the optimized structure are substantial due to the larger size of their atoms. For example, the bond length of carbon-halogen atom, *l*(C-R) (where R = F, Cl, Br) of dehalogenated acetate are 1.365 Å, 1.803 Å and 1.971 Å, respectively. Despite the presence of the halogen atoms, the bond length of carbon-hydrogen, *l*(C-H), that is subject to be attacked by HO• does not differ. When it comes to the pre-reactive complex and transition state structures, the hydrogen bonds between the H-atom of the HO• and the oxygen of carboxylic functional group are produced. This hydrogen bond is approximately 1.6-1.7 Å and 1.8-1.9 Å for the pre-reactive complex and transition state, respectively, for the halogenated acetates. Because of this hydrogen bond, the angle ∠HOH at the transition state is smaller (<90 degree) for the halogenated acetates than typical angle (≈90 degree (Minakata et al., 2010)). The angle ∠CHO of the abstracted H-atom becomes larger as the halogenated atoms become larger. One of the distinctive differences in the transition state structures when the halogenated atoms are employed is the length of the oxygen of the HO• and the abstracted hydrogen (i.e., *l*(O-H)). For

example, the *l*(O-H) is 1.358 Å for acetate while it is 1.450 Å and 1.464Å, respectively, for difluoroacetate and dibromoacetate.

Table 4.5: Geometry of HO• and H_2O

		O-H, Å	< HOH, degree
HO•	vacuo	0.976	
	water	0.977	
H_2O	vacuo	0.962	103.726
	water	0.964	102.918

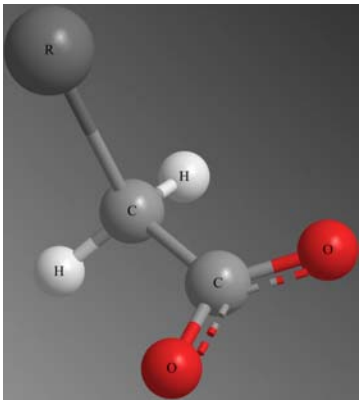

Figure 4.9: Schematic picture of acetate with R functional group

Table 4.6: Geometry of acetate and halogenated acetate

	C-C, Å	C=O, Å	C-H, Å	C-R, Å	< HCC, degree	< RCC, degree	< OCC, degree	< OCO, degree
CH_3COO-	1.538	1.262	1.093/1.097		111.454/107.544		117.033	125.913
CH_2ClCOO-	1.548	1.256	1.089	1.830	112.143	109.405	116.160	127.681
$CHCl_2COO$-	1.566	1.244/1.251	1.085	1.803/1.815		112.020	117.653	129.751
Cl_3CCOO-	1.608	1.240		1.796/1.813		112.492/106.547	114.278	131.387
CHF_2COO-	1.552	1.252	1.097	1.365	111.564	111.039	115.446	129.041
$CHBr_2COO$-	1.563	1.242/1.254	1.085	1.971/1.969	112.085	110.879/111.540	112.305	129.547
Br_3CCOO-	1.609	1.240		1.966/1.985		112.729/106.263	114.344	131.274

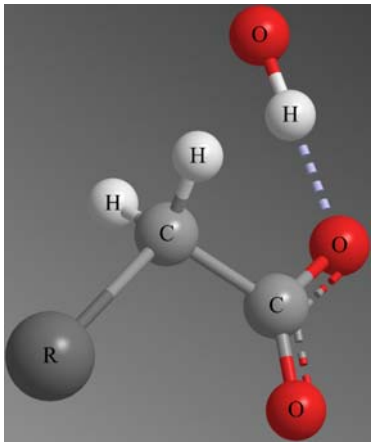

Figure 4.10: Schematic picture of pre-reactive complex between HO• with acetate, R is functional group

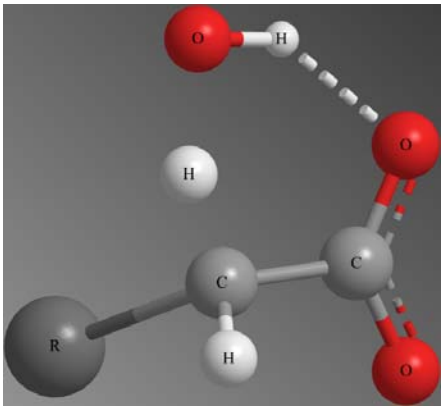

Figure 4.11: Schematic picture of transition state between HO• with acetate, R is functional group

Table 4.7: Geometry of transition states for the reaction of HO• with halogenated acetate

		H-bond		Abstracted H-atom				H-CR_2COO-			
		O-H, Å	Dihedral H-O-H-O	C-H(R), Å	O-H(R), Å	< CH(R)O, degree	< H(R)OH, degree	C-C, Å	C=O, Å	< HCC, degree	< OCO, degree
HO…H…CH_2COO-	vacuo	1.915	-0.004	1.221	1.346	158.276	85.376	1.551	1.251/1.250	107.703	129.448
	water	1.896	-1.763	1.209	1.358	156.416	87.246	1.528	1.255/1.261	108.139	126.483
HO…H…CHClCOO-	vacuo			1.150	1.547	151.046	90.718	1.609	1.230/1.242	108.881	134.663
	water	1.929	4.014	1.188	1.395	151.648	88.277	1.549	1.261/1.243	105.759	128.447
HO…H…CCl_2COO-	water										
HO…Cl…CCl_2COO-	water			2.233	1.922	173.330	99.168	1.595	1.238	96.884	132.364
HO…H…CF_2COO-	water	1.923	-1.850	1.174	1.450	154.948	87.701	1.570	1.252/1.243	108.453	130.194
HO…H…CBr_2COO-	water	1.874	2.218	1.155	1.464	155.259	87.622	1.574	1.254/1.238	109.639	129.701
HO…Br…CBr_2COO-	water			2.315	2.030	162.343	100.687	1.588	1.240	101.334	131.465

4.4.3.3 Linear Free Energy Relationships

As was previously observed for neutral compounds (Minakata and Crittenden, 2010), we obtained a linear correlation: $\log k_I - \log k_R = -0.272\ (\Delta G^{act}_I - \Delta G^{act}_R) + 0.062$ (N=8, r^2=0.817). The reaction of HO• with acetate was used for the reference reaction. The LFER includes the literature-reported HO• reaction rate constants including formate, acetate, propionate, malonate, succinate and lactate as well as our experimentally obtained rate constants for a series of halogenated acetates (i.e., chloroacetate, difluoroacetate, dibromoacetate). All free energies of activation for these acetates are quantum mechanically calculated in this study and summarized in Table 4.1. Transition state for dichloroacetate could not be located. It is anticipated that quantum mechanically calculated free energy of activation for pyruvate and the reported rate constants might have been overestimated. We are able to identify three transition states for the reaction of HO• with pyruvate and all free energies of activation are similar (i.e., 9.7 kcal/mol, 12.0 kcal/mol, and 12.1 kcal/mol). These calculated values seem to be reasonable if compared to the structurally-similar compounds. In contrast, Ervens et al (2003) reported five temperature-dependent HO• reaction rate from 288K to 328 K using a laser photolysis technique. It is not clear whether the different techniques produce different rate constants. Yet, we did not include the pyruvic acetate for the correlation.

Our quantum mechanically obtained free energies of activation for various carboxylic acetates turn to be acceptable. Eight out of 10 compounds indicate that the calculated aqueous phase free energies of activation are within ±2.0 kcal/mol as compared to those that are obtained from the experiments, while the calculated aqueous phase free energy of activation for formate and propionate show 2.23 kcal/mol and 2.19 kcal/mol of difference from the experimental values. Considering the general error

arising from the G4 gaseous phase calculations (i.e., 0.83 kcal/mol, Curtiss et al., 2007) and uncertainty for calculating free energy of transition state, these results should be within the reasonable range. Sample deviation (SD) that is obtained from equation (4.44) is 0.27 for 10 ionic compounds (N=10).

$$\mathrm{SD} = \sqrt{\frac{1}{N-1}\sum_{i=1}^{N}\left(\frac{\Delta G_{\mathrm{rxn}}^{\mathrm{act},i} - \left(\Delta G_{\mathrm{rxn,aq}}^{\neq,i} + \Delta G_{\mathrm{extra}}^{i}\right)}{\Delta G_{\mathrm{rxn}}^{\mathrm{act},i}}\right)^{2}} \tag{4.44}$$

We have shown that G4 with the SMD model calculates the acceptable aqueous phase free energy of solvation. From next sections, we will examine significant contribution of the free energy of solvation, in particular for the ionized compounds: 1) entropic contribution and 2) electrostatic contribution.

4.4.3.4 Entropy Contribution

The entropic contribution to the free energy of activation is significant for ionic compounds because solvent is re-organized after significant change in the interactions (i.e., hydrogen-bonding) between ionized compounds and implicitly expressed water molecules. Nonelectrostatic interactions represent cavity formation, dispersion interactions, and changes in solvent structure (Marenich et al., 2009) between solute and water molecules. The nonelectrostatic energies of activation ($\Delta E_{\text{non-ES}}^{\text{act}}$) that are calculated at G4 with the SMD model for the reactions of HO• with halogenated acetates range from -0.84 to -0.14 kcal/mol (Table 4.8). Although these interactions are smaller contribution to free energies of activation, this is due to significant cancellation between enthalpic and entropic contributions (Ashcraft et al., 2007). As Ashcraft et al. (2007) addressed, for example, neglecting nonelectrostatic energies would introduce 4.45 kcal/mol of entropic term (i.e., entropy of cavitation) of water. Accordingly, the entropic

contribution should be considered independently by assuming that the dispersion interaction is enthalpic, and the cavity formation and the changes in solvent structure are completely entropic. It is noted that the nonelectrostatic enrgy of activation as well as the change in cavity volume weakly correlated with the experimentally obtained entropy of activation (see Figure 4.12).

The entropic contribution that arises from the cavity formation examines the effect of confining the solute in the accessible free volume of the solution and can be estimated using a methodology outlined by Pierotti (Pierotti, 1963; Hofinger and Zerbetto, 2003) as shown in equation (4.45). This approach has been shown to work for calculating cavitation entropy by Ashcraft et al. (2007).

$$\Delta G_{\text{cav}} = K_0 + K_1 r_{\text{cav}} + K_2 r_{\text{cav}}{}^2 + K_3 r_{\text{cav}}{}^3 \tag{4.45}$$

$$K_0 = RT\left[-\ln(1-y) + \frac{9}{2}\left(\frac{y}{1-y}\right)^2\right] - \frac{4\pi r_{\text{water}}{}^3 P}{3}$$

$$K_1 = -\frac{RT}{2r_{\text{water}}}\left[6\left(\frac{y}{1-y}\right) + 18\left(\frac{y}{1-y}\right)^2\right] + 4\pi r_{\text{water}}{}^2 P$$

$$K_2 = \frac{RT}{4r_{\text{water}}{}^2}\left[12\left(\frac{y}{1-y}\right) + 18\left(\frac{y}{1-y}\right)^2\right] + 4\pi r_{\text{water}} P$$

$$K_3 = \frac{4\pi P}{3}$$

$$y = \frac{4\pi\rho r_{\text{water}}{}^3}{3}$$

where r_{water} is the hard-sphere radius of a water molecule and taken to be 1.35 Å that is approximately half the distance to the first peak in the experimental oxygen-oxygen radial distribution function for water (Ashcraft et al., 2007; Narten and Levy, 1971), ρ is

the number density of the solvent, molecules/Å^3, P is the pressure (1 atm = 0.01458 cal/mol·Å^3), R is the gas constant, and T is the temperature. The cavity radius is estimated from the volume of cavity that is calculated at G4 with SMD. The entropy of cavitation can relate to the free energy through a temperature derivative as shown in equation (4.46):

$$\Delta S_{\text{cav}} = -\left(\frac{\partial \Delta G_{\text{cav}}}{\partial T}\right)_P \tag{4.46}$$

Table 4.8: Calculated cavitation entropy of activation, change in cavity volume, nonelectrostatic energy of activation and experimentally obtained entropy of activation

	$\Delta S^{\neq}_{\text{cav}}$	$\Delta V^{\neq}$	$\Delta E^{\text{act}}_{\text{non-ES}}$	$\Delta S^{\text{act}}_{\text{rxn}}$
	cal/mol K	Å^3	kcal/mol	cal/mol K
HCOO-	-17.38	-2.38	-0.80	-10.7±0.96[a]
CH3COO-	-14.32	-4.03	-0.71	-12.7[a]
CH3CH2COO-	-8.58	-4.72	-0.78	-7.88±0.48[a]
HOOCCH2COO-	-5.61	-2.53	-0.45	-17.2±2.15[a]
-OOC(CH2)2COO-	6.57	-3.82	-0.76	-11.5±0.96[a]
CH3COCOO-	-7.92	-4.18	-0.84	-5.02±0.48[a]
CH2ClCOO-	3.33	-4.31	-0.74	-11.50
CHCl2COO-	9.45		n.a.	-7.00±0.15
F2HCCOO-	-9.30	-3.72	-0.69	16.9±0.92
Br2HCCOO-	n.a.	-5.43	-0.69	-3.51±0.10

a: Ervens et al., 2003

Table 4.8 summarizes the calculated cavitation entropy of activation, the change in cavity volume, and nonelectstatic energy of activation and experimentally obtained entropy of activation. The calculated cavitation entropy is consistent with the values that were obtained by Ashcraft et al. (2007). Aqueous phase entropy contains solvent ordering entropy (Leung et al., 2004) in addition to the cavity entropy. Ashcraft et al. (2007) estimated the typical solvent ordering entropy of ground sate molecules from -2 to

+5 cal/mol K that were obtained by fitting empirical parameters with a few available experimental entropy data. However, this approch is not feasible for transition state due to the lack of experimental values. Nevertheless, the cavitation entropy of activation turns out to be dominant in the entropy of activation.

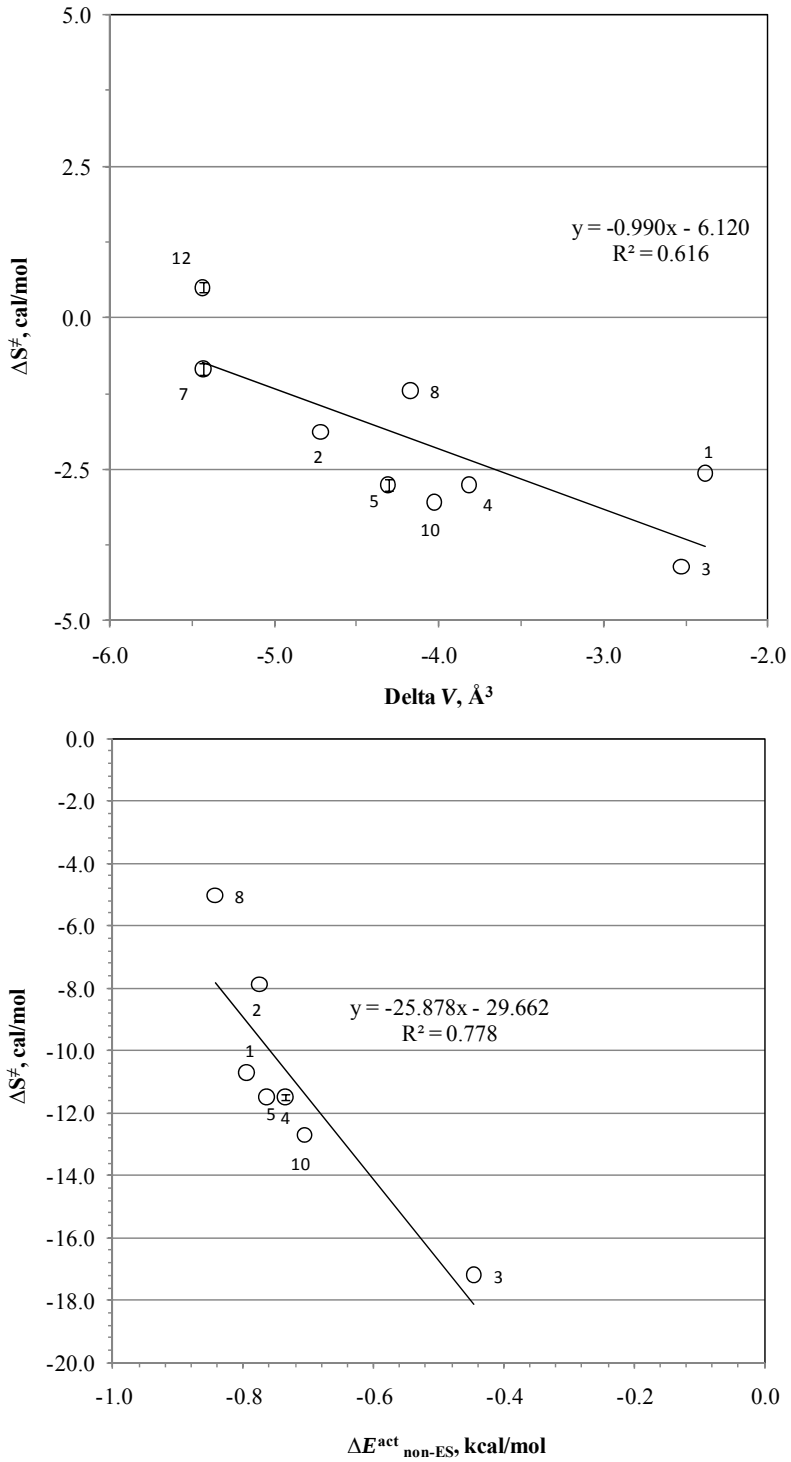

Figure 4.12: Experimentally obtained free energies of entropies versus quantum mechanically calculated change in cavity, ΔV_{cav}, $Å^3$ (top), and non-electrostatic energy of activation (bottom) at G4 with the SMD model for series of acetate

4.4.3.5 Charge Distribution and Reaction Mechanisms

The analysis of atomic charge distributions on each element enables one to understand the effects of different functional groups to the molecular reactivity in progression from reactants → transition state → products. In Figures 4.13 and 4.14, the charges obtained from a natural population analysis (NPA) (Foster and Weinhold, 1980) at MP2/aug-cc-pVTZ//B3LYP/6-31G(2df,p) with the SMD model for the reactions of HO• with CH_3COO^- in the gaseous and aqueous phases and a series of halogenated acetates in the aqueous phase, respectively.

For the reactions of HO• with CH_3COO^-, the analysis confirms that as the abstracted hydrogen of acetate becomes more positive at the transition state and the oxygen of HO• becomes more negative at the transition state. The negative charge on the oxygen of hydroxyl radical indicates that this oxygen can be a hydrogen bond acceptor. This development of negative charge on the oxygen of the HO• affords the opportunity for the solvent to stabilize the transition state through its polarity and/or ability to participate in hydrogen bonding. In contrast, the hydrogen on the hydroxyl radical (not involved in the reaction) bears substantial positive charge in the reactant, transition state, and product. Although this hydrogen can also participate in hydrogen bonding, this interaction does not affect the relative energies because the charge on this hydrogen remains almost constant in the progression from reactant to transition state to product. In the aqueous phase, the degree of the polarizability at the transition state is less substantial, which implies that smaller barrier height and faster reactions. The carboxylic functional group is known to manifest the inductive effects of electrons from the C-H bond due to electron-withdrawing properties of oxygen, although the resonance stabilization afforded by the lone pair of electrons offset this inductive effect. Because

oxygen is more electronegative than carbon and hydrogen, in the transition state for hydrogen abstraction, electron density is pulled toward the oxygen of the hydroxyl radical, giving it a partial negative charge and a partial positive charge on the alkyl portion of the transition state. The carboxylic functional group in the aqueous phase becomes less negative due to the impact of surrounding continuum water molecules, whereas little change in charge distribution of carboxylic functional group in the gaseous phase is observed.

vacuo:

$$\underbrace{\overset{0.399}{H}\ \overset{-0.399}{O}}_{0.000}\bullet + \left[\overset{0.157}{H} - \overset{-0.639}{C}\ \overset{0.157}{H}\ \overset{0.162}{H}\ \underbrace{COO^-}_{-0.838}\right] \rightarrow \left[\overset{0.494}{H}\ \overset{-0.627}{O} \cdots \overset{0.193}{H} \cdots \overset{-0.556}{C}\ \overset{0.168}{H_2}\ \underbrace{COO^-}_{-0.84}\right]^{\neq} \rightarrow \bullet \overset{-0.306}{C}\ \overset{0.115}{H_2}\ \underbrace{COO^-}_{-0.924} + \underbrace{\overset{0.461}{H}\ \overset{-0.922}{O}\ \overset{0.461}{H}}_{0.000}$$

SMD:

$$\underbrace{\overset{0.449}{H}\ \overset{-0.449}{O}}_{0.000}\bullet + \left[\overset{0.192}{H} - \overset{-0.653}{C}\ \overset{0.192}{H}\ \overset{0.206}{H}\ \underbrace{COO^-}_{-0.935}\right] \rightarrow \left[\overset{0.498}{H}\ \overset{-0.614}{O} \cdots \overset{0.199}{H} \cdots \overset{-0.580}{C}\ \overset{0.207}{H_2}\ \underbrace{COO^-}_{-0.917}\right]^{\neq} \rightarrow \bullet \overset{-0.289}{C}\ \overset{0.160}{H_2}\ \underbrace{COO^-}_{-1.03} + \underbrace{\overset{0.498}{H}\ \overset{-0.996}{O}\ \overset{0.498}{H}}_{0.000}$$

Figure 4.13: Charge distributions of reactants, transition states and products for the gaseous and aqueous phases HO• reactions with acetate

Figure 4.14 compares the charge distributions of halogenated acetates in the aqueous phase. Halogenated atoms (i.e., F, Cl, and Br) significantly affect the charge distributions and hence the activation energies and reaction rates. When the electron-negative halogenated functional groups are accommodated besides carboxylic functional groups, the transition state is less polarized because the functional group competes for electron density; there is less transfer of negative charge to the oxygen of the hydroxyl

radical and hydrogen bonding interactions are expected to be weaker. Fluorine atom that has more negative charge produces the least positive charge on the abstracted hydrogen, and the largest barrier height and smallest rate constant is obtained. Bromine affects the charge distribution in the process from reactant to transition state to product in the same manner as is observed for acetate. The abstracted hydrogen becomes slightly positive and the oxygen of hydroxyl radical becomes more negative than the reactants that have chlorine and fluorine. Nevertheless, the significant large rate constants for dibromoacetate suggest the electron-transfer reaction between the bromine atom and hydroxyl radical to produce a $2\sigma/1\sigma^*$ two-center–three-electron (2c-3e) adduct containing two bonding σ and one antibonding σ^* electrons (Asmus and Bonifačič, 1999)

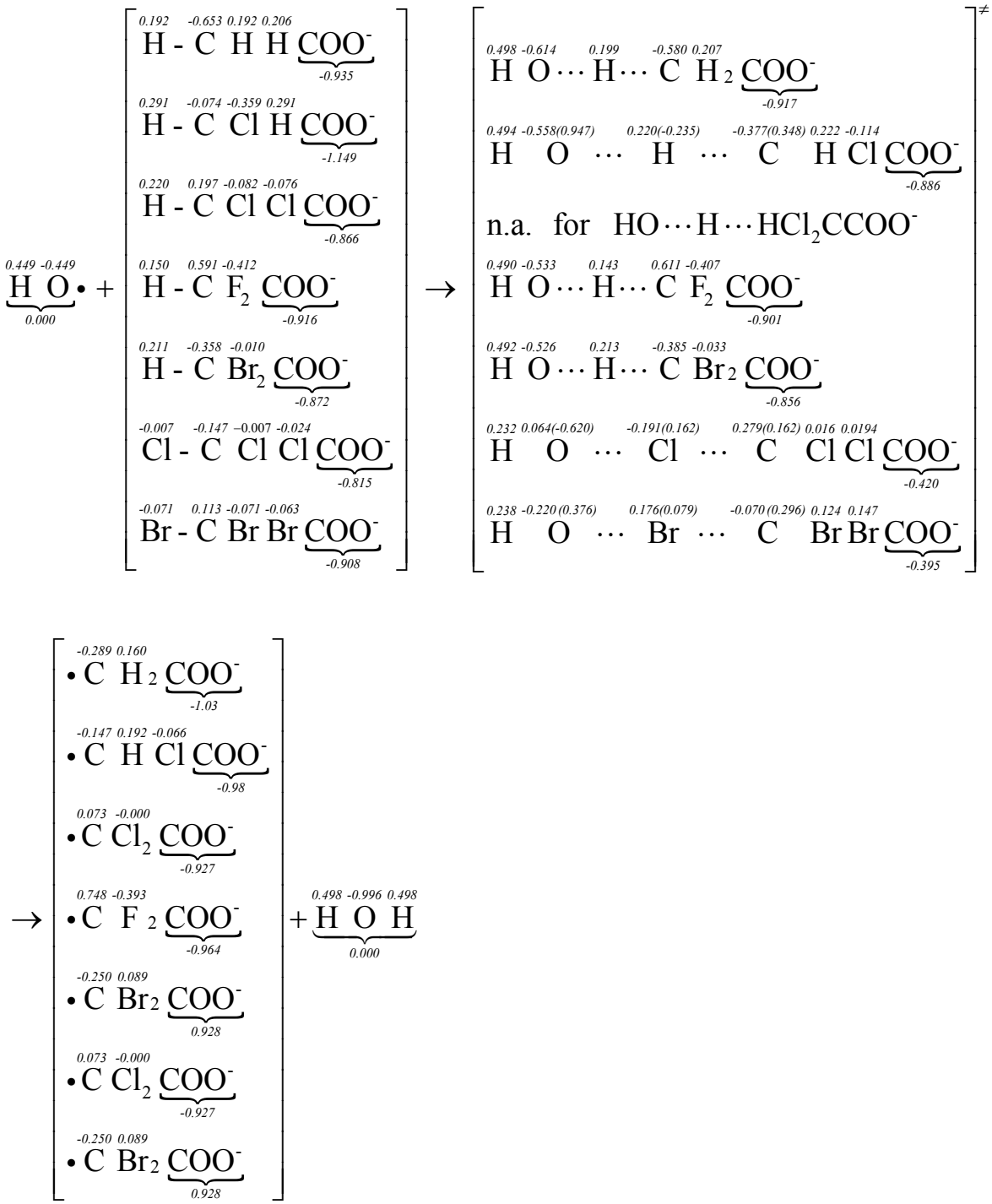

Figure 4.14: Charge distributions of reactants, transition states and products for the aqueous phases HO• reactions with halogenated acetate

To investigate the dominant reaction mechanisms, we examine spin populations from the natural population analysis (NPA) at MP2/aug-cc-pVTZ//B3LYP/6-31G(2df,p) with the SMD model. For the H-atom abstraction, the spin populations that are shown in the parentheses at the transition state are concentrated on the two atoms which undergo the H exchange, while the transition states of Cl_3CCOO^- and Br_3CCOO^- locate the spin populations mainly on one of the garments. The former indicates the three-center three-electron bond and corresponds to H-atom abstraction. The latter indicates the electron transfer as was observed by for iodine and bromine-atom-containing compounds. Such electron transfer interaction may take place both by inter- and intra-molecular coordination through overlap of p-orbitals. In general, fully halogenated compounds are practically inert toward the HO• (Lal et al., 1988). Nevertheless, we observe significant temperature-dependent reactivity for perhalocarbons such as Cl_3CCOO- and Br_3CCOO-. These perhalocarbons are good halogen donors to chlorine and bromine radical under the abstraction of halogen atom (Kerr, 1973). Fliount et al (1997) concluded that HO• at least indirectly particulate in the degradation mechanism (equation (4.47)), which is induced by the reaction with bromide liberated in the H• and e_{aq}^- induced processes.

$$HO\bullet + 2Br^- \rightarrow Br_2\bullet^- + OH^- \quad (4.47)$$

The $Br_2\bullet$- compounds are in equilibrium state with bromine radical in equation (4.48)

$$Br_2\bullet^- \leftrightarrow Br\bullet + Br^- \quad (4.48)$$

Accordingly, Br• induces either Br^- atom abstraction from the Br_3CCOO^- or oxidize the carboxyl function in a one-electron transfer process (Fliount et al., 1997).

$$Br\bullet + Br_3CCOO\text{-} \rightarrow Br_2 + \bullet Br_2CCOO \quad (4.49)$$

$$Br\bullet + Br_3CCOO\text{-} \rightarrow Br\text{-} + Br_3CCOO\bullet \quad (4.49)$$

However, at neutral pH and in the N_2O saturated solution, all e^-_{aq} is supposed to be converted into hydroxyl radicals according to the following equation and the reaction forming H• in equation is not present at neutral pH but in very acidic condition.

$$e_{aq}^- + N_2O + H_2O \rightarrow HO\bullet + OH^- + N_2 \quad (4.50)$$

$$H^+ + e_{aq}^- \rightarrow H\bullet \quad (4.51)$$

Therefore, we exclude the possibility of the reactions involving Br^- substitutions. Accordingly, it is very likely that HO• reacts with one of the halogenated atoms in perhalocarbons via electron-transfer.

4.4.3.6 Addition of Explicit Water Molecules

It is reported that water molecule is able to stabilize the developing negative charge on the hydroxyl radical in the transition state by acting as a hydrogen bond donor (Mitroka et al., 2010; Vöhringer-Martinez et al, 2007). An addition of explicit water molecules to the implicit polarizable continuum model has been reported to predict the absolute solvation free energies more accurately for a series of charged ions by considering short-range interactions between solvent and solute (Kim et al., 2009; Jaque et al., 2007; Pliego and Riveros, 2001). The SMD model that is used for this study includes the short-range interaction. However, the SMD does not include the explicit nonbulk electrostatic contribution that represents the deviation of short-range electrostatics from bulk electrostatics (Liu et al., 2010). Accordingly, we included a limited number of explicit water molecules (n=1~3) upon the transition state search and see differences in calculating the free energies of activations. As Mitroka et al. (2010) observed for the barriers of reaction of HO• with CH_4, addition of explicit water molecule(s) significantly decreases the barrier height of the reactions of HO• with a

series of halogenated acetates (Figure 4.15). The effect of individual water molecules appear to be additive. Three conformations of explicit one water molecule are found (Figure 4.16). Hydrogen of all explicit water molecules forms a hydrogen-bond with either oxygen of hydroxyl radical or carboxylic functional group. A total of two hydrogen bonds are observed for each configuration. When two and three explicit water molecules are added, carboxylic functional groups produce two and three hydrogen bonds, respectively, with hydrogen of hydroxyl radical and hydrogen of water molecules.

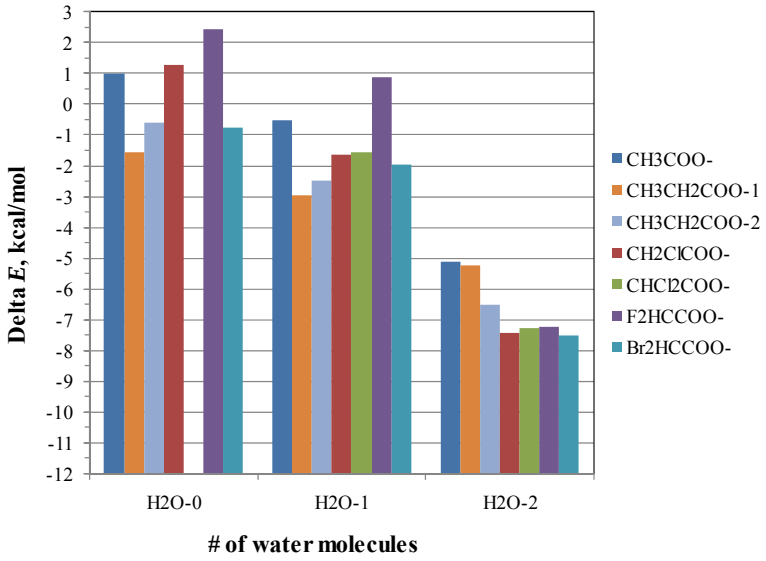

Figure 4.15: Comparison of observed barrier height for the reactions of HO• with a series of halogenated acetates in the absence of presence of explicit water molecule(s). Note that the transition state of the reaction of HO• with $CHCl_2COO^-$ could not be located.

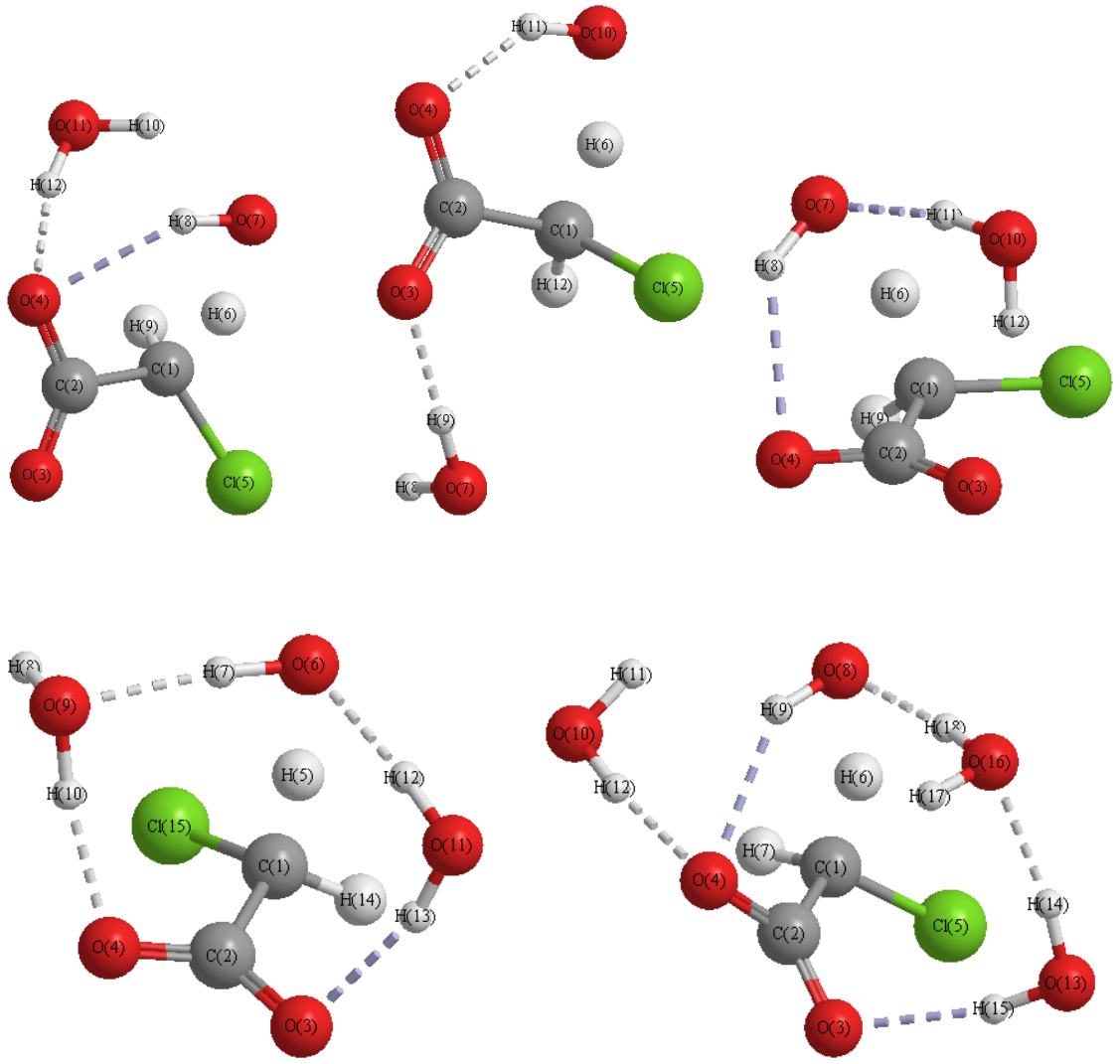

Figure 4.16: Optimized transition state for the reaction of HO• with chloroacetate in the presence of explicit water molecule(s). The dotted line represents hydrogen bond.

Addition(s) of explicit water molecules significantly change the charge distributions when compared to the case obtained from the absence of water molecules. Regardless several configurations of explicit water molecule(s), the charge distributions (Figure 4.17) revealed that the abstracted hydrogen-atom becomes less positive as

increasing explicit water molecules and the transition state becomes less polarized. As a result of this, the barrier heights become smaller with an increase of explicit water molecules. The presence of an explicit water molecule decreases the negative charges of a carboxylic functional group as well as a chlorine atom by almost half due to a hydrogen bond. When two or three water molecules are added, the degree of polarizability of transition state does not appear to be as much distinctive as the degree where one implicit water molecule is employed.

We establish the LFER using the calculated free energy of activation that is obtained by including explicit water molecules (Figure 4.1). The clear linear relation becomes closer to the LFER that is obtained from the experimental investigation. This observation suggests that the inclusion of explicit water molecule in addition to the SMD solvation model provides the actual solvation phenomena and the calculated free energies of activation that is a driving force can be quantum mechanically calculated. This approach may be used for the other reaction mechanisms to establish a library of reaction rate constants for a mechanistic modeling in AOPs.

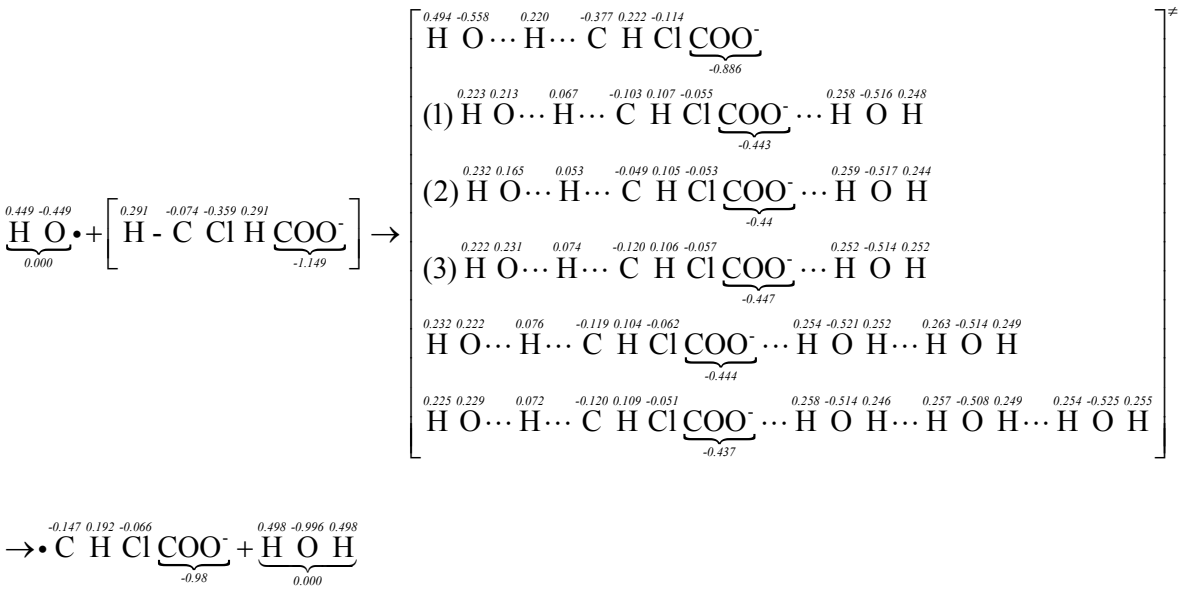

Figure 4.17: Charge distributions of reactants, transition states and products for the aqueous phases HO• reactions with chloroacetate in the absence and presence of explicit water molecule(s). The transition state in the presence of one explicit water molecule shows three conformations

4.5 Conclusions

Temperature-dependent aqueous phase HO• reaction rate constants enables us to obtain Arrhenius parameters and calculate thermochemical properties of activation. With the experimentally obtained free energies of activation and logarithms of the reaction rate constants, we established linear free energy relationships (LFERs) for a series of halogenated acetates. The experimentally obtained free energies of activation are compared with quantum mechanical calculations that utilize *Ab initio* quantum mechanical approaches and the SMD solvation model. Quantum mechanical calculations revealed that effects that arise from halogenated functional groups and hydrogen bonding in process of solvation. We found that an addition of explicit water molecule(s) to

implicit SMD solvation model provides the LFER that is consistent with that is established from the experiments.

4.6 Acknowledgement

This work was supported by the National Science Foundation Award 0854416 from the National Science Foundation. Any opinions, findings, conclusions, or recommendations expressed in this publication are those of the authors and do not necessarily reflect the view of the supporting organizations. Authors appreciate the support from the Hightower Chair and the Georgia Research Alliance at the Georgia Institute of Technology. Authors also appreciate Dr. Matthew Wolf at the College of Computing in Georgia Tech and Dr. Ron Huchinsons at Office of Information Technology for the high performance and clustered computing resources. We gratefully acknowledge the contribution of Mary Kate Varnau for her editorial assistance.

4.7 Appendices

Appendic F contains all optimized structures for reactants, transition states, complex and products at G4 with SMD.

4.8 Literature Cited

A division of the American Chemical Society. CAS (Chemical Abstract Service). http://www.cas.org/expertise/cascontent/index.html (accessed June 12, 2009).

Aquino, A.J.A.; Tunega, D.; Haberhauer, G.; Gerzaberk, M.H.; Lischka, H. Solvent effects on hydrogen bonds – A theoretical study. *J. Phys. Chem. A*. 2002, *106*, 1862-1871.

Ardura, D.; López, R.; Sordo, T.L. Relative gibbs energies in solution through continuum models: Effect of the loss of translational degrees of freedom in bimolecular reactions on gibbs energy barriers. J. Phys. Chem. B. 2005, 109, 23618-23623.

Asmus, K.-D.; Bonifačič, M. In Sulfur-Centered Reactive Intermediates as Studied by Radiation Chemical and Complementary Techniques; Chapter 5. 141-191. Alfassi, Z. B. Eds. The Chemistry of Free Radicals S-Centered Radicals. 1999. Chichester, U.K.

Beckwith, A.L.J.; Bowry, V.W.; Ingold, K.U. Kinetics of nitroxide radical trapping. 1. Solvent effects. J. Am. Chem. Soc. 1992, 114, 4983-4992.
Benson, S.W. The Foundations of Chemical Kinetics. McGraw-Hill: New York. 1982.

Bielski, B.H.J.; Cabelli, D.E. Highlights of current research involving superoxide and perhydroxyl radicals in aqueous solutions. *Int. J. Radiat. Biol*. 1991, *59*(2), 291-319.

Brezonik, P.L. Chemical kinetics and process dynamics in aqueous systems. Lewis Publishers. 2002.

Buxton, V. B.; Greenstock, C. L.; Helman, W. P.; Ross, A. B. Critical review of rate constants for reactions of hydrated electrons, hydrogen atoms and hydroxyl radicals (•OH/•O^-) in aqueous solution. *J. Phys. Chem. Ref. Data*. 1988, *17* (2) 513-795.

Charbonneau, P.; Knapp, B. 1995, A User's guide to PIKAIA 1.0, *NCAR Technical Note 418+IA*, National Center for Atmospheric Research, Boulder.

Chartfield, D.C.; Friedman, R.S.; Schwenke, D.W.; Truhlar, D.G. Control of chemical reactivity by quantized transition states. *J. Phys. Chem*. 1992, *96*, 2414-2421.

Chin, M.; Wine, P.H. Aquatic and Surface Photochemistry, G.R. Helz, R.G. Zepp and D.G. Crosby (eds.), CRC Press, Inc., Boca Raton, FL, 1994, p.85-96.

Cossi, M.; Rega, N.; Scalmani, G.; Barone, V. Energies, structures, and electronic properties of molecules in solution with the C-PCM solvation model. *J. Comp. Chem*. 2003, *24*(6), 669-681.

Cramer, J.C. Essentials of Computational Chemistry. Theories and Models. 2nd ed. John Wiley & Sons, Ltd. 2004. England.

Crittenden, J.C.; Hu, S.; Hand, D.W.; Green, S.A. A kinetic model for H_2O_2/UV process in a completely mixed batch reactor. *Wat. Res*. 1999, *33*(10), 2315-2328.

Curtiss, L.A. Gaussian-2 theory for molecular energies of first- and second-row compounds, *J. Chem. Phys.* 1991, *94*(11), 7221-7230.

Curtiss, L.A.; Redfern, P.C.; Raghavachari, K. Gaussian-4 theory. *J. Chem. Phys.*, 2007, 126, 084108.

Curtiss, L.A.; Redfern, P.C.; Rassolov, V.; Pople, J.A. Gaussian-3(G3) theory for molecules containing first and second-row atoms, *J. Chem. Phys.* 1998, *109*(18), 7764-7776.

Eisenberg, J.N.S.; Mckone, T.E. Decision tree method for the classification of chemical pollutants: Incorporation of across-chemical variability and within-chemical uncertainty. *Environ. Sci. Technol*. 1998, *32*, 3396-3404.

Eljarrat, E.; Barceló, D. Priority lists for persistent organic pollutants and emerging contaminants based on their relatice toxic potency in environmental samples. *Trends in Analytical Chem*. 2003, *22*(10), 655-665.

Ervens, B.; Gligorovski, S.; Herrmann, H. Teperature-dependent rate constants for hydroxyl radical reactions with organic compounds in aqueous solution. *Phys. Chem. Chem. Phys*., 2003, *5*, 1811-1824.

Eyring, H.; Gershinowitz, H.; Sun, C.E. The absolute rate of homogeneous atomic reactions. *J. Chem. Phys*. 1935, *3*, 786-796.

Evans, M.; Polanyı´, M. Inertia and driving force of chemical reactions. *Trans. Faraday Soc.* 1938, *34*, 11-29.

Fliount, R.; Makogon, O.; Guldi, D.M.; Asmus, K-D. Radical-mediated degradation mechanisms of tribromo- and other trishalogenated acetic acids in oxygen-free solutions as studied by radiation chemistry methods. J. Chem. Soc., Perkin Trans. 2. 1997, 1535-1545.

Foester, J.P.; Weinhold, F. Natural hybrid orbitals. *J. Am. Chem. Soc*. 1980, *102*, 7211-7218.

Galano, A.; Macías-Ruvalcaba, N.A.; Campos, O.N.M.; Pedraza-Chaverri, J. Mechanism of the OH radical scavenging activity of nordihydroguaiaretic acid: A combined theoretical and experimental study. J. Phys. Chem. B. 114, 6625-6635.

Gaussian 09, Revision A.1, Frisch, M. J.; Trucks, G. W.; Schlegel, H. B.; Scuseria, G. E.; Robb, M. A.; Cheeseman, J. R.; Scalmani, G.; Barone, V.; Mennucci, B.; Petersson, G. A.; Nakatsuji, H.; Caricato, M.; Li, X.; Hratchian, H. P.; Izmaylov, A. F.; Bloino, J.; Zheng, G.; Sonnenberg, J. L.; Hada, M.; Ehara, M.; Toyota, K.; Fukuda, R.; Hasegawa, J.; Ishida, M.; Nakajima, T.; Honda, Y.; Kitao, O.; Nakai, H.; Vreven, T.; Montgomery, Jr., J. A.; Peralta, J. E.; Ogliaro, F.; Bearpark, M.; Heyd, J. J.; Brothers, E.; Kudin, K. N.; Staroverov, V. N.; Kobayashi, R.; Normand, J.; Raghavachari, K.; Rendell, A.; Burant, J. C.; Iyengar, S. S.; Tomasi, J.; Cossi, M.; Rega, N.; Millam, N. J.; Klene, M.; Knox, J. E.; Cross, J. B.; Bakken, V.; Adamo, C.; Jaramillo, J.; Gomperts, R.; Stratmann, R. E.; Yazyev, O.; Austin, A. J.; Cammi, R.; Pomelli, C.; Ochterski, J. W.; Martin, R. L.; Morokuma, K.; Zakrzewski, V. G.; Voth, G. A.; Salvador, P.; Dannenberg, J. J.; Dapprich, S.; Daniels, A. D.; Farkas, Ö.; Foresman, J. B.; Ortiz, J. V.; Cioslowski, J.; Fox, D. J. Gaussian, Inc., Wallingford CT, 2009.

Gligorovski, S.; Herrmann, H. Kinetics of reactions of OH with organic carbonyl compounds in aqueous solution. *Phys. Chem. Chem. Phys*. 2004, *6*, 4118-4126.

Gligorovski, S.; Rousse, D.; George, C.H.; Herrmann, H. Rate constants for the OH reactions with oxygenated organic compounds in aqueous solution. *Int. J. Chem. Kinet*. 2009, *41*, 309-326.

Goldberg, D.E. Genetic algorithms in search, optimization, and machine learning. Addison-Wesley Publishing Company, INC. Massachusetts, U.S.A. 1989.

Herrmann, H. Kinetics of aqueous phase reactions relevant for atmospheric chemistry. *Chem. Rev*. 2003, *103*, 4691-4716.

Hindmarsh, A.C.; Gear, C.W. Ordinary differential equation system solver. UCID-30001 Rev. 3 Lawrence Livermore Laboratory, Livermore, Ca. 1974.

Hofinger, S.; Zerbetto, F. On the cavitation energy of water.*Eur. J. Chem.* 2003, *9*, 566.

Huber, M.M.; Canonica, S.; Park, G-Y.; Von Gunten, U. Oxidation of pharmaceuticals during ozonation and advanced oxidation processes. *Environ. Sci. Technol*. 2003, *37*, 1016-1024.

Hug, G.L.; Wang, Y.; Schöneich, C.; Jiang, P.-Y.; Fessenden, R.W. Multiple time scales in pulse radiolysis. Application to bromide solutions and dipeptides. Rad. Phys. Chem. 1999, 54, 559-566.

Jaque, P.; Marenich, A.V.; Cramer, C.J.; Truhlar, D.G. Computational electrochemistry: The aqueous Ru3+|Ru2+ reduction potential. *J. Phys. Chem. C*. 2007, *111*, 5783-5799.

Karelson, M. Molecular Descriptors in QSAR/QSPR. John Wiley & Sons, INC. New York, 2000.

Kelly, C.P.; Cramer, C.J.; Truhlar, D.G. Aqueous solvation free energies of ions and ion –water clusters based on an accurate value for the absolute aqueous solvation free energy of the proton. *J. Phys. Chem. B*. 2006, *110*, 16066-16081.

Kim, Y.; Marenich, A.V.; Zheng, J.; Kim, K-H.; Kolodziejska-Huben, M.; Rostkowski, M.; Paneth, P.; Truhlar, D.G. Mechanistic analysis of the base-catalyzed HF elimination from 4-fluoro-4-(4'-nitrophenyl)butane-2-one based on liquid-phase kinetic isotope effects calculated by dynamic modeling with multidimensional tunneling. *J. Chem. Theory Comput*. 2009, *5*, 59-67.

Klamt, A. Estimation of gas-phase hydroxyl radical rate constants of oxygenated compounds based on molecular orbital calculations. *Chemosphere*. 1996, *32*(4), 717-726.

Klamt, A.; Jonas, V.; Bürger, T.; Lohrenz, J.C.W. Refinement and parametrization of COSMO-RS. *J.Phys.Chem. A*. 1998, *102*, 5074-5085.

Lal, M.; Schoeneich, C.; Moenig, J.; Asmus, K.-D. Rate constants for the reaction of halogenated organic radicals. *Int. J. Radiat. Biol*. 1988, *54*, 773-785.

Leung, B. O.; Reid, D. L.; Armstrong, D. A.; Rauk, A. Entropies in solution from entropies in the gas phase. *J. Phys.Chem. A.* 2004, *108*, 2720-2725.

Li, K.; Crittenden, J.C. Computerized pathway elucidation for hydroxyl radical-induced chain reaction mechanisms in aqueous phase Advanced Oxidation Processes. *Environ. Sci. Technol*. 2009, *43*, 2831-2837.

Li, K.; Hokanson, D.R.; Crittenden, J.C.; Trussell, R.R.; Minakata, D. Evaluating UV/H_2O_2 processes for methyl tert-butyl ether and tertiary butyl alcohol removal. *Wat. Res*. 2008, *42*(20), 5045-5053.

Li, K.; Stefan, M.I.; Crittenden, J.C. Trichloroethene degradation by UV/H_2O_2 advanced oxidation process: product study and kinetic modeling. *Environ. Sci. Technol*. 2007, *41*, 1696-1703.

Li, K.; Stefan, M.I.; Crittenden, J.C. UV photolysis of trichloroethylene: Product study and kinetic modeling. *Environ. Sci. Technol*. 2004, *38*, 6685-6693.

Li, X.; Frisch, M.J. Energy-represented DIIS within a hybrid geometry optimization method. *J. Chem. Theory and Comput.* 2006, 2, 835-839.

Liptak, M. D.; Shields, G. C. Accurate p*K*a Calculations for Carboxylic Acids Using Complete Basis Set and Gaussian-n Models Combined with CPCM Continuum Solvation Methods. *J. Am. Chem. Soc.* 2001, *123*, 7314-7319.

Liu, J.; Kelly, C.P.; Goren, A.C.; Marenich, A.V.; Cramer, C.J.; Truhlar, D.G.; Zhan, C-G. Free energies of solvation with surface, volume, and local electrostatic effects and atomic surface tensions to represent the first solvation shell. *J. Chem. Theory. Comput*. 2010, *6*, 1109-1117.

Mader, E.A.; Davidson, E.R.; Mayer, J.M. Large ground-state entropy changes for hydrogen atom transfer reactions of iron complexes. *JACS*. 2007, *129*, 5153-5166.

Marenich, A. V.; Kelly, C. P.; Thompson, J. D.; Hawkins, G. D.; Chambers, C. C.; Giesen, D. J.; Winget, P.; Cramer, C. J.; Truhlar, D. G. *Minnesota Solvation Database – version 2009*, University of Minnesota, Minneapolis, 2009.

Marenich, A.V.; Cramer, C.J.; Truhlar, D.G. Universal solvation model based on solute electron density and on a continuum model of the solvent defined by the bulk dielectric constant and atomic surface tensions. *J. Phys. Chem. B*. 2009, *113*, 6378-6396.

Mezyk, S.P.; Bartels, D.M. Rate constant and activation energy measurement for the reaction of atomic hydrogen with thiocyanate and azide in aqueous solution. *J. Phys. Chem. A*. 2005, *109*, 11823-11827.

Milosavljevic, B.H.; LaVerne, J.A. Pulse radiolysis of aqueous thiocyanate solution. *J. Phys. Chem. A*. 2005, *109*, 165-168.

Minakata, D.; Crittenden, J.C. Linear free energy relationships between the aqueous phase hydroxyl radical reaction rate constants and the free energy of activation. *Environ. Sci. & Technol*. 2010 Submitted.

Minakata, D.; Li, K.; Westerhoff, P.; Crittenden, J. Development of a group contribution method to predict aqueous phase hydroxyl radical (HO•) reaction rate constants. *Environ. Sci. & Technol*. 2009, *43*, 6220-6227.

Monod, A.; Poulain, L.; Grubert, S.; Voisin, D.; Wortham, H. Kinetics of OH-initiated oxidation of oxygenated organic compounds in the aqueous phase: new rate constants, structure-activity relationships and atmospheric implications. *Atmos. Environ*. 2005, *39*, 7667-7688.

Narten, A. H.; Levy, H. A. Liquid water: Molecular correlation functions from X-ray diffraction. *J. Chem. Phys.* 1971, *55*, 2263.

Neta, P.; Simic, M.; Hayon, E. Pulse radiolysis of aliphatic acids in aqueous solutions. I. Simple monocarboxylic acids. *J. Phys. Chem*. 1969, *73*(12), 4207-4213.

Okuno, Y. Theoretical investigation of the mechanism of the Baeyer-Villiger reaction in nonpolar solvents. *Chemistry: a European Journal*. 1997, 3, 212.

Partington, J.R. An advanced Treatise on Physical Chemisty, Longmans, Green and Co. London. 1951. Vol.2 pp2. And Vol.5 pp390.

Pascual-Ahuir, J. L.; Silla, E. GEPOL: An improved description of molecular surfaces. I. Building the spherical surface set. *J. Comput. Chem.* 1990, *11*, 1047.

Peng, C.; Ayala, P.Y.; Schlegel, H.B.; Frisch, M.J. Using redundant internal coordinates to optimize equilibrium geometries and transition states. *J. Comp. Chem. 1996, 17, 49-86.*

Peng, C.; Schlegel, H.B. Combining Synchronous Transit and Quasi-Newton Methods for Finding Transition States. *Israel J. Chem*. 1993, *33,* 449-54.

Pfaendtner, J.; Broadbelt, L. J. Elucidation of structure-reactivity relationships in hindered phenols via quantum chemistry and transition state theory. *Chem. Eng. Sci.* 2007, *62*, 5232-5239.

Pfaendtner, J.; Broadbelt, L. J. Mechanistic modeling of lubricant degradation. 2. The autooxidation of decane and octane. *Ind. Eng. Chem. Res*. 2008, *47*, 2897-2904.

Pfaendtner, J.; Broadbelt, L. J. Mechanistic modeling of lubricant degradation. 1. Structure-reactivity relationships for free-radical oxidation. *Ind. Eng. Chem. Res*. 2008, *47*, 2886-2896.

Pierotti, R. A. The solubility of gases in liquids. *J. Phys. Chem.* 1963, *67*, 1840-1845.
Pitzer, K.S.; Gwinn, W. Energy levels and thermodynamic functions for molecules with internal rotation. *J. Chem. Phys*. 1942, *10*, 428-440.

Pliego, J.R.; Riveros, J.M. The cluster-continuum model for the calculation of the solvation free energy of ionic species. *J. Phys. Chem. A*. 2001, *105*, 7241-7247.

Pople, J.A.; Gordon, M.H.; Fox, D.J. Gaussian-1 theory: A general procedure for prediction of molecular energies. *J. Chem. Phys.* 1989, *90*(10), 5622-2629.

Pu, J.; Gao, J.; Truhlar, D.G. Multidimensional tunneling, recrossing, and the transmission coefficient for enzymatic reactions. *Chem. Rev*. 2006, *106*, 3140-3169.

Richardson, S. D. Water Analysis: Emerging contaminants and current issues. *Anal. Chem*., 2009, *81*, 4645-4677.

Rosenfeldt, E.J.; Linden, K.G. Degradation of endocrine disrupting chemicals bisphenol A, ethinyl estradiol, and estradiol during UV photolysis and advanced oxidation processes. *Environ. Sci. Technol*. 2004, *38*, 5476-5483.

Schlegel, H.B. Optimization of equilibrium geometries and transition structures. *J. Comp. Chem*. 1982, *3*(2), 214-218.

Schwarz, H. A determination of some rate constants for the radical processes in the radiation chemistry of water. 1962, *66*, 255-262.

Spinks, J. W. T.; Woods, R. J. *An Introduction to Radiation Chemistry*: John Wiley & Sons: New York, 1964; Chapter 8, pp 237-308.

Štefanić, I.; Ljubić, M.; Bonifačić, M.; Sabljić, A.; Asmus, K.-D. A surprisingly complex aqueous chemistry of the simplest amino acid. A pulse radiolysis and theoretical study on H/D kinetic isotope effects in the reaction of glycine anions with hydroxyl radicals. *Phys. Chem. Chem. Phys*. 2009, *11*, 2256-2267.

Tanko, J. M.; Suleman, N. K. Solvent Effects in the Reactions of Neutral Free Radicals. In Energetics of Organic Free Radicals; Martinho Simo˜es, J. A., Greenburg, A., Liebman, J. F., Eds.; SEARCH Series 4; Blackie: Glasgow, 1996; pp 244-293.

Van Cauter, K.; Van Speybroeck, V.; Vansteenkiste, P.; Reyniers, M. F.; Waroquier, M. Ab initio study of free-radical polymerization: Polyethylene propagation kinetics. *Chem. Phys. Chem.* 2006, *7*, 131-140.

Vöhringer-Martinez, E.; Hansmann, B.; Hernandez, H.; Francisco, J.S.; Troe, J.; Abel, B. Water catalysis of a radical-molecule gas-phase reaction. *Science*. 2007, *315*, 497-501.

von Sonntag, C.; Schuchmann, H.-P. In., Alfassi, Z. B. *Peroxyl Radicals*; John Wiley and Sons Ltd.: New York, 1997; p 173.

Westerhoff, P.; Yoon, Y.; Snyder, S.; Wert, E. Fate of endocrine-disruptor, pharmaceutical, and personal care product chemicals during simulated drinking water treatment processes. *Environ. Sci. Technol*. 2005, *39*, 6649-6663.

Whitman, K.; Lyons, S. Miller, R.; Nett, D.; Treas, P.; Zante, A.; Fessenden, R. W.; Thomas, M. D.; Wang, Y. In *Proceedings of the '95 Particle Accelerator Conference and International Conference on High Energy Accelerators*, Dallas, Texas, May 1-5, 1995.

Wigner, E. Z. *f. physic. Chemie* B19, 203, 1932.

Wold, S.; Sjöström, M. Liner Free Energy Relationships as Tools for Investigating Chemical Similarity- Theory and Practice. 1-54 in Chapman, N.B.; Shorter, J. Correlation Analysis in Chemistry Recent Advances. Plenum Press New York and Longdon, 1978.

Woo, Y-T.; Lai, D.; McLain, J.L.; Manibusan, M.L.; Dellarco, V. Use of mechanism-based structure-activity relationships analysis in carcinogenic potential ranking for drinking water disinfection by-products. Environ. Health Perspectives. 2002, 110, 75-87.

CHAPTER 5

Implications and Future Studies

The GCM is innovative because it is the first comprehensive tool to predict the aqueous phase HO• reaction rate constant and it includes a wide range of functional groups and four reaction mechanisms: 1) H-atom abstraction by HO•, 2) HO• addition to alkenes, 3) HO• addition to aromatic compounds, and 4) HO• interactions with S-, N-, or P-atom-containing compounds. The GCM's predictability (i.e., $0.5 \leq k_{cal}/k_{exp} \leq 2.0$) is an acceptable range in terms of predicting reaction rate constants. The GCM provides a user-friendly Microsoft excel spread sheet and an executed FORTRAN program named GCM Identifier.f90. These tools enable one to calculate the aqueous phase HO• reaction rate constants with a minimum input of structural information of a compound of interest. This will help researchers and water treatment engineers estimate the "reactivity" when coming across a new chemical compound in application of AOPs. With newly obtained HO• reaction rate constants, we should be able to update the GCM to include missing functional groups that have not been employed in the original GCM.

The LFERs that have been developed using sophisticated quantum mechanical approaches bridge kinetic information that is obtained from experiments with theoretically calculated thermochemical properties (i.e., free energy of activation). The application of the LFERs to chemical reactivity is a new concept. The theoretically calculated free energy of activation was validated with those that were obtained from the experimental investigations. Aqueous phase molecular modeling using quantum mechanical approaches is a challenging task due to water molecules. Nevertheless, our

methodologies that utilize combinations of gaseous phase *Ab initio* quantum mechanical calculations with implicit solvation model have been shown to calculate aqueous phase free energy of activation with acceptable errors as compared to those that were obtained from experiments. This proof of concept study should be applied to other reaction mechanisms where few experimental reaction rate constants are available. Figures 5.1-5.3 demonstrate the aqueous phase free energy profiles that are calculated at G3 and COSMO-RS for the HO• induced reactions with methane. Figure 5.1 includes the hydrogen-atom abstraction by HO•, oxygen addition followed by peroxy radical reaction mechanisms that are predicted by the reaction pathway generator. Figure 5.2 shows 1.2-H shift of oxyl radical in the absence and presence of a water molecule. Figure 5.3 shows the hydrolysis reactions of formaldehyde with one and two water molecules assisted. These energy profiles are in good agreement with the gaseous phase potential energy profiles for the reaction of HO• with methane (Green, 1994), although he did not locate transition states for any reactions. For example, Green (1994) obtained approximately 30 kcal/mol of gaseous phase reaction energy for $CH_3 + O_2 \rightarrow CH_3OO\bullet$ while we obtained 30.0 kcal/mol of aqueous phase free energy of reaction for this exorthermic reaction. Furthermore, he calculated approximately 60 kcal/mol of reaction energy for the gaseous phase uni-molecular reaction of $CH_3OO\bullet \rightarrow CH_3O\bullet + O$, whereas we obtained 53.7 kcal/mol of aqueous phase free energy of reaction. The similar agreements were observed for other reactions for $CH_3OO\bullet \rightarrow H_2C\bullet OOH$ and $H_2C\bullet OOH \rightarrow CH_2O + HO$. Although these free energy profiles are limited to the HO• induced reactions with methane, same procedures should be applied for other reactions to build LFERs and establish a library of rate constant predictions for the reactions that take place in AOPs.

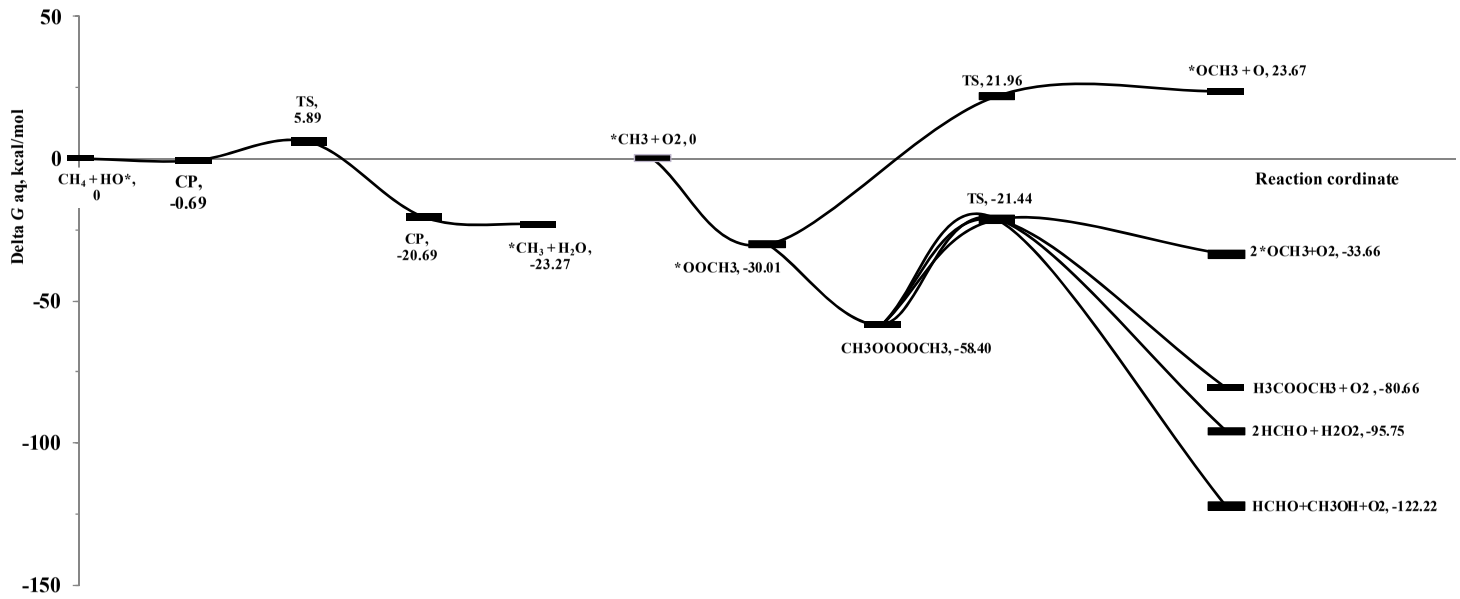

Figure 5.1: Aqueous phase free energy change profiles for the reactions that are initiated by HO•

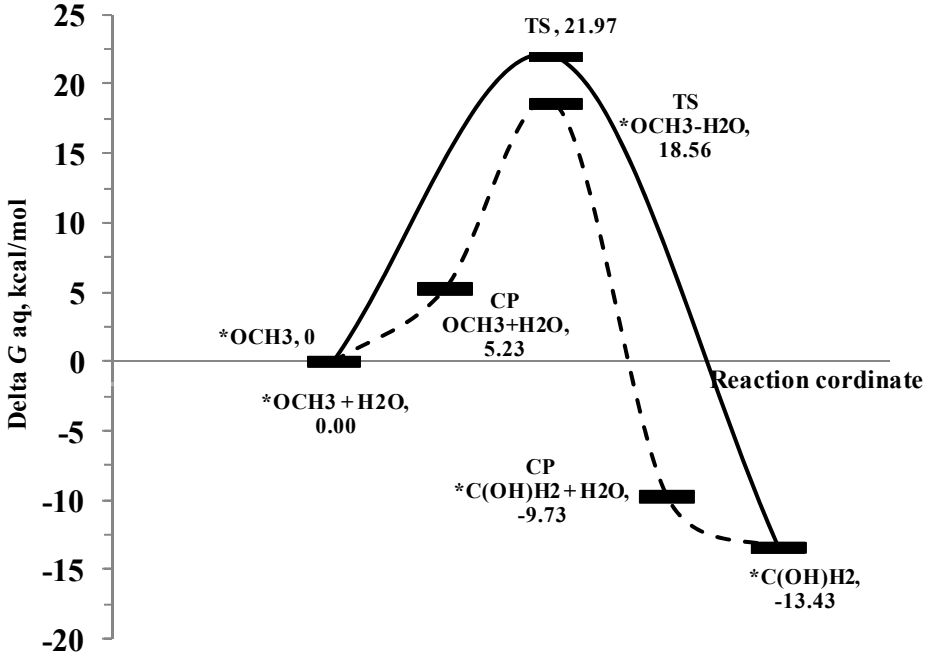

Figure 5.2: Aqueous phase free energy change profiles for 1,2-H shift reaction of oxyl radical in the absence or presence of a water molecule

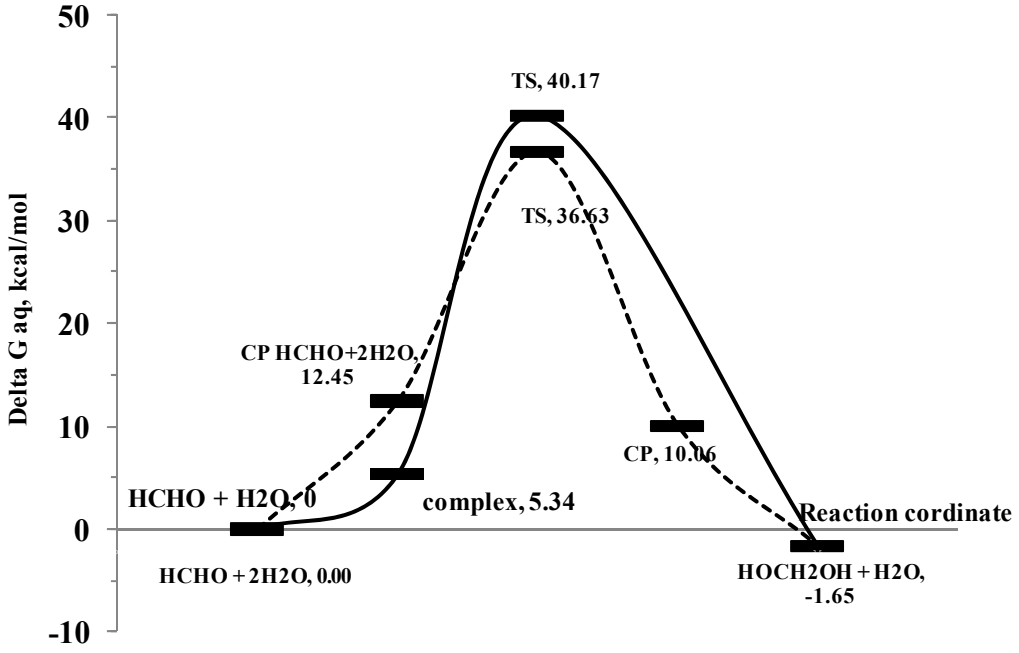

Figure 5.3: Aqueous phase free energy change profiles for hydrolysis reaction of formaldehyde with one and two water molecules assisted

There are significant differences in basic principle, theory, approach, and reaction mechanism that are applied between the GCM and LFERs. While the GCM shows the predicatability: $0.5 \leq k_{cal}/k_{exp} \leq 2.0$ (i.e., difference of factor 2), the LFER indicates: $0.2 \leq k_{cal}/k_{exp} \leq 5.0$ (i.e., difference of factor 5). The GCM includes a wide range of functional groups and four HO• reaction mechanisms (i.e., H-atom abstraction, HO• adition to alkenes and aromatic compounds, and HO• interaction with S-, N-, or P-atom-containing compounds). The LFERs include aliphatic hydrocarbons, oxygenated and halogenated compounds for H-atom abstraction from C-H bond and HO• addition to alkenes. While the GCM utilizes overall reaction rate constant using Benson's thermochemical and rate constant additivity, the LFERs consider the lowest energy point of aqueous phase free energy of activation among different transition states and conformers. The GCM does not include electron-electron interactions in the process from reactants to transition state, whereas the LFERs consider transition state energy based on *Ab initio* quantum mechanical calculations. Both the GCM and LFERs used single-functional-group compounds for calibration and multi-functional-group compounds for prediction. The GCM shows applicability of predicting rate constant for a limited number of emerging contaminants, whereas the LFERs do not because of many possible transition states and conformers. The largest molecules that the LFERs include are $HOOCCH_2COOH$ for neutral, and Br_2HCCOO^- and $^-OOC(CH_2)_2COO^-$ for ionized compounds. These aliphatic saturated compounds would be comprised of 8 equivalent carbon-atoms if all elements are carbons and hydrogens. Considerable efforts have to be made to deal with emerging contaminant using the LFERs. Although the GCM shows better predicatability of aqueous phase HO• reaction rate constants for compounds with multi-functional-groups

than the LFERs, the LFERs can be applied to other reaction mechanisms based on *Ab initio* reaction rate constant predictions. As a consequence, the LFERs approach should be used for the reaction rate constant predictors of mechanistic modeling in aqueous phase AOPs.

Application of computational chemistry using quantum mechanical approaches to water treatment engineering is not common. With recent improvement in high performance computing resources, aqueous phase molecular simulations in relatively larger molecules become feasible. The proof of concept approach using the LFERs implicates the validity of application of computational chemistry to chemical reactivity that is observed in water treatment engineering. The LFERs may be applied not only AOPs technology but also other oxidation and disinfection processes (e.g., chlorination, ozonation, manganese).

To apply water treatment, mechanics modeling must include the effect of natural organic matter (NOM). Our modeling only represents a starting point by developing the theoretical approach and modeling framework in water containing only the target compound. NOM reactions with radical species are complex (Westerhoff et al., 1999; von Gunten, 2003) and they could be added in the future, if the knowledge-base on the structural and chemical characteristics of NOM become available. To date, the impact of NOM on target compound destruction has been considered by accounting for NOM quenching of hydroxyl radical (Westerhoff et al., 2007; 1999; Elovitz et al., 2000) and UV light absorption (Li et al., 2008; Weishaar et al., 2003). This approach could also be applied to the by-products that are formed. However, a considerable amount of effort

remains to understand the byproduct formation of target compounds in the presence of NOM (Weber et al., 2005).

A contribution of this dissertation to engineering field is significant. This dissertation shows an application of existing scientific disciplines to water treatment engineering field by shedding light on developing tools to predict aqueous phase HO• reaction rate constants for aqueous phase AOPs. In general, when a ciritical chemical contaminant is identified, it is typical to measure the rate constant with chemical oxidant experimentally or estimate the rate constant on the basis of structurally similar compounds. For engineering design, an over-design is a typical strategy using a safety factor. This approach is also applied for intermediates and byproducts by extending retention time and scaling reactor volume. However, considering a number of chemical contaminants that emerge in industries, this approach is not practical in particular for fate of intermediate and byproducts. The reaction rate constant predictors that have been developed in this study enable water treatment engineers to screen reactivity of a new contaminant in the application of AOPs. Once the mechanistic model is developed based on a library of reaction rate constant predictors, it will be used to help engineers assess the treatment efficiency of a parent contaminant and evaluate the fate of intermediate and byproducts in aqueous phase AOPs.

Literature Cited

Elovitz, M. S.; von Gunten, U; Kaiser H-P. Hydroxyl radical/ozone ratios during ozonationprocesses. II. The effect of temperature, pH, alkalinity, and DOM properties. *Ozone. Sci. Eng*. 2000, *22*, 123-150.

Li, K.; Hokanson, D.R.; Crittenden, J.C.; Trussell, R.R.; Minakata, D. Evaluating UV/H2O2 processes for methyl tert-butyl ether and tertiary butyl alcohol removal: Effect of pretreatment options and light sources. *Wat. Res*. 2008, 42, 5045-5053.

von Gunten, U. Ozonation of drinking water: Part I. Oxidation kinetics and product formation. *Wat. Res*. 2003, *37*, 1443-1467.

Weber, J.R. W.; Huang, Q.; Pinto, A. Reduction of disinfection byproduct formation by molecular reconfiguration of the fulvic constituents of natural background organic mater. *Environ. Sci. Technol*. 2005, *39*, 6446-6452.

Weishaar, J. L.; Aiken, G. R.; Bergamaschi, B. A.; Fram, M. S.; Fujii, R.; Mopper, K. Evaluation of specific ultraviolet absorbance as an indicator of the chemical composition and reactivity of dissolved organic carbon. *Environ. Sci. Technol.* 2003, *37*, 4702-4708.

Westerhoff, P.; Aiken, G.; Amy, G.; Debroux, J. Relationships between the structure of natural organic matter and its reactivity towards molecular ozone and hydroxyl radicals. *Wat. Res.* 1999, *33* (10), 2265-2276.

Westerhoff, P.; Mezyk, S.P.; Cooper, W.J.; Minakata, D. Electron pulse radiolysis determination of hydroxyl radical rate constants with Suwannee river fulvic acid and other dissolved organic matter isolates. *Environ. Sci. & Technol*. 2007, *41*, 4610-4646.

APPENDIX A: GENETIC ALGORITHM

```
MODULE Genetic_Algorithm
IMPLICIT NONE

!    Common block to make iseed visible to rninit (and to save
!    it between calls)
! COMMON /rnseed/ iseed
INTEGER, SAVE  :: iseed


CONTAINS


SUBROUTINE pikaia(ff,n,ctrl,x,f,STATUS)

! Code converted using TO_F90 by Alan Miller
! Date: 2001-07-09  Time: 15:54:13

!=========================================================
==========
!  Optimization (maximization) of user-supplied "fitness" function ff
!  over n-dimensional parameter space  x  using a basic genetic algorithm
!  method.

!  Paul Charbonneau & Barry Knapp
!  High Altitude Observatory
!  National Center for Atmospheric Research
!  Boulder CO 80307-3000
!  USA
!  <paulchar@hao.ucar.edu>
!  <knapp@hao.ucar.edu>

!  Web site:
!  http://www.hao.ucar.edu/public/research/si/pikaia/pikaia.html

!  Version 1.0   [ 1995 December 01 ]

!  Genetic algorithms are heuristic search techniques that incorporate in a
!  computational setting, the biological notion of evolution by means of
!  natural selection.  This subroutine implements the three basic operations
!  of selection, crossover, and mutation, operating on "genotypes" encoded as
!  strings.

!  References:

!    Charbonneau, Paul.  "Genetic Algorithms in Astronomy and Astrophysics."
!       Astrophysical J. (Supplement), vol 101, in press (December 1995).

!    Goldberg, David E.  Genetic Algorithms in Search, Optimization,
!       & Machine Learning.  Addison-Wesley, 1989.

!    Davis, Lawrence, ed.  Handbook of Genetic Algorithms.
!       Van Nostrand Reinhold, 1991.
!=========================================================
==========
!  USES: ff, urand, setctl, report, rnkpop, select, encode, decode,
!       cross, mutate, genrep, stdrep, newpop, adjmut

INTEGER, INTENT(IN)   :: n
REAL, INTENT(IN OUT)  :: ctrl(12)
REAL, INTENT(OUT)     :: x(n)
REAL, INTENT(OUT)     :: f
INTEGER, INTENT(OUT)  :: STATUS

INTERFACE
  FUNCTION ff(n, x) RESULT(fn_val)
    IMPLICIT NONE
    INTEGER, INTENT(IN)  :: n
    REAL, INTENT(IN)     :: x(:)
    REAL                 :: fn_val
  END FUNCTION ff
END INTERFACE

! EXTERNAL ff

!  Input:
!  o Integer  n  is the parameter space dimension, i.e., the number
!    of adjustable parameters.

!  o Function  ff  is a user-supplied scalar function of n variables, which
!    must have the calling sequence f = ff(n,x), where x is a real parameter
!    array of length n.  This function must be written so as to bound all
!    parameters to the interval [0,1]; that is, the user must determine
!    a priori bounds for the parameter space, and ff must use these bounds
!    to perform the appropriate scalings to recover true parameter values in
!    the a priori ranges.

!    By convention, ff should return higher values for more optimal
!    parameter values (i.e., individuals which are more "fit").

!    For example, in fitting a function through data points, ff
!    could return the inverse of chi**2.

!    In most cases initialization code will have to be written
!    (either in a driver or in a separate subroutine) which loads
!    in data values and communicates with ff via one or more labeled
!    common blocks.  An example exercise driver and fitness function
!    are provided in the accompanying file, xpkaia.f.


!  Input/Output:


!  o Array  ctrl  is an array of control flags and parameters, to
!    control the genetic behavior of the algorithm, and also printed
!    output.  A default value will be used for any control variable
!    which is supplied with a value less than zero.  On exit, ctrl
!    contains the actual values used as control variables.  The
!    elements of ctrl and their defaults are:

!      ctrl( 1) - number of individuals in a population (default
!                 is 100)
!      ctrl( 2) - number of generations over which solution is
!                 to evolve (default is 500)
!      ctrl( 3) - number of significant digits (i.e., number of
!                 genes) retained in chromosomal encoding (default
!                 is 6)  (Note: This number is limited by the
!                 machine floating point precision.  Most 32-bit
!                 floating point representations have only 6 full
!                 digits of precision.  To achieve greater preci-
!                 sion this routine could be converted to double
!                 precision, but note that this would also require
!                 a double precision random number generator, which
!                 likely would not have more than 9 digits of
!                 precision if it used 4-byte integers internally.)
!      ctrl( 4) - crossover probability; must be  <= 1.0 (default is 0.85)
!      ctrl( 5) - mutation mode; 1/2=steady/variable (default is 2)
!      ctrl( 6) - initial mutation rate; should be small (default is 0.005)
!                 (Note: the mutation rate is the probability that any one
!                 gene locus will mutate in any one generation.)
!      ctrl( 7) - minimum mutation rate; must be >= 0.0 (default is 0.0005)
!      ctrl( 8) - maximum mutation rate; must be <= 1.0 (default is 0.25)
!      ctrl( 9) - relative fitness differential; range from 0
!                 (none) to 1 (maximum).  (default is 1.)
!      ctrl(10) - reproduction plan; 1/2/3=Full generational
!                 replacement/Steady-state-replace-random/Steady-
!                 state-replace-worst (default is 3)
!      ctrl(11) - elitism flag; 0/1=off/on (default is 0)
!                 (Applies only to reproduction plans 1 and 2)
!      ctrl(12) - printed output 0/1/2=None/Minimal/Verbose (default is 0)


! Output:


!  o Array  x(1:n)  is the "fittest" (optimal) solution found,
!    i.e., the solution which maximizes fitness function ff

!  o Scalar  f  is the value of the fitness function at x

!  o Integer  status  is an indicator of the success or failure
!    of the call to pikaia (0=success; non-zero=failure)


! Constants

INTEGER, PARAMETER :: nmax = 200, pmax = 128, dmax = 6

!  o NMAX is the maximum number of adjustable parameters (n <= NMAX)

!  o PMAX is the maximum population (ctrl(1) <= PMAX)

!  o DMAX is the maximum number of Genes (digits) per Chromosome
!       segement (parameter) (ctrl(3) <= DMAX)


!    Local variables
INTEGER :: np, nd, ngen, imut, irep, ielite, ivrb, k, ip, ig, ip1,  &
          ip2, NEW, newtot
REAL :: pcross, pmut, pmutmn, pmutmx, fdif

REAL :: ph(nmax,2), oldph(nmax,pmax), newph(nmax,pmax)

INTEGER :: gn1(nmax*dmax), gn2(nmax*dmax)
INTEGER :: ifit(pmax), jfit(pmax)
REAL :: fitns(pmax)

!    User-supplied uniform random number generator
```

```
! REAL :: urand
! EXTERNAL urand

! Function urand should not take any arguments.  If the user wishes to be able
! to initialize urand, so that the same sequence of random numbers can be
! repeated, this capability could be implemented with a separate subroutine,
! and called from the user's driver program.  An example urand function
! (and initialization subroutine) which uses the function ran0 (the "minimal
! standard" random number generator of Park and Miller [Comm. ACM 31, 1192-
! 1201, Oct 1988; Comm. ACM 36 No. 7, 105-110, July 1993]) is provided.


!    Set control variables from input and defaults
CALL setctl(ctrl, n, np, ngen, nd, pcross, pmutmn, pmutmx, pmut, imut, fdif, &
        irep, ielite, ivrb, STATUS)
IF (STATUS /= 0) THEN
  WRITE (*, *) ' Control vector (ctrl) argument(s) invalid'
  RETURN
END IF

!    Make sure locally-dimensioned arrays are big enough
IF (n > nmax .OR. np > pmax .OR. nd > dmax) THEN
  WRITE (*, *) ' Number of parameters, population, or genes too large'
  STATUS = -1
  RETURN
END IF

!    Compute initial (random but bounded) phenotypes
DO  ip = 1, np
  DO  k = 1, n
    oldph(k,ip) = urand()
  END DO
  fitns(ip) = ff(n, oldph(:,ip))
END DO

!    Rank initial population by fitness order
CALL rnkpop(np,fitns,ifit,jfit)

!    Main Generation Loop
DO  ig = 1, ngen

!      Main Population Loop
  newtot = 0
  DO  ip = 1, np / 2

!        1. pick two parents
    CALL select(np,jfit,fdif,ip1)
    30 CALL select(np,jfit,fdif,ip2)
    IF (ip1 == ip2) GO TO 30

!        2. encode parent phenotypes
    CALL encode(n,nd,oldph(1,ip1),gn1)
    CALL encode(n,nd,oldph(1,ip2),gn2)

!        3. breed
    CALL cross(n,nd,pcross,gn1,gn2)
    CALL mutate(n,nd,pmut,gn1)
    CALL mutate(n,nd,pmut,gn2)

!        4. decode offspring genotypes
    CALL decode(n,nd,gn1,ph(1,1))
    CALL decode(n,nd,gn2,ph(1,2))

!        5. insert into population
    IF (irep == 1) THEN
      CALL genrep(nmax,n,np,ip,ph,newph)
    ELSE
      CALL stdrep(ff,nmax,n,np,irep,ielite,ph,oldph,fitns,ifit, jfit,NEW)
      newtot = newtot + NEW
    END IF

!      End of Main Population Loop
  END DO

!      if running full generational replacement: swap populations
  IF (irep == 1) CALL newpop(ff,ielite,nmax,n,np,oldph,newph,ifit,  &
      jfit,fitns,newtot)

!      adjust mutation rate?
  IF (imut == 2) CALL adjmut(np,fitns,ifit,pmutmn,pmutmx,pmut)

!      print generation report to standard output?
  IF (ivrb > 0) CALL report(ivrb,nmax,n,np,nd,oldph,fitns,ifit,pmut,ig,newtot)

!    End of Main Generation Loop
END DO

!    Return best phenotype and its fitness
DO  k = 1, n
  x(k) = oldph(k,ifit(np))
END DO
f = fitns(ifit(np))
RETURN
END SUBROUTINE pikaia

!*****************************************************************
***

SUBROUTINE setctl(ctrl,n,np,ngen,nd,pcross,pmutmn,pmutmx,pmut,  &
          imut,fdif,irep,ielite,ivrb,STATUS)
!=================================================================
==========
!    Set control variables and flags from input and defaults
!=================================================================
=========

!    Input
!    Input/Output
REAL, INTENT(IN OUT)  :: ctrl(12)
INTEGER, INTENT(IN)   :: n

!    Output
INTEGER, INTENT(OUT)  :: np
INTEGER, INTENT(OUT)  :: ngen
INTEGER, INTENT(OUT)  :: nd
REAL, INTENT(OUT)     :: pcross
REAL, INTENT(OUT)     :: pmutmn
REAL, INTENT(OUT)     :: pmutmx
REAL, INTENT(OUT)     :: pmut
INTEGER, INTENT(OUT)  :: imut
REAL, INTENT(OUT)     :: fdif
INTEGER, INTENT(OUT)  :: irep
INTEGER, INTENT(OUT)  :: ielite
INTEGER, INTENT(OUT)  :: ivrb
INTEGER, INTENT(OUT)  :: STATUS


!    Local
INTEGER :: i
REAL, SAVE  :: dfault(12) = (/ 100., 500., 5., .85, 2., .005, .0005, .25,  &
                1., 1., 1., 0. /)

DO  i = 1, 12
  IF (ctrl(i) < 0.) ctrl(i) = dfault(i)
END DO

np = ctrl(1)
ngen = ctrl(2)
nd = ctrl(3)
pcross = ctrl(4)
imut = ctrl(5)
pmut = ctrl(6)
pmutmn = ctrl(7)
pmutmx = ctrl(8)
fdif = ctrl(9)
irep = ctrl(10)
ielite = ctrl(11)
ivrb = ctrl(12)
STATUS = 0

!    Print a header
IF (ivrb > 0) THEN

  WRITE (*,5000) ngen, np, n, nd, pcross, pmut, pmutmn, pmutmx, fdif
  IF (imut == 1) WRITE (*,5100) 'Constant'
  IF (imut == 2) WRITE (*,5100) 'Variable'
  IF (irep == 1) WRITE (*,5200) 'Full generational replacement'
  IF (irep == 2) WRITE (*,5200) 'Steady-state-replace-random'
  IF (irep == 3) WRITE (*,5200) 'Steady-state-replace-worst'
END IF

!    Check some control values
IF (imut /= 1 .AND. imut /= 2) THEN
  WRITE (*,5300)
  STATUS = 5
END IF

IF (fdif > 1.) THEN
  WRITE (*,5400)
  STATUS = 9
END IF

IF (irep /= 1 .AND. irep /= 2 .AND. irep /= 3) THEN
  WRITE (*,5500)
  STATUS = 10
END IF

IF (pcross > 1.0 .OR. pcross < 0.) THEN
  WRITE (*,5600)
  STATUS = 4
END IF

IF (ielite /= 0 .AND. ielite /= 1) THEN
  WRITE (*,5700)
  STATUS = 11
```

```
END IF

IF (irep == 1 .AND. imut == 1 .AND. pmut > 0.5 .AND. ielite == 0) THEN
  WRITE (*,5800)
END IF

IF (irep == 1 .AND. imut == 2 .AND. pmutmx > 0.5 .AND. ielite == 0) THEN
  WRITE (*,5900)
END IF

IF (fdif < 0.33 .AND. irep /= 3) THEN
  WRITE (*,6000)
END IF

IF (MOD(np,2) > 0) THEN
  np = np - 1
  WRITE (*,6100) np
END IF

RETURN
5000 FORMAT (/' ', 60('*') /   &
   ' *', t16, 'PIKAIA Genetic Algorithm Report ', t60, '*' / &
   ' ', 60('*') //  &
   '  Number of Generations evolving: ', i4 /  &
   '      Individuals per generation: ', i4 /  &
   '    Number of Chromosome segments: ', i4 /  &
   '    Length of Chromosome segments: ', i4 /  &
   '          Crossover probability: ', f9.4 /   &
   '          Initial mutation rate: ', f9.4 /   &
   '          Minimum mutation rate: ', f9.4 /   &
   '          Maximum mutation rate: ', f9.4 /   &
   '    Relative fitness differential: ', f9.4)
5100 FORMAT ('                  Mutation Mode: '/ a)
5200 FORMAT ('              Reproduction Plan: '/ a)
5300 FORMAT (' ERROR: illegal value for imut (ctrl(5))')
5400 FORMAT (' ERROR: illegal value for fdif (ctrl(9))')
5500 FORMAT (' ERROR: illegal value for irep (ctrl(10))')
5600 FORMAT (' ERROR: illegal value for pcross (ctrl(4))')
5700 FORMAT (' ERROR: illegal value for ielite (ctrl(11))')
5800 FORMAT (' WARNING: dangerously high value for pmut (ctrl(6));' /  &
   ' (Should enforce elitism with ctrl(11)=1.)')
5900 FORMAT (' WARNING: dangerously high value for pmutmx (ctrl(8));' /
&
   ' (Should enforce elitism with ctrl(11)=1.)')
6000 FORMAT (' WARNING: dangerously low value of fdif (ctrl(9))')
6100 FORMAT (' WARNING: decreasing population size (ctrl(1)) to np='/ i4 )
END SUBROUTINE setctl

!*****************************************************************
***

SUBROUTINE report(ivrb, ndim, n, np, nd, oldph, fitns, ifit, pmut, ig, nnew)

!    Write generation report to standard output

!    Input:
INTEGER,  INTENT(IN)  :: ivrb
INTEGER,  INTENT(IN)  :: ndim
INTEGER,  INTENT(IN)  :: n
INTEGER,  INTENT(IN)  :: np
INTEGER,  INTENT(IN)  :: nd
REAL, INTENT(IN)      :: oldph(ndim, np)
REAL, INTENT(IN)      :: fitns(np)
INTEGER, INTENT(IN)   :: ifit(np)
REAL, INTENT(IN)      :: pmut
INTEGER, INTENT(IN)   :: ig
INTEGER, INTENT(IN)   :: nnew

!    Output: none

!    Local
REAL, SAVE  :: bestft = 0.0, pmutpv = 0.0
INTEGER  :: ndpwr, k
LOGICAL  :: rpt

rpt = .false.

IF (pmut /= pmutpv) THEN
  pmutpv = pmut
  rpt = .true.
END IF

IF (fitns(ifit(np)) /= bestft) THEN
  bestft = fitns(ifit(np))
  rpt = .true.
END IF

IF (rpt .OR. ivrb >= 2) THEN

!       Power of 10 to make integer genotypes for display
  ndpwr = nint(10.**nd)

  WRITE (*, '(/i6, i6, f10.6, 4f10.6)') ig, nnew, pmut,  &
     fitns(ifit(np)), fitns(ifit(np-1)), fitns(ifit(np/2))
  DO  k = 1, n
    WRITE (*, '(22x, 3i10)') nint(ndpwr*oldph(k, ifit(np))),  &
      nint(ndpwr*oldph(k, ifit(np-1))), nint(ndpwr*oldph(k, ifit(np/2)))
  END DO

END IF
RETURN
END SUBROUTINE report

!*****************************************************************
*****
!                    GENETICS MODULE
!*****************************************************************
*****

!    ENCODE:    encodes phenotype into genotype
!               called by: PIKAIA

!    DECODE:    decodes genotype into phenotype
!               called by: PIKAIA

!    CROSS:     Breeds two offspring from two parents
!               called by: PIKAIA

!    MUTATE:    Introduces random mutation in a genotype
!               called by: PIKAIA

!    ADJMUT:    Implements variable mutation rate
!               called by: PIKAIA

!*****************************************************************
*****

SUBROUTINE encode(n, nd, ph, gn)
!=================================================================
=============
!    encode phenotype parameters into integer genotype
!    ph(k) are x, y coordinates [ 0 < x, y < 1 ]
!=================================================================
=============


INTEGER, INTENT(IN)   :: n
INTEGER, INTENT(IN)   :: nd
REAL, INTENT(IN OUT)  :: ph(n)
INTEGER, INTENT(OUT)  :: gn(n*nd)

!    Inputs:



!    Output:


!    Local:
INTEGER :: ip, i, j, ii
REAL :: z

z = 10. ** nd
ii = 0
DO  i = 1, n
  ip = INT(ph(i)*z)
  DO  j = nd, 1, -1
    gn(ii+j) = MOD(ip, 10)
    ip = ip / 10
  END DO
  ii = ii + nd
END DO

RETURN
END SUBROUTINE encode

!*****************************************************************
*****

SUBROUTINE decode(n, nd, gn, ph)
!=================================================================
=============
!    decode genotype into phenotype parameters
!    ph(k) are x, y coordinates [ 0 < x, y < 1 ]
!=================================================================
=============


INTEGER, INTENT(IN)  :: n
INTEGER, INTENT(IN)  :: nd
INTEGER, INTENT(IN)  :: gn(n*nd)
REAL, INTENT(OUT)    :: ph(n)

!    Inputs:
```

```
!    Output:


!    Local:
INTEGER :: ip, i, j, ii
REAL :: z

z = 10. ** (-nd)
ii = 0
DO  i = 1, n
  ip = 0
  DO  j = 1, nd
    ip = 10 * ip + gn(ii+j)
  END DO
  ph(i) = ip * z
  ii = ii + nd
END DO

RETURN
END SUBROUTINE decode

!*****************************************************************
*****

SUBROUTINE cross(n, nd, pcross, gn1, gn2)
!=================================================================
============
!    breeds two parent chromosomes into two offspring chromosomes
!    breeding occurs through crossover starting at position ispl
!=================================================================
============
!    USES: urand

!    Inputs:
INTEGER, INTENT(IN)      :: n
INTEGER, INTENT(IN)      :: nd
REAL, INTENT(IN)         :: pcross

!    Input/Output:
INTEGER, INTENT(IN OUT)  :: gn1(n*nd)
INTEGER, INTENT(IN OUT)  :: gn2(n*nd)

!    Local:
INTEGER :: i, ispl, t

!    Function
! REAL :: urand
! EXTERNAL urand


!    Use crossover probability to decide whether a crossover occurs
IF (urand() < pcross) THEN

!       Compute crossover point
  ispl = INT(urand()*n*nd) + 1

!       Swap genes at ispl and above
  DO  i = ispl, n * nd
    t = gn2(i)
    gn2(i) = gn1(i)
    gn1(i) = t
  END DO
END IF

RETURN
END SUBROUTINE cross


!*****************************************************************
*****

SUBROUTINE mutate(n, nd, pmut, gn)
!=================================================================
============
!    Mutations occur at rate pmut at all gene loci
!=================================================================
============
!    USES: urand

!    Input:
INTEGER, INTENT(IN)      :: n
INTEGER, INTENT(IN)      :: nd
REAL, INTENT(IN)         :: pmut

!    Input/Output:
INTEGER, INTENT(IN OUT)  :: gn(n*nd)


!    Local:
INTEGER :: i

!    Function:
! REAL :: urand
! EXTERNAL urand

!    Subject each locus to mutation at the rate pmut
DO  i = 1, n * nd
  IF (urand() < pmut) THEN
    gn(i) = INT(urand()*10.)
  END IF
END DO

RETURN
END SUBROUTINE mutate

!*****************************************************************
*****

SUBROUTINE adjmut(np, fitns, ifit, pmutmn, pmutmx, pmut)
!=================================================================
============
!    dynamical adjustment of mutation rate; criterion is relative
!    difference in absolute fitnesses of best and median individuals
!=================================================================
============

!    Input:
INTEGER, INTENT(IN)   :: np
REAL, INTENT(IN)      :: fitns(:)
INTEGER, INTENT(IN)   :: ifit(:)
REAL, INTENT(IN)      :: pmutmn
REAL, INTENT(IN)      :: pmutmx

!    Input/Output:
REAL, INTENT(IN OUT)  :: pmut

!    Local:
REAL  :: rdif
REAL, PARAMETER  :: rdiflo = 0.05, rdifhi = 0.25, delta = 1.5

rdif = ABS(fitns(ifit(np)) - fitns(ifit(np/2))) / (fitns(ifit(np)) +  &
       fitns(ifit(np/2)))
IF (rdif <= rdiflo) THEN
  pmut = MIN(pmutmx, pmut*delta)
ELSE IF (rdif >= rdifhi) THEN
  pmut = MAX(pmutmn, pmut/delta)
END IF

RETURN
END SUBROUTINE adjmut

!*****************************************************************
*****
!                    REPRODUCTION MODULE
!*****************************************************************
*****

!  SELECT:   Parent selection by roulette wheel algorithm
!            called by: PIKAIA

!  RNKPOP:   Ranks initial population
!            called by: PIKAIA, NEWPOP

!  GENREP:   Inserts offspring into population, for full
!            generational replacement
!            called by: PIKAIA

!  STDREP:   Inserts offspring into population, for steady-state
!            reproduction
!            called by: PIKAIA
!            calls:     FF

!  NEWPOP:   Replaces old generation with new generation
!            called by: PIKAIA
!            calls:     FF, RNKPOP

!*****************************************************************
*****

SUBROUTINE select(np, jfit, fdif, idad)
!=================================================================
============
!    Selects a parent from the population, using roulette wheel
!    algorithm with the relative fitnesses of the phenotypes as
!    the "hit" probabilities [see Davis 1991, chap. 1].
!=================================================================
============
!    USES: urand

!    Input:
INTEGER, INTENT(IN)   :: np
INTEGER, INTENT(IN)   :: jfit(np)
REAL, INTENT(IN)      :: fdif

!    Output:
INTEGER, INTENT(OUT)  :: idad
```

```
!     Local:
INTEGER :: np1, i
REAL :: dice, rtfit

!     Function:
! REAL :: urand
! EXTERNAL urand


np1 = np + 1
dice = urand() * np * np1
rtfit = 0.
DO  i = 1, np
  rtfit = rtfit + np1 + fdif * (np1-2*jfit(i))
  IF (rtfit >= dice) THEN
    idad = i
    GO TO 20
  END IF
END DO
!     Assert: loop will never exit by falling through

20 RETURN
END SUBROUTINE select

!*****************************************************************
*****

SUBROUTINE rnkpop(n, arrin, indx, rank)
!=================================================================
!     Calls external sort routine to produce key index and rank order
!     of input array arrin (which is not altered).
!=================================================================
!     USES: rqsort

!     Input
INTEGER, INTENT(IN)   :: n
REAL, INTENT(IN)      :: arrin(:)

!     Output
INTEGER, INTENT(OUT)  :: indx(:)
INTEGER, INTENT(OUT)  :: rank(:)


!     Local
INTEGER :: i

!     External sort subroutine
! EXTERNAL rqsort


!     Compute the key index
CALL rqsort(n, arrin, indx)

!     ...and the rank order
DO  i = 1, n
  rank(indx(i)) = n - i + 1
END DO
RETURN
END SUBROUTINE rnkpop

!*****************************************************************
******

SUBROUTINE genrep(ndim, n, np, ip, ph, newph)
!=================================================================
!     full generational replacement: accumulate offspring into new
!     population array
!=================================================================

!     Input:
INTEGER, INTENT(IN)  :: ndim
INTEGER, INTENT(IN)  :: n
INTEGER, INTENT(IN)  :: np
INTEGER, INTENT(IN)  :: ip
REAL, INTENT(IN)     :: ph(ndim, 2)

!     Output:
REAL, INTENT(OUT)    :: newph(ndim, np)


!     Local:
INTEGER :: i1, i2, k


!     Insert one offspring pair into new population
i1 = 2 * ip - 1
i2 = i1 + 1
DO  k = 1, n
  newph(k, i1) = ph(k, 1)
  newph(k, i2) = ph(k, 2)
END DO

RETURN
END SUBROUTINE genrep

!*****************************************************************
*****

SUBROUTINE stdrep(ff, ndim, n, np, irep, ielite, ph, oldph, fitns, ifit, jfit, nnew)
!=================================================================
!     steady-state reproduction: insert offspring pair into population
!     only if they are fit enough (replace-random if irep=2 or
!     replace-worst if irep=3).
!=================================================================
!     USES: ff, urand

!     Input:
INTEGER, INTENT(IN)      :: ndim
INTEGER, INTENT(IN)      :: n
INTEGER, INTENT(IN)      :: np
INTEGER, INTENT(IN)      :: irep
INTEGER, INTENT(IN)      :: ielite
REAL, INTENT(IN)         :: ph(ndim, 2)

!     Input/Output:
REAL, INTENT(IN OUT)     :: oldph(ndim, np)
REAL, INTENT(IN OUT)     :: fitns(np)
INTEGER, INTENT(IN OUT)  :: ifit(np)
INTEGER, INTENT(IN OUT)  :: jfit(np)

!     Output:
INTEGER, INTENT(OUT)     :: nnew

INTERFACE
  FUNCTION ff(n, x) RESULT(fn_val)
    IMPLICIT NONE
    INTEGER, INTENT(IN)  :: n
    REAL, INTENT(IN)     :: x(:)
    REAL                 :: fn_val
  END FUNCTION ff
END INTERFACE

! EXTERNAL ff

!     Local:
INTEGER :: i, j, k, i1, if1
REAL :: fit

!     External function
! REAL :: urand
! EXTERNAL urand


nnew = 0
loop70:  DO  j = 1, 2

!       1. compute offspring fitness (with caller's fitness function)
  fit = ff(n, ph(:, j))

!       2. if fit enough, insert in population
  DO  i = np, 1, -1
    IF (fit > fitns(ifit(i))) THEN

!           make sure the phenotype is not already in the population
      IF (i < np) THEN
        DO  k = 1, n
          IF (oldph(k, ifit(i+1)) /= ph(k, j)) GO TO 20
        END DO
        CYCLE loop70
      END IF

!           offspring is fit enough for insertion, and is unique

!           (i) insert phenotype at appropriate place in population
      20 IF (irep == 3) THEN
        i1 = 1
      ELSE IF (ielite == 0 .OR. i == np) THEN
        i1 = INT(urand()*np) + 1
      ELSE
        i1 = INT(urand()*(np-1)) + 1
      END IF
      if1 = ifit(i1)
      fitns(if1) = fit
      DO  k = 1, n
        oldph(k, if1) = ph(k, j)
      END DO

!           (ii) shift and update ranking arrays
      IF (i < i1) THEN
```

```
!              shift up
      jfit(if1) = np - i
      DO  k = i1 - 1, i + 1, -1
        jfit(ifit(k)) = jfit(ifit(k)) - 1
        ifit(k+1) = ifit(k)
      END DO
      ifit(i+1) = if1
     ELSE

!              shift down
      jfit(if1) = np - i + 1
      DO  k = i1 + 1, i
        jfit(ifit(k)) = jfit(ifit(k)) + 1
        ifit(k-1) = ifit(k)
      END DO
      ifit(i) = if1
     END IF
     nnew = nnew + 1
     CYCLE loop70
   END IF
  END DO

END DO loop70

RETURN
END SUBROUTINE stdrep

!*****************************************************************
*****

SUBROUTINE newpop(ff, ielite, ndim, n, np, oldph, newph, ifit, jfit, fitns,
nnew)
!=================================================================
==========
!    replaces old population by new; recomputes fitnesses & ranks
!=================================================================
==========
!    USES: ff, rnkpop

!    Input:
INTEGER, INTENT(IN)   :: ielite
INTEGER, INTENT(IN)   :: ndim
INTEGER, INTENT(IN)   :: n
INTEGER, INTENT(IN)   :: np

!    Input/Output:
REAL, INTENT(IN OUT)  :: oldph(ndim, np)
REAL, INTENT(IN OUT)  :: newph(ndim, np)

!    Output:
INTEGER, INTENT(OUT)  :: ifit(np)
INTEGER, INTENT(OUT)  :: jfit(np)
REAL, INTENT(OUT)     :: fitns(np)
INTEGER, INTENT(OUT)  :: nnew

INTERFACE
  FUNCTION ff(n, x) RESULT(fn_val)
    IMPLICIT NONE
    INTEGER, INTENT(IN)  :: n
    REAL, INTENT(IN)     :: x(:)
    REAL                 :: fn_val
  END FUNCTION ff
END INTERFACE

! EXTERNAL ff

!    Local:
INTEGER :: i, k

nnew = np

!    if using elitism, introduce in new population fittest of old
!    population (if greater than fitness of the individual it is
!    to replace)
IF (ielite == 1 .AND. ff(n, newph(:, 1)) < fitns(ifit(np))) THEN
  DO  k = 1, n
    newph(k, 1) = oldph(k, ifit(np))
  END DO
  nnew = nnew - 1
END IF

!    replace population
DO  i = 1, np
  DO  k = 1, n
    oldph(k, i) = newph(k, i)
  END DO

!       get fitness using caller's fitness function
  fitns(i) = ff(n, oldph(:, i))
END DO

!    compute new population fitness rank order

CALL rnkpop(np, fitns, ifit, jfit)

RETURN
END SUBROUTINE newpop

!*****************************************************************
*****

FUNCTION urand() RESULT(fn_val)
!=================================================================
==========
!  Return the next pseudo-random deviate from a sequence which is
!  uniformly distributed in the interval [0, 1]

!  Uses the function ran0, the "minimal standard" random number
!  generator of Park and Miller (Comm. ACM 31, 1192-1201, Oct 1988;
!  Comm. ACM 36 No. 7, 105-110, July 1993).
!=================================================================
==========

!    Input - none

!    Output
REAL  :: fn_val

!    Local
! INTEGER :: iseed
! REAL :: ran0
! EXTERNAL ran0

!    Common block to make iseed visible to rninit (and to save
!    it between calls)
! COMMON /rnseed/ iseed

fn_val = ran0()
RETURN
END FUNCTION urand

!*****************************************************************
*****

SUBROUTINE rninit(seed)
!=================================================================
==========
!    Initialize random number generator urand with given seed
!=================================================================
==========

!    Input
INTEGER, INTENT(IN)  :: seed

!    Output - none

!    Local
! INTEGER  :: iseed

!    Common block to communicate with urand
! COMMON /rnseed/ iseed

!    Set the seed value
iseed = seed
IF (iseed <= 0) iseed = 123456
RETURN
END SUBROUTINE rninit

!*****************************************************************
*****

FUNCTION ran0() RESULT(fn_val)
!=================================================================
==========
!  "Minimal standard" pseudo-random number generator of Park and Miller.
!  Returns a uniform random deviate r s.t. 0 < r < 1.0.
!  Set seed to any non-zero integer value to initialize a sequence, then do
!  not change seed between calls for successive deviates in the sequence.

!  References:
!    Park, S. and Miller, K., "Random Number Generators: Good Ones
!      are Hard to Find", Comm. ACM 31, 1192-1201 (Oct. 1988)
!    Park, S. and Miller, K., in "Remarks on Choosing and Implementing
!      Random Number Generators", Comm. ACM 36 No. 7, 105-110 (July 1993)
!=================================================================
==========
! *** Declaration section ***

!    Output:
REAL  :: fn_val

!    Constants:

INTEGER, PARAMETER  :: a = 48271, m = 2147483647, q = 44488, r = 3399

REAL, PARAMETER :: scale = 1./m, eps = 1.2E-7, rnmx = 1. - eps
```

```
!     Local:
INTEGER  :: j

! *** Executable section ***

j = iseed / q
iseed = a * (iseed - j*q) - r * j
IF (iseed < 0) iseed = iseed + m
fn_val = MIN(iseed*scale, rmmx)

RETURN
END FUNCTION ran0

!*****************************************************************
*****

SUBROUTINE rqsort(n, a, p)
!=================================================================
=============
!  Return integer array p which indexes array a in increasing order.
!  Array a is not disturbed.  The Quicksort algorithm is used.

!  B. G. Knapp, 86/12/23

!  Reference: N. Wirth, Algorithms and Data Structures/
!  Prentice-Hall, 1986
!=================================================================
=============

INTEGER, INTENT(IN)   :: n
REAL, INTENT(IN)      :: a(:)
INTEGER, INTENT(OUT)  :: p(:)

!     Constants

INTEGER, PARAMETER :: lgn = 32, q = 11
!        (LGN = log base 2 of maximum n;
!         Q = smallest subfile to use quicksort on)

!     Local:
REAL :: x
INTEGER :: stackl(lgn), stackr(lgn), s, t, l, m, r, i, j

!     Initialize the stack
stackl(1) = 1
stackr(1) = n
s = 1

!     Initialize the pointer array
DO  i = 1, n
  p(i) = i
END DO

20 IF (s > 0) THEN
  l = stackl(s)
  r = stackr(s)
  s = s - 1

  30 IF ((r-l) < q) THEN

!          Use straight insertion
    DO  i = l + 1, r
      t = p(i)
      x = a(t)
      DO  j = i - 1, l, -1
        IF (a(p(j)) <= x) GO TO 50
        p(j+1) = p(j)
      END DO
      j = l - 1
      50 p(j+1) = t
    END DO
  ELSE

!          Use quicksort, with pivot as median of a(l), a(m), a(r)
    m = (l+r) / 2
    t = p(m)
    IF (a(t) < a(p(l))) THEN
      p(m) = p(l)
      p(l) = t
      t = p(m)
    END IF
    IF (a(t) > a(p(r))) THEN
      p(m) = p(r)
      p(r) = t
      t = p(m)
      IF (a(t) < a(p(l))) THEN
        p(m) = p(l)
        p(l) = t
        t = p(m)
      END IF
    END IF

!          Partition
    x = a(t)
    i = l + 1
    j = r - 1
    70 IF (i <= j) THEN
      80 IF (a(p(i)) < x) THEN
        i = i + 1
        GO TO 80
      END IF
      90 IF (x < a(p(j))) THEN
        j = j - 1
        GO TO 90
      END IF
      IF (i <= j) THEN
        t = p(i)
        p(i) = p(j)
        p(j) = t
        i = i + 1
        j = j - 1
      END IF
      GO TO 70
    END IF

!          Stack the larger subfile
    s = s + 1
    IF (j-l > r-i) THEN
      stackl(s) = l
      stackr(s) = j
      l = i
    ELSE
      stackl(s) = i
      stackr(s) = r
      r = j
    END IF
    GO TO 30
  END IF
  GO TO 20
END IF
RETURN
END SUBROUTINE rqsort

END MODULE Genetic_Algorithm
```

APPENDIX B: SURVEY OF LITERATURE-REPORTED EXPERIMENTAL AQUEOUS PHASE HYDROXYL RADICAL REACTION RATE CONSTANTS

During the past three decades, the HO• rate constants with a number of organic compounds were experimentally investigated. There is currently one critical review available on the HO• rate constants (Buxton et al., 1988). However, there is no comprehensive report available to cover the experimental data which have been reported since 1988. One of the main objectives for this survey of the experimentally reported HO• rate constants is for the group contribution method to predict HO• rate constant with emerging contaminants. For the accurate parameter calibration, selection and critical review of the original data is inevitable. The data used here were referred to Buxton et al (1988), University Notre Dame, The Radiation Chemistry Data Center (RCDC) (http://www.rad.nd.edu/rcdc/index.html), and each literature on the peer-reviewed paper.

Table A-B1: Survey of HO• rate constants with alkane

chemcial formura	compound	$k_{HO\bullet}$ (M-1 s-1)	references	experimental method	evaluation method	pH	Temp. (K)	$k_{HO\bullet}$ (cm3 molecules^{-1} s^{-1}) in gas at 298K	Exp. Solvation free energy (kJ/mol) at 298 K	Exp. Solvation free energy (kcal/mol) at 298K
CH4	methane	1.20E+08	Getoff 1989	pulse radiolysis	C.K.		N.R.	8.50E+09	8.37	2.00
		1.00E+08	Hickel, 1975	pulse radiolysis	D.K.		298.0			
		1.20E+08	Stevens et al., 1972	pulse radiolysis	D.K.	5.5	N.R.			
CH3-CH3	ethane	1.40E+09	Getoff 1989	pulse radiolysis	C.K.		N.R.	3.40E+11	7.66	1.83
		1.80E+09	Hickel, 1975	pulse radiolysis	C.K.	4.4	298.0			
CH3-CH2-CH3	*n* -propane	2.30E+09	Getoff 1989	pulse radiolysis	C.K.	7.5-8.5	N.R.	1.26E+12	8.21	1.96
		3.60E+09	Rudakov 1981	Fenton reaction	steady-state	2.0				
CH3-(CH2)2-CH3	*n* -butane	2.90E+09	Getoff 1989	pulse radiolysis	C.K.	7.5-8.5	N.R.	2.56E+12	8.71	2.08
		4.60E+09	Rudakov 1981	Fenton reaction	steady-state	2.0				
CH3-(CH2)3-CH3	*n*- pentane	5.40E+09	Rudakov 1981	Fenton reaction	steady-state	2.0		4.06E+12	9.76	2.33
CH3-(CH2)4-CH3	*n* -hexane	6.60E+09	Rudakov 1981	Fenton reaction	steady-state	2.0		5.55E+12	10.43	2.49
CH3-(CH2)5-CH3	*n* -heptane	7.70E+09	Rudakov 1981	Fenton reaction	steady-state	2.0		7.18E+12	10.97	2.62
CH3-(CH2)6-CH3	*n* -octane	9.10E+09	Rudakov 1981	Fenton reaction	steady-state	2.0		8.86E+12	12.10	2.89
CH3-CH(CH3)-CH3	2-methylpropane	4.60E+09	Rudakov 1981	Fenton reaction	steady-state	2.0		2.67E+12	9.71	2.32
CH3-CH2-CH(CH3)-CH3	2-methylbutane	5.20E+09	Rudakov 1981	Fenton reaction	steady-state	2.0		3.87E+12		
CH3-CH2-CH(CH2-CH3)-CH2-CH3	3-ethylpentane	5.90E+09	Rudakov 1981	Fenton reaction	steady-state	2.0				
CH3-C(CH3)2-CH2-CH(CH3)-CH3	2,2,4-Trimethylpentane	6.10E+09	Rudakov 1981	Fenton reaction	steady-state	2.0		3.90E+12	11.93	2.85

Table A-B2: Survey of HO• rate constants with alcohol

chemcial formura	compound	$k_{HO\bullet}$ (M-1 s-1)	references	experimental method	evaluation method	pH		Exp. Solvation free energy (kJ/mol) at 298 K	Exp. Solvation free energy (kcal/mol) at 298K
CH3-OH	methanol	9.70E+08	Buxton 1988				selected values	-21.39	-5.11
		8.30E+08	Motohashi and Saito, 1993	γ radiolysis	C.K.	7.5 293-298 K			
			Elliot and McCracken, 1989	Pulse radiolysis	C.K.		Ea = 4.8 kJ/mol, log(A)=9.856, T = 293-353 K		
		1.00E+09					T=293 K		
		1.10E+09					303 K		
		1.20E+09					313 K		
		1.30E+09					323 K		
		1.40E+09					333 K		
		1.40E+09					343 K		
		1.50E+09					353 K		
		1.00E+09	Wolfenden and Willson, 1982	Pulse radiolysis	C.K.	6.0	temperature: N.D.		
		9.70E+08	Willson et al., 1971	Pulse radiolysis	C.K.				
		9.50E+08	Baxendale and Khan, 1969	Pulse radiolysis	C.K.				
		8.30E+08	Neta and Dorfman, 1968	Pulse radiolysis	C.K.		$k_{reference}$ = 5.9E9		
		8.30E+08	Neta and Dorfman, 1968	Pulse radiolysis	C.K.		$k_{reference}$ = 2.6E9		
		8.30E+08	Neta and Dorfman, 1968	Pulse radiolysis	C.K.		$k_{reference}$ = 7.9E9		
		8.80E+08	Adams et al., 1965	Pulse radiolysis	C.K.	10.7	$k_{reference}$ = 3.9E8		
		7.80E+08	Adams et al., 1965	Pulse radiolysis	C.K.	7.0	$k_{reference}$ = 1.1E10		
		1.20E+09	Adams et al., 1965	Pulse radiolysis	D.M	2.0			
		8.00E+08	Adams et al., 1965	Pulse radiolysis	D.M	7.0			

CH3-CH2-OH	ethanol	1.90E+09	Buxton 1988				selected values	-20.98	-5.01
						7.5			
		2.20E+09	Motohashi and Saito, 1993	γ radiolysis	C.K.	293-298 K			
		1.90E+09	Park and Getoff, 1992	Pulse radiolysis	C.K.	9.0			
		1.90E+09	Wolfenden and Willson, 1982	Pulse radiolysis	C.K.	6.0	temperature: N.D.		
		1.90E+09	Matheson et al., 1973	Pulse radiolysis	C.K.	298 K			
		2.10E+09	Willson et al., 1971	Pulse radiolysis	C.K.				
		2.10E+09	Buxton, 1970	Pulse radiolysis	C.K.	11.0			
		1.60E+09	Baxendale and Khan, 1969	Pulse radiolysis	C.K.				
		1.80E+09	Neta and Dorfman, 1968	Pulse radiolysis	C.K.		$k_{reference}$ = 7.9E9		
		1.80E+09	Neta and Dorfman, 1968	Pulse radiolysis	C.K.		$k_{reference}$ = 2.6E9		
		1.80E+09	Neta and Dorfman, 1968	Pulse radiolysis	C.K.		$k_{reference}$ = 5.9E9		
		2.00E+09	Heckel et al., 1966	Pulse radiolysis	C.K.				
		2.20E+09	Adams et al., 1965	Pulse radiolysis	C.K.				
		2.80E+09	Matthews and Sangster, 1965	γ radiolysis	C.K.	3-10.5, N.R.			
		1.80E+09	Adams et al., 1965	Pulse radiolysis	C.K.	7.0			
		1.90E+09	Adams et al., 1965	Pulse radiolysis	C.K.	7, 10.7			
		2.80E+09	Adams et al., 1965	Pulse radiolysis	C.K.	2.0			
		1.90E+08	Adams et al., 1965	Pulse radiolysis	C.K.	7.0			
		2.10E+09	Ervens et al., 2003	Laser-photolysis	C.K.	298 K	Ea = 10±5 kJ/mol, A = (1.0±0.1)e11 M-1s-1		
		1.60E+09				283 K			
		1.70E+09				288 K			
		2.10E+09				298 K			
		2.40E+09				308 K			
		2.40E+09				318 K			
						pH 1-2			
		2.10E+09	Monod et al., 2005	Photo-fenton	C.K.	298 K	Ea = 6.9±1.2 kJ/mol, A = (3.2±)e11 M-1s-1		
		1.80E+09				276 K			
		1.70E+09				285 K			
		2.10E+09				298 K			
		2.60E+09				328 K			
CH3-(CH2)2-OH	1-propanol	2.80E+09	Buxton 1988				average of 3 values	-20.22	-4.83
		3.00E+09	Willson et al., 1971	Pulse radiolysis	C.K.				
		2.90E+09	Adams et al., 1965	Pulse radiolysis	C.K.	10.7			
		2.50E+09	Adams et al., 1965	Pulse radiolysis	C.K.	7.0			
						pH = 6.0			
		3.20E+09	Ervens et al., 2003	Laser-photolysis	C.K.	298 K	Ea = (8±6) kJ/mol, A = (5.6±0.6)e10 M-1 s-1		
		3.30E+09				288 K			
		3.20E+09				298 K			
		4.20E+09				308 K			
		4.30E+09				318 K			
		4.40E+09				328 K			
						pH 1-2			
		2.70E+09	Monod et al., 2005	Photo-fenton	C.K.	298 K	Ea = 6.5±1.7 kJ/mol, A = 4.4e10 M-1s-1		
		2.80E+09				276.0			
		2.70E+09				298.0			
		3.80E+09				323.0			
		4.20E+09				339.0			
CH3-(CH2)3-OH	1-butanol	4.20E+09	Buxton 1988				average of 3 values	-19.76	-4.72
		4.50E+09	Willson et al., 1971	Pulse radiolysis	C.K.				
		4.30E+09	Adams et al., 1965	Pulse radiolysis	C.K.	7.0	$k_{reference}$ = 3.9E8		
		3.70E+09	Adams et al., 1965	Pulse radiolysis	C.K.	7.0	$k_{reference}$ = 1.1E10		
		4.20E+09	Monod et al., 2005	Photo-fenton	C.K.				
						pH 5.8			
		4.10E+09	Ervens et al., 2003	Laser photolysis	C.K.	298 K	Ea = (8±1) kJ/mol, A = (1.0±0.1)e11 M-1s-1		
CH3-(CH2)4-OH	1-pentanol	3.70E+09	Reuvers 1973	Pulse radiolysis	C.K.		$k_{reference}$ = 1.1E10	-18.71	-4.47
		4.00E+09	Reuvers 1973	Pulse radiolysis	C.K.		$k_{reference}$ = 1.0E10		
CH3-(CH2)5-OH	1-hexyanol	7.00E+09	Scholes and Willson, 1967	γ radiolysis	C.K.	-2.0		-18.25	-4.36
CH3-(CH2)6-OH	1-heptanol	7.40E+09	Scholes and Willson, 1967	γ radiolysis	C.K.	-2.0		-17.75	-4.24
CH3-CH(OH)-CH3	2-propanol	1.90E+09	Buxton 1988				selected values	-19.93	-4.76
						7.5			
		1.60E+09	Motohashi and Saito, 1993	γ radiolysis	C.K.	293-298 K			
		2.30E+09	Elliot and Simsons, 1984	Pulse radiolysis	C.K.	292 K	Ea = 5 kJ/mol, log(A)=10.256, T = 292-352 K		
		1.90E+09	Wolfenden and Willson, 1982	Pulse radiolysis	C.K.	6.0	temperature: N.D.		
		2.30E+09	Willson et al., 1971	Pulse radiolysis	C.K.				
		1.90E+09	Greenstock et al., 1968	Pulse radiolysis	C.K.	2.0-10.0			
						7.0			
		1.90E+09	Thomas, 1965	Pulse radiolysis	C.K.	298 K			
						pH 1-2			
		1.90E+09	Monod et al., 2005	Photo-fenton	C.K.	298 K			
						pH 5.8			
		4.10E+09	Ervens et al., 2003	Laser photolysis	C.K.	298 K	Ea = (8±2) kJ/mol, A = (6.1±0.3)e10 M-1s-1		
CH3-CH(OH)-CH2-CH3	2-butanol	3.10E+09	Adams et al., 1965	Pulse radiolysis	C.K.	7.0	$k_{reference}$ = 1.1E10		
						pH 5.8			
		3.50E+09	Ervens et al., 2003	Laser photolysis	C.K.	298 K	Ea = (8±3) kJ/mol, A = (7.4±0.3)e11 M-1s-1		
CH3-CH2-CH(OH)-CH2-CH3	3-pentanol	2.10E+09	Snook and Hamilton, 1974	Fenton reaction	C.K.	-1.8			
(CH3)3-C-OH	tert-butanol	7.20E+08	Elliot and Simons, 1989		C.K.		Ea = 10 kJ/mol		
		5.00E+08	Ervens et al., 2003	Laser photolysis	C.K.	298 K	Ea = (10±3) kJ/mol, A = (3.3±0.1)e10 M-1s-1		
		1.80E+09				283 K			
		2.30E+09				288 K			
		2.40E+09				298 K			
		3.00E+09				308 K			
		2.70E+09				318 K			
		3.30E+09				328 K			
						pH 1-2			
		7.00E+08	Monod et al., 2005	Photo-fenton	C.K.	298 K			
		4.20E+08	Logan, 1989		C.K.				
		4.80E+08	Motohashi and Saito, 1993						
		5.90E+08	Willson et al., 1971						
		6.00E+08	Buxton et al., 1988				*recommended values*		
		6.00E+08	Wolfenden and Willson, 1982		C.K.				
		7.60E+08	Gordon et al., 1977		D.K.				
		6.00E+08	Buxton 1988				selected values		
						7.5			
		4.80E+08	Motohashi and Saito, 1993	γ radiolysis	C.K.	293-298 K			
		6.60E+08	Elliot and Simsons, 1984	Pulse radiolysis	C.K.	292 K	Ea = 10 kJ/mol, log(A)=10.609, T = 292-352 K		
		6.00E+08	Wolfenden and Willson, 1982	Pulse radiolysis	C.K.	6.0			
		7.60E+08	Gordon et al., 1977	Pulse radiolysis	D.K.	7.0			
		5.90E+08	Willson et al., 1971	Pulse radiolysis	C.K.				
		4.20E+08	Adams et al., 1965	Pulse radiolysis	C.K.	7.0			
CH3-CH2-C(CH3)(OH)-CH3	2-methyl-2-butanol	1.90E+09	Anbar 1966	γ radiolysis	C.K.	9.0			
CH3-CH(CH3)-CH2-OH	2-methyl-1-propanol	3.30E+09	Buxton 1988				average of 3 values	-18.88	-4.51
		2.90E+09	Reuvers 1973	Pulse radiolysis	C.K.		$k_{reference}$ = 1.0E10		
		3.60E+09	Reuvers 1973	Pulse radiolysis	C.K.		$k_{reference}$ = 1.1E10		
		3.30E+09	Adams et al., 1965	Pulse radiolysis	C.K.	7.0			
CH3-C(CH3)2-CH2-OH	2,2-dimethyl-1-propanol	5.20E+09	Walling 1975	Fenton reaction	steady-state	<2			
CH3-CH2-CH(CH3)-CH2-OH	3-methyl-1-butanol	3.80E+09	Reuvers 1973	Pulse radiolysis	C.K.		$k_{reference}$ = 1.0E10		
		3.70E+09	Reuvers 1973	Pulse radiolysis	C.K.		$k_{reference}$ = 1.1E10		

Table A-B3: Survey of HO• rate constants with poly-alcohol

chemcial formura	compound	$k_{HO\bullet}$ (M-1 s-1)	references	experimental method	evaluation method	pH	
HO-CH2-OH	dihydroxymethane	7.60E+08	Chin 1994	Flash photolysis	C.K.	297 K	Ea = 8.5 kJ/mol, log(A)=10.37, T = 279-319 K, pH = 1.5-5.7
		1.00E+09	Hart et al., 1964		C.K.		
		1.30E+09	Merz and Waters, 1949	Fenton reaction	C.K.	1.0	
HO-CH2-CH2-OH	ethyleneglycol	2.40E+09	Matheson 1973	Pulse radiolysis	C.K.		
		1.70E+09	Willson et al., 1971	Pulse radiolysis	C.K.		
		1.70E+09	Adams 1965	Pulse radiolysis	C.K.	7.0	$k_{reference}$ = 1.0E10
		1.40E+09	Adams 1965	Pulse radiolysis	C.K.	7.0	$k_{reference}$ = 1.1E10
HO-(CH2)3-OH	1,3-propanediol	2.50E+09	Anbar 1966	γ radiolysis	C.K.	9.0	
HO-(CH2)4-OH	1.4-butanediol	3.20E+09	Adams 1965	Pulse radiolysis	C.K.	7.0	
HO-(CH2)5-OH	1,5-pentanediol	3.60E+09	Anbar 1966	γ radiolysis	C.K.	9.0	
HO-(CH2)6-OH	1,6-hexyanediol	4.70E+09	Anbar 1966	γ radiolysis	C.K.	9.0	
CH3-CH(OH)2	1,1-ethanediol	1.20E+09	Shuchmann 1988	Pulse radiolysis	C.K.		
CH3-CH(OH)-CH2-OH	1,2-propanediol	1.70E+09	Adams 1965	Pulse radiolysis	C.K.	7.0	
CH3-CH(OH)-CH2-CH2-OH	1,3-butanediol	2.20E+09	Adams 1965	Pulse radiolysis	C.K.	7.0	
CH3-CH(OH)-CH(OH)-CH3	2,3-butanediol	1.30E+09	Adams 1965	Pulse radiolysis	C.K.	7.0	
CH3-CH(OH)-CH2-CH(OH)-CH3	2,4-pentanediol	2.30E+09	Ulanski 1994	Pulse radiolysis	C.K.		
HO-CH2-CH(OH)-CH2-OH	glycerol	2.00E+09	Reuvers 1973	Pulse radiolysis	C.K.		$k_{reference}$ = 1.1E10
		1.80E+09	Reuvers 1973	Pulse radiolysis	C.K.		$k_{reference}$ = 1.0E10
		2.10E+09	Willson et al., 1971	Pulse radiolysis	C.K.		
		1.90E+09	Adams 1965	Pulse radiolysis	C.K.	10.7	
		1.50E+09	Adams 1965	Pulse radiolysis	C.K.	7.0	
		2.10E+09	Adams 1965	Pulse radiolysis	C.K.		contains 0.04 M NasCO3-
HO-CH2-[CH(OH)]3-CH2-OH	arabinitol	1.80E+09	Moore 1979	Pulse radiolysis	C.K.	7.0	
HO-CH2-[CH(OH)]4-CH2-OH	mannitol	1.70E+09	Buxton 1988	Fenton reaction	C.K.	7.4	T = 310 K
		1.40E+09	Ching et al., 1993	Fenton reaction	C.K.	7.4	T = 310 K
		1.90E+09	Motohashi and Saito, 1993	γ radiolysis	C.K.	7.5 293- 298 K	
C(CH2OH)4	pentaerythritol	3.30E+09	Anbar 1966	γ radiolysis	C.K.	9.0	
CH2OH-CHOH-CHOH-CH2OH	erythritol	1.50E+09	Moore 1979	Pulse radiolysis	C.K.	7.0	
HOCH2COOH	glycolic acid	5.40E+08	Scholes 1967				

Table A-B4: Survey of HO• rate constants with ether

chemcial formura	compound	$k_{HO\bullet}$ (M-1 s-1)	references	experimental method	evaluation method	pH		Exp. Solvation free energy (kJ/mol) at 298K	Exp. Solvation free energy (kcal/mol) at 298K
CH3-O-CH3	dimethylether	1.00E+09	Eibenberger 1980	Pulse radiolysis	C.K.			-8.04	-1.92
CH3-CH2-O-CH2-CH3	diethylether	2.90E+09	Eibenberger 1980	Pulse radiolysis	C.K.			-7.37	-1.76
(CH3)3-C-O-CH3	tert-butyl-methyl-ether (MTBE)	1.60E+09	Eibenberger 1980	Pulse radiolysis	C.K.			-9.25	-2.21
(CH3)3-C-O-CH2-CH3	tert-butyl-ethyl-ether (ETBE)	1.80E+09	Mezyk 2001	Pulse radiolysis	C.K.	pH 2.0 295±2 K			
		1.50E+09	Monod et al., 2005	Photo-fenton	C.K.	pH 1-2 298 K	Ea = 4.8±4.7kJ/mol, A = 1.2e10 M-1s-1		
		1.70E+09				279			
		1.50E+09				286.0			
		1.50E+09				297.0			
		1.30E+09				309.5			
		2.40E+09				320			
		2.30E+09				333			
(CH3)2-HC-O-CH-(CH3)2	diisopropyl ether (DIPE)	2.49E+09	Mezyk 2001	Pulse radiolysis	T.S.	pH 2.0 295±2 K			
		3.70E+09	Schuchmann and von Sonntag, 1987	Pulse radiolysis	C.K.	N.D.			
$C_2H_5C(CH_3)_2OCH_3$	tert-amyl methyl ether (TAME)	2.37E+09	Mezyk 2001	Pulse radiolysis	T.S.	pH 2.0 295±2 K			
CH2(OCH3)2	dimethoxymethane	1.20E+09	Eibenberger 1980	Pulse radiolysis	C.K.				
CH3CH(OCH3)2	1,1-dimethoxyethane	2.20E+09	Eibenberger 1980						
CH2(OC2H5)2	diethoxymethane	1.60E+09	Anbar 1966	γ radiolysis	C.K.	9.0			
CH3-O-CH2-O-CH3		3.20E+08	Neta						
CH3-O-CH2-CH2-OH	2-methoxyethanol	1.30E+09	Anbar 1966	γ radiolysis	C.K.	9.0			
C2H5-O-CH2-CH2-OH	2-ethoxyethanol	1.70E+09	Anbar 1966	γ radiolysis	C.K.	9.0			
CH3-O-CH2-CH2-O-CH3	ethylene glycol dimethyl ether	1.60E+09	Anbar 1966	γ radiolysis	C.K.	9.0			
CH3CH2-O-CH2CH2-O-CH2CH3	ethylene glycol diethyl ether	2.30E+09	Anbar 1966	γ radiolysis	C.K.	9.0			
CH3CH2-O-CH2CH2-CH2CH2-O-CH2CH3	diethylene glycol diethyl ether	3.20E+09	Anbar 1966	γ radiolysis	C.K.	9.0			
HO-CH2-CH2-O-CH2-CH2-OH	diethylene glycol	2.10E+09	Anbar 1966	γ radiolysis	C.K.	9.0			
CH3-C(CH3)(OCH3)CH2-OH	2-methyl-2-methoxy propanol	8.40E+08	Mezyk 2004						

Table A-B5: Survey of HO• rate constants with ester

chemcial formura	compound	$k_{HO\bullet}$ (M-1 s-1)	references	experimental method	evaluation method	pH	
HCOO-CH2-CH3	ethyl formate	3.90E+08	Adams 1965	Pulse radiolysis	C.K.		
		3.30E+08	Gligorovski and Hermann, 2004	Photo-fenton	C.K.	298 K	Ea = 10±4 kJ/mol, A = 1.8±0.1 e10 M-1s-1 288-328 K G** = 24±11 kJ/mol H** = 7±3 kJ/mol S** = -(57±4) kJ/mol
CH3-COO-CH3	methyl acetate	1.20E+08	Adams 1965	Pulse radiolysis	C.K.	2.0	
CH3-COO-CH2-CH3	ethyl acetate	4.00E+08	Adams 1965	Pulse radiolysis	C.K.		
CH3-COO-CH2-CH2-CH3	propyl acetate	1.40E+09	Adams 1965	Pulse radiolysis	C.K.		
CH3-COO-(CH2)3-CH3	n-butylacetate	1.80E+09	Monod et al., 2005	Photo-fenton	C.K.	298 K	Ea = 8.3±1.7kJ/mol, A = 5.3e10 M-1s-1
		1.30E+09				278	
		1.80E+09				288.0	
		1.80E+09				297.0	
		1.90E+09				307.0	
		2.30E+09				318.0	
CH3-COO-CH(CH3)2	iso-propyl acetate	4.50E+08	Adams 1965	Pulse radiolysis	C.K.	2.0	
CH3-CH2-COO-CH3	methyl propionate	4.50E+08	Buxton 1988	Pulse radiolysis	C.K.		
		3.20E+08	Biro and Wojnarovits, 1992	Pulse radiolysis	C.K.		
CH3-CH2-COO-CH2-CH3	ethyl propionate	8.70E+08	Adams 1965				
CH3-(CH2)2-COO-CH3	methyl butyrate	1.70E+09	Adams 1965	Pulse radiolysis	C.K.		
CH3-(CH2)2-COO-CH2-CH3	ethyl butyrate	1.60E+09	Adams 1965	Pulse radiolysis	C.K.		
CH3-COO-CH2CH2OH	2-hydroxyethyl acetate	9.10E+08	Matsusige et al., 1975	Pulse radiolysis	C.K.	T = 293 K	
CH3CH2-O-CO-CH2-COO-CH2CH3	diethyl malonate	6.50E+08	Adams 1965	Pulse radiolysis	C.K.		
CH3CH2-O-CO-(CH2)2-COO-CH2CH3	diethylsuccinate	7.80E+08	Adams 1965	Pulse radiolysis	C.K.		
CH3-O-CH2-COO-CH3	methyl methoxy acetate	1.80E+09	Massaut 1988	Pulse radiolysis	C.K.	-7.0	

Table A-B6: Survey of HO• rate constants with aldehyde

chemcial formura	compound	$k_{HO\bullet}$ (M-1 s-1)	references	experimental method	evaluation method	pH	
HCHO	form aldehyde	1.00E+09					
CH3-CHO	acetaldehyde	3.60E+09	Schuchmann and von Sonntag, 1988	Pulse radiolysis	C.K.	pH = 5.0 '- 293 K	
		9.50E+08	Merz and Waters, 1949	Fenton reaction	C.K.	1.0	
CH3-CH2-CHO	propionaldehyde	2.20E+09	Mezyk 1994	Pulse radiolysis	C.K.	pH =5.2 T = 298 K	Ea = 28 kJ/mol, Log(A)=14.207, T=276-313 K
		2.80E+09	Hesper and Hermann	Photo-fenton	C.K.	pH =6.0 298 K	Ea = 11±3 kJ/mol, A = 2.6±0.1 e11 M-1s-1
CH3-CH2-CH2-CHO	butyraldehyde	3.90E+09	Adams 1965	Pulse radiolysis	C.K.	2.0	
		3.90E+09	Hesper and Hermann	Photo-fenton	C.K.	pH =5.9 298 K	Ea = 8±3 kJ/mol, A = 8.1±0.3 e10 M-1s-1
(CH3)2-CH-CHO	isobutyl aldehyde	2.90E+09	Gligorovski and Hermann, 2004	Photo-fenton	C.K.	298 K	Ea = 6±3 kJ/mol, A = 3.0±0.1 e10 M-1s-1 288-328 K G** = 19±10 kJ/mol H** = 3.3±1.7 kJ/mol S** = -(53±3) kJ/mol
CHO-CHO	glyoxal	6.60E+07	Draganic and Marcovic	Radiolysis	C.K.	1.3	Ea = 13 1
CH3-CO-CHO	methyl glyoxal	5.30E+08	Monod et al., 2005	Photo-fenton	C.K.	pH 1-2 298 K	Ea = 9.1±2.5kJ/mol, A = 2.0e10 M-1s-1
		5.30E+08				276.0	
		3.10E+08				276.0	
		5.30E+08				288.0	
		4.80E+08				288.0	
		5.30E+08				298.0	
		4.60E+08				298.0	
		7.00E+08				318.0	
		6.70E+08				318.0	
(CH3)3-C-O-CHO	tertbutylformate (TBA)	4.10E+08	Onstein 1999	UV/H2O2	C.K.	pH = 7.0 T = 298 K	
CH3-C(CH3)(OCH3)-CHO	2-methyl-2-methoxy-propanal	3.99E+09	Mezyk 2004				
HO-C(CH3)2-CHO	hydroxy-iso-butylaldehyde	3.00E+09	Acero 1991				

Table A-B7: Survey of HO• rate constants with carbonyl

chemcial formura	compound	$k_{HO\bullet}$ (M-1 s-1)	references	experimental method	evaluation method	pH		Exp. Solvation free energy (kJ/mol) at 298K	Exp. Solvation free energy (kcal/mol) at 298K
CH3-CO-CH3	acetone	1.10E+08	Buxton et al., 1988					-16.12	-3.85
		1.30E+08	Wolfenden and Willson, 1982	Pulse radiolysis	C.K.	6.0			
		1.40E+08	Willson et al., 1971	Pulse radiolysis	C.K.				
		8.30E+07	Thomas 1965	Pulse radiolysis	C.K.				
		9.70E+07	Adams 1965	Pulse radiolysis	C.K.				
		2.10E+08	Ervens et al., 2003	Laser photolysis	C.K.	298 K	E_a = (15±11) kJ/mol, A = (3.4±0.4)e11 M-1s-1		
		1.30E+08				283 K			
		1.20E+08				288 K			
		2.10E+08				298 K			
		2.20E+08				308 K			
		2.70E+08				318 K			
						pH 1-2			
		1.10E+08	Monod et al., 2005	Photo-fenton	C.K.	298 K	Ea = 11.6±4kJ/mol, A = 1.6±)e10 M-1s-1		
		8.00E+07				276.0			
		1.10E+08				298.0			
		1.20E+08				298.0			
		1.30E+08				301.0			
		1.30E+08				317.0			
		1.70E+08				323.0			
						pH =6.0			
		1.30E+08	Hesper and Hermann	Photo-fenton	C.K.	298 K	Ea = 16±3 kJ/mol, A = 8.4±0.4 e10 M-1s-1		
CH3-CH2-CO-CH3	2-butanone	6.60E+08	Mezyk 1994	Pulse radiolysis		5.2, T=297K	Ea = 12 kJ/mol, Log(A)=11.009, T = 275-340 K	-15.24	-3.64
		9.00E+08	Adams 1965	Pulse radiolysis	C.K.				
						pH 1-2			
		8.10E+08	Monod et al., 2005	Photo-fenton	C.K.	298 K	Ea = 13.3±2.5kJ/mol, A = 26.2e11 M-1s-1		
		5.30E+08				276.0			
		7.80E+08				276.0			
		7.40E+08				288.0			
		8.10E+08				298.0			
		9.00E+08				298.0			
		1.03E+09				318.0			
		1.02E+09				328.0			
							Ea = 15±8 kJ/mol, A = 5.1±0.6 e11 M-1s-1 278-348 K G** = 21±13 kJ/mol H** = 13±6 kJ/mol		
		1.50E+09	Gligorovski and Herrmann, 2004	Photo-fenton	C.K.	298 K	S** = -(29±3) kJ/mol		
		1.80E+09	George et al, 2003	Teflon wavelength			Ea = 31±6kJ/mol, A = 4.1 0.3 e14 M-1s-1		
CH3-CH2-CH2-CO-CH3	2-pentanone	1.90E+09	Adams 1965	Pulse radiolysis	C.K.			-14.78	-3.53
						pH 1-2			
(CH3)2-CH-CH2-CO-CH3	methyl-iso-butyl ketone	2.10E+09	Monod et al., 2005	Photo-fenton	C.K.	298 K	Ea = 10±2.5kJ/mol, A = 1.3e11 M-1s-1		
		2.10E+09				276.0			
		2.10E+09				298.0			
		3.50E+09				323.0			
		4.40E+09				339.0			
CH3-CH2-CO-CH2-CH3	3-pentanone	1.40E+09	Adams 1965	Pulse radiolysis	C.K.			-14.28	-3.41
CH3-CO-CO-CH3	2,3-butanedion	1.70E+08	Lilie 1968	Pulse radiolysis	C.K.				
							Ea = 24±5 kJ/mol, A = 4.3±0.3 e11 M-1s-1 288-328 K G** = 25±7 kJ/mol H** = 22±4 kJ/mol		
		2.80E+08	Gligorovski and Herrmann, 2004	Photo-fenton	C.K.	298 K	S** = -(11±1) kJ/mol		
CH3-CO-CH2-CO-CH3	2,4-pentanone	9.90E+09	Broszkiewicz 1982	Pulse radiolysis	C.K.	6.4			
							Ea = 12±5 kJ/mol, A = 1.1±0.1 e11 M-1s-1 288-328 K G** = 22±10 kJ/mol H** = 10±4 kJ/mol		
CH3-CO-CH2CH2-CO-CH3	acetonyl acetone	7.60E+08	Gligorovski and Herrmann, 2004	Photo-fenton	C.K.	298 K	S** = -(42±3) kJ/mol		
CH3-CO-CH(OH)-CH3	3-hydro-2-butanone	1.20E+09	Lilie 1968	Pulse radiolysis	C.K.				
		8.50E+08	Adams et al., 1965	Pulse radiolysis	C.K.	2.0			
						pH =508			
		2.90E+09	Hesper and Hermann	Photo-fenton	C.K.	298 K	Ea = 11±3 kJ/mol, A = 2.9±0.1 e11 M-1s-1		
CH3-CO-CHO	methyl glyoxal	1.10E+09	Ervens et al., 2003	Laser photolysis	C.K.	298 K	E_a = (15±6) kJ/mol, A = (2.9±0.3)e11 M-1s-1		
		1.10E+09				288 K			
		1.10E+09				298 K			
		1.50E+09				308 K			
		1.80E+09				318 K			
		2.00E+09				328 K			

Table A-B8: Survey of HO• rate constants with carboxylic acid

chemical formula	compound	$k_{HO\bullet}$ (M-1 s-1)	references	experimental method	evaluation method	pH		Exp. Solvation free energy (kJ/mol) at 298K	Exp. Solvation free energy (kcal/mol) at 298K
H-COOH	formic acid	1.30E+08	Buxton 1988				average of 2 values		
		1.40E+08	Thomas 1965	Pulse radiolysis	C.K.				
		1.30E+08	Adams et al., 1965	Pulse radiolysis	C.K.	1.0			
		1.00E+08	Chan and Wine, 1994	Flash photolysis	C.K.	T=297 K	Ea = 8.2 kJ/mol, Log(A)=9.469, T=279-319K, pH=0.3-1.0		
HCOO-	formate ion	3.20E+09	Buxton 1988				selected value		
		3.10E+09	Chan and Wine, 1994	Flash photolysis	C.K.	T = 297 K pH = 5.7	Ea = 10 kJ/mol, Log(A)=11.3, T=279-319K, pH=0.3-1.0		
		3.20E+09	Motohashi and Saito, 1993	γ radiolysis	C.K.	7.5 293-298 K			
		4.30E+09	Elliot et al., 1990	Pulse radiolysis	C.K.	T = 298 K	Ea = 4.0 kJ/mol, log(A)=10.335, T=293-473 K		
		5.10E+09	Logan, 1989	Flash photolysis/ oxidative quenching	C.K.	9.0			
		3.80E+09	Elliot and Simsons, 1984	Pulse radiolysis	C.K.	T=292 K	Ea = 8.5 kJ/mol, log(A)=11.101, T=292-352 K		
		3.50E+09	Wolfenden and Willson, 1982	Pulse radiolysis	C.K.	6.0			
		3.20E+09	Willson et al, 1971	Pulse radiolysis	C.K.				
		2.20E+09	Baxendale and Khan, 1969	Pulse radiolysis	C.K.				
		4.10E+09	Buxton, 1969	Pulse radiolysis	C.K.	11.0	pH 11 and 13		
		2.60E+09	Thomas, 1965	Pulse radiolysis	C.K.	7.0			
CH3-COOH	acetic acid	1.70E+07	Chin 1994	Flash photolysis	C.K.	pH = -1.8 T = 297 K	Ea = 11kJ/mol, Log(A)= 9.18, T = 279-319 K	-28.05	-6.70
		9.20E+06	Thomas 1965	Pulse radiolysis	D.K.	1.0			
		1.50E+07	Thomas 1965	Pulse radiolysis	C.K.	1.0			
		2.30E+07	Adams et al., 1965	Pulse radiolysis	C.K.				
CH3-COO-	acetate ion	7.30E+07	Chin and Wine, 1994	flash photolysis	C.K.	pH = 6.3 T = 297 K	Ea = 15 kJ/mol, Log(A)=10.45, T= 279-319 K		
		7.40E+07	Schuler, 1981	Pulse radiolysis	C.K.	10.7			
		1.00E+08	Fisher and Hamill, 1973	Pulse radiolysis	C.K.				
		7.90E+07	Willson et al, 1971	Pulse radiolysis	C.K.				
		8.50E+07	Willson et al, 1971	Pulse radiolysis	P.B.K.				
CH3-CH2-COOH	propionic acid	6.20E+08	Scholes 1967	γ radiolysis	C.K.	-2.0		-27.09	-6.47
		3.80E+08	Merz and Waters, 1949	Fenton reaction	C.K.	1.0			
		3.20E+08	Ervens et al., 2003	Laser photolysis	C.K.	298 K	Ea = (19±8) kJ/mol, A = (7.6±0.9)e11 M-1s-1		
		2.90E+08				288 K			
		3.20E+08				298 K			
		4.70E+08				308 K			
		5.20E+08				318 K			
		7.70E+08				328 K			
CH3CH2-COO-	propionate	1.20E+09	Logan, 1989	Flash photolysis/ oxidative quenching	C.K.	9.0			
		8.20E+08	Anbar et al., 1966	γ radiolysis	C.K.	9.0			
		7.20E+08	Ervens et al., 2003	Laser photolysis	C.K.	298 K	Ea = (13±4) kJ/mol, A = (3.2±0.2)e11 M-1s-1		
		6.60E+08				288 K			
		7.20E+08				298 K			
		8.90E+08				308 K			
		1.10E+09				318 K			
		1.40E+09				328 K			
CH3-(CH2)2-COOH	butyric acid	2.20E+09	Scholes 1967	γ radiolysis	steay-state method	-2.0			
CH3-CH2-CH2-COO-	butyrate ion	2.00E+09	Anbar et al., 1966	γ radiolysis	C.K.	9.0			
CH3-(CH2)6-COOH	caprylic acid	4.80E+09	Scholes 1967	γ radiolysis	steay-state method	-2.0			
CH3-(CH2)7-COOH	Azelaic acid	5.40E+09	Scholes and Willson, 1967	γ radiolysis	steay-state method	-2.0			
(CH3)2CHCH2COOH	3-methylbutyric acid	1.40E+09	Merz and Waters, 1949	Fenton reaction	C.K.	1.0			
(CH3)3-C-COOH	tri-methyl-acetic acid	6.50E+08	Neusser 1994	Pulse radiolysis	C.K.				
(CH3)-C-COO-	tri-methyl-acetate ion	6.50E+08	Buchanan et al., 1976	fenton reaction	steay-state method	-2.0			
		1.50E+09	Anbar et al., 1966	γ radiolysis	steay-state method	9.0			
CH3-C(CH3)(OCH3)-COOH	2-methyl-2-methoxy-propanoic acid	7.73E+08	Mertz 2002						
CH3-CH(OH)-COOH	lactic acid	4.30E+08	Adams 1965						
		5.24E+08	Martin et al., 2008	pulse radiolysis	C.K.		24C, Ea = 9.31+-0.45 kJ/mole, pH = -6		
		7.70E+08			C.K.		22.2C, Ea = 10.76+-0.35 kJ/mole, pH = - 3.6		
CH3CH2CH(OH)COOH	2-hydroxybutyric acid	1.30E+09	Merz 1949	Fenton reaction	C.K.	1.0			
HO-CH2-(CHOH)4-COOH	glucuronic acid	1.30E+09	Phillips 1970	Pulse radiolysis	C.K.				
HOCH2COOH	glycolic acid	5.40E+08	Scholes 1967	γ radiolysis	steay-state method	-2.0	pKa = 3.83		
CHOCOOH	glyoxylic acid	3.60E+08	Ervens et al., 2003	Laser photolysis	C.K.	298 K	Ea = (8±3) kJ/mol, A = (8.1±0.4)e9 M-1s-1		
		3.50E+08				288 K			
		3.60E+08				298 K			
		4.20E+08				308 K			
		4.50E+08				318 K			
		5.10E+08				328 K			
CHOCOO-	glyoxylate	2.60E+09	Ervens et al., 2003	Laser photolysis	C.K.	298 K	Ea = (36±8) kJ/mol, A = (6.0±0.4)e15 M-1s-1		
		1.90E+09				288 K			
		2.60E+09				298 K			
		5.00E+09				308 K			
		7.60E+09				318 K			
		1.10E+10				328 K			
CH3COCOOH	pyruvic acid	1.20E+08	Ervens et al., 2003	Laser photolysis	C.K.	298 K	Ea = (25±4) kJ/mol, A = (1.0±0.1)e12 M-1s-1		
		9.00E+07				288 K			
		1.20E+08				298 K			
		1.50E+08				308 K			
		2.10E+08				318 K			
		2.80E+08				328 K			
CH3COCOO-	pyruvate	7.00E+08	Ervens et al., 2003	Laser photolysis	C.K.	298 K	Ea = (19±4) kJ/mol, A = (1.3±0.1)e12 M-1s-1		
		6.00E+08				288 K			
		7.00E+08				298 K			
		9.00E+08				308 K			
		1.20E+09				318 K			
		1.50E+09				328 K			
		8.00E+08	Merz and Waters, 1949	Fenton reaction	steay-state method	1.0			

Table A-B9: Survey of HO• rate constants with poly-carboxylic acid

chemcial formura	compound	$k_{HO\bullet}$ (M-1 s-1)	references	experimental method	evaluation method	pH	
HOOC-COOH	oxalic acid	1.40E+06	Getoff 1971	pulse radiolysis	C.K.	0.2	pKa = 1.25, 4.28
-OOC-COOH	oxalate ion, hydrogen	4.70E+07	Getoff et al., 1971	pulse radiolysis	C.K.	3.0	
		1.90E+08	Ervens et al., 2003	Laser photolysis	C.K.	pH =3 298 K	*Ea = (23* ±4) kJ/mol, A = (2.5±0.1)e1 M-1s-1
		1.30E+08				288 K	
		1.90E+08				298 K	
		2.60E+08				308 K	
		3.20E+08				318 K	
		4.50E+08				328 K	
-OOC-COO-	oxalate ion	7.70E+06	Getoff et al., 1971	pulse radiolysis	C.K.	6.0	
		1.60E+08	Ervens et al., 2003	Laser photolysis	C.K.	pH = 8 298 K	*Ea = (36* ±10) kJ/mol, A = (4.6±0.5)e14 M-1s-1
		1.10E+08				288 K	
		1.60E+08				298 K	
		3.30E+08				308 K	
		5.00E+08				318 K	
		6.40E+08				328 K	
HOOC-CH2-COOH	malonic acid	1.60E+07	Walling 1975	fenton reaction	C.K.	1.0	pKa = 2.85, 5.69
		2.40E+07	Scholes and Willson, 1967	γ radiolysis	steay-state method	-2.0	pKa= 2.8, 5.7
-OOC-CH2-COO-	malonate ion	2.40E+08	Logan, 1989	flash photolysis/ oxidative quenching	C.K.	9.0	
		8.00E+07	Ervens et al., 2003	Laser photolysis	C.K.	pH = 9 298 K	*Ea = (38* ±19) kJ/mol, A = (2.1±0.6)e9 M-1s-1
HOOC-CH2-COO-	malonate ion	6.00E+07	Ervens et al., 2003	Laser photolysis	C.K.	pH = 8 298 K	*Ea = (11* ±5) kJ/mol, A = (3.2±0.4)e9 M-1s-1
		3.00E+07				283 K	
		3.80E+07				288 K	
		6.00E+07				298 K	
		3.60E+07				308 K	
		4.50E+07				318 K	
		3.00E+08	Adams 1965	pulse radiolysis	C.K.		
HOOC-(CH2)2-COOH	succinic acid	3.10E+08	Cabelli 1985	pulse radiolysis	P.B.K		pKa= 4.16, 5.61
		1.10E+08	Ervens et al., 2003	Laser photolysis	C.K.	pH = 8 298 K	*Ea = (11* ±6) kJ/mol, A = (8±1)e9 M-1s-1
		4.00E+08				288 K	
		5.00E+08				298 K	
		5.10E+08				308 K	
		6.70E+08				318 K	
		7.30E+08				328 K	
-OOC-(CH2)2-COO-	succinate ion	7.60E+08	Logan, 1989	flash photolysis/ oxidative quenching	C.K.	9.0	
		5.00E+08	Ervens et al., 2003	Laser photolysis	C.K.	pH = 8 298 K	*Ea = (11* ±5) kJ/mol, A = (5±0.4)e10 M-1s-1
		9.90E+07				288 K	
		1.10E+08				298 K	
		1.30E+08				308 K	
		1.30E+08				318 K	
		1.80E+08				328 K	
HOOC-(CH2)3-COOH	glutaric acid	8.30E+08	Scholes and Willson, 1967	γ radiolysis	steay-state method	-2.0	
HOOC-(CH2)4-COOH	adipic acid	2.00E+09	Scholes and Willson, 1967	γ radiolysis	steay-state method	-2.0	
HOOC-(CH2)6-COOH	saberic acid	4.80E+09	Scholes and Willson, 1967	γ radiolysis	steay-state method	-2.0	
HOOC-(CH2)7-COOH	azelaic acid	5.40E+09	Scholes and Willson, 1967				
HOOC-(CH2)8-COOH	sabacic acid	6.40E+09	Scholes and Willson, 1967				
HOOC-CH(OH)-COOH	tartoronic acid	1.70E+08	Schuchmann 1995	γ radiolysis	steay-state method	-2.0	
	tartarate ion	1.40E+09	Logan 1989	flash photolysis/ oxidative quenching	C.K.	9.0	
		6.80E+08	Kraljic, 1967	γ radiolysis	C.K.	9.0	
HOOC-CH2-CH(OH)-COOH	malic acid	8.20E+08	Cabelli 1985				
HOOC-CH(OH)-CH(OH)-COOH	tartaric acid	7.00E+08	Scholes 1967				
HOOC-CH2-C(COOH)(OH)-CH2-COOH	citric acid	5.00E+07	Adams 1965	pulse radiolysis	C.K.	1.0	pKa = 3.08, 4.74, 5.40

Table A-B10: Survey of HO• rate constants with alkyl halides

Chemcial Formura	Compound	$k_{HO\bullet}$ (M-1 s-1)	references	experimental method	evaluation method	pH	Exp. Solvation free energy (kJ/mol) at 298K	Exp. Solvation free energy (kcal/mol) at 298K
Cl-CH2-COOH	chloroacetic acid	4.30E+07	Adams 1965					
		2.75E+07	Mao et al., 1991	TiO2/UV	C.K.			
CH3-Cl	monochloromethane	5.50E+07	Milosavljevic et al., 2005	Pulse radiolysis	C.K.		-2.34	-0.56
Cl2-CH2	dichloromethane	9.00E+07	Haag and Yao, 1992	Chemical reaction	C.K.	pH = 8.5 T = 297 K	-5.69	-1.36
		9.00E+07	Getoff, 1991	Pulse radiolysis	C.K.	pH = 8.6 T = 303 K		
		5.80E+07	Emmi et al., 1985	Pulse radiolysis	P.B.K	pH = -10		
		1.00E+08	Cohen and Benson, 1987					
Br2-CH2	dibromomethane	9.00E+07	Haag and Yao, 1992	Chemical reaction	C.K.	pH = 8.5 T = 297 K		
		9.90E+07	Haag and Yao, 1992	Chemical reaction	C.K.	pH = 3 T = 297 K		
BrCl2CH	bromodichloromethane	7.10E+07	Mezyk et al., 2006	Pulse radiolysis	C.K.			
CHBr2Cl	chlorodibromomethane	8.30E+07	Mezyk et al., 2006	Pulse radiolysis	C.K.			
CHCl3	chloroform	5.00E+07	Haag and Yao, 1992	Photolysis	C.K.	pH = 2.8 T = 297 K	-4.48	-1.07
		7.40E+06	Chutny, 1966	Radiolysis	C.K.			
		9.50E+06	Bednar and Teply, 1960	fenton reaction	C.K.	pH = 0.4		
		1.80E+07	Bednar and Teply, 1960	Beta-radiolysis	C.K.	pH = 0.4		
		1.40E+07	Anbar et al., 1966	gamma-radiolysis	C.K.	pH = 9.0		
I2-CH2	diiodomethane	2.10E+09	Mohan and Moorthy, 1990	Pulse radiolysis	P.B.K in N2O saturated solution	pH = 6.0		
		6.30E+09	Mohan and Moorthy, 1990	Pulse radiolysis	P.B.K	pH = 1.5		
		6.00E+09			P.B.K	pH = 3.0		
BrClCH2	bromochloromethane	2.50E+09	Maity et al., 1995	Pulse radiolysis	P.B.K.	PH <0, acid catalyzed		
ClICH2	chloroiodomethane	4.00E+09	Mohan and Mittal, 1992	Pulse radiolysis	T.S.			
CHBr3	tribromomethane	1.50E+08	Mezyk 2006					
		1.00E+08	Lal and Mahal, 1992	Pulse radiolysis	C.K.	pH = 7.0		
ClCH2-CH2Br	1-bromo-2-chloroethane	4.50E+09	Maity et al., 1995	Pulse radiolysis	P.B.K.	PH <0, acid catalyzed		
CH3-CH2Br	bromoethane	1.30E+08	Lal and Mahal, 1992	Pulse radiolysis	C.K.	pH = 7.0		
BrCH2-CH2Br	1,2-dibromoethane (1,2-DBE)	2.60E+08	Lal and Mahal, 1992	Pulse radiolysis	C.K.	pH = 7.0		
		2.10E+08	Lat et al, 1988	Pulse radiolysis	C.K.	pH = 7.0		
Br2CH-CHBr2	1,1,2,2-tetrabromoethane	2.20E+08	Lal and Mahal, 1992	Pulse radiolysis	C.K.	pH = 7.0		
CH3-CHCl2	1,1-dichloroethane (1,1-DCE)	1.30E+08	Lat et al, 1988	Pulse radiolysis	C.K.	pH = 7.0		
		1.30E+08	Milosavljevic et al., 2005	Pulse radiolysis	C.K.			
CH2Cl-CH2Cl	1,2-dichloroethane (1,2-DCE)	7.90E+08	Getoff 1990	Pulse radiolysis	C.K.	pH = -6.5		
		2.00E+08	Lat et al, 1988	Pulse radiolysis	C.K.	pH = 7.0		
		2.20E+08	Milosavljevic et al., 2005	Pulse radiolysis	C.K.			
ClCH2-CHCl2	1,1,2-trichloroethane (1,1,2-TCE)	1.10E+08	Lat et al, 1988	Pulse radiolysis	C.K.	pH = 7.0	-8.16	-1.95
		3.00E+08	Haag and Yao, 1992	Photolysis	C.K.	pH = 2.8 T = 297 K		
		3.00E+08	Milosavljevic et al., 2005	Pulse radiolysis	C.K.			
CCl3-CH3	1,1,1-trichloroethane (1,1,1-TCE)	1.00E+08	Getoff 1989	Photolysis	C.K.	pH = 6.7	-1.05	-0.25
		4.00E+07	Lat et al, 1988	Pulse radiolysis	C.K.	pH = 7.0		
Cl3C-CH2Cl	1,1,1-2-tetrachloroethane 1,1,1,2-TetCE	1.80E+07	Mao et al., 1991	TiO2/UV	C.K.		-4.81	-1.15
		1.00E+07	Milosavljevic et al., 2005	Pulse radiolysis	C.K.			
CHCl2-CHCl2	1,1,2,2-tetrachloroethane (1,1,2,2-TetCE)	2.50E+08	Milosavljevic et al., 2005	Pulse radiolysis	C.K.			
Cl3C-CHCl2	pentachloroethane (PCE)	1.00E+07	Mao et al., 1991	TiO2/UV	C.K.			
CCl3-CHO		3.10E+09	Ross 1977					
CF3-CHCl2	2,2-dichloro-1,1,1-trifluoroethane	1.30E+07	Lal 1988					
CH3CH2CH2-Br	1-bromopropane	1.70E+08	Lal and Mahal, 1992	Pulse radiolysis	C.K.	pH = 7.0		
CH3CH2CH2-Cl	1-chloropropane	2.50E+09	Getoff 1991	Pulse radiolysis	C.K.	pH = 7.5-8.5	-1.13	-0.27
CHCl-CHCl-CH2Br	1,2-dichloro-3-bromopropane	7.30E+08	Haag and Yao, 1992	Photolysis	C.K.	pH = 2.8 T = 297 K		
CH2Cl-CHCl-CH3	1,2-dichloropropane	2.00E+00	Haag and Yao, 1992	Photolysis	C.K.	pH = 2.8 T = 297 K		
CH2(Cl)-CH2-CH2(Br)	1-bromo-3-chloropropane	2.00E+09	Maity et al., 1995	Pulse radiolysis	P.B.K.	PH <0, acid catalyzed		
(CH3)3-C-Br	2-methyl-2-bromopropane	2.20E+08	Lal and Mahal, 1992	Pulse radiolysis	C.K.	pH = 7.0		
Cl-CH2CH2CH2-I	1-chloro-2-iodo-propane	4.70E+09	Mohan and Mittal, 1992	Pulse radiolysis	T.S.			
CH2Br-CH2-CH2Br	1,3-dibromopropane	4.10E+09	Mohan 1993					

CH3-(CH2)3-Br	1-bromobutane	1.50E+08	Lal and Mahal, 1992	Pulse radiolysis	C.K.	pH = 7.0		
CH3-CH2-CHBr-CH3	2-bromobutane	1.50E+08	Lal and Mahal, 1992	Pulse radiolysis	C.K.	pH = 7.0		
CH3-(CH2)3-Cl	1-chlorobutane	3.40E+09	Getoff, 1991	Pulse radiolysis	C.K.	T = 303 K		
Br-(CH2)4-Br	1,4-dibromobutane	6.50E+09	Mohan et al, 1993	Pulse radiolysis	P.B.K.	PH <0, acid catalyzed T = 298 K		
CH3-(CH2)4-Br	1-bromopentane	1.20E+08	Lal and Mahal, 1992	Pulse radiolysis	C.K.	pH = 7.0		
Br-(CH2)5-Br	1,5-dibromopentane	8.50E+09	Mohan et al, 1993	Pulse radiolysis	P.B.K.	PH <0, acid catalyzed T = 298 K		
Br-(CH2)6-Br	1,6-dibromohexane	1.70E+10	Mohan et al, 1993	Pulse radiolysis	P.B.K.	PH <0, acid catalyzed T = 298 K		
Br-CH2-CH2-OH	2-bromoethanol	3.50E+08	Haag and Yao, 1992	Photolysis	C.K.	pH = 2.8 T = 297 K		
Cl-CH2-CH2-OH	2-chloroethanol	9.50E+08	Anbar and Neta, 1967	Gamma-radiolysis	C.K.	pH = 8.5		
CCl3-CH2-OH	2,2,2-trichloroethanol	4.20E+08	Walling et al., 1974	Fenton		pH <2		
CF3-CH2-OH	2,2,2-trifluoroethanol	2.30E+08	Walling et al., 1974	Fenton		pH <2		
CCl3-CH(OH)2	chloral hydrate	3.10E+09	Erikson et al., 1973	Pulse radiolysis	C.K.			
Cl-CH2-CH(OCH3)2	2-chloro-1,1-dimethoxyethane	1.50E+09	Eibenberger 1980	Pulse radiolysis	R.M.			
CCl3-CN		3.90E+07	Lat et al, 1988	Pulse radiolysis	C.K.	pH = 7.0		
CF3-CHClBr	Halothane	1.30E+07	Lat et al, 1988	Pulse radiolysis	C.K.	pH = 7.0		
CHF2-O-CF2-CHClF	Enflurane	9.50E+06	Lat et al, 1988	Pulse radiolysis	C.K.	pH = 7.0		
CF3-CHCl-O-CHF2	Isoflurane	2.40E+07	Lat et al, 1988	Pulse radiolysis	C.K.	pH = 7.0		
H3C-O-CF2-CHCl2	Methoxyflurane	8.30E+07	Lat et al, 1988	Pulse radiolysis	C.K.	pH = 7.0		
ICH2COOH	Iodoacetic acid	5.70E+09	Gilbert et al., 1974	Pulse radiolysis	C.K.	pH = 1.0		
NH2Cl		5.20E+08	Poskrebyshev et al., 2003	Pulse radiolysis	C.K.	pH = 9.0 T = 295 K		

Table A-B11: Survey of HO• rate constants with nitro compounds

chemcial formura	compound	$k_{HO\bullet}$ (M-1 s-1)	references	experimental method	evaluation method	pH		Exp. Solvation free energy (kJ/mol) 298K	Exp. Solvation free energy (kcal/mol) 298K
CH3-CH2-CH2-NO2	1-nitropropane	2.50E+08	Bors et al., 1993	Pulse radiolysis	C.K.		$k_{reference}$ = 1.3E10	-13.98	-3.34
(CH3)2-CH-NO2	2-nitropropane	8.00E+07	Bors et al., 1993	Pulse radiolysis	C.K.		$k_{reference}$ = 1.3E10	-13.15	-3.14
CH2ClNO2	chloronitromethane	1.94E+08	Mezyk et al., 2006	Pulse radiolysis	C.K.	pH = 7.0 T = 293 K			
CHCl2NO2	dichloronitromethane	5.12E+08	Mezyk et al., 2006	Pulse radiolysis	C.K.	pH = 7.0 T = 293 K			
CH2BrNO2	bromonitromethane	8.36E+07	Cole et al., 2006	Pulse radiolysis	C.K.	pH = 7.0 T = 293 K			
CHBr2NO2	dibromonitromethane	4.75E+08	Mezyk et al., 2006	Pulse radiolysis	C.K.	pH = 7.0 T = 293 K			
CHBrClNO2	bromochloronitromethane	4.20E+08	Mezyk et al., 2006	Pulse radiolysis	C.K.	N.R.			
Cl3C-NO2	chloropicrim	4.97E+07	Cole et al., 2006	Pulse radiolysis	C.K.				
CH2-NO2-	aci-Nitromethane anion	8.50E+09	Asmus and Taub, 1968	Pulse radiolysis	P.B.K.	10.5			

Table A-B12: Survey of HO• rate constants with nitrile

chemcial formura	compound	$k_{HO\bullet}$ (M-1 s-1)	references	experimental method	evaluation method	pH	Exp. Solvation free energy (kJ/mol) 298K	Exp. Solvation free energy (kcal/mol) 298K
CH3-CN	acetonitrile	2.20E+07	Neta 1975	Pulse radiolysis	D.M.	3.5		
CN-CN	cyanogen	<1.0E7	Draganic et al., 1971	Pulse radiolysis	T.S.			
CH3-CH2-CN	propionitrile	9.30E+07	Draganic et al., 1973	γ radiolysis	C.K.		-16.12	-3.85
NC-CH2-CH2-CN	succino nitrile	3.00E+07	Draganic et al., 1973	γ radiolysis	C.K.			
CCl3CN	trichloroacetonitrile	3.90E+07						
H2N-CN	cyanamide	8.70E+06	Draganic et al., 1979	γ radiolysis	C.K.			
H-CN	hydrogen cyanide	6.00E+07	Buechler et al., 1976	Pulse radiolysis	P.B.K.	3.5		

Table A-B13: Survey of HO• rate constants with amine

chemical formula	compound	$k_{HO\bullet}$ (M-1 s-1)	references	experimental method	evaluation method	pH		Exp. Solvation free energy (kJ/mol) at 298K	Exp. Solvation free energy (kcal/mol) at 298K
NH2-OH	hydroxy amine	9.50E+09	Simic and Hayon, 1971	Pulse radiolysis	C.K.	pH = 8.0 T = 295 K	$k_{reference}$ = 1.1E10		
		9.50E+09	Poskrebyshev et al., 2003	Pulse radiolysis	C.K.	pH = 9.0 T = 295 K			
NH3OH+	hydroxyl ammonium ion	<5.0E8	Simic and Hayon, 1971	Pulse radiolysis	C.K.	pH = 4.0 T = 295 K	$k_{reference}$ = 1.1E10		
CH3-NH2	methyl amine	1.80E+09	Getoff and Schwoerer, 1971	Pulse radiolysis	C.K.	10.5 295 K	pH = 2.0-13.1	-19.09	-4.56
		4.10E+09	Getoff and Schwoerer, 1971	Pulse radiolysis	C.K.	11.1 295 K	pH= 9.7-12.8		
		5.70E+09	Wigger et al., 1969	Pulse radiolysis	C.K.				
CH3-NH3+	methyl ammonium ion	3.50E+07	Getoff and Schwoerer, 1970	Pulse radiolysis	C.K.	295 K	pH = 2.0 and 7.0		
		9.10E+07	Wigger et al., 1969	Pulse radiolysis	C.K.				
CH3-CH2-NH2	ethyl amine	6.40E+09	Getoff and Schwoerer, 1973	Pulse radiolysis	C.K.	pH = 8.5	$k_{reference}$ = 3.9E9	-18.84	-4.50
		6.40E+09	Getoff and Schwoerer, 1973	Pulse radiolysis	C.K.		$k_{reference}$ = 1.1E10		
		1.30E+10	Simic et al., 1971	Pulse radiolysis	C.K.				
CH3-CH2-NH3+	ethyl ammonium ion	5.90E+08	Getoff and Schwoerer, 1973	Pulse radiolysis	C.K.	pH = 13	$k_{reference}$ = 1.1E10		
		3.30E+08	Getoff and Schwoerer, 1973	Pulse radiolysis	C.K.	pH = 13	$k_{reference}$ = 3.9E9		
		3.00E+08	Simic et al., 1971	Pulse radiolysis	C.K.	3.1	$k_{reference}$ = 1.1E10		
CH3-CH2-CH2-NH2	propyl amine	7.30E+09	Getoff and Schwoerer, 1973	Pulse radiolysis	C.K.		$k_{reference}$ = 1.1E10	-18.38	-4.39
		5.80E+09	Getoff and Schwoerer, 1973	Pulse radiolysis	C.K.		$k_{reference}$ = 3.9E9		
CH3-(CH2)2-NH3+	propyl ammonium ion	8.20E+08	Getoff and Schwoerer, 1973	Pulse radiolysis	C.K.	pH = 13	$k_{reference}$ = 3.9E9		
		1.40E+09	Getoff and Schwoerer, 1973	Pulse radiolysis	C.K.	pH = 13	$k_{reference}$ = 1.1E10		
		7.50E+08	Getoff and Schwoerer, 1970	Pulse radiolysis	C.K.		$k_{reference}$ = 1.1E10		
CH3-(CH2)3-NH2	N-butyl amine	8.20E+09	Getoff and Schwoerer, 1973	Pulse radiolysis	C.K.	pH = 8.5	$k_{reference}$ = 3.9E9	-17.96	-4.29
			Getoff and Schwoerer, 1973	Pulse radiolysis	C.K.	pH = 8.5	$k_{reference}$ = 1.1E10		
		1.00E+10	Pramanick and Bhattacharyya, 1986	Fenton reaction	C.K.	1.0 298K	$k_{reference}$ = 1.2E10		
CH3-(CH2)4-NH2	N-amyl amine	7.00E+09	Getoff and Schwoerer, 1973	Pulse radiolysis	C.K.	pH = 8.5	$k_{reference}$ = 3.9E9		
		9.00E+09	Getoff and Schwoerer, 1973	Pulse radiolysis	C.K.	pH = 8.5	$k_{reference}$ = 1.1E10		
		8.90E+09	Getoff and Schwoerer, 1973	Pulse radiolysis	C.K.	pH = 8.5	$k_{reference}$ = 1.0E10		
CH3-(CH2)5-NH2	Hexylamine	1.31E+10	Pramanick and Bhattacharyya, 1986	Fenton reaction	C.K.	1.0 298K	$k_{reference}$ = 1.2E10		
CH3-(CH2)7-NH2	N-octylamine	1.46E+10	Pramanick and Bhattacharyya, 1986	Fenton reaction	C.K.	1.0 298K	$k_{reference}$ = 1.2E10		
N-C4H9-NH3+	butylammonium ion	3.20E+09	Getoff and Schwoerer, 1973	Pulse radiolysis	C.K.	pH = 8-13.1	$k_{reference}$ = 1.0E10		
		2.50E+09	Getoff and Schwoerer, 1973	Pulse radiolysis	C.K.		$k_{reference}$ = 3.9E9		
		3.10E+09	Getoff and Schwoerer, 1973	Pulse radiolysis	C.K.	pH = 8-13.1	$k_{reference}$ = 1.1E10		
		5.50E+09	Getoff and Schwoerer, 1970	Pulse radiolysis	C.K.	4 295 K	$k_{reference}$ = 1.1E10		
H2N-CH2-CH2-NH2	ethylenediamine	5.50E+09	Lati and Meyerstein, 1972	Pulse radiolysis	C.K.	10 pH 8.0, 8.5, 9.0	$k_{reference}$ = 1.1E10		
(CH3)3-C-NH2	tert-butyl amine	6.00E+09	Simic et al., 1971	Pulse radiolysis	C.K.		$k_{reference}$ = 1.1E10		
(CH3)3-C-NH3+	tert-butyl ammonium ion	7.00E+08	Simic et al., 1971	Pulse radiolysis	C.K.	3.2	$k_{reference}$ = 1.1E10		
		2.40E+08	Getoff and Schwoerer, 1970	Pulse radiolysis	C.K.	4 295 K	$k_{reference}$ = 1.1E10		
N-C5H11-NH3+	amyl ammonium ion	4.70E+09	Getoff and Schwoerer, 1973	Pulse radiolysis	C.K.	pH = 8-13.1	$k_{reference}$ = 1.1E10		
		6.80E+09	Getoff and Schwoerer, 1973	Pulse radiolysis	C.K.	pH = 8-13.1	$k_{reference}$ = 1.0E10		
		3.40E+09	Getoff and Schwoerer, 1973	Pulse radiolysis	C.K.	pH = 8-13.1	$k_{reference}$ = 3.9E9		
		9.80E+09	Getoff and Schwoerer, 1973	Pulse radiolysis	C.K.	pH = 8-13.1	$k_{reference}$ = 1.1E10		
(CH3)2-CH-NH2	iso-propyl amine	1.30E+10	Simic et al., 1971	Pulse radiolysis	C.K.		$k_{reference}$ = 1.1E10		
(CH3)2-CH-NH3+	iso-propyl ammonium ion	5.00E+08	Simic et al., 1971	Pulse radiolysis	C.K.	3.0	$k_{reference}$ = 1.1E10		
		4.70E+08	Getoff and Schwoerer, 1970	Pulse radiolysis	C.K.	4 295 K	$k_{reference}$ = 1.1E10		
(CH3)2-N-NH2	1,1-dimethyl hydrazine	1.60E+10	Hayson and Simic, 1972	Pulse radiolysis	C.K.	9.7	$k_{reference}$ = 1.1E10		
CH3-NH-CH3	dimethylamine (DMA)	8.90E+09	Lee et al., 2007	photolysis	C.K.	pH = 7.0, 10, 11.5		-17.96	-4.29
CH3-NH2+-CH3	dimethyl ammonium ion	6.00E+07	Lee et al., 2007	photolysis	C.K.	pH = 7.0, 10, 11.5			
CH3-NH-NH-CH3	1,2-dimethyl hydrazine	1.40E+10	Hayson and Simic, 1972	Pulse radiolysis	C.K.	10.1	$k_{reference}$ = 1.1E10		
CH3-(CH2)3-NH-(CH2)3-CH3	dibutyl amine	1.81E+10	Pramanick 1986						
(C2H5)2-N-OH	N,N-diethyl hydroxyl amine	1.30E+09	Saunders and Gorse, 1979	Pulse radiolysis	P.B.K.	9.0			
CH3-O-NH2	O-methyl hydroxy amine	1.40E+10	Simic and Hayon, 1971	Pulse radiolysis	C.K.	pH =9.1 T = 295 K	$k_{reference}$ = 1.1E10		
CH3-O-NH3+	O-methyl hydroxyl ammonium amine	<4.0E8	Simic and Hayon, 1971	Pulse radiolysis	C.K.	4.5	$k_{reference}$ = 1.1E10		
(CH3(CH2)3)3-N	tributyl amine	1.67E+10	Pramanick and Bhattacharyya, 1986	Fenton reaction	C.K.	1.0 298K	$k_{reference}$ = 1.2E10		
(C2H5)3-N	triethyl amine	1.00E+10	Simic et al., 1971	Pulse radiolysis	C.K.		$k_{reference}$ = 1.1E10		
(C2H5)3-NH+	triethyl ammonium ion	3.50E+08	Simic et al., 1971	Pulse radiolysis	C.K.	3.6	$k_{reference}$ = 1.1E10		
(CH3)3-N	trimethyl amine	1.30E+10	Simic et al., 1971	Pulse radiolysis	C.K.		$k_{reference}$ = 1.1E10	-13.52	-3.23
(CH3)3-NH+	Trimethyl ammonium ion	4.00E+08	Simic et al., 1971	Pulse radiolysis	C.K.	7.5	$k_{reference}$ = 1.1E10		
(CH3)2-N-CHO	Dimethyl formamide	1.70E+09	Simic et al., 1971	Pulse radiolysis	C.K.		$k_{reference}$ = 1.1E10		
(CH3)2-N-CH2CH2-OH	Dimethylethanolamine (DMEA)	6.50E+09	Lee et al., 2007	photolysis	C.K.	pH = 7.0, 10, 11.5			
	Dimethylethanol ammonium ion	4.70E+08	Lee et al., 2007	photolysis	C.K.	pH = 7.0, 10, 11.5			
(HO-CH2-CH2)3-N	triethanolamine	8.00E+09	Schwarz 1982	Pulse radiolysis	C.K.		$k_{reference}$ = 1.1E10		
(CH2COOH)3-N	Nitrilotriacetic acid	2.10E+09	Borggaard 1972	Fenton reaction	C.K.	0.0	$k_{reference}$ = 5.9E9		
(HOCH2CH2)3-N	Nitrilotriethanol	8.00E+09	Schwarz 1982	Pulse radiolysis	C.K.				
HOOC-CH2-NH-CH2-COOH	Iminodiacetic acid	4.90E+07	Bhattacharyya and Saha, 1976	γ radiolysis	C.K.	1.0	2.5, 9.4		
	2,2-bis(hydroxymethyl)-2,2',2"-nitrilotriethanol	3.00E+09	Raap 1978	Pulse radiolysis					
(HO-CH2)3C-NH2	2-amino-2-propane-1,3-diol	1.50E+09	Buxton 1988	Pulse radiolysis					
(COOH-CH2-N(CH2)COOH-CH2)2	Ethylenediamine tetra acetic acid	2.00E+09	Bernd and von Sonntag, 1998						
H2N-C(=NH)-NH-CN	dicyandiamide	7.20E+06	Draganic et al., 1979	γ radiolysis	C.K.	5.0	$k_{reference}$ = 3.2E9		
(CH3)2-N-CS-S-	dimethylthiocarbamate	4.20E+09	Lee et al., 2007	γ radiolysis	C.K.	pH = 10			

Table A-B14: Survey of HO• rate constants with NDMA and related compounds

chemcial formura	compound	$k_{HO\bullet}$ (M-1 s-1)	references	experimental method	evaluation method	pH
(CH3)2-N-NO	N-nitrosodimethylamine (NDMA)	4.30E+08	Mezyk et al., 2006	Pulse radiolysis	C.K.	pH = 7.0 T = 294 K
		4.50E+08	Lee et al., 2007	O3/H2O2	C.K.	pH = 294 K
(CH3-CH2)2-N-NO	N-nitrosodiethylamine	6.99E+08	Mezyk et al., 2006	Pulse radiolysis	C.K.	pH = 7.0 T = 294 K
(CH3-CH2-CH2)2-N-NO	N-nitrosodipropylamine	2.30E+09	Landsman et al., 2007	Pulse radiolysis	C.K.	pH = 7.0 T = 292 K
(CH3-CH2-CH2-CH2)2-N-NO	N-nitrosodibutylamine	4.71E+09	Landsman et al., 2007	Pulse radiolysis	C.K.	pH = 7.0 T = 292 K
(CH3-CH2)(CH3)-N-NO	N-nitrosomethylethylamine	4.95E+08	Mezyk et al., 2006	Pulse radiolysis	C.K.	pH = 7.0 T = 294 K
(CH3-CH2-CH2-CH2)(CH3-CH2)-N-NO	N-nitrosoethylbutylamine	3.10E+09	Landsman et al., 2007	Pulse radiolysis	C.K.	pH = 7.0 T = 292 K
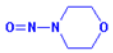	N-nitrosomorpholine	1.75E+09	Landsman et al., 2007	Pulse radiolysis	C.K.	pH = 7.0 T = 292 K
	N-nitrosopyrrolidine	1.75E+09	Landsman et al., 2007	Pulse radiolysis	C.K.	pH = 7.0 T = 292 K
	N-nitrosopiperidine	2.98E+09	Landsman et al., 2007	Pulse radiolysis	C.K.	pH = 7.0 T = 292 K
	N-nitrosohexamethyleneimine	4.35E+09	Landsman et al., 2007	Pulse radiolysis	C.K.	pH = 7.0 T = 292 K
(CH3)2-N-NO2	dimethylnitramine	5.44E+08	Mezyk et al., 2006	Pulse radiolysis	C.K.	pH = 7.0 T = 294 K
(CH3)(CH3CH2)-N-NO2	methyl ethyl nitramine	7.60E+08	Mezyk et al., 2006	Pulse radiolysis	C.K.	pH = 7.0 T = 294 K
(CH3-CH2)2-N-NO2	diethyl nitramine	8.67E+08	Mezyk et al., 2006	Pulse radiolysis	C.K.	pH = 7.0 T = 294 K

Table A-B15: Survey of HO• rate constants with amide

chemcial formura	compound	$k_{HO\bullet}$ (M-1 s-1)	references	experimental method	evaluation method	pH	
H2N-CN	cyanamide	8.70E+06	Draganic et al., 1978	γ radiolysis	C.K.		$k_{reference}$ =1.9E9
CH3-CO-NH2	acetamide	1.90E+08	Hayon et al., 1970	Pulse radiolysis	C.K.	5.5	$k_{reference}$ = 1.1E10
CH3-CO-NH-C-(CH3)3	N-tert-butyl-acetamide	1.10E+09	Hayon et al., 1971	Pulse radiolysis	C.K.	5.0-6.0	$k_{reference}$ = 1.1E10
CH3-CO-N-(CH3)2	N,N-dimethyl acetamide	3.50E+09	Hayon et al., 1970	Pulse radiolysis	C.K.	5.5	$k_{reference}$ = 1.1E10
H-CO-N-(CH3)2	N,N-dimethyl formamide	1.70E+09	Hayon et al., 1970	Pulse radiolysis	C.K.	5.5	$k_{reference}$ = 1.1E10
(CH3)3-C-CO-N-(CH3)2	N,N-dimethyl pivalamide	3.90E+09	Hayon et al., 1971	Pulse radiolysis	C.K.		$k_{reference}$ = 1.1E10
H2N-CH2-CO-NH2	2-aminoacetamide	2.80E+09	Rao and Hayon, 1975	Pulse radiolysis	P.B.K.	10	
HO-CH2-CO-NH2	glycolamide	1.10E+09	Bell et al, 1975	Pulse radiolysis	C.K.	8.5	$k_{reference}$ = 1.1E10
HO-CH(CH3)-CO-NH2	2-hydroxypropionamide	1.30E+09	Bell et al, 1975	Pulse radiolysis	C.K.	4.5	$k_{reference}$ =1.3E9
(CH3)2-CH-CO-NH2	2-methylpropionamide	1.60E+09	Hayon et al., 1971	Pulse radiolysis	C.K.	5.0-6.0	$k_{reference}$ = 1.1E10
CH3-CO-NH-CH3	N-methylacetamide	1.60E+09	Hayon et al., 1970	Pulse radiolysis	C.K.	5.5	$k_{reference}$ = 1.1E10
H-CO-NH-CH3	N-methyl-formamide	1.20E+09	Hayon et al., 1970	Pulse radiolysis	C.K.	5.5	$k_{reference}$ = 1.1E10
(CH3)2-CH-CO-NH-CH3	N-butylformamide	1.90E+09	Hayon et al., 1971	Pulse radiolysis	C.K.	5.0-6.0	$k_{reference}$ = 1.1E10
(CH3)3-C-CO-NH-CH3	N-methyl-pivalamide	2.40E+09	Hayon et al., 1971	Pulse radiolysis	C.K.	5.0-6.0	$k_{reference}$ = 1.1E10
CH3-CH2-CO-NH-CH3	N-methyl-propionamide	1.40E+09	Hayon et al., 1971	Pulse radiolysis	C.K.	5.0-6.0	$k_{reference}$ = 1.1E10
C2H5-CO-NH2	propionamide	7.00E+08	Hayon et al., 1971	Pulse radiolysis	C.K.	5.0-6.0	$k_{reference}$ = 1.1E10
(CH3)3-CO-NH2	trimethylacetamide	1.50E+09	Hayon et al., 1971	Pulse radiolysis	C.K.	5.0-6.0	$k_{reference}$ = 1.1E10
H2N-CH2-CO-NH2	glycinamide	2.80E+09	Rao and Hayon, 1975	Pulse radiolysis	P.B.K.	10	
(CH3)2-CH-CO-NH2	isobutyramide	1.60E+09	Hayon et al., 1971	Pulse radiolysis	C.K.	5.0-6.0	$k_{reference}$ = 1.1E10
(CH3)2-CH-CO-NH-CH3	N-methylisobutyramide	1.90E+09	Hayon et al., 1971	Pulse radiolysis	C.K.	5.0-6.0	$k_{reference}$ = 1.1E10

Table A-B16: Survey of HO• rate constants with sulphide

chemcial formura	compound	$k_{HO\bullet}$ (M-1 s-1)	references	experimental method	evaluation method	pH		exp. solvation energy, kJ/mol	exp. solvation energy, kcal/mol
H3C-S-CH3	dimethyl sulfide	1.90E+10	Bonifacic et al., 1975	Pulse radiolysis	P.B.K.			-6.45	-1.54
H3C-S-S-CH3	di-methyl-di-sulfides	1.70E+10	Bonifacic et al., 1975	Pulse radiolysis	P.B.K. R.T.	-4.0		-7.66	-1.83
H3C-CH2-S-CH2-CH3	di-ethyl-sulfides	1.40E+10	Bonifacic et al., 1975	Pulse radiolysis	P.B.K.			-5.99	-1.43
H3C-CH2-S-S-CH2-CH3	di-ethyl-di-sulfides	1.40E+10	Bonifacic et al., 1975	Pulse radiolysis	P.B.K. R.T.	-4.0		-6.82	-1.63
(CH3)2-CH-S-S-CH-(CH3)2	di-ethyl-methyl-di-sulfides	2.00E+10	Bonifacic et al., 1975	Pulse radiolysis	P.B.K.	-4.0			
(CH3)3-C-S-S-C-(CH3)3	di-tert-butyl-sulfides	6.50E+09	Bonifacic et al., 1975	Pulse radiolysis	P.B.K. R.T.	-4.0			
CH3-S-CH2-CH2-OH	2-methylthio-ethanol	7.90E+09	Schoeneich and Bobrowski, 1993	Pulse radiolysis	P.B.K.	T=298 K			
H3C-S-CH2-CH2-CHO	methional	8.20E+09	Bors et al., 1976	Pulse radiolysis	C.K.				
HO-CH2-CH2-S-CH2-CH2-OH	2,2'-thiodiethanol	1.40E+10	Mohan and Mittal, 1991	Pulse radiolysis	P.B.K.	6.0			
		8.10E+09	Schoeneich and Bobrowski, 1993	Pulse radiolysis	P.B.K.	T =298 K			
		2.00E+10	Mohan and Mittal, 1991	Pulse radiolysis	C.K.	6.0	$k_{reference}$ = 1.1E10		
HO-CH2CH2CH2-S-CH2CH2CH2-OH	3,3'-thiodiethanol	1.40E+10	Mohan and Mittal, 1991			6.0			
	3,3'-thiodipropanol	1.40E+10	Mohan and Mittal, 1991	Pulse radiolysis	P.B.K.	pH = 6.0 T =296 K			
HOOC-CH2-S-CH2-COOH	thiodiacetic acid	6.00E+09	Adams et al., 1965						
S=C=S	carbon disulfides	8.00E+09	Roebke et al., 1973	Pulse radiolysis	C.K.	7.6	$k_{reference}$ = 1.1E10		

Table A-B17: Survey of HO• rate constants with sulfoxide

chemcial formura	compound	$k_{HO\bullet}$ (M-1 s-1)	references	experimental method	evaluation method	pH	
CH3-SO-CH3	di-methyl-sulfoxide	6.50E+09	Milne 1989	Flash photolysis	C.K.	4.0-5.0	
		7.00E+09	Veltwisch et al., 1980	Pulse radiolysis	C.D.	pH = 2.0 R.T.	
		5.80E+09	Reuvers et al., 1973	Pulse radiolysis	C.K.		$k_{reference}$ = 1.1E10
		7.00E+09	Meissner et al., 1967	Pulse radiolysis	C.K.		$k_{reference}$ = 1.1E10
CH3-CH2-SO-CH2-CH3	di-ethyl-sulfoxide	6.50E+09	Veltwisch et al., 1980	Pulse radiolysis	D.K.	pH = 2.0 R.T.	
CH3-CH2-CH2-SO-CH2-CH2-CH3	di-propyl-sulfoxide	6.30E+09	Veltwisch et al., 1980	Pulse radiolysis	D.K.	pH = 2.0 R.T.	
(CH3)2CH-SO-CH(CH3)2	di(1-methyl-ethyl)sulfoxide	6.80E+09	Veltwisch et al., 1980	Pulse radiolysis	D.K.	pH = 2.0 R.T.	
(CH3-CH2-CH2-CH2)2-SO	di-butyl-sulfoxide	8.00E+09	Veltwisch et al., 1980	Pulse radiolysis	D.K.	pH = 2.0 R.T.	
(CH3)3-C-SO-C-(CH3)3	di-tert-butyl-sulfoxide	5.30E+09	Veltwisch et al., 1980	Pulse radiolysis	D.K.	pH = 2.0 R.T.	
CH3-SO-CH2-S-CH3	methyl methyl thiomethyl sulfoxide	4.80E+09	Sumiyoshi 1982	Pulse radiolysis	P.B.K.		
HO-CH2CH2-SO-CH2CH2-OH	di(2-hydroxyethyl) sulfoxide	5.30E+09	Veltwisch et al., 1980	Pulse radiolysis	D.K.	pH = 2.0 R.T.	
(CH3)2-CH-SO-CH-(CH3)2	diisopropyl sulfoxide	6.80E+09	Veltwisch et al., 1980	Pulse radiolysis	D.K.	pH = 2.0 R.T.	
C4H8OS	tetramethylene sulfoxides	7.00E+09	Veltwisch et al., 1980	Pulse radiolysis	D.K.	pH = 2.0 R.T.	

Table A-B18: Survey of HO• rate constants with thiol

chemcial formura	compound	$k_{HO\bullet}$ (M-1 s-1)	references	experimental method	evaluation method	pH		
HS-CH2-CH2-OH	mercaptoethanol	6.80E+09	Jayson et al., 1971	Pulse radiolysis	C.K.	6.5	$k_{reference}$ = 1.0E10	
-S-CH2-CH2-OH	2-hydroxyethylsulfide ion	4.00E+09	Karmann et al., 1969	Pulse radiolysis	P.B.K.	11		
HS-CH2-COOH	mercaptoacetic acid	1.20E+09	Merz and Waters, 1949	Fenton reaction	C.K.	1	$k_{reference}$ = 4.3E8	
CH3-CH(SH)-COO-	2-mercaptopropionate ion	1.70E+10	Hoffman and Hayon, 1973	Pulse radiolysis	R.M.	7.2	$k_{reference}$ = 1.1E10	pKa = 4, 10.7
		1.60E+10			R.M.	10.8		
HS-CH2-CH2-COOH	3-mercaptopropionate ion	3.00E+10	Hoffman and Hayon, 1973	Pulse radiolysis	R.M.	6	$k_{reference}$ = 1.1E10	pKa= 4.3, 10.3
		2.10E+10				10.7		
HS-CH2-COOCH3	methyl thioglycolate	2.10E+10	Hoffman 1973	Pulse radiolysis	C.K.	5.1	$k_{reference}$ = 1.1E10	pKa = 7.8
		1.80E+10				10.6		
HS-CH2-CH(OH)-CH(OH)-CH2-SH	dithiothreitol	1.50E+10	Akhlaq and von Sonntag, 1987	Pulse radiolysis	P.B.K.	4		
	glutatione	2.30E+10	Misik et al., 1993	photolysis	C.K.	6.8	$k_{reference}$ = 4.3E9	
		9.00E+09	Liphard et al., 1990	Pulse radiolysis	C.K.	pH = 8.0 T = 291 K	$k_{reference}$ = 5.2E9	
		1.30E+10	Eriksen and Fransson, 1988			7.8	$k_{reference}$ = 1.1E10	pKa = 2.5, 3.7, 9.2, 9.5
		4.00E+10				10.6		
		1.30E+10	Quintiliani et al., 1977	Pulse radiolysis	C.K.	5.5	$k_{reference}$ = 1.1E10	pH 8 and 9.2
		1.40E+10	Adams et al., 1965	Pulse radiolysis	C.K.	1	$k_{reference}$ = 1.1E10	pKa = 2.12, 3.53, 8.66, 9.62

Table A-B19: Survey of HO• rate constants with urea

chemcial formura	compound	$k_{HO\bullet}$ (M-1 s-1)	references	experimental method	evaluation method	pH	
H2N-CS-NH2	thiourea	1.20E+10	Wang et al., 1999	pulse radiolysis	B.D.K		
H2N-CO-NH2	urea	7.90E+05	Masuda et al., 1980	γ radiolysis	C.K.		$k_{reference}$ = 1.2E10
(CH3)2N-CS-N(CH3)2	tetramethyl thiourea	8.00E+09	Wang et al., 1999	pulse radiolysis	B.D.K		
CH3-NH-CS-NH-CH3	1,3-dimethyl thiourea	1.20E+09	Fessenden 1981	pulse radiolysis	P.B.K.		
CH3-NH-CO-NH-CH3	1,3-dimethylurea	2.60E+09	Fessenden 1981	pulse radiolysis	C.K.		$k_{reference}$ = 1.9E9
CH3-NH-CO-NH2	methylurea	2.00E+09	Miller and Cornwell, 1998	chemical reaction	C.K.		
(CH3)2-N-CO-N-(CH3)2	tetramethyl urea	5.20E+09	Liphard et al., 1990	pulse radiolysis	C.K.	pH = 8.0 T = 291 K	$k_{reference}$ = 1.1E10
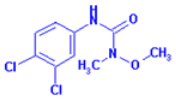	Linuron	5.60E+09	Benitez et al., 2007	photo Fenton	C.K.	T = 293 K pH = 3.3	
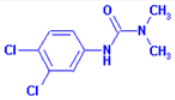	diuron	7.10E+09	Benitez et al., 2007	photo Fenton	C.K.	T = 293 K pH = 3.3	
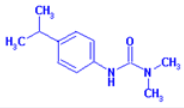	isoproturon	5.70E+09	Benitez et al., 2007	photo Fenton	C.K.	T = 293 K pH = 3.3	
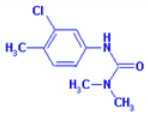	chlortoluron	7.50E+09	Benitez et al., 2007	photo Fenton	C.K.	T = 293 K pH = 3.3	

Table A-B20: Survey of HO• rate constants with phosphate-containing compounds

chemcial formura	compound	$k_{HO\bullet}$ (M-1 s-1)	references	experimental method	evaluation method	pH
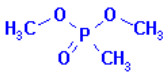	dimethyl methylphosphonate (DMMP)	2.00E+08	Aguila et al., 2001	Pulse radiolysis	C.K.	pH = 7.0 298 K
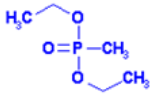	Diethyl methylphosphonate (DEMP)	6.00E+08	Aguila et al., 2001	Pulse radiolysis	C.K.	pH = 7.0 298 K
	trimethyl phosphate	1.20E+08	von Sonntag et al., 1972	Pulse radiolysis	C.K.	
	triethyl phosphate	2.90E+09	Greenstock and Shierman, 1975	gamma-radiolysis	C.K.	pH = -7.0
	tributyl phosphate	1.00E+10	Clay and Witort, 1974	gamma-radiolysis	C.K.	pH = 1.2

Table A-B21: Survey of HO• rate constants with unsaturated alkene

chemcial formura	compound	$k_{HO\cdot}$ (M-1 s-1)	references	experimental method	evaluation method	pH		k HO gas (cm3/molecule-sec)
H2C=CHCH2OH	allyl alcohol	5.90E+09	Maruthamuthu 1980	Pulse radiolysis	C.K.	-7.0	$k_{reference}$ = 1.1E10	2.59E-11
H2C=CHCH2CN	allyl cyanide	6.90E+09	Maruthamuthu 1980	Pulse radiolysis	C.K.	-7.0	$k_{reference}$ = 1.1E10	
CH3CH=CHCHO	crotonaldehyde	5.80E+09	Lilie 1970	Pulse radiolysis	C.K.		$k_{reference}$ = 1.1E10	3.60E-11
CH3CH2CH=CH2	1-butene	7.00E+09	Thomas 1967	Pulse radiolysis	C.K.		$k_{reference}$ = 1.1E10	3.14E-11
H2C=CHCOCH3	1-butene-3-one	8.50E+09	Lilie 1970	Pulse radiolysis	C.K.		$k_{reference}$ = 1.1E10	
		8.50E+08	Kumar et al., 1990	Pulse radiolysis	C.K.	6.8		
Cis HOOC-CH=CH-COOH	maleic acid	6.00E+09	Cabelli 1985	Pulse radiolysis	P.B.K.	4.0-10.5 298K		
Trans HOOC-CH=CH-COOH	fumaric acid	6.00E+09	Cabelli 1985	Pulse radiolysis	P.B.K.	4.0-10.5 298K	pKa = 3.03, 4.44	
H2C=CHCN	acrilonitrile	5.30E+09	Kumar 1988	Pulse radiolysis	C.K.	-7.0	$k_{reference}$ = 1.1E10	1.99E-11
		5.20E+09	Maruthamuthu 1980	Pulse radiolysis	C.K.	-7.0	$k_{reference}$ = 1.1E10	
		2.80E+09	Buxton et al., 1979	Pulse radiolysis	C.K.	10.9	$k_{reference}$ = 3.9E8	
H2C=CHCHO	acrolein	7.00E+09	Lilie 1970	Pulse radiolysis	C.K.		$k_{reference}$ = 1.1E10	1.99E-11
H2C=CHCONH2	acrylamide	5.90E+09	Buxton et al., 1988				average of 4 values	
		5.80E+09	Kumar et al., 1988	Pulse radiolysis	C.K.	7.0	$k_{reference}$ = 1.1E10	
		4.70E+09	Maruthamuthu 1980	Pulse radiolysis	C.K.	-7.0	$k_{reference}$ = 1.1E10	
		5.30E+09	Willson et al., 1971	Pulse radiolysis	C.K.		$k_{reference}$ = 1.0E10	
		6.80E+09	Willson et al., 1971	Pulse radiolysis	P.B.K.			
		6.60E+09	Chambers et al., 1970	Pulse radiolysis	C.K.	-12.0	$k_{reference}$ = 3.9E8	
H2C=CH-OH	vinyl alcohol	1.50E+08	Ulanski, 1994	Pulse radiolysis	C.K.		$k_{reference}$ = 1.1E10	
H2C=CHCOOH	acrylic acid	1.50E+09	Walling 1973	Fenton reaction	C.K.	1.0	$k_{reference}$ = 9.7E8	
H2C=CHCH=CH2	butadiene	7.00E+09	Thomas 1967	Pulse radiolysis	C.K.	298 K	$k_{reference}$ = 1.1E10	6.66E-11
trans ClCH=CHCl	trans 1,2-dichloroethylene	7.30E+09	Koester and Asmus, 1971	Pulse radiolysis	P.B.K.	-6.5		
		7.30E+09	Koester and Asmus, 1971	Pulse radiolysis	C.K.	-6.5	$k_{reference}$ = 1.1E10	
ClCH=CHCl	dichloroethylene	3.80E+09	Getoff 1991	Pulse radiolysis	C.K.	8.6	$k_{reference}$ = 1.1E10	1.09E-11
		5.00E+09	Koester and Asmus, 1971			-6.5		
		4.40E+09	Koester and Asmus, 1971			-6.5		
NCN=C(NH2)2	dicyandiamide		Draganic et al., 1979	γ radiolysis	C.K.	5	$k_{reference}$ = 3.9E9	
H3C-C=CH-HC=CH-CH2OH	2,4-hexadien-1-ol	9.80E+09	Simic 1973	Pulse radiolysis	P.B.K.	7.0		
CH2=CHCOOCH2CH2OH	2-hydroxyethyl acrylate	1.10E+10	Safrany 1993	Pulse radiolysis	C.K.		$k_{reference}$ = 1.1E10	
(CH3)2C=CH2	isobutylene	5.40E+09	Thomas 1967	Pulse radiolysis	C.K.	298 K	$k_{reference}$ = 1.1E10	5.14E-11
H2C=C(CH3)CN	methacrylonitrile	1.20E+10	Kumar et al., 1988	Pulse radiolysis	C.K.	-7.0	$k_{reference}$ = 1.1E10	2.60E-11
		1.10E+10	Maruthamuthu 1980	Pulse radiolysis	C.K.	-7.0	$k_{reference}$ = 1.1E10	
H2C=C(CH3)COOCH3	methyl methacrylate	1.10E+10	Kumar 1988	Pulse radiolysis	C.K.	-7.0	$k_{reference}$ = 1.1E10	
		1.20E+10	Maruthamuthu 1980	Pulse radiolysis	C.K.	-7.0	$k_{reference}$ = 1.1E10	
H2C=CH-CH(OH)-CH=CH2	1,4-pentadien-3-ol	1.00E+10	Simic 1973	Pulse radiolysis	P.B.K.	7.0		
CH3CH=CH2	propylene	7.00E+09	Thomas 1967	Pulse radiolysis	C.K.			2.63E-11
ClCH=CCl2	trichloroethylene	2.90E+09	Getoff 1991	Pulse radiolysis	C.K.	8.6	$k_{reference}$ = 1.1E10	2.36E-12
		3.30E+09	Getoff 1989	Pulse radiolysis	C.K.		$k_{reference}$ = 1.1E10	
		4.00E+09	Koester and Asmus, 1971	Pulse radiolysis	P.B.K.			
		4.30E+09	Koester and Asmus, 1971	Pulse radiolysis	C.K.		$k_{reference}$ = 1.1E10	
Cl2C=CCl2	tetrachloroethylene	2.00E+09	Getoff 1991	Pulse radiolysis	C.K.	8.5	$k_{reference}$ = 1.1E10	1.67E-13
		4.90E+08	Getoff 1990	Pulse radiolysis	C.K.		$k_{reference}$ = 1.1E10	
		2.80E+09	Koester and Asmus, 1971	Pulse radiolysis	C.K.	-6.5	$k_{reference}$ = 1.1E10	
		2.30E+09	Koester and Asmus, 1971	Pulse radiolysis	P.B.K.	-6.5		
H2C=CHCl	vinyl chloride	1.20E+10	Koester 1971	Pulse radiolysis	C.K.	-6.5	$k_{reference}$ = 1.1E10	6.96E-12
H2C=CCl2	vinylidine chloride	6.80E+09	Koester 1971	Pulse radiolysis	C.K.	-6.5	$k_{reference}$ = 1.1E10	
H2C=C(CH3)-CO-NH2	methyl acrylamide	1.30E+10	Kumar et al., 1988	Pulse radiolysis	C.K.	-7.0	$k_{reference}$ = 1.1E10	
	crocetin	2.30E+10	Bors et al., 1982	Pulse radiolysis	D.K.	5.9		
(H2C=CH)2SO2	vinyl sulfone	4.10E+09	Kumar et al 1990	Pulse radiolysis	C.K.	7.0		
		4.00E+09	Kumar et al 1990	Pulse radiolysis	P.B.K.	6.8		
H2C=CH2	ethylene	4.40E+09	Thomas 1967	Pulse radiolysis	C.K.		$k_{reference}$ = 1.1E10	8.52E-12
		1.70E+09	Cullis et al 1967	Pulse radiolysis	C.K.		$k_{reference}$ = 1.1E10	
$NCN=C(NH_2)_2$	dcyandiamide	7.20E+06	Draganic et al., 1979	γ radiolysis	C.K.	5.0	$k_{reference}$ = 3.2E9	
	2,5-dimethyl-3-hexyne-2,5-diol	3.30E+09	Walling 1973	Fenton reaction	C.K.	1.0	$k_{reference}$ = 9.7E8	

Table A-B22: Survey of HO• rate constants with benzene and benzene derivatives

chemcial formura	compound	$k_{HO\bullet}$ (M-1 s-1)	references	experimental method	evaluation method	pH	k HO gas
C6H6	benzene	7.60E+09					1.23E-12
C6H5-CH3	toluene	5.10E+09	Roder et al., 1990	Pulse radiolysis	P.B.K.		5.96E-12
		3.00E+09	Dorfman et al., 1964	Pulse radiolysis	P.B.K.	pH = 3.0	
C6H5-CH2CH3	ethylbenzene	7.50E+09	Sehested and Holcman, 1979	Pulse radiolysis		pH = 7.0	7.10E-12
C6H5-OH	phenol	6.60E+09	Field et al., 1982	Pulse radiolysis	P.B.K.	pH = 7.0	2.63E-11
		1.40E+10	Land and Ebert, 1967	Pulse radiolysis	P.B.K.	pH = -7.6	
		1.80E+10	Adames et al., 1965	Pulse radiolysis	C.K.	pH = 6-7	
C6H5-F	fluorobenzene	5.70E+09	Mohan and Mittal, 1995	Pulse radiolysis	P.B.K.	pH = 7.0	6.90E-13
		1.00E+10	Koester and Asmus, 1973	Pulse radiolysis	C.K.		
C6H5Cl	chlorobenzene	5.60E+09	Ashton et al., 1995	Pulse radiolysis	P.B.K.	T = 293 K	7.70E-13
		4.30E+09	Kochany and Bolton, 1992	Photolysis	C.K.	pH = 3.5, 7.0	
		4.50E+09	Shevchuk et al., 1969	γ-radiolysis	C.K.	pH = 9.0	
		6.50E+09	Matthews and Sangster, 1965	γ-radiolysis	C.K.	pH = 10.7	
C6H5-Br	bromobenezene	5.20E+09	Mohan and Mittal, 1995	Pulse radiolysis	P.B.K.	pH = 7.0	7.70E-13
		7.40E+09	Mohan and Mittal, 1995	Pulse radiolysis	C.K.	pH = 7.0	
		1.00E+10	Mohan and Mittal, 1995	Pulse radiolysis	P.B.K.	pH <0	
		8.90E+09	Mohan and Mittal, 1995	Pulse radiolysis	P.B.K.	pH <0	
		4.40E+09	Merga et al., 1994	Pulse radiolysis	P.B.K.	pH = 7.0	
		4.90E+09	Kochany and Bolton, 1992	Photolysis	C.K.	pH = 3.5	
		4.80E+09	Kochany and Bolton, 1992	Photolysis	C.K.	pH = 7.0	
C6H5-I	iodobenzene	5.70E+09	Kochany and Bolton, 1992	Photolysis	C.K.	pH = 3.5	1.10E-12
		5.30E+09	Kochany and Bolton, 1992	Photolysis	C.K.	pH = 7.0	
		3.10E+09	Mohan and Moorthy, 1989	Pulse radiolysis	C.K.		
		5.00E+09	Shevchuk et al., 1969	γ-radiolysis	C.K.	pH = 9.0	
C6H5-CN	benzonitrile	3.90E+09	Chutny and Swallow, 1970	Pulse radiolysis	C.K.		3.30E-13
		4.90E+09	Neta and Dorfman, 1968	Pulse radiolysis	P.B.K.	pH = 7.0	
C6H5-NO2	nitrobenzene	3.90E+09	Buxton et al., 1988			selected values	1.40E-13
		4.00E+09	Ashton et al., 1995	Pulse radiolysis	P.B.K.		
		3.20E+09	Neta and Dorfman, 1968	Pulse radiolysis	P.B.K.	pH = 7.0	
		4.70E+09	Asmus et al., 1967	Pulse radiolysis	P.B.K.		
		3.50E+09	Asmus et al., 1967	Pulse radiolysis	P.B.K.		
C6H5-NH2	aniline	1.70E+10					
C6H5-CHO	benzaldehyde	4.40E+09	Shevchuk et al., 1969	γ-radiolysis	C.K.	pH = 9.0	1.29E-11
C6H5-COOH	benzoic acid	1.80E+09	Ashton et al., 1995	Pulse radiolysis	P.B.K.	T = 293 K	
		4.30E+09	Wander et al., 1968	Pulse radiolysis	P.B.K.	pH <- 3	
C6H5-COCH3	acetophenone	6.40E+09	Willson et al., 1971	Pulse radiolysis	P.B.K.		2.74E-12
		5.90E+09	Willson et al., 1971	Pulse radiolysis	P.B.K.		
		6.50E+09	Neta and Dorfman, 1968	Pulse radiolysis	P.B.K.	pH = 7.0	
C6H5-NO	nitrosobenzene	1.80E+10	Asmus et al., 1966	Pulse radiolysis	C.K.	pH = 7.0	
C6H5-CONH2	benzamide	4.60E+09	Anbar et al., 1966	γ-radiolysis	C.K.	pH = 9.0	
		2.90E+09	Merz and Waters, 1949	Fenton reaction	C.K.	pH = 1.0	
C6H5-SOCH3	methyl phenyl sulfoxide	9.70E+09	Veltwish et al., 1980	Pulse radiolysis			
C6H5-CH(CH3)2	cumene	7.50E+09	Sehested and Holcman, 1979	Pulse radiolysis	C.K.	pH = 7.0	6.50E-12
C6H5-CH2OH	benzylalcohol	8.40E+09	Neta and Dorfman, 1968	Pulse radiolysis	P.B.K.	pH = 7.0	2.29E-11
C6H5-NH-CO-CH3	acetanilide	5.20E+09	Anbar et al., 1966	γ-radiolysis	C.K.	pH = 9.0	
C6H5-SO2NH2	benzensulfonamide	2.80E+09	Phillips et al., 1973	γ-radiolysis	C.K.		
		2.90E+09	Anbar et al., 1966	γ-radiolysis	C.K.	pH = 9.0	
C6H5-SO3H	benzenesulfonic acid	2.10E+09	Merz and Waters, 1949	Fenton reaction	C.K.	pH = 1.0	
C6H5-S-CH3	thioanisole	3.50E+09	Mohan and Mittal, 1997	Pulse radiolysis	P.B.K.		
C6H5-NH-OH	phenyl hydroxylamine	1.50E+10	Wigger et al., 1967	Pulse radiolysis	P.B.K.		
C6H5-SO-C2H5	Ethyl phenyl sulfoxide	8.40E+09	Veltwish et al., 1980	Pulse radiolysis			
C6H5-SO-CH(CH3)2	isopropyl phyenyl sulfoxide	1.00E+10	Veltwish et al., 1980	Pulse radiolysis			
C6H5-CH2CH2-C(CH3)2-OH	2-methyl-4-phenyl-2-butanol	5.90E+09	Snook and Hamilton, 1974	Fenton reaction		pH = -1.8	
C6H5-CHOHCH(CH3)2	2-methyl-1-phenyl-1-propanol	9.50E+09	Snook and Hamilton, 1974	Fenton reaction		pH = -1.8	
C6H5-CH(OH)C(CH3)3	2,2-dimethyl-1-phenyl-1-propanol	9.90E+09	Snook and Hamilton, 1974	Fenton reaction		pH = -1.8	
C6H5-CHOHCH3	phenylethanol	1.10E+10	Snook and Hamilton, 1974	Fenton reaction		pH = -1.8	
C6H5-CH(OCH3)CH(CH3)2	1-methoxy-2-methyl-1-phenylpropane	7.40E+09	Snook and Hamilton, 1974	Fenton reaction		pH = -1.8	
C6H5-CH(OH)(CH2-CH3)	1-phenyl-1-propanol	1.00E+10	Snook and Hamilton, 1974	Fenton reaction		pH = -1.8	
C6H5-CH2-CH2--OH	1-phenyl-2-propanol	2.10E+10	Snook and Hamilton, 1974	Fenton reaction		pH = -1.8	
		5.80E+09	Reuvers et al., 1973	Pulse radiolysis	C.K.		
		7.00E+09	Reuvers et al., 1973	Pulse radiolysis	C.K.		
C2H5CH-C6H5-OH	2-phenyl-2-propanol	4.60E+09	Snook and Hamilton, 1974	Fenton reaction		pH = -1.8	
C6H5-CH2-CH2CH2-CH(OH)-CH3	1-phenyl-3-butanol	2.00E+10	Snook and Hamilton, 1974	Fenton reaction		pH = -1.8	
C6H5-O-CH3	anisol	5.40E+09	O'Neill et al., 1975	Pulse radiolysis	P.B.K.	pH = 6.5	1.73E-11
(C6H5)2-CO	benzophenone	9.00E+09	Brede et al., 1975	Pulse radiolysis	P.B.K.		
		8.70E+09	Land 1968	Pulse radiolysis	P.B.K.		
(C6H5)2-NH	diphenylamine	1.00E+10	Schmidt et al., 1985	Pulse radiolysis	P.B.K.	pH=3-9	1.94E-10
		1.30E+10	Shevchuk et al., 1969	γ-radiolysis	C.K.	pH = 9.0	
(C6H5)2-SO	diphenyl sulfoxide	6.30E+09	Veltwish et al., 1980	Pulse radiolysis			
(C6H5)2-S	diphenylsulfides	1.30E+10	Engman et al., 1994	Pulse radiolysis	P.B.K.	pH = 7.0	
-O-COOH	phenoxyacetic acid	1.00E+10	Zona et al., 2002	Pulse radiolysis	P.B.K.	T = 295 K	
CH3-CH(OH)-C6H5	1-phenyl-1-propanol	1.00E+10	Snook and Hamilton, 1974	Fenton reaction		pH = -1.8	

2	HO-C6H4-CH3	o-cresol	1.10E+10	Savel'eva et al., 1972	γ-radiolysis	C.K.	pH = 9.0	4.20E-11
	HO-C6H4-CH3	p-cresol	1.20E+10	Feitelson and Hayon, 1973	Pulse radiolysis	C.K.	pH = 5.5	4.70E-11
	H3C-C6H4-CH3	o-xylene	6.70E+09					
	H3C-C6H4-CH3	m-xylene	7.50E+09					
	H3C-C6H4-CH3	p-xylene	7.00E+09					
	C6H4-Cl2	1,2-dichlorobenzene	2.50E+09	Merga et al., 1994	Pulse radiolysis	P.B.K.	pH = 7.0	4.20E-13
			3.90E+09	Kochany and Bolton 1992	Photolysis	C.K.	pH = 3.5	
			4.00E+09	Kochany and Bolton 1992	Photolysis	C.K.	pH= 7.0	
	C6H4-Cl2	1,3-dichlorobenzene	5.70E+09	Merga et al., 1994	Pulse radiolysis	P.B.K.	pH = 7.0	7.20E-13
			5.80E+09	Kochany and Bolton 1992	Photolysis	C.K.	pH = 3.5	
			5.70E+09	Kochany and Bolton 1992	Photolysis	C.K.	pH= 7.0	
	C6H4-Cl2	1,4-dichlorobenzene	5.30E+09	Kochany and Bolton 1992	Photolysis	C.K.	pH = 3.5	3.20E-13
			5.40E+09	Kochany and Bolton 1992	Photolysis	C.K.	pH= 7.0	
	C6H4-(OH)2	1,2-benzenediol	1.10E+10	Savel'eva et al., 1972	γ-radiolysis	C.K.	pH = 9.0	1.04E-10
	1,3-C6H4 (OH)2	resorcinol	1.20E+10	Savel'eva et al., 1972	γ-radiolysis	C.K.	pH = 9.0	
	HO-C6H4-Cl	2-chlorophenol	1.20E+10	Getoff and Solar, 1986	Pulse radiolysis	P.B.K.	pH = 6.5-7.7	
	HO-C6H4-Cl	3-chlorophenol	7.20E+09	Savel'eva et al., 1972	γ-radiolysis	C.K.	pH = 9.0	
	HO-C6H4-Cl	4-chlorophenol	9.30E+09	Satafford et al., 1994	Pulse radiolysis	P.B.K.	pH = 6.0	
	H3C-C6H4-OH	2-methyl phenol	1.10E+10	Savel'eva et al., 1972	γ-radiolysis	C.K.	pH = 9.0	4.20E-11
	H3C-C6H4-OH	4-methyl phenol	1.20E+10	Feitelson and Hayon, 1973	Pulse radiolysis	C.K.	pH = 5.5	4.70E-11
	HO-C6H4-O-CH3	2,3-methoxyphenol	2.00E+10	O'Neil and Steenken, 1977	Pulse radiolysis	C.K.	pH = 6-7	
	HO-C6H4-O-CH3	3,5-methoxyphenol	3.20E+10	O'Neil and Steenken, 1977	Pulse radiolysis	C.K.	pH = 6-7	
	HO-C6H4-O-CH3	2,6-methoxyphenol	2.60E+10	O'Neil and Steenken, 1977	Pulse radiolysis	C.K.	pH = 6-7	
	H5C2-C6H4-CH(OH)-CH3	2-p-1-(p-ethylphenyl)ethanol	1.30E+10	Snook and Hamilton, 1974	Fenton reaction		pH = -1.8	
	HO-C6H4-NO2	4-nitrophenol	3.80E+09	Cercek and Ebert, 1968	Pulse radiolysis	P.B.K.	pH = 7.0	
	4-CH3-C6H4-CN	4-tolunitrile	1.20E+10	Holcman and Sehested, 1979	Pulse radiolysis	P.B.K.	pH = 7.0	
	1,4-C6H4(CN)2	1,4-dicyanobenzene	7.80E+08	Robinson and Schulte-Frohlinde, 1973	Pulse radiolysis	C.K.		
							pH= 7.0	
	4-F-C6H4-CN	p-fluorobenzonitrile	3.50E+09	Klever and Schulte-Frohlinde, 1976	Pulse radiolysis	C.K.	T = 292 K	
	4-Br-C6H4-CH(CH3)-OH	1-(p-bromophenyl)ethanol	6.10E+09	Snook and Hamilton, 1974	Fenton reaction		pH = -1.8	
	(CH3)3-C-C6H4-OH	tert-butylphenol	1.90E+10	Savel'eva et al., 1972	γ-radiolysis	C.K.	pH = 9.0	
	1,2-C6H4(OH)2	1,2-catechol	1.10E+10	Savel'eva et al., 1972	γ-radiolysis	C.K.	pH = 9.0	
	C6H4-F2	o-difluorobenzene	7.50E+09	Koester and Asmus, 1973	Pulse radiolysis	C.K.		
	C6H4-F2	p-difluorobenzene	1.00E+10	Koester and Asmus, 1973	Pulse radiolysis	C.K.		
	C6H4-(OCH3)2	1,2-dimethoxybenzene	5.20E+09	O'Neill et al., 1975	Pulse radiolysis	P.B.K.	pH = 6.5	
	C6H4-(OCH3)2	1,3-dimethoxybenzene	7.20E+09	O'Neill et al., 1975	Pulse radiolysis	P.B.K.	pH = 6.5	
	C6H4-(OCH3)2	1,4-dimethoxybenzene	7.00E+09	O'Neill et al., 1975	Pulse radiolysis	P.B.K.	pH = 6.5	
							pH = -6	
	4-O2N-C6H4-NH2	p-nitroaniline	1.40E+10	van der Linde, 1977	Pulse radiolysis	C.K.	T = 295 K	
	CH3-C6H4-CN	p-tolunitrile	1.20E+10					
	4-Cl-C6H4NO2	1-chloro-4-nitrobenzene	1.30E+09	Guittonneau et al., 1990	Photolysis	C.K.	pH = 7.5	
	4-O2N-C6H4-COCH3	4-nitroacetophenone	3.30E+09	Whillans 1977	Pulse radiolysis	P.B.K.	pH=6.5	
			2.80E+09	Michaels et al., 1976	Pulse radiolysis	P.B.K.	pH = 6.6	
							pH = -6	
	4-O2N-C6H4NH2	4-nitroaniline	1.40E+10	van der Linde, 1977	Pulse radiolysis	C.K.	T = 295 K	
3	(HO)2-C6H3-Cl	4-chlorocatecohol	7.00E+09					
	C6H3-(OH)3	phloroglucinol	1.00E+10	Wang et al., 1994	Pulse radiolysis	P.B.K.	pH = 5.8	
		1,2,3-trimethyl benzene	7.00E+09					
		1,2,4-trimethyl benzene	6.20E+09					
		1,3,5-trimethyl benzene (mesitylene)	6.40E+09					
	3,4-(HO)2-C6H3-CHO	dihydroxybenzaldehyde	8.30E+09	Bors et al., 1979	Pulse radiolysis	C.K.	pH = 7.0	
	(HO)2-C6H3-COCH3	2,4-dihydroxyacetophenone	3.00E+10	Bors et al., 1984	Pulse radiolysis	C.K.		
	(HO)2-C6H3-COCH3	2,5-dihydroxyacetophenone	8.00E+09	Bors et al., 1984	Pulse radiolysis	C.K.		
	(HO)2-C6H3-COCH3	3,4-dihydroxyacetophenone	1.00E+10	Bors et al., 1984	Pulse radiolysis	C.K.	pH = 7.0	
	(NO2)2-C6H3-OCH3	3,5-dinitroanisole	4.00E+09	Tamminga et al., 1979	Pulse radiolysis	P.B.K.		
	C6H3-(OCH3)3	1,2,3-trimethoxybenzene	7.00E+09	Sehested et al., 1975	Pulse radiolysis	P.B.K.	pH= -7.0	
	C6H3-(OCH3)3	1,2,4-trimethoxybenzene	6.20E+09	Sehested et al., 1975	Pulse radiolysis	P.B.K.	pH= -7.0	
	C6H3-(OCH3)3	1,3,5-trimethoxybenzene	8.10E+09					
	HO-C6H4-CH3O	2,3-dimethoxyphenol	2.00E+10					
	HO-C6H4-CH3O	2,4-dimethoxyphenol	2.60E+10					
	HO-C6H4-CH3O	3,5-dimethoxyphenol	2.00E+10					
	-F, -F, -F	1,3,5-trifluorobenzene	4.10E+09					
	-F, -F, -F	1,2,3-trifluorobenzene	3.70E+09					
	-F, -F, -F	1,2,4-trifluorobenzene	3.90E+09					
	-Cl, -Cl, -OH	2,4-dichlrophenol	7.10E+09	Zona et al., 2002	Pulse radiolysis	P.B.K	T = 295 K	
	-OH, -OH, -OH	1,2,4-trihydroxybenzene	8.60E+09	Oturan et al., 2000	Electron-fenton			
	-OH, -OH, -C(CH3)3	tert-butyl hydroquinone	6.30E+09	Dohmann and Bergmann 1995	Pulse radiolysis	C.K.	pH = 6.8, T = 295 K	
4	C6H2(CH3)4	1,2,3,4-tetramethylbenzen	7.20E+09	Sehested et al., 1975	Pulse radiolysis	P.B.K.	pH= -7.0	
	C6H2(CH3)4	1,2,3,5-tetramethylbenzene	7.10E+09	Sehested et al., 1975	Pulse radiolysis	P.B.K.	pH= -7.0	
	C6H2(CH3)4	1,2,4,5-tetramethylbenzene	7.10E+09	Sehested et al., 1975	Pulse radiolysis	P.B.K.	pH= -7.0	
	-Cl, -Cl, -Cl, -OH	2,4,5-trichlorophenol	1.20E+10	Draper et al., 1989	Pulse radiolysis	P.B.K	pH = 3.0	
	-Cl, -Cl, -O-COOH	2,4-dichlorophenoxyacetic acid	6.60E+09	Zona et al., 2002	Pulse radiolysis	P.B.K	T = 295 K	
	1,2,4,5-Cl, OH, OH, Cl	2,5-dichlorohydroquinone	2.10E+10	Al-Suhyban and Hughes, 1988	Gamma-radiolysis	C.K.	pH = -0	
			2.50E+10	Al-Suhyban and Hughes, 1988	Gamma-radiolysis	C.K.	pH = -0	
			1.10E+10	Al-Suhyban and Hughes, 1988	Gamma-radiolysis	C.K.	pH = -0	
5		pentafluorobenzene	7.00E+09	Koester and Asmus, 1973	Pulse radiolysis	C.K.		
		pentamethylbenzene	7.50E+09	Sehested et al., 1975	Pulse radiolysis	C.K.	pH = - 7	
6	-F, -F, -F, -F, -OH, -OH	tetrafluorohydroquinone	3.10E+09	Tripathi and Schuler 1983	Pulse radiolysis	P.B.K	pH = -10.5	
		hexafluorobenzene	1.40E+09	Shoute and Mittal, 1993	Pulse radiolysis	C.K.	pH = 7.0	
			3.00E+09	Koester and Asmus, 1973	Pulse radiolysis	C.K.		
		hexamethylbenzene	7.20E+09	Sehested et al., 1975	Pulse radiolysis	p.b.K	pH= -7.0	
		pentafluoroiodobenzene	1.20E+09	Mohan and Mittal 1995	Pulse radiolysis	P.B.K.		
	F, F, F, F,F, -COCH3	pentafluoroacetophenone (PFA)	1.50E+09					
	F, F, F, F, F, CHO	pentafluorobenzaldehyde	2.00E+09					
	F, F, F, F, F, -COOH	pentafluorobenzoic acid	1.10E+09					
	F, F, F, F,F -NH2	pentafluoroaniline	9.60E+09					
	F,F,F,F,F, -OH	pentafluorophenol	9.50E+09					

Table A-B23: Survey of HO• rate constants with pyridine and pyridine derivatives

chemcial formura	compound	HO• (M-1 s-	references	experimental method	evaluation method	pH
	pyridine	3.00E+09	Solar et al., 1993	Pulse radiolysis	P.B.K.	pH = 10
		4.50E+09	Cohen and Meyerstein, 1976	Pulse radiolysis	P.B.K.	pH = 5.9
		1.80E+09	Simic and Ebert, 1971	Pulse radiolysis	P.B.K.	pH = 7.0
		3.00E+09	Cercek and Ebert, 1967	Pulse radiolysis	P.B.K.	pH = 7.0
	2-methyl pyridine	2.50E+09	Schevchuck 1969	Gamma-radiolysis	C.K.	pH = 9.0
	3-methyl pyridine	2.40E+09	Schevchuck 1969	Gamma-radiolysis	C.K.	pH = 9.0
		6.00E+09	Solar et al., 1993	Pulse radiolysis	P.B.K.	pH = 10
	2,4-dimethyl pyridine	3.10E+09	Schevchuck 1969	Gamma-radiolysis	C.K.	pH = 9.0
	2,6-dimethyl pyridine	7.30E+09	Solar et al., 1993	Pulse radiolysis	P.B.K.	pH = 10
		3.00E+09	Schevchuck 1969	Gamma-radiolysis	C.K.	pH = 9.0
	3,5-dimethyl pyridine	8.00E+09	Solar et al., 1993	Pulse radiolysis	P.B.K.	pH = 10
	2,4,6-trimethylpyridine	2.50E+09	Zakatova et al., 1969	Gamma-radiolysis	C.K.	pH = 6.5
		6.50E+09	Solar et al., 1993	Pulse radiolysis	P.B.K.	pH = 10
-NH2	2-pyridine amine	8.40E+09	Shevchuk et al., 1969	Gamma-radiolysis	C.K.	pH = 9.0
-NH2	4-pyridine amine	5.00E+09	Schevchuck 1969	Gamma-radiolysis	C.K.	pH = 9.0
	2-bromopyridine	2.40E+09	Schevchuck 1969	Gamma-radiolysis	C.K.	pH = 9.0
	3-bromopyridine	1.10E+09	Schevchuck 1969	Gamma-radiolysis	C.K.	pH = 9.0
	2-chloropyridine	1.80E+09	Schevchuck 1969	Gamma-radiolysis	C.K.	pH = 9.0
	4-chloropyridine	3.10E+09	Schevchuck 1969	Gamma-radiolysis	C.K.	pH = 9.0
	3-cyanopyridine	7.50E+08	Schevchuck 1969	Gamma-radiolysis	C.K.	pH = 9.0
	3-hydroxy pyridine	8.90E+09	Neik 1991			
	3-pyridinol	5.40E+09	Schevchuck 1969	Gamma-radiolysis	C.K.	pH = 9.0
	4-pyridinol	1.10E+10	Naik and Morthy 1993	Pulse radiolysis	P.B.K.	pH = 6.8
	4-pyridinecarboxyamide	1.60E+09	Cohen and Meyerstein 1976	Pulse radiolysis	P.B.K.	pH=5.9
-COOH	nicotinamide 3-pyridinenicotineamide	1.40E+09	Cohen and Meyerstein 1976	Pulse radiolysis	P.B.K.	pH=5.9
		1.50E+09				
	nicotinic acid (3-pyridinecarboxylic acid)	2.20E+07	Simic and Ebert, 1971	Pulse radiolysis	P.B.K.	pH =9.0
		2.60E+08	Simic and Ebert, 1971	Pulse radiolysis	P.B.K.	pH = 3.1
	4-pyridinecarboxylic acid	6.00E+07	Solar 1991			
	2-pyridine carboxylic acid	2.00E+08	Dey et al., 1992	Pulse radiolysis	P.B.K.	pH = 3.8
	4,4'-bipyridine	5.30E+09	Simic 1971	Pulse radiolysis	P.B.K.	pH=9.3
	2,2'-bipyridine	6.20E+09	Simic and Ebert, 1971	Pulse radiolysis	P.B.K.	pH=9.3
	3,5-pyridinedicarboxylic acid	1.00E+08	Solar et al., 1991			
	2,6-pyridinedicarboxylic acid	5.00E+08	Solar et al., 1991			
	4-ethyl-5-hydroxy-2-methylpyridine	1.40E+09	Zakatova et al., 1969	Gamma-radiolysis	C.K.	pH = 6.5
	pyridine-N-oxide	3.00E+09	Neta et al., 1980	Pulse radiolysis	P.B.K.	pH=7.0
	3-methylpyridine-N-oxide	4.20E+09	Neta et al., 1980	Pulse radiolysis	P.B.K.	pH=7.0
	4-methylpyridine-N-oxide	2.80E+09	Neta et al., 1980	Pulse radiolysis	P.B.K.	pH=7.0
	picrolam (4-Amino-3,5,6-trichloro-2-pyridinecarboxylic acid)	3.40E+09	Haag and Yao, 1992	Fenton reaction	C.K.	pH = 2.1-3.7 T = 297 K
	4-ethyl-5-hydroxy-2-methylpyridine	1.40E+09	Zakatova 1969			
	2,4,6-trimethyl-3-hydroxypyridine	2.50E+09	Zakatova et al., 1969	Gamma-radiolysis	C.K.	pH = 6.5
	2-pyridone	1.10E+10	Naik and Moorthy, 1991	Pulse radiolysis	P.B.K.	pH= 6.8
		6.50E+09	Steenken and O'Neill, 1979	Pulse radiolysis	C.K.	pH = 6-7
	4-pyridone	5.30E+09	Steenken and O'Neill, 1979	Pulse radiolysis	C.K.	pH = 6-7
	pyridoxine 3,4-pyridinedimethanol, 5-hydroxy-6-methyl	4.30E+09	Moorthy and Hayon 1975	Pulse radiolysis	P.B.K.	pH=3.6
		6.30E+09				pH=7.2
		7.40E+09				pH=10.5
	pyrimidine	1.60E+08	Masuda et al., 1975	gamma radiolysis	C.K.	pH=6-7 T=290
	Alfa-(2-pyridyl)-tert-butyl nitrone	9.60E+09	Sridhar et al., 1984	Pulse radiolysis	P.B.K.	
	Alfa-(3-pyridyl)-tert-butyl nitrone	4.60E+09	Sridhar et al., 1984	Pulse radiolysis	P.B.K.	
	Alfa-(4-pyridyl)-tert-butyl nitrone	8.30E+09	Sridhar et al., 1984	Pulse radiolysis	P.B.K.	
	a-(2-Pyridyl 1-oxide)-*N*-*tert*-butylnitrone	3.20E+09	Neta et al., 1980	Pulse radiolysis	P.B.K.	pH=7.0
	a-(3-Pyridyl 1-oxide)-*N*-*tert*-butylnitrone	4.80E+09	Neta et al., 1980	Pulse radiolysis	P.B.K.	pH=7.0
	a-(4-Pyridyl 1-oxide)-*N*-*tert*-butylnitrone	3.50E+09	Neta et al., 1980	Pulse radiolysis	P.B.K.	pH=7.0

Table A-B24: Survey of HO• rate constants with cyclo-compounds

compound	$k_{HO\bullet}$ (M-1 s-1)	references	experimental method	evaluation method	pH
cycloheptane	7.70E+09	Rudakov et al., 1981	Fenton reaction	C.K.	pH = 2.0
cycloheptanol	1.70E+09	Snook and Hamilton, 1974	Fenton reaction	C.K.	pH = - 1.8
cycloheptanol-1d	1.30E+09	Snook and Hamilton, 1974	Fenton reaction	C.K.	pH = - 1.8
cycloheptatoriene	1.00E+10	Schoeneshoefer, 1971	Pulse radiolysis	C.K.	
cyclohexane	6.10E+09	Rudakov et al., 1981	Fenton reaction	C.K.	pH = 2.0
cyclopentane	4.50E+09	Rabani et al., 1974	Pulse radiolysis	C.K.	
	3.00E+09	Soeylemez and Schuler, 1974	Pulse radiolysis	C.K.	
methylcyclopentane	7.00E+09	Rudakov et al., 1981	Fenton reaction	C.K.	pH = 2.0
tetrahydrofuran	4.00E+09				
1,3-dioxolane	4.00E+09				
1,4-dioxalene	3.10E+09	Eigenberger, 1980	Pulse radiolysis	C.K.	
	2.50E+09	Thomas, 1965	Pulse radiolysis	C.K.	pH=7.0
1,4-dioxolane	4.00E+09	Eigenberger, 1980	Pulse radiolysis	C.K.	
cyclohexene	8.80E+09	Michael and Hart, 1970	Pulse radiolysis	C.K.	pH = 7.0
cyclopentene	7.00E+09	Soeylemez and Schuler, 1974	Pulse radiolysis	C.K.	
1,4-dithiane	1.80E+10	Asmus et al., 1977	Pulse radiolysis	P.B.K.	pH = -7.0
1,3-cyclohexadiene	9.90E+09	Michael and Hart, 1970	Pulse radiolysis	C.K.	pH = 7.0
1,4-cyclohexadiene	7.70E+09	Michael and Hart, 1970	Pulse radiolysis	C.K.	pH = 7.0
cycloserine	9.00E+09	Tanaka et al., 1984	Pulse radiolysis	C.K.	pH = 6.5
	1.20E+10		Pulse radiolysis	C.K.	pH = 9-11
1,3,5-trioxane	1.50E+09	Eigenberger, 1980	Pulse radiolysis	C.K.	
2-methyl-1,3-dioxalane	3.50E+09	Eigenberger, 1980	Pulse radiolysis	C.K.	
tetramethylene sulfoxide	7.00E+09	Veltwish et al., 1980	Pulse radiolysis		

Table A-B25: Survey of HO• rate constants with furan and related compounds

chemcial formura	compound	$k_{HO\bullet}$ (M-1 s-1)	references	experimental method	evaluation method	pH
	furan	3.90E+09	Lilie 1971	Pulse radiolysis	C.K.	
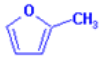	2-methyl furan	1.90E+10	Savel'eva et al., 1973	gamma-radiolysis	C.K.	pH = 9.0
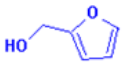	2-furfuryl alcohol	1.50E+10	Savel'eva 1973			
	2-furaldehyde	7.80E+09	Savel'eva et al., 1973	gamma-radiolysis	C.K.	pH = 9.0
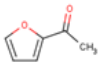	2-acetyl furan	4.50E+09	Vysotskaya et al., 1983	gamma-radiolysis	C.K.	pH = 9.0
	2-furancarboxamide	5.50E+09	Vysotskaya et al., 1983	gamma-radiolysis	C.K.	pH = 9.0
	phenylfuran	1.60E+10	Vysotskaya et al., 1983	gamma-radiolysis	C.K.	pH = 9.0
	5-phenylfurfural	5.90E+09	Vysotskaya et al., 1983	gamma-radiolysis	C.K.	pH = 9.0

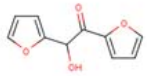	furoin	1.30E+10	Aguer and Richard, 1993	Photolysis	C.K.	pH = 6.3
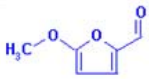	5-hydroxymethylfurfuryl	5.80E+09	Vysotskaya et al., 1983	gamma-radiolysis	C.K.	pH = 9.0
	5-methylfurfural	7.20E+09	Vysotskaya et al., 1983	gamma-radiolysis	C.K.	pH = 9.0
	5-bromofurfural	3.90E+09	Vysotskaya et al., 1983	gamma-radiolysis	C.K.	pH = 9.0
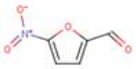	nitrofuraldehyde	5.50E+09	Greenstock and Dunlop, 1973	Pulse radiolysis	P.B.K.	pH = 7.0
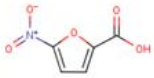	nitrofuroic acid	5.30E+09	Greenstock and Dunlop, 1973	Pulse radiolysis	P.B.K.	pH = 7.0
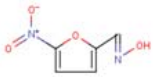	nifuroxime	1.00E+10	Greenstock and Dunlop, 1973	Pulse radiolysis	P.B.K.	pH = 7.0
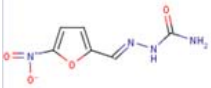	nitrofurazone	1.06E+10	Greenstock and Dunlop, 1973	Pulse radiolysis	P.B.K.	pH = 7.0
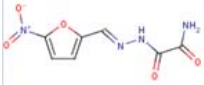	furamazone	1.03E+10	Greenstock and Dunlop, 1973	Pulse radiolysis	P.B.K.	pH = 7.0
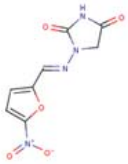	furadantin	9.30E+09	Greenstock and Dunlop, 1973	Pulse radiolysis	P.B.K.	pH = 7.0
	tetrahydrofuran	4.00E+09	Eigenberger, 1980	Pulse radiolysis	C.K.	

Table A-B26: Survey of HO• rate constants with indole and indole derivatives

chemcial formura	compound	$k_{HO\bullet}$ (M-1 s-1)	references	experimental method	evaluation method	pH
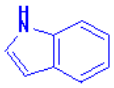	indole	3.20E+10	Iddon et al., 1971	Pulse radiolysis	P.B.K.	pH = 9.0
		1.37E+10	Roberts et al., 1998	photolysis	C.K.	pH 7.0
	1,2-dimethylindole	1.00E+10	Iddon 1971	Pulse radiolysis	P.B.K.	pH = 9.0
	1,3-dimethylindole	1.10E+10	Iddon 1971	Pulse radiolysis	P.B.K.	pH = 9.0
	2,3-dimethylindole	1.30E+10	Iddon 1971	Pulse radiolysis	P.B.K.	pH = 9.0
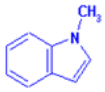	1-methylindole	1.50E+10	Iddon 1971	Pulse radiolysis	P.B.K.	pH = 9.0
		1.20E+10	Solar et al., 1991	Pulse radiolysis	P.B.K.	pH = 7- 10
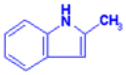	2-methylindole	3.40E+10	Iddon 1971	Pulse radiolysis	P.B.K.	pH = 9.0
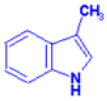	3-methylindole	3.30E+10	Iddon 1971	Pulse radiolysis	P.B.K.	pH = 9.0
	indole-3-acetic acid	6.50E+09	Shetiya et al., 1972	Pulse radiolysis	C.K.	
	indole-3-propionic acid	8.50E+09	Shetiya et al., 1972	Pulse radiolysis	C.K.	
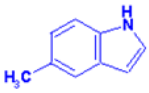	5-methylindole	1.70E+10	Iddon 1971	Pulse radiolysis	P.B.K.	pH = 9.0
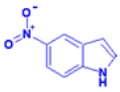	5-nitroindole	1.00E+10	Iddon 1971	Pulse radiolysis	P.B.K.	pH = 9.0
	5-chloroindole	2.00E+10	Iddon 1971	Gamma radiolysis	C.K.	pH = 9.0
	5-aminoindole	3.30E+10	Iddon et al., 1971	Gamma radiolysis	C.K.	pH = 9.0
	5-bromoindole	1.60E+10	Iddon et al., 1971	Gamma radiolysis	C.K.	pH = 9.0
	5-cyanoindole	1.10E+10	Iddon et al., 1971	Gamma radiolysis	C.K.	pH = 9.0
	5-hydroxyindole	1.70E+10	Iddon et al., 1971	Pulse radiolysis	P.B.K.	pH = 9.0
		1.67E+10	Roberts et al., 1998	photolysis	C.K.	pH 7.0
	5-methoxy indole	1.50E+10	Iddon 1971	Pulse radiolysis	P.B.K.	pH = 9.0
		1.39E+10	Roberts et al., 1998	photolysis	C.K.	pH 7.0
	Indole-5-acetic acid	7.90E+09	Iddon 1971	Pulse radiolysis	P.B.K.	pH = 9.0
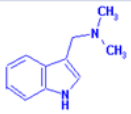	2-(dimethylaminomethyl)-indole (gramine)	3.00E+10	Lee et al., 2007	Gamma radiolysis	C.K.	pH = 8, 9, 10
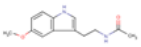	Melatonin	1.32±0.08 e10	Roberts et al., 1998	photolysis	C.K.	pH = 7.0
		2.7 ± 0.3 e10	Matuszak et al 1996	Fenton	ESR	

	Tryptophan	1.25E+10	Roberts et al., 1998	photolysis	C.K.	pH = 7.0
		1.30E+10	Buxton et al., 1988			average 3 values
	6-chloromelatonin	0.82 ± 0.06 e10	Roberts et al., 1998	photolysis	C.K.	pH = 7.0
		1.95±0.1 e10	Matuszak et al 1996	Fenton	ESR	
	6-hydroxy-melatonin	1.1±0.3 e10	Matuszak et al 1996	Fenton	ESR	
	5-methoxytryptamine	2.3±0.3 e10	Matuszak et al 1996	Fenton	ESR	
	5-hydroxytryptamine	1.7±0.3 e10	Matuszak et al 1996	Fenton	ESR	

Table A-B27: Survey of HO• rate constants with uracil

chemcial formura	compound	$k_{HO\bullet}$ (M-1 s-1)	references	experimental method	evaluation method	pH
	Uracil	5.70E+09	Buxton et al., 1988	selected and recommended values	average of 7 values	
		6.00E+09	Chapman et al., 1973	Pulse radiolysis	P.B.K.	
		6.50E+09	Patterson and Bansal, 1972	Pulse radiolysis	P.B.K.	pH = 7.0
		4.80E+09	Patterson and Bansal, 1972	Pulse radiolysis	C.K.	pH = 7.0
		4.70E+09	Willson et al., 1971	Pulse radiolysis	C.K.	
		7.50E+09	Scholes et al., 1965	Pulse radiolysis	C.K.	pH = -2
		8.70E+09				pH = -5
		5.20E+09				pH = -7.4
	5-azauracil	7.00E+09	Rosenthal et al., 1983	Pulse radiolysis	C.K.	pH = 8.0
	6-azauracil	4.50E+09	Rosenthal et al., 1983	Pulse radiolysis	C.K.	pH = 8.0
	5-bromouracil	5.20E+09	Myint et al., 1987	Pulse radiolysis	P.B.K.	pH = 7.0
		4.00E+09	Patterson and Bansal, 1972	Pulse radiolysis	P.B.K.	pH = 7.0
		3.60E+09	Zimbrick et al., 1969	Pulse radiolysis	P.B.K.	pH = 7.0

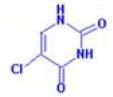	5-chlorouracil	5.50E+09	Patterson and Bansal, 1972	Pulse radiolysis	P.B.K.	pH = 7.0
		5.80E+09				pH = 11.0
		5.20E+09	Patterson and Bansal, 1972	Pulse radiolysis	P.B.K.	pH = 7.0
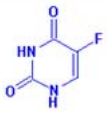	5-fluorouracil	5.20E+09	Patterson and Bansal, 1972	Pulse radiolysis	P.B.K.	pH = 7.0
		5.50E+09	Patterson and Bansal, 1972	Pulse radiolysis	P.B.K.	pH = 7.0
		6.00E+09				pH = 11.0
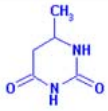	dihydro-6-methyluracil	1.30E+09	Barszcz and Fielden, 1974	Pulse radiolysis	C.K.	pH = 7.0
		1.00E+09	Barszcz and Fielden, 1974	Pulse radiolysis	C.K.	pH = 7.0
	5-nitro-6-methyluracil	5.30E+09	Neta and Greenstock, 1973	Pulse radiolysis	P.B.K.	pH = 5.9
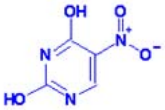	5-nitrouracil	5.40E+09	Neta and Greenstock, 1973	Pulse radiolysis	P.B.K.	pH = 5.9
		7.40E+09	Neta and Greenstock, 1973	Pulse radiolysis	D.K.	pH = 5.9
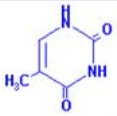	thymine	6.40E+09	Buxton et al., 1988	selected values		
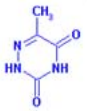	6-azathymine	2.80E+09	Rosenthal et al., 1983	Pulse radiolysis	C.K.	pH = 8.0
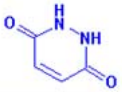	maleic hydrazide	2.90E+09	Eriksen et al., 1983	Pulse radiolysis	P.B.K.	pH = 3.5
	isouramil	5.00E+09	Chevion and Ilan, 1980	Pulse radiolysis	P.B.K.	pH= 5.3-8.0
	cytosine	6.30E+09	ssung and von Sonntag, 19	Pulse radiolysis	P.B.K.	pH = 7.0
		6.80E+09	Michaels and Hunt, 1973	Pulse radiolysis	P.B.K.	pH = 7.0
		6.20E+09	Theard et al., 1970	Pulse radiolysis	P.B.K.	pH = 5.8
		7.50E+09	Scholes et al., 1965	Pulse radiolysis	C.K.	pH = -5
		4.90E+09			C.K.	pH = -7.5
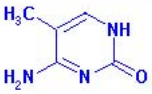	5-methylcytosine	6.00E+09	ssung and von Sonntag, 19	Pulse radiolysis	P.B.K.	pH = 7.0
		3.60E+09	Eriksen et al., 1983	Pulse radiolysis	C.K.	
	6-azacytosine	4.50E+09	Rosenthal et al., 1983	Pulse radiolysis	C.K.	pH = 8.0
	5-azacytosine	2.10E+09	Rosenthal et al., 1983	Pulse radiolysis	C.K.	pH = 8.0
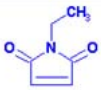	N-ethylmaleimide	9.00E+09	Hayon and Simic, 1972	Pulse radiolysis	P.B.K.	pH = 6.0
	6-methyl uracil	5.70E+09	gannadham and Steenken, 19	Pulse radiolysis	P.B.K.	pH = 5-6

Table A-B28: Survey of HO• rate constants with imidazole

chemcial formura	compound	$k_{HO\bullet}$ (M-1 s-1)	references	experimental method	evaluation method	pH
	imidazole	3.90E+09	Ching et al., 1993	Fenton reaction	C.K.	pH = 7.4 T = 310 K
		3.90E+09	Aruoma et al., 1989	Thermal	C.K.	pH = 7.4
		1.20E+10	Rao et al., 1975	Pulse radiolysis	P.B.K.	p H = 10.9
	1-methyl imidazole	8.10E+09	Rao et al., 1975	Pulse radiolysis	P.B.K.	pH = 9.4
	xanthine	5.20E+09	Santamaria et al., 1984	Pulse radiolysis	P.B.K.	pH = 7.8
	theophilline	6.30E+09	Powers 1986	Pulse radiolysis	P.B.K.	
	theobromine	5.80E+09	Powers 1986	Pulse radiolysis	P.B.K.	
	1-hypoxanthine	6.50E+09	Santamaria et al., 1984	Pulse radiolysis	P.B.K.	pH = 7.8
	isoguanine	1.20E+10	Masuda et al., 1975	Gamma-radiolysis	C.K.	pH = 11.0 T = 290 K
	guanine	9.20E+09	Masuda et al., 1975	Gamma-radiolysis	C.K.	pH = 10 T = 290 K
	caffeine	6.90E+09	Kesavan and Powers, 1985	Pulse radiolysis	C.K.	
	allopurinol	7.00E+08	Passquier 1989			
	purine	3.00E+08	Masuda 1975			
	6-methyl purine	4.60E+08	Vieira and Steenken 1987	Pulse radiolysis	C.K.	pH= 6.2 T = 298 K
	6-methoxy purine	2.00E+09	Vieira and Steenken 1987	Pulse radiolysis	C.K.	pH= 6.8 T = 298 K
	2-aminopurine	3.00E+09	Manoj et al 2006	Pulse radiolysis	C.K.	pH = 7.0
	adenine	5.80E+09	Theard et al., 1970	Pulse radiolysis	P.B.K.	pH = 5.7
		6.30E+09	Scholes et al., 1965	Pulse radiolysis	C.K.	pH = -5.3
		5.10E+09	Scholes et al., 1965	Pulse radiolysis	C.K.	pH = -7.4
	N,N-dimethyladenine	7.10E+09	Vieira and Steenken 1987	Pulse radiolysis	C.K.	pH= 7.8 T = 298 K
	2-mercaptopurine	4.40E+09	Czaudema 1984			
	6-mercaptopurine	7.00E+09	Czaudema 1984			
	carbendazim	2.20E+09	Mazellier 2003			

Table A-B29: Survey of HO• rate constants with thiophene

compound	$k_{HO\bullet}$ (M-1 s-1)	references	experimental method	evaluation method	pH
thiophene	8.20E+09	Saunders et al., 1978	Pulse radiolysis	P.B.K.	pH = -7
	4.10E+09	Saunders et al., 1978	Pulse radiolysis	P.B.K.	pH = -10
	3.30E+09	Lilie 1971	Pulse radiolysis	C.K.	
2,5-dimethylthiophene	7.20E+09	Saunders et al., 1978	Pulse radiolysis	P.B.K.	pH = -7
2-methylthiophene	3.20E+09	Saunders et al., 1978	Pulse radiolysis	P.B.K.	pH = 11
3-methylthiophene	3.20E+09	Saunders et al., 1978	Pulse radiolysis	P.B.K.	pH = 11
2,2'-bithiophene	1.60E+10	Saunders et al., 1978	Pulse radiolysis	P.B.K.	pH = -7
2-iodo-3,5-dinitrothiophene	2.10E+09	Breccia et al 1990	Pulse radiolysis	C.K.	pH = -7
3-nitro-2-(4-nitrophenoxy)thiophene	1.30E+09	Breccia et al 1990	Pulse radiolysis	C.K.	pH = -7
tetrahydrothiophene	1.40E+10	Bonifacic et al., 1975	Pulse radiolysis	P.B.K.	

Table A-B30: Survey of HO• rate constants with triazine

chemcial formura	compound	$k_{HO\bullet}$ (M-1 s-1)	references	experimental method	evaluation method	pH	
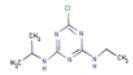	atrazine	2.00E+09	Charmosta 1993				
	cyanuric acid	2.00E+07	De laat 1994				
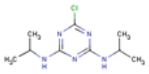	propazine	1.20E+09	Charmosta 1993				
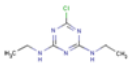	simazine	2.10E+09	Charmosta 1993				
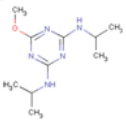	prometone	2.50E+09	Shemer 2006				

	1,3,5-triazine	3.40E+09	Joseph et al., 2000				
	2,4,6-trimethoxy-1,3,5-triazine	2.06E+08	Joseph et al., 2000				
	dioxohexahydrotriazine	1.61E+09	Joseph et al., 2000				
	simetone	4.70E+09	De Laat et al 1994	chemical re	O3/H2O2	pH = 7.5	T = 295K
	ametryne	2.60E+10	De Laat et al 1994	chemical re	O3/H2O2	pH = 7.5	T = 295K
	simetryne	2.60E+10	De Laat et al 1994	chemical re	O3/H2O2	pH = 7.5	T = 295K
	terbutazine	2.80E+09	De Laat et al 1994	chemical re	O3/H2O2	pH = 7.5	T = 295K
	cyanazine	1.90E+09	De Laat et al 1994	chemical re	O3/H2O2	pH = 7.5	T = 295K
	2-chloro-4,6-diamino-s-triazine	5.00E+07	De Laat et al., 1994	chemical re	O3/H2O2	pH = 7.5-8.1	T = 293K

-The end of HO• rate constant survey

Literature Cited

Adams, G.E.; Boag, J.W.; Michael, B.D. Reactions of the hydroxyl radical. part 2. – determination of absolute rate constants. Trans. Faraday Soc. 1965, **61**, 1417-1424.

Aguer, J.P.; Richard, C. Toxicol. Environ. Chem. 1993, 39, 217-227.

Aguila, A.; O'Shea, K.E.; Tobien, T.; Asmus, K-D. Reactions of hydroxyl radical with dimethyl methylphosphonate and diethyl methylphosphonate. A fundamental mechanistic study. J. Phys. Chem. A. 2001, 105, 7834-7839.

Akhlaq, M.S.; von Sonntag, C. Z. Naturforsch., C, Biosci. 1987, **42C**, 134-140.

Al-Suhybani, A.A.; Hughes, G. Arab Gulf J. Sci. Res. 1988, A 6, 85-103.

Anbar, M.; Meyerstein, D.; Neta, P. Reactivity of aliphatic compounds towards hydroxyl radicals. J. Chem. Soc. (B) 1966, 745-747.

Anbar, M.; Neta, P. J. Chem. Soc. Pt. A, 1967, 834-837.

Aruoma, O.I.; Laughton, M.J.; Halliwell, B. Biochem. J. 1989, 264, 863-869.

Ashton, L.; Buxton, G.V.; Stuart, C.R. Temperature dependence of the rate of reaction of OH with some aromatic compounds in aqueous solution. J. Chem. Soc. Faraday. Trans. 1995, 91(11), 1631-1633.

Asmus, K.-D.; Taub, I.A. Spectrum and kinetics of the hydroxynitromethane anion radical in pulse-irradiated alkaline nitromethane solutions. J. Phys. Chem. 1966, 72(10), 3382-3387.

Barszcz, D.; Fielden, E.M.Int. J. Radiat. Biol. Relat. Stud. Phys., Chem. Med. 1974, 25, 539-553.

Baxendale, J.H.; Khan, A.A. Int. J. Radiat. Phys. Chem. 1969, **1**, 11-24.

Bednar, J.; Teply, J. Collect. Czech. Chem. Commun. 1960, **25**, 842-851.

Bell, J.A.; Grunwald, E.; Hayon, E. Kinetics of deprotonation of organic free radicals in water. Reaction of HOCHCOO2-, HOCHCONH2, and HOCCH3CONH2 with various bases. J. Am. Chem. Soc. 1975, 97(11), 2995-3000.

Benitez, F.J.; Real, F.J.; Acero, J.L.; Garcia, C.; Llanos, E.M. Kinetics of phenylurea herbicides oxidation by Fenton and photo-Fenton processes. J. Chem. Technol. Biotechnol. 2007, 82, 65-73.

Bonifačić, M.; Möckel, H.; Bahnemann, D.; Asmus, K-D. Formation of positive ions and other primary species in the oxidation of sulphides by hydroxyl radicals. J. Chem. Soc. Perkin I. 1975, 675-685.

Borggaard, O.K. Acta Chem. Scand. 1972, **26**, 3393-3394.

Bors, W.; Michel, C.; Dalke, C.; Stettmaier, K.; Saran, M.; Andrae, U. Radical intermediates during the oxidation of nitropropanes. The formation of NO2 from 2-nitropropane, its reactivity with nucleosides, and implications for the genotoxicity of 2-nitropropane. Chem. Res. Toxicol. 1993, 6, 302-309.

Bors, W.; Lengfelder, E.; Saran, M.; Fuchs, C.; Michel, C. Biochem. Biophys. Res. Commun. 1976, **70**, 81-87.

Bors, W.; Saran, M.; Michel, C. Pulse-radiolytic investigations of catechols and catecholamines. 4. 3,4-dihydroxybenzaldehyde and 3,4-dihydroxyacetophenone. J. Phys. Chem. 1979, 83(24), 3084-3088.

Bors, W.; Saran, M.; Michel, C. Int. J. Radiat. Biol. Relat. Stud. Phys., Chem. Med. 1982, **41**, 493-501.

Bors, W.; Michel, C.; Erben-Russ, M.; Kreileder, B.; Tait, D.; Saran, M. Oxygen Radicals Chem. Biol., W. Bors, M. Saran and D. Tait (eds.), de Gruyter, Berlin, Fed. Rep. Germany, Pub. 1984, p.95-9.

Breccia, A.; Busi, F.; Gattavecchia, E. Tamba, M. Radiat. Environ. Biophys. 1990, 29, 153-160.

Brede, O.; Helmstreit, W.; Mehnert, R. Z. Phys. Chem. (Leipzig), 1975, **256**, 513-521.

Buechler, Hch.; Buehler, R.E.; Cooper, R. J. Phys. Chem. 1976, **80**, 1549-1553.

Buxton, G.V. Trans. Faraday Soc. 1970, **66**, 1656-1660.

Buxton, G.V.; Greenstock, C.L.; Helman, W.P.; Ross, A.B. Critical review of rate constants for reactions of hydrated electrons, hydrogen atoms and hydroxyl radicals (•OH/•O-) in aqueous solution. *J. Phys. Chem. Ref. Data*. 1988, *17* (2) 513-795.

Cabelli, D.E.; Bielski, B.H.J. Z. Naturforsch., B, Anorg. Chem., Org. Chem. 1985, **40B**, 1731-1737.

Cercek, B.; Ebert, M. Trans. Faraday Soc. 1967, 63, 1687-1698.

Cercek, B.; Ebert, M. Adv. Chem. Ser. 1968, **81**, 210-221.

Chambers, K.W.; Collinson, E.; Dainton, F.S. Trans. Faraday Soc. 1970, **66**, 142-162.

Chevion, M.; Ilan, Y.A. DOE/EV/03221-63, 1980, 16p.

Chin, M.; Wine, P.H. Aquatic and Surface Photochemistry, G.R. Helz, R.G. Zepp and D.G. Crosby (eds.), CRC Press, Inc., Boca Raton, FL, 1994, p.85-96

Ching, T.-L.; Haenen, G.R.M.M.; Bast, A. Cimetidine and other H2 receptor antagonists as powerful hydroxyl radical scavengers. Chem.-Biol. Interact. 1993, **86**, 119-127.

Chutny, B. Collect. Czech. Chem. Commun. 1966, **31**, 358-361.

Chutny, B.; Swallow, A.J. Trans. Faraday Soc. 1970, **66**, 2847-2854.

Clay, P.G.; Witort, M. Radiochem. Radioanal. Lett. 1974, **19**, 101-107.

Cohen, N.; Benson, S.W. Empirical correlations for rate coefficients for reactions of OH with haloalkanes. J. Phys. Chem. 1987, 91, 171-175.

Cohen, H.; Meyerstein, D. J. Chem. Soc., Dalton Trans. 1976, 1976-1979.

Cole, S.K.; Cooper, W.J.; Fox, R.; Gardinali, P.R.; Mezyk, S.P.; Mincher, B.J.; O'Shea, K.E. Free radical chemistry of disinfection byproducts. 2. Rate constants and degradation mechanisms of trichloronitromethane (Chloropcrin). Environ. Sci. Technol. 2007, 41, 863-869.

Cullis, C.F.; Francis, J.M.; Raef, Y.; Swallow, A.J. Proc. R. Soc. London, Ser. A, 1967, **300**, 443-454.

Czauderna, M.; Wagner-Czauderna, E. J. Radioanal Nucl. Chem. 1984, 81, 283-289.

De laat, J.; Chramosta, N.; Rore, M.; Suty, H.; Pouillot, M. Rate constants for reaction of hydroxyl radicals with some degradation by-products of atrazine by O3 or O3/H2O2. Environ. Technol. 1994, 15, 419-428.

Dey, G.R.; Naik, D.B.; Kishore, K.; Moorthy, P.N. J. Radioanal. Nucl. Chem. 1992, 163, 391-400.

Dorfman, L.M.; Taub, I.A.; Harter, D.A. Rate constants for the reaction of the hydroxyl radical with aromatic molecules. J. Chem. Phys. 1964, 41, 2954-2955

Dohrmann, J.K.; Bergmann, B. J. Phys. Chem. 1995, **99**, 1218-1227.

Draganic, I.G.; Draganic, Z.D.; Holroyd, R.A. Pulse radiolysis of aqueous cyanogens solution. J. Phys. Chem. 1971, 75(5), 608-612.

Draganic, I.; Draganic, Z.; Petkovic, Lj.; Nikolic, A. The radiation chemistry of aqueous solutions of simple RCN compounds. J. Am. Chem. Soc. 1973, 95(22), 7193-7199.

Draganic, Z.D.; Draganic, I.G.; Jovanovic, S.V. Radiat. Res. 1978, **75**, 508-518.

Draganic, Z.D.; Draganic, I.G.; Sehested, K. Radiation chemistry of aqueous solutions of dicyandamide. J. Phys. Chem. 1979, 83(2), 220-224.

Draper, R.B.; Fox, M.A.; Pelizzetti, E.; Serpone, N. Pulse radiolysis of 2,4,5-trichlorophenol: Formation, kinetics, and properties of hydroxytrichlorocyclohexadienyl, trichlorophenoxyl, and dihydroxytrichlorocyclohexadienyl radicals. J. Phys. Chem. 1989, 93, 1938-1944.

Eibenberger, J. Pulse radiolytic investigations concerning the formation and the oxidation of organic radicals in aqueous solution. 1980, Ph.D. Thesis. Vienna University, Austria.

Elliot, A.J.; McCracken, D.R. Effect of temperature on O•- reactions and equilibria: A pulse radiolysis study. Radiat.Phys.Chem. 1989, 33(1), 69-74.

Elliot, A.J.; McCracken, D.R.; Buxton, G.V.; Wood, N.D. J. Chem. Soc., Faraday Trans. 1990, **86**, 1539-1547.

Elliot, A.J.; Simsons, A.S. Radiat. Phys. Chem. 1984, **24**, 229-231.

Emmi, S.S.; Beggiato, G.; Casalbore-Miceli, G.; Fuochi, P.G. J. Radioanal. Nucl. Chem., Lett. 1985, **93**, 189-197.

Engman, L.; Lind, J.; Merényi, G. Redox properties of diaryl chalcogenides and their oxides. J. Phys. Chem. 1994, 98, 3174-3182.

Eriksen, T.; Henglein, A.; Stockhausen, K. J. Chem. Soc., Faraday Trans. 1. 1973, **69**, 337-345.

Eriksen, T.; Lind, J.; Merenyi, G.J. Chem. Soc., Faraday Trans. 1983, 1 79, 1503-1511.

Ervens, B.; Gligorovski, S.; Herrmann, H. Teperature-dependent rate constants for hydroxyl radical reactions with organic compounds in aqueous solution. Phys. Chem. Chem. Phys., 2003, 5, 1811-1824.

Feitelson, J.; Hayon, E. Electron ejection and electron capture by phenolic compounds. J. Phys. Chem. 1973, 77(1), 10-15.

Field, R.J.; Raghavan, N.V.; Brummer, J.G. A pulse radiolysis investigation of the reactions of BrO2• with Fe(CN)64-, Mn(II), phenoxide ion, and phenol. J. Phys. Chem. 1982, **86**, 2443-2449.

Fisher, M.M.; Hamill, W.H. Electronic processes in pulse-irradiated aqueous and alcoholic systems. J. Phys. Chem. **77**, 171-177 (1973)

George, C.; Rousse, D.; Perraudin, E.; Strekowski, R. A new approach for studying aqueous phase OH kinetics: Application of Teflon waveguides. Phys. Chem. Chem. Phys. 2003, 5, 1562-1569.

Getoff, N.; Schwoerer, F. Int. J. Radiat. Phys. Chem. 1970, **2**, 81-89.
Simic, M.; Neta, P.; Hayon, E. Int. J. Radiat. Phys. Chem. 1971, **3**, 309-320.

Getoff, N.; Schwörer, F.; Markovic, V.M.; Sehested, K.; Nielsen, S.O. Pulse radiolysis of oxalic acid and oxylates. J. Phys. Chem. 1971, 75(6), 749-755.

Getoff, N.; Schwoerer, F. Int. J. Radiat. Phys. Chem. 1973, **5**, 101-111.

Getoff, N. Advancements of radiation induced degradation of pollutants in drinking and waste water. Appl.Radiat.Isot. 1989, 40(7), 585-594.

Getoff, N. Section 5.2. solid and liquid waste treatment. Decomposition of biological resistant pollutants in water by irradiation. Radiat. Phys. Chem. 1990, 35(1-3), 432-439.

Getoff, N. Radiation- and photoinduced degradation of pollutants in water. A comparative study. Radiat. Phys. Chem. 1991, 37(5/6), 673-680.

Gilbert, B.C.; Norman, R.O.C.; Sealy, R.C. J. Chem. Soc., Perkin Trans. 2. 1974, 1435-1441.

Gligorovski, S.; Herrmann, H. Kinetics of reactions of OH with organic carbonyl compounds in aqueous solution. Phys. Chem. Chem. Phys. 2004, 6, 4118-4126.

Greenstock, C.L.; Shierman, E. Int. J. Radiat. Biol. Relat. Stud. Phys., Chem. Med. 1975, **28**, 1-11.

Greenstock, C.L.; Dunlop, I. Pulse radiolysis studies of nitrofurans. Radiation chemistry of nifuroxime. J. Phys. Chem. 1973, 77(15), 1834-1838.

Guittonneau, S.; de Laat, J.; Dore, M.; Duguet, J.P.; Suty, H. Environ. Technol. 1990, **11**, 57-70.

Haag, W.R.; Yao, C.C.D. Rate constants for reaction of hydroxyl radicals with several drinking water contaminants. Environ. Sci. Technol. 1992, 26, 1005-1013.

Heckel, E.; Henglein, A.; Beck, G. Ber. Bunsenges. Phys. Chem. 1966, **70**, 149-154.

Hickel, B. Absorption spectra and kinetics of methyl and ethyl radicals in water. J.Phys.Chem. 1975, 79(11), 1054-1059.

Hissung, A.; von Sonntag, C.Z. Naturforsch., Teil B, 1978, 33B, 321-328.

Hoffman, M.Z.; Hyon, E. Pulse radiolysis study of sulfhydryl compounds in aqueous solution. J. Phys. Chem. 1973, 77(8), 990-996.

Iddon, B.; Phillips, G.O.; Robbins, K.E. Radiation chemistry of aqueous solutions of indole and its derivatives. J.Chem. Soc. (B). 1971, 1887-1892.

Jayson, G.G.; Stirling, D.A.; Swallow, A.J. Int. J. Radiat. Biol. Relat. Stud. Phys., Chem. Med. 1971, **19**, 143-156.

Joseph, J.M.; Jacob, T.A.; Manoj, V.M.; Arvindakumar, C.T. Oxidative degradation of triazine derivatives in aqueous medium: A radiation and photochemical study. J. Agric. Food Chem. 2000, 48, 3704-3709.

Karmann, W.; Granzow, A.; Meissner, G.; Henglein, A. Int. J. Radiat. Phys. Chem. 1969, **1**, 395-405.

Kesavan, P.C.; Powers, E.L.Int. J. Radiat. Biol. Relat. Stud. Phys., Chem. Med. 1985, 48, 223-233.

Klever, H.; Schulte-Frohlinde, D. Ber. Bunsenges. Phys. Chem. 1976, **80**, 1259-1265.

Kochany, J.; Bolton, J.R. Mechanism of photodegradation of aqueous organic pollutants. 2. Measurement of the primary rate constants for reaction of •OH radicals with benzene and some halobenzenes using an EPR spin-trapping method following the photolysis of H2O2. Environ. Sci. Technol. 1992, 26, 262-265.

Koester, R.; Asmus, K.-D. Z. Naturforsch. Teil B, 1971, **26**, 1108-1116.

Kraljic, I. The Chemistry of Ionization and Excitation, Johnson, G.R.A. and Scholes, G. (eds.), Taylor and Francis Ltd, London, 1967, p.303-9.

Kumar, M.; Rao, M.H.; Moorthy, P.N. J. Macromol. Sci., Chem. 1990, **A27**, 299-308.

Kumar, M.; Rao, M.H.; Moorthy, P.N.; Rao, K.N. Radiat. Eff. Express **1**, 1988, 167-173.

Lal and Mahal, 1992 Medical Biochemical and Chemical Aspects of Free Radicals, O. Hayaishi, E. Niki, M. Kondo and T. Yoshikawa (eds.), Elsevier, Amsterdam, The Netherlands, 1989, Vol. 1, p.425-32

Lal, M.; Schoeneich, C.; Moenig, J.; Asmus, K.-D. Int. J. Radiat. Biol. 1988, **54**, 773-785.

Land, E.J.; Ebert, M. Trans. Faraday Soc. 1967, **63**, 1181-1190.

Land, E.J. Proc. R. Soc. London, Ser. A, 1968, **305**, 457-471.

Landsman, N.A.; Swancutt, K.L.; Bradford, C.N.; Cox, C.R.; Kiddle, J.J.; Mezyk, S.P. Free radical chemistry of advanced oxidation processes removal of nitrosamines in water. Environ. Sci. Technol. 2007, 41, 5818-5823.

Lati, J.; Meyerstein, D. Trivalent nickel. II. A pulse radiolytic study of the formation and decomposition of the ethylenediamine and glycine complexes in aqueous solution. Inorganic. Chem. 1972, 11(10), 2397-2401.

Lee, C.; Schmidt, C.; Yoon, J.; von Gunten, U. Oxidation of N-nitrosodimethylamine (NDMA) precursors with ozone and chlorine dioxide: Kinetics and effect on NDMA formation potential. Environ. Sci. Technol. 2007, 41, 2056-2063.

Lilie, J.; Beck, G.; Henglein, A. Ber. Bunsenges. Phys. Chem. 1968, **72**, 529-533.

Lilie, J.; Henglein, A. Ber. Bunsenges. Phys. Chem. 1970, **74**, 388-393.

Lilie, J. Z. Naturforsch. Teil B. 1971, 26, 197-202

Logan, S.R. J. Chem. Soc., Perkin Trans. 2, 1989, 751-754.

Maity, D.K.; Mohan, H.; Chattopadhyay, S.; Mittal, J. P. Formation, stability, and reactivity of radical cations of 1-bromo-n-chloroalkanes in aqueous solution: A pulse radiolysis study. J. Phys. Chem. 1995, 99, 12195-12203.

Mao, Y.; Schöneich, C.; Asmus, K-D. Identification of organic acids and other intermediates in oxidative degradation of chlorinated ethanes on TiO2 surfaces en Route to mineralization. A combined photocatalytic and radiation chemical study. J. Phys. Chem. 1991, 95, 10080-10089.

Maruthamuthu, P. Makromol. Chem., Rapid Commun. 1980, **1**, 23-25.

Massaut, B.; Tilquin, B.; Hickel, B. Bull. Soc. Chim. Belg. 1988, **97**, 1031-1036.

Masuda, T.; Minemura, A.; Yamauchi, K.; Kondo, M. J. Radiat. Res. 1980, **21**, 149-156.

Masuda, T.; Shinohara, H.; Kondo, M. J. Radiat. Res. 1975, 16, 153-161.

Matheson, M.S.; Mamou, A.; Silverman, J.; Rabani, J. Reaction of hydroxyl radicals with polyethylene oxide in aqueous solution. J. Phys. Chem. 1973, **77**, 2420-2424.

Matheson, M.S.; Silverman, A.M.J.; Rabani, J. Reaction of hydroxyl radicals with polyethylene oxide in aqueous solution. J. Phys. Chem. 1973, 77(20), 2420-2424.

Matsushige, T.; Koltzenburg, G.; Schulte-Frohlinde, D. Ber. Bunsenges. Phys. Chem. 1975, **79**, 657-661.

Mattews, R.W.; Sangster, D.F. Measurement by benzoate radiolytic decarboxylation of relative rate constants for hydroxyl radical reactions. J. Phys. Chem. 1965, **69**, 1938-1946.

Matuszak, Z.; Reszka, K.J.; Chignell, C.F. Reaction of melatonin and related indoles with hydroxyl radicals: EPR and spin trapping investigations. Free Radical Biology &

Medicine. 1997, 23(3), 367-372.

Mazellier, P.; Leroy, E.; De laat, J.; Legube, B. Degradation of carbendazim by UV/H2O2 investigated by kinetic modeling. Environ. Chem. Lett. 2003, 1, 68-72.

Merga, G.; Rao, B.S.M.; Mohan, H.; Mittal, J. P. Reactions of OH and SO4•- with some halobenzenes and halotoluenes: A radiation chemical study. J. Phys. Chem. 1994, 98, 9158-9164.

Merz, J.H.; Waters, W.A. A Electronic transfer reactions. The mechanism of oxidation of alcohols with fenton's reagent. 1949, 179-188.

Mezyk, S.P.; Helgeson, T.; Cole, S.K.; Cooper, W.J.; Fox, R.V.; Gardinali, P.R.; Mincher, B.J. Free radical chemistry of disinfection-byproducts. 1. Kinetics of hydrated electron and hydroxyl radical reactions with halonitromethanes in water. J. Phys. Chem. A. 2006, 110, 2176-2180.

Mezyk, S.P.; Ewing, D.B.; Kiddle, J.J.; Madden, K.P. Kinetics and mechanisms of the reactions of hydroxyl radicals and hydrated electrons with nitrosamines and nitramines in water. J. Phys. Chem. A, 2006, 110, 4732-4737.

Mezyk, S.P.; Cooper, W.J.; Bartels, D.M.; O'Shea, K.E.; Wu, T. Radiation chemistry of alternative fuel oxygenates: Substituted ethers. J. Phys. Chem. A. 2001, 105, 3521-3526.

Mezyk, S.P.; Jones, J.; Cooper, W.J.; Tobien, T.; Nickelsen, M.G.; Adams, J.W.; O'Shea, K.E.; Bartels, D.M.; Wishart, J.F.; Tornatore, P.M.; Newman, K.S.; Gregoire, K.; Weidman, D.J. Environ. Sci. & Technol. 2004, 38, 3994-4001.

Mezyk, S.P. Rate constant and activation energy determination for reaction of e-(aq) and •OH with 2-butanone and propanal. Can. J. Chem. 1994, **72**, 1116-1119.

Michaels, H.B.; Rasburn, E.J.; Hunt, J.W. Radiat. Res. 1976, **65**, 250-267.

Michaels, H.B.; Hunt, J.W. Radiat. Res. 1973, 56, 57-70.

Michael, B.D.; Hart, E.J. J. Phys. Chem. 1970, 74, 2878-2884.

Miller, J.S.; Cornwell, D.G. The role of cryoprotective agents as hydroxyl radical scavengers. Cryoobiology. 1978, 15, 585-588.

Milne, P.J. Ph.D., Thesis, Univ. Miami, Coral Gables, FL, 1989, 265p.

Milosavljevic, B.H.; LaVerne, J.A. Pulse radiolysis of aqueous thiocyanate solution. J. Phys. Chem. A. 2005, 109, 165-168.

Mohan, H.; Mittal, J.P. Structure-reactivity studies on the nature of transients formed on reaction of OH radicals with chloroiodoalkanes in aqueous solution. J. Chem. Soc. Perkin. Trans. 2. 1992, 1731-1736.

Mohan, H.; Mittal, J.P. Radiat. Phys. Chem. 1991, **38**, 45-50.

Mohan, H.; Mittal, J. Formation and reactivity of the radical cation of bromobenzene in aqueous solution: A pulse radiolysis study. J. Phys. Chem. 1995, 99, 6519-6524.

Mohan, H.; Moorthy, P.N. Formation of radical cations of polyiodomethanes: A pulse radiolysis study. J. Chem. Soc. Perkin. Trans. 2. 1990, 277-282.

Monod, A.; Poulain, L.; Grubert, S.; Voisin, D.; Wortham, H. Kinetics of OH-initiated oxidation of oxygenated organic compounds in the aqueous phase: new rate constants, atructure-activity relationships and atmospheric implications. Atmosph. Environ. 2005, 39, 7667-7688.

Moore, J.S.; Kemsley, K.G.; Davies, J.V.; Phillips, G.O. Radiation Biology and Chemistry. Research Developments, H.E. Edwards, S. Navaratnam, B.J. Parsons and G.O. Phillips (eds.), Elsevier, New York, 1979, p.99-113 (1979).

Moorthy, P.N.; Hayon, E. One-electron redox reactions of water-soluble vitamins. III. Pyridoxine and pyridoxal phosphate (Vitamin B6). J. Am. Chem. Soc. 1975, 97(8), 2048-2052.

Motohashi, N.; Saito, Y. Competitive measurement of rate constants for hydroxyl radical reactions using radiolytic hydroxylation of benzoate. Chem. Pharm. Bull. 1993, **41**, 1842-1845.

Myint, P.; Deeble, D.J.; Beaumont, P.C.; Blake, S.M.; Phillips, G.O. Biochim. Biophys. Acta, 1987, 925, 194-202.

Naik, D.B.; Moorthy, P.N. Radiat. Phys. Chem. 1993, 41, 817-824.

Naik, D.B.; Moorthy, P.N. Proc. Indian Acad. Sci., Chem. Sci. 1991, 103, 667-675.

Neta, P.; Dorfman, L.M. Pulse radiolysis studies. XIII. Rate constants for the reaction of hydroxyl radicals with aromatic compounds in aqueous solutions. Radiat. Chem. 1968, 222-230.

Neta, P.; Greenstock, C.L. Radiat. Res. 1973, 54, 35-48.

Nauser, T.; Buehler, R.E. J. Chem. Soc., Faraday Trans. 1994, **90**, 3651-3656.

O'Neill, P.; Steenken, S.; Schulte-Frohlinde, D. J. Phys. Chem. 1975, **79**, 2773-2779.

Onstein, P.; Stefan, M.I.; Bolton, J.R. Competition kinetics method for the determination of rate constants for the reaction of hydroxyl radicals with organic pollutants using the UV/H2O2 advanced oxidation technology: The rate constants for the tert-butyl formate ester and 2,4-dinitrophenol. J. AOT. 1999, 4, 231-236.

Park, H-R.; Getoff, N. Radiolysis of aqueous ethanol in the presence of CO. Z. Naturforsch., A, Phys. Sci. 1992. **47A**, 985-991.

Pasquier, C.; Pierce, B.; Willson, R.L. Medical Biochemical and Chemical Aspects of Free Radicals, O. Hayaishi, E. Niki, M. Kondo and T. Yoshikawa (eds.), Elsevier, Amsterdam, The Netherlands, 1989, Vol. 1, p.425-32

Patterson, L.K.; Bansal, K.M. J. Phys. Chem. 1972, 76, 2392-2399.

Poskrebyshev, G.A.; Huie, R.E.; Neta, P. Radiolysis reactions of monochloramine in aqueous solutions. J. Phys. Chem. A. 2003, 107, 7423-7428.

Powers, E.L.Int. J. Radiat. Biol. Relat. Stud. Phys., Chem. Med. 1986, 50, 983-993.

Rao, P.S.; Hayon, E. Reaction of hydroxyl radicals with oligopeptides in aqueous solutions. A pulse radiolysis study. J. Phys. Chem. 1975, 79(2), 109-115.

Rao, P.S.; Simic, M.; Hayon, E. J. Phys. Chem. 1975, 79, 1260-1263.
Reuvers, A.P.; Greenstock, C.L.; Borsa, J.; Chapman, J.D. Int. J. Radiat. Biol. Relat. Stud. Phys., Chem. Med. 1973, **24**, 533-536.

Roberts, J.E.; Hu, D-N.; Wishart, J.F. Pulse radiolysis studies of melatonin and chloromelatonin. J. Photochem. Photobiology B. Biology 42, 1998, 125-132.
Robinson, E.A.; Schulte-Frohlinde, D. J. Chem. Soc., Faraday Trans. 1, 1973, **69**, 707-718.

Roder, M.; Wojnarovits, L.; Foldiak, G. Radiat. Phys. Chem. 1990, **36**, 175-176.
Rosenthal, I.; Riesz, P.; Faraggi, M. Int. J. Radiat. Biol. Relat. Stud. Phys., Chem. Med. 1983, 44, 463-468.

Ross, F.; Ross, A.B. Selected specific rates of reactions of transients from water in aqueous solution. III. Hydroxyl radical and perhydroxyl radical an their radical ions. NSRDS-NBS 59,

Rudakov, E.S.; Volkova, L.K.; Tret'yakov, V.P. React. Kinet. Catal. Lett. 1981, **16**, 333-337.

Santamaria, J.; Pasquier, C.; Ferradini, C.; Pucheault, J.Radiat. Res. 1984, 97, 452-461.

Saunders, B.B.; Gorse, Jr. R.A. Reactions of diethylhydroxylamine with radiolytically produced radicals in aqueous solutions. J. Phys. Chem. 1979, 83(13), 1696-1701.

Saunders, B.B.; Kaufman, P.C.; Matheson, M.S. Reactions of thiophene with radiolytically produced radicals. 1. The hydroxyl radical. J. Phys. Chem. 1978, 82(2), 142-150.

Savel'eva, O.S.; Shevchuk, L.G.; Vysotskaya, N.A. J. Org. Chem. USSR, 1972, **8**, 283-286.

Savel'eva, O.S.; Shevchuk, L.G.; Vysotskaya, N.A. J. Org. Chem. USSR, 1973, 9, 759-761.

Schöneich, C.; Bobrowski, K. Intramolecular hydrogen transfer as the key step in the dissociation of hydroxyl radical adducts of (Alkylthio)ethanol derivatives. J. Am. Chem. Soc. 1993, 115, 6538-6547.

Scholes, G.; Willson, R.L. Trans. Faraday Soc. 1967, **63**, 2983-2993.

Schuchmann, M.N.; von Sonntag, C. Hydroxyl radical-induced oxidation of diisopropyl ether in oxygenated aqueous solution. A product and pulse radiolysis study. Z. Naturforsch. 1987, 42b, 495-502.

Schuchmann, M.N.; von Sonntag, C. J. The rapid hydration of the acetyl radical. A pulse radiolysis study of acetaldehyde in aqueous solution. Am. Chem. Soc. 1988, **110**, 5698-5701.

Schmidt, K.H.; Bromberg, A.; Meisel, D. Oxidation of diphenylamine by OH radicals and excitation of the diphenylamino and OH adduct radicals. J. Phys. Chem. 1985, 89. 4352-4357.

Sehested, K.; Holcman, J. Reactions of the radical cations of methylated benzene derivatives in aqueous solution. J. Phys. Chem. 1978, 82(6), 651-653.

Sehested, K.; Holcman, J. Nukleonika 1979, **24**, 941-950.

Sehested, K.; Cortitzen, H.; Christense, H.C.; Hart, E.J. Rates of reaction of O-, OH, and H with methylated benzenes in aqueous solution. Optical spectra of radicals. 1975, 79(4), 310-315.

Shemer, H.; Sharpless, C.M.; Elovitz, M.S.; Linden, K.G. Relative rate constants of contaminant candidate list pesticides with hydroxyl radicals. Environ. Sci. Technol. 2006, 40, 4460-4466.

Shevchuk, L.G.; Zhikharev, V.S.; Vysotskaya, N.A. J. Org. Chem. USSR, 1969, **5**, 1606-1608.

Schoeneshoefer, M. Z. Naturforsch. Teil B, 1971, 26, 1120-1124.

Simic, M.; Ebert, M. Int. J. Radiat. Phys. Chem. 1971, 3, 259-272.

Simic, M.; Neta, P.; Hayon, E. Int. J. Radiat. Phys. Chem. 1971, **3**, 309-320.

Simic, M.; Hayon, E. Intermediates produced from the one-electron oxidation and reduction of hydroxylamines. Acid-base properties of the amino, hydroxyamino, and methoxyamino radicals. J. Am. Chem. Soc. 1971, 93(23), 5982-5986.

Snook, M.E.; Hamilton, G.A. Oxidation and fragmentation of some phenyl-substituted alcohols and ethers by peroxydisulfate and fenton's reagent. J.A.C.S. 1974, 96(3), 860-869.

Soeylemez, T.; Schuler, R.H. J. Phys. Chem. 1974, 78, 1052-1062.

Solar, S.; Getoff, N. Oxidation of tryptophan and N-methylindole by N3, Br2- and (SCN)2- radicals in light and heavy-water solutions: A pulse radiolysis study. J. Phys. Chem. 1991, 95, 3639-3643.

Sridhar, R.; Beaumont, P.C.; Powers, E.L. Oxygen Radicals Chem. Biol., W. Bors, M.

Saran and D. Tait (eds.), de Gruyter, Berlin, Fed. Rep. Germany, Pub. 1984, p.101-7

Steenken, S.; O'Neill, P. J. Phys. Chem. 1979, 83, 2407-2412.

Stevens, G.C.; Clarke, R.M.; Hart, E. Radiolysis of aqueous methane solutions. J.Phys.Chem. 1972, 76(25), 3863-3867.

Sumiyoshi, T.; Miura, N.; Aikawa, M.; Katayama, M. Bull. Chem. Soc. Jpn. 1982, **55**, 2347-2351.

Tamminga, J.J.; van den Ende, C.A.M.; Warman, J.M.; Hummel, A. Recl. Trav. Chim. Pays-Bas, 1979, **98**, 305-315.

Tanaka, M.; Sakuma, H.; Kohanawa, O.; Fukaya, S.; Katayama, M. Bull. Chem. Soc. Jpn. 1984, 57, 3403-3407.

Thomas, J.K. Trans. Faraday Soc. 1965, **61**, 702-707.

Thomas, J.K. Pulse radiolysis of aqueous solutions of methyl iodide and methyl bromide. The reactions of iodine atoms and methyl radicals in water. J. Phys. Chem. 1967, 71(6), 1919-1925.

Tripathi, G.N.R.; Schuler, R.H. J. Phys. Chem. 1983, 87, 3101-3105.

Ulanski, P.; Bothe, E.; Rosiak, J.M.; von Sonntag, C. Macromol. Chem. Phys. 1994, **195**, 1443-1461.

Ulanski, P.; von Sonntag, C. The OH radical-induced chain reactions of methanol with hydrogen peroxide and with peroxodisulfate. Perkin transaction, 1994.

Veltwisch, D.; Janata, E.; Asmus, K-D. Primary processes in the reaction of OH•-radicals with sulphoxides. J.C.S. Perkin II. 1980, 146-153.

van der Linde, H.J. Radiat. Phys. Chem. 1977, **10**, 199-206.

von Sonntag, C.; Ansorge, G.; Sugimori, A.; Omori, T.; Koltzenburg, G.; Schulte-Frohlinde, D.
Z. Naturforsch. Teil B, 1972, **27**, 471-472.

Vysotskaya, N.A.; Shevchuk, L.G.; Gavrilova, S.P.; Badovskaya, L.A.; Kul'nevich, V.G. J. Org. Chem. USSR, 1983, 19, 1352-1354.

Walling, C.; El-Taliawi, G.M. Fenton's reagent. II. Reactions of carbonyl compounds and α,β-unsaturated acids. J. Am. Chem. Soc. 1973, 95(3), 844-847.

Walling, C.; El-Taliawi, G.M.; Johnson, R.A. Fenton's reagent. IV. Structure and reactivity relations in the reactions of hydroxyl radicals and the redox reactions of radicals. J. Am. Chem. Soc. 1974, 96(1), 133-139.

Wander, R.; Neta, P.; Dorfman, L.M. Pulse radiolysis studies. XII. Kinetics and spectra f the cyclohexadienyl radicals in aqueous benzoic acid solution. J. Phys. Chem. 1968, 72(8), 2946-2949.

Wang, W-f.; Schuchmann, M.N.; Schuchmann, H-P.; Knolle, W.; von Sonntag, J.; von Sonntag, C. Radical cations in the OH-radical-induced oxidation of thiourea and tetramethylthiourea in aqueous solution. J. Am. Chem. Soc. 1999, 121, 238-245.

Wang, D.; Gyoergy, I.; Hildenbrand, K.; von Sonntag, C. J. Chem. Soc., Perkin Trans. 2, 1994, 45-55.

Whillans, D.W. Radiat. Phys. Chem. 1977, **10**, 335-340.

Wigger, A.; Gruenbein, W.; Henglein, A.; Land, E.J. Z. Naturforsch. Teil B, 1969, **24**, 1262-1267.

Willson, R.L.; Greenstock, C.L.; Adams, G.E.; Wageman, R.; Dorfman, L.M. The standardization of hydroxyl radical rate data from radiation chemistry.
Int.J.Radiat.Phys.Chem. 1971, 3, 211-220.

Wolfenden, B.S.; Willson, R.L. J. Chem. Soc., Perkin Trans. 2, 1982, 805-812.

Zakatova, N.V.; Minkhadzhiddinova, D.P.; Sharpatyi, V.A. Bull. Acad. Sci. USSR, Div. Chem. Sci. (Engl. Transl.), 1969, 1520.

Zimbrick, J.D.; Ward, J.F.; Myers, L.S.Jr. Int. J. Radiat. Biol. Relat. Stud. Phys., Chem. Med. 1969, 16, 505-523.

Zona, R.; Solar, S.; Sehested, K.; Holcman, J.; Mezyk, S.P. OH-radical induced oxidation of phenoxyacetic acid and 2,4-dichlorophenoxyacetic acid. Primary radical steps and products. J. Phys. Chem. A. 2002, 106, 6743-6749.

APPENDIX C: FORTRAN 90 PROGRAM SOURCE CODE OF GROUP CONTRIBUTION METHOD IDENTIFIER

```
!*****************************************************************************
!  GCM Identifier.f90
!
!  FUNCTIONS: GCMIdentifier
!
!*******************************************************************************************************
!                                                                                                      *
!  PROGRAM: GCM Identifier  ver.1.0 (June, 2009)                                                       *
!                                                                                                      *
!  by Daisuke Minakata and John C. Crittenden                                                          *
!  Department of Civil and Environmental Engineering, Georgia Institute of Technology                  *
!                                                                                                      *!
This program enables you to calculate an aqueous phase HO radical reaction rate                      *
!  constant that includes:                                                                             *
!   1)H-atom abstraction from a C-H bond of saturated aliphatic or cyclic compounds                    *
!   2)HO radical addition to unsaturated alkenes                                                       *
!   3)HO radical addition to aromatic compounds                                                        *
!   4)HO interaction with S,N,or P-atom containing compounds                                           *
!  based on a group contribution method (GCM) that is described in a paper:                           *
!                                                                                                      *
!  Daisuke,M.;Li,K.;Westerhoff,P.;Crittenden,J.C.                                                      *
!  Development of a Group Contribution Method (GCM) to Predict Aqueous Phase Hydroxyl                  *
!  Radical (HO*) Reaction Rate Constants. Environ.Sci.Technol. 2009                                    *
!                                                                                                      *
!  If you have any difficulties in running this program or come across technical                       *
!  issues, please email to Daisuke Minakata:                                                           *
!  Daisuke.Minakata@gatech.edu                                                                         *
!                                                                                                      *
!  Nomenclature:                                                                                       *
!                                                                                                      *
!  NPRIMCH,NSECNCH,NTERTCH  : # of primary,secondary,tertiary C-H bond(s)                              *
!  NALCOL,NCABXL            : # of alcohol and carboxylic functional group(s)                          *
!  NS,NSS,NSH               : # of -S-,-S-S-,-SH- functional group(s)                                  *
!  NCN,NNO2                 : # of -CN and -NO2 functional group(s)                                    *
!  NCONH2,NCONH,NCON        : # of -CO-NH2, -CO-NH-, -CO-N< functional group(s)                        *
!  NNH2,NNH,NN              : # of -NH2,_>NH-, >N- functional group(s)                                 *
!  NNCON                    : # of -N-CO-N- functional group(s)                                        *
!  NP                       : # of ->P- functional group(s)                                            *
!  X1(I)              : group contribution factor of functional group R1 for primary C-H bond          *
!  X2(J),X3(J)        : group contribution factor of functional group R1 and R2 for secondary C-H bond  *
!  X4(K),X5(K),X6(K)  : group contribution factor of functional group R1,R2,and R3 for tertiary C-H bond*
!  NADDALK1           : # of basic structure of HH>C=C<H                                               *
!  NADDALK2           : # of basic structure of HH>C=C<                                                *
!  NADDALK3           : # of basic structure of H>C=C<H(cis)                                           *
!  NADDALK4           : # of basic structure of H>C=C<H(trans)                                         *
!  NADDALK5           : # of basic structure of H>C=C<                                                 *
!  NADDALK6           : # of basic structure of >C=C<                                                  *
!  NBEBC6H5           : # of -C6H5 structure (benzene ring with one functional group)                  *
!  BENC6H4O           : # of -C6H4 structure (benzene ring with 2 functional groups at ortho-position)  *
!  BENC6H4M           : # of -C6H4 structure (benzene ring with 2 functional groups at meta-position)   *
!  BENC6H4P           : # of -C6H4 structure (benzene ring with 2 functional groups at para-position)   *
!  BENC6H3A           : # of -C6H3 structure (benzene ring with 3 functional groups at 1,2,3-positions) *
!  BENC6H3B           : # of -C6H3 structure (benzene ring with 3 functional groups at 1,2,4-positions) *
!  BENC6H3C           : # of -C6H3 structure (benzene ring with 3 functional groups at 1,3,5-positions) *
!  BENC6H2A      : # of -C6H2 structure (benzene ring with 4 functional groups at 1,2,3,4-positions)    *
!  BENC6H2B      : # of -C6H2 structure (benzene ring with 4 functional groups at 1,2,3,5-positions)    *
!  BENC6H2C      : # of -C6H2 structure (benzene ring with 4 functional groups at 1,2,4,5-positions)    *
!  BENC6HC       : # of -C6H  structure (benzene ring with 5 functional groups at 1,2,3,4,5-positions)  *
!  BENC6         : # of -C6   structure (benzene ring with 6 functional groups at 1,2,3,4,5,6-positions)*
!  PYR1,PYR2,PYR3: # of pyridine structures with a fucntional group at 2-,3-,4-position,respectively    *
!  PYR4,PYR5     : # of pyridine structures with two functional groups at 2,6- and 3,5-positions        *
!  PYR6          : # of pyridine structures with three functional groups at 2,4,6-positions            *
!  FUR1,FUR2     : # of furan structures with one and two functional groups at 2- and 2,5-positions     *
!  IMI           : # of imidazole basic structure                                                     *
!  TRI           : # of triazine basic structure                                                      *
!  OVALLRATE     : overall HO* reaction rate constant, M-1s-1                                         *
!  HABSTRATE     : partial HO* rate constant for H-atom abstraction                                   *
!  INTRATE       : partial HO* rate constant to interact with S-,N-,or P-atom containing compounds     *
!  ADDALKRATE    : partial HO* rate constant for HO* to add alkene                                    *
!  ADDARMRATE    : partial HO* rate constant for HO* to add aromatic compounds                        *
!*******************************************************************************************************

PROGRAM GCMIdentifier

IMPLICIT NONE

INTEGER         :: I, J, K
INTEGER         :: L1,L2,L3,L4,L5,L6
INTEGER         :: B1,B2,B3,B4,B5,B6
```

```
INTEGER          :: P1,P2,P3,P4,P5,P6
INTEGER          :: F1,F2
INTEGER          :: I1
INTEGER          :: T1

REAL             :: NPRIMCH, NSECNCH, NTERTCH, NALCOL, NCABXL
REAL             :: NS,NSS,NSO,NSH,NCN,NNO2,NCONH2,NCONH,NCON,NNH2,NNH,NN,NNCON,NP
REAL             :: NADDALK1,NADDALK2,NADDALK3,NADDALK4,NADDALK5,NADDALK6
REAL             :: NBENC6H5
REAL             :: BENC6H4,BENC6H4O,BENC6H4M,BENC6H4P
REAL             :: BENC6H3,BENC6H3A,BENC6H3B,BENC6H3C
REAL             :: BENC6H2,BENC6H2A,BENC6H2B,BENC6H2C,BENC6H,BENC6
REAL             :: PYR1,PYR2,PYR3,PYR4,PYR5,PYR6
REAL             :: FUR1,FUR2
REAL             :: IMI
REAL             :: TRZ

REAL, PARAMETER            :: NMAXN =100
REAL, PARAMETER            :: NMAXFUN = 197

REAL, DIMENSION(0:NMAXFUN) :: z
REAL, DIMENSION(0:NMAXFUN) :: y
REAL, DIMENSION(0:NMAXFUN) :: X1,X2,X3,X4,X5,X6
REAL, DIMENSION(0:NMAXFUN) :: Y1,Y2,Y3,Y4,Y5,Y6,Y7,Y8,Y9,Y10,Y11,Y12,Y13,Y14
REAL, DIMENSION(0:NMAXFUN) :: Z1,Z2,Z3,Z4,Z5,Z6,Z7,Z8,Z9,Z10
REAL, DIMENSION(0:NMAXFUN) :: Z11,Z12,Z13,Z14,Z15,Z16,Z17,Z18,Z19,Z20
REAL, DIMENSION(0:NMAXFUN) :: Z21,Z22,Z23,Z24,Z25,Z26,Z27,Z28,Z29,Z30
REAL, DIMENSION(0:NMAXFUN) :: Z31,Z32,Z33,Z34,Z35,Z36,Z37,Z38,Z39,Z40
REAL, DIMENSION(0:NMAXFUN) :: Z41,Z42,Z43,Z44,Z45,Z46,Z47,Z48,Z49,Z50
REAL, DIMENSION(0:NMAXFUN) :: Z51,Z52,Z53,Z54,Z55,Z56,Z57

REAL, DIMENSION(0:NMAXN)   :: PRATEPRIM, PRATESECN, PRATETERT

REAL, DIMENSION(0:NMAXN)   :: PRATEADDALK1,PRATEADDALK2,PRATEADDALK3
REAL, DIMENSION(0:NMAXN)   :: PRATEADDALK4,PRATEADDALK5,PRATEADDALK6
REAL, DIMENSION(0:NMAXN)   :: PRATEADDBEN1
REAL, DIMENSION(0:NMAXN)   :: PRATEADDBEN2
REAL, DIMENSION(0:NMAXN)   :: PRATEADDBEN2ORTH,PRATEADDBEN2META,PRATEADDBEN2PARA
REAL, DIMENSION(0:NMAXN)   :: PRATEADDBEN3
REAL, DIMENSION(0:NMAXN)   :: PRATEADDBEN3A,PRATEADDBEN3B,PRATEADDBEN3C
REAL, DIMENSION(0:NMAXN)   :: PRATEADDBEN4
REAL, DIMENSION(0:NMAXN)   :: PRATEADDBEN4A,PRATEADDBEN4B,PRATEADDBEN4C
REAL, DIMENSION(0:NMAXN)   :: PRATEADDBEN5,PRATEADDBEN6
REAL, DIMENSION(0:NMAXN)   :: PRATEADDPYR1,PRATEADDPYR2,PRATEADDPYR3
REAL, DIMENSION(0:NMAXN)   :: PRATEADDPYR4,PRATEADDPYR5,PRATEADDPYR6
REAL, DIMENSION(0:NMAXN)   :: PRATEADDFUR1,PRATEADDFUR2
REAL, DIMENSION(0:NMAXN)   :: PRATEADDIMI1
REAL, DIMENSION(0:NMAXN)   :: PRATEADDTRZ1

REAL             :: OVALLRATE,HABSTRATE,ADDALKRATE,GRATEALCOL,GRATECABXL
REAL             :: INTRATE
REAL             :: GRATES,GRATESS,GRATESO,GRATESH,GRATECN,GRATENO2,GRATECONH2
REAL             :: GRATECONH,GRATECON,GRATENH2,GRATENH,GRATEN,GRATENCON,GRATEP
REAL             :: ADDARMRATE,PRATEADDBEN,PRATEADDPYR,PRATEADDFUR,PRATEADDIMI,PRATEADDTRZ


CHARACTER*80               :: fn_output

!**parameters**
y(1)=    1.17401           !'-CH2-
y(2)=    1.17401           !'-CH<
y(3) =   1.17401           !'>C<
y(4) =   0.57803           !'-OH
y(5)=    1.17580E+08                !k prim
y(6)=    5.10970E+08                !k sec
y(7) =   1.99026E+09                !k tert
y(8) =   9.99996E+07                !k OH
y(9)=    1.12000           !'-CH3
y(10)=   0.55103           !'-O- AND -C-O-
y(11)=   0.15399           !'-CO
y(12)=   0.15399           !'-CH2-CO-
y(13)=   0.15399           !'-CH-CO-
y(14)=   0.60162           !'-CHO
y(15)=   0.04300           !'-COOR
y(16)=   0.00000           !'-OCOR
y(17)=   0.04300           !'-COOH
y(18)=   7.00463E+05                !kCOOH
y(19)=   0.00000           !'-F
y(20)=   0.20319           !'-Cl
y(21)=   0.37668           !'-Br
y(22)=   0.10180           !'-CF3
y(23)=   0.00000           !'-CF2-
y(24)=   0.11225           !'-CCl3
y(25)=   2.38950           !'-S
y(26)=   2.38950           !'-S-S-
y(27)=   2.36093E+09                !'k -S-
y(28)=   3.67296E+09                !'k -S-S-
y(29)=   0.44480           !'-SO-
```

```
y(30)=   1.91952E+09                !'k -SO-
y(31) =  2.38950           !'-SH-
y(32) =  9.93380E+08                !k-SH-
y(33) =  0.00292           !'-CN
y(34) =  5.54903E+06                !k-CN
y(35)=   0.00000           !'-NO2
y(36)=   1.32607E+08                !k-NO2
y(37) =  0.15399           !'-CO-NH2
y(38) =  0.15399           !'-CO-NH-
y(39)=   0.15399           !'-CO-N<
y(40)=   9.98120E+07                !k -CO-NH2
y(41)=   5.00446E+08                !k -CO-NH-
y(42)=   9.98491E+08                !k -CO-N<
y(43)=   1.62857           !'-NH2
y(44)=   3.99837E+09                !k-NH2
y(45)=   1.62857           !'-NH
y(46)=   1.62857           !'-N<
y(47)=   0.01054           !'-N-NO
y(48)=   0.17649           !'-N-NO2
y(49)=   1.00820E+08                !k-NH-
y(50)=   3.53248E+09                !k-N<
y(51)=   0.00000E+00                !k-N-NO
y(52)=   0.00000E+00                !k-N-NO2
y(53)=   0.10281           !'-PO
y(54)=   2.57962E+07                !k PO, PO3
y(55)=   1.00000           !'-H
y(56)=   0.36000           !'=O
y(57)=   0.15399           !->C-CO-
y(58)=   3.18576           !-N-CO-
y(59)=   0.00004           !-P<-
y(60)=   0.86006           !-RS5
y(61)=   0.05199           !-RS3
y(62)=   0.94498           !-O-second
y(63)=   0.00000           !-O-fluorinated
y(64)=   0.00000           !-O-C-C-fluorinated
y(65)=   0.36708           !-CH2Br
y(66)=   0.36708           !-CH2Cl
y(67)=   0.36708           !-CHCl2
y(68)=   0.36708           !-CHBr2
y(69)=   0.36708           !-CHCl-
y(70)=   0.00000           !-CH2CN
y(71)=   0.00000           !-CH2-NO2
y(72)=   0.00000           !-CH-NO2
y(73)=   0.00000           !-CH2-O-
y(74)=   9.99990E+09                !k HH>C=C<H-1
y(75)=   1.01020E+08                !k HH>C=C<H-2
y(76)=   9.78771E+10                !k HH>C=C< -1
y(77)=   3.16106E+09                !k HH>C=C< -2
y(78)=   3.01102E+10                !k H>C=C<H (cis)
y(79)=   0.51475           !-CN(uns)
y(80)=   0.38893           !-CH2-(uns)
y(81)=   0.59969           !-CO-(uns)
y(82)=   0.00000           !-OH(uns)
y(83)=   0.59969           !-CHO(uns)
y(84)=   0.23449           !-COOH(uns)
y(85)=   0.23449           !-COOR(uns)
y(86)=   0.21000           !-Cl(uns)
y(87)=   0.17115           !-CH3(uns)
y(88)=   0.59969           !-CO-NH2(uns)
y(89)=   1.00000           !>C=C<
y(90)=   1.00000           !-C6H5
y(91)=   1.02285E+09                !k-C6H5-2,6
y(92)=   1.29419E+09                !k-C6H5-3,5
y(93)=   9.14417E+08                !k-C6H5-4
y(94)=   1.00078           !-CH2-(Ar)
y(95)=   1.26917           !-OH(Ar)
y(96)=   0.97265           !-F(Ar)
y(97)=   0.97811           !-Cl(Ar)
y(98)=   0.87842           !-Br(Ar)
y(99)=   0.82106           !'-I(Ar)
y(100)=  0.41111           !'-CN(Ar)
y(101)=  0.40518           !-NO2(Ar)
y(102)=  0.67178           !-CHO(Ar)
y(103)=  0.67967           !-COOH(Ar)
y(104)=  0.98129           !-CO-(Ar)
y(105)=  0.84219           !-CONH2 (Ar)
y(106)=  0.65601           !-SO- (Ar)
y(107)=  0.85532           !-NH-CO-(Ar)
y(108)=  0.37331           !-SO3H (Ar)
y(109)=  1.10547           !-NH- (Ar)
y(110)=  1.00078           !-CH< (Ar)
y(111)=  1.03424           !-O- (Ar)
y(112)=  1.00078           !-CH3 (Ar)
y(113)=  1.00078           !>C< (Ar)
y(114)=  1.48110           !-NH2 (Ar)
y(115)=  1.78102E+09                !k-C6H4 (o-Ar)-3,6
y(116)=  7.05874E+08                !k-C6H4 (o-Ar)-4,5
y(117)=  9.88668E+08                !k-C6H4 (m-Ar)-2
```

```
y(118)=  1.69648E+09                !k-C6H4 (m-Ar)-4,6
y(119)=  1.90707E+09                !k-C6H4 (m-Ar)-5
y(120)=  7.12780E+08                !k-C6H4 (p-Ar)-2,6
y(121)=  1.92019E+09                !k-C6H4 (p-Ar)-2,6
y(122)=  2.15116E+09                !k-C6H3 (1,2,3-Ar)-4,6
y(123)=  1.63538E+09                !k-C6H3 (1,2,3-Ar)-5
y(124)=  2.79648E+09                !k-C6H3 (1,2,4-Ar)-3
y(125)=  3.06673E+08                !k-C6H3 (1,2,4-Ar)-5
y(126)=  1.13033E+09                !k-C6H3 (1,2,4-Ar)-6
y(127)=  1.67605E+09                !k-C6H3 (1,3,5-Ar)
y(128)=  1.97249           !-OH  (Pyr)
y(129)=  0.01078           !-COOH (Pyr)
y(130)=  1.00000           !-pyr
y(131)=  9.89963E+08                !k(2-pyr)-3,6
y(132)=  2.92815E+08                !k(2-pyr)-4,5
y(133)=  4.56050E+08                !k(3-pyr)-2
y(134)=  8.22558E+08                !k(3-pyr)-4,6
y(135)=  2.49180E+07                !k(3-pyr)-5
y(136)=  7.90881E+08                !k(4-pyr)-2,6
y(137)=  8.88526E+08                !k(4-pyr)-3,5
y(138)=  1.02552E+09                !k(2,6-pyr)-3,5
y(139)=  7.31676E+08                !k(2,6-pyr)-4
y(140)=  3.70768E+09                !k(3,5-pyr)-2,6
y(141)=  7.92572E+08                !k(3,5-pyr)-4
y(142)=  7.61212E+08                !k(2,4,6-pyr)-3,5
y(143)=  0.49841           !-CONH2(Pyr)
y(144)=  0.96179           !-CH3 (Pyr)
y(145)=  1.74733           !-NH2 (Pyr)
y(146)=  0.60347           !-Br  (Pyr)
y(147)=  0.81204           !-Cl  (Pyr)
y(148)=  0.33275           !-CN  (Pyr)
y(149)=  1.00000           !-fur
y(150)=  3.92420E+09                !-k(2-fur)-3
y(151)=  4.81346E+09                !-k(2-fur)-4
y(152)=  1.41939E+09                !-k(2-fur)-5
y(153)=  1.23883           !-CH3 (fur)
y(154)=  1.23883           !-CH2-(fur)
y(155)=  0.64680           !-CHO (fur)
y(156)=  5.70629E+09                !-k(5-furfural)-3
y(157)=  5.70629E+09                !-k(5-furfural)-4
y(158)=  0.60013           !-COOH (fur)
y(159)=  1.02225           !-O-  (5-furfural)
y(160)=  0.77850           !-NO2 (5-furfural)
y(161)=  0.90311           !-CH-CN-(fur)
y(162)=  408844.05370      !k-N-CO-N
y(163)=  0.00000           !-CO(cyclic)(uns)
y(164)=  0.00000           !-N<(uns)
y(165)=  0.00000               !k H>C=C< -1
y(166)=  0.00000               !k H>C=C< -2
y(167)=  0.00000           !-Br (uns)
y(168)=  0.00000           !-F  (uns)
y(169)=  0.00000           !-NO2(uns)
y(170)=  5.14211E+11                !k >C=C<
y(171)=  0.00000           !-NH2(uns)
y(172)=  1.00000           !-Iimid
y(173)=  1.70508E+09                !k(imid)-1
y(174)=  1.08285E+09                !k(imid)-2
y(175)=  0.40621           !-CO-   (fur)
y(176)=  0.61015           !-CONH2-(fur)
y(177)=  0.94316           !-C6H5  (fur)
y(178)=  0.64680           !-Br    (fur)
y(179)=  1.23883           !-CH<   (fur)
y(180)=  4.13229E+06                !k(triazine)
y(181)=  0.00000           !-OH (Triazine)
y(182)=  0.21404           !-O  (Triazine)
y(183)=  0.99757           !-Cl (Triazine)
y(184)=  4.94660           !-NH2(Triazine)
y(185)=  0.04155           !-NH-(Triazine)
y(186) =1.82626            !-S- (Triazine)
y(187)=  5.21229E+10       ! H>C=C<H (trans)
y(188)=  3.11655E+08                !kC6H6
y(189)=  7.06349E+09                !kC6H5
y(190)=  3.68416E+09                !kC6H4-1,2,3,4
y(191)=  2.80386E+09                !kC6H4-1,2,3,5
y(192)=  3.52577E+09                !kC6H4-1,2,4,5
y(193)=  0.68103           !->C-O-
y(194)=  1.61412           !-N< (imid)
y(195)=  0.73095           !-CO (imid)
y(196)=  1.42538           !-NH-(imid)
y(197)=  1.16621           !-Alk(imid)

!**end of parameters**

!*****************************************************************************************
!H-atom abstraction reaction from C-H bond
!*****************************************************************************************

OPEN(7, file='GCM_INPUT.txt', status='unknown')
```

```
PRINT*, "*************************************************************"
PRINT*, "H-atom abstraction"
PRINT*, "*************************************************************"

!The effect of functional groups includes alkane, oxygenated, alkyl halides,
!S-, N-, or P-atom containing functional groups.

!Primary C-H bond(s) (kprim*Xi)
    PRINT*, "The number of primary C-H bonds presented in the molecule"
    READ (7,*) NPRIMCH
    IF (NPRIMCH == 0.0) THEN
         PRATEPRIM(NPRIMCH)=0.0

    ELSE IF (NPRIMCH >= 1.) THEN
        PRINT*, "Input group contribution factors of functional groups X of R1 &
                & from the supplement material Tables"
        DO 10 I=1,NPRIMCH
        READ(7,*) X1(I)
            PRATEPRIM(NPRIMCH)=PRATEPRIM(NPRIMCH)+3*y(5)*X1(I)      !kCH3R1
10      CONTINUE
    END IF

!Secondary C-H bond(s) (ksec*Xi*Xi)
    PRINT*, "The number of secondary C-H bonds presented in the molecule"
    READ (7,*) NSECNCH
    IF (NSECNCH == 0.0) THEN
         PRATESECN(NSECNCH)=0.0

    ELSE IF (NSECNCH >= 1.) THEN
        PRINT*, "Input group contribution factors of functional groups X of R1 &
                & and X of R2 from the supplement material Tables"
            DO 20 J=1,NSECNCH
            READ(7,*) X2(J)
            READ(7,*) X3(J)
            PRATESECN(NSECNCH)=PRATESECN(NSECNCH)+2*y(6)*X2(J)*X3(J)   !kCH2R1R2
20          CONTINUE
    END IF

!Tertiary C-H bond(s) (ktert*Xi*Xi*Xi)
    PRINT*, "The number of tertiary C-H bonds presented in the molecule"
    READ (7,*) NTERTCH
    IF (NTERTCH == 0.0) THEN
         PRATETERT(NTERTCH)=0.0

    ELSE IF (NTERTCH >= 1.) THEN
        PRINT*, "Input group contribution factors of functional groups X of R1,R2,and R3 &
                & from the supplement material Tables"
             DO 30 K=1,NTERTCH
             READ(7,*) X4(K)
             READ(7,*) X5(K)
             READ(7,*) X6(K)
             PRATETERT(NTERTCH)=PRATETERT(NTERTCH)+y(7)*X4(K)*X5(K)*X6(K)   !kCHR1R2R3
30           CONTINUE
    END IF

!Group rate constants for alcohol and carboxylic functional group,kR4
    PRINT*, "The number of alcohol functional group presented in the molecule"
    READ(7,*) NALCOL
    GRATEALCOL=NALCOL*y(8)             !k-OH

    PRINT*, "The number of carboxylic functional group presented in the molecule"
    READ(7,*) NCABXL
    GRATECABXL=NCABXL*y(18)             !k-COOH

 !HO* rate constant for H-atom abstraction
    HABSTRATE=PRATEPRIM(NPRIMCH)+PRATESECN(NSECNCH)+PRATETERT(NTERTCH)+GRATEALCOL+GRATECABXL

!*****************************************************************************************
!HO radical interaction with S, N, P-atom containing compounds
!*****************************************************************************************

PRINT*, "*************************************************************"
PRINT*, "HO radical interaction with S, N, P-atom containing compounds"
PRINT*, "*************************************************************"

!Group rate constant for S-atom containing compounds
    PRINT*, "The number of -S-"
    READ(7,*) NS
    GRATES=NS*y(27)         !k-S-

    PRINT*, "The number of -S-S-"
    READ(7,*) NSS
    GRATESS=NSS*y(28)       !k-S-S-

    PRINT*, "The number of -SO-"
    READ(7,*) NSO
    GRATESO=NSO*y(30)       !k-SO-
```

```
    PRINT*, "The number of -SH-"
    READ(7,*) NSH
    GRATESH=NSH*y(32)       !k-SH-

!Group rate constant for N-atom containing compounds
    PRINT*, "The number of -CN"
    READ(7,*) NCN
    GRATECN=NCN*y(34)           !k-CN

    PRINT*, "The number of -NO2"
    READ(7,*) NNO2
    GRATENO2=NNO2*y(36)         !k-NO2

    PRINT*, "The number of -CO-NH2"
    READ(7,*) NCONH2
    GRATECONH2=NCONH2*y(40)     !k-CO-NH2

    PRINT*, "The number of -CO-NH-"
    READ(7,*) NCONH
    GRATECONH=NCONH*y(41)       !k-CO-NH-

    PRINT*, "The number of -CO-N<"
    READ(7,*) NCON
    GRATECON=NCON*y(42)         !k-CO-N<

    PRINT*, "The number of -NH2"
    READ(7,*) NNH2
    GRATENH2=NNH2*y(44)         !k-NH2

    PRINT*, "The number of -NH-"
    READ(7,*) NNH
    GRATENH=NNH*y(49)           !k-NH-

    PRINT*, "The number of -N<"
    READ(7,*) NN
    GRATEN=NN*y(50)             !k-N<

    PRINT*, "The number of -N-CO-N"
    READ(7,*) NNCON
    GRATENCON=NNCON*y(162)      !k-N-CO-N

!Group rate constant for P-atom containing compounds
    PRINT*, "The number of -PO, PO3"
    READ(7,*) NP
    GRATEP=NP*y(54)             !k-P<-

!k for interaction with S-, N-, or P-atom containing compounds

    INTRATE=GRATES+GRATESS+GRATESO+GRATESH+GRATECN+GRATENO2+GRATECONH2+GRATECONH+GRATECON &
&    +GRATENH2+GRATENH+GRATEN+GRATENCON+GRATEP

!*********************************************************************************************
!HO radical addition to alkenes
!*********************************************************************************************

PRINT*, "*************************************************************"
PRINT*, "HO radical addition to alkenes"
PRINT*, "*************************************************************"

    PRINT*, "Basic structure that includes C=C bond are: &
    &(1)HH>C=C<H, (2)HH>C=C<,(3)H>C=C<H(cis),(4)H>C=C<H(trans),(5)H>C=C<, and (6) >C=C<"
    PRINT*, "The number of basic structure 'HH>C=C<H' presented in the molecule"
    READ (7,*) NADDALK1
        IF (NADDALK1 == 0.0) THEN
            PRATEADDALK1(NADDALK1)=0.0

        ELSE IF (NADDALK1 >= 1.) THEN
            PRINT*, "Input group contribution factor, Y of R1 "
            DO 40 L1=1,NADDALK1
            READ (7,*) Y1(L1)
                PRATEADDALK1(NADDALK1)=PRATEADDALK1(NADDALK1)+(y(74)+y(75))*Y1(L1)
40          CONTINUE
        END IF

    PRINT*, "The number of basic structure 'HH>C=C<' presented in the molecule"
    READ(7,*) NADDALK2
        IF (NADDALK2 == 0.0) THEN
            PRATEADDALK2(NADDALK2)=0.0

        ELSE IF (NADDALK2 >= 1.) THEN
            PRINT*, "Input group contribution factors, Y of R1 and R2"
            DO 50 L2=1,NADDALK2
            READ (7,*) Y2(L2)
            READ (7,*) Y3(L2)
                PRATEADDALK2(NADDALK2)=PRATEADDALK2(NADDALK2)+(y(76)+y(77))*Y2(L2)*Y3(L2)
50          CONTINUE
        END IF
```

```
    PRINT*, "The number of basic structure 'H>C=C<H(cis)' presented in the molecule"
    READ(7,*) NADDALK3
        IF (NADDALK3 == 0.0) THEN
            PRATEADDALK3(NADDALK3)=0.0

        ELSE IF (NADDALK3 >= 1.) THEN
            PRINT*, "Input group contribution factors, Y of R1 and R2"
            DO 60 L3=1,NADDALK3
            READ (7,*) Y4(L3)
            READ (7,*) Y5(L3)
                PRATEADDALK3(NADDALK3)=PRATEADDALK3(NADDALK3)+2*y(78)*Y4(L3)*Y5(L3)
60          CONTINUE
        END IF

    PRINT*, "The number of basic structure 'H>C=C<H(trans)' presented in the molecule"
    READ(7,*) NADDALK4
        IF (NADDALK4 == 0.0) THEN
        PRATEADDALK4(NADDALK4)=0.0

        ELSE IF (NADDALK4 >= 1.) THEN
            PRINT*, "Input group contribution factors, Y of R1 and R2"
            DO 70 L4=1,NADDALK4
            READ (7,*) Y6(L4)
            READ (7,*) Y7(L4)
                PRATEADDALK4(NADDALK4)=PRATEADDALK4(NADDALK4)+2*y(187)*Y6(L4)*Y7(L4)
70          CONTINUE
        END IF

    PRINT*, "The number of basic structure 'H>C=C<' presented in the molecule"
    READ(7,*) NADDALK5
        IF (NADDALK5 == 0.0) THEN
        PRATEADDALK5(NADDALK5)=0.0

        ELSE IF (NADDALK5 >= 1.) THEN
            PRINT*, "Input group contribution factors, Y of R1, R2, and R3"
            DO 80 L5=1,NADDALK5
            READ (7,*) Y8(L5)
            READ (7,*) Y9(L5)
            READ (7,*) Y10(L5)
                PRATEADDALK5(NADDALK5)=PRATEADDALK5(NADDALK5)+2*(y(165)+y(166))*Y8(L5)*Y9(L5)*Y10(L5)
80          CONTINUE
        END IF

    PRINT*, "The number of basic structure '>C=C<' presented in the molecule"
    READ(7,*) NADDALK6
        IF (NADDALK6 == 0.0) THEN
        PRATEADDALK6(NADDALK6)=0.0

        ELSE IF (NADDALK6 >= 1.) THEN
            PRINT*, "Input group contribution factors, Y of R1,R2,R3,and R4"
            DO 90 L6=1,NADDALK6
            READ (7,*) Y11(L6)
            READ (7,*) Y12(L6)
            READ (7,*) Y13(L6)
            READ (7,*) Y14(L6)
                PRATEADDALK6(NADDALK6)=PRATEADDALK6(NADDALK6)+y(170)*Y11(L6)*Y12(L6)*Y13(L6)*Y14(L6)
90          CONTINUE
        END IF

    ADDALKRATE=PRATEADDALK1(NADDALK1)&
   & +PRATEADDALK2(NADDALK2) &
   & +PRATEADDALK3(NADDALK3) &
   & +PRATEADDALK4(NADDALK4) &
   & +PRATEADDALK5(NADDALK5) &
   & +PRATEADDALK6(NADDALK6)

!*****************************************************************************************
!HO addition to aromatic compounds
!*****************************************************************************************

PRINT*, "*************************************************************"
PRINT*, "HO addition to aromatic compounds"
PRINT*, "*************************************************************"
PRINT*, " "

!Benzene

PRINT*, "The # of -C6H5 with one functional group"
    READ(7,*) NBENC6H5
        IF (NBENC6H5 == 0.0) THEN
            PRATEADDBEN1(NBENC6H5)=0.0
        ELSE IF (NBENC6H5 >= 1.) THEN
            PRINT*, "Input group contribution factor, Z of R1"
                DO 100 B1=1,NBENC6H5
                READ(7,*) Z1(B1)
                PRATEADDBEN1(NBENC6H5)=PRATEADDBEN1(NBENC6H5)+(2*y(91)+2*y(92)+y(93))*Z1(B1)     !k-C6H5
100             CONTINUE
```

```
        END IF

PRINT*, "The # of -C6H4 with one functional group at 'ortho-' position"
    READ(7,*) BENC6H4O
        IF (BENC6H4O == 0.0) THEN
            PRATEADDBEN2ORTH(BENC6H4O)=0.0
        ELSE IF (BENC6H4O >= 1.) THEN
            PRINT*, "Input group contribution factors, Z of R1 and R2"
                DO 110 B2=1,BENC6H4O
                READ(7,*) Z2(B2)
                READ(7,*) Z3(B2)
                PRATEADDBEN2ORTH(BENC6H4O)=PRATEADDBEN2ORTH(BENC6H4O)+(2*y(115)+2*y(116))*Z2(B2)*Z3(B2) !k-
C6H4(ortho)
110             CONTINUE
        END IF

PRINT*, "The # of -C6H4 with one functional group at 'meta-' position"
    READ(7,*) BENC6H4M
        IF (BENC6H4M == 0.0) THEN
            PRATEADDBEN2META(BENC6H4M)=0.0
        ELSE IF (BENC6H4M >= 1.) THEN
            PRINT*, "Input group contribution factors, Z of R1 and R2"
                DO 120 B2=1,BENC6H4M
                READ(7,*) Z4(B2)
                READ(7,*) Z5(B2)
                PRATEADDBEN2META(BENC6H4M)=PRATEADDBEN2META(BENC6H4M)+(y(117)+2*y(118)+y(119))*Z4(B2)*Z5(B2)
!k-C6H4(meta)
120             CONTINUE
        END IF

PRINT*, "The # of -C6H4 with one functional group at 'para-' position"
    READ(7,*) BENC6H4P
        IF (BENC6H4P == 0.0) THEN
            PRATEADDBEN2PARA(BENC6H4P)=0.0
        ELSE IF (BENC6H4P >= 1.) THEN
            PRINT*, "Input group contribution factors, Z of R1 and R2"
                DO 130 B2=1,BENC6H4P
                READ(7,*) Z6(B2)
                READ(7,*) Z7(B2)
                PRATEADDBEN2PARA(BENC6H4P)=PRATEADDBEN2PARA(BENC6H4P)+(2*y(120)+2*y(121))*Z6(B2)*Z7(B2) !k-
C6H4(para)
130             CONTINUE
        END IF

PRATEADDBEN2(BENC6H4)= PRATEADDBEN2ORTH(BENC6H4O)+PRATEADDBEN2META(BENC6H4M)+PRATEADDBEN2PARA(BENC6H4P)


PRINT*, "The # of -C6H3 with one functional group at (1,2,3-Ar) position (called position A)"
    READ(7,*) BENC6H3A
        IF (BENC6H3A == 0.0) THEN
            PRATEADDBEN3A(BENC6H3A)=0.0
        ELSE IF (BENC6H3A >= 1.) THEN
            PRINT*, "Input group contribution factors, Z of R1,R2 and R3"
                DO 140 B3=1,BENC6H3A
                READ(7,*) Z8(B3)
                READ(7,*) Z9(B3)
                READ(7,*) Z10(B3)
                PRATEADDBEN3A(BENC6H3A)=PRATEADDBEN3A(BENC6H3A)+(2*y(122)+y(123))*Z8(B3)*Z9(B3)*Z10(B3)  !k-
C6H3(1,2,3-Ar)
140             CONTINUE
        END IF

PRINT*, "The # of -C6H3 with one functional group at (1,2,4-Ar) position (called position B)"
    READ(7,*) BENC6H3B
        IF (BENC6H3B == 0.0) THEN
            PRATEADDBEN3B(BENC6H3B)=0.0
        ELSE IF (BENC6H3B >= 1.) THEN
            PRINT*, "Input group contribution factors, Z of R1,R2 and R3"
                DO 150 B3=1,BENC6H3B
                READ(7,*) Z11(B3)
                READ(7,*) Z12(B3)
                READ(7,*) Z13(B3)
                PRATEADDBEN3B(BENC6H3B)=PRATEADDBEN3B(BENC6H3B)+(y(124)+y(125)+y(126))*Z11(B3)*Z12(B3)*Z13(B3)
!k-C6H3(1,2,4-Ar)
150             CONTINUE
        END IF

PRINT*, "The # of -C6H3 with one functional group at (1,3,5-Ar) position (called position C)"
    READ(7,*) BENC6H3C
        IF (BENC6H3C == 0.0) THEN
            PRATEADDBEN3C(BENC6H3C)=0.0
        ELSE IF (BENC6H3C >= 1.) THEN
            PRINT*, "Input group contribution factors, Z of R1,R2 and R3"
                DO 160 B3=1,BENC6H3C
                READ(7,*) Z14(B3)
                READ(7,*) Z15(B3)
                READ(7,*) Z16(B3)
```

```
                PRATEADDBEN3C(BENC6H3C)=PRATEADDBEN3C(BENC6H3C)+(3*y(127))*Z14(B3)*Z15(B3)*Z16(B3)   !k-
C6H3(1,3,5-Ar)
160             CONTINUE
        END IF

PRATEADDBEN3(BENC6H3)= PRATEADDBEN3A(BENC6H3A)+PRATEADDBEN3B(BENC6H3B)+PRATEADDBEN3C(BENC6H3C)


PRINT*, "The # of -C6H2 with one functional group at (1,2,3,4-Ar) position (called position A)"
    READ(7,*) BENC6H2A
        IF (BENC6H2A == 0.0) THEN
            PRATEADDBEN4A(BENC6H2A)=0.0
        ELSE IF (BENC6H2A >= 1.) THEN
            PRINT*, "Input group contribution factors, Z of R1,R2,R3 and R4"
                DO 170 B4=1,BENC6H2A
                READ(7,*) Z17(B4)
                READ(7,*) Z18(B4)
                READ(7,*) Z19(B4)
                READ(7,*) Z20(B4)
                PRATEADDBEN4A(BENC6H2A)=PRATEADDBEN4A(BENC6H2A)+(2*y(190))*Z17(B4)*Z18(B4)*Z19(B4)*Z20(B4)!k-
C6H2(1,2,3,4-Ar)
170             CONTINUE
        END IF

PRINT*, "The # of -C6H2 with one functional group at (1,2,3,5-Ar) position (called position B)"
    READ(7,*) BENC6H2B
        IF (BENC6H2B == 0.0) THEN
            PRATEADDBEN4B(BENC6H2B)=0.0
        ELSE IF (BENC6H2B >= 1.) THEN
            PRINT*, "Input group contribution factors, Z of R1,R2,R3 and R4"
                DO 180 B4=1,BENC6H2B
                READ(7,*) Z21(B4)
                READ(7,*) Z22(B4)
                READ(7,*) Z23(B4)
                READ(7,*) Z24(B4)
                PRATEADDBEN4B(BENC6H2B)=PRATEADDBEN4B(BENC6H2B)+(2*y(191))*Z21(B4)*Z22(B4)*Z23(B4)*Z24(B4)
!k-C6H2(1,2,3,5-Ar)
180             CONTINUE
        END IF

PRINT*, "The # of -C6H2 with one functional group at (1,2,4,5-Ar) position (called position C)"
    READ(7,*) BENC6H2C
        IF (BENC6H2C == 0.0) THEN
            PRATEADDBEN4C(BENC6H2C)=0.0
        ELSE IF (BENC6H2C >= 1.) THEN
            PRINT*, "Input group contribution factors, Z of R1,R2,R3 and R4"
                DO 190 B4=1,BENC6H2C
                READ(7,*) Z25(B4)
                READ(7,*) Z26(B4)
                READ(7,*) Z27(B4)
                READ(7,*) Z28(B4)
                PRATEADDBEN4C(BENC6H2C)=PRATEADDBEN4C(BENC6H2C)+(2*y(192))*Z25(B4)*Z26(B4)*Z27(B4)*Z28(B4)
!k-C6H2(1,2,4,5-Ar)
190             CONTINUE
        END IF

PRATEADDBEN4(BENC6H2)=PRATEADDBEN4A(BENC6H2A)+PRATEADDBEN4B(BENC6H2B)+PRATEADDBEN4C(BENC6H2C)


PRINT*, "The # of -C6H with functional groups at (1,2,3,4,5-Ar) position"
    READ(7,*) BENC6H
        IF (BENC6H == 0.0) THEN
            PRATEADDBEN5(BENC6H)=0.0
        ELSE IF (BENC6H >= 1.) THEN
            PRINT*, "Input group contribution factors, Z of R1,R2,R3,R4 and R5"
                DO 200 B5=1,BENC6H
                READ(7,*) Z29(B5)
                READ(7,*) Z30(B5)
                READ(7,*) Z31(B5)
                READ(7,*) Z32(B5)
                READ(7,*) Z33(B5)
                PRATEADDBEN5(BENC6H)=PRATEADDBEN5(BENC6H)+y(189)*Z29(B5)*Z30(B5)*Z31(B5)*Z32(B5)*Z33(B5)
!k-C6H(1,2,3,4,5-Ar)
200             CONTINUE
        END IF

PRINT*, "The # of -C6 with functional groups at (1,2,3,4,5,6-Ar) position"
    READ(7,*) BENC6
        IF (BENC6 == 0.0) THEN
            PRATEADDBEN6(BENC6)=0.0
        ELSE IF (BENC6 >= 1.) THEN
            PRINT*, "Input group contribution factors, Z of R1,R2,R3,R4,R5 and R6"
                DO 210 B6=1,BENC6
                READ(7,*) Z34(B6)
                READ(7,*) Z35(B6)
                READ(7,*) Z36(B6)
                READ(7,*) Z37(B6)
                READ(7,*) Z38(B6)
```

```
                READ(7,*) Z39(B6)

PRATEADDBEN6(BENC6)=PRATEADDBEN6(BENC6)+6*y(188)*Z34(B6)*Z35(B6)*Z36(B6)*Z37(B6)*Z38(B6)*Z39(B6)        !k-
C6(1,2,3,4,5,6-Ar)
210             CONTINUE
        END IF

    PRATEADDBEN= PRATEADDBEN1(NBENC6H5) &
    &           +   PRATEADDBEN2(BENC6H4) &
    &           +   PRATEADDBEN3(BENC6H3) &
    &           +   PRATEADDBEN4(BENC6H2) &
    &           +   PRATEADDBEN5(BENC6H)  &
    &           +   PRATEADDBEN6(BENC6)                     !overall rate constant for benzene-derivatives

! Pyridine with functional groups

  PRINT*, "The # of pyridine ring with functional group at (2-pyr) position"
    READ(7,*) PYR1
        IF (PYR1 == 0.0) THEN
            PRATEADDPYR1(PYR1)=0.0
        ELSE IF (PYR1 >= 1.) THEN
            PRINT*, "Input group contribution factors, Z of R1"
                DO 220 P1=1,PYR1
                READ(7,*) Z40(P1)
                PRATEADDPYR1(PYR1)=PRATEADDPYR1(PYR1)+(2*y(131)+2*y(132))*Z40(P1)           !k(2-pyr)
220             CONTINUE
        END IF

  PRINT*, "The # of pyridine ring with functional group at (3-pyr) position"
    READ(7,*) PYR2
        IF (PYR2 == 0.0) THEN
            PRATEADDPYR2(PYR2)=0.0
        ELSE IF (PYR2 >= 1.) THEN
            PRINT*, "Input group contribution factors, Z of R1"
                DO 230 P2=1,PYR2
                READ(7,*) Z41(P2)
                PRATEADDPYR2(PYR2)=PRATEADDPYR2(PYR2)+(y(133)+2*y(134)+y(135))*Z41(P2)       !k(3-pyr)
230             CONTINUE
        END IF

  PRINT*, "The # of pyridine ring with functional group at (4-pyr) position"
    READ(7,*) PYR3
        IF (PYR3 == 0.0) THEN
            PRATEADDPYR3(PYR3)=0.0
        ELSE IF (PYR3 >= 1.) THEN
            PRINT*, "Input group contribution factors, Z of R1"
                DO 240 P3=1,PYR3
                READ(7,*) Z42(P3)
                PRATEADDPYR3(PYR3)=PRATEADDPYR3(PYR3)+(2*y(136)+2*y(137))*Z42(P3)            !k(4-pyr)
240             CONTINUE
        END IF

  PRINT*, "The # of pyridine ring with functional group at (2,6-pyr) position"
    READ(7,*) PYR4
        IF (PYR4 == 0.0) THEN
            PRATEADDPYR4(PYR4)=0.0
        ELSE IF (PYR4 >= 1.) THEN
            PRINT*, "Input group contribution factors, Z of R1 and R2"
                DO 250 P4=1,PYR4
                READ(7,*) Z43(P4)
                READ(7,*) Z44(P4)
                PRATEADDPYR4(PYR4)=PRATEADDPYR4(PYR4)+(2*y(138)+y(139))*Z43(P4)*Z44(P4)      !k(2,6-pyr)
250             CONTINUE
        END IF

  PRINT*, "The # of pyridine ring with functional group at (3,5-pyr)  position"
    READ(7,*) PYR5
        IF (PYR5 == 0.0) THEN
            PRATEADDPYR5(PYR5)=0.0
        ELSE IF (PYR5 >= 1.) THEN
            PRINT*, "Input group contribution factors, Z of R1 and R2"
                DO 260 P5=1,PYR5
                READ(7,*) Z45(P5)
                READ(7,*) Z46(P5)
                PRATEADDPYR5(PYR5)=PRATEADDPYR5(PYR5)+(2*y(140)+y(141))*Z45(P5)*Z46(P5)      !k(3,5-pyr)
260             CONTINUE
        END IF

  PRINT*, "The # of pyridine ring with functional group at (2,4,6-pyr)   position"
    READ(7,*) PYR6
        IF (PYR6 == 0.0) THEN
            PRATEADDPYR6(PYR6)=0.0
        ELSE IF (PYR6 >= 1.) THEN
            PRINT*, "Input group contribution factors, Z of R1,R2 and R3"
                DO 270 P6=1,PYR6
                READ(7,*) Z47(P6)
                READ(7,*) Z48(P6)
                READ(7,*) Z49(P6)
```

```
                PRATEADDPYR6(PYR6)=PRATEADDPYR6(PYR6)+3*y(142)*Z47(P6)*Z48(P6)*Z49(P6)        !k(2,4,6-pyr)
270             CONTINUE
        END IF

PRATEADDPYR = PRATEADDPYR1(PYR1)   + &
&               PRATEADDPYR2(PYR2) + &
&               PRATEADDPYR3(PYR3) + &
&               PRATEADDPYR4(PYR4) + &
&               PRATEADDPYR5(PYR5) + &
&               PRATEADDPYR6(PYR6)

! furan

  PRINT*, "The # of pyridine ring with functional group at (2-fur)   position"
    READ(7,*) FUR1
        IF (FUR1 == 0.0) THEN
            PRATEADDFUR1(FUR1)=0.0
        ELSE IF (FUR1 >= 1.) THEN
            PRINT*, "Input group contribution factors, Z of R1"
                DO 280 F1=1,FUR1
                READ(7,*) Z50(F1)
                PRATEADDFUR1(FUR1)=PRATEADDFUR1(FUR1)+(y(150)+y(151)+y(152))*Z50(F1)        !k(2-fur)
280             CONTINUE
        END IF

  PRINT*, "The # of pyridine ring with functional group at (5-furfural)   position"
    READ(7,*) FUR2
        IF (FUR2 == 0.0) THEN
            PRATEADDFUR2(FUR2)=0.0
        ELSE IF (FUR2 >= 1.) THEN
            PRINT*, "Input group contribution factors, Z of R1 and R2"
                DO 290 F2=1,FUR2
                READ(7,*) Z51(F2)
                READ(7,*) Z52(F2)
                PRATEADDFUR2(FUR2)=PRATEADDFUR2(FUR2)+(y(156)+y(157))*Z51(F2)*Z52(F2)   !k(5-furfural)
290             CONTINUE
        END IF

PRATEADDFUR = PRATEADDFUR1(FUR1) + PRATEADDFUR2(FUR2)

!imidazole

  PRINT*, "The # of imidazole with 2 functional groups at 4,5-positions"
    READ(7,*) IMI
        IF (IMI == 0.0) THEN
            PRATEADDIMI1(IMI)=0.0
        ELSE IF (IMI >= 1.) THEN
            PRINT*, "Input group contribution factors, Z of R1 and R2"
                DO 300 I1=1,IMI
                READ(7,*) Z53(I1)
                READ(7,*) Z54(I1)
                PRATEADDIMI1(IMI)= PRATEADDIMI1(IMI)+(2*y(173)+y(174))*Z53(I1)*Z54(I1)    !k(imidazole)
300             CONTINUE
        END IF

PRATEADDIMI = PRATEADDIMI1(IMI)

!triazine

  PRINT*, "The # of triazine with 3 functional groups at 2,4,6-positions"
    READ(7,*) TRZ
        IF (TRZ == 0.0) THEN
            PRATEADDTRZ1(TRZ)=0.0

        ELSE IF (TRZ >= 1) THEN
            PRINT*, "Input group contribution factors, Z of R1, R2 and R3"
                DO 310 T1=1,TRZ
                READ(7,*) Z55(T1)
                READ(7,*) Z56(T1)
                READ(7,*) Z57(T1)
                PRATEADDTRZ1(TRZ)= PRATEADDTRZ1(TRZ)+3*y(180)*Z55(T1)*Z56(T1)*Z57(T1)      !k(triazine)
310             CONTINUE
        END IF

PRATEADDTRZ =PRATEADDTRZ1(TRZ)

    ADDARMRATE=PRATEADDBEN+PRATEADDPYR+PRATEADDFUR+PRATEADDIMI+PRATEADDTRZ

    CLOSE(7)

!*****************************************************************************************
!Calculate overall reaction rate constant for a given molecule
!*****************************************************************************************
   OVALLRATE=HABSTRATE+INTRATE+ADDALKRATE+ADDARMRATE

    OPEN(8, file='output.txt', status='unknown')
    WRITE(8,*) "Calculated HO radical reaction rate constant,M-1s-1"
    WRITE(8,*) " "
```

```
    WRITE(8,*) "Overall rate constant"
    WRITE(8,*) OVALLRATE
    WRITE(8,*) " "
    WRITE(8,*) "Partial rate constant for each reaction mechanism"
    WRITE(8,*) "H-atom abstraction"
    WRITE(8,*) HABSTRATE
    WRITE(8,*) "HO radical addition to alkene"
    WRITE(8,*) ADDALKRATE
    WRITE(8,*) "HO radical addition to aromatic compound"
    WRITE(8,*) ADDARMRATE
    WRITE(8,*) "HO radical interaction"
    WRITE(8,*) INTRATE

    CLOSE(8)

END PROGRAM GCMIdentifier
```

APPENDIX D: ENERGY OF HIGHEST OCCUPIED MOLECULAR ORBITAL AND LOWEST UNOCCUPIED MOLECULAR ORBITAL

chemical formula of compound	name of compound	k HO	log k	HOMO	HOMO-SOMO	LUMO
CH4	methane	1.20E+08	8.08	-13.30875	-11.47875	4.660697
CH3-CH3	ethane	1.80E+09	9.26	-11.76554	-9.93554	4.116723
CH3-CH2-CH3	propane	3.60E+09	9.56	-11.32619	-9.49619	3.920865
CH3-CH(CH3)-CH3	2-methylpropane	4.60E+09	9.66	-11.29054	-9.46054	3.833211
CH3-(CH2)2-CH3	!butane	4.60E+09	9.66	-11.17067	-9.34067	3.828838
CH3-(CH2)3-CH3	!pentane	5.40E+09	9.73	-11.11003	-9.28003	3.775402
CH3-(CH2)4-CH3	!hexane	6.60E+09	9.82	-11.08502	-9.25502	3.737725
CH3-(CH2)5-CH3	!heptane	7.70E+09	9.89	-11.07213	-9.24213	3.681164
CH3-(CH2)6-CH3	!octane	9.10E+09	9.96	-11.06686	-9.23686	3.638226
CH3-CH2-CH(CH3)-CH3	!2-methylbutane	5.20E+09	9.72	-11.1809	-9.3509	3.745211
CH3-CH2-CH(CH2-CH3)-CH2-CH3	!3-ethylpentane	5.90E+09	9.77	-10.99532	-9.16532	3.679372
CH3-C(CH3)2-CH2-CH(CH3)-CH3	!2,2,4-Trimethylpentane	6.10E+09	9.79	-11.02812	-9.19812	3.626539
CH3-OH	methanol	9.70E+08	8.99	-11.13453	-9.30453	3.77894
CH3-CH2-OH	!ethanol	2.10E+09	9.32	-10.87574	-9.04574	3.564502
CH3-(CH2)2-OH	!1-propanol	3.20E+09	9.51	-10.84639	-9.01639	3.48847
CH3-(CH2)3-OH	!1-butanol	4.20E+09	9.62	-10.84564	-9.01564	3.426211
(CH3)3-C-OH	!tert-butanol	7.00E+08	8.85	-10.99061	-9.16061	3.437299
CH3-(CH2)5-OH	!1-hexyanol	7.00E+09	9.85	-10.84862	-9.01862	3.369371
CH3-(CH2)6-OH	!1-heptanol	7.40E+09	9.87	-10.84806	-9.01806	3.352759
CH3-CH(OH)-CH3	!2-propanol	1.90E+09	9.28	-10.89775	-9.06775	3.491269
CH3-CH(CH3)-CH2-OH	!2-methyl-1-propanol	3.30E+09	9.52	-10.87454	-9.04454	3.455483
CH3-CH2-C(CH3)(OH)-CH3	!2-methyl-2-butanol	1.90E+09	9.28	-10.94695	-9.11695	3.453075
CH3-C(CH3)2-CH2-OH	!2,2-dimethyl-1-propanol	5.20E+09	9.72	-10.86936	-9.03936	3.439935
CH3-CH2-CH(CH3)-CH2-OH	!3-methyl-1-butanol	3.80E+09	9.58	-10.82195	-8.99195	3.42855
CH3-CH(OH)-CH2-CH3	!2-butanol	3.50E+09	9.54	-10.79586	-8.96586	3.505121
CH3-C(CH3)(OH)-CH2-CH3	!tert-amyl alcohol	1.90E+09	9.28	-10.80912	-8.97912	3.44938
HO-CH2-OH	!dihydroxymethane	1.30E+09	9.11	-10.74605	-8.91605	3.001253
HO-CH2-CH2-OH	!ethyleneglycol	2.40E+09	9.38	-10.82728	-8.99728	3.02301
CH3-CH(OH)2	!1,1-ethanediol	1.20E+09	9.08	-11.29653	-9.46653	-3.253182
CH3-CH(OH)-CH2-OH	!1,2-propanediol	1.70E+09	9.23	-10.82385	-8.99385	3.179295
HO-(CH2)3-OH	!1,3-propanediol	2.50E+09	9.40	-10.91272	-9.08272	3.090769
CH3-CH(OH)-CH2-CH2-OH	!1,3-butanediol	2.20E+09	9.34	-10.94984	-9.11984	3.147903
HO-(CH2)4-OH	!1.4-butanediol	3.20E+09	9.51	-10.91242	-9.08242	3.141693
CH3-CH(OH)-CH(OH)-CH3	!2,3-butanediol	1.30E+09	9.11	-10.7055	-8.8755	3.165536
HO-(CH2)5-OH	!1,5-pentanediol	3.60E+09	9.56	-10.88223	-9.05223	3.169252
CH3-CH(OH)-CH2-CH(OH)-CH3	!2,4-pentanediol	2.30E+09	9.36	-10.89812	-9.06812	3.126363
HO-(CH2)6-OH	!1,6-hexyanediol	4.70E+09	9.67	-10.87071	-9.04071	3.194863
HO-CH2-CH(OH)-CH2-OH	!glycerol	2.00E+09	9.30	-10.81248	-8.98248	3.024266
CH3CH(OCH3)2	!1,1-dimethoxyethane	2.20E+09	9.34	-10.70728	-8.87728	2.766965
CH3-O-CH3	!dimethylether	1.00E+09	9.00	-10.61215	-8.78215	3.250377
CH3-O-CH2-O-CH3	!methylene glycol diethyl ether	3.20E+08	8.51	-10.38339	-8.55339	2.447473
CH3-CH2-O-CH2-CH3	!diethylether	2.90E+09	9.46	-10.39318	-8.56318	2.981373
(CH3)2HC-O-CH(CH3)2	!diisopropyl ether	2.49E+09	9.40	-10.33819	-8.50819	2.889881
	mtbe	1.60E+09	9.20	-10.43097	-8.60097	2.988416
(CH3)3-C-O-CH2-CH3	!tert-butyl-ethyl-ether	1.80E+09	9.26	-10.30765	-8.47765	2.888528
$C_2H_5C(CH_3)_2OCH_3$	!tert-amyl methyl ether	2.37E+09	9.37	-10.41498	-8.58498	2.955497
CH3CH2-O-CH2CH2-CH2CH2-O-CH2CH3	!diethylene glycol diethyl ether	3.20E+09	9.51	-10.41134	-8.58134	2.684676
CH3CH2-O-CH2CH2-O-CH2CH3	!ethylene glycol diethyl ether	2.30E+09	9.36	-10.40904	-8.57904	2.443595
CH3-O-CH2-CH2-O-CH3	!ethylene glycol dimethyl ether	1.60E+09	9.20	-10.50665	-8.67665	2.526982
CH2(OC2H5)2	!diethoxymethane	1.60E+09	9.20	-10.27684	-8.44684	2.340627
CH2(OCH3)2	!dimethoxymethane	1.20E+09	9.08	-10.38339	-8.55339	2.447473
CH3-C(CH3)(OCH3)CH2-OH	!2-methyl-2-methoxy propanol	8.40E+08	8.92	-10.29167	-8.46167	3.011841
CH3-O-CH2-CH2-OH	!2-methoxyethanol	1.30E+09	9.11	-10.57917	-8.74917	2.720358
C2H5-O-CH2-CH2-OH	!2-ethoxyethanol	1.70E+09	9.23	-10.48799	-8.65799	2.643535
HO-CH2-CH2-O-CH2-CH2-OH	!diethylene glycol	2.10E+09	9.32	-10.58134	-8.75134	2.384354
CH3-CO-CO-CH3	!2,3-butanedion	2.80E+08	8.45	-10.42726	-8.59726	-0.5169114
CH3-CH2-CO-CH3	!2-butanone	8.10E+08	8.91	-10.51649	-8.68649	0.8809061
CH3-CO-CH3	acetone	1.10E+08	8.04	-10.66836	-8.83836	0.8443826
CH3-CH2-CH2-CO-CH3	!2-pentanone	1.90E+09	9.28	-10.53028	-8.70028	0.8842067
CH3-CH2-CO-CH2-CH3	!3-pentanone	1.40E+09	9.15	-10.39733	-8.56733	0.9147174
CH3-CO-CH(OH)-CH3	!3-hydro-2-butanone	2.90E+09	9.46	-10.4004	-8.5704	0.6729621
(CH3)2-CH-CH2-CO-CH3	!methyl-iso-butyl ketone	2.10E+09	9.32	-10.50366	-8.67366	0.8847981
CH3-CO-CH2CH2-CO-CH3	acetonyl acetone	7.60E+08	8.88	-10.55812	-8.72812	0.5975642
HCHO	formaldehyde	1.00E+09	9.00	-10.78296	-8.95296	0.7926633
CH3-CHO	!acetaldehyde	9.50E+08	8.98	-10.72027	-8.89027	0.8346022
CH3-CH2-CHO	!propionaldehyde	2.20E+09	9.34	-10.58833	-8.75833	0.8641795
CH3-CH2-CH2-CHO	!butyraldehyde	3.90E+09	9.59	-10.59022	-8.76022	0.8685883
(CH3)2-CH-CHO	isobutyl aldehyde	2.90E+09	9.46	-10.4711	-8.6411	0.9016389
CH3-C(CH3)(OCH3)-CHO	!2-methyl-2-methoxy-propanal	3.99E+09	9.60	-10.19846	-8.36846	0.751712
HO-C(CH3)2-CHO	!hydroxy-iso-butylaldehyde	3.00E+09	9.48	-10.51888	-8.68888	0.5663642
CH3-CO-CHO	!methyl glyoxal	5.30E+08	8.72	-10.44341	-8.61341	-0.5637148
HCOOCH2CH3	ethyl formate	3.90E+08	8.59	-11.50189	-9.67189	1.023383
CH3-COO-CH3	!methyl acetate	1.20E+08	8.08	-11.40985	-9.57985	1.099622
CH3-COO-CH2-CH3	!ethyl acetate	4.00E+08	8.60	-11.24806	-9.41806	1.148494
CH3-COO-CH2-CH2-CH3	!propyl acetate	1.40E+09	9.15	-11.18701	-9.35701	1.153689
CH3-CH2-COO-CH3	!methyl propionate	4.50E+08	8.65	-11.23087	-9.40087	1.145877
CH3-CH2-COO-CH2-CH3	!ethyl propionate	8.70E+08	8.94	-11.22122	-9.39122	1.196556
CH3-COO-CH2CH2OH	!2-hydroxyethyl acetate	9.10E+08	8.96	-11.04306	-9.21306	1.060454
CH3COOCH(CH3)2	!isopropyl acetate	4.50E+08	8.65	-11.1843	-9.3543	1.194501

CH3-COO-(CH2)3-CH3	!n-butylacetate	1.80E+09	9.26	-11.17429	-9.34429	1.152853
CH3-(CH2)2-COO-CH3	methyl butyrate	1.70E+09	9.23	-11.24771	-9.41771	1.149702
CH3-(CH2)2-COO-CH2-CH3	ethyl butyrate	1.60E+09	9.20	-11.19034	-9.36034	1.199758
CH3CH2-O-CO-CH2-COO-CH2CH3	diethyl malonate	6.50E+08	8.81	-11.22127	-9.39127	0.7714942
CH3CH2-O-CO-(CH2)2-COO-CH2CH3	diethylsuccinate	7.80E+08	8.89	-11.1582	-9.3282	0.9063339
CH3-O-CH2-COO-CH3	methyl methoxy acetate	1.80E+09	9.26	-11.03721	-9.20721	1.063044
H-COOH	formic acid	1.30E+08	8.11	-11.81994	-9.98994	0.9572287
CH3-COOH	acetic acid	1.70E+07	7.23	-11.61804	-9.78804	0.9760237
CH3-CH2-COOH	!propionic acid	3.20E+08	8.51	-11.43741	-9.60741	1.01772
CH3-(CH2)2-COOH	!butyric acid	2.20E+09	9.34	-11.44889	-9.61889	1.024579
CH3-(CH2)6-COOH	caprylic acid	4.80E+09	9.68	-11.25724	-9.42724	1.024105
CH3-(CH2)7-COOH	Azelaic acid	5.40E+09	9.73	-11.2154	-9.3854	1.023791
(CH3)2CHCH2COOH	!3-methylbutyric acid	1.40E+09	9.15	-11.41208	-9.58208	1.040318
(CH3)3-C-COOH	!tri-methyl-acetic acid	6.50E+08	8.81	-11.23537	-9.40537	1.124628
CH3-C(CH3)(OCH3)-COOH	!2-methyl-2-methoxy-propanoic acid	7.73E+08	8.89	-10.63404	-8.80404	0.9379864
HOCH2COOH	!glycolic acid	5.40E+08	8.73	-11.65826	-9.82826	0.8873319
CH3-CH(OH)-COOH	!lactic acid	4.30E+08	8.63	-11.28919	-9.45919	0.7232831
CH3CH2CH(OH)COOH	!2-hydroxybutyric acid	1.30E+09	9.11	-11.26127	-9.43127	1.089727
HO-CH2-(CHOH)4-COOH	!glucuronic acid	1.30E+09	9.11	-10.82001	-8.99001	0.6729594
CHOCOOH	glyoxylic acid	5.90E+08	8.77	-11.3587	-9.5287	-0.7367213
CH3COCOOH	pyruvic acid	1.20E+08	8.08	-11.17299	-9.34299	-0.5833086
CH3-COCHO	pyruvic aldehyde	6.49E+08	8.81	-10.44303	-8.61303	-0.563917
HOOC-CH2-COOH	!malonic acid	1.60E+07	7.20	-11.74597	-9.91597	-0.5409926
HOOC-(CH2)2-COOH	!succinic acid	1.10E+08	8.04	-11.597	-9.767	0.7170363
HOOC-(CH2)3-COOH	!glutaric acid	8.30E+08	8.92	-11.55724	-9.72724	0.8186073
HOOC-(CH2)4-COOH	!adipic acid	2.00E+09	9.30	-11.33201	-9.50201	0.7043018
HOOC-(CH2)6-COOH	!saberic acid	4.80E+09	9.68	-11.44787	-9.61787	0.9421537
HOOC-(CH2)7-COOH	!azelaic acid	5.40E+09	9.73	-11.27873	-9.44873	0.9605793
HOOC-(CH2)8-COOH	!sabacic acid	6.40E+09	9.81	-11.24963	-9.41963	0.9912882
HOOC-CH(OH)-CH(OH)-COOH	!tartaric acid	7.00E+08	8.85	-11.41339	-9.58339	0.4464404
HOOC-CH2-C(COOH)(OH)-CH2-COOH	!citric acid	5.00E+07	7.70	-11.64445	-9.81445	0.3078744
HOOC-CH(OH)-COOH	!tartoronic acid	1.70E+08	8.23	-11.81043	-9.98043	0.2966391
HOOC-CH2-CH(OH)-COOH	!malic acid	8.20E+08	8.91	-11.53031	-9.70031	0.4883153
Cl-CH2-COOH	chloroacetic acid	4.30E+07	7.63	-11.57351	-9.74351	0.6216664
CH3-Cl	monochloromethane	5.50E+07	7.74	-11.33756	-9.50756	1.599236
Cl2-CH2	dichloromethane	5.80E+07	7.76	-11.38951	-9.55951	0.5949168
Br2-CH2	dibromomethane	9.90E+07	8.00	-10.95719	-9.12719	-0.05173813
BrCl2CH	bromodichloromethane	7.10E+07	7.85	-11.47995	-9.64995	-0.6316573
Cl3C-CHCl2	pentachlroethane	1.00E+07	7.00	-11.86976	-10.03976	-0.6803114
CHBr2Cl	chlorodibromomethane	8.30E+07	7.92	-11.16707	-9.33707	-0.7282994
CHBr3	tribromomethane	1.50E+08	8.18	-11.07151	-9.24151	-0.7477874
BrCH2-CH2Br	1,2-dibromoethane	2.60E+08	8.41	-11.01309	-9.18309	0.00074076
CH3-CHCl2	1,1-dichloroethane	1.30E+08	8.11	-11.42285	-9.59285	0.5827897
CH2Cl-CH2Cl	1,2-dichloroethane	2.00E+08	8.30	-11.41638	-9.58638	0.6849483
Br2CH-CHBr2	1,1,2,2-tetrabromoethane	2.20E+08	8.34	-10.94151	-9.11151	-0.6516382
Cl3C-CH2Cl	1,1,1-2-tetrachloroethane	1.80E+07	7.26	-11.79226	-9.96226	0.4848345
ClCH2-CHCl2	1,1.-2-trichloroethane	1.10E+08	8.04	-11.56405	-9.73405	0.17132
CCl3-CH3	1,1,1-trichloroethane	1.00E+08	8.00	-11.99181	-10.16181	-0.2648686
CH3CH2CH2-Cl	1-chloropropane	2.50E+09	9.40	-11.13376	-9.30376	1.519827
CH2Cl-CHCl-CH2Br	1,2-dichloro-3-bromopropane	7.30E+08	8.86	-11.04351	-9.21351	0.2836433
CH2Br-CH2-CH2Br	1,3-dibromopropane	4.10E+09	9.61	-10.88648	-9.05648	0.3616003
CH2Cl-CHCl-CH3	1,2-dichloropropane	4.00E+08	8.60	-11.28917	-9.45917	1.114866
CH3-(CH2)3-Cl	1-chlorobutane	3.40E+09	9.53	-11.13331	-9.30331	1.510461
Br-CH2-CH2-OH	2-bromoethanol	3.50E+08	8.54	-10.8385	-9.0085	0.6344152
Cl-CH2-CH2-OH	2-chloroethanol	9.50E+08	8.98	-11.14609	-9.31609	1.293984
CCl3-CH2-OH	2,2,2-trichloroethanol	4.20E+08	8.62	-11.68246	-9.85246	-0.2747993
CF3-CH2-OH	2,2,2-trifluoroethanol	2.30E+08	8.36	-12.0465	-10.2165	1.395035
CCl3-CH(OH)2	chloral hydrate	3.10E+09	9.49	-11.71673	-9.88673	-0.2992691
CF3-CHClBr	Halothane	1.30E+07	7.11	-12.26293	-10.43293	-0.3346105
CHCl3	chloroform	1.40E+07	7.15	-11.77096	-9.94096	-0.3031954
CF3-CHCl2	2,2-dichloro-1,1,1-trifluoroethane	1.30E+07	7.11	-12.07176	-10.24176	-0.3564039
CHF2-O-CHCl-CF3	Isoflurane	2.40E+07	7.38	-12.10108	-10.27108	-0.2714219
CHF2-O-CF2-CHFCl	Enflurane	9.50E+06	6.98	-12.26368	-10.43368	-0.4409282
CH3-O-CF2-CHCl2	Methoxyflurane	8.30E+07	7.92	-11.42938	-9.59938	-0.0711531
H3C-S-CH3	dimethyl sulfide	1.90E+10	10.28	-8.480959	-6.650959	0.93672
H3C-S-S-CH3	di-methyl-di-sulfides	1.70E+10	10.23	-8.187714	-6.357714	-1.5168
H3C-CH2-S-CH2-CH3	di-ethyl-sulfides	1.40E+10	10.15	-8.442901	-6.612901	0.8614488
H3C-CH2-S-S-CH2-CH3	di-ethyl-di-sulfides	1.40E+10	10.15	-8.125221	-6.295221	-1.456254
(CH3)2-CH-S-S-CH-(CH3)2	di-ethyl-methyl-di-sulfides	2.00E+10	10.30	-8.066539	-6.236539	-1.357738
CH3-S-CH2-CH2-OH	2-methylthio-ethanol	7.90E+09	9.90	-8.585316	-6.755316	0.7303413
H3C-S-CH2-CH2-CHO	methional	8.20E+09	9.91	-8.758738	-6.928738	0.5407815
HO-CH2-CH2-S-CH2-CH2-OH	2,2'-thiodiethanol	2.00E+10	10.30	-8.684018	-6.854018	0.5429511
HO-CH2CH2CH2-S-CH2CH2CH2-OH	3,3'-thiodiethanol	1.40E+10	10.15	-8.554573	-6.724573	0.6732906
HOOC-CH2-S-CH2-COOH	thiodiacetic acid	6.00E+09	9.78	-9.59493	-7.76493	-0.6227674
CH3-SO-CH3	di-methyl-sulfoxide	6.50E+09	9.81	-9.53044	-7.70044	0.8079428
CH3-CH2-SO-CH2-CH3	di-ethyl-sulfoxide	6.50E+09	9.81	-9.461343	-7.631343	0.7123829
CH3-CH2-CH2-SO-CH2-CH2-CH3	di-propyl-sulfoxide	6.30E+09	9.80	-9.464796	-7.634796	0.7194619
(CH3)2CH-SO-CH(CH3)2	di(1-methyl-ethyl)sulfoxide	6.80E+09	9.83	-9.361073	-7.531073	0.6316707
(CH3)3-C-SO-C-(CH3)3	di-tert-butyl-sulfoxide	5.30E+09	9.72	-9.243156	-7.413156	0.4398249
(CH3-CH2-CH2-CH2)2-SO	di-butyl-sulfoxide	8.00E+09	9.90	-9.461222	-7.631222	0.7111593
CH3-SO-CH2-S-CH3	methyl methyl thiomethyl sulfoxide	4.80E+09	9.68	-8.76255	-6.93255	0.2166057
HO-CH2CH2-SO-CH2CH2-OH	di(2-hydroxyethyl) sulfoxide	5.30E+09	9.72	-9.734745	-7.904745	0.4641739
(CH3)2-CH-SO-CH-(CH3)2	diisopropyl sulfoxide	6.80E+09	9.83	-9.355276	-7.525276	0.6113388
HS-CH2-CH2-OH	mercaptoethanol	6.80E+09	9.83	-9.041336	-7.211336	0.6572682
HS-CH2-COOH	mercaptoacetic acid	1.20E+09	9.08	-9.267602	-7.437602	0.1983789
HS-CH2-COOCH3	methyl thioglycolate	2.10E+10	10.32	-9.195185	-7.365185	0.2886098
HS-CH2-CH(OH)-CH(OH)-CH2-SH	dithiothreitol	1.50E+10	10.18	-8.908919	-7.078919	0.4106834
CH3-CN	acetonitrile	2.20E+07	7.34	-12.46419	-10.63419	1.66406
CN-CN	cyanogen	1.00E+07	7.00	-13.30628	-11.47628	-0.2375803
CH3-CH2-CN	propionitrile	9.30E+07	7.97	-11.99011	-10.16011	1.708873

NC-CH2-CH2-CN	succino nitrile	3.00E+07	7.48	-12.31428	-10.48428	1.026906
CCl3CN	trichloroacetonitrile	3.90E+07	7.59	-12.533	-10.703	-0.9552739
H2N-CN	cyanamide	8.70E+06	6.94	-10.79421	-8.96421	1.619838
H-CN	hydrogen cyanide	6.00E+07	7.78	-13.67734	-11.84734	1.725668
CH3-CH2-CH2-NO2	1-nitropropane	2.50E+08				
(CH3)2-CH-NO2	2-nitropropane	8.00E+07				
CH2ClNO2	chloronitromethane	1.94E+08				
CHCl2NO2	dichloronitromethane	5.12E+08				
CH2BrNO2	bromonitromethane	8.36E+07				
CHBr2NO2	dibromonitromethane	4.75E+08				
CHBrClNO2	bromochloronitromethane	4.20E+08				
CH3-CO-NH2	acetamide	1.90E+08	8.28	-10.53649	-8.70649	1.531495
HO-CH2-CO-NH2	glycolamide	1.10E+09	9.04	-10.51591	-8.68591	1.455724
HO-CH(CH3)-CO-NH2	2-hydroxypropionamide	1.30E+09	9.11	-10.57368	-8.74368	1.365525
(CH3)2-CH-CO-NH2	2-methylpropionamide	1.60E+09	9.20	-10.47292	-8.64292	1.61425
C2H5-CO-NH2	propionamide	7.00E+08	8.85	-10.493	-8.663	1.577841
(CH3)3-C-CO-NH2	trimethylacetamide	1.50E+09	9.18	-10.45896	-8.62896	1.638468
(CH3)2-CH-CO-NH2	isobutyramide	1.60E+09	9.20	-10.47933	-8.64933	1.60468
CH3-CO-NH-C-(CH3)3	N-tert-butyl-acetamide	1.10E+09	9.04	-9.884847	-8.054847	1.600515
CH3-CO-NH-CH3	N-methylacetamide	1.60E+09	9.20	-9.912984	-8.082984	1.52948
(CH3)2-CH-CO-NH-CH3	N-butylformamide	1.90E+09	9.28	-9.872602	-8.042602	1.582228
(CH3)3-C-CO-NH-CH3	N-methyl-pivalamide	2.40E+09	9.38	-9.848647	-8.018647	1.652937
CH3-CH2-CO-NH-CH3	N-methyl-propionamide	1.40E+09	9.15	-9.882551	-8.052551	1.576084
(CH3)2-CH-CO-NH-CH3	N-methylisobutyramide	1.90E+09	9.28	-9.878726	-8.048726	1.565597
H-CO-N-(CH3)2	N,N-dimethyl formamide	1.70E+09	9.23	-10.07748	-8.24748	1.513837
H-CO-NH-CH3	N-methyl-formamide	1.20E+09	9.08	-10.03077	-8.20077	1.559681
CH3-CO-N-(CH3)2	N,N-dimethyl acetamide	3.50E+09	9.54	-9.494224	-7.664224	1.487585
(CH3)3-C-CO-N-(CH3)2	N,N-dimethyl pivalamide	3.90E+09	9.59	-9.429583	-7.599583	1.598679
H2N-CH2-CO-NH2	2-aminoacetamide	2.80E+09	9.45	-10.27474	-8.44474	1.551645
CH3-NH2	methyl amine	5.70E+09	9.76	-9.752981	-7.922981	3.811647
CH3-CH2-NH2	ethyl amine	6.40E+09	9.81	-9.686995	-7.856995	3.65019
CH3-(CH2)3-NH2	N-butyl amine	8.20E+09	9.91	-9.691511	-7.861511	3.527124
CH3-CH2-CH2-NH2	propyl amine	7.30E+09	9.86	-9.688557	-7.858557	3.586944
H2N-CH2-CH2-NH2	ethylenediamine	5.50E+09	9.74	-9.748913	-7.918913	3.280833
(CH3)3-C-NH2	tert-butyl amine	6.00E+09	9.78	-9.835228	-8.005228	3.530262
CH3-(CH2)4-NH2	N-amyl amine	7.00E+09	9.85	-9.693243	-7.863243	3.490922
CH3-(CH2)5-NH2	Hexylamine	1.30E+10	10.11	-9.692966	-7.862966	3.464632
CH3-(CH2)7-NH2	N-octylamine	1.46E+10	10.16	-9.692657	-7.862657	3.432262
(CH3)2-CH-NH2	iso-propyl amine	1.30E+10	10.11	-9.842072	-8.012072	3.619046
CH3-O-NH2	O-methyl hydroxy amine	1.40E+10	10.15	-10.53077	-8.70077	2.763594
CH3-NH-CH3	dimethylamine	8.90E+09	9.95	-9.387733	-7.557733	3.479749
CH3-(CH2)3-NH-(CH2)3-CH3	dibutyl amine	1.80E+10	10.26	-9.289158	-7.459158	3.121498
HOOC-CH2-NH-CH2-COOH	Iminodiacetic acid	4.90E+07	7.69	-10.31659	-8.48659	0.5947785
(C2H5)2-N-OH	N,N-diethyl hydroxyl amine	1.30E+09	9.11	-9.712082	-7.882082	2.628267
(CH3(CH2)3)3-N	tributyl amine	1.70E+10	10.23	-8.953861	-7.123861	2.807584
(C2H5)3-N	triethyl amine	1.00E+10	10.00	-8.957604	-7.127604	2.879667
(CH3)3-N	trimethyl amine	1.30E+10	10.11	-9.122827	-7.292827	3.192113
(HO-CH2-CH2)3-N	triethanolamine	8.00E+09	9.90	-9.283858	-7.453858	2.262806
(CH2COOH)3-N	Nitrilotriacetic acid	2.10E+09	9.32	-10.20437	-8.37437	0.384091
(HOCH2CH2)3-N	Nitrilotriethanol	8.00E+09	9.90	-9.276757	-7.446757	2.266425
(CH3)2-N-NH2	1,1-dimethyl hydrazine	1.60E+10	10.20	-9.472585	-7.642585	2.755817
(HO-CH2)3C-NH2	2-amino-2-propane-1,3-diol	1.50E+09	9.18	-10.04871	-8.21871	2.835901
(CH3)2-N-NO	N-nitrosodimethylamine	4.30E+08	8.63	-10.0307	-8.2007	0.8459922
CH3-CH2-N(CH3)-N=O	methylethylnitrosamine	4.95E+08	8.69	-9.960921	-8.130921	0.9187226
CH3-CH2-N(N=O)-CH2-CH3	diethylnitrosamine	6.99E+08	8.84	-9.868942	-8.038942	1.004807
(CH3)2-N-NO2	dimethylnitramine	5.44E+08				
(CH3-CH2)2-N-NO2	diethyl nitramine	8.67E+08				
(CH3)(CH3CH2)-N-NO2	methyl ethyl nitramine	7.60E+08				
(CH3)(CH3-O-)2-P=O	dimethyl methylphosphonate (DMMP)	2.00E+08	8.30	-11.41011	-9.58011	1.029427
(CH3)(CH3CH2)(CH3CH2O)-PO	Diethyl methylphosphonate (DEMP)	6.00E+08	8.78	-10.9066	-9.0766	1.6096
PO4-(CH3)3	trimethyl phosphate	1.20E+08	8.08	-11.73312	-9.90312	0.503187
PO4-(CH2-CH3)3	triethyl phosphate	2.90E+09	9.46	-11.39699	-9.56699	0.6473161
PO4-(CH2-CH2-CH3)3	tributyl phosphate	1.00E+10	10.00	-11.28924	-9.45924	0.6307454
	cycloheptane	7.70E+09			1.83	
	cycloheptanol	1.70E+09			1.83	
	cyclohexane	6.10E+09			1.83	
	cyclopentane	4.50E+09			1.83	
	tetrahydrofuran	4.00E+09			1.83	
	1,4-dioxane	3.10E+09			1.83	
	1,4-dithiane	1.80E+10			1.83	
	1,3,5-trioxane	1.50E+09			1.83	
	tetramethylene sulfoxide	7.00E+09			1.83	
	2-methyl-1,3-dioxalane	3.50E+09			1.83	
	1,3-dioxolane	4.00E+09			1.83	
	ethylene oxide	6.80E+07			1.83	
	1,2-epoxybutane	7.80E+08			1.83	
	1,2-epoxypropane	2.50E+08			1.83	
	2,3-epoxypropanol	4.70E+08			1.83	
H2C=CHCH2OH	allyl alcohol	5.90E+09	9.77	-10.04281	-8.21281	1.21865
H2C=CHCH2CH3	1-butene	7.00E+09	9.85	-9.925002	-8.095002	1.369879

H2C=CHCOCH3	1-butene-3-one	8.50E+09	9.93	-10.64627	-8.81627	-0.06871939
H2C=CHCONH2	acrylamide	5.90E+09	9.77	-10.55344	-8.72344	0.1649501
H2C=CHCHO	acrolein	7.00E+09	9.85	-10.69461	-8.86461	-0.138328
H2C=CHCOOH	acrylic acid	1.50E+09	9.18	-11.172	-9.342	-0.1215594
H2C=CHCOOCH2CH2OH	2-hydroxyethyl acrylate	1.10E+10	10.04	-11.02822	-9.19822	-0.06259909
H2C=CHCl	vinyl chloride	1.20E+10	10.08	-10.20941	-8.37941	0.8561512
H2C=CHCH2CN	allyl cyanide	6.90E+09	9.84	-10.50379	-8.67379	0.824497
H2C=CHCN	acrilonitrile	5.30E+09	9.72	-10.8575	-9.0275	0.04998269
H2C=CHCH3	propylene	7.00E+09	9.85	-9.982217	-8.152217	1.351431
H2C=CCl2	vinylidine chloride	6.80E+09	9.83	-10.18964	-8.35964	0.3793356
H2C=C(CH3)-CO-NH2	methyl acrylamide	1.30E+10	10.11	-10.42105	-8.59105	0.1893389
H2C=C(CH3)COOCH3	methyl methacrylate	1.10E+10	10.04	-10.36607	-8.53607	-0.03770118
(CH3)2C=CH2	isobutylene	5.40E+09	9.73	-9.594924	-7.764924	1.277581
H2C=C(CH3)CN	methacylonitrile	1.20E+10				
H2C=C(CH3)COOCH3	methyl methacrylate	1.10E+10				
CH3CH=CHCHO	crotonaldehyde	5.80E+09	9.76	-10.44213	-8.61213	-0.141633
HOOC-CH=CH-COOH (cis)	maleic acid	6.00E+09				
ClCH=CHCl (cis)	dichloroethylene	3.80E+09				
HOOC-CH=CH-COOH (trans)	fumaric acid	6.00E+09	9.78	-11.6333	-9.8033	-1.204368
ClCH=CHCl (trans)	dichloroethylene	4.40E+09	9.64	-10.01435	-8.18435	0.3390446
Cl2C=CCl2	tetrachloroethylene	2.00E+09	9.30	-9.899768	-8.069768	-0.4371864
	1,4-cyclohexadiene	7.70E+09				
	cyclopentene	7.00E+09				
	cyclohexene	8.80E+09				
	trichloroethene	2.90E+09	9.46	-9.955593	-8.125593	-0.06103172
	etheylene	4.40E+09	9.64	-10.55205	-8.72205	1.438299
	Uracil	5.70E+09	9.76	-9.971515	-8.141515	-0.3183682
	5-azauracil	7.00E+09	9.85	-11.05554	-9.22554	-0.5902089
	6-azauracil	4.50E+09	9.65	-10.55661	-8.72661	-0.6103272
	5-bromouracil	4.00E+09	9.60	-9.806242	-7.976242	-0.6673521
	5-chlorouracil	5.50E+09	9.74	-9.756308	-7.926308	-0.601387
	5-fluorouracil	5.20E+09	9.72	-9.81127	-7.98127	-0.6562816
	dihydro-6-methyluracil	1.30E+09	9.11	-10.52412	-8.69412	0.4678679
	5-nitro-6-methyluracil	5.30E+09				
	5-nitrouracil	5.40E+09				
	thymine	6.40E+09	9.81	-9.607611	-7.777611	-0.2941526
	6-azathymine	2.80E+09	9.45	-10.17861	-8.34861	-0.5449313
	maleic hydrazide	2.90E+09	9.46	-9.948973	-8.118973	-1.067842
	isouramil	5.00E+09	9.70	-8.735811	-6.905811	-0.07312837
	cytosine	6.30E+09	9.80	-9.383221	-7.553221	-0.09800104
	5-methylcytosine	6.00E+09	9.78	-9.156627	-7.326627	-0.07697516
	6-azacytosine	4.50E+09	9.65	-9.936148	-8.106148	-0.4477363
	5-azacytosine	2.10E+09	9.32	-9.973156	-8.143156	-0.09400064
	N-ethylmaleimide	9.00E+09	9.95	-10.52536	-8.69536	-1.103325
	6-methyl uracil	5.70E+09				
C6H5-CH2CH3	ethylbenzene	7.50E+09	9.88	-9.363271	-7.533271	0.5302613
C6H5-OH	phenol	6.60E+09	9.82	-9.115282	-7.285282	0.3974596
C6H5-F	fluorobenzene	5.70E+09	9.76	-9.545124	-7.715124	0.1636994
C6H5Cl	chlorobenzene	4.30E+09	9.63	-9.560975	-7.730975	0.1546716
C6H5-Br	bromobenezene	4.80E+09	9.68	-9.601476	-7.771476	0.05965194
C6H5-I	iodobenzene	5.30E+09	9.72	-9.647136	-7.817136	0.06134555
C6H5-CN	benzonitrile	3.90E+09	9.59	-10.02129	-8.19129	-0.3946016
C6H5-NO2	nitrobenzene	3.90E+09				
C6H5-CHO	benzaldehyde	4.40E+09	9.64	-10.00277	-8.17277	-0.4348125
C6H5-COOH	benzoic acid	4.30E+09	9.63	-10.08448	-8.25448	-0.4684967
C6H5-COCH3	acetophenone	6.40E+09	9.81	-9.936084	-8.106084	-0.361914
C6H5-CONH2	benzamide	4.60E+09	9.66	-9.942663	-8.112663	-0.2145394
C6H5-SOCH3	methyl phenyl sulfoxide	9.70E+09	9.99	-9.260956	-7.430956	-0.1992762
C6H5-CH2OH	benzylalcohol	8.40E+09	9.92	-9.382318	-7.552318	0.4754084
C6H5-NH-CO-CH3	acetanilide	5.20E+09	9.72	-8.765536	-6.935536	0.3259316
C6H5-SO3H	benzenesulfonic acid	2.10E+09	9.32	-10.42274	-8.59274	-0.8968664
C6H5-NH-OH	phenyl hydroxylamine	1.50E+10	10.18	-8.098616	-6.268616	0.7375505
C6H5-CH2CH2-C(CH3)2-OH	2-methyl-4-phenyl-2-butanol	5.90E+09	9.77	-9.287429	-7.457429	0.5829438
C6H5-CHOHCH(CH3)2	2-methyl-1-phenyl-1-propanol	9.50E+09	9.98	-9.383857	-7.553857	0.5120207
C6H5-CHOHCH3	phenylethanol	1.10E+10	10.04	-9.387175	-7.557175	0.5058496
C6H5-CH(OH)(CH2-CH3)	1-phenyl-1-propanol	1.00E+10	10.00	-9.455846	-7.625846	0.4862124
C6H5-CH2-CH2--OH	1-phenyl-2-propanol	2.10E+10	10.32	-9.473491	-7.643491	0.4123215
C6H5-O-CH3	anisol	5.40E+09	9.73	-9.004682	-7.174682	0.4837376
-O-COOH	phenoxyacetic acid	1.00E+10	10.00	-9.617941	-7.787941	0.0243417
(C6H5)2-CO	benzophenone	9.00E+09	9.95	-9.84922	-8.01922	-0.6259145
(C6H5)2-NH	diphenylamine	1.00E+10	10.00	-8.042634	-6.212634	0.1528785
(C6H5)2-SO	diphenyl sulfoxide	6.30E+09	9.80	-9.223753	-7.393753	-0.2421511
C6H5-CH3	toluene	5.10E+09	9.71	-9.330592	-7.500592	0.520049
C6H5-NH2	aniline	1.70E+10	10.23	-8.21347	-6.38347	0.7582679
H3C-C6H4-CH3	o-xylene	6.70E+09	9.83	-9.168906	-7.338906	0.5253025
H3C-C6H4-CH3	m-xylene	7.50E+09	9.88	-9.190805	-7.360805	0.5293261
H3C-C6H4-CH3	p-xylene	7.00E+09	9.85	-9.061137	-7.231137	0.4863504
C6H4-Cl2	1,2-dichlorobenzene	4.00E+09	9.60	-9.601684	-7.771684	-0.1421155
C6H4-Cl2	1,3-dichlorobenzene	5.70E+09	9.76	-9.681361	-7.851361	-0.1582009
C6H4-Cl2	1,4-dichlorobenzene	5.40E+09	9.73	-9.524891	-7.694891	-0.2155087
C6H4-(OCH3)2	1,2-dimethoxybenzene	5.20E+09	9.72	-8.629187	-6.799187	0.4657356
C6H4-(OCH3)2	1,3-dimethoxybenzene	7.20E+09	9.86	-8.865617	-7.035617	0.4848553
C6H4-(OCH3)2	1,4-dimethoxybenzene	7.00E+09	9.85	-8.551408	-6.721408	0.3840715
(CH3)3-C-C6H4-OH	tert-butylphenol	1.90E+10	10.28	-8.894211	-7.064211	0.47087
CN, CN	1,4-dicyanobenzene	7.80E+08	8.89	-10.342550	-8.51255	-1.166878
F, F	o-difluorobenzene	7.50E+09	9.88	-9.632658	-7.802658	-0.1913946
F, F	p-difluorobenzene	1.00E+10	10.00	-9.490196	-7.660196	-0.2138308
-CH3, -CH3, -CH3	1,2,3-trimethyl benzene	7.00E+09	9.85	-9.135165	-7.305165	0.5717542
	1,2,4-trimethyl benzene	6.20E+09	9.79	-8.964077	-7.134077	0.5046272
	1,3,5-trimethyl benzene (mesitylene)	6.40E+09	9.81	-9.1668	-7.3368	0.5768769

-OCH3, -OCH3, -OCH3	1,2,3-trimethoxybenzene	7.00E+09	9.85	-8.57087	-6.74087	0.5082324
	1,2,4-trimethoxybenzene	6.20E+09	9.79	-8.390726	-6.560726	0.4095613
	1,3,5-trimethoxybenzene	8.10E+09	9.91	-8.96364	-7.13364	0.539712
-OH, -OH, -OH	1,2,4-trihydroxybenzene	8.60E+09	9.93	-8.685031	-6.855031	0.1685672
-OH, -OH, -C(CH3)3	tert-butyl hydroquinone	6.30E+09	9.80	-8.623081	-6.793081	0.2502026
-Cl, -Cl, -OH	2,4-dichlrophenol	7.10E+09	9.85	-9.230422	-7.400422	-0.1966052
-Cl, -Cl, -O-COOH	2,4-dichlorophenoxyacetic acid	6.60E+09	9.82	-9.627147	-7.797147	-0.550822
-F, -F, -F	1,3,5-trifluorobenzene	4.10E+09	9.61	-10.07859	-8.24859	-0.4993107
-F, -F, -F	1,2,3-trifluorobenzene	3.70E+09	9.57	-9.935002	-8.105002	-0.5078655
-F, -F, -F	1,2,4-trifluorobenzene	3.90E+09	9.59	-9.673085	-7.843085	-0.5498641
-OH, -OH, -OH	phloroglucinol	1.00E+10	10.00	-9.235044	-7.405044	0.3088495
	1,2,3,4-tetramethylbenzene	7.20E+09	9.86	-8.902376	-7.072376	0.5368509
	1,2,3,4-tetrafluorobenzene	8.00E+09	9.90	-9.940006	-8.110006	-0.8556418
	1,2,3,5-tetramethylbenzene	7.10E+09	9.85	-8.910298	-7.080298	0.5395229
	1,2,4,5-tetramethylbenzene	7.00E+09	9.85	-8.819628	-6.989628	0.5005955
	1,2,4,5-tetramethoxybenzene	7.00E+09	9.85	-8.115336	-6.285336	0.3806553
-Cl, -Cl, -Cl, -OH	2,4,5-trichlorophenol	1.20E+10	10.08	-9.322358	-7.492358	-0.5108725
1,2,4,5-Cl, OH, OH, Cl	2,5-dichlorohydroquinone	2.10E+10	10.32	-8.982342	-7.152342	-0.4068606
	pentafluorobenzene	7.00E+09	9.85	-10.06738	-8.23738	-1.183294
	pentamethylbenzene	7.50E+09	9.88	-8.787662	-6.957662	0.542161
F, F, F, F,F, -COCH3	pentafluoroacetophenone (PFA)	1.50E+09	9.18	-10.20297	-8.37297	-1.681022
F, F, F, F, F, CHO	pentafluorobenzaldehyde	2.00E+09	9.30	-10.28462	-8.45462	1.775973
F, F, F,F, F, -COOH	pentafluorobenzoic acid	1.10E+09	9.04	-10.31038	-8.48038	-1.830766
F, F, F, F,F -NH2	pentafluoroaniline	9.60E+09	9.98	-9.102796	-7.272796	-0.9412494
F,F,F,F,F, -OH	pentafluorophenol	9.50E+09	9.98	-9.939639	-8.109639	-1.2963
	pentafluoroiododobenzene	1.20E+09	9.08	-10.2148	-8.3848	-1.469127
	hexafluorobenzene	1.40E+09	9.15	-10.37	-8.53846	-1.479236
	hexamethylbenzene	7.20E+09	9.86	-8.750388	-6.920388	0.5751311
-F, -F, -F, -F, -OH, -OH	tetrafluorohydroquinone	3.10E+09	9.49	-9.549725	-7.719725	-1.13147
-CH3	2-methyl pyridine	2.50E+09	9.40	-9.628386	-7.798386	0.1505354
-CH3	3-methyl pyridine	2.40E+09	9.38	-9.638089	-7.808089	0.133376
-NH2	2-pyridine amine	8.40E+09	9.92	-8.570785	-6.740785	0.4871594
-NH2	4-pyridine amine	5.00E+09	9.70	-8.903617	-7.073617	0.4037449
-Br	2-bromopyridine	2.40E+09	9.38	-9.892888	-8.062888	-0.303153
-Br	3-bromopyridine	1.10E+09	9.04	-9.874868	-8.044868	-0.3221716
-Cl	2-chloropyridine	1.80E+09	9.26	-9.879027	-8.049027	-0.2294526
-Cl	4-chloropyridine	3.10E+09	9.49	-10.22018	-8.39018	-0.1355081
-CN	3-cyanopyridine	7.50E+08				
-OH	2-pyridone	6.50E+09	9.81	-9.435832	-7.605832	0.1213861
-OH	3-pyridinol	5.40E+09	9.73	-9.452283	-7.622283	0.02146091
-OH	4-pyridinol	1.10E+10	10.04	-9.949773	-8.119773	0.01668134
-COOH	2-pyridine carboxylic acid	2.60E+07	7.41	-10.38682	-8.55682	-0.7652425
-COOH	3-pyridinecarboxylic acid	2.20E+07	7.34	-10.41877	-8.58877	-0.820963
-COOH	4-pyridinecarboxylic acid	6.00E+07	7.78	-10.32512	-8.49512	-0.7771906
-pyr	4,4'-bipyridine	5.30E+09	9.72	-9.923306	-8.093306	-0.7677598
-pry	2,2'-bipyridine	6.20E+09	9.79	-9.186643	-7.356643	-0.5373726
-CONH2	4-pyridinecarboxyamide	1.60E+09	9.20	-10.22076	-8.39076	-0.5112579
-CONH2	3-pyridinecarboxyamide	1.40E+09	9.15	-10.28491	-8.45491	-0.5768472
	2,6-dimethyl pyridine	3.00E+09	9.48	-9.394721	-7.564721	0.1760146
	3,5-dimethyl pyridine	8.00E+09	9.90	-9.435932	-7.605932	0.1378607
	2,4,6-trimethylpyridine	2.50E+09	9.40	-9.357427	-7.527427	0.2376713
	furan	3.90E+09	9.59	-9.317534	-7.487534	0.7230756
	2-methyl furan	1.90E+10	10.28	-9.007906	-7.177906	0.7199911
	2-furfuryl alcohol	1.50E+10	10.18	-9.174876	-7.344876	0.6181119
	2-furaldehyde	7.80E+09	9.89	-9.735093	-7.905093	-0.4559993
	2-acetyl furan	4.50E+09	9.65	-9.664335	-7.834335	-0.3647549
	2-furancarboxamide	5.50E+09	9.74	-9.674635	-7.844635	-0.1558389
	phenylfuran	1.60E+10	10.20	-8.600646	-6.770646	-0.2524168
	5-phenylfurfural	5.90E+09	9.77	-8.954058	-7.124058	-0.8471305
	furoin	1.30E+10	10.11	-9.411239	-7.581239	-0.6307386
	5-hydroxymethylfurfuryl	5.80E+09	9.76	-9.119494	-7.289494	-0.385334
	5-methylfurfural	7.20E+09	9.86	-9.245028	-7.415028	-0.5071848
	5-bromofurfural	3.90E+09	9.59	-9.726897	-7.896897	-0.7652646
	nitrofuraldehyde	5.50E+09				
	nitrofuroic acid	5.30E+09				
	nifuroxime	1.00E+10				
	nitrofurazone	1.06E+10				
	furamazone	1.03E+10				
	furadantin	9.30E+09				
	tetrahydrofuran	4.00E+09	9.60	-10.20846	-8.37846	3.116479
	indole	3.20E+10	10.51	-8.403031	-6.573031	0.3000424
		1.37E+10				
	1,2-dimethylindole	1.00E+10				
	1,3-dimethylindole	1.10E+10				
	2,3-dimethylindole	1.30E+10	10.11	-8.121906	-6.291906	0.3036284
	1-methylindole	1.50E+10	10.18	-8.30021	-6.47021	0.3248031
		1.20E+10				
	2-methylindole	3.40E+10	10.53	-8.274981	-6.444981	0.2980896
	3-methylindole	3.30E+10	10.52	-8.238073	-6.408073	0.3067786
	indole-3-acetic acid	6.50E+09	9.81	-8.843916	-7.013916	-0.1644274
	indole-3-propionic acid	8.50E+09	9.93	-8.529186	-6.699186	0.0819269
	5-methylindole	1.70E+10	10.23	-8.347065	-6.517065	0.325323
	5-nitroindole	1.00E+10				
	5-chloroindole	2.00E+10	10.30	-8.612524	-6.782524	0.041292
	5-aminoindole	3.30E+10	10.52	-7.651357	-5.821357	0.4400067
	5-bromoindole	1.60E+10	10.20	-8.654009	-6.824009	0.02258883
	5-cyanoindole	1.10E+10	10.04	-8.847144	-7.017144	-0.2170322
	5-hydroxyindole	1.70E+10	10.23	-8.301017	-6.471017	0.1543591
	5-methoxy indole	1.50E+10	10.18	-8.218704	-6.388704	0.2132235
	Indole-5-acetic acid	7.90E+09	9.90	-8.803644	-6.973644	-0.2380285

	2-(dimethylaminomethyl)-indole (gramine)	3.00E+10	10.48	-8.288119	-6.458119	0.2996526
	Melatonin	1.32E+10	10.12	-8.383657	-6.553657	-0.02848179
	Tryptophan	1.25E+10	10.10	-8.469387	-6.639387	0.1268472
	6-chloromelatonin	8.20E+09	9.91	-8.748535	-6.918535	-0.3210769
	6-hydroxy-melatonin	1.10E+10	10.04	-8.474654	-6.644654	-0.07347865
	5-methoxytryptamine	2.30E+10	10.36	-8.175366	-6.345366	0.1698762
	5-hydroxytryptamine	1.70E+10	10.23	-8.252984	-6.422984	0.113479
	indoline	3.80E+10	10.58	-8.012069	-6.182069	0.6960114
	imidazole	3.90E+09	9.59	-9.159063	-7.329063	0.9772351
	1-methyl imidazole	8.10E+09	9.91	-9.068705	-7.238705	0.9551286
	xanthine	5.20E+09	9.72	-9.335711	-7.505711	-0.5102662
	theophilline	6.30E+09	9.80	-9.065549	-7.235549	-0.3744477
	theobromine	5.80E+09	9.76	-9.017918	-7.187918	-0.4077799
	1-hypoxanthine	6.50E+09	9.81	-9.499949	-7.669949	-0.6002567
	isoguanine	1.20E+10	10.08	-8.931677	-7.101677	-0.4709503
	guanine	9.20E+09	9.96	-8.599816	-6.769816	-0.1587732
	caffeine	6.90E+09	9.84	-8.946396	-7.116396	-0.3416989
	allopurinol	7.00E+08	8.85	-9.623034	-7.793034	-0.5682302
	purine	3.00E+08	8.48	-9.641496	-7.811496	-0.566691
	6-methyl purine	4.60E+08	8.66	-9.579273	-7.749273	-0.5272966
	6-methoxy purine	2.00E+09	9.30	-9.537105	-7.707105	-0.503417
	2-aminopurine	3.00E+09	9.48	-8.430102	-6.600102	0.2551631
	adenine	5.80E+09	9.76	-8.665549	-6.835549	-0.5752795
	N,N-dimethyladenine	7.10E+09				
	2-mercaptopurine	4.40E+09	9.64	-8.669272	-6.839272	-1.05871
	6-mercaptopurine	7.00E+09	9.85	-8.826919	-6.996919	-1.121564
	carbendazim	2.20E+09	9.34	-8.719607	-6.889607	-0.1053538
	thiophene	8.20E+09	9.91	-9.217519	-7.387519	0.2388409
	2,5-dimethylthiophene	7.20E+09	9.86	-8.960532	-7.130532	0.192614
	2-methylthiophene	3.20E+09	9.51	-9.167394	-7.337394	0.2153039
	3-methylthiophene	3.20E+09	9.51	-8.960335	-7.130335	0.2716238
	2,2'-bithiophene	1.60E+10	10.20	-8.582865	-6.752865	-0.5731946
	2-iodo-3,5-dinitrothiophene	2.10E+09				
	3-nitro-2-(4-nitrophenoxy)thiophene	1.30E+09				
	tetrahydrothiophene	1.40E+10				
	atrazine	2.00E+09	9.30	-9.4324	-7.6024	0.02653915
	cyanuric acid	2.00E+07	7.30	-11.16566	-9.33566	-0.5236035
	simazine	2.10E+09	9.32	-9.322888	-7.492888	0.1204403
	prometone	2.50E+09	9.40	-9.356476	-7.526476	0.3281624
	1,3,5-triazine	3.40E+09	9.53	-11.31689	-9.48689	-0.5514946
	2,4,6-trimethoxy-1,3,5-triazine	2.06E+08	8.31	-10.63024	-8.80024	-0.1619785
	dioxohexahydrotriazine	1.61E+09	9.21	-10.3639	-8.5339	0.5279263
	simetone	4.70E+09	9.67	-9.172058	-7.342058	0.5188141
	ametryne	2.60E+10	10.41	-8.658154	-6.828154	0.193481
	simetryne	2.60E+10	10.41	-8.596725	-6.766725	0.3103282
	terbutazine	2.80E+09	9.45	-9.291797	-7.461797	0.1537872
	cyanazine	1.90E+09	9.28	-9.554059	-7.724059	-0.1189912
	2-chloro-4,6-diamino-s-triazine	5.00E+07	7.70	-9.729335	-7.899335	-0.01503109

APPENDIX E: QUANTUM MECHANICALLY OPTIMIZED STRUCTURES IN THE GASEOUS AND AQUEOUS PHASES FOR NEUTRAL COMPOUNDS

The structure on the left is optimized geometry of molecules and radicals in the gaseous phase using G1, G2 and G3 methods (i.e., geometry optimization is conducted with MP2(Full)/6-31G(d). The optimized geometry includes numbers and labels of each atom as well as atomic charges that were obtained from Mulliken's charge distribution (charges were shown in the parentheses). The Z-matrix is also given for the gaseous phase optimizes structure. The vector indicates direction of the dipole moment. The structure on the right is optimized geometry that is used for calculating free energy of solvation.

H_2O

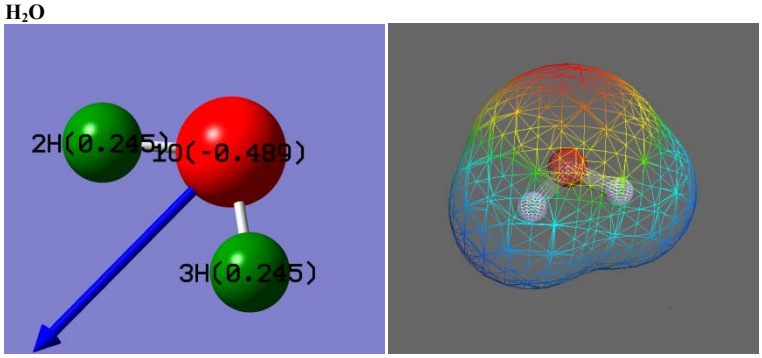

Row	Highlight	Tag	Symbol	NA	NB	NC	Bond	Angle	Dihedral
1	No	1	O						
2	No	2	H	1			0.9685687		
3	No	3	H	1	2		0.9685687	103.9827963	

HO•

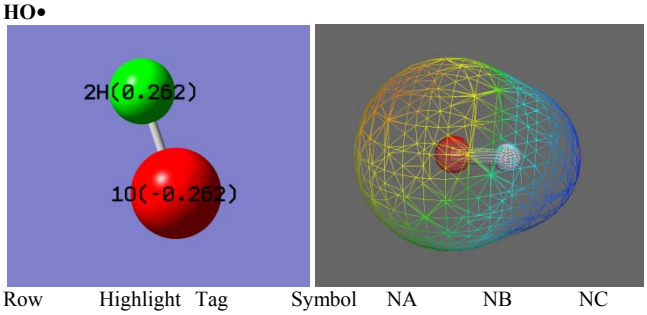

Row	Highlight	Tag	Symbol	NA	NB	NC	Bond	Angle	Dihedral
1	No	1	O						
2	No	2	H	1			0.9789630		

CH_4

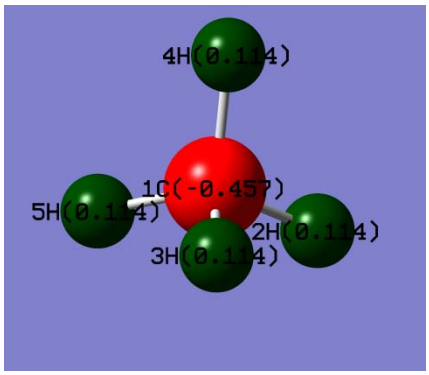

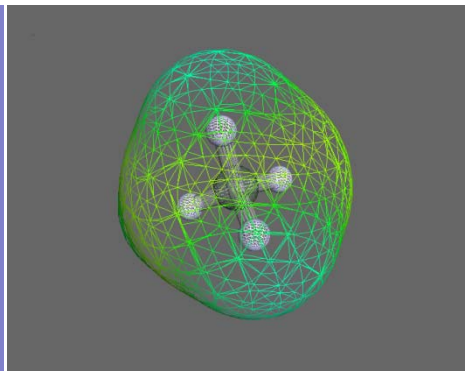

Row	Highlight	Tag	Symbol	NA	NB	NC	Bond	Angle	Dihedral
1	No	1	C						
2	No	2	H	1			1.0894409		
3	No	3	H	1	2		1.0894409	109.4712206	
4	No	4	H	1	2	3	1.0894409	109.4712206	120.0000000
5	No	5	H	1	2	3	1.0894409	109.4712206	-120.0000000

CH_4 in CPCM

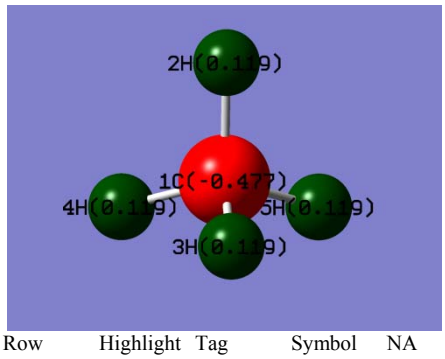

Row	Highlight	Tag	Symbol	NA	NB	NC	Bond	Angle	Dihedral
1	No	1	C						
2	No	2	H	1			1.0898653		
3	No	3	H	1	2		1.0898653	109.4712206	
4	No	4	H	1	2	3	1.0898653	109.4712206	120.0000000
5	No	5	H	1	2	3	1.0898653	109.4712206	-120.0000000

TS CH_4-HO•

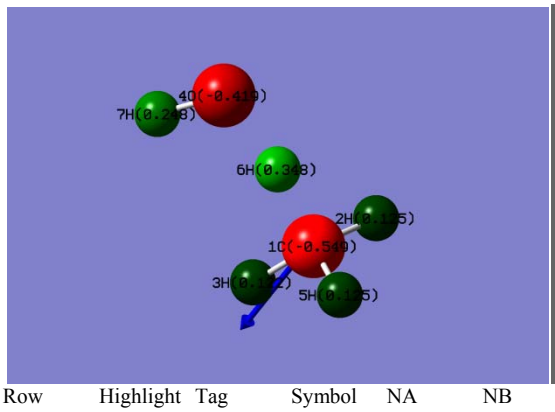

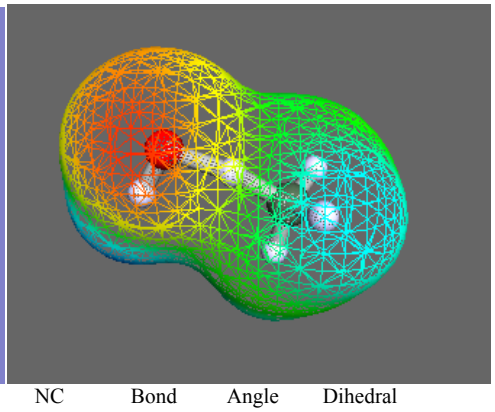

Row	Highlight	Tag	Symbol	NA	NB	NC	Bond	Angle	Dihedral
1	No	1	C						
2	No	2	H	1			1.0872222		
3	No	3	H	1	2		1.0874447	112.3121608	
4	No	4	O	1	2	3	2.4821739	108.2078863	-112.1310642
5	No	5	H	1	4	3	1.0871626	108.0680387	-118.7274897
6	No	6	H	1	4	3	1.2259716	5.8798364	177.7599752
7	No	7	H	4	1	5	0.9778787	93.7778328	-115.7543397

TS CH_4-HO• in CPCM

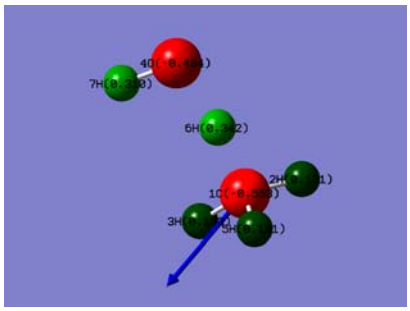

Row	Highlight	Tag	Symbol	NA	NB	NC	Bond	Angle	Dihedral
1	No	1	C						
2	No	2	H	1			1.0879907		
3	No	3	H	1	2		1.0875847	112.3822663	
4	No	4	O	1	3	2	2.4923043	101.9002896	115.9528627
5	No	5	H	1	4	3	1.0876671	107.9830162	-118.6674389
6	No	6	H	1	4	3	1.2203932	5.5259278	170.5837115
7	No	7	H	4	1	3	0.9855481	93.3845049	20.390555

C_2H_6

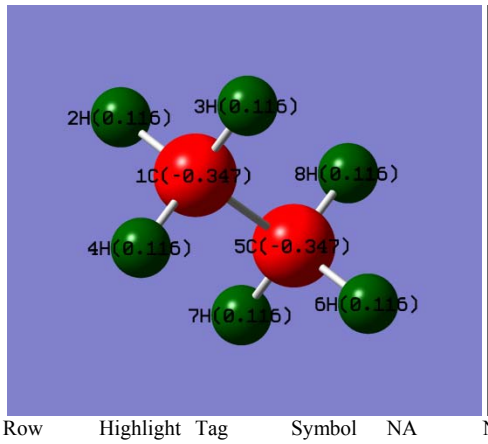

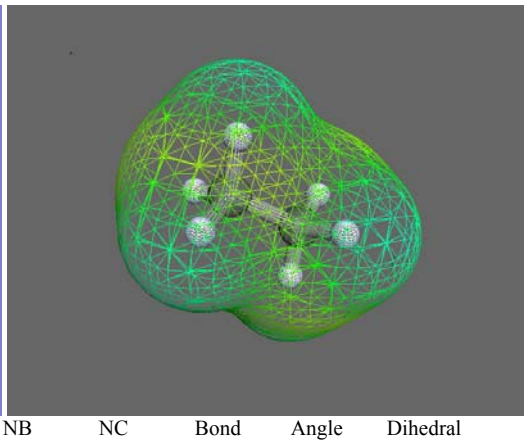

Row	Highlight	Tag	Symbol	NA	NB	NC	Bond	Angle	Dihedral
1	No	1	C						
2	No	2	H	1			1.0926187		
3	No	3	H	1	2		1.0926182	107.6918168	
4	No	4	H	1	3	2	1.0926182	107.6917705	-115.8851506
5	No	5	C	1	3	4	1.5243840	111.1968744	-122.0574157
6	No	6	H	5	1	3	1.0926187	111.1968643	59.9999827
7	No	7	H	5	1	3	1.0926182	111.1968744	180.0000000
8	No	8	H	5	1	3	1.0926182	111.1968744	-60.0000346

C_2H_6 in CPCM

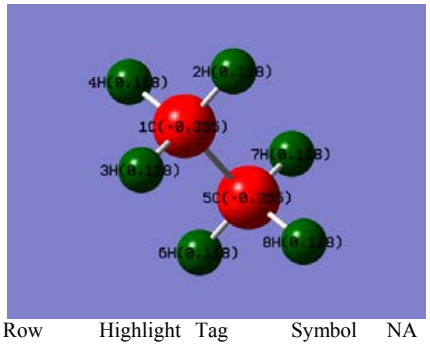

Row	Highlight	Tag	Symbol	NA	NB	NC	Bond	Angle	Dihedral
1	No	1	C						
2	No	2	H	1			1.0927988		
3	No	3	H	1	2		1.0927989	107.7186035	
4	No	4	H	1	2	3	1.0927989	107.7186035	115.9437789
5	No	5	C	1	2	3	1.5245500	111.1716097	-122.0281106

6	No	6	H	5	1	2	1.0927988	111.1716097	180.0000000
7	No	7	H	5	1	2	1.0927989	111.1716064	-60.0000058
8	No	8	H	5	1	2	1.0927989	111.1716064	60.0000058

C2H6-HO• (TS)

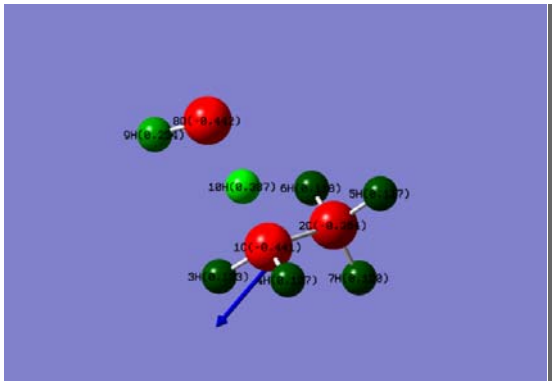

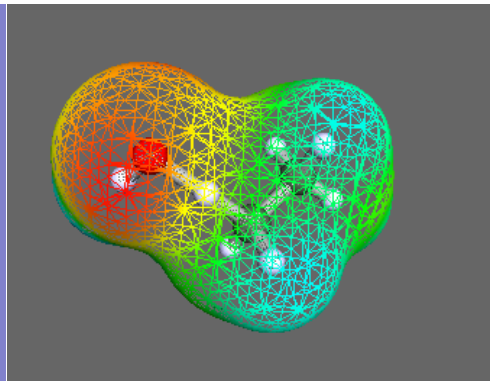

Row	Highlight	Tag	Symbol	NA	NB	NC	Bond	Angle	Dihedral
1	No	1	C						
2	No	2	C	1			1.5121286		
3	No	3	H	1	2		1.0912071	113.6682857	
4	No	4	H	1	2	3	1.0910596	114.2188748	127.7562112
5	No	5	H	2	1	4	1.0917678	111.0371481	-54.7657081
6	No	6	H	2	1	4	1.0918400	111.0009418	-174.8915413
7	No	7	H	2	1	4	1.0947889	110.7332447	65.1588403
8	No	8	O	1	2	5	2.5028296	106.2598884	66.0474791
9	No	9	H	8	1	2	0.9782489	94.7559645	123.0541796
10	No	10	H	1	2	8	1.2077062	107.2009548	-5.9397381

C2H6-HO• (TS) in CPCM

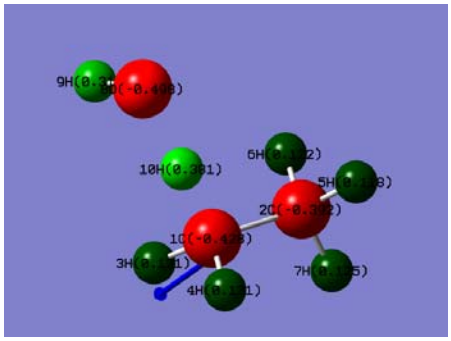

Row	Highlight	Tag	Symbol	NA	NB	NC
	Bond	Angle	Dihedral			
1	No	1	C			
2	No	2	C	1		
3	No	3	H	1	2	
4	No	4	H	1	2	3
5	No	5	H	2	1	3
6	No	6	H	2	1	3
7	No	7	H	2	1	3
8	No	8	O	1	2	5
9	No	9	H	8	1	2
10	No	10	H	1	2	8

2	No	2	C	1			1.5124070		
3	No	3	H	1	2		1.0909110	113.7540938	
4	No	4	H	1	2	3	1.0914026	114.0286441	127.7111756
5	No	5	H	2	1	3	1.0922465	111.1776478	177.0724345
6	No	6	H	2	1	3	1.0923069	111.1290542	56.5376858
7	No	7	H	2	1	3	1.0946419	110.5379493	-63.1725075
8	No	8	O	1	2	5	2.5142659	107.0738524	64.9934139
9	No	9	H	8	1	2	0.9856625	93.5742160	99.2063519
10	No	10	H	1	2	8	1.2043211	108.1494394	-5.2162835

Propane (C3H8)

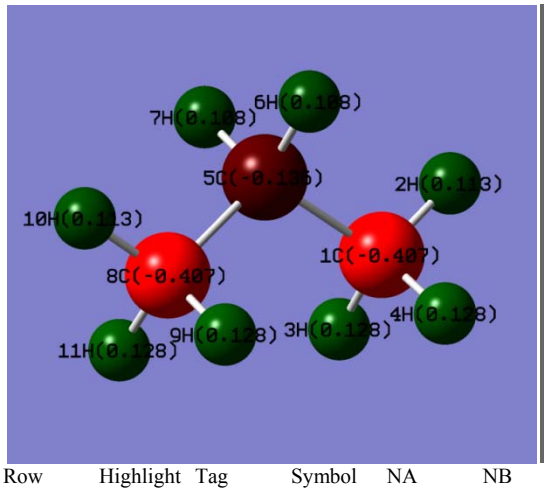

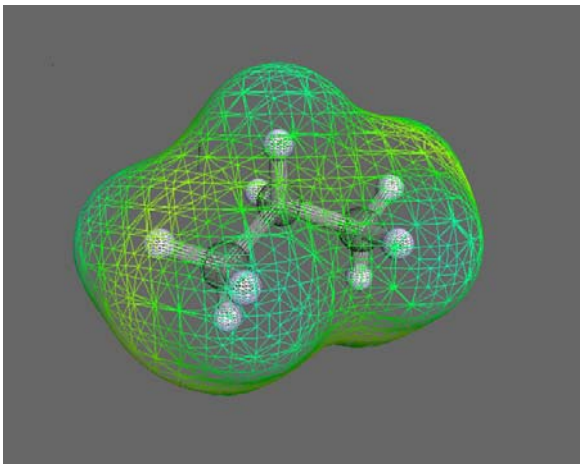

Row	Highlight	Tag	Symbol	NA	NB	NC	Bond	Angle	Dihedral
1	No	1	C						
2	No	2	H	1			1.0935214		
3	No	3	H	1	2		1.0941869	107.8892763	
4	No	4	H	1	2	3	1.0941869	107.8892763	116.0891868
5	No	5	C	1	2	3	1.5244470	111.5646994	-121.9554066
6	No	6	H	5	1	2	1.0957086	109.4934811	-58.0825182
7	No	7	H	5	1	2	1.0957086	109.4934811	58.0825182
8	No	8	C	5	1	2	1.5244470	112.3912434	180.0000000
9	No	9	H	8	5	1	1.0941869	110.8247706	59.7543721
10	No	10	H	8	5	1	1.0935214	111.5646994	180.0000000
11	No	11	H	8	5	1	1.0941869	110.8247706	-59.7543721

Propane (C3H8) in CPCM

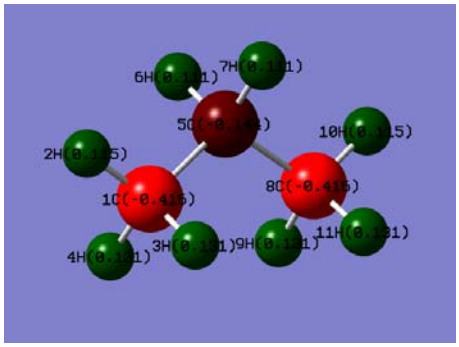

Row	Highlight	Tag	Symbol	NA	NB	NC
	Bond	Angle	Dihedral			
1	No	1	C			
2	No	2	H	1		
	1.0937473					
3	No	3	H	1	2	
	1.0943707	107.9190969				
4	No	4	H	1	2	3
	1.0943707	107.9190969		116.1691046		
5	No	5	C	1	2	3
	1.5245619	111.5441765		-121.9154477		
6	No	6	H	5	1	2
	1.0958923	109.4874306		-58.1158106		
7	No	7	H	5	1	2
	1.0958923	109.4874306		58.1158106		
8	No	8	C	5	1	2
	1.5245619	112.3595737		180.0000000		
9	No	9	H	8	5	1
	1.0943707	110.7870249		59.7559666		
10	No	10	H	8	5	1
	1.0937473	111.5441765		180.0000000		
11	No	11	H	8	5	1
	1.0943707	110.7870249		-59.7559666		

C3H8-HOradical TS1

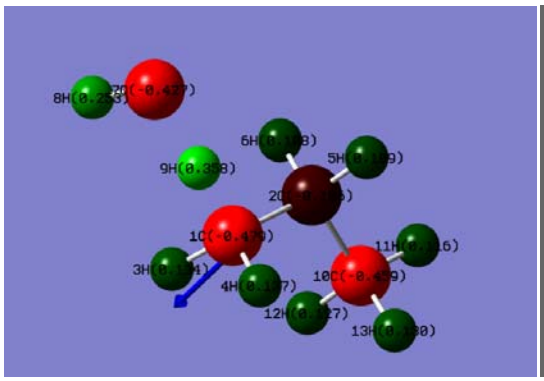

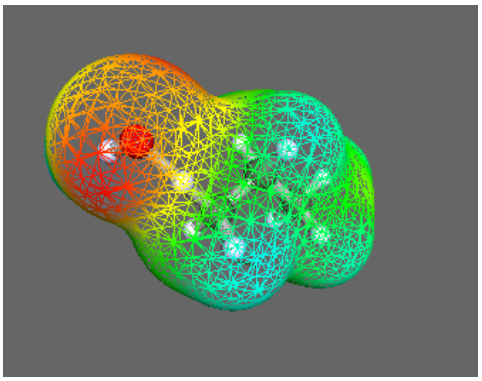

Row	HighlighTag		Symbol	NA	NB	NC	Bond	Angle	Dihedral
	X		Y		Z				
1	No	1	C						
	-0.0325510		0.2175070		0.0381640				
2	No	2	C	1			1.5128566		
	-0.0410990		0.0618470		1.5429670				
3	No	3	H	1	2		1.0924672	113.4266290	
	0.8844720		-0.1464900		-0.4309410				
4	No	4	H	1	2	3	1.0923491	113.8677853	127.1121200
	-0.9060470		-0.2140400		-0.4557980				
5	No	5	H	2	1	4	1.0944431	109.3238599	-57.7998579
	-0.9457640		0.5243410		1.9497670				
6	No	6	H	2	1	4	1.0945838	109.3701413	-174.0220832
	0.8057810		0.6087640		1.9693350				
7	No	7	O	1	2	5	2.5008216	105.6002886	63.2878354
	0.0705780		2.6805190		-0.3826030				
8	No	8	H	7	1	2	0.9782996	94.3325698	111.3218865
	0.9795680		2.6558570		-0.7434340				
9	No	9	H	1	2	7	1.2086780	107.7123036	-6.1521522
	-0.1065520		1.3981550		-0.2098210				
10	No	10	C	2	1	7	1.5276746	111.9506633	-174.8674707
	0.0241260		-1.4047110		1.9657470				
11	No	11	H	10	2	1	1.0934315	111.0525937	-179.9354835
	0.0159730		-1.5002290		3.0549680				
12	No	12	H	10	2	1	1.0937973	110.9718650	59.9813511
	0.9360390		-1.8795550		1.5924770				
13	No	13	H	10	2	1	1.0936548	110.9173422	-59.8961560
	-0.8300050		-1.9629080		1.5721010				

C3H8-HOradical TS1 in CPCM

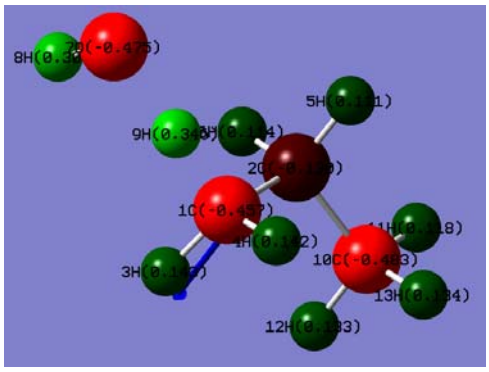

Row	Highlight	Tag	Symbol	NA	NB	NC
	Bond	Angle	Dihedral			
1	No	1	C			
2	No	2	C	1		
	1.5131575					
3	No	3	H	1	2	
	1.0920588	113.5431386				
4	No	4	H	1	2	3
	1.0927679	113.5548832		127.1889193		
5	No	5	H	2	1	3
	1.0949335	109.4384084		174.3154433		
6	No	6	H	2	1	3
	1.0951149	109.5082425		57.6701216		
7	No	7	O	1	2	5
	2.5130171	105.3287268		61.1486800		
8	No	8	H	7	1	2
	0.9858586	93.3994955		81.4417255		
9	No	9	H	1	2	7
	1.2048159	108.6646019		-4.6192586		
10	No	10	C	2	1	7
	1.5276409	111.7839674		-177.1877546		
11	No	11	H	10	2	1
	1.0935963	111.0176666		179.9707344		
12	No	12	H	10	2	1
	1.0937742	110.8774186		59.8789003		
13	No	13	H	10	2	1
	1.0937718	110.8318383		-59.9789099		

C3H8-HOradical TS2 Staggered

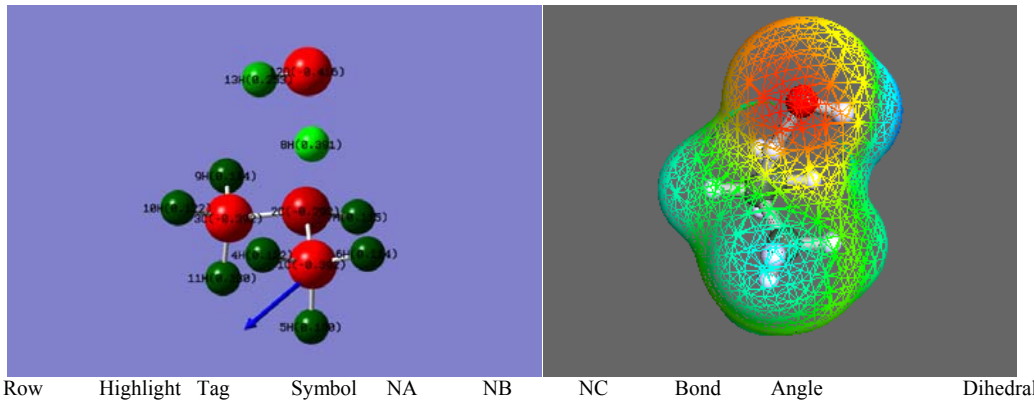

Row	Highlight	Tag	Symbol	NA	NB	NC	Bond	Angle	Dihedral
	X		Y		Z				
1	No	1	C						
	0.0433560		0.0689040		0.0687530				
2	No	2	C	1			1.5142781		
	0.0513010		0.3885390		1.5488910				
3	No	3	C	2	1		1.5142773	114.9252361	
	1.3124570		-0.0167780		2.2825390				
4	No	4	H	1	2	3	1.0941535	111.0394491	-55.7235557
	0.9066980		0.5149650		-0.4340810				
5	No	5	H	1	2	3	1.0955269	110.4307196	63.4931515
	0.0923740		-1.0141150		-0.0888740				
6	No	6	H	1	2	3	1.0924229	111.3956270	-176.3823785
	-0.8627670		0.4414060		-0.4145390				
7	No	7	H	2	1	3	1.0943691	111.7177012	-128.6323876
	-0.8466520		0.0129140		2.0491210				
8	No	8	H	2	1	3	1.1946103	107.8346214	120.2829200
	-0.0779770		1.5700700		1.6687470				
9	No	9	H	3	2	1	1.0924224	111.3954823	176.3828806
	1.2830960		0.2965230		3.3286590				
10	No	10	H	3	2	1	1.0941525	111.0393256	55.7244715
	2.1974900		0.4278320		1.8175570				
11	No	11	H	3	2	1	1.0955274	110.4307597	-63.4925662
	1.4369980		-1.1048950		2.2566330				
12	No	12	O	2	1	3	2.5265637	105.4546130	115.6800906
	-0.0310940		2.9096030		1.6937060				
13	No	13	H	12	2	1	0.9786268	93.3027968	-60.9838358
	0.8140420		3.0213350		1.2131110				

C3H8-HOradical TS2 Staggered in CPCM

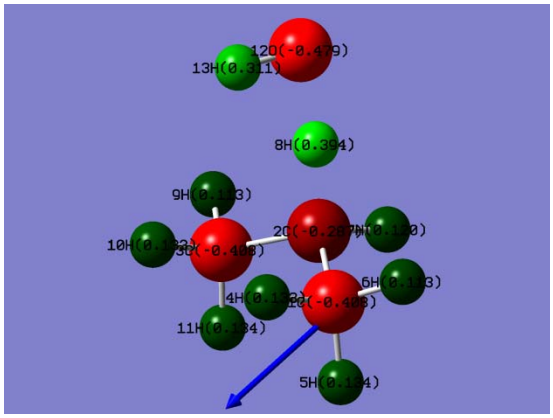

Row	Highlight	Tag	Symbol	NA	NB	NC	Bond	Angle	Dihedral
1	No	1	C						
2	No	2	C	1			1.5145279		
3	No	3	C	2	1		1.5145172	114.7540663	
4	No	4	H	1	2	3	1.0939767	110.9092943	-56.3259880
5	No	5	H	1	2	3	1.0954579	110.2365389	62.9396907
6	No	6	H	1	2	3	1.0928617	111.4739686	-177.0866494
7	No	7	H	2	1	3	1.0947827	111.7005124	-128.4427383
8	No	8	H	2	1	3	1.1921016	107.7510164	120.0141617
9	No	9	H	3	2	1	1.0928587	111.4773812	177.1198786
10	No	10	H	3	2	1	1.0939732	110.9112134	56.3515872
11	No	11	H	3	2	1	1.0954658	110.2315031	-62.9101292
12	No	12	O	2	1	3	2.5397858	105.7935971	116.2062476

13	No	13	H	12	2	1	0.9859455	93.5745839	-61.2079970

C3H8-HOradical TS3 Eclipsed

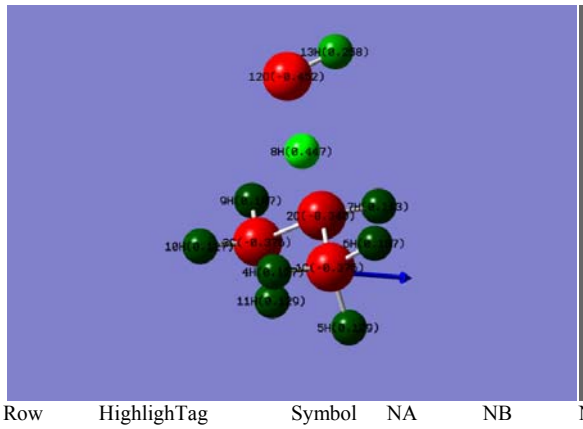

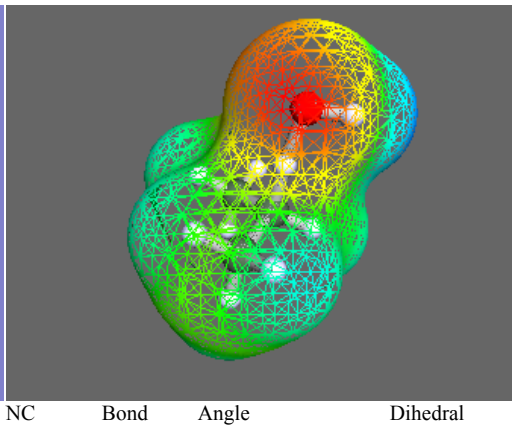

Row	HighlighTag		Symbol	NA	NB	NC	Bond	Angle	Dihedral
	X		Y		Z				
1	No	1	C						
	-0.0747120		0.0015510		0.0293220				
2	No	2	C	1			1.5143162		
	0.0059960		-0.1314570		1.5356250				
3	No	3	C	2	1		1.5143170	114.9391899	
	1.3989850		0.0009400		2.1145970				
4	No	4	H	1	2	3	1.0930913	110.6337006	-56.1264376
	0.3561290		0.9516370		-0.2971150				
5	No	5	H	1	2	3	1.0958220	110.4296167	63.3317263
	0.4830440		-0.8069760		-0.4564950				
6	No	6	H	1	2	3	1.0925403	111.4862733	-176.4772267
	-1.1085760		-0.0409510		-0.3213390				
7	No	7	H	2	1	3	1.0946535	111.6655672	-128.5232437
	-0.4937400		-1.0391950		1.8885300				
8	No	8	H	2	1	3	1.1935836	106.3221937	117.3315285
	-0.6319220		0.7708870		1.9867100				
9	No	9	H	3	2	1	1.0925400	111.4864054	176.4770368
	1.3843910		-0.0419810		3.2061960				
10	No	10	H	3	2	1	1.0930908	110.6337582	56.1260916
	1.8507870		0.9510140		1.8178110				
11	No	11	H	3	2	1	1.0958221	110.4294562	-63.3320260
	2.0428990		-0.8076270		1.7507010				
12	No	12	O	2	1	3	2.5309497	107.7985225	120.2251068
	-1.4301800		1.6884500		2.5510280				
13	No	13	H	12	2	1	0.9785029	95.1465910	117.6903135
	-2.0523290		1.0743000		2.9905940				

C4H10 –Anti Staggered

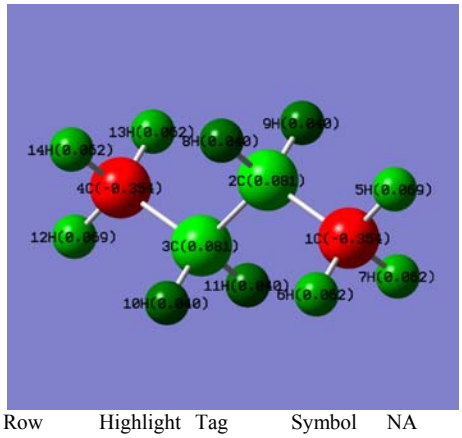

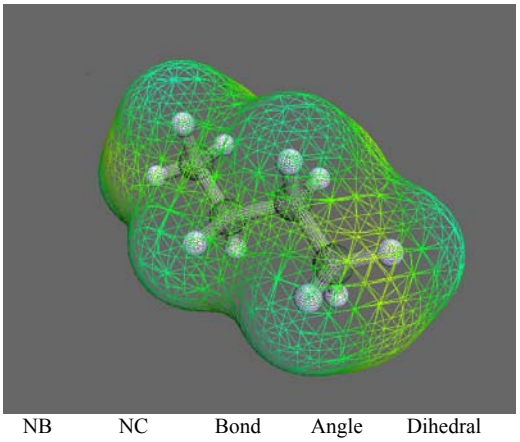

Row	Highlight	Tag	Symbol	NA	NB	NC	Bond	Angle	Dihedral
1	No	1	C						
2	No	2	C	1			1.5321572		

3	No	3	C	2	1		1.5340227	113.3152872	
4	No	4	C	3	2	1	1.5321572	113.3152872	179.9897384
5	No	5	H	1	2	3	1.0963616	111.4699916	179.9922033
6	No	6	H	1	2	3	1.0973113	111.1566451	-59.8714373
7	No	7	H	1	2	3	1.0973127	111.1563104	59.8562027
8	No	8	H	2	1	3	1.0997736	109.4617689	122.0840238
9	No	9	H	2	1	3	1.0997730	109.4626456	-122.0849654
10	No	10	H	3	2	1	1.0997738	109.1506682	57.7319241
11	No	11	H	3	2	1	1.0997736	109.1503755	-57.7519577
12	No	12	H	4	3	2	1.0963616	111.4699917	179.9929895
13	No	13	H	4	3	2	1.0973123	111.1563656	59.8568402
14	No	14	H	4	3	2	1.0973122	111.1565532	-59.8707356

C4H10 –Gauche staggered dihedral angle = 60 degrees

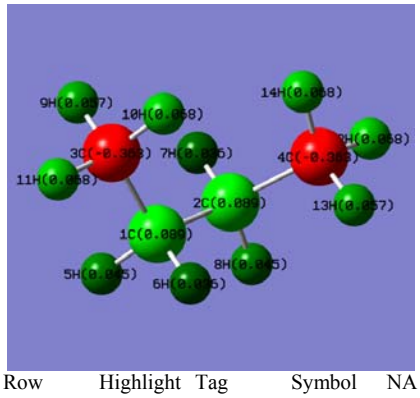

Row	Highlight	Tag	Symbol	NA	NB	NC	Bond	Angle	Dihedral
1	No	1	C						
2	No	2	C	1			1.5379280		
3	No	3	C	1	2		1.5334313	114.3669905	
4	No	4	C	2	1	3	1.5334313	114.3669905	65.6963061
5	No	5	H	1	3	2	1.0987111	108.8644577	-121.7647513
6	No	6	H	1	3	2	1.0998727	109.4242987	122.7025278
7	No	7	H	2	1	3	1.0998727	109.0825461	-57.1914798
8	No	8	H	2	1	3	1.0987111	108.6859982	-172.4411496
9	No	9	H	3	1	2	1.0976039	110.9970755	57.7114576
10	No	10	H	3	1	2	1.0959628	111.9223309	-62.5025121
11	No	11	H	3	1	2	1.0963244	111.0736279	177.4453780
12	No	12	H	4	2	1	1.0963244	111.0736279	177.4453780
13	No	13	H	4	2	1	1.0976040	110.9971056	57.7115029
14	No	14	H	4	2	1	1.0959628	111.9223309	-62.5025121

C4H10 – Gauche staggered dihedral angle = 300 degrees

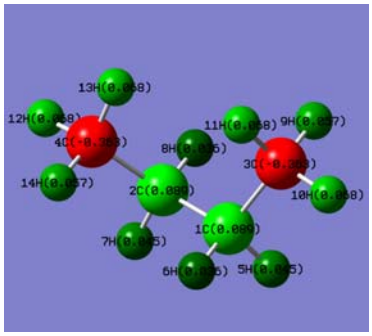

Row	Highlight	Tag	Symbol	NA	NB	NC	Bond	Angle	Dihedral
1	No	1	C						
2	No	2	C	1			1.5379307		
3	No	3	C	1	2		1.5334312	114.3675327	
4	No	4	C	2	1	3	1.5334312	114.3675327	-65.6947700
5	No	5	H	1	3	2	1.0987106	108.8645205	121.7648434
6	No	6	H	1	3	2	1.0998727	109.4241333	-122.7026963
7	No	7	H	2	1	3	1.0987110	108.6857893	172.4424429
8	No	8	H	2	1	3	1.0998727	109.0824772	57.1931298

9	No	9	H	3	1	2	1.0976037	110.9968063	-57.7119838
10	No	10	H	3	1	2	1.0963243	111.0740412	-177.4453703
11	No	11	H	3	1	2	1.0959625	111.9226271	62.5018985
12	No	12	H	4	2	1	1.0963243	111.0740412	-177.4453703
13	No	13	H	4	2	1	1.0959625	111.9226271	62.5018985
14	No	14	H	4	2	1	1.0976037	110.9968063	-57.7119838

C4H10-HO radical TS1 Anti staggered dihedral angle = 180 degrees

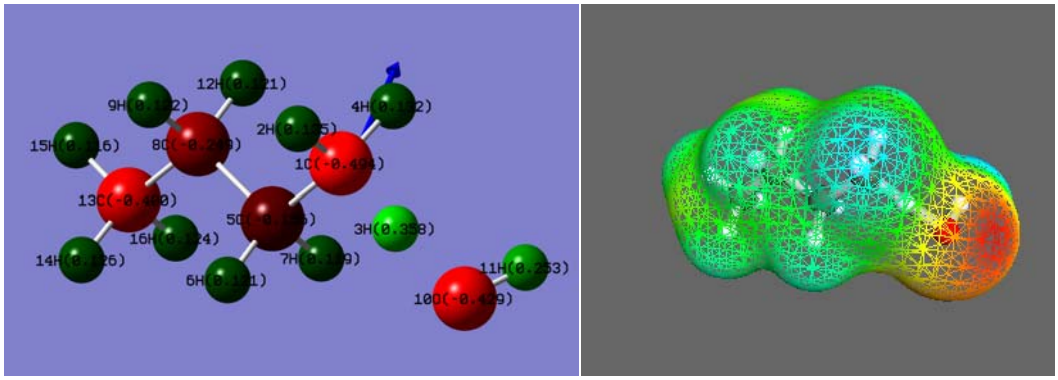

Row	Highlight	Tag	Symbol	NA	NB	NC	Bond	Angle	Dihedral
	X		Y		Z				
1	No	1	C						0.1559880
	-0.3339080		0.2062360						
2	No	2	H	1			1.0923054		0.1948660
	-0.7102210		1.2309350						
3	No	3	H	1	2		1.2082820	104.0702091	1.2646150
	-0.5437720		-0.2260240						
4	No	4	H	1	2	3	1.0924193	110.2097568	-114.1283246
	0.0184570		0.7498190		0.2071610				
5	No	5	C	1	2	4	1.5126185	113.8918024	-128.8250075
	-0.8296950		-1.0651190		-0.6779440				
6	No	6	H	5	1	2	1.0957321	109.4930405	-57.8052260
	-0.5793240		-2.1316230		-0.7005830				
7	No	7	H	5	1	2	1.0958993	109.5477781	-174.1917212
	-0.7372040		-0.7027290		-1.7080480				
8	No	8	C	5	1	2	1.5286063	112.4233245	63.9625355
	-2.2739030		-0.8935440		-0.2073460				
9	No	9	H	8	5	1	1.0965051	109.1804691	-57.9354940
	-2.3620320		-1.2549410		0.8241330				
10	No	10	O	1	5	8	2.5020159	105.8700432	-175.0338900
	2.3888880		-0.6028790		-0.8900740				
11	No	11	H	10	1	5	0.9783016	94.2494371	110.8215550
	2.4592990		0.3394550		-1.1432990				
12	No	12	H	8	5	1	1.0966710	109.2198494	58.0117652
	-2.5212080		0.1746030		-0.1830660				
13	No	13	C	8	5	1	1.5248897	112.4472733	-179.9452924
	-3.2679410		-1.6315780		-1.0975610				
14	No	14	H	13	8	5	1.0938284	110.8337676	59.8290218
	-3.0548630		-2.7043480		-1.1124930				
15	No	15	H	13	8	5	1.0934273	111.3842702	179.9950557
	-4.2944220		-1.4973780		-0.7455520				
16	No	16	H	13	8	5	1.0938949	110.8595867	-59.8213593
	-3.2147690		-1.2660370		-2.1272010				

C4H10-HO radical TS2 Anti staggered dihedral angle = 180 degrees

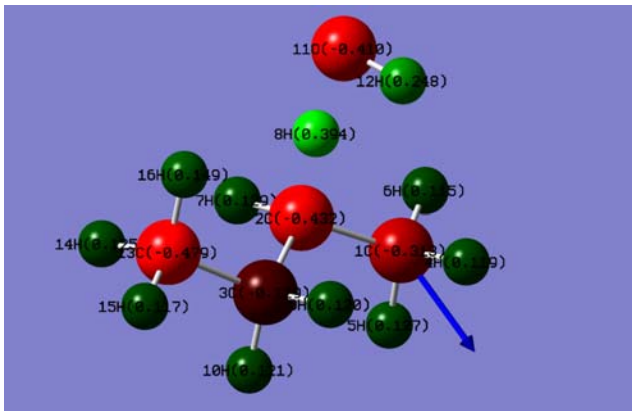

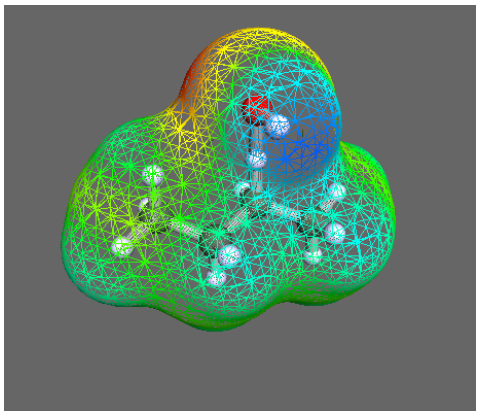

Row	Highlight	Tag	Symbol	NA	NB	NC	Bond	Angle	Dihedral
	X		Y		Z				
1	No	1	C						0.0024170
	-0.0040110		-0.0054770						
2	No	2	C	1			1.5146005		-0.0026490
	-0.0040300		1.5091150						
3	No	3	C	2	1		1.5157896	115.3944001	1.3644270
	0.0099950		2.1637330						
4	No	4	H	1	2	3	1.0941601	111.0828823	-55.6590334
	0.5709780		0.8448190		-0.3971560				
5	No	5	H	1	2	3	1.0954732	110.4089637	63.5638021
	0.4701810		-0.9186190		-0.3859380				
6	No	6	H	1	2	3	1.0926284	111.4416984	-176.3815052
	-1.0118260		0.0497750		-0.4082860				
7	No	7	H	2	1	3	1.0957680	111.8437213	-128.6396151
	-0.6309280		-0.8049430		1.9147150				
8	No	8	H	2	1	3	1.1943153	108.1660887	119.9228278
	-0.5800100		0.9736300		1.8795530				
9	No	9	H	3	2	1	1.0972654	109.1248295	54.2281210
	1.9417350		0.8570780		1.7723800				
10	No	10	H	3	2	1	1.0985396	108.6096820	-60.9899972
	1.9079650		-0.8949690		1.8597660				
11	No	11	O	2	1	3	2.5319514	106.4512793	114.4243772
	-1.0317280		2.1965370		2.2227530				
12	No	12	H	11	2	1	0.9789753	92.7531108	-56.0194648
	-0.3797140		2.7205050		1.7141000				
13	No	13	C	3	2	1	1.5244932	112.7421404	176.6647490
	1.2889830		0.0910560		3.6841990				
14	No	14	H	13	3	2	1.0938864	110.7349786	60.9552732
	0.7604860		-0.7753090		4.0924760				
15	No	15	H	13	3	2	1.0932797	111.3615186	-178.9478261
	2.2861940		0.1184230		4.1315040				
16	No	16	H	13	3	2	1.0923251	110.1536287	-58.3694989
	0.7462970		0.9894700		3.9867190				

C5H12 – Anti Staggered

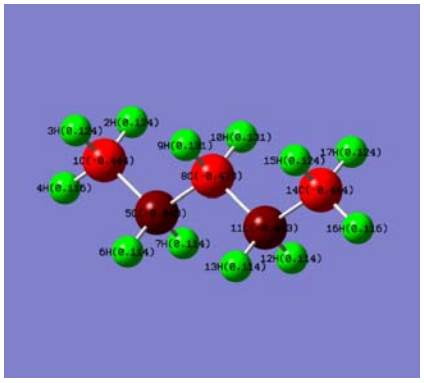

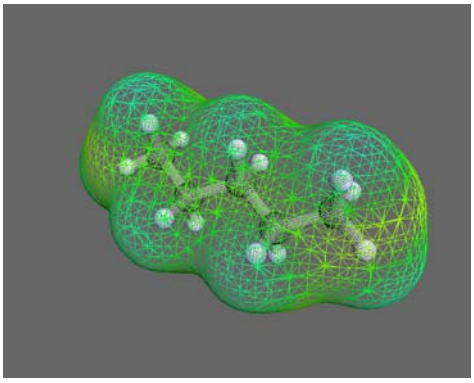

Row	Highlight	Tag	Symbol	NA	NB	NC	Bond	Angle	Dihedral
1	No	1	C						
2	No	2	H	1			1.0941147		
3	No	3	H	1	2		1.0941147	107.7270407	
4	No	4	H	1	2	3	1.0936558	107.8641759	116.1928710
5	No	5	C	1	4	2	1.5247509	111.5347065	-121.9483950
6	No	6	H	5	1	4	1.0969419	109.6239889	-58.1490982
7	No	7	H	5	1	4	1.0969419	109.6239889	58.1490982
8	No	8	C	5	1	4	1.5250730	112.8138762	180.0000000
9	No	9	H	8	5	1	1.0983327	109.2500797	57.8959964
10	No	10	H	8	5	1	1.0983327	109.2500797	-57.8959964
11	No	11	C	8	5	1	1.5250730	113.3827266	180.0000000
12	No	12	H	11	8	5	1.0969419	109.1446217	57.8790304
13	No	13	H	11	8	5	1.0969419	109.1446217	-57.8790304
14	No	14	C	11	8	5	1.5247509	112.8138762	180.0000000
15	No	15	H	14	11	8	1.0941147	110.8476816	59.7907381
16	No	16	H	14	11	8	1.0936558	111.5347065	180.0000000
17	No	17	H	14	11	8	1.0941147	110.8476816	-59.7907381

C5H12-HO radical TS2

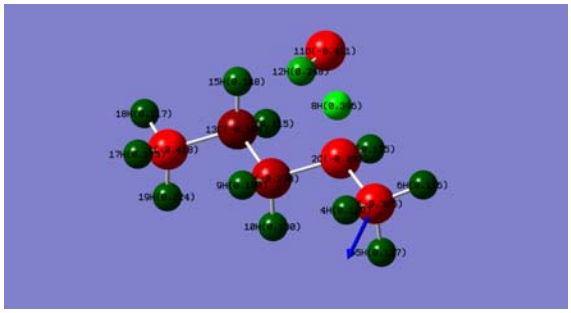

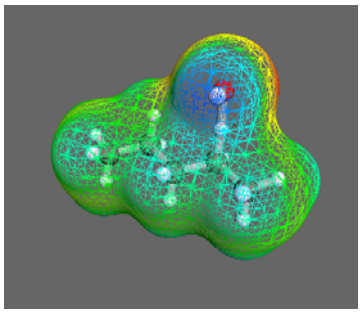

Row	Highlight	Tag	Symbol	NA	NB	NC	Bond	Angle	Dihedral
	X	Y	Z						
1	No	1	C						
	0.0586670		-0.1079310		0.0323560				
2	No	2	C	1			1.5148027		
	0.0126980		0.3936000		1.4609850				
3	No	3	C	2	1		1.5156857	115.3536642	
	1.2829570		0.1884970		2.2620330				
4	No	4	H	1	2	3	1.0941294	111.0736256	-55.6960832
	0.8949050		0.3379990		-0.5144270				
5	No	5	H	1	2	3	1.0954672	110.4014780	63.5291712
	0.1935080		-1.1949020		0.0133740				
6	No	6	H	1	2	3	1.0926808	111.4342469	-176.4089237
	-0.8638950		0.1279770		-0.5035340				
7	No	7	H	2	1	3	1.0957260	111.8088149	-128.6245046
	-0.8638340		0.0138420		1.9977260				
8	No	8	H	2	1	3	1.1941364	108.0840701	119.9975845
	-0.2038480		1.5676480		1.4348920				
9	No	9	H	3	2	1	1.0986229	109.3109568	54.1485102
	2.1303820		0.6278600		1.7181550				
10	No	10	H	3	2	1	1.0998254	108.7742229	-61.1952153
	1.4901590		-0.8896690		2.3271580				
11	No	11	O	2	1	3	2.5322745	106.2776912	114.5289204
	-0.2187300		2.9114560		1.3222180				
12	No	12	H	11	2	1	0.9789901	92.6885645	-57.3843380
	0.5999140		3.0037370		0.7933250				
13	No	13	C	3	2	1	1.5253494	113.2703521	176.5470135
	1.2138330		0.7844090		3.6644600				
14	No	14	H	13	3	2	1.0967702	108.9978229	58.7084155
	0.3765810		0.3273240		4.2057430				
15	No	15	H	13	3	2	1.0948879	108.5453599	-56.8432734
	0.9820620		1.8510320		3.5785700				
16	No	16	C	13	3	2	1.5242680	112.6579605	-179.3031566
	2.5039520		0.5851080		4.4513940				
17	No	17	H	16	13	3	1.0942294	110.9043236	59.9546344
	3.3490330		1.0580460		3.9419770				

18	No	18	H	16	13	3	1.0934021	111.3674358	-179.9955998	
	2.4313360		1.0195990		5.4521300					
19	No	19	H	16	13	3	1.0942427	111.0069678	-59.7900784	
	2.7348660		-0.4786300		4.5632300					

C5H12-HO radical TS2

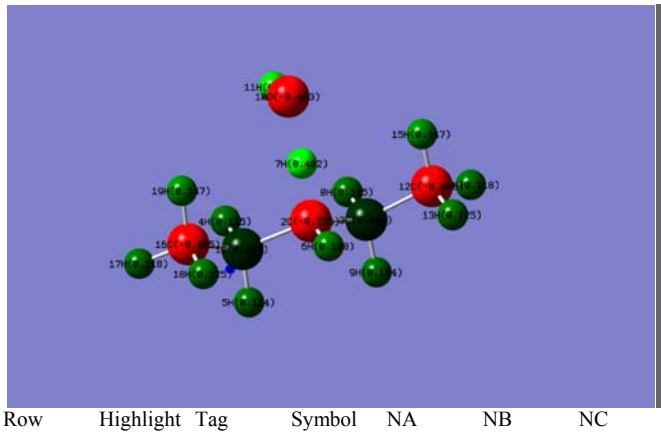

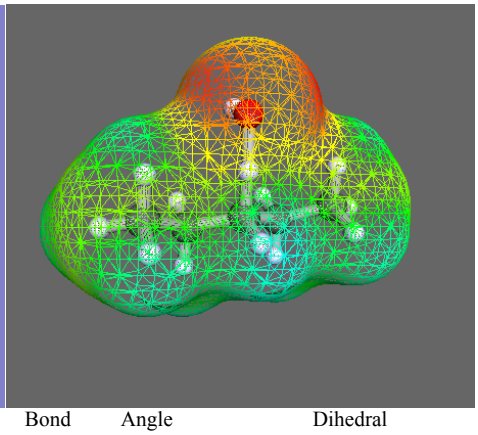

Row	Highlight	Tag	Symbol	NA	NB	NC	Bond	Angle	Dihedral
	X		Y		Z				
1	No	1	C						
	-0.0063080		-0.0055230		-0.0068700				
2	No	2	C	1			1.5158948		
	0.0086040		-0.0211430		1.5088710				
3	No	3	C	2	1		1.5158944	116.0438591	
	1.3768580		-0.0048090		2.1612130				
4	No	4	H	1	2	3	1.0972577	109.1922739	-53.6524343
	0.5900780		0.8431390		-0.3647400				
5	No	5	H	1	2	3	1.0984113	108.6877984	61.6507080
	0.4997130		-0.9090150		-0.3731380				
6	No	6	H	2	1	3	1.0971678	111.4678989	-129.0416688
	-0.6170430		-0.8291120		1.9082820				
7	No	7	H	2	1	3	1.1935739	107.3606085	120.0494014
	-0.5749260		0.9513640		1.8808140				
8	No	8	H	3	2	1	1.0972578	109.1922203	53.6533250
	1.9524850		0.8438520		1.7708250				
9	No	9	H	3	2	1	1.0984113	108.6877527	-61.6497199
	1.9225510		-0.9082720		1.8571060				
10	No	10	O	2	1	3	2.5372809	104.6362355	114.7281672
	-1.0495740		2.1841550		2.1831960				
11	No	11	H	10	2	1	0.9792808	92.1361885	-61.2472471
	-0.3478070		2.6998330		1.7353230				
12	No	12	C	3	2	1	1.5248530	112.6511420	176.0599108
	1.3014030		0.0747020		3.6821210				
13	No	13	H	12	3	2	1.0938417	110.7260061	60.9528907
	0.7748440		-0.7932150		4.0894850				
14	No	14	H	12	3	2	1.0933377	111.3882059	-178.9218054
	2.2984470		0.1043580		4.1297940				
15	No	15	H	12	3	2	1.0925555	110.2229687	-58.3400171
	0.7563660		0.9712210		3.9868600				
16	No	16	C	1	2	3	1.5248530	112.6510925	-176.0589554
	-1.4173620		0.0733220		-0.5794840				
17	No	17	H	16	1	2	1.0933382	111.3882413	178.9220501
	-1.4031270		0.1024660		-1.6723410				
18	No	18	H	16	1	2	1.0938421	110.7259913	-60.9526831
	-2.0084590		-0.7946170		-0.2732540				
19	No	19	H	16	1	2	1.0925552	110.2230744	58.3402661
	-1.9236780		0.9698710		-0.2140790				

CH3OH

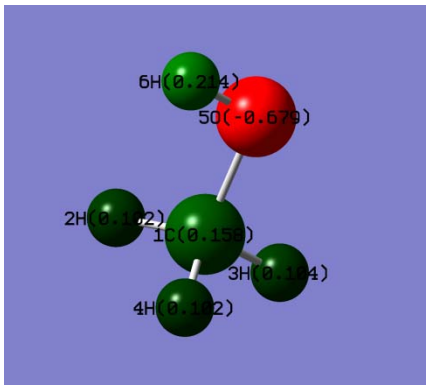

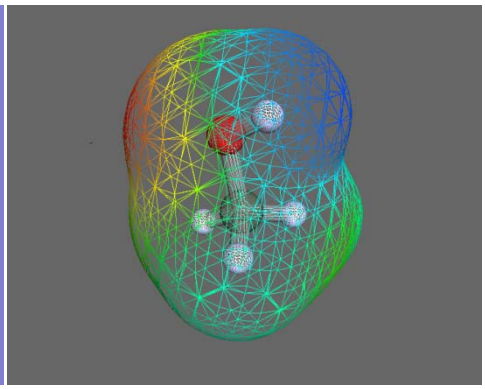

Row	Highlight	Tag	Symbol	NA	NB	NC	Bond	Angle	Dihedral
1	No	1	C						
2	No	2	H	1			1.0968545		
3	No	3	H	1	2		1.0896819	108.4853977	
4	No	4	H	1	3	2	1.0968546	108.4853671	118.0037697
5	No	5	O	1	3	4	1.4228698	106.3070105	120.9981242
4	No	6	H	5	1	3	0.9699425	107.4141935	-180.0000000

CH3OH – HO radical TS1

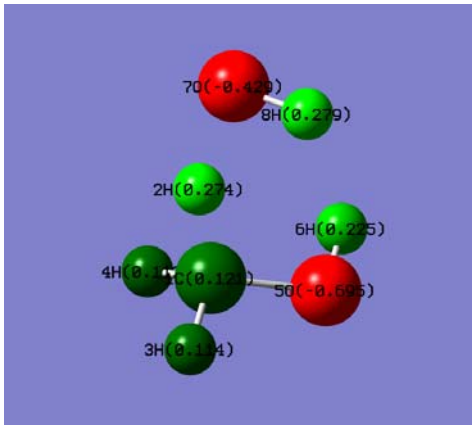

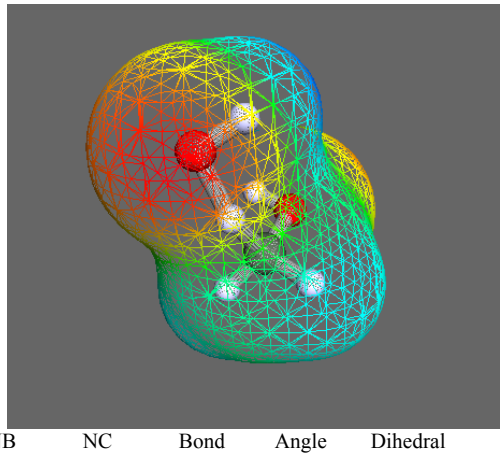

Row	Highlight	Tag	Symbol	NA	NB	NC	Bond	Angle	Dihedral
1	No	1	C						
2	No	2	H	1			1.2038477		
3	No	3	H	1	2		1.0884908	107.2998703	
4	No	4	H	1	3	2	1.0947782	111.9656768	-114.3114758
5	No	5	O	1	3	4	1.3997471	108.3019882	-126.9658518
6	No	6	H	5	1	3	0.9717456	107.5303200	177.1109864
7	No	7	O	1	5	6	2.4775111	96.8954253	-63.7284073
8	No	8	H	7	1	5	0.9789196	87.9839098	-41.7137783

CH3CH2OH

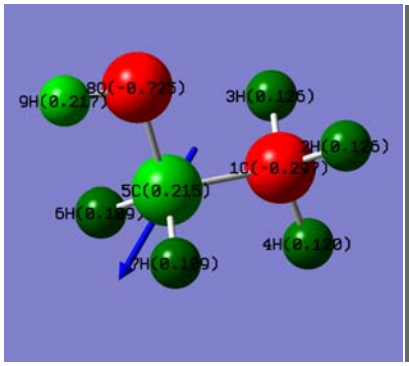

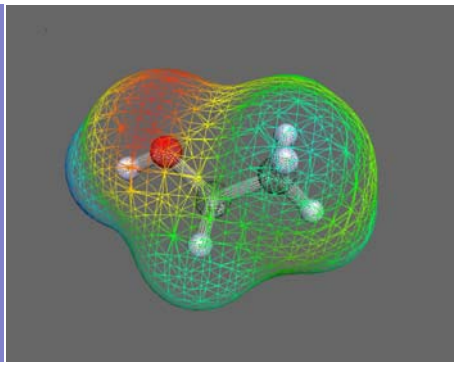

Row	Highlight	Tag	Symbol	NA	NB	NC	Bond	Angle	Dihedral
1	No	1	C						
2	No	2	H	1			1.0917693		
3	No	3	H	1	2		1.0917693	108.4336302	
4	No	4	H	1	2	3	1.0933220	108.8317448	118.2399256
5	No	5	C	1	2	3	1.5118586	109.9733025	-120.2807483
6	No	6	H	5	1	2	1.0991518	110.2207610	-179.6193158
7	No	7	H	5	1	2	1.0991518	110.2207610	-61.0358765
8	No	8	O	5	1	2	1.4275846	107.0229441	59.6724039
9	No	9	H	8	5	1	0.9711288	107.7063937	180.0000000

CH3CH2OH – HO radical TS1

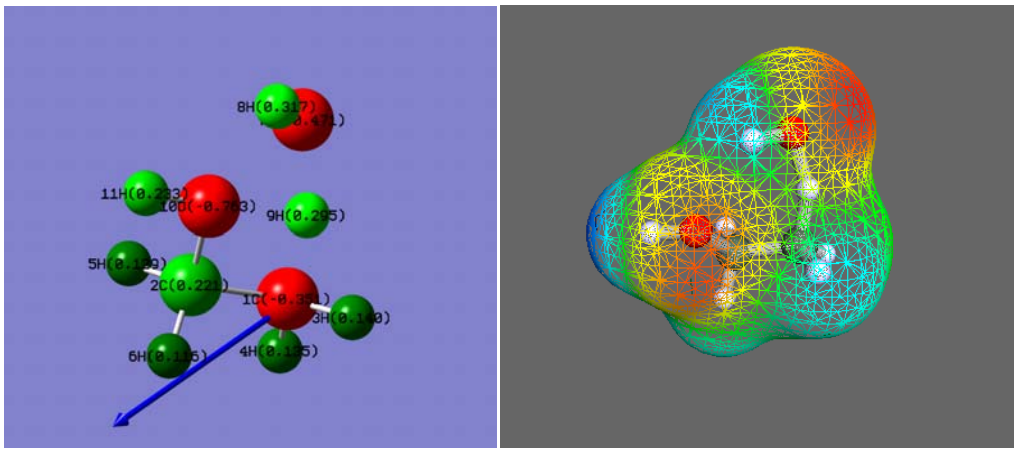

Row	Highlight	Tag	Symbol	NA	NB	NC	Bond	Angle	Dihedral
1	No	1	C						
2	No	2	C	1			1.5023386		
3	No	3	H	1	2		1.0895662	113.0671477	
4	No	4	H	1	2	3	1.0906044	113.4836227	129.3531768
5	No	5	H	2	1	3	1.0968851	109.9842882	177.8321676
6	No	6	H	2	1	3	1.0990223	110.4713632	-62.8216968
7	No	7	O	1	2	5	2.4399043	94.6184081	66.5649571
8	No	8	H	7	1	2	0.9813564	84.9858821	38.7730367
9	No	9	H	1	2	7	1.2325561	106.1098348	-4.3034523
10	No	10	O	2	1	7	1.4332197	106.9336453	-53.8526620
11	No	11	H	10	2	1	0.9718047	107.9883587	176.8713599

C2H5OH – HO radical TS2

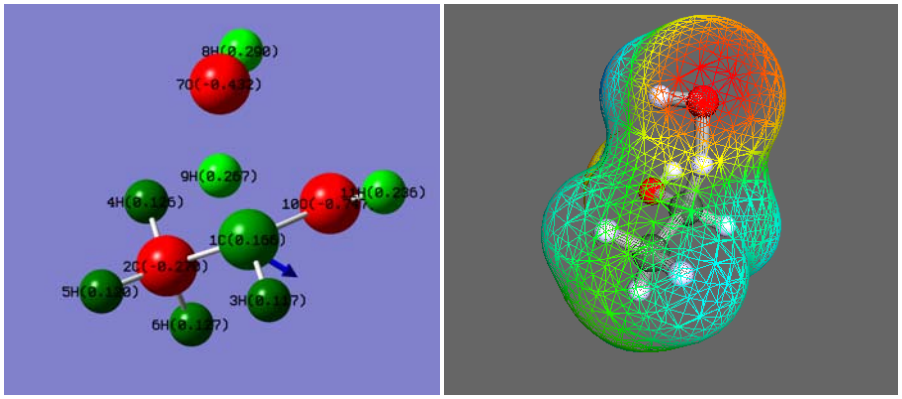

Row	Highlight	Tag	Symbol	NA	NB	NC	Bond	Angle	Dihedral
1	No	1	C						
2	No	2	C	1			1.5039172		
3	No	3	H	1	2		1.0975523	113.3662599	
4	No	4	H	2	1	3	1.0916567	110.0804241	176.1610098
5	No	5	H	2	1	3	1.0920903	110.5426179	55.8579099
6	No	6	H	2	1	3	1.0933156	109.9040588	-64.4988262
7	No	7	O	1	2	4	2.4933828	114.3272003	47.9292776
8	No	8	H	7	1	2	0.9790070	84.8379173	-78.9898282

9	No	9	H	1	2	7	1.1951128	108.7925255	12.9107047
10	No	10	O	1	2	7	1.4083560	109.0732246	-105.4350453
11	No	11	H	10	1	2	0.9726559	107.7340914	-175.3957615

CH3CH(OH)CH3

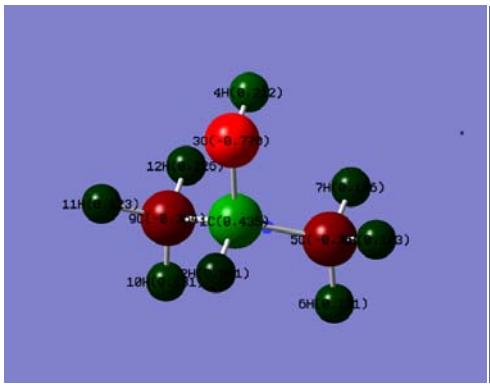

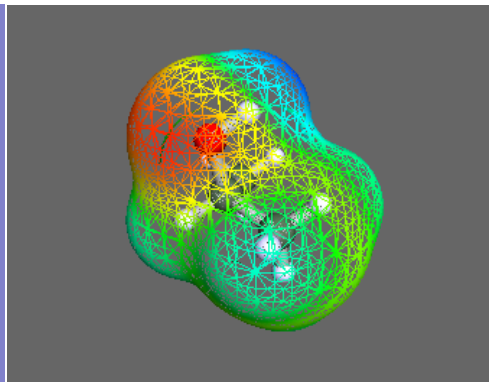

Row	Highlight	Tag	Symbol	NA	NB	NC	Bond	Angle	Dihedral
1	No	1	C						
2	No	2	H	1			1.0945247		
3	No	3	O	1	2		1.4321065	103.8323702	
4	No	4	H	3	1	2	0.9735367	106.6518738	180.0000000
5	No	5	C	1	3	4	1.5204977	110.8135562	62.8245860
6	No	6	H	5	1	3	1.0939508	111.3457674	175.0794265
7	No	7	H	5	1	3	1.0960337	110.1478691	-65.2933847
8	No	8	H	5	1	3	1.0920798	110.1395835	54.2136940
9	No	9	C	1	3	5	1.5204977	110.8135512	-125.6496640
10	No	10	H	9	1	3	1.0939512	111.3457942	-175.0798977
11	No	11	H	9	1	3	1.0920789	110.1396264	-54.2141367
12	No	12	H	9	1	3	1.0960345	110.1478506	65.2928914

CH3CH(OH)CH3-HO radical TS1

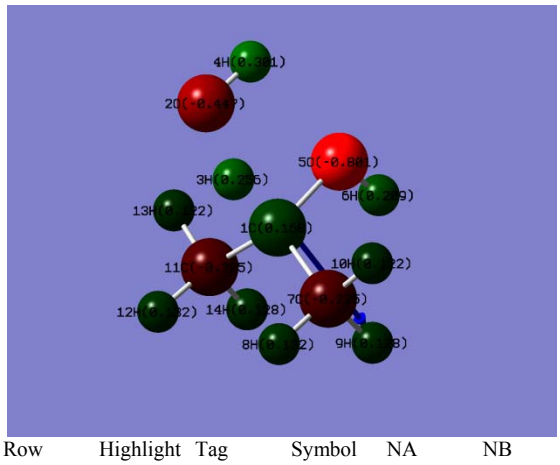

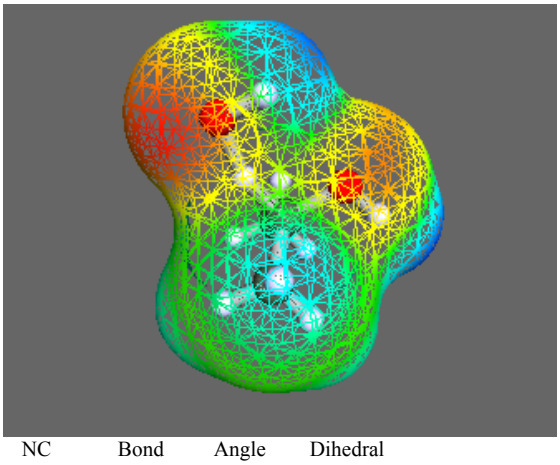

Row	Highlight	Tag	Symbol	NA	NB	NC	Bond	Angle	Dihedral
1	No	1	C						
2	No	2	O	1			2.4737132		
3	No	3	H	1	2		1.2001575	11.0939544	
4	No	4	H	2	1	3	0.9793677	85.1890685	179.9719699
5	No	5	O	1	2	4	1.4218821	90.6419651	-0.0228165
6	No	6	H	5	1	2	0.9747216	107.6080243	179.9579748
7	No	7	C	1	5	2	1.5104417	112.1769066	-113.9491624
8	No	8	H	7	1	5	1.0928020	111.1528970	173.8379491
9	No	9	H	7	1	5	1.0976914	109.9299261	-66.5218701
10	No	10	H	7	1	5	1.0914047	109.9914931	52.9968809
11	No	11	C	1	5	7	1.5104431	112.1764915	-132.1048449
12	No	12	H	11	1	5	1.0928038	111.1530722	-173.8362622
13	No	13	H	11	1	5	1.0914034	109.9907923	-52.9955984
14	No	14	H	11	1	5	1.0976868	109.9292862	66.5219428

CH3CH(OH)CH3-HO radical TS2

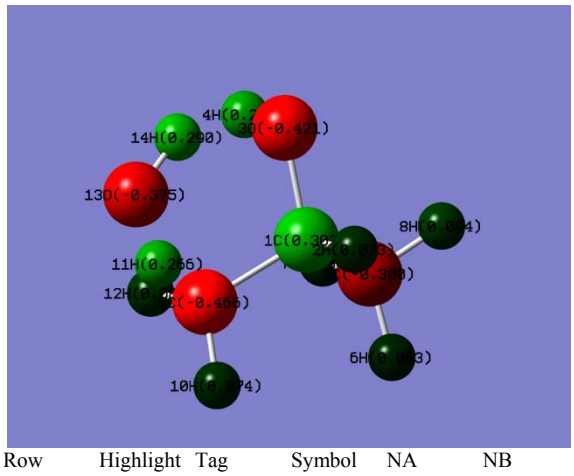

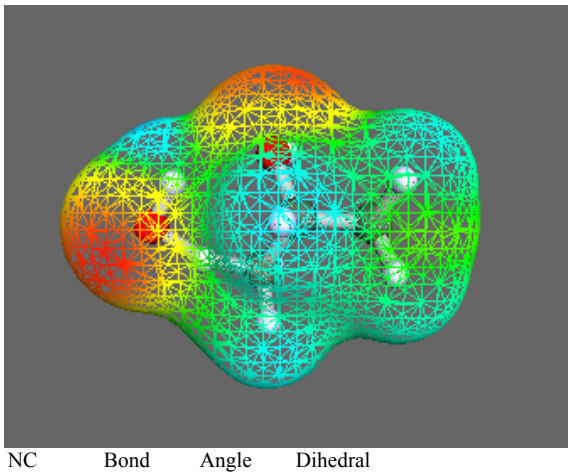

Row	Highlight	Tag	Symbol	NA	NB	NC	Bond	Angle	Dihedral
1	No	1	C						
2	No	2	H	1			1.0934059		
3	No	3	O	1	2		1.4389027	103.7476566	
4	No	4	H	3	1	2	0.9746230	107.0358163	177.2071921
5	No	5	C	1	3	4	1.5202769	110.6774752	59.5952352
6	No	6	H	5	1	3	1.0933420	111.0506524	175.4533188
7	No	7	H	5	1	3	1.0955069	110.3123697	-64.9326732
8	No	8	H	5	1	3	1.0922432	110.0319615	54.8471519
9	No	9	C	1	3	5	1.5115119	110.6212202	-125.6077553
10	No	10	H	9	1	3	1.0914989	113.9299139	-167.8965256
11	No	11	H	9	1	3	1.2353394	106.4245284	-52.1344445
12	No	12	H	9	1	3	1.0930579	113.2107121	63.5791964
13	No	13	O	9	1	3	2.4401073	95.3305833	-47.8606546
14	No	14	H	13	9	1	0.9821730	84.8209609	28.3006272

CH3CH2CH2OH

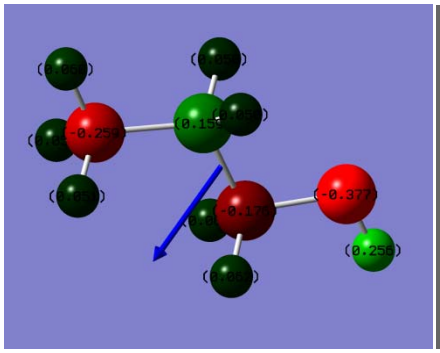

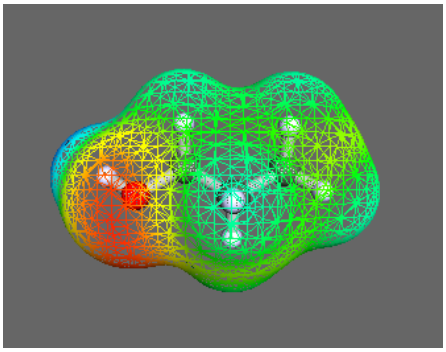

Row	Highlight	Tag	Symbol	NA	NB	NC	Bond	Angle	Dihedral
1	No	1	C						
2	No	2	H	1			1.0941560		
3	No	3	H	1	2		1.0941560	107.8352063	
4	No	4	H	1	2	3	1.0927606	107.7350489	116.0310913
5	No	5	C	1	4	2	1.5243322	111.0921520	-121.9516110
6	No	6	H	5	1	4	1.0945291	110.5489994	-59.0706892
7	No	7	H	5	1	4	1.0945291	110.5489994	59.0706892
8	No	8	C	5	1	4	1.5139923	112.2538545	180.0000000
9	No	9	H	8	5	1	1.1004484	109.8402438	-59.0153234
10	No	10	H	8	5	1	1.1004484	109.8402438	59.0153234
11	No	11	O	8	5	1	1.4268389	107.4866833	180.0000000
12	No	12	H	11	8	5	0.9711543	107.7196839	180.0000000

CH3CH2CH2OH – HO radical TS1

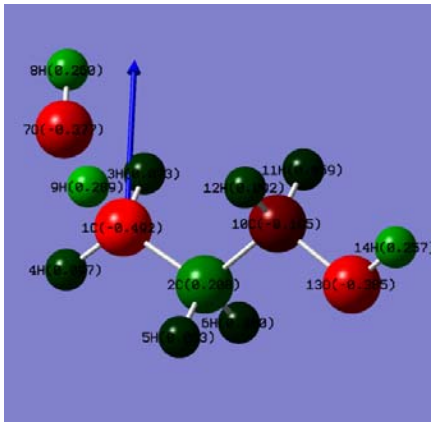

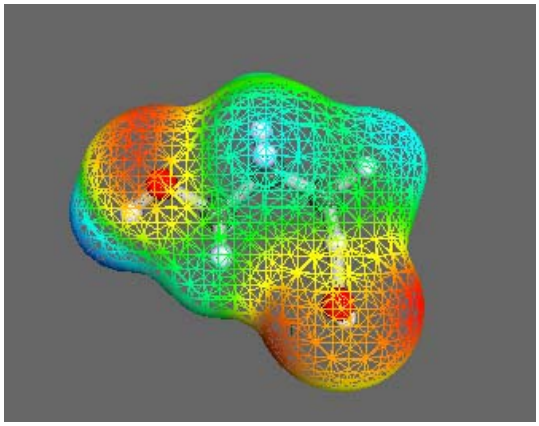

Row	Highlight	Tag	Symbol	NA	NB	NC	Bond	Angle	Dihedral
1	No	1	C						
2	No	2	C	1			1.5127586		
3	No	3	H	1	2		1.0924449	113.4737611	
4	No	4	H	1	2	3	1.0911710	114.1637085	127.6346597
5	No	5	H	2	1	4	1.0936299	110.4552188	-52.6738246
6	No	6	H	2	1	4	1.0968135	109.7768999	65.0767062
7	No	7	O	1	2	5	2.5067090	106.3480969	68.9677462
8	No	8	H	7	1	2	0.9786676	94.5458576	127.5502869
9	No	9	H	1	2	7	1.2082473	107.2891869	-6.5514013
10	No	10	C	2	1	7	1.5152490	112.4437913	-52.4266629
11	No	11	H	10	2	1	1.1011909	109.7615563	-56.9659973
12	No	12	H	10	2	1	1.0968458	109.3800430	61.2018196
13	No	13	O	10	2	1	1.4266437	107.0574951	-177.5348809
14	No	14	H	13	10	2	0.9711710	107.6555344	-174.0480329

CH3CH2CH2OH – HO radical TS2

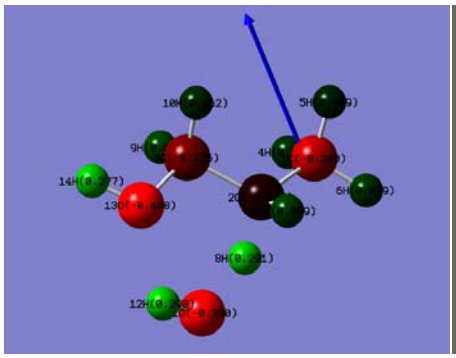

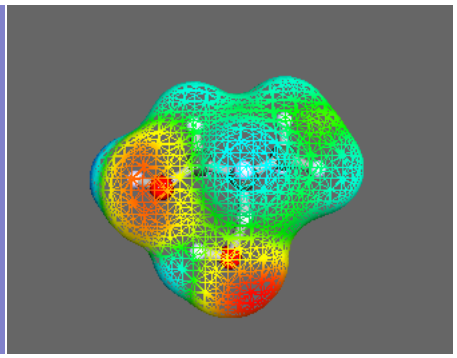

Row	Highlight	Tag	Symbol	NA	NB	NC	Bond	Angle	Dihedral
1	No	1	C						
2	No	2	C	1			1.5128786		
3	No	3	C	2	1		1.5057892	114.5115137	
4	No	4	H	1	2	3	1.0931198	110.8446095	-58.2479206
5	No	5	H	1	2	3	1.0962056	110.8721257	61.7950168
6	No	6	H	1	2	3	1.0918590	111.0189829	-178.3523709
7	No	7	H	2	1	3	1.0929829	113.5831518	-128.7880286
8	No	8	H	2	1	3	1.2164573	107.4774475	116.1610284
9	No	9	H	3	2	1	1.0980917	109.6064709	53.2352373
10	No	10	H	3	2	1	1.1000450	110.1046648	-65.5891268
11	No	11	O	2	1	3	2.4605201	115.0979758	106.7652571
12	No	12	H	11	2	1	0.9814307	85.6160929	-157.2606964
13	No	13	O	3	2	1	1.4327330	107.4433488	173.8727232
14	No	14	H	13	3	2	0.9718779	107.9607077	-177.5731559

CH3CH2CH2OH- HO radical TS3

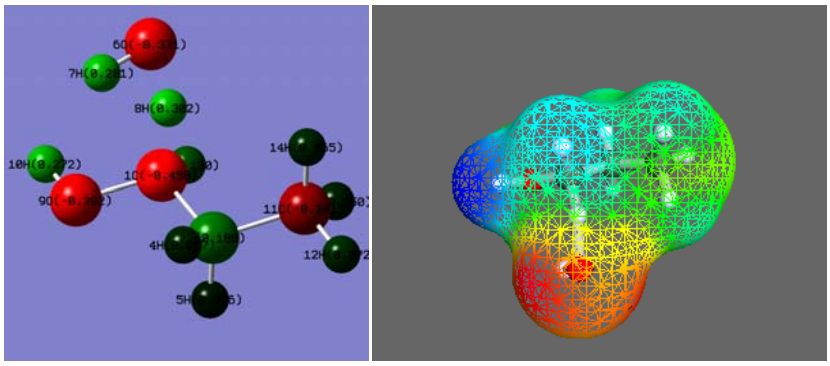

Row	Highlight	Tag	Symbol	NA	NB	NC	Bond	Angle	Dihedral
1	No	1	C						
2	No	2	C	1			1.5063747		
3	No	3	H	1	2		1.0990527	112.9242365	
4	No	4	H	2	1	3	1.0944997	108.0072984	-178.8481418
5	No	5	H	2	1	3	1.0959800	108.4325626	-63.3496562
6	No	6	O	1	2	4	2.5122367	105.9717191	54.3689557
7	No	7	H	6	1	2	0.9792625	84.2238367	-85.9066756
8	No	8	H	1	2	6	1.1919149	107.0970749	12.1417889
9	No	9	O	1	2	6	1.4081089	109.6857740	-106.3828819
10	No	10	H	9	1	2	0.9723044	108.0844703	-171.5316767
11	No	11	C	2	1	9	1.5240738	111.7781682	-173.7102265
12	No	12	H	11	2	1	1.0924355	110.9338027	-179.8749798
13	No	13	H	11	2	1	1.0939917	111.1597014	-59.9558782
14	No	14	H	11	2	1	1.0927221	110.3673065	60.0968194

HOCH2OH

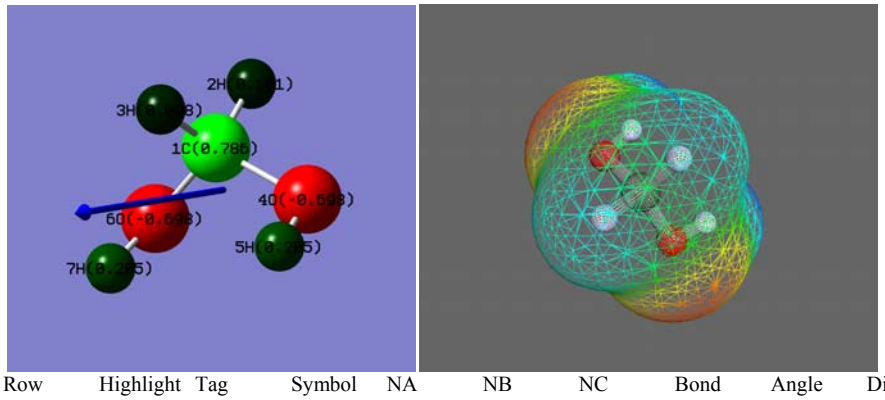

Row	Highlight	Tag	Symbol	NA	NB	NC	Bond	Angle	Dihedral
1	No	1	C						
2	No	2	H	1			1.0876852		
3	No	3	H	1	2		1.0998989	109.8207858	
4	No	4	O	1	2	3	1.4090658	105.6811084	-119.2772254
5	No	5	H	4	1	2	0.9715133	108.4019332	168.8641615
6	No	6	O	1	4	5	1.4090633	114.2387721	-75.3987018
7	No	7	H	6	1	4	0.9715152	108.4013314	75.3388620

HOCH2OH – HO radical TS

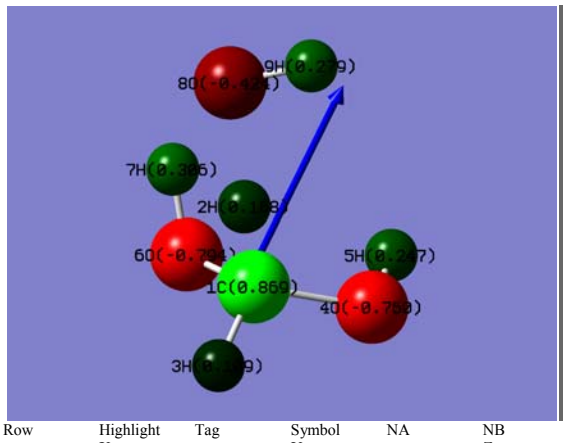

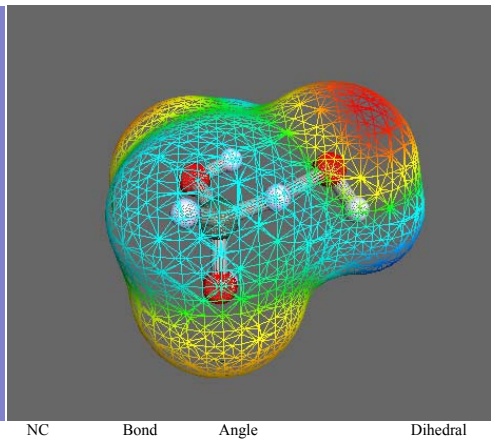

Row	Highlight X	Tag	Symbol Y	NA	NB Z	NC	Bond	Angle		Dihedral	
1	No 0.1988810	1	C 0.1362680		0.0369840						
2	No 0.1557360	2	H -0.0440340	1 1.2100650			1.1876402				
3	No 0.2088190	3	H -0.2433000	1	2		1.0923834	107.3703458			1.2521990
4	No -0.2935460	4	O	1	3	2	1.3900685	108.1370790	119.2121830	-0.4204750	1.3360340
5	No -0.4157220	5	H	4	1	3	0.9737081	106.2263408	155.3839825	-1.3643400	1.1303660
6	No -0.5318510	6	O	1	4	5	1.3901238	113.4628063	30.8083466	-0.4103820	-0.9762380
7	No 0.1882870	7	H	6	1	4	0.9757679	106.1050159	-104.8578795	-0.9033650	-1.4126920
8	No 2.2389920	8	O	1	4	6	2.4662317	109.4098404	-97.1057960	-0.6103300	-0.6244140
9	No 2.6014300	9	H	8	1	4	0.9789731	100.3516194	-20.2889496	-0.9523160	0.2182440

HOCH2COOH

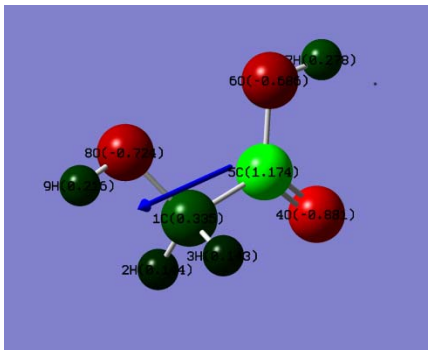

Row	Highlight	Tag	Symbol	NA	NB	NC	Bond	Angle	Dihedral
1	No	1	C						
2	No	2	H	1			1.0970410		
3	No	3	H	1	2		1.0999262	107.4289122	
4	No	4	O	1	2	3	2.3979114	87.1292757	97.1240562
5	No	5	C	4	1	2	1.2184705	32.0357808	140.2546603
6	No	6	O	5	4	1	1.3472568	123.9062207	177.5767191
7	No	7	H	6	5	4	0.9802106	105.0171897	0.9501190
8	No	8	O	1	5	4	1.4142418	110.7189190	-164.9411026
9	No	9	H	8	1	5	0.9713649	107.2570992	-177.8786515

HOCH2COOH HO radical TS1 CIS

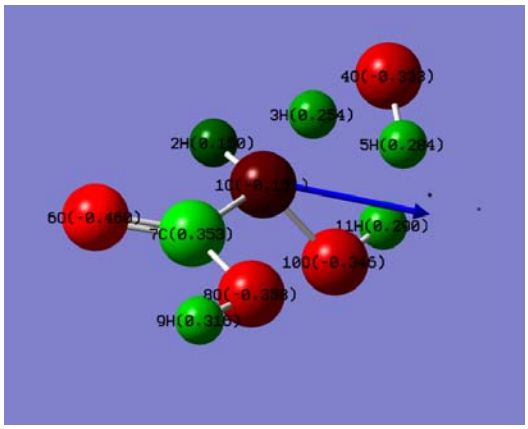

Row	Highlight	Tag	Symbol	NA	NB	NC	Bond	Angle	Dihedral
1	No	1	C						
2	No	2	H	1			1.0951105		
3	No	3	H	1	2		1.2094779	106.0140503	
4	No	4	O	1	2	3	2.4783639	118.5865102	-2.9970869
5	No	5	H	4	1	2	0.9806188	85.1626498	175.2842370
6	No	6	O	1	4	5	2.4096351	110.6528951	78.2697466
7	No	7	C	6	1	4	1.2152195	30.7622863	-69.1089389
8	No	8	O	7	6	1	1.3545339	124.0395531	176.4447715
9	No	9	H	8	7	6	0.9800054	105.6796663	1.1791849
10	No	10	O	1	7	6	1.3956714	110.5775747	-137.6542236
11	No	11	H	10	1	7	0.9728860	107.7205115	-175.2084566

HOCH2COOH HO radical TS2 TRANS

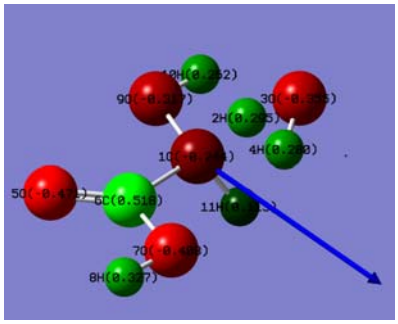

Row	Highlight	Tag	Symbol	NA	NB	NC	Bond	Angle	Dihedral
1	No	1	C						
2	No	2	H	1			1.2109027		
3	No	3	O	2	1		1.3237389	162.7612156	
4	No	4	H	3	2	1	0.9797667	97.0281894	-12.1375357
5	No	5	O	1	3	2	2.4296451	114.5305362	-117.0609105
6	No	6	C	5	1	3	1.2096211	29.6525702	-52.9631031
7	No	7	O	6	5	1	1.3673317	123.8006960	179.8624238
8	No	8	H	7	6	5	0.9795665	105.7381198	0.4798498
9	No	9	O	1	6	5	1.3879629	109.4890313	5.4493437
10	No	10	H	9	1	6	0.9722802	107.9305419	-176.5790685
11	No	11	H	1	9	6	1.0977355	115.0918893	125.3040287

HOCH2COOH HO radical TS3 TRANS

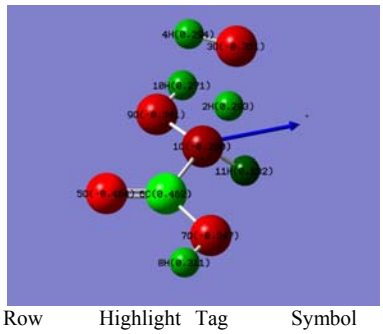

Row	Highlight	Tag	Symbol	NA	NB	NC	Bond	Angle	Dihedral
1	No	1	C						
2	No	2	H	1			1.2072233		
3	No	3	O	2	1		1.3334878	154.8166096	
4	No	4	H	3	2	1	0.9803086	96.2210473	32.3837369
5	No	5	O	1	3	2	2.4204299	106.3446544	100.3798600
6	No	6	C	5	1	3	1.2123115	30.1537344	-99.0276128
7	No	7	O	6	5	1	1.3565686	124.4387946	177.2556052
8	No	8	H	7	6	5	0.9794983	105.9078124	-1.6291804
9	No	9	O	1	6	5	1.3922683	109.6734151	-16.4653433
10	No	10	H	9	1	6	0.9727647	107.4362443	-178.5759779
11	No	11	H	1	9	6	1.0957524	115.2475164	127.7223199

(CH3)3COH

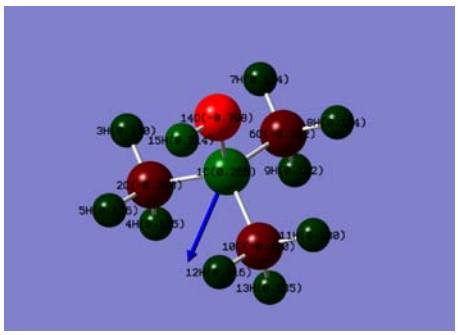

Row	Highlight	Tag	Symbol	NA	NB	NC	Bond	Angle	Dihedral
1	No	1	C						
2	No	2	C	1			1.5240164		
3	No	3	H	2	1		1.0928655	109.8394691	
4	No	4	H	2	1	3	1.0941526	111.3375715	120.6753134
5	No	5	H	2	1	3	1.0959763	110.5082670	-119.4825216
6	No	6	C	1	2	3	1.5184442	111.0063412	-58.3020152
7	No	7	H	6	1	2	1.0928013	109.8924893	58.3923256
8	No	8	H	6	1	2	1.0928013	109.8924893	177.5651625
9	No	9	H	6	1	2	1.0934961	110.7924333	-62.0212560
10	No	10	C	1	6	2	1.5240164	111.0063412	124.0425119
11	No	11	H	10	1	6	1.0928655	109.8394691	58.3020152
12	No	12	H	10	1	6	1.0959763	110.5082670	177.7845368
13	No	13	H	10	1	6	1.0941526	111.3375715	-62.3732982
14	No	14	O	1	6	10	1.4380370	104.4870544	117.9787440
15	No	15	H	14	1	6	0.9738932	106.9316679	180.0000000

(CH3)3COH HO radical TS

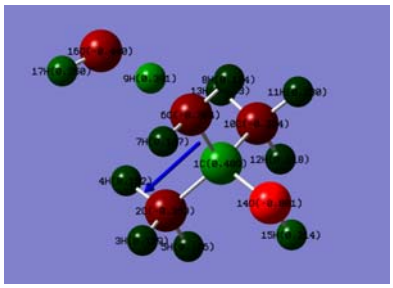

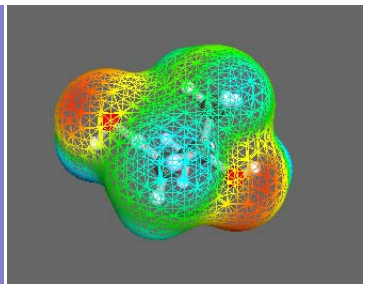

Row	Highlight	Tag	Symbol	NA	NB	NC	Bond	Angle	Dihedral
1	No	1	C						
2	No	2	C	1			1.5229251		
3	No	3	H	2	1		1.0934409	109.8124513	
4	No	4	H	2	1	3	1.0923804	110.6065089	120.8494068
5	No	5	H	2	1	3	1.0954871	110.3385564	-119.2523708
6	No	6	C	1	2	4	1.5130697	110.9447170	61.6817545
7	No	7	H	6	1	2	1.0914456	112.6995902	53.9810690
8	No	8	H	6	1	2	1.0914449	112.9025981	-178.9540495
9	No	9	H	6	1	2	1.2125368	106.7436117	-64.1299152
10	No	10	C	1	6	2	1.5225587	110.6393145	123.9513059
11	No	11	H	10	1	6	1.0930075	109.8627173	58.6412109
12	No	12	H	10	1	6	1.0957246	110.3085472	178.0488763
13	No	13	H	10	1	6	1.0931204	110.8011313	-62.0291147
14	No	14	O	1	6	10	1.4391230	103.6704440	118.0817965
15	No	15	H	14	1	6	0.9746298	106.7538551	-179.0105829
16	No	16	O	6	1	14	2.4980835	103.6352300	-176.7174221
17	No	17	H	16	6	1	0.9790306	95.1808429	112.0265432

CH(CH3)(OH)2

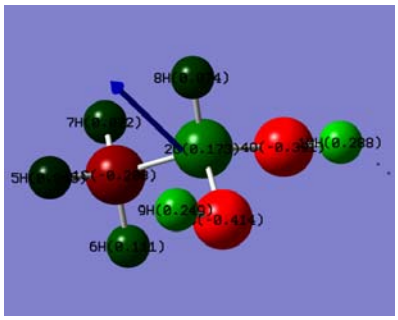

Row	Highlight	Tag	Symbol	NA	NB	NC	Bond	Angle	Dihedral
1	No	1	C						
2	No	2	C	1			1.5094213		
3	No	3	O	2	1		1.4252415	112.1695092	
4	No	4	O	2	1	3	1.3991234	107.3932665	116.9415979
5	No	5	H	1	2	4	1.0932583	110.5392698	179.9503068
6	No	6	H	1	2	4	1.0910572	108.2569900	60.2806661
7	No	7	H	1	2	4	1.0920666	110.4499256	-59.4908537
8	No	8	H	2	1	4	1.1044354	110.8364731	121.1517750
9	No	9	H	3	2	1	0.9724113	107.8936482	-77.6711664
10	No	10	H	4	2	1	0.9736420	106.2686278	-169.2478189

CH(CH3)(OH)2 – HO radical TS1

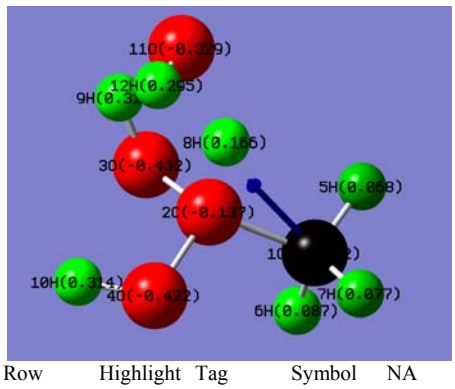

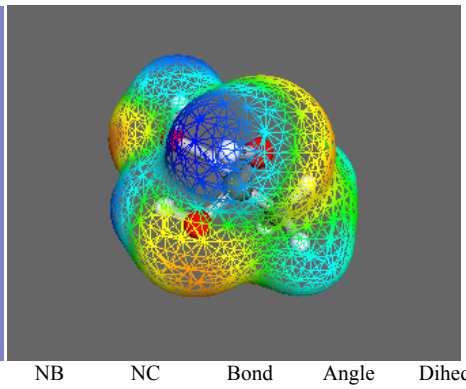

Row	Highlight	Tag	Symbol	NA	NB	NC	Bond	Angle	Dihedral
1	No	1	C						
2	No	2	C	1			1.5041828		
3	No	3	O	2	1		1.3980250	112.0064362	
4	No	4	O	2	1	3	1.4003918	109.8123055	124.6989713
5	No	5	H	1	2	3	1.0905492	110.0615550	62.0079550
6	No	6	H	1	2	3	1.0929730	108.0274672	-57.3902550
7	No	7	H	1	2	3	1.0909496	110.2488532	-176.5824822
8	No	8	H	2	1	4	1.1836928	109.3471803	119.2299422
9	No	9	H	3	2	1	0.9762702	105.8005732	-134.4234459
10	No	10	H	4	2	1	0.9737564	105.7323765	-146.5385279
11	No	11	O	2	1	4	2.4785407	126.6793954	129.7782285
12	No	12	H	11	2	1	0.9792436	97.0391411	-114.1794939

CH(CH3)(OH)2 – HO radical TS2

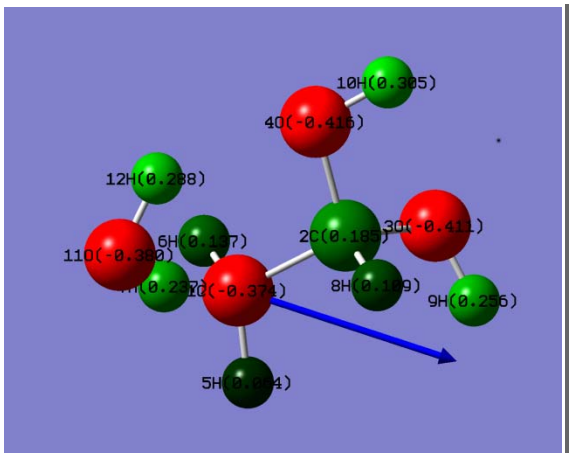

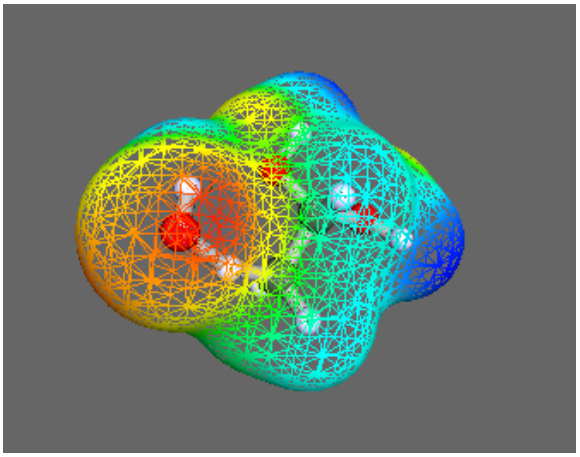

Row	Highlight	Tag	Symbol	NA	NB	NC	Bond	Angle	Dihedral
1	No	1	C						
2	No	2	C	1			1.5026100		
3	No	3	O	2	1		1.4221271	112.2811071	
4	No	4	O	2	1	3	1.4053750	106.9042848	116.5673226
5	No	5	H	1	2	4	1.0906063	113.4563899	-173.5839719
6	No	6	H	1	2	4	1.0892224	111.3804411	57.7760201
7	No	7	H	1	2	4	1.2350812	106.3684718	-58.4725431
8	No	8	H	2	1	4	1.1018320	110.5831879	120.6410020
9	No	9	H	3	2	1	0.9726412	107.9670600	-81.3120885
10	No	10	H	4	2	1	0.9741157	106.6651175	-170.5078582
11	No	11	O	1	2	4	2.4407213	94.8426117	-55.8877525
12	No	12	H	11	1	2	0.9806644	86.6157685	41.0663074

HCHO

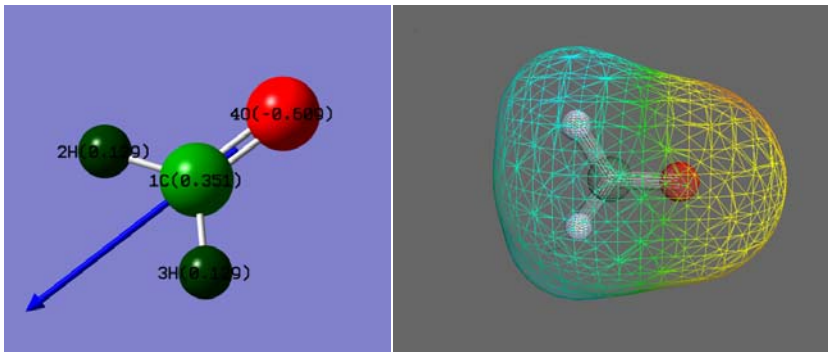

Row	Highlight	Tag	Symbol	NA	NB	NC	Bond	Angle	Dihedral
1	No	1	C						
2	No	2	H	1			1.1043225		
3	No	3	H	1	2		1.1043225	115.6011365	
4	No	4	O	1	2	3	1.2198430	122.1994317	180.0000000

HCHO – HO radical TS

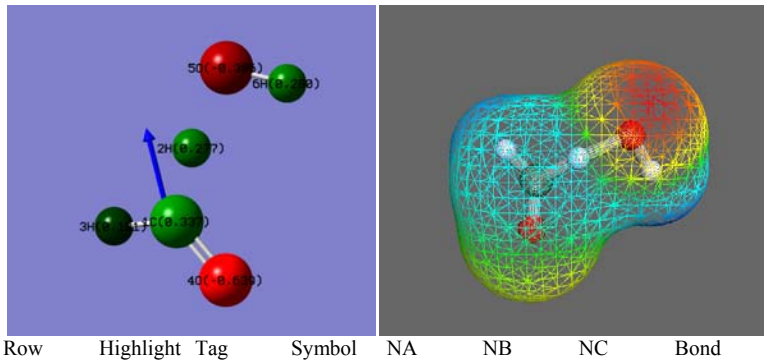

Row	Highlight	Tag	Symbol	NA	NB	NC	Bond	Angle	Dihedral
1	No	1	C						
2	No	2	H	1			1.1998889		
3	No	3	H	1	2		1.1091725	111.7452108	
4	No	4	O	1	3	2	1.1952081	125.1360572	-177.3085725
5	No	5	O	1	4	3	2.4917876	121.2087436	-159.7078145
6	No	6	H	5	1	4	0.9796013	93.9601645	2.8033658

CH3CHO

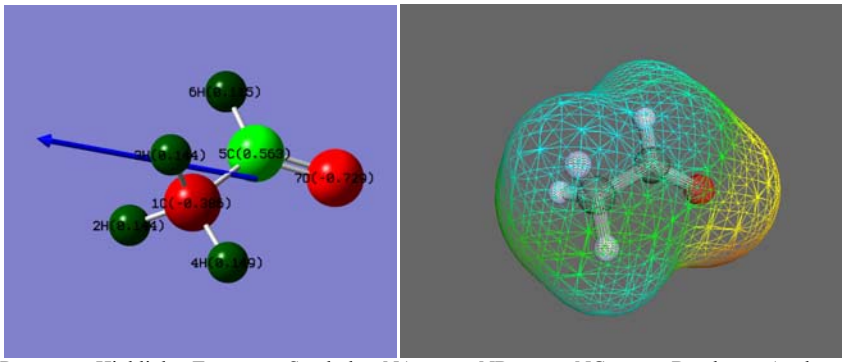

Row	Highlight	Tag	Symbol	NA	NB	NC	Bond	Angle	Dihedral
1	No	1	C						
2	No	2	H	1			1.0947733		
3	No	3	H	1	2		1.0947755	107.1749445	
4	No	4	H	1	2	3	1.0901317	110.0324659	119.6212762
5	No	5	C	1	4	3	1.5015846	109.8276211	121.0638792
6	No	6	H	5	1	4	1.1089830	115.3459493	179.9886512
7	No	7	O	5	1	4	1.2224501	124.3297801	-0.0136633

CH3CHO – HO radical TS1

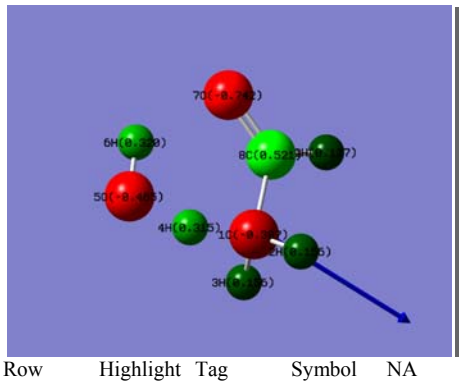

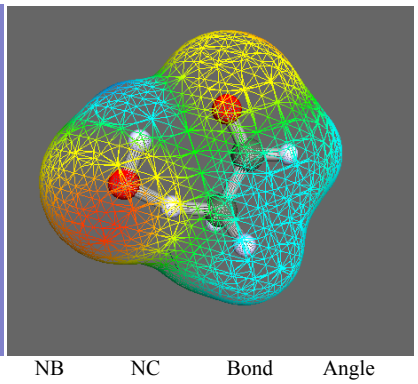

Row	Highlight	Tag	Symbol	NA	NB	NC	Bond	Angle	Dihedral
1	No	1	C						
2	No	2	H	1			1.0921518		
3	No	3	H	1	2		1.0921546	110.7358071	
4	No	4	H	1	2	3	1.2505394	106.5940369	115.5585872
5	No	5	O	1	2	3	2.4366564	111.5088477	124.7884456
6	No	6	H	5	1	2	0.9819134	87.6365699	117.8300549
7	No	7	O	1	5	6	2.4120172	73.0182122	0.0062510
8	No	8	C	7	1	5	1.2242153	30.6766591	179.9928383
9	No	9	H	8	7	1	1.1070746	119.8299023	179.9979513

CH3CHO – HO radical TS2

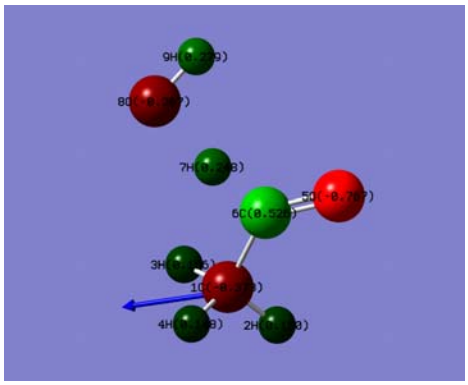

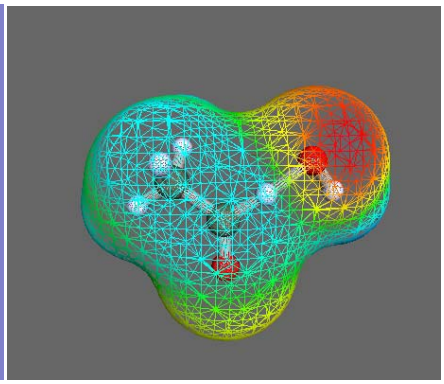

Row	Highlight	Tag	Symbol	NA	NB	NC	Bond	Angle	Dihedral
	X	Y	Z						
1	No	1	C						
	-0.0123370		0.0703640		-0.0352760				
2	No	2	H	1			1.0904408		
	-0.0691130		-0.1357170		1.0340080				
3	No	3	H	1	2		1.0929583	110.9520188	
	1.0169880		0.2766090		-0.3394320				
4	No	4	H	1	2	3	1.0935891	110.5071639	119.0960818
	-0.3578190		-0.7930320		-0.6107120				
5	No	5	O	1	2	4	2.4315897	86.8133469	119.6883917
	-1.5576560		1.9026830		0.3736550				
6	No	6	C	5	1	2	1.2054713	29.3255167	178.0649927
	-0.8644510		1.2594230		-0.3739040				
7	No	7	H	6	5	1	1.1944195	120.8052529	-178.0457185
	-0.7665880		1.5578260		-1.5263000				
8	No	8	O	6	5	1	2.5341742	120.2623842	-162.9257261
						-0.2077640		2.1998790	-2.6336260
9	No	9	H	8	6	5			
						0.9794425	93.6627437	5.7499330	-
0.6119510						3.0744320		-2.4572810	

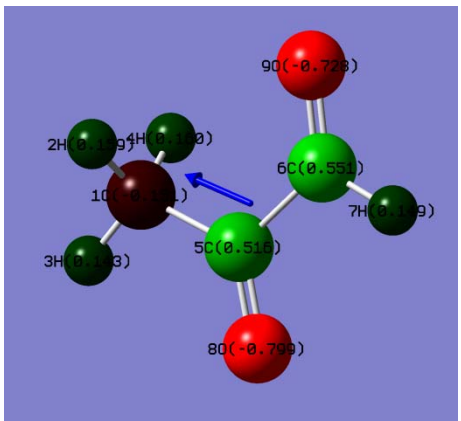

CH3COCHO

Row	Highlight	Tag	Symbol	NA	NB	NC	Bond	Angle	Dihedral
1	No	1	C						
2	No	2	H	1			1.0935787		
3	No	3	H	1	2		1.0896056	110.3219881	
4	No	4	H	1	3	2	1.0935838	110.3173060	-117.7034927
5	No	5	C	1	3	4	1.4990048	109.5788890	-121.1452959
6	No	6	C	5	1	3	1.5218312	117.1138262	-179.9739652
7	No	7	H	6	5	1	1.1059837	114.1577589	-179.9994603
8	No	8	O	5	1	6	1.2281004	125.1263403	-179.9967228
9	No	9	O	6	5	1	1.2230842	122.6896867	0.0003627

CH3COCHO-HOradical TS1

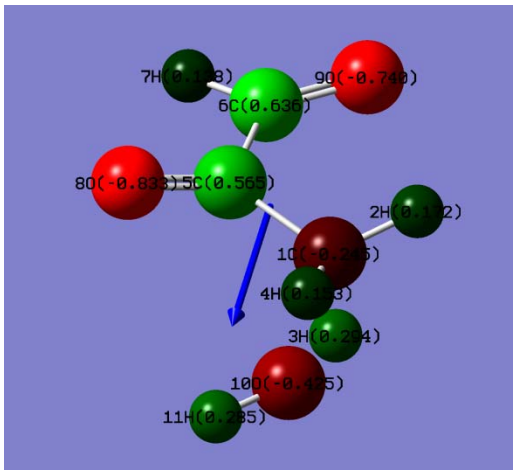

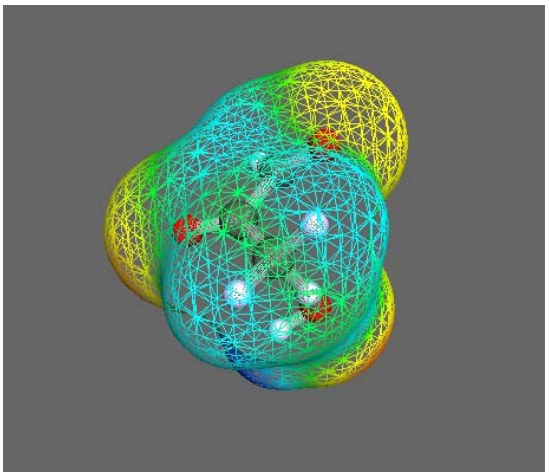

Row	Highlight	Tag	Symbol	NA	NB	NC	Bond	Angle	Dihedral
1	No	1	C						
2	No	2	H	1			1.0886815		
3	No	3	H	1	2		1.2481002	103.5165864	
4	No	4	H	1	2	3	1.0879395	115.7773833	118.0283824
5	No	5	C	1	4	2	1.4998351	113.5968071	-135.4350744
6	No	6	C	5	1	4	1.5553826	114.6909736	168.7600823
7	No	7	H	6	5	1	1.1088956	112.8067475	162.4500085
8	No	8	O	5	1	6	1.1986216	126.0702681	177.9881369
9	No	9	O	6	5	1	1.1978521	122.7021906	-20.1206492
10	No	10	O	1	5	8	2.3878360	82.5527627	98.6749401
11	No	11	H	10	1	5	0.9813396	94.4849431	-75.9111752

CH3COCHO-HOradical TS2

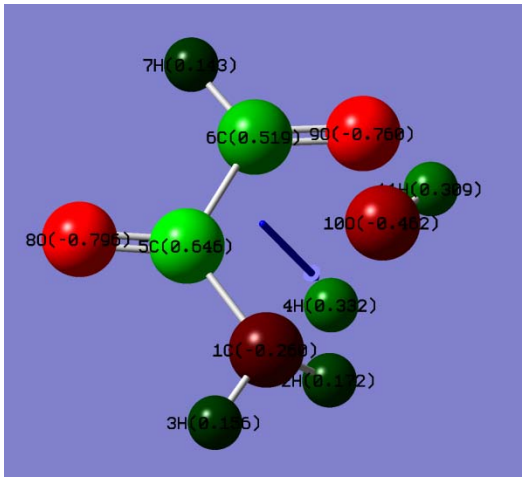

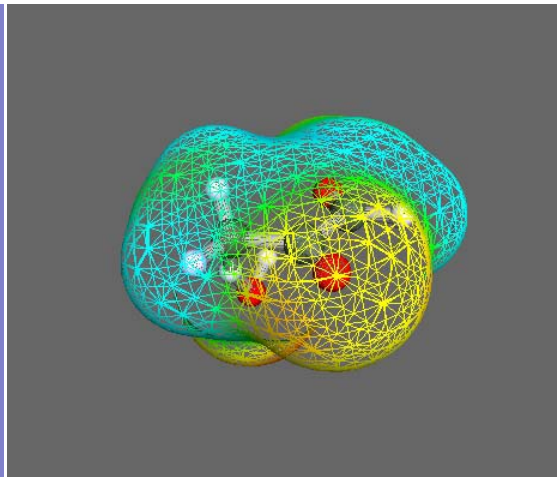

Row	Highlight	Tag	Symbol	NA	NB	NC	Bond	Angle	Dihedral
1	No	1	C						
2	No	2	H	1			1.0898525		

3	No	3	H	1	2		1.0882820	114.5100852	
4	No	4	H	1	3	2	1.2537801	105.5063179	-115.8996371
5	No	5	C	1	3	2	1.5013281	112.4912609	131.5785438
6	No	6	C	5	1	3	1.5661333	115.4564998	179.4036012
7	No	7	H	6	5	1	1.1082900	112.2560061	177.8631111
8	No	8	O	5	1	6	1.1880689	126.5462975	179.6266902
9	No	9	O	6	5	1	1.2020879	123.7022434	-0.9869822
10	No	10	O	1	5	8	2.4183871	92.6442261	-119.7637367
11	No	11	H	10	1	5	0.9810850	92.1264387	-78.9423099

CH3COCHO-HOradical TS3

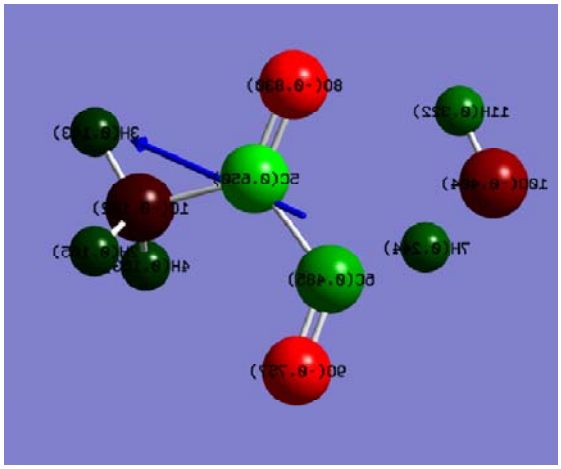

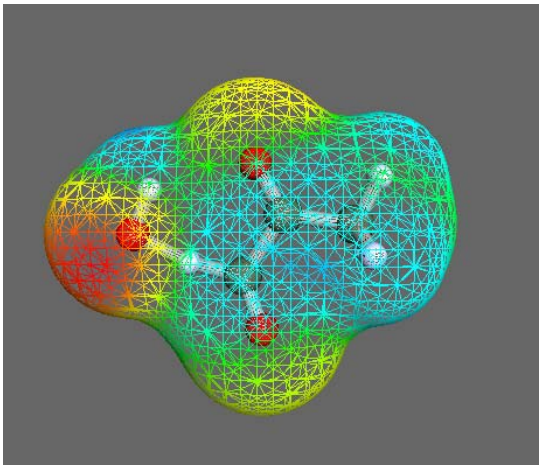

Row	Highlight	Tag	Symbol	NA	NB				
	NC	Bond	Angle	Dihedral					
1	No	1	C						
2	No	2	H	1			1.0935503		
3	No	3	H	1	2		1.0893375	110.5846966	
4	No	4	H	1	3	2	1.0936836	110.6198336	-118.1875497
5	No	5	C	1	3	2	1.4958448	109.8349372	120.6093385
6	No	6	C	5	1	3	1.5611351	115.8773507	178.7953853
7	No	7	H	6	5	1	1.2233674	110.6638218	-172.1137211
8	No	8	O	5	1	6	1.2165418	126.3625699	178.8419312
9	No	9	O	6	5	1	1.1859733	124.4381423	12.5995865
10	No	10	O	6	5	1	2.4515706	101.8167983	173.2089785
11	No	11	H	10	6	5	0.9813976	89.4313241	2.5666983

CH3COCHO-HOradical TS4

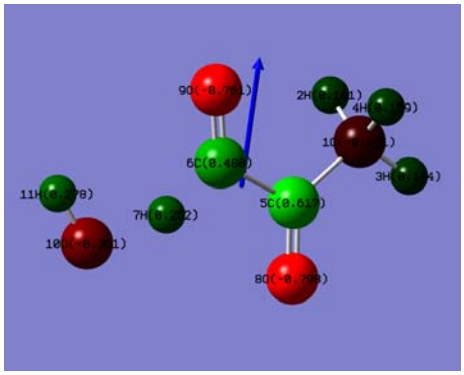

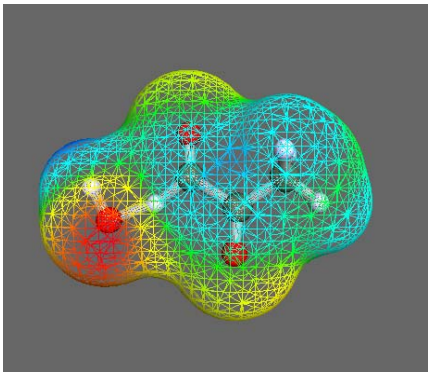

Row	Highlight	Tag	Symbol	NA	NB	NC	Bond	Angle	Dihedral
1	No	1	C						
2	No	2	H	1			1.0937243		
3	No	3	H	1	2		1.0894837	110.3545182	
4	No	4	H	1	3	2	1.0932174	110.7141446	-118.2519502

5	No	5	C	1	3	2	1.4996733	109.4360733	120.6197257
6	No	6	C	5	1	3	1.5643106	115.0908868	177.4129540
7	No	7	H	6	5	1	1.2150091	111.1312403	174.4726842
8	No	8	O	5	1	6	1.2116475	126.6913929	-179.8178451
9	No	9	O	6	5	1	1.1893590	124.7990155	-2.7108374
10	No	10	O	6	5	1	2.4677087	116.3428064	157.8012160
11	No	11	H	10	6	5	0.9800394	90.1968317	-166.2043528

CHOCOOHTS1

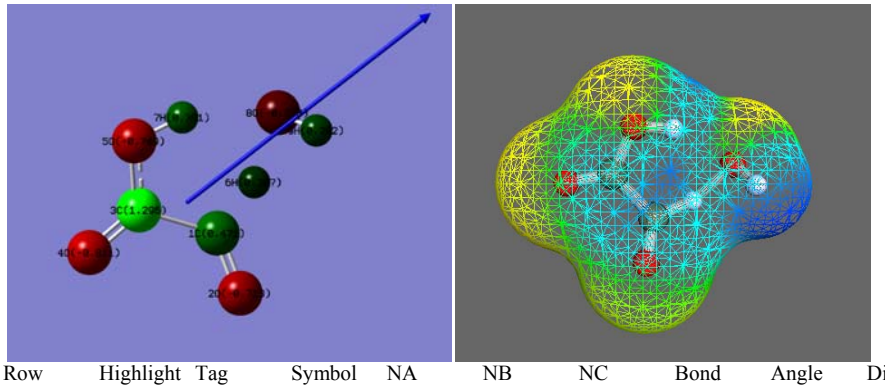

Row	Highlight	Tag	Symbol	NA	NB	NC	Bond	Angle	Dihedral
1	No	1	C						
2	No	2	O	1			1.1851101		
3	No	3	C	1	2		1.5568824	125.4279199	
4	No	4	O	3	1	2	1.2074225	120.8423297	-25.1066722
5	No	5	O	3	1	2	1.3356306	113.4704566	154.9377726
6	No	6	H	1	2	3	1.1965928	122.6821845	176.7152248
7	No	7	H	5	3	1	0.9893896	110.1876172	0.7303834
8	No	8	O	1	2	3	2.5007390	132.0264866	152.1300853
9	No	9	H	8	1	2	0.9805869	94.8774707	-29.9711572

CHOCOOH2 TS

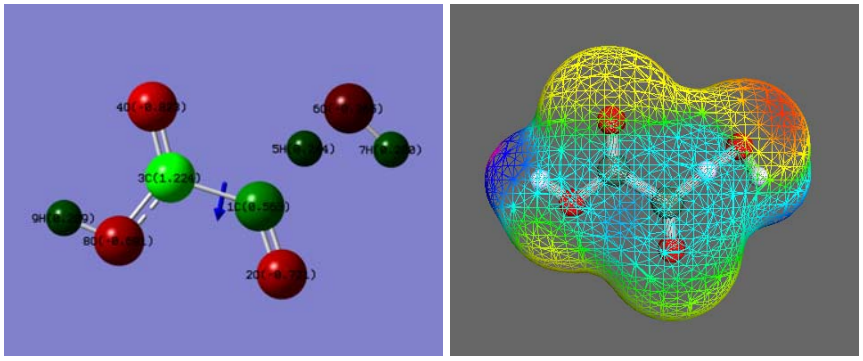

Row	Highlight	Tag	Symbol	NA	NB	NC	Bond	Angle	Dihedral
1	No	1	C						
2	No	2	O	1			1.1844955		
3	No	3	C	1	2		1.5429563	125.9895771	
4	No	4	O	3	1	2	1.2116698	122.1640841	177.7697924
5	No	5	H	1	2	3	1.2206465	124.2809118	-176.0976115
6	No	6	O	1	2	3	2.4211603	118.3418254	-155.8183066
7	No	7	H	6	1	2	0.9804081	91.3738688	-1.8079368
8	No	8	O	3	1	2	1.3428085	110.9920979	-1.5809055
9	No	9	H	8	3	1	0.9811953	106.4019610	179.4826963

CHOCOOH3 TS

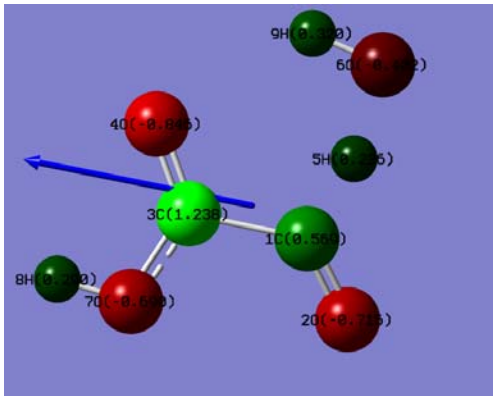

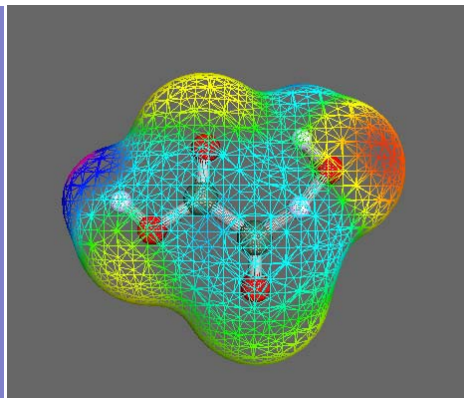

Row	Highlight	Tag	Symbol	NA	NB	NC	Bond	Angle	Dihedral
1	No	1	C						
2	No	2	O	1			1.1808558		
3	No	3	C	1	2		1.5445538	125.4834757	
4	No	4	O	3	1	2	1.2159505	121.4665208	-161.3685960
5	No	5	H	1	2	3	1.2260045	124.7448414	-173.5999176
6	No	6	O	1	2	3	2.4132845	128.2546172	-150.9368612
7	No	7	O	3	1	2	1.3361274	111.8841065	18.7612097
8	No	8	H	7	3	1	0.9816802	106.9371032	179.8471544
9	No	9	H	6	1	2	0.9812156	90.6434389	157.4748845

CH3OCH3

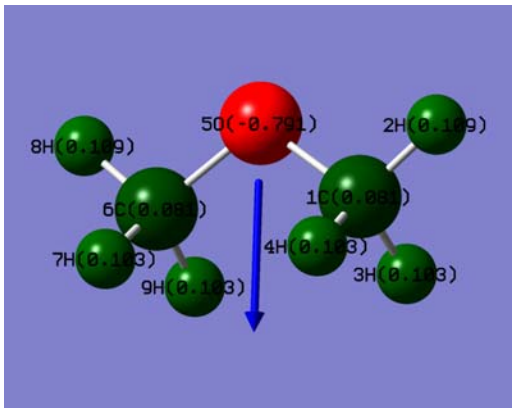

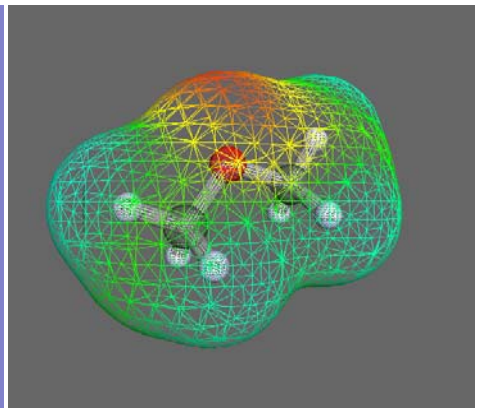

Row	Highlight	Tag	Symbol	NA	NB	NC	Bond	Angle	Dihedral
1	No	1	C						
2	No	2	H	1			1.0902799		
3	No	3	H	1	2		1.0990990	109.2142928	
4	No	4	H	1	2	3	1.0990990	109.2142928	118.4599173
5	No	5	O	1	2	3	1.4137364	106.9383951	-120.7700414
6	No	6	C	5	1	2	1.4137364	111.0638283	180.0000000
7	No	7	H	6	5	1	1.0990990	111.4848934	60.6862676
8	No	8	H	6	5	1	1.0902799	106.9383951	180.0000000
9	No	9	H	6	5	1	1.0990990	111.4848934	-60.6862676

CH3OCH3 – HO radical TS1

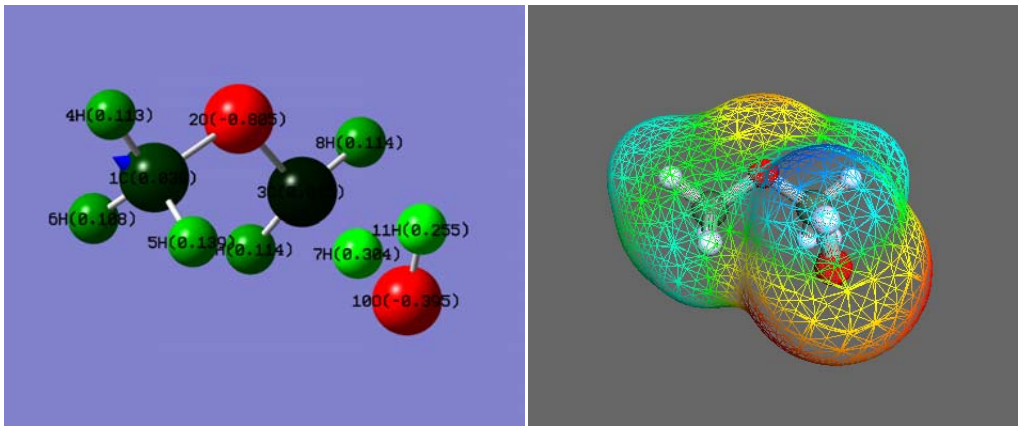

Row	Highlight	Tag	Symbol	NA	NB	NC	Bond	Angle	Dihedral
1	No	1	C						
2	No	2	O	1			1.4251529		
3	No	3	C	2	1		1.3895895	111.6702339	
4	No	4	H	1	2	3	1.0893377	106.5390958	178.4636446
5	No	5	H	1	2	3	1.0944757	110.4699934	58.6754934
6	No	6	H	1	2	3	1.0971728	110.8027705	-62.4696541
7	No	7	H	3	2	1	1.2020677	110.3130895	-67.2083619
8	No	8	H	3	2	1	1.0894797	108.7576942	175.4326005
9	No	9	H	3	2	1	1.0977400	113.5806282	49.7073160
10	No	10	O	3	2	1	2.5188556	100.5348622	-68.3511257
11	No	11	H	10	3	2	0.9792526	89.0893548	-44.0476632

CH3COCH3

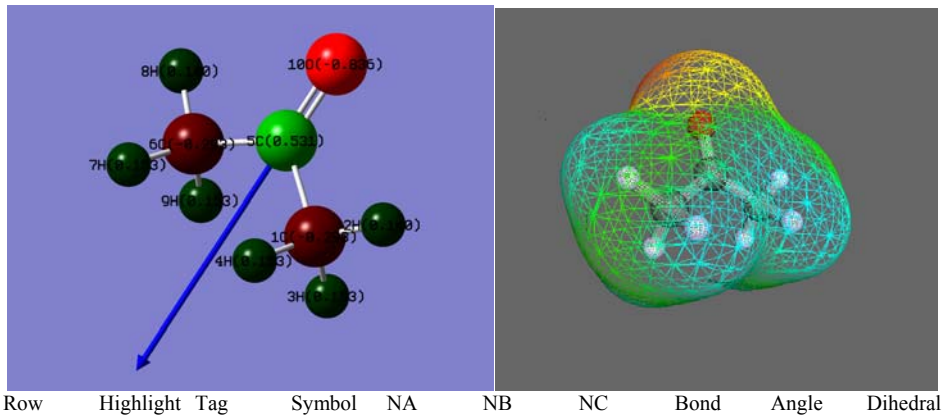

Row	Highlight	Tag	Symbol	NA	NB	NC	Bond	Angle	Dihedral
1	No	1	C						
2	No	2	H	1			1.0901252		
3	No	3	H	1	2		1.0947335	109.7540519	
4	No	4	H	1	2	3	1.0947399	109.7522556	117.5608639
5	No	5	C	1	2	4	1.5117777	109.4746061	121.2159950
6	No	6	C	5	1	2	1.5117777	116.4810552	179.9643218
7	No	7	H	6	5	1	1.0947399	110.3159398	59.1611567
8	No	8	H	6	5	1	1.0901252	109.4746061	-179.9643218
9	No	9	H	6	5	1	1.0947335	110.3208048	-59.0844909
10	No	10	O	5	1	6	1.2263390	121.7594724	179.9970677

CH3COCH3 – HO radical TS

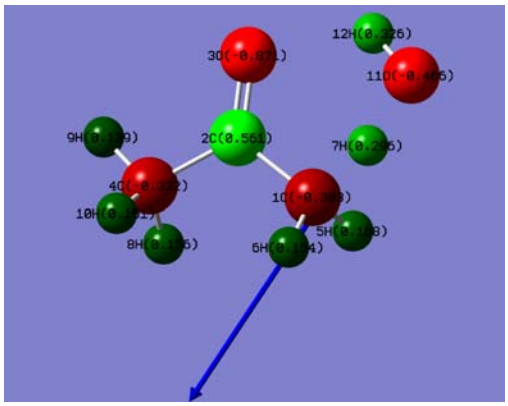

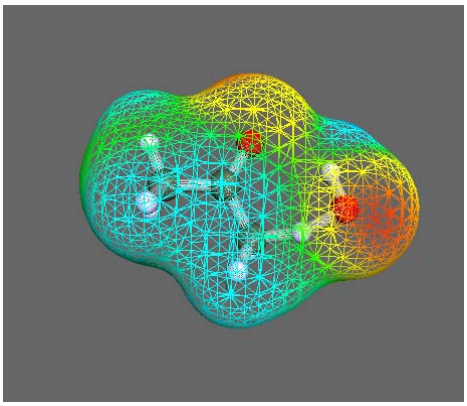

Row	Highlight	Tag	Symbol	NA	NB	NC	Bond	Angle	Dihedral
1	No	1	C						
2	No	2	C	1			1.5055640		
3	No	3	O	2	1		1.2286113	121.7844034	
4	No	4	C	2	1	3	1.5080519	116.5263024	178.9039486
5	No	5	H	1	2	3	1.0920767	111.9005967	-95.5194196
6	No	6	H	1	2	3	1.0911983	113.9361876	137.6113249
7	No	7	H	1	2	3	1.2466390	107.4017726	19.4168979
8	No	8	H	4	2	1	1.0940676	110.4743674	-52.9555144
9	No	9	H	4	2	1	1.0900482	109.5645950	-174.4338683
10	No	10	H	4	2	1	1.0946215	109.6940475	65.1218663
11	No	11	O	1	2	3	2.4339047	98.0337682	14.1749117
12	No	12	H	11	1	2	0.9823571	86.4455218	-12.5038966

CH3COCOCH3

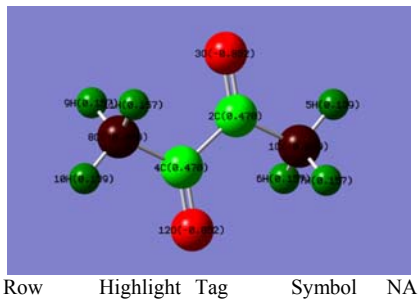

Row	Highlight	Tag	Symbol	NA	NB	NC	Bond	Angle	Dihedral
1	No	1	C						
2	No	2	C	1			1.5011788		
3	No	3	O	2	1		1.2284470	124.1940116	
4	No	4	C	2	1	3	1.5336417	116.6291839	-179.9991151
5	No	5	H	1	2	3	1.0898314	109.3195266	0.0029425
6	No	6	H	1	2	3	1.0932219	110.0366937	-121.3744199
7	No	7	H	1	2	3	1.0932231	110.0358886	121.3793921
8	No	8	C	4	2	1	1.5011788	116.6291839	180.0000000
9	No	9	H	8	4	2	1.0932231	110.0358886	58.6197231
10	No	10	H	8	4	2	1.0898314	109.3195266	179.9961727
11	No	11	H	8	4	2	1.0932219	110.0366937	-58.6264649
12	No	12	O	4	2	1	1.2284470	119.1768045	-0.0008383

CH3COCOCH3 HO radical TS

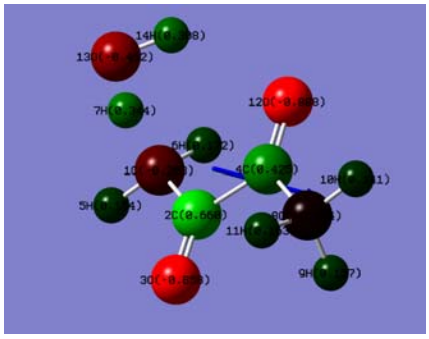

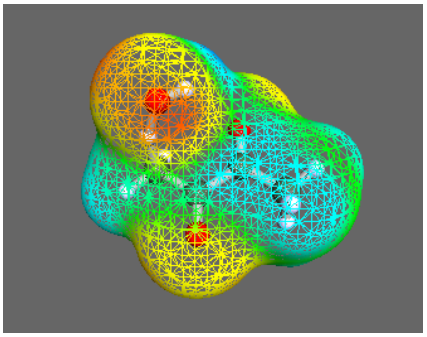

Row	Highlight	Tag	Symbol	NA	NB	NC	Bond	Angle	Dihedral
1	No	1	C						
2	No	2	C	1			1.5018949		
3	No	3	O	2	1		1.1941576	125.1114211	
4	No	4	C	2	1	3	1.5665340	115.3872849	-179.9439121
5	No	5	H	1	2	3	1.0885213	112.0482661	-0.9621441
6	No	6	H	1	2	3	1.0891957	113.9611905	-133.0269904
7	No	7	H	1	2	3	1.2494046	104.1344543	112.5133348
8	No	8	C	4	2	1	1.4962037	115.2304388	-177.1243307
9	No	9	H	8	4	2	1.0932388	109.7882060	58.0438643
10	No	10	H	8	4	2	1.0893630	109.6007943	179.8763329
11	No	11	H	8	4	2	1.0932520	109.3617152	-58.4661361
12	No	12	O	4	2	1	1.2188519	119.8741866	2.2232633
13	No	13	O	1	2	3	2.4242745	93.6894507	118.3720772
14	No	14	H	13	1	2	0.9810665	90.6432439	77.3135759

HCOOH

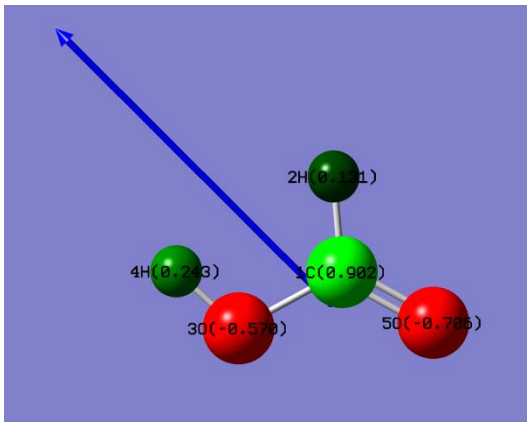

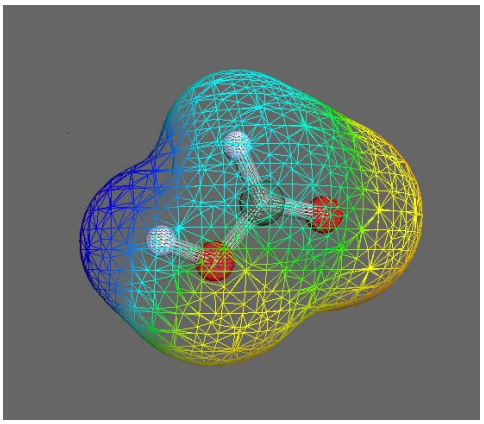

Row	Highlight	Tag	Symbol	NA	NB	NC	Bond	Angle	Dihedral
1	No	1	C						
2	No	2	H	1			1.1041223		
3	No	3	O	1	2		1.3563320	113.6632436	
4	No	4	H	3	1	2	0.9744820	109.0455535	-0.0039058
5	No	5	O	1	3	4	1.2060386	122.4892356	179.9963460

HCOOH – HO radical TS1

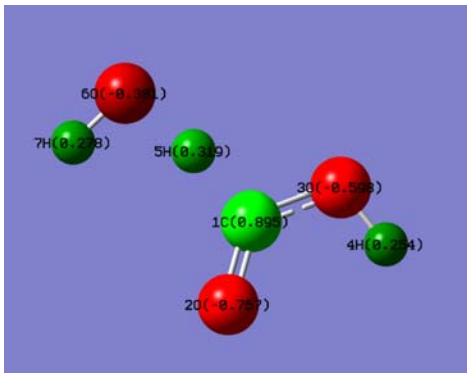

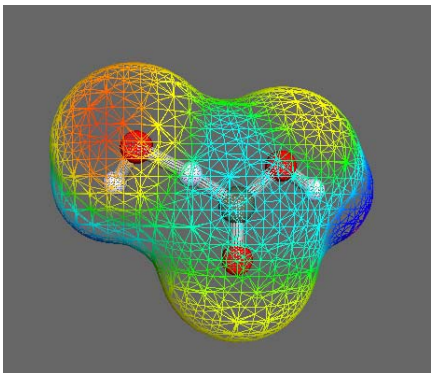

Row	Highlight	Tag	Symbol	NA	NB	NC	Bond	Angle	Dihedral
1	No	1	C						
2	No	2	O	1			1.2036211		
3	No	3	O	1	2		1.3401178	128.0904617	
4	No	4	H	3	1	2	0.9826149	106.7556303	-0.4699168
5	No	5	H	1	2	3	1.2280037	124.4852270	178.8689552
6	No	6	O	1	2	3	2.4721854	121.2520425	168.3232221
7	No	7	H	6	1	2	0.9798319	92.4687800	-18.6044480

CH3COOH

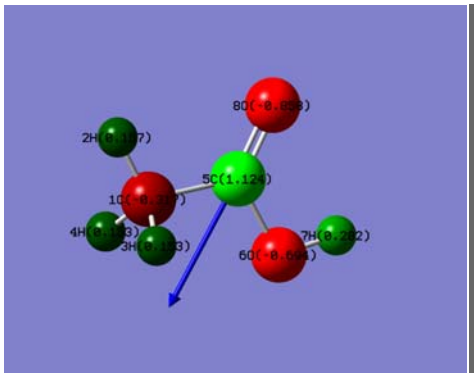

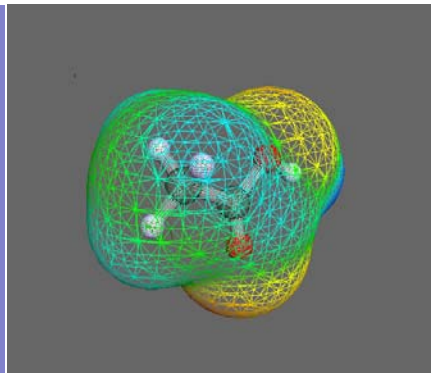

Row	Highlight	Tag	Symbol	NA	NB	NC	Bond	Angle	Dihedral
1	No	1	C						
2	No	2	H	1			1.0884592		
3	No	3	H	1	2		1.0922158	110.1913043	
4	No	4	H	1	2	3	1.0922145	110.1918801	118.6718828
5	No	5	C	1	2	3	1.5000958	109.2979924	-120.6631144
6	No	6	O	5	1	2	1.3612256	110.9704813	-179.9955921
7	No	7	H	6	5	1	0.9792418	105.3981012	-179.9967961
8	No	8	O	5	1	6	1.2168656	126.4406452	-179.9993039

CH3COOH – HO radical TS

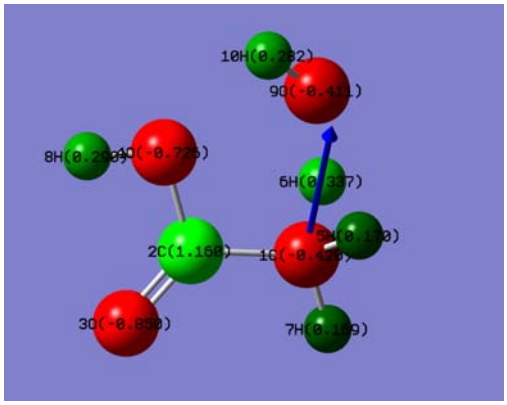

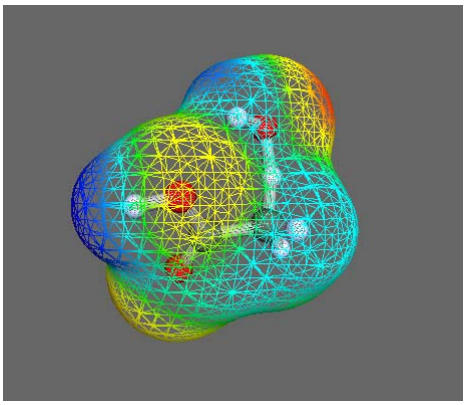

Row	Highlight	Tag	Symbol	NA	NB	NC	Bond	Angle	Dihedral
1	No	1	C						
2	No	2	C	1			1.4894306		
3	No	3	O	2	1		1.2143774	126.5124009	
4	No	4	O	2	1	3	1.3664787	110.7191133	-179.7006338
5	No	5	H	1	2	3	1.0891367	112.9517672	-123.3053690
6	No	6	H	1	2	3	1.2374797	106.7555954	122.4806756
7	No	7	H	1	2	3	1.0871782	112.0116014	6.3904978
8	No	8	H	4	2	1	0.9796669	105.7384773	179.6398951
9	No	9	O	1	2	3	2.4525945	99.1712344	129.1151106
10	No	10	H	9	1	2	0.9798345	88.6814300	39.1485394

CH3CH2COOH

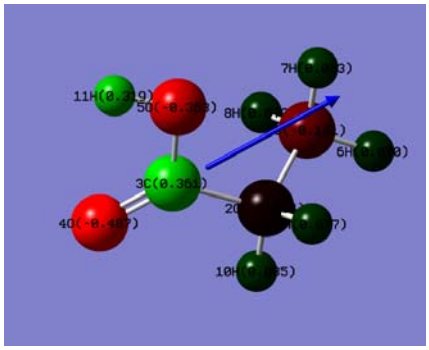

Row	Highlight	Tag	Symbol	NA	NB	NC	Bond	Angle	Dihedral
1	No	1	C						
2	No	2	C	1			1.5293694		
3	No	3	C	2	1		1.5033478	112.1105703	
4	No	4	O	3	2	1	1.2178407	126.4197012	119.0565305
5	No	5	O	3	2	1	1.3624786	111.2231393	-60.4358735
6	No	6	H	1	2	3	1.0924303	110.2318374	-178.1820138
7	No	7	H	1	2	3	1.0908435	110.7830822	61.6328208
8	No	8	H	1	2	3	1.0929111	110.7412847	-58.7043642
9	No	9	H	2	1	3	1.0949355	109.9043388	-120.1281290
10	No	10	H	2	1	3	1.0914486	111.4092628	119.8860049
11	No	11	H	5	3	2	0.9793973	105.4011527	179.3696902

CH3CH2COOH HO radical TS1

CH3CH2COOH HO radical TS2

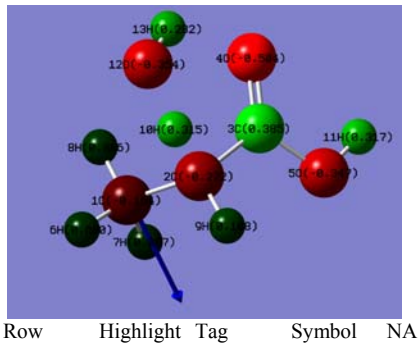

Row	Highlight	Tag	Symbol	NA	NB	NC	Bond	Angle	Dihedral
1	No	1	C						
2	No	2	C	1			1.5171245		
3	No	3	C	2	1		1.4952908	112.6808579	
4	No	4	O	3	2	1	1.2220241	124.7223594	75.2281025
5	No	5	O	3	2	1	1.3528961	112.3943039	-102.6897673
6	No	6	H	1	2	3	1.0914859	110.3071137	-174.3513811
7	No	7	H	1	2	3	1.0945599	110.6033196	65.6989357
8	No	8	H	1	2	3	1.0916212	110.1474372	-54.5733381
9	No	9	H	2	1	3	1.0909794	114.1834008	-129.3860029

10	No	10	H	2	1	3	1.2276152	106.6955486	113.8350890
11	No	11	H	5	3	2	0.9807815	105.9572461	178.4546518
12	No	12	O	2	1	3	2.4471972	102.9113785	102.6802720
13	No	13	H	12	2	1	0.9815543	86.6440291	-92.4010817

HOOCCH2COOH

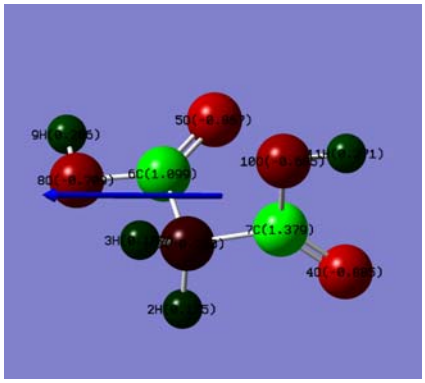

Row	Highlight	Tag	Symbol	NA	NB	NC	Bond	Angle	Dihedral
1	No	1	C						
2	No	2	H	1			1.0927516		
3	No	3	H	1	2		1.0932098	108.5593005	
4	No	4	O	1	2	3	2.4223473	86.0211361	127.9006381
5	No	5	O	1	4	2	2.4300314	90.3966950	-116.3383840
6	No	6	C	5	1	4	1.2155404	30.2599641	163.2247692
7	No	7	C	4	1	6	1.2150285	30.3650339	87.3474994
8	No	8	O	6	5	1	1.3554494	123.7261605	-178.9385506
9	No	9	H	8	6	5	0.9798487	105.8342807	0.4134014
10	No	10	O	7	4	1	1.3547549	123.8663076	-179.7831706
11	No	11	H	10	7	4	0.9795981	105.9332817	3.1983458

HOOCCH2COOH HOradical TS

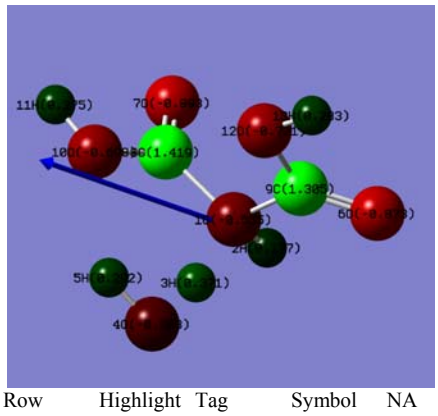

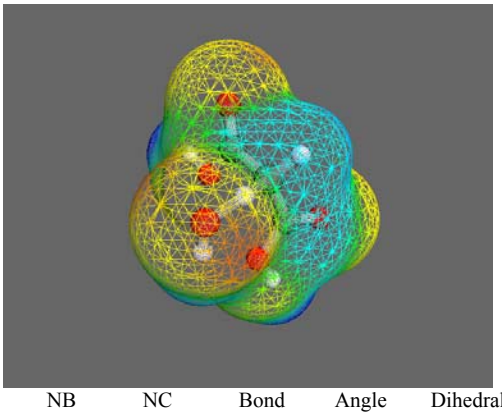

Row	Highlight	Tag	Symbol	NA	NB	NC	Bond	Angle	Dihedral
1	No	1	C						
2	No	2	H	1			1.0893268		
3	No	3	H	1	2		1.2409196	105.3457853	
4	No	4	O	1	2	3	2.4466970	115.7920422	0.9276214
5	No	5	H	4	1	2	0.9807696	89.9845468	-147.9819511
6	No	6	O	1	4	5	2.4063482	103.0025226	118.7624380
7	No	7	O	1	6	4	2.4058312	124.3570621	154.8372467
8	No	8	C	7	1	6	1.2147152	30.9298388	-123.9838432
9	No	9	C	6	1	8	1.2133690	30.8779700	43.0603078
10	No	10	O	8	7	1	1.3584630	123.4512644	179.6722539
11	No	11	H	10	8	7	0.9803507	106.1442371	-2.0519639
12	No	12	O	9	6	1	1.3552302	124.0304969	178.4996519
13	No	13	H	12	9	6	0.9803428	105.7399374	-0.2354131

CH3COCOOHTS1

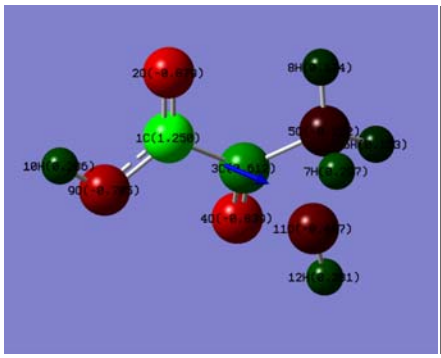

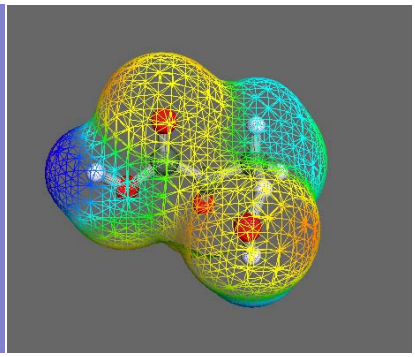

Row	Highlight	Tag	Symbol	NA	NB	NC	Bond	Angle	Dihedral
1	No	1	C						
2	No	2	O	1			1.2172899		
3	No	3	C	1	2		1.5429636	122.9440705	
4	No	4	O	3	1	2	1.1978954	121.6825923	-159.4758658
5	No	5	C	3	1	2	1.5007389	113.3032065	22.4173908
6	No	6	H	5	3	1	1.0881023	112.7287309	-170.0286246
7	No	7	H	5	3	1	1.2442963	100.3275478	75.4023791
8	No	8	H	5	3	1	1.0881834	114.8854715	-34.7003907
9	No	9	O	1	2	3	1.3407225	125.4713227	-178.5731039
10	No	10	H	9	1	2	0.9804859	105.9776710	-1.0723084
11	No	11	O	5	3	1	2.3969746	84.2168861	76.9326639
12	No	12	H	11	5	3	0.9812745	94.3619482	71.1229745

CH3COCOOHTS2

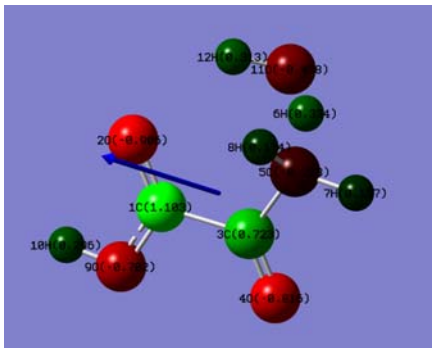

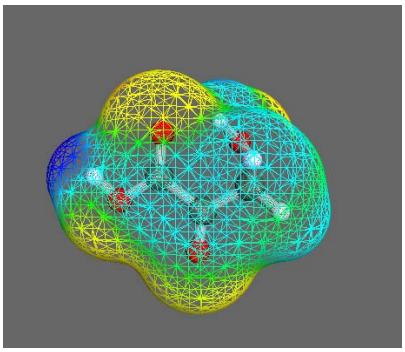

Row	Highlight	Tag	Symbol	NA	NB	NC	Bond	Angle	Dihedral
1	No	1	C						
2	No	2	O	1			1.2208926		
3	No	3	C	1	2		1.5573403	123.5714412	
4	No	4	O	3	1	2	1.1866441	120.7047253	-175.6181400
5	No	5	C	3	1	2	1.5023031	113.7053635	4.0827766
6	No	6	H	5	3	1	1.2511776	104.3498540	-67.4088433
7	No	7	H	5	3	1	1.0883924	111.6866625	179.3143385
8	No	8	H	5	3	1	1.0892818	114.0679313	47.5542323
9	No	9	O	1	2	3	1.3356794	124.9539327	178.6845448
10	No	10	H	9	1	2	0.9809219	106.3251403	1.1626251
11	No	11	O	5	3	1	2.4229221	93.7493441	-61.9569114
12	No	12	H	11	5	3	0.9809427	91.3553722	77.1649028

CH3COOCH3

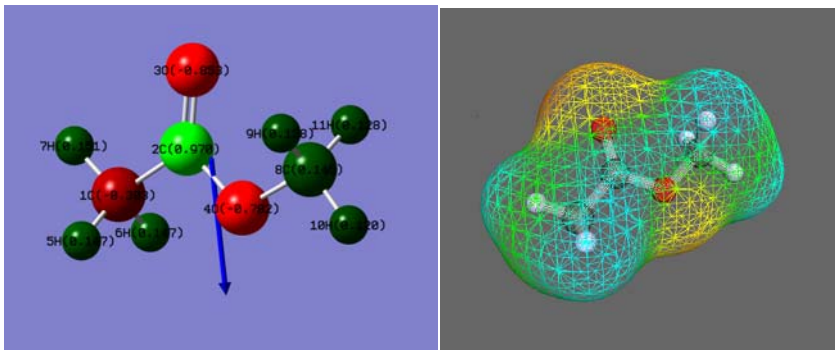

Row	Highlight	Tag	Symbol	NA	NB	NC	Bond	Angle	Dihedral
1	No	1	C						
2	No	2	C	1			1.5027391		
3	No	3	O	2	1		1.2181509	126.0569676	
4	No	4	O	2	1	3	1.3561766	110.4972898	-180.0000000
5	No	5	H	1	2	3	1.0922014	109.8395561	-120.8656378
6	No	6	H	1	2	3	1.0921981	109.8412655	120.8790459
7	No	7	H	1	2	3	1.0888599	109.2509199	0.0056337
8	No	8	C	4	2	1	1.4395437	114.0130884	179.9979556
9	No	9	H	8	4	2	1.0908298	110.4519754	60.4163792
10	No	10	H	8	4	2	1.0879822	105.1342580	-179.9844068
11	No	11	H	8	4	2	1.0908259	110.4527969	-60.3844166

CH3COOCH3 – HO radical TS1

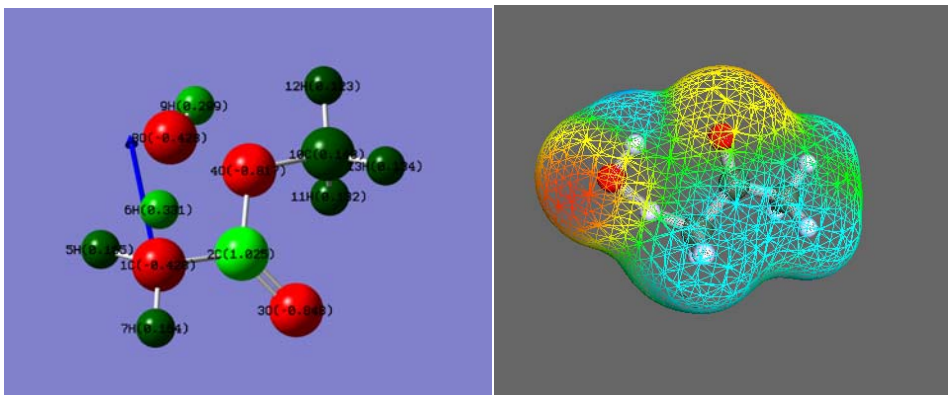

Row	Highlight	Tag	Symbol	NA	NB	NC	Bond	Angle	Dihedral
1	No	1	C						
2	No	2	C	1			1.4922357		
3	No	3	O	2	1		1.2159572	126.0076102	
4	No	4	O	2	1	3	1.3612357	110.4295258	179.9733343
5	No	5	H	1	2	3	1.0893003	112.9650391	-121.4232276
6	No	6	H	1	2	3	1.2358720	107.0764075	124.1744188
7	No	7	H	1	2	3	1.0876450	111.9142996	7.9436848
8	No	8	O	1	2	3	2.4505545	99.2607238	131.2005430
9	No	9	H	8	1	2	0.9798090	87.5358915	37.8548815
10	No	10	C	4	2	1	1.4430558	114.0274778	-179.8384672
11	No	11	H	10	4	2	1.0901444	110.1887612	60.0763777
12	No	12	H	10	4	2	1.0875957	105.1106400	179.5857816
13	No	13	H	10	4	2	1.0903331	110.2963202	-60.7452764

CH3COOCH3 – HO radical TS2

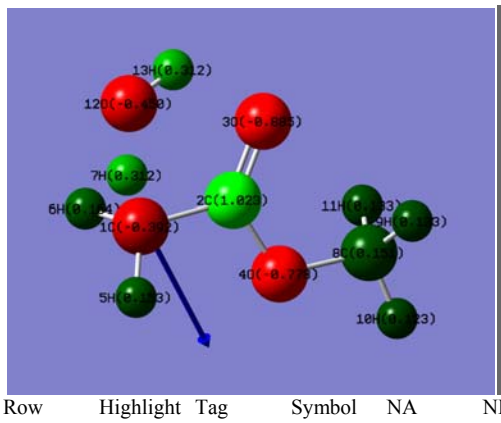

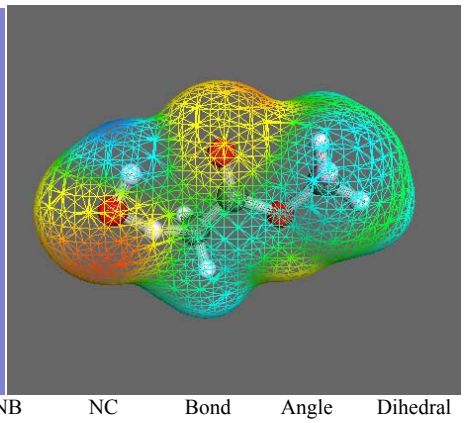

Row	Highlight	Tag	Symbol	NA	NB	NC	Bond	Angle	Dihedral
1	No	1	C						
2	No	2	C	1			1.4949241		
3	No	3	O	2	1		1.2229080	124.4781692	
4	No	4	O	2	1	3	1.3461609	111.7432995	-178.9023791
5	No	5	H	1	2	3	1.0879876	114.0157648	-154.8316040
6	No	6	H	1	2	3	1.0897070	112.0091700	75.8852728
7	No	7	H	1	2	3	1.2447802	105.5490695	-37.1199107
8	No	8	C	4	2	1	1.4440845	114.2452788	179.1027316
9	No	9	H	8	4	2	1.0901796	110.1776737	59.8823707
10	No	10	H	8	4	2	1.0873015	104.9559379	179.4645416
11	No	11	H	8	4	2	1.0902288	110.2320446	-60.9531515
12	No	12	O	1	2	3	2.4334984	96.6345123	-30.0065880
13	No	13	H	12	1	2	0.9816709	86.3187519	23.5203040

HCOOCH2CH3

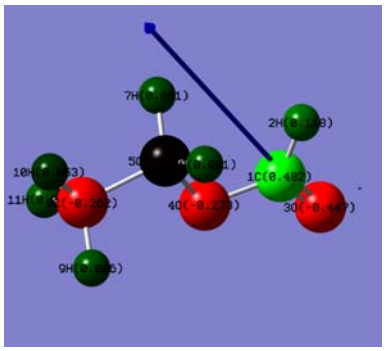

Row	Highlight	Tag	Symbol	NA	NB	NC	Bond	Angle	Dihedral
1	No	1	C						
2	No	2	H	1			1.1050675		
3	No	3	O	1	2		1.2087678	123.8441364	
4	No	4	O	1	3	2	1.3518149	122.7612858	-179.9985757
5	No	5	C	4	1	3	1.4451956	115.6276743	-179.9931114
6	No	6	H	5	4	1	1.0954452	109.4744929	-59.4510993
7	No	7	H	5	4	1	1.0954439	109.4730020	59.5222408
8	No	8	C	5	4	1	1.5097912	106.7494065	-179.9646086
9	No	9	H	8	5	4	1.0913141	110.2529297	59.9620530
10	No	10	H	8	5	4	1.0931940	110.0993417	-179.9984530
11	No	11	H	8	5	4	1.0913130	110.2530732	-59.9591154

HCOOCH2CH3 HO radical TS1

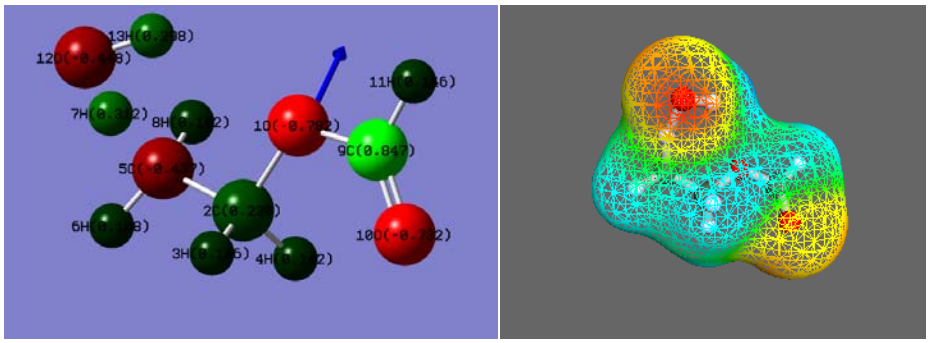

Row	Highlight	Tag	Symbol	NA	NB	NC	Bond	Angle	Dihedral
1	No	1	O						
2	No	2	C	1			1.4519350		
3	No	3	H	2	1		1.0923530	108.8036687	
4	No	4	H	2	1	3	1.0939440	108.7490185	-117.7083883
5	No	5	C	2	1	3	1.4995910	106.6224730	120.9894109
6	No	6	H	5	2	1	1.0908166	112.6668061	-173.5472990
7	No	7	H	5	2	1	1.2272670	107.2766652	-59.1022278
8	No	8	H	5	2	1	1.0895729	113.5605978	57.8526635
9	No	9	C	1	2	5	1.3514412	114.4972811	-176.3622202
10	No	10	O	9	1	2	1.2126471	125.5472186	0.5137662
11	No	11	H	9	1	2	1.0976255	109.1182118	-179.6762258
12	No	12	O	5	2	1	2.4535112	97.3844765	-55.2817482
13	No	13	H	12	5	2	0.9793030	88.5129711	45.3191008

HCOOCH2CH3 HO radical TS2

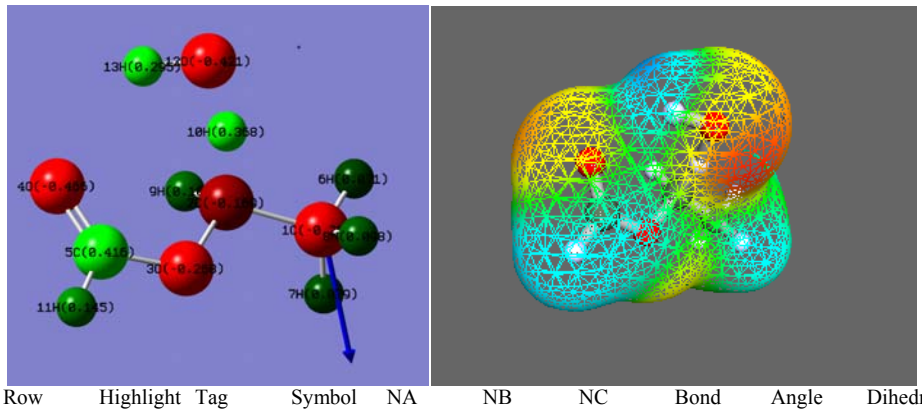

Row	Highlight	Tag	Symbol	NA	NB	NC	Bond	Angle	Dihedral
1	No	1	C						
2	No	2	C	1			1.5006247		
3	No	3	O	2	1		1.4284157	108.6508717	
4	No	4	O	3	2	1	2.2817821	90.0598079	177.3492905
5	No	5	C	4	3	2	1.2162561	28.5743682	178.9475934
6	No	6	H	1	2	3	1.0921164	109.7206463	-178.1513248
7	No	7	H	1	2	3	1.0937710	110.4947336	61.9585841
8	No	8	H	1	2	3	1.0910621	110.2968179	-58.3338128
9	No	9	H	2	1	3	1.0923785	115.4686200	-124.7613222
10	No	10	H	2	1	3	1.2156622	108.4373096	117.4633158
11	No	11	H	5	4	3	1.0962852	124.8794421	-179.6647542
12	No	12	O	2	1	3	2.4837717	114.9498177	115.8607010
13	No	13	H	12	2	1	0.9804726	90.6706262	179.2353614

CH2ClCOOH

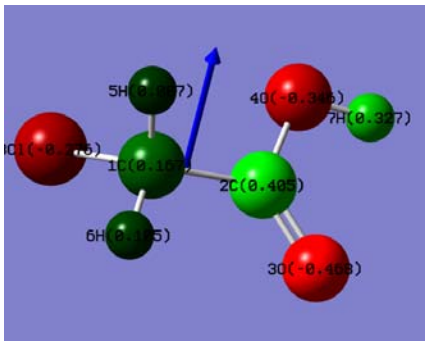

Row	Highlight	Tag	Symbol	NA	NB	NC	Bond	Angle	Dihedral
1	No	1	C						
2	No	2	C	1			1.5094908		
3	No	3	O	2	1		1.2161251	124.5068589	
4	No	4	O	2	1	3	1.3512828	111.4196727	-178.6615377
5	No	5	H	1	2	3	1.0908101	109.9215359	123.7953732
6	No	6	H	1	2	3	1.0879670	108.3301299	2.8693689
7	No	7	H	4	2	1	0.9796137	106.0347377	-179.1905166
8	No	8	Cl	1	2	3	1.7785385	111.2932112	-116.6344609

CH2ClCOOH HO radical TS1

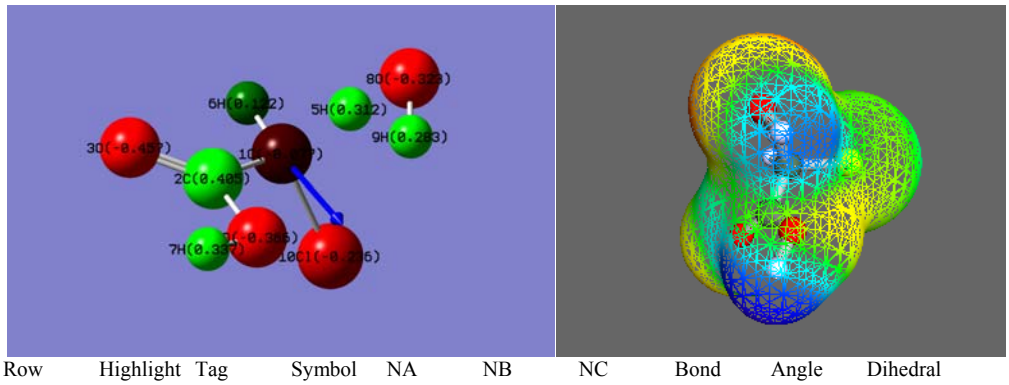

Row	Highlight	Tag	Symbol	NA	NB	NC	Bond	Angle	Dihedral
1	No	1	C						
2	No	2	C	1			1.5012159		
3	No	3	O	2	1		1.2138316	124.4672956	
4	No	4	O	2	1	3	1.3555007	111.3497999	-177.9006199
5	No	5	H	1	2	3	1.2247764	106.0978940	116.2959797
6	No	6	H	1	2	3	1.0884376	110.7067620	1.5758338
7	No	7	H	4	2	1	0.9799570	106.1052436	179.3284970
8	No	8	O	1	2	3	2.4565258	96.4733473	120.0241796
9	No	9	H	8	1	2	0.9804083	90.3147225	52.1394805
10	No	10	Cl	1	2	3	1.7496174	114.3105537	-125.2313749

CH3Cl

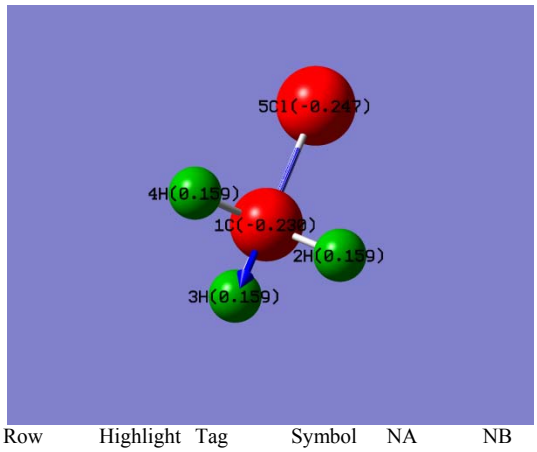

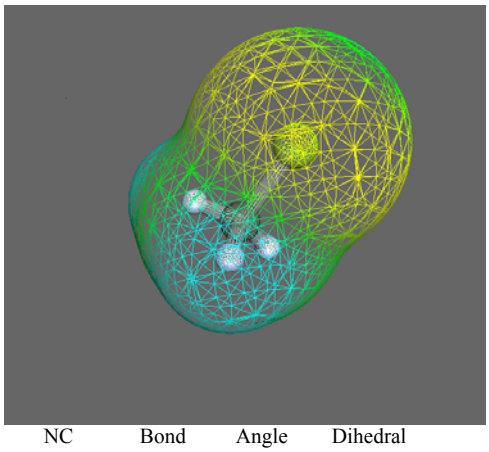

Row	Highlight	Tag	Symbol	NA	NB	NC	Bond	Angle	Dihedral
1	No	1	C						
2	No	2	H	1			1.0877290		
3	No	3	H	1	2		1.0877290	110.0324504	
4	No	4	H	1	3	2	1.0877290	110.0324426	-121.4015994
5	No	5	Cl	1	3	4	1.7769510	108.9039889	-119.2991989

CH3Cl – HO radical TS

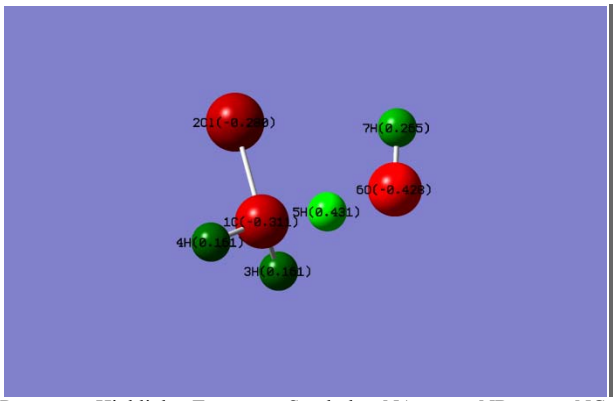

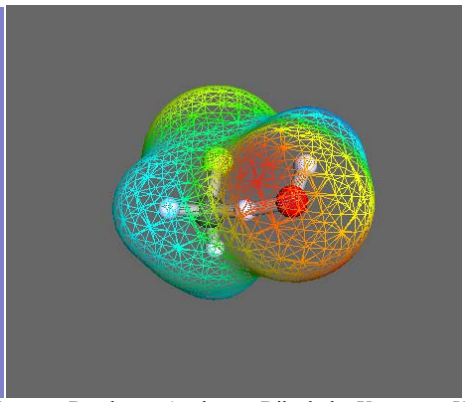

Row	Highlight	Tag	Symbol	NA	NB	NC	Bond	Angle	Dihedral	X	Y
	Z										
1	No	1	C								
	0.0324910		0.0735030		-0.0457330						
2	No	2	Cl	1			1.7520008				
	0.1157880		-0.4216530		1.6327750						
3	No	3	H	1	2		1.0872864	111.0892923			
	1.0157050		0.3437340		-0.4231680						
4	No	4	H	1	3	2	1.0872861	113.3221376	125.8900901		
	-0.7120910		0.8531100		-0.1871600						
5	No	5	H	1	4	3	1.2221837	105.7499757	-115.3856490		
	-0.3386700		-0.8679740		-0.7310020						
6	No	6	O	1	4	3	2.4851296	107.9550848	-119.5131191		
	-0.7310980		-1.9471280		-1.2744930						
7	No	7	H	6	1	4	0.9790502	94.0925270	-118.5730562		
	-0.7847980		-2.5021410		-0.4697470						

CH2Cl2

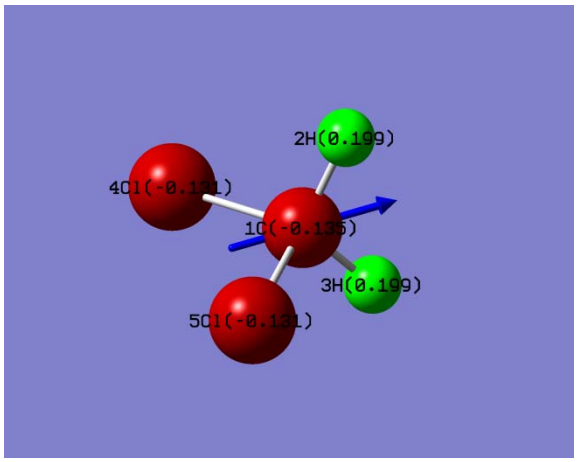

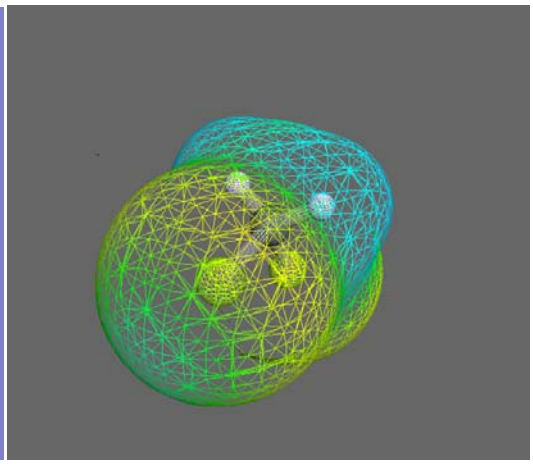

Row	Highlight	Tag	Symbol	NA	NB	NC	Bond	Angle	Dihedral
1	No	1	C						
2	No	2	H	1			1.0862404		
3	No	3	H	1	2		1.0862404	110.8247119	
4	No	4	Cl	1	2	3	1.7672268	108.2594556	-118.5866069
5	No	5	Cl	1	2	3	1.7672268	108.2594556	118.5866069

CH2Cl2 – HO radical TS

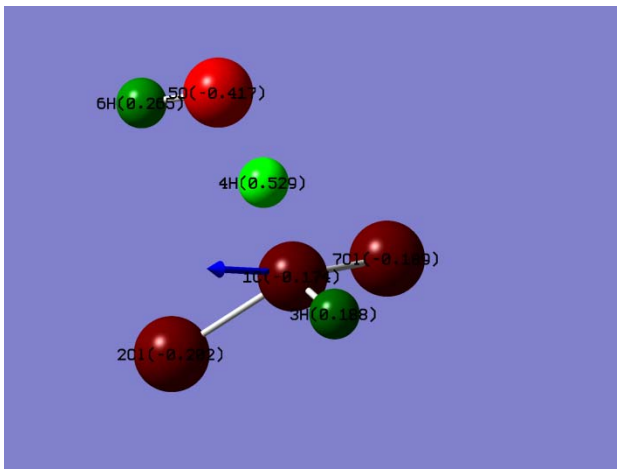

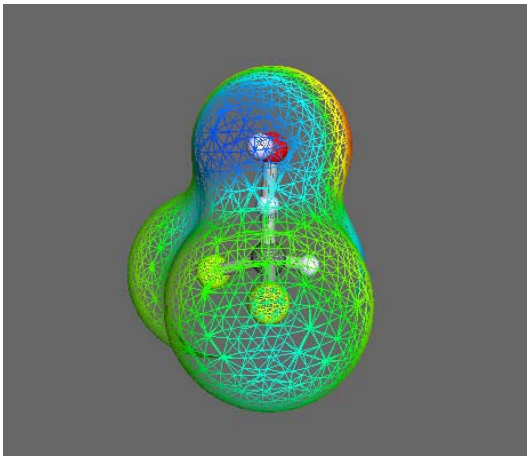

Row	Highlight	Tag	Symbol	NA	NB	NC	Bond	Angle	Dihedral
	X		Y		Z				
1	No	1	C						
	-0.0057280		-0.1091990		0.0055960				
2	No	2	Cl	1			1.7511287		
	-0.1553290		0.0513630		1.7429190				
3	No	3	H	1	2		1.0877137	110.1069232	
	1.0262330		0.0531160		-0.2974410				
4	No	4	H	1	3	2	1.2149568	105.7887293	116.9100713
	-0.6477250		0.7794530		-0.5181000				
5	No	5	O	1	3	4	2.4825617	105.2337461	-5.2017575
	-1.2631220		1.8328320		-0.8947310				
6	No	6	H	5	1	3	0.9796106	96.0766436	-130.4129373
	-1.7235690		2.0547050		-0.0590290				
7	No	7	Cl	1	5	6	1.7434552	111.6813655	109.4648495
	-0.6047400		-1.6166730		-0.6334210				

CHCl3

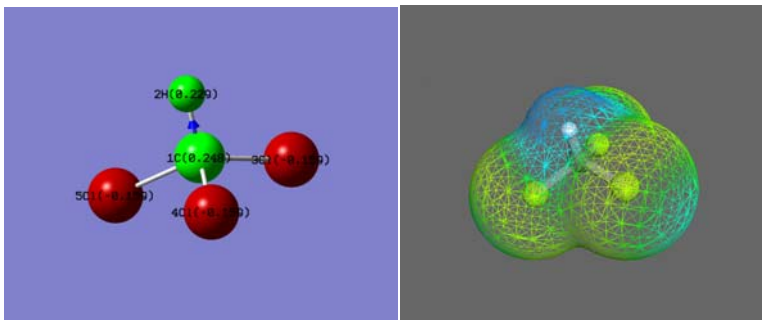

Row	Highlight	Tag	Symbol	NA	NB	NC	Bond	Angle	Dihedral
1	No	1	C						
2	No	2	H	1			1.0859050		
3	No	3	Cl	1	2		1.7647550	107.6496419	
4	No	4	Cl	1	2	3	1.7647553	107.6496388	120.0000136
5	No	5	Cl	1	2	3	1.7647553	107.6496388	-120.0000136

CHCl3 – HO radical TS

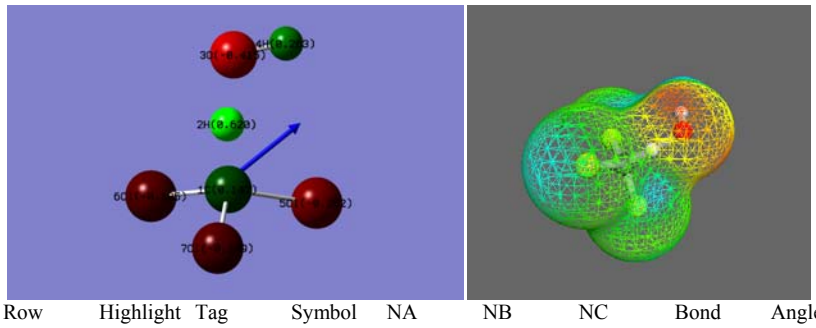

Row	Highlight	Tag	Symbol	NA	NB	NC	Bond	Angle	Dihedral
	X		Y		Z				
1	No	1	C						
	0.1502290		-0.0582220		-0.0270430				
2	No	2	H	1			1.2113901		
	0.0516450		-0.2064140		1.1712000				
3	No	3	O	2	1		1.2769738	173.6870009	
	0.0284220		-0.2481900		2.4472790				
4	No	4	H	3	2	1	0.9798502	100.5435918	-2.1135074
	0.6084120		0.5117800		2.6621360				
5	No	5	Cl	1	3	2	1.7560589	103.9788259	178.5991999
	1.1146520		1.3846800		-0.2947460				
6	No	6	Cl	1	3	2	1.7462661	107.2965739	59.3529605
	-1.4846470		0.1159630		-0.6155030				
7	No	7	Cl	1	3	2	1.7464857	107.3267641	-62.1560496
	0.9339120		-1.5013450		-0.6215590				

CH3CH2Cl

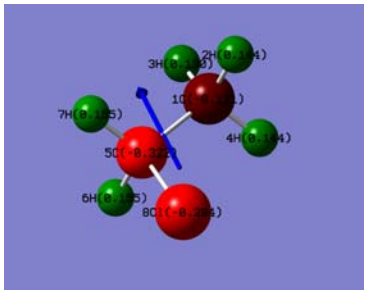

Row	Highlight	Tag	Symbol	NA	NB	NC	Bond	Angle	Dihedral
1	No	1	C						
2	No	2	H	1			1.0911363		
3	No	3	H	1	2		1.0936868	108.5403635	
4	No	4	H	1	2	3	1.0911363	108.4727189	117.7514409

5	No	5	C	1	2	4	1.5142665	110.8805834	121.9808439
6	No	6	H	5	1	2	1.0898889	111.4966144	-179.4768387
7	No	7	H	5	1	2	1.0898889	111.4966144	58.9138472
8	No	8	Cl	5	1	2	1.7884778	111.3615489	-60.2814958

CH3CH2Cl – HO radical TS1

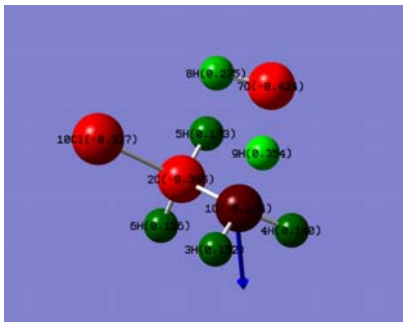

Row	Highlight	Tag	Symbol	NA	NB	NC	Bond	Angle	Dihedral
1	No	1	C						
2	No	2	C	1			1.5032899		
3	No	3	H	1	2		1.0896395	113.8753135	
4	No	4	H	1	2	3	1.0917653	112.0153383	128.1599262
5	No	5	H	2	1	3	1.0899236	111.1001021	173.7985897
6	No	6	H	2	1	3	1.0918229	111.3672397	-64.4830810
7	No	7	O	1	2	5	2.4669892	99.8996084	56.6551953
8	No	8	H	7	1	2	0.9794829	92.8822734	51.1119198
9	No	9	H	1	2	7	1.2250699	108.3895233	-1.1202039
10	No	10	Cl	2	1	7	1.7893247	111.3920030	-62.6629434

CH3CH2Cl – HO radical TS2

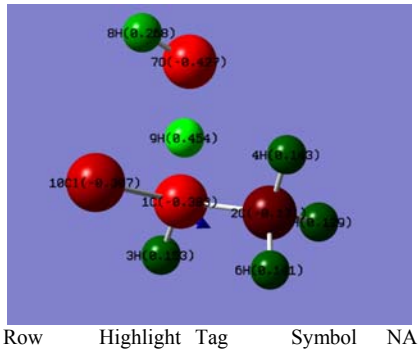

Row	Highlight	Tag	Symbol	NA	NB	NC	Bond	Angle	Dihedral
1	No	1	C						
2	No	2	C	1			1.5049328		
3	No	3	H	1	2		1.0901565	114.5197724	
4	No	4	H	2	1	3	1.0909805	110.6289370	175.7387864
5	No	5	H	2	1	3	1.0928555	109.2691819	56.1917135
6	No	6	H	2	1	3	1.0933084	110.7149981	-63.6118216
7	No	7	O	1	2	4	2.4962237	105.4874952	54.6166151
8	No	8	H	7	1	2	0.9792778	94.6454734	-119.7317749
9	No	9	H	1	2	7	1.2065970	107.2838764	5.0402959
10	No	10	Cl	1	2	7	1.7663821	113.4053603	-113.2349317

CH3CHCl2

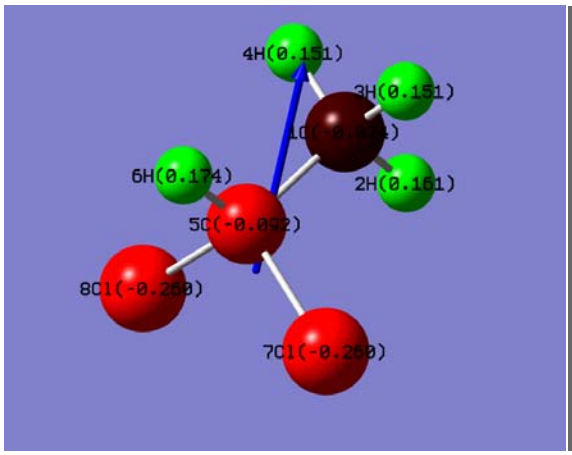

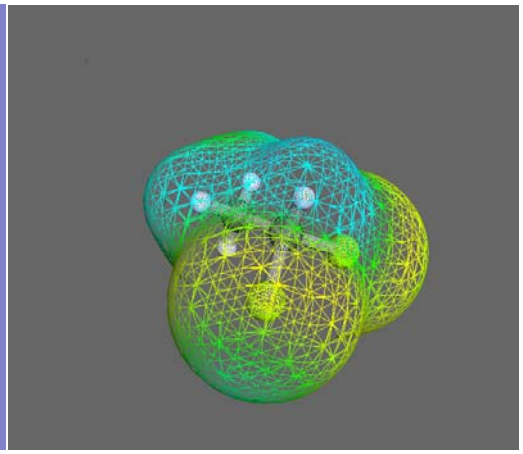

Row	Highlight	Tag	Symbol	NA	NB	NC	Bond	Angle	Dihedral
1	No	1	C						
2	No	2	H	1			1.0908771		
3	No	3	H	1	2		1.0919994	109.0825710	
4	No	4	H	1	2	3	1.0919994	109.0825710	119.1869561
5	No	5	C	1	2	3	1.5109931	110.2710716	-120.4065220
6	No	6	H	5	1	2	1.0883920	111.9302385	180.0000000
7	No	7	Cl	5	1	2	1.7794330	110.6057807	61.5123423
8	No	8	Cl	5	1	2	1.7794330	110.6057807	-61.5123423

CH3CHCl2 – HO radical TS1

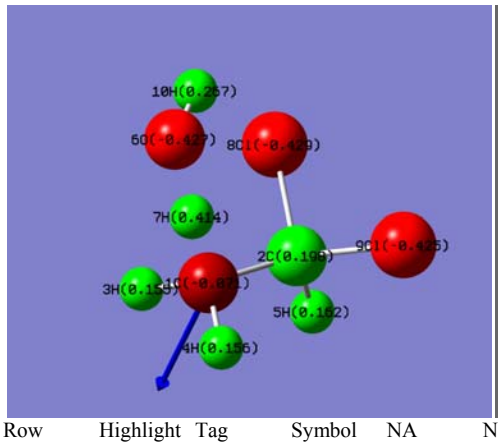

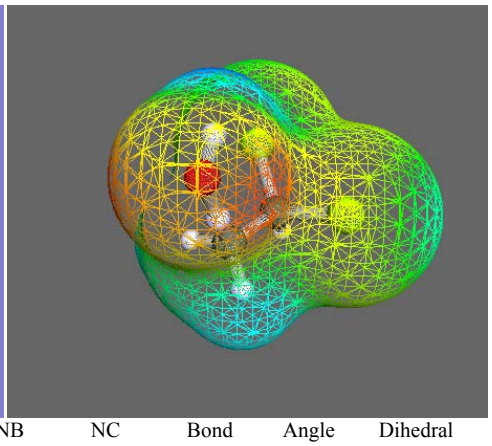

Row	Highlight	Tag	Symbol	NA	NB	NC	Bond	Angle	Dihedral
	X		Y		Z				
1	No	1	C						
	-0.0276110		0.2066110		0.0593180				
2	No	2	C	1			1.5014390		
	-0.0316170		-0.0434420		1.5397830				
3	No	3	H	1	2		1.0896014	112.2921220	
	0.9049620		-0.1052720		-0.4100090				
4	No	4	H	1	2	3	1.0903501	112.1879770	127.7839306
	-0.9032840		-0.2180090		-0.4323710				
5	No	5	H	2	1	3	1.0903419	111.4010516	-61.8089081
	0.0681180		-1.1057850		1.7641170				
6	No	6	O	1	2	5	2.4705273	106.1452560	-174.0140478
	-0.0138670		2.6609360		-0.2228260				
7	No	7	H	1	2	6	1.2359139	109.4743844	-5.0522321
	-0.1232970		1.4202400		-0.1538300				
8	No	8	Cl	2	1	6	1.7836693	110.6013411	-56.4022039
	1.3620090		0.7555100		2.3149980				
9	No	9	Cl	2	1	6	1.7741652	111.1014339	67.1773257
	-1.5556860		0.4914530		2.2737880				
10	No	10	H	6	1	2	0.9794300	94.3868087	34.4060462
	0.5374100		2.8244070		0.5700510				

CH3CHCl2 – HO radical TS2

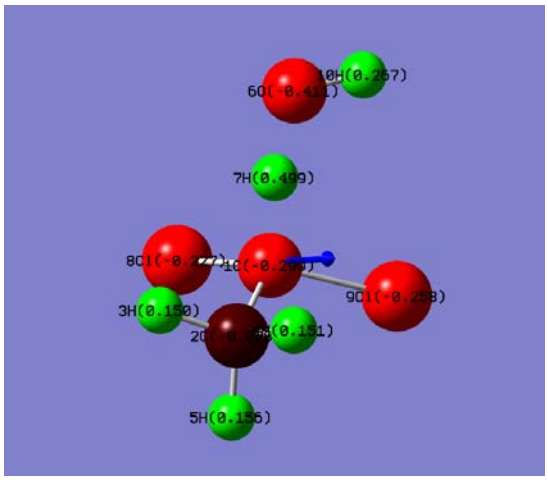

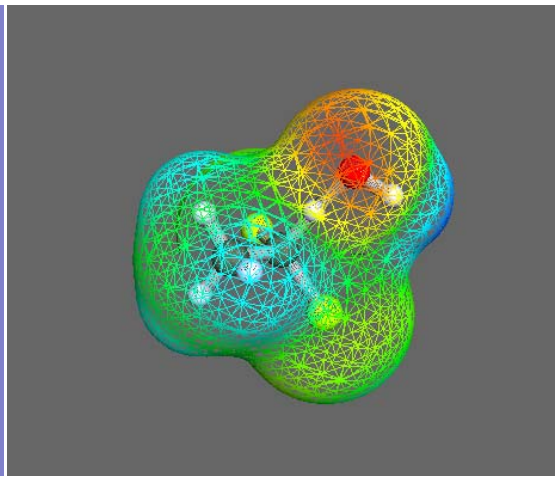

Row	Highlight	Tag	Symbol	NA	NB	NC	Bond	Angle	Dihedral
	X	Y		Z					
1	No	1	C						
	0.0244230		0.1069860		0.0067020				
2	No	2	C	1			1.5052920		
	0.0026630		-0.0214720		1.5063450				
3	No	3	H	2	1		1.0914012	109.2988725	
	1.0244570		0.0241900		1.8871450				
4	No	4	H	2	1	3	1.0911716	109.3102293	-119.3826392
	-0.4383670		-0.9813190		1.7799170				
5	No	5	H	2	1	4	1.0925503	110.3008634	-120.3950279
	-0.5840990		0.7876310		1.9476260				
6	No	6	O	1	2	4	2.4882174	103.9378935	-53.8150454
	1.1954530		-1.9523320		-0.7543000				
7	No	7	H	1	2	6	1.2017934	107.0300721	-5.4757959
	0.6761720		-0.8101330		-0.4157000				
8	No	8	Cl	1	2	6	1.7573117	112.8485940	-121.2136875
	0.8441930		1.5614010		-0.5417490				
9	No	9	Cl	1	2	6	1.7649431	112.3146979	111.1022024
	-1.5838730		-0.0510320		-0.7028320				
10	No	10	H	6	1	2	0.9797790	96.9942978	132.2224337
	0.5538320		-2.2040040		-1.4506840				

CH2ClCH2Cl – boat

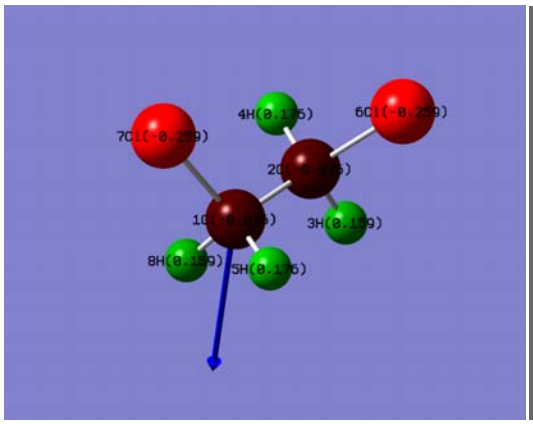

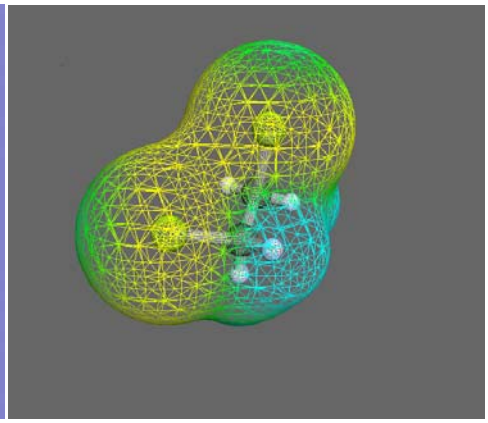

Row	Highlight	Tag	Symbol	NA	NB	NC	Bond	Angle	Dihedral
1	No	1	C						
2	No	2	C	1			1.5119986		
3	No	3	H	2	1		1.0921124	108.9078275	
4	No	4	H	2	1	3	1.0902277	110.8564046	120.1042807
5	No	5	H	1	2	4	1.0902276	110.8564070	-173.6858870
6	No	6	Cl	2	1	5	1.7781063	112.4999430	-52.7826806
7	No	7	Cl	1	2	4	1.7781066	112.4999585	-52.7826231

8	No	8	H	1	2	4	1.0921130	108.9077971	66.2098964

CH2ClCH2Cl – HO radical TS (Trans)

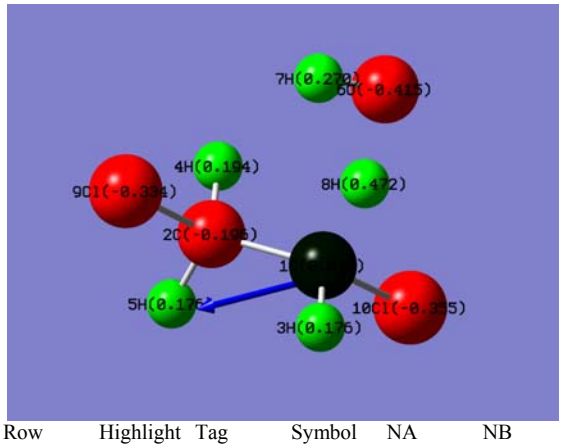

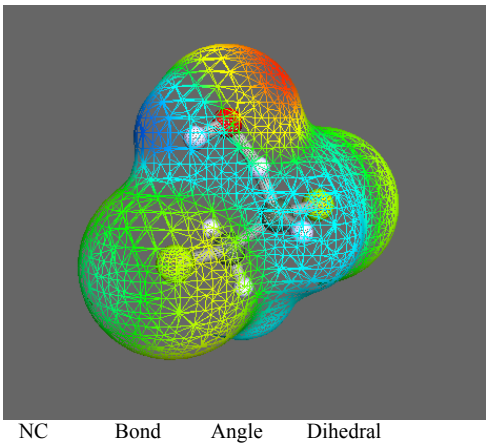

Row	Highlight	Tag	Symbol	NA	NB	NC	Bond	Angle	Dihedral
	X		Y	Z					
1	No	1	C						
	-0.0100540		0.1983470		-0.0691370				
2	No	2	C	1			1.5066266		
	-0.0129980		0.1115420		1.4349840				
3	No	3	H	1	2		1.0897852	113.6753738	
	0.8534300		-0.2776990		-0.5332570				
4	No	4	H	2	1	3	1.0897307	110.5477013	174.0547901
	-0.8377790		0.6904180		1.8498960				
5	No	5	H	2	1	3	1.0910674	110.9667871	-64.1557857
	-0.0910810		-0.9251430		1.7660660				
6	No	6	O	1	2	4	2.4731566	101.2075065	57.5265326
	0.1461050		2.6430250		-0.409236				
7	No	7	H	6	1	2	0.9798107	94.6153745	51.8982601
	0.9243750		2.7544190		0.1755000				
8	No	8	H	1	2	6	1.2186213	108.1105547	-1.8441375
	0.0275580		1.3759070		-0.3805460				
9	No	9	Cl	2	1	6	1.7832887	109.7235590	-61.7187827
	1.5119710		0.7746720		2.0790700				
10	No	10	Cl	1	2	6	1.7543515	111.2983900	-118.0274282
	-1.4978300		-0.4378190		-0.7470490				

CH2ClCHCl2

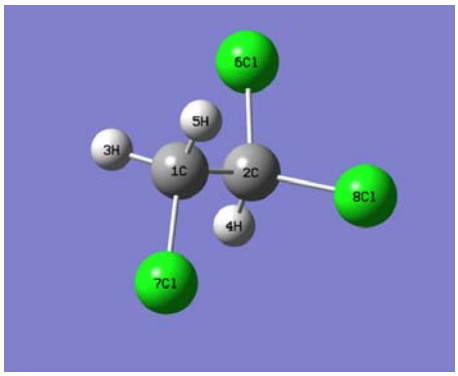

Row	Highlight	Tag	Symbol	NA	NB	NC	Bond	Angle	Dihedral
1	No	1	C						
2	No	2	C	1			1.5168772		
3	No	3	H	1	2		1.0901456	108.8895603	
4	No	4	H	2	1	3	1.0887532	111.1326960	-64.7307969
5	No	5	H	1	2	4	1.0900974	110.1021473	174.9913964
6	No	6	Cl	2	1	5	1.7782149	107.9208978	-67.4655462
7	No	7	Cl	1	2	4	1.7744198	111.3561989	54.1250595
8	No	8	Cl	2	1	5	1.7683108	111.7625514	54.9222831

CH2ClCHCl2 HOradical TS1

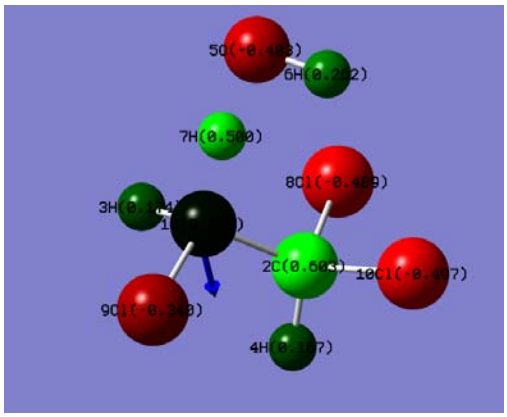

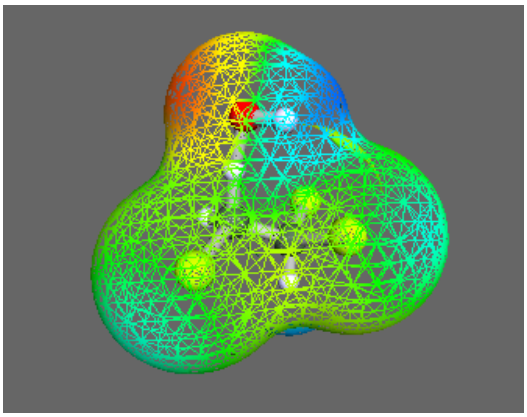

Row	Highlight	Tag	Symbol	NA	NB	NC	Bond	Angle	Dihedral
1	No	1	C						
2	No	2	C	1			1.5109455		
3	No	3	H	1	2		1.0903640	111.2077299	
4	No	4	H	2	1	3	1.0903264	110.6840951	-70.5592840
5	No	5	O	1	2	4	2.4762647	104.5799625	173.9350415
6	No	6	H	5	1	2	0.9800030	96.0821947	-40.3888306
7	No	7	H	1	2	5	1.2277895	109.1528235	1.0311048
8	No	8	Cl	2	1	5	1.7710556	108.7896241	-67.9924207
9	No	9	Cl	1	2	5	1.7478353	113.1937528	-119.5318075
10	No	10	Cl	2	1	5	1.7744753	111.6648240	55.1499028

CH2ClCHCl2 HO radical TS2

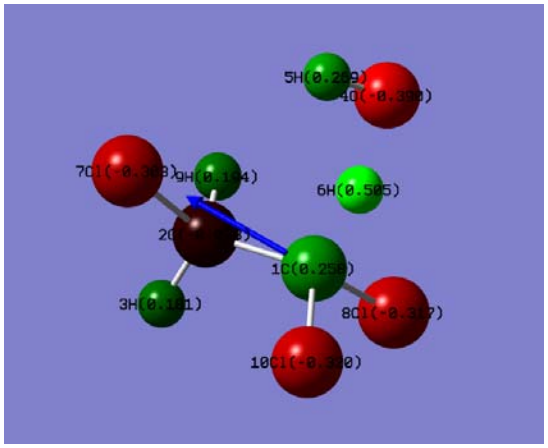

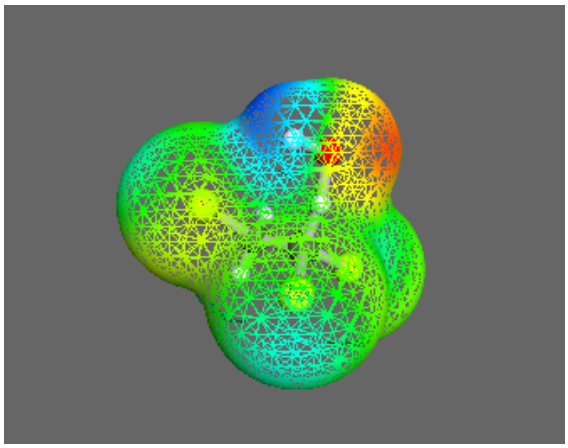

Row	Highlight	Tag	Symbol	NA	NB	NC	Bond	Angle	Dihedral
1	No	1	C						
2	No	2	C	1			1.5130735		
3	No	3	H	2	1		1.0912663	110.1046968	
4	No	4	O	1	2	3	2.4704625	101.1542019	-178.8051425
5	No	5	H	4	1	2	0.9804164	96.5060224	54.4975987
6	No	6	H	1	2	4	1.2132998	108.3993736	0.3528316
7	No	7	Cl	2	1	4	1.7753986	111.8495331	-58.2200061
8	No	8	Cl	1	2	4	1.7556444	109.4203996	-113.5855786
9	No	9	H	2	1	4	1.0898361	108.4694968	60.7664424
10	No	10	Cl	1	2	4	1.7498596	113.6941090	119.4693609

CH2ClCH2Cl (Trans)

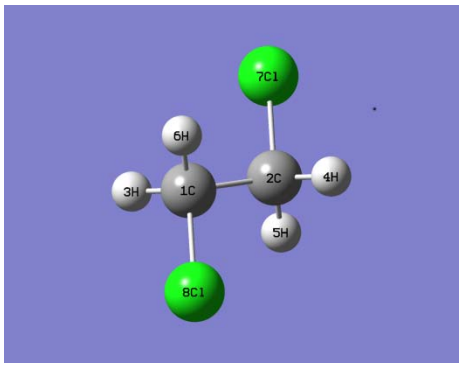

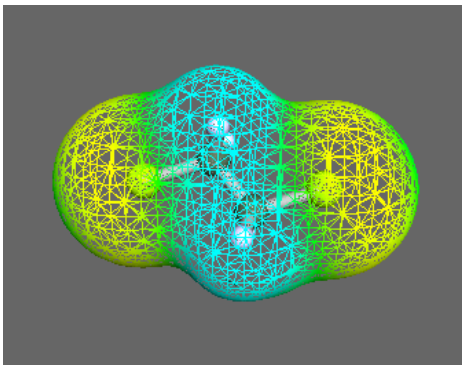

Row	Highlight	Tag	Symbol	NA	NB	NC	Bond	Angle	Dihedral
1	No	1	C						
2	No	2	C	1			1.5400000		
3	No	3	H	1	2		1.0700000	109.4712206	
4	No	4	H	2	1	3	1.0700000	109.4712206	180.0000000
5	No	5	H	2	1	3	1.0700000	109.4712206	-60.0000000
6	No	6	H	1	2	4	1.0700000	109.4712206	60.0000000
7	No	7	Cl	2	1	3	1.7600000	109.4712206	60.0000000
8	No	8	Cl	1	2	4	1.7600000	109.4712206	-60.0000000

CH2ClCH2Cl (Cis)

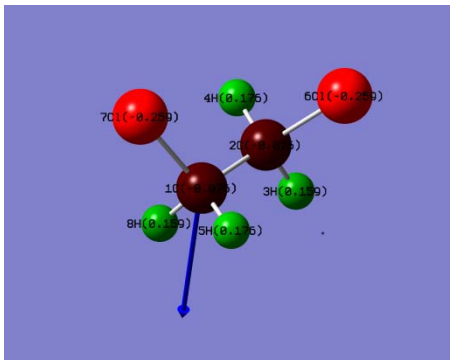

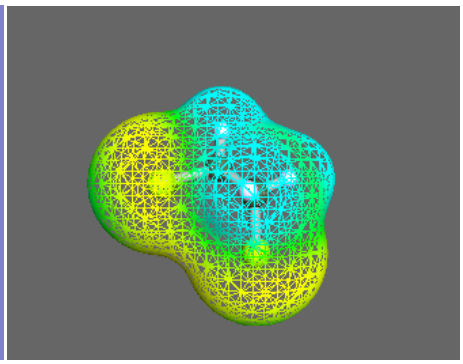

Row	Highlight	Tag	Symbol	NA	NB	NC	Bond	Angle	Dihedral
1	No	1	C						
2	No	2	C	1			1.5119986		
3	No	3	H	2	1		1.0921124	108.9078275	
4	No	4	H	2	1	3	1.0902277	110.8564046	120.1042807
5	No	5	H	1	2	4	1.0902276	110.8564070	-173.6858870
6	No	6	Cl	2	1	5	1.7781063	112.4999430	-52.7826806
7	No	7	Cl	1	2	4	1.7781066	112.4999585	-52.7826231
8	No	8	H	1	2	4	1.0921130	108.9077971	66.2098964

CH2ClCH2Cl – HO radical (trans) TS1

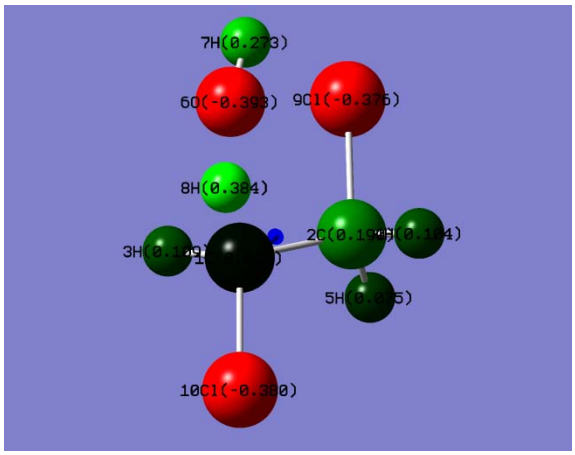

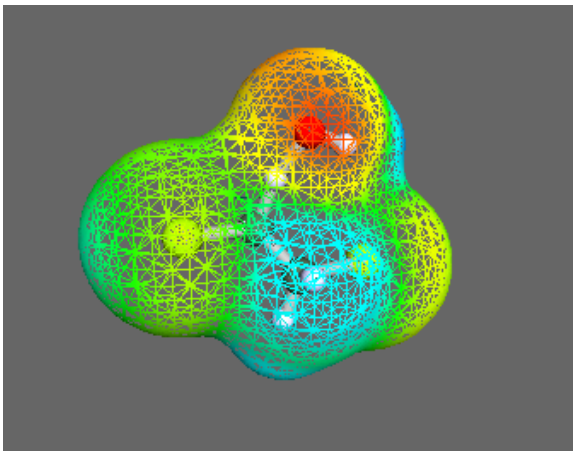

Row	Highlight	Tag	Symbol	NA	NB	NC	Bond	Angle	Dihedral
1	No	1	C						
2	No	2	C	1			1.5066266		
3	No	3	H	1	2		1.0897852	113.6753738	
4	No	4	H	2	1	3	1.0897307	110.5477013	174.0547901
5	No	5	H	2	1	3	1.0910675	110.9667858	-64.1558417
6	No	6	O	1	2	4	2.4731566	101.2075065	57.5265326
7	No	7	H	6	1	2	0.9798107	94.6153745	51.8982601
8	No	8	H	1	2	6	1.2186213	108.1105547	-1.8441375
9	No	9	Cl	2	1	6	1.7832887	109.7235590	-61.7187827
10	No	10	Cl	1	2	6	1.7543519	111.2984201	-118.0274300

CH2ClCH2Cl – HO radical (cis) TS1

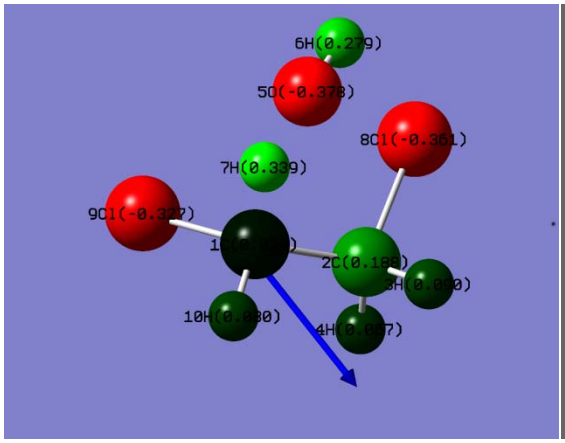

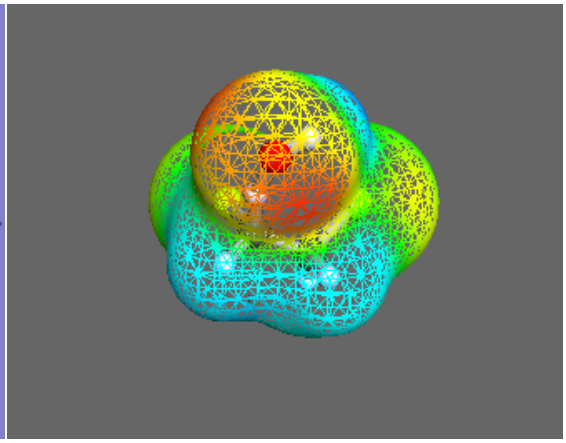

Row	Highlight	Tag	Symbol	NA	NB	NC	Bond	Angle	Dihedral
1	No	1	C						
2	No	2	C	1			1.5050036		
3	No	3	H	2	1		1.0910882	108.5964796	
4	No	4	H	2	1	3	1.0913956	110.8358083	120.4819549
5	No	5	O	1	2	3	2.4641412	99.5787976	59.0109702
6	No	6	H	5	1	2	0.9802269	95.2649328	52.3894629
7	No	7	H	1	2	5	1.2174241	108.5507430	2.0954192
8	No	8	Cl	2	1	5	1.7802993	112.6854229	-60.0646009
9	No	9	Cl	1	2	5	1.7517221	114.7901356	123.4056003
10	No	10	H	1	2	5	1.0917959	111.0924393	-111.1665033

CH3CCl3

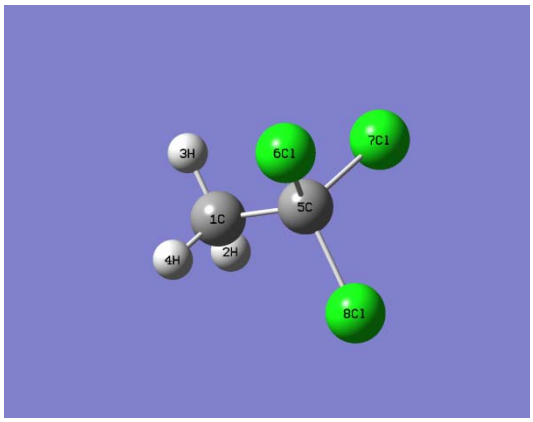

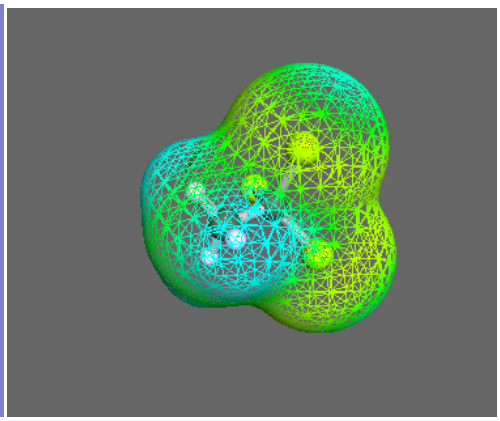

Row	Highlight	Tag	Symbol	NA	NB	NC	Bond	Angle	Dihedral
1	No	1	C						
2	No	2	H	1			1.0905158		
3	No	3	H	1	2		1.0905157	109.5219404	
4	No	4	H	1	3	2	1.0905159	109.5219461	-120.1244757
5	No	5	C	1	3	2	1.5140080	109.4204475	119.9377611
6	No	6	Cl	5	1	3	1.7779700	109.7548355	60.0007784
7	No	7	Cl	5	1	3	1.7779700	109.7548353	-59.9992220
8	No	8	Cl	5	1	3	1.7779700	109.7548355	-179.9992223

CH3CCl3 – HO radical TS

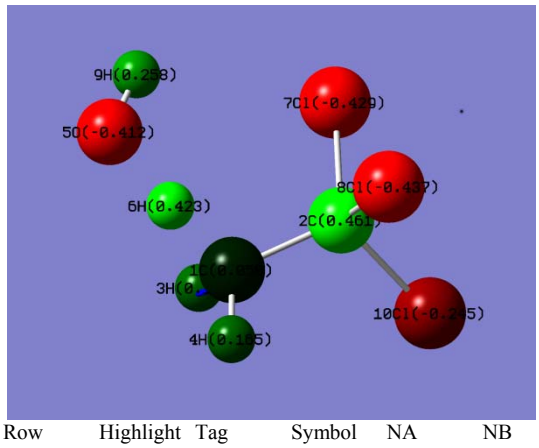

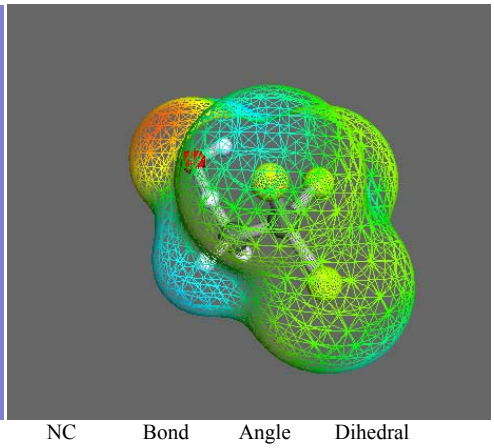

Row	Highlight	Tag	Symbol	NA	NB	NC	Bond	Angle	Dihedral
1	No	1	C						
2	No	2	C	1			1.5024000		
3	No	3	H	1	2		1.0888800	112.0342601	
4	No	4	H	1	2	3	1.0898778	111.8816660	127.6150424
5	No	5	O	1	2	4	2.4710284	107.2773068	119.8874851
6	No	6	H	1	2	5	1.2360656	108.9726029	-5.2873635
7	No	7	Cl	2	1	5	1.7824080	109.8150769	-56.0299808
8	No	8	Cl	2	1	5	1.7711787	110.2745857	64.6367054
9	No	9	H	5	1	2	0.9794129	95.2478020	44.3930191
10	No	10	Cl	2	1	5	1.7815958	108.9671773	-175.2002589

CH3Br

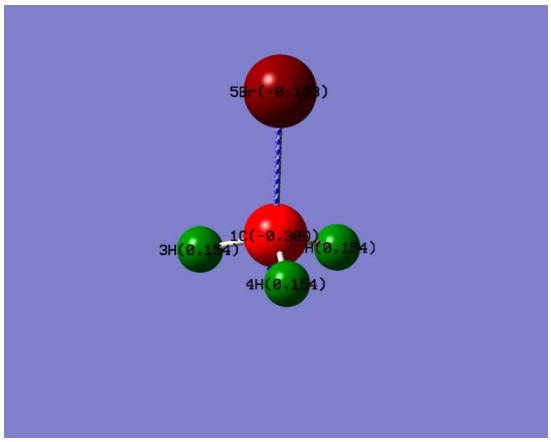

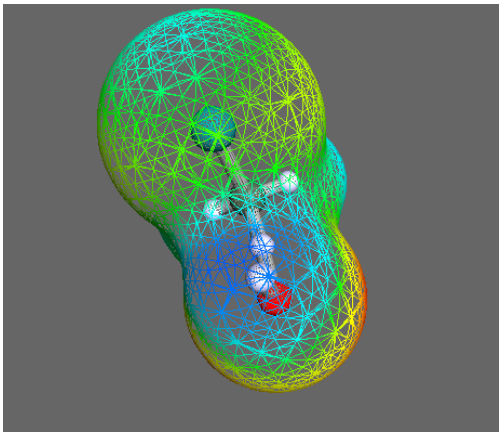

Row	Highlight	Tag	Symbol	NA	NB	NC	Bond	Angle	Dihedral
1	No	1	C						
2	No	2	H	1			1.0862788		
3	No	3	H	1	2		1.0862789	111.0426788	
4	No	4	H	1	2	3	1.0862789	111.0426788	124.0707756
5	No	5	Br	1	2	3	1.9473380	107.8499575	-117.9646122

CH3Br – HO radical TS

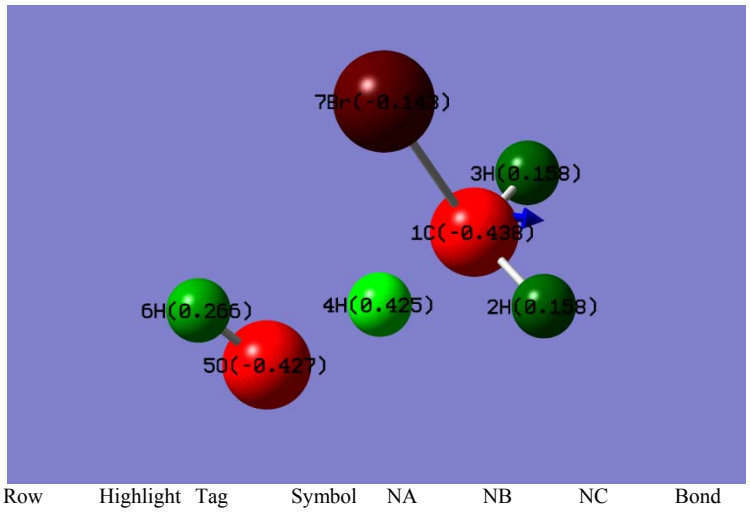

Row	Highlight	Tag	Symbol	NA	NB	NC	Bond	Angle	Dihedral
	X	Y	Z						
1	No	1	C						
	0.0491390		-0.2921990		0.0283690				
2	No	2	H	1			1.0862658		
	-0.0528140		0.1313230		1.0234610				
3	No	3	H	1	2		1.0862657	114.3360206	
	0.8599350		0.1313300		-0.5574690				
4	No	4	H	1	3	2	1.2263685	106.9266693	-118.1415359
	0.2971220		-1.4846700		0.1715370				
5	No	5	O	1	3	2	2.4731808	109.5212113	-123.3297328
	0.3447850		-2.7417060		0.1990500				
6	No	6	H	5	1	3	0.9792476	92.3404240	-116.9364571
	-0.4896700		-2.9163670		-0.2827220				
7	No	7	Br	1	5	6	1.9207136	102.3226799	0.0000000
	-1.6093710		-0.1452210		-0.9291710				

Cl3CCH2OH

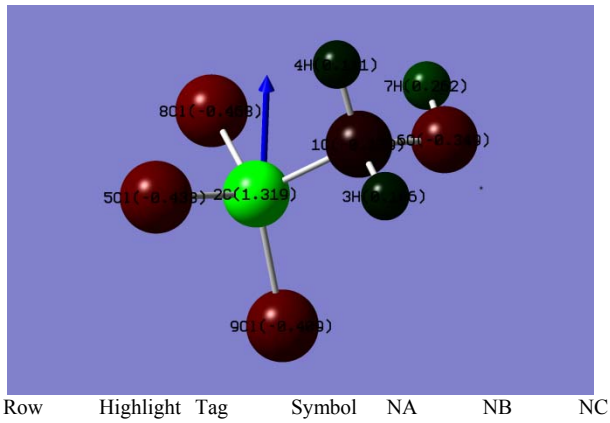

Row	Highlight	Tag	Symbol	NA	NB	NC	Bond	Angle	Dihedral
1	No	1	C						
2	No	2	C	1			1.5335867		
3	No	3	H	1	2		1.0913822	107.6846724	
4	No	4	H	1	2	3	1.0973225	107.1480734	-117.2935364
5	No	5	Cl	2	1	3	1.7734588	108.1316605	61.1079515
6	No	6	O	1	2	5	1.4018894	112.8179634	178.8680906
7	No	7	H	6	1	2	0.9734488	107.9948965	69.8939248
8	No	8	Cl	2	1	6	1.7814366	108.7367106	-62.1988726
9	No	9	Cl	2	1	6	1.7642039	110.4121851	58.1798906

Cl3CCH2OH HO radical TS

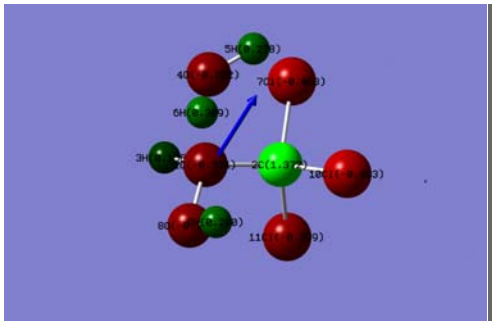

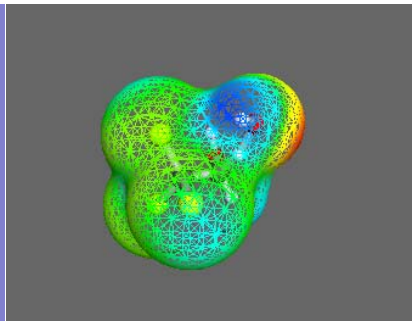

Row	Highlight	Tag	Symbol	NA	NB	NC	Bond	Angle	Dihedral
1	No	1	C						
2	No	2	C	1			1.5274641		
3	No	3	H	1	2		1.0919652	109.6846873	
4	No	4	O	1	2	3	2.4733662	106.3843271	-127.4725164
5	No	5	H	4	1	2	0.9799560	101.0246597	13.8384514
6	No	6	H	1	2	4	1.2131248	107.1067499	11.9549261
7	No	7	Cl	2	1	4	1.7745413	108.0359265	-68.7275897
8	No	8	O	1	2	4	1.3791064	114.6208846	-108.8461149
9	No	9	H	8	1	2	0.9756838	107.8633988	75.2486606
10	No	10	Cl	2	1	8	1.7762146	109.8199747	-57.9027964
11	No	11	Cl	2	1	8	1.7681130	109.4694984	62.4748744

F3CCH2OH

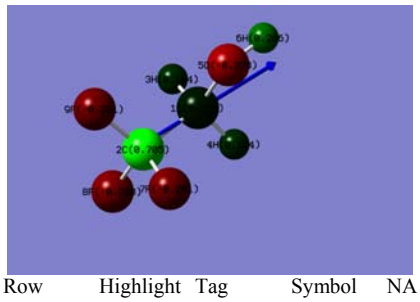

Row	Highlight	Tag	Symbol	NA	NB	NC	Bond	Angle	Dihedral
1	No	1	C						
2	No	2	C	1			1.5058334		
3	No	3	H	1	2		1.0968709	107.2564124	
4	No	4	H	1	2	3	1.0968711	107.2563894	-116.8412035
5	No	5	O	1	2	4	1.4126789	107.0150114	-121.5794106
6	No	6	H	5	1	2	0.9707617	107.8345825	179.9981277
7	No	7	F	2	1	5	1.3449296	111.8863841	-60.6537225
8	No	8	F	2	1	5	1.3544677	109.2676077	180.0000000
9	No	9	F	2	1	5	1.3449298	111.8864193	60.6534961

F3CCH2OH HO radical TS

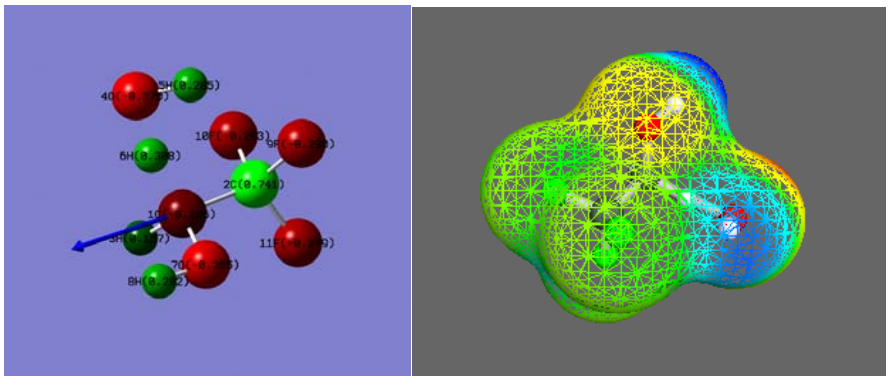

Row	Highlight	Tag	Symbol	NA	NB	NC	Bond	Angle	Dihedral
1	No	1	C						
2	No	2	C	1			1.5023487		
3	No	3	H	1	2		1.0964099	110.5900838	
4	No	4	O	1	2	3	2.4807611	102.5931580	-123.0019222
5	No	5	H	4	1	2	0.9799622	89.8680009	-44.7171935
6	No	6	H	1	2	4	1.2149770	104.8162542	9.7324067
7	No	7	O	1	2	4	1.3888087	108.5494433	-109.2649915
8	No	8	H	7	1	2	0.9723831	108.2406961	176.5180444
9	No	9	F	2	1	7	1.3512365	110.9783731	-61.6406116
10	No	10	F	2	1	7	1.3478948	109.7329275	179.1577485
11	No	11	F	2	1	7	1.3442371	112.1101086	58.9139403

F3CCHCl2

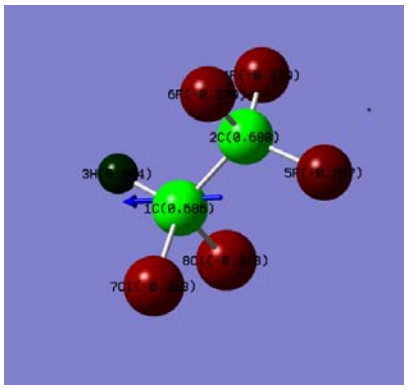

Row	Highlight	Tag	Symbol	NA	NB	NC	Bond	Angle	Dihedral
1	No	1	C						
2	No	2	C	1			1.5250954		
3	No	3	H	1	2		1.0895117	107.6924175	
4	No	4	F	2	1	3	1.3443289	109.6523384	-59.1598382
5	No	5	F	2	1	3	1.3370348	112.2614980	180.0000000
6	No	6	F	2	1	3	1.3443289	109.6523384	59.1598382
7	No	7	Cl	1	2	5	1.7611848	109.9344492	62.0994997
8	No	8	Cl	1	2	5	1.7611848	109.9344492	-62.0994997

F3CCHCl2 HO radical

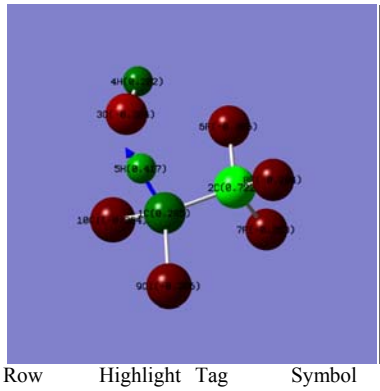

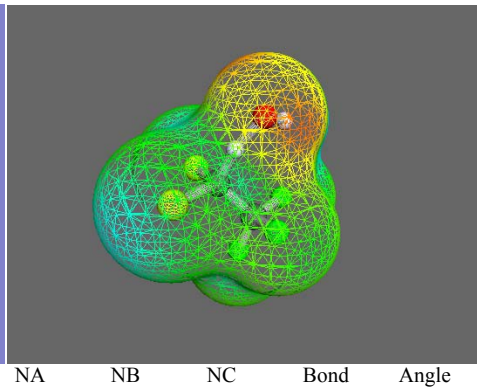

Row	Highlight	Tag	Symbol	NA	NB	NC	Bond	Angle	Dihedral
1	No	1	C						
2	No	2	C	1			1.5219714		
3	No	3	O	1	2		2.4655809	98.5185758	
4	No	4	H	3	1	2	0.9803378	94.6128922	51.2303835
5	No	5	H	1	2	3	1.2226738	104.9388942	-3.1462954
6	No	6	F	2	1	3	1.3500087	109.2216145	-54.0426387
7	No	7	F	2	1	3	1.3387568	112.0096053	-174.0350790
8	No	8	F	2	1	3	1.3382468	110.4495563	64.6615850
9	No	9	Cl	1	2	3	1.7386192	111.7182616	-118.3596625
10	No	10	Cl	1	2	3	1.7425130	111.2483853	112.8510728

APPENDIX F: OPTIMIZED MOLECULAR STRUCTURES FOR IONIZED COMPOUNDS

All molecular and radical structures were optimized at B3LYP/6-31G(d) with the SMD solvation model.

HO•

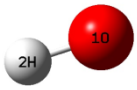

vacuo

Row	Highlight	Tag	Symbol	NA	NB	NC	Bond	Angle	Dihedral
1	No	1	O						
2	No	2	H	1			0.9762090		

Water

Row	Highlight	Tag	Symbol	NA	NB	NC	Bond	Angle	Dihedral
1	No	1	O						
2	No	2	H	1			0.9773250		

H2O

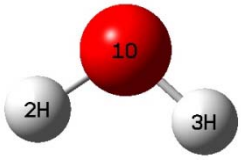

vacuo

Row	Highlight	Tag	Symbol	NA	NB	NC	Bond	Angle	Dihedral
1	No	1	O						
2	No	2	H	1			0.9618832		
3	No	3	H	1	2		0.9618832	103.7261688	

Water

Row	Highlight	Tag	Symbol	NA	NB	NC	Bond	Angle	Dihedral
1	No	1	O						
2	No	2	H	1			0.9640429		
4	No	3	H	1	2		0.9640429	102.9177762	

HCOO-

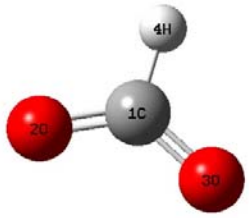

Row	Highlight	Tag	Symbol	NA	NB	NC	Bond	Angle	Dihedral
1	No	1	C						
2	No	2	O	1			1.2550634		
3	No	3	O	1	2		1.2550634	128.1753288	
4	No	4	H	1	2	3	1.1242020	115.9123356	180.0000000

Complex with HO radical

Row	Highlight	Tag	Symbol	NA	NB	NC	Bond	Angle	Dihedral
1	No	1	C						
2	No	2	O	1			1.2585671		
3	No	3	O	1	2		1.2426905	129.3906941	
4	No	4	H	1	3	2	1.1386801	116.3282890	-179.9919976
5	No	5	O	2	1	3	2.6949660	80.9193196	-179.9988671
6	No	6	H	5	2	1	0.9923476	18.3260707	-179.9635181

TS with HO radical

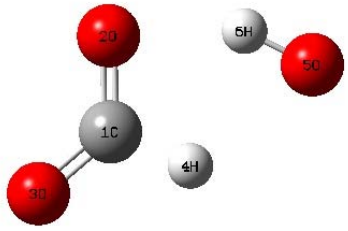

Row	Highlight	Tag	Symbol	NA	NB	NC	Bond	Angle	Dihedral
1	No	1	C						
2	No	2	O	1			1.2581365		
3	No	3	O	1	2		1.2427858	129.4619970	
4	No	4	H	1	3	2	1.1389483	116.2965404	-179.9922118
5	No	5	O	2	1	3	2.6986388	80.7398273	-179.9466891
6	No	6	H	5	2	1	0.9919989	18.2605580	179.9948910

CH3COO-

Vacuo

Row	Highlight	Tag	Symbol	NA	NB	NC	Bond	Angle	Dihedral
1	No	1	C						
2	No	2	C	1			1.5775575		
3	No	3	O	2	1		1.2509454	114.9722656	
4	No	4	O	2	1	3	1.2509454	114.9722656	178.4757704
5	No	5	H	1	2	3	1.0999228	109.4005594	-89.2378852
6	No	6	H	1	2	3	1.0968652	111.4835090	152.3856557
7	No	7	H	1	2	3	1.0968652	111.4835090	29.1385738

water

Row	Highlight	Tag	Symbol	NA	NB	NC	Bond	Angle	Dihedral
1	No	1	C						
2	No	2	C	1			1.5381280		
3	No	3	O	2	1		1.2615947	117.0329928	
4	No	4	O	2	1	3	1.2615947	117.0329928	178.4478910
5	No	5	H	1	2	3	1.0971857	108.9690579	-89.2239455
6	No	6	H	1	2	3	1.0936022	111.4545713	152.2491371
7	No	7	H	1	2	3	1.0936022	111.4545713	29.3029719

TS with HO radical

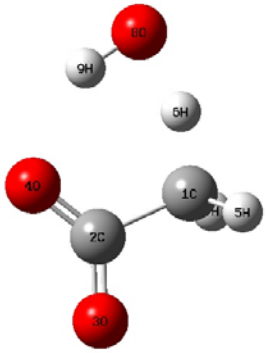

Vacuo

Row	Highlight	Tag	Symbol	NA	NB	NC	Bond	Angle	Dihedral
1	No	1	C						
2	No	2	C	1			1.5510952		
3	No	3	O	2	1		1.2502555	112.3189423	
4	No	4	O	2	1	3	1.2519399	118.2334446	-179.9977424
5	No	5	H	1	2	3	1.0958753	112.1746029	-61.5417468
6	No	6	H	1	2	3	1.2208910	107.7031099	-179.9680425
7	No	7	H	1	2	3	1.0958783	112.1750326	61.6120591
8	No	8	O	1	2	3	2.5207054	96.3063367	-179.9819007
9	No	9	H	8	1	2	0.9849539	75.0481290	-0.0123990

Water

Row	Highlight	Tag	Symbol	NA	NB	NC	Bond	Angle	Dihedral
1	No	1	C						
2	No	2	C	1			1.5280346		
3	No	3	O	2	1		1.2559018	114.5045609	
4	No	4	O	2	1	3	1.2611523	119.0089665	179.7328949
5	No	5	H	1	2	3	1.0937174	112.4158599	-67.2522530
6	No	6	H	1	2	3	1.2086949	108.1379106	175.6565575
7	No	7	H	1	2	3	1.0934116	112.6242146	58.0953272
8	No	8	O	1	2	3	2.5126693	95.7018024	176.8238598

9	No	9	H	8	1	2	0.9838074	76.1624308	2.7390343

Complex with HO radical

C-centered radical

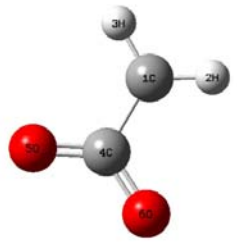

Vacuo

Row	Highlight	Tag	Symbol	NA	NB	NC	Bond	Angle	Dihedral
1	No	1	C						
2	No	2	H	1			1.0902437		
3	No	3	H	1	2		1.0902437	117.9487411	
4	No	4	C	1	2	3	1.5050900	121.0256292	179.9918772
5	No	5	O	4	1	2	1.2598142	115.3171301	-179.9969839
6	No	6	O	4	1	5	1.2598142	115.3171301	-179.9976589

Water

Row	Highlight	Tag	Symbol	NA	NB	NC	Bond	Angle	Dihedral
1	No	1	C						
2	No	2	H	1			1.0856116		
3	No	3	H	1	2		1.0856116	118.6337914	
4	No	4	C	1	2	3	1.4764340	120.6831037	179.9873162
5	No	5	O	4	1	2	1.2697253	117.1773322	-179.9825063
6	No	6	O	4	1	5	1.2697253	117.1773322	179.9779574

CH3CH2COO-

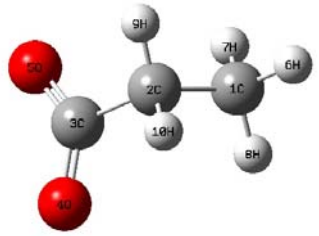

Row	Highlight	Tag	Symbol	NA	NB	NC	Bond	Angle	Dihedral
1	No	1	C						
2	No	2	C	1			1.5360833		
3	No	3	C	2	1		1.5404047	110.2710645	
4	No	4	O	3	2	1	1.2624316	117.1295327	88.8554160
5	No	5	O	3	2	1	1.2624316	117.1295327	-88.8554160
6	No	6	H	1	2	3	1.0946555	111.6018322	180.0000000
7	No	7	H	1	2	3	1.0955269	110.7100780	59.7675066
8	No	8	H	1	2	3	1.0955269	110.7100780	-59.7675066
9	No	9	H	2	1	3	1.0951392	109.6338437	-120.6538505
10	No	10	H	2	1	3	1.0951392	109.6338437	120.6538505

TS1 with HO radical

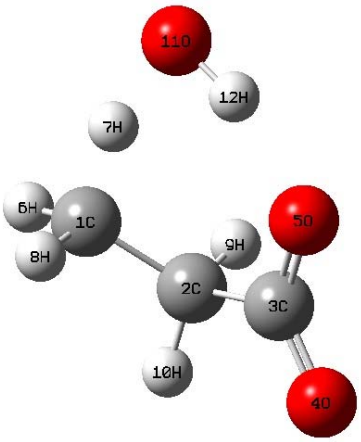

Row	Highlight	Tag	Symbol	NA	NB	NC	Bond	Angle	Dihedral
1	No	1	C						
2	No	2	C	1			1.5166227		
3	No	3	C	2	1		1.5437957	115.4912876	
4	No	4	O	3	2	1	1.2528578	117.5361363	135.7475264
5	No	5	O	3	2	1	1.2710693	117.6775527	-45.7072506
6	No	6	H	1	2	3	1.0935773	113.4921807	177.1262219
7	No	7	H	1	2	3	1.2104353	109.1054363	62.3693225
8	No	8	H	1	2	3	1.0933971	114.1845714	-54.3496337
9	No	9	H	2	1	3	1.0979495	109.2974250	-121.4964796
10	No	10	H	2	1	3	1.0963933	109.5286654	122.1385009
11	No	11	O	1	2	3	2.5177083	99.7147303	57.5222945
12	No	12	H	11	1	2	0.9969321	80.0397309	-35.0554035

TS2 with HO radical

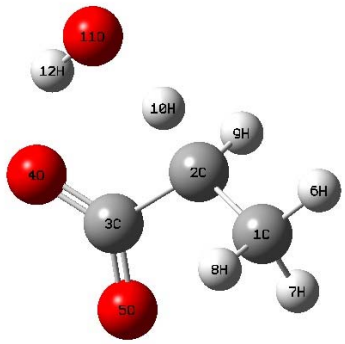

Row	Highlight	Tag	Symbol	NA	NB	NC	Bond	Angle	Dihedral
1	No	1	C						
2	No	2	C	1			1.5183687		
3	No	3	C	2	1		1.5389144	116.6666720	
4	No	4	O	3	2	1	1.2659345	117.6140437	146.2870691
5	No	5	O	3	2	1	1.2539746	116.4140641	-35.2114387
6	No	6	H	1	2	3	1.0942175	111.2638770	-177.9587991
7	No	7	H	1	2	3	1.0955904	110.0060705	62.6634576
8	No	8	H	1	2	3	1.0946498	111.6212624	-56.7811035
9	No	9	H	2	1	3	1.0969845	111.7672112	-126.6358661
10	No	10	H	2	1	3	1.1874217	109.5940514	119.5865156
11	No	11	O	2	1	3	2.5415235	122.1513552	113.1554881
12	No	12	H	11	2	1	0.9874917	74.4311783	-136.9934852

HOOCCH2COO-

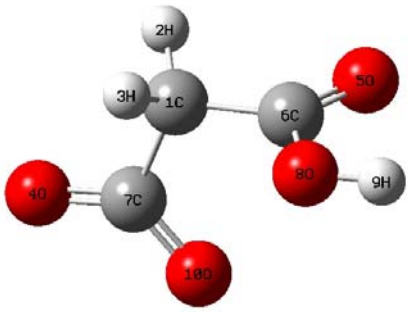

Row	Highlight	Tag	Symbol	NA	NB	NC	Bond	Angle	Dihedral
1	No	1	C						
2	No	2	H	1			1.0919131		
3	No	3	H	1	2		1.0928234	108.7089955	
4	No	4	O	1	2	3	2.3866726	92.4339024	94.1299402
5	No	5	O	1	4	2	2.4160556	134.5926824	-88.6907370
6	No	6	C	5	1	4	1.2157487	30.2405367	-114.3507801
7	No	7	C	4	1	6	1.2520942	36.3396028	3.0793609
8	No	8	O	6	5	1	1.3513626	121.9441766	178.5147668
9	No	9	H	8	6	5	0.9714622	107.6302017	-1.7269216
10	No	10	O	7	4	1	1.2560180	127.6934860	-179.8467560

TS with HO radical

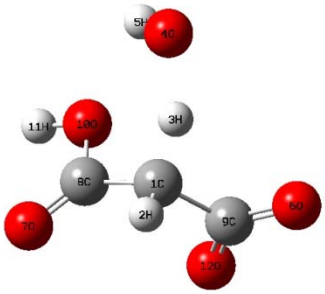

Row	Highlight	Tag	Symbol	NA	NB	NC	Bond	Angle	Dihedral
1	No	1	C						
2	No	2	H	1			1.0924433		
3	No	3	H	1	2		1.1598393	106.9172807	
4	No	4	O	1	2	3	2.6056028	107.1033397	-11.6708063
5	No	5	H	4	1	2	0.9736023	88.5209567	-142.2121043
6	No	6	O	1	4	5	2.3951069	96.4033201	112.9720186
7	No	7	O	1	6	4	2.4132763	143.4134275	149.0217665
8	No	8	C	7	1	6	1.2135524	30.3655586	-92.8287395
9	No	9	C	6	1	8	1.2470365	35.2638777	-28.2978764
10	No	10	O	8	7	1	1.3489363	122.5314779	179.3556370
11	No	11	H	10	8	7	0.9716740	108.0603792	-0.7090864
12	No	12	O	9	6	1	1.2565433	128.3537788	-178.2602802

-OOC(CH2)2COO-

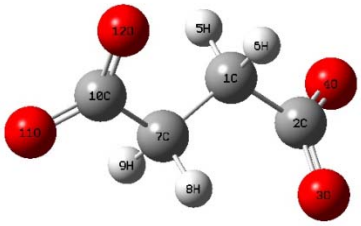

Row	Highlight	Tag	Symbol	NA	NB	NC	Bond	Angle	Dihedral
1	No	1	C						
2	No	2	C	1			1.5425311		
3	No	3	O	2	1		1.2627867	117.6455338	
4	No	4	O	2	1	3	1.2622101	117.0252997	-178.6035986
5	No	5	H	1	2	4	1.0952041	108.7235034	19.9613289
6	No	6	H	1	2	4	1.0978928	107.3670860	-94.4287553
7	No	7	C	1	2	4	1.5281905	114.6586359	144.9565202
8	No	8	H	7	1	2	1.0979207	108.5378356	50.1312946
9	No	9	H	7	1	2	1.0961668	110.8698372	-65.4150279
10	No	10	C	7	1	2	1.5427915	115.9885491	170.7340996
11	No	11	O	10	7	1	1.2626856	116.2697926	157.9210145
12	No	12	O	10	7	1	1.2619949	118.2483009	-23.7391386

TS with HO radical

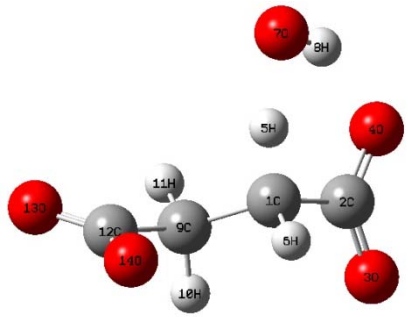

Row	Highlight	Tag	Symbol	NA	NB	NC	Bond	Angle	Dihedral
1	No	1	C						
2	No	2	C	1			1.5354765		
3	No	3	O	2	1		1.2559343	115.2447347	
4	No	4	O	2	1	3	1.2650251	118.6768659	178.9744781
5	No	5	H	1	2	3	1.1756462	106.8664621	168.2561618
6	No	6	H	1	2	3	1.0943640	111.1538695	53.6392821
7	No	7	O	1	2	3	2.5665761	93.6729949	173.5863438
8	No	8	H	7	1	2	0.9873967	73.6645127	5.7890455
9	No	9	C	1	2	3	1.5210262	113.7176105	-72.1890023
10	No	10	H	9	1	2	1.0998748	108.1093495	57.7285740
11	No	11	H	9	1	2	1.0945251	110.6759695	-58.8970925
12	No	12	C	9	1	2	1.5465868	114.4938551	176.7422645
13	No	13	O	12	9	1	1.2596336	116.6579626	144.0981760
14	No	14	O	12	9	1	1.2602205	117.1407214	-37.4032980

CH3COCOO-

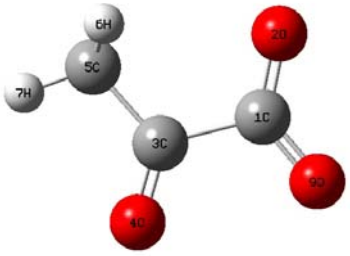

Row	Highlight	Tag	Symbol	NA	NB	NC	Bond	Angle	Dihedral
1	No	1	C						
2	No	2	O	1			1.2549675		
3	No	3	C	1	2		1.5659240	115.6765700	
4	No	4	O	3	1	2	1.2182862	120.2943832	179.8498092
5	No	5	C	3	1	2	1.5053558	117.1659645	-0.1475589
6	No	6	H	5	3	1	1.0949808	109.6755998	-58.1420397
7	No	7	H	5	3	1	1.0915551	110.8515249	-179.9706614
8	No	8	H	5	3	1	1.0950132	109.6594646	58.2217870
9	No	9	O	1	2	3	1.2518151	128.3911953	179.9850526

TS1 with HO radical

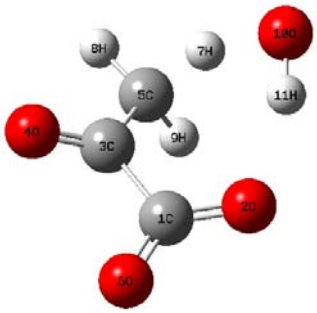

Row	Highlight	Tag	Symbol	NA	NB	NC	Bond	Angle	Dihedral
1	No	1	C						
2	No	2	O	1			1.2626159		
3	No	3	C	1	2		1.5594437	115.9143612	
4	No	4	O	3	1	2	1.2189010	120.4081934	-151.8839381
5	No	5	C	3	1	2	1.4951665	117.8426138	27.4028054
6	No	6	O	1	2	3	1.2449116	127.8979246	-179.2176411
7	No	7	H	5	3	1	1.1999998	106.5918585	-66.7387385
8	No	8	H	5	3	1	1.0914360	113.0366364	176.9251190
9	No	9	H	5	3	1	1.0918415	113.1049464	46.8571471
10	No	10	O	5	3	1	2.5221940	101.3141202	-55.5891304
11	No	11	H	10	5	3	0.9905959	79.2984677	42.5171028

TS2 with HO radical

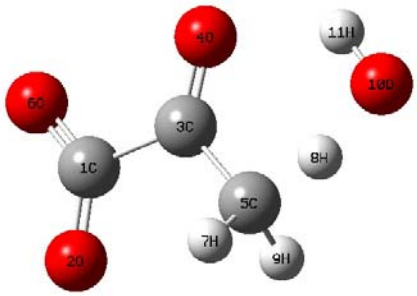

Row	Highlight	Tag	Symbol	NA	NB	NC	Bond	Angle	Dihedral
1	No	1	C						
2	No	2	O	1			1.2525088		
3	No	3	C	1	2		1.5737290	115.1331492	
4	No	4	O	3	1	2	1.2165636	120.7245743	-179.8080359
5	No	5	C	3	1	2	1.4978901	116.1862529	0.1873813
6	No	6	O	1	2	3	1.2471084	129.4615356	-179.9908581
7	No	7	H	5	3	1	1.0931580	112.7548152	-62.7626332
8	No	8	H	5	3	1	1.2185471	106.7306339	-179.9484629
9	No	9	H	5	3	1	1.0931799	112.7585742	62.8596704
10	No	10	O	5	3	1	2.5130241	97.4388951	-179.9367400
11	No	11	H	10	5	3	0.9755587	84.9630577	-0.0329154

TS3 with HO radical

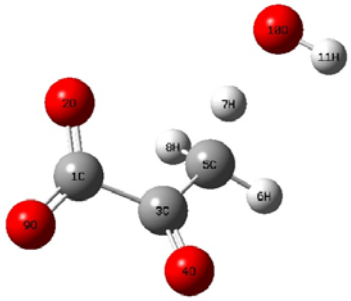

Row	Highlight	Tag	Symbol	NA	NB	NC	Bond	Angle	Dihedral
1	No	1	C						
2	No	2	O	1			1.2537626		
3	No	3	C	1	2		1.5627193	114.4422475	
4	No	4	O	3	1	2	1.2161745	121.1235365	156.9921080
5	No	5	C	3	1	2	1.5013119	116.8554745	-21.5094253
6	No	6	H	5	3	1	1.0907082	111.9955452	-172.8853233
7	No	7	H	5	3	1	1.1605194	107.1617455	68.0693831
8	No	8	H	5	3	1	1.0926504	112.2486185	-45.8874473
9	No	9	O	1	2	3	1.2485253	129.3895235	178.7962420
10	No	10	O	5	3	1	2.5937781	119.9332147	74.0447129
11	No	11	H	10	5	3	0.9733447	91.1625811	94.9216081

CH2ClCOO-

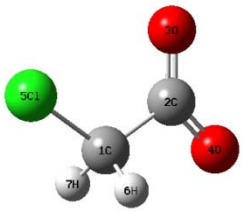

Vacuo

Row	Highlight	Tag	Symbol	NA	NB	NC	Bond	Angle	Dihedral
1	No	1	C						
2	No	2	C	1			1.5752444		
3	No	3	O	2	1		1.2344772	119.8737514	
4	No	4	O	2	1	3	1.2515686	107.5244686	179.9731942
5	No	5	Cl	1	2	3	1.8603508	117.8293234	0.0719315
6	No	6	H	1	2	3	1.0902969	110.1583898	-119.8222031
7	No	7	H	1	2	3	1.0902376	110.1740153	119.9949164

Water

Row	Highlight	Tag	Symbol	NA	NB	NC	Bond	Angle	Dihedral
1	No	1	C						
2	No	2	C	1			1.5481317		
3	No	3	O	2	1		1.2556149	116.1596306	
4	No	4	O	2	1	3	1.2556149	116.1596306	-179.9175053
5	No	5	H	1	2	3	1.0886566	112.1431210	-153.0209849
6	No	6	Cl	1	2	3	1.8303334	109.4045555	89.9587527
7	No	7	H	1	2	3	1.0886566	112.1431210	-27.0615098

Complex with HO radical

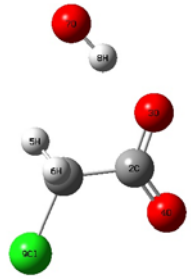

Row	Highlight	Tag	Symbol	NA	NB	NC	Bond	Angle	Dihedral
1	No	1	C						
2	No	2	C	1			1.5414481		
3	No	3	O	2	1		1.2713132	112.2881324	
4	No	4	O	2	1	3	1.2399959	121.2039058	179.2547634
5	No	5	H	1	2	4	1.0889505	110.2480352	-125.4327657
6	No	6	H	1	2	4	1.0904509	109.5615779	115.0135448
7	No	7	O	3	2	1	2.6443644	119.5129659	-8.5129590
8	No	8	H	7	3	2	1.0119314	0.9610633	73.9283606
9	No	9	Cl	1	2	4	1.8152501	115.0492819	-4.8096037

TS with HO radical

Vacuo

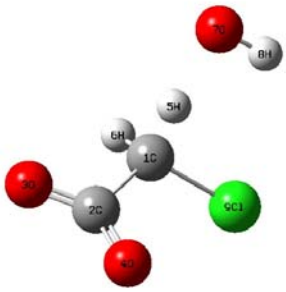

Row	Highlight	Tag	Symbol	NA	NB	NC	Bond	Angle	Dihedral
1	No	1	C						
2	No	2	C	1			1.6091372		
3	No	3	O	2	1		1.2426074	108.5931464	
4	No	4	O	2	1	3	1.2302228	116.7438707	-179.9388399
5	No	5	H	1	2	4	1.1502500	108.8809057	-90.9488159
6	No	6	H	1	2	4	1.0888002	111.2215127	148.9694571
7	No	7	O	1	2	4	2.6137537	125.4140268	-93.2061725
8	No	8	H	7	1	2	0.9693297	84.1984783	129.1460848
9	No	9	Cl	1	2	4	1.8262714	115.3302438	28.1335865

Water

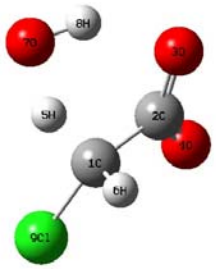

Row	Highlight	Tag	Symbol	NA	NB	NC	Bond	Angle	Dihedral
1	No	1	C						
2	No	2	C	1			1.5490139		
3	No	3	O	2	1		1.2609953	112.6846406	
4	No	4	O	2	1	3	1.2431340	118.8323252	178.0069770
5	No	5	H	1	2	4	1.1879932	105.7592796	-139.7647843
6	No	6	H	1	2	4	1.0910173	112.0041811	105.4224276
7	No	7	O	1	2	4	2.5049616	95.2910834	-151.1827970
8	No	8	H	7	1	2	0.9830256	76.4723383	-20.7009990
9	No	9	Cl	1	2	4	1.7853926	117.1338791	-20.3040185

C-centered radical

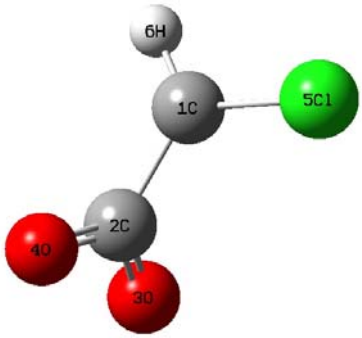

Vacuo

Row	Highlight	Tag	Symbol	NA	NB	NC	Bond	Angle	Dihedral
1	No	1	C						

2	No	2	C	1			1.5400000		
3	No	3	O	2	1		1.2583997	120.0000084	
4	No	4	O	2	1	3	1.2583997	120.0000084	180.0000000
5	No	5	Cl	1	2	3	1.7600003	119.9999953	-90.0000000
6	No	6	H	1	2	3	1.0699998	120.0000049	90.0000000

Water

Row	Highlight	Tag	Symbol	NA	NB	NC	Bond	Angle	Dihedral
1	No	1	C						
2	No	2	H	1			1.0826116		
3	No	3	C	1	2		1.4843939	123.1430277	
4	No	4	O	3	1	2	1.2665587	113.1923429	-0.0147631
5	No	5	O	3	1	4	1.2578403	119.3869355	-179.9926978
6	No	6	Cl	1	3	5	1.7274363	122.3809700	0.0142807

CHCl2COO-

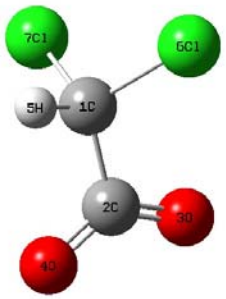

Row	Highlight	Tag	Symbol	NA	NB	NC	Bond	Angle	Dihedral
1	No	1	C						
2	No	2	C	1			1.5656471		
3	No	3	O	2	1		1.2448135	117.6529044	
4	No	4	O	2	1	3	1.2512878	112.6135584	-178.8254779
5	No	5	H	1	2	3	1.0851345	112.0201207	-162.0688165
6	No	6	Cl	1	2	3	1.8033894	113.1960861	-41.4406990
7	No	7	Cl	1	2	3	1.8150036	108.6703341	81.0815042

CF2HCOO-

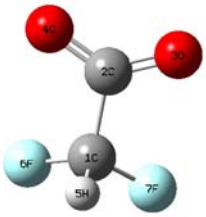

Row	Highlight	Tag	Symbol	NA	NB	NC	Bond	Angle	Dihedral
1	No	1	C						
2	No	2	C	1			1.5517666		
3	No	3	O	2	1		1.2516483	115.4457044	
4	No	4	O	2	1	3	1.2516483	115.4457044	-177.2798390
5	No	5	H	1	2	3	1.0971657	111.5641672	88.6399195
6	No	6	F	1	2	3	1.3652214	111.0385490	-150.7604380
7	No	7	F	1	2	3	1.3652214	111.0385490	-31.9597230

TS with HO radical

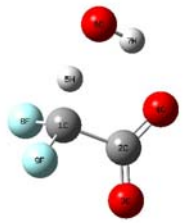

Row	Highlight	Tag	Symbol	NA	NB	NC	Bond	Angle	Dihedral
1	No	1	C						
2	No	2	C	1			1.5703663		
3	No	3	O	2	1		1.2434208	114.7702453	
4	No	4	O	2	1	3	1.2522968	115.0198139	178.7012624
5	No	5	H	1	2	3	1.1742339	108.4531101	161.8686820
6	No	6	O	1	2	3	2.5627562	95.7394320	167.5393038
7	No	7	H	6	1	2	0.9826917	76.8231207	9.2856247
8	No	8	F	1	2	3	1.3515027	110.4803389	-79.3868168
9	No	9	F	1	2	3	1.3457961	112.4225468	40.7829840

Complex with HO radical

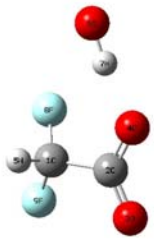

Row	Highlight	Tag	Symbol	NA	NB	NC	Bond	Angle	Dihedral
1	No	1	C						
2	No	2	C	1			1.5500215		
3	No	3	O	2	1		1.2427695	117.0621110	
4	No	4	O	2	1	3	1.2624901	115.1010379	-177.5279988
5	No	5	H	1	2	3	1.0964875	111.5536537	99.3519928
6	No	6	O	4	2	1	2.6708772	127.7171888	-5.3657013
7	No	7	H	6	4	2	1.0052466	4.7642940	-9.4321344
8	No	8	F	1	2	3	1.3662393	110.4091153	-140.3601527
9	No	9	F	1	2	3	1.3602113	111.1124934	-21.8150262

CHBr2COO-

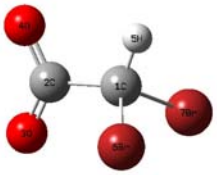

Row	Highlight	Tag	Symbol	NA	NB	NC	Bond	Angle	Dihedral
1	No	1	C						
2	No	2	C	1			1.5628049		
3	No	3	O	2	1		1.2429244	118.1488796	
4	No	4	O	2	1	3	1.2540700	112.3045276	179.9432597
5	No	5	H	1	2	3	1.0846822	112.0850574	177.0543878
6	No	6	Br	1	2	3	1.9710809	110.8798414	-65.3459698
7	No	7	Br	1	2	3	1.9697655	111.5409224	58.9131591

TS with HO radical

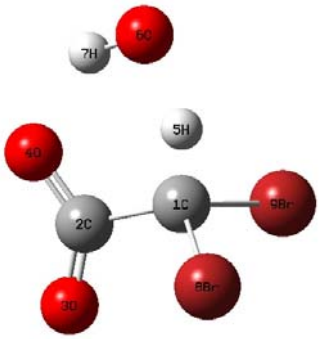

Row	Highlight	Tag	Symbol	NA	NB	NC	Bond	Angle	Dihedral
1	No	1	C						
2	No	2	C	1			1.5736965		
3	No	3	O	2	1		1.2381014	116.7084030	
4	No	4	O	2	1	3	1.2549333	113.5848866	-179.2272607
5	No	5	H	1	2	3	1.1550823	109.6391434	-170.8637617
6	No	6	O	1	2	3	2.5593156	95.9405052	-172.9842796
7	No	7	H	6	1	2	0.9853682	76.7475184	-5.4706171
8	No	8	Br	1	2	3	1.9464828	113.5768894	-53.6356266
9	No	9	Br	1	2	3	1.9508318	110.9002174	74.0198459

Complex with HO radical

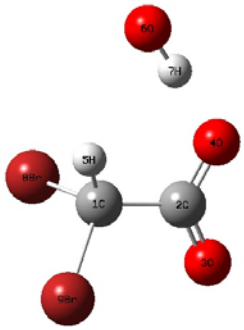

Row	Highlight	Tag	Symbol	NA	NB	NC	Bond	Angle	Dihedral
1	No	1	C						
2	No	2	C	1			1.5573584		
3	No	3	O	2	1		1.2355314	119.2034666	
4	No	4	O	2	1	3	1.2653863	112.8572086	179.1001393
5	No	5	H	1	2	3	1.0844485	112.3427260	160.1417410
6	No	6	O	4	2	1	2.6544761	120.7398695	2.2710869
7	No	7	H	6	4	2	1.0086689	1.2625004	-170.1657539
8	No	8	Br	1	2	3	1.9728431	108.3871553	-84.4551998
9	No	9	Br	1	2	3	1.9563724	113.3814880	39.6135639

Cl3CCOO-

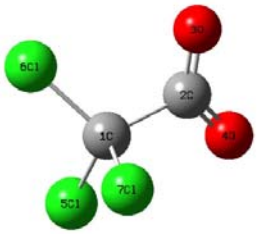

Row	Highlight	Tag	Symbol	NA	NB	NC	Bond	Angle	Dihedral
1	No	1	C						
2	No	2	C	1			1.6079327		

3	No	3	O	2	1		1.2395986	114.2781014	
4	No	4	O	2	1	3	1.2395986	114.2781014	177.5697398
5	No	5	Cl	1	2	3	1.7965239	112.4923515	152.4544617
6	No	6	Cl	1	2	3	1.7965239	112.4923515	29.9757985
7	No	7	Cl	1	2	3	1.8130073	106.5479112	-88.7848699

TS with HO radical

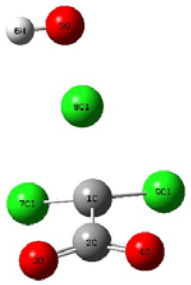

Row	Highlight	Tag	Symbol	NA	NB	NC	Bond	Angle	Dihedral
1	No	1	C						
2	No	2	C	1			1.5951577		
3	No	3	O	2	1		1.2383651	113.7955073	
4	No	4	O	2	1	3	1.2384431	113.8390222	-179.9905400
5	No	5	O	1	2	3	4.1484445	98.6945749	87.8847622
6	No	6	H	5	1	2	0.9703815	96.8868790	-75.3987414
7	No	7	Cl	1	2	3	1.7422407	116.9932103	-21.5463998
8	No	8	Cl	5	1	2	1.9221380	3.5851927	54.2978442
9	No	9	Cl	1	2	3	1.7419665	116.9522388	-159.2518383

Complex with HO radical

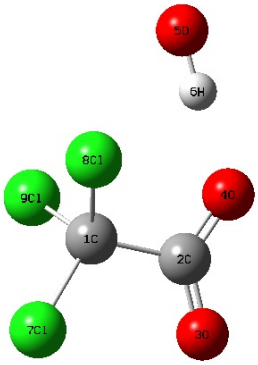

Row	Highlight	Tag	Symbol	NA	NB	NC	Bond	Angle	Dihedral
1	No	1	C						
2	No	2	C	1			1.6014530		
3	No	3	O	2	1		1.2323167	116.1979169	
4	No	4	O	2	1	3	1.2507084	113.8881331	178.6448953
5	No	5	O	4	2	1	2.6966306	129.0528315	-5.7580770
6	No	6	H	5	4	2	0.9987912	1.3363413	-38.9898071
7	No	7	Cl	1	2	3	1.7897837	113.0144083	13.2840877
8	No	8	Cl	1	2	3	1.8022551	110.7388587	134.6891610
9	No	9	Cl	1	2	3	1.8068883	107.4300566	-106.5112721

Br3CCOO-

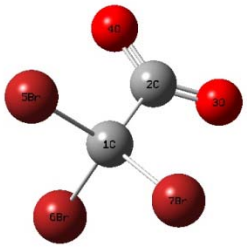

Row	Highlight	Tag	Symbol	NA	NB	NC	Bond	Angle	Dihedral
1	No	1	C						
2	No	2	C	1			1.6093380		
3	No	3	O	2	1		1.2397784	114.3439929	
4	No	4	O	2	1	3	1.2397784	114.3439929	178.0177619
5	No	5	Br	1	2	3	1.9666868	112.7295554	152.1996410
6	No	6	Br	1	2	3	1.9858430	106.2631754	-89.0088809
7	No	7	Br	1	2	3	1.9666868	112.7295554	29.7825971

TS with HO radical

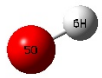

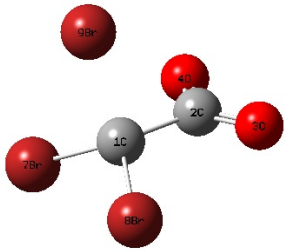

Row	Highlight	Tag	Symbol	NA	NB	NC	Bond	Angle	Dihedral
1	No	1	C						
2	No	2	C	1			1.5878183		
3	No	3	O	2	1		1.2407005	114.4002643	
4	No	4	O	2	1	3	1.2403319	114.1281171	-179.1745253
5	No	5	O	1	2	4	4.2939175	96.7103908	-81.8046552
6	No	6	H	5	1	2	0.9696590	97.2549790	-12.5775321
7	No	7	Br	1	2	4	1.9195969	115.9370431	27.0408122
8	No	8	Br	1	2	4	1.9223453	116.4974291	161.6079055
9	No	9	Br	5	1	2	2.0298329	9.4131163	-124.6074093

With explicit water molecules
CH3COO-HO radical with H2O

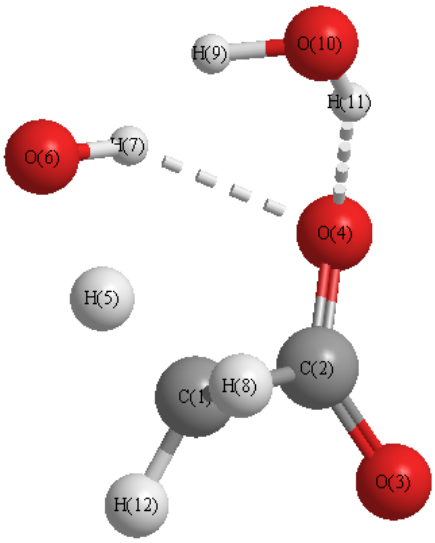

Row	Highlight	Tag	Symbol	NA	NB	NC	Bond	Angle	Dihedral
1	No	1	C						
2	No	2	C	1			1.5256830		
3	No	3	O	2	1		1.2511343	115.4972265	
4	No	4	O	2	1	3	1.2684329	118.3686942	-178.6133261
5	No	5	H	1	2	3	1.1927183	107.9165597	-157.2877667
6	No	6	O	1	2	3	2.5446747	96.2629490	-161.4390055
7	No	7	H	6	1	2	0.9813051	77.4841644	-3.2964981
8	No	8	H	1	2	3	1.0939441	111.7135185	87.6443150
9	No	9	H	6	1	2	2.1360446	82.7531439	-81.3959709
10	No	10	O	4	2	1	2.8485567	105.2651192	43.2533692
11	No	11	H	10	4	2	0.9752104	13.1699577	108.6079219
12	No	12	H	1	2	3	1.0921768	113.5579843	-38.6536063

CH3COO-HO radical with 2H2O

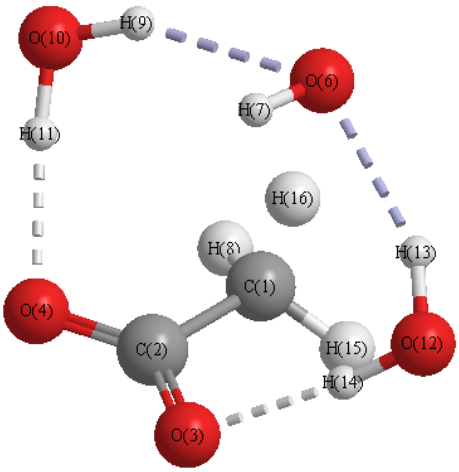

Row	Highlight	Tag	Symbol	NA	NB	NC	Bond	Angle	Dihedral
1	No	1	C						
2	No	2	C	1			1.5284823		
3	No	3	O	2	1		1.2616253	117.2950031	
4	No	4	O	2	1	3	1.2616285	117.2919902	178.6902178
5	No	5	H	1	2	3	1.1458407	106.3521210	-89.2752632
6	No	6	O	1	2	3	2.7002049	99.5746892	-89.2868748
7	No	7	H	6	1	2	0.9761757	89.6100565	0.0821367
8	No	8	H	1	2	3	1.0914172	113.2629049	155.2544585
9	No	9	H	6	1	2	2.1997977	74.9142114	-77.1203951
10	No	10	O	4	2	1	2.8024035	106.3104570	-38.9050104
11	No	11	H	10	4	2	0.9799320	4.5077156	147.6737411
12	No	12	O	3	2	1	2.8024963	106.3569528	38.7077413

13	No	13	H	12	3	2	0.9665530	98.2562453	17.4590543
14	No	14	H	12	3	2	0.9799526	4.4917050	-148.1018470
15	No	15	H	1	2	3	1.0914219	113.2583334	26.1861669

CH3COO-HO radical with 3H2O

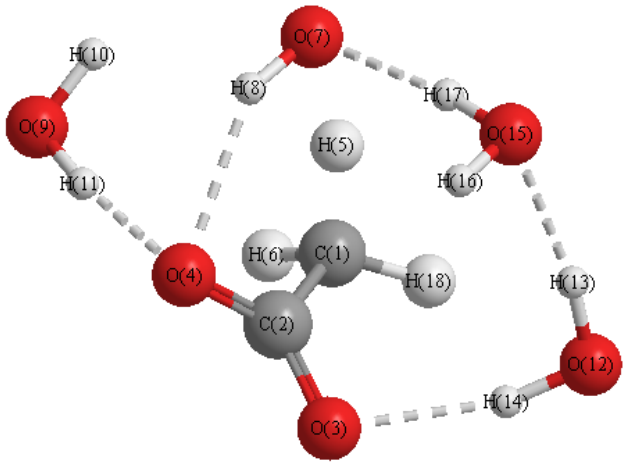

Row	Highlight	Tag	Symbol	NA	NB	NC	Bond	Angle	Dihedral
1	No	1	C						
2	No	2	C	1			1.5229610		
3	No	3	O	2	1		1.2565091	117.2455939	
4	No	4	O	2	1	3	1.2663150	117.4555116	-179.4591039
5	No	5	H	1	2	3	1.1757682	106.1477464	-137.0471603
6	No	6	H	1	2	3	1.0933328	112.0114102	109.0025616
7	No	7	O	1	2	3	2.5707080	92.6084612	-139.3448038
8	No	8	H	7	1	2	0.9808329	78.1698363	-21.8552554
9	No	9	O	4	2	1	2.7920121	111.7940015	28.9246153
10	No	10	H	9	4	2	0.9641775	97.4620467	-76.5188126
11	No	11	H	9	4	2	0.9799621	4.6234241	114.5285949
12	No	12	O	3	2	1	2.8329509	102.4384407	49.1320250
13	No	13	H	12	3	2	0.9755149	91.6153362	38.9775675
14	No	14	H	12	3	2	0.9752189	10.2131495	-151.0225459
15	No	15	O	7	1	2	2.8614477	83.3829979	69.3852990
16	No	16	H	15	7	1	0.9651689	99.1970173	-85.4562221
17	No	17	H	15	7	1	0.9780379	4.7776619	125.7554167
18	No	18	H	1	2	3	1.0899800	114.1759379	-20.1045845

Transition state 1 for CH2ClCOO-HOradical with one explicit water molecule

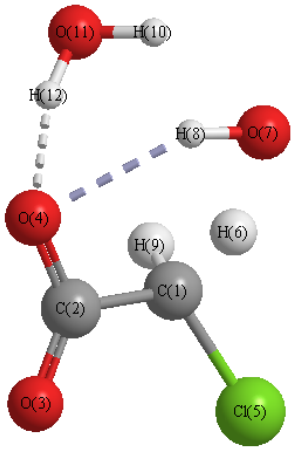

Row	Highlight	Tag	Symbol	NA	NB	NC	Bond	Angle	Dihedral
1	No	1	C						
2	No	2	C	1			1.5475214		
3	No	3	O	2	1		1.2394262	119.6604251	
4	No	4	O	2	1	3	1.2662344	112.4695166	-179.1603558
5	No	5	Cl	1	2	3	1.7847655	117.0041526	-12.2709455
6	No	6	H	1	2	3	1.1671555	106.3018382	-131.5537679

7	No	7	O	1	2	3	2.5653721	97.3405346	-142.7348999
8	No	8	H	7	1	2	0.9777407	81.2305794	-12.0994126
9	No	9	H	1	2	3	1.0905617	111.7744333	113.7182258
10	No	10	H	7	1	2	2.2375272	80.4390501	-89.0916997
11	No	11	O	4	2	1	2.8078004	113.9790319	26.6889318
12	No	12	H	11	4	2	0.9781067	8.8540233	113.3866772

Transition state 2 for CH2ClCOO-HOradical with one explicit water molecule

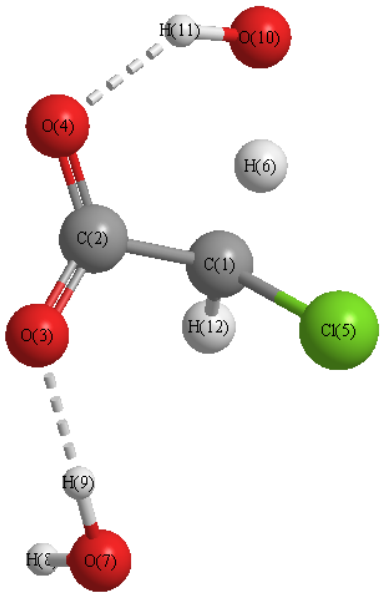

Row	Highlight	Tag	Symbol	NA	NB	NC	Bond	Angle	Dihedral
1	No	1	C						
2	No	2	C	1			1.5458216		
3	No	3	O	2	1		1.2561478	115.5712626	
4	No	4	O	2	1	3	1.2514596	117.3080085	-178.9562023
5	No	5	Cl	1	2	4	1.7898016	112.7746913	116.4824970
6	No	6	H	1	2	4	1.1884166	108.5289309	-0.7352169
7	No	7	O	3	2	1	2.7644767	115.2068258	-22.0508014
8	No	8	H	7	3	2	0.9635350	100.7940086	-85.9718912
9	No	9	H	7	3	2	0.9813089	2.9784560	128.9459821
10	No	10	O	1	2	4	2.5151850	95.9935869	-2.6458366
11	No	11	H	10	1	2	0.9836370	77.8044742	1.7531963
12	No	12	H	1	2	4	1.0905829	113.1108242	-120.6212563

Transition state 3 for CH2ClCOO-HOradical with one explicit water molecule

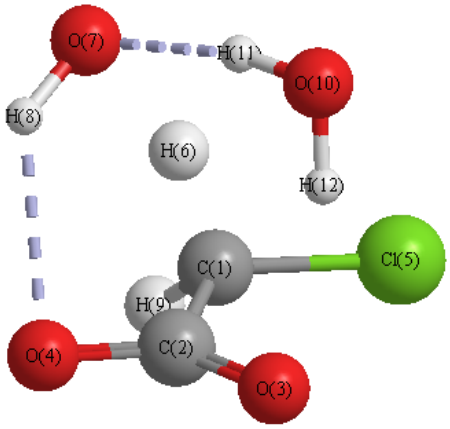

Row	Highlight	Tag	Symbol	NA	NB	NC	Bond	Angle	Dihedral
1	No	1	C						
2	No	2	C	1			1.5476838		

3	No	3	O	2	1		1.2493552	119.5303303	
4	No	4	O	2	1	3	1.2547724	111.6770602	176.9400648
5	No	5	Cl	1	2	3	1.7850288	117.4462625	8.1600013
6	No	6	H	1	2	3	1.1579584	103.6678494	-109.4297928
7	No	7	O	1	2	3	2.5960454	89.3710907	-116.0678121
8	No	8	H	7	1	2	0.9782609	79.2705642	-35.5873799
9	No	9	H	1	2	3	1.0895021	112.9224309	135.6605467
10	No	10	O	7	1	2	2.9612695	77.2891756	61.9191818
11	No	11	H	10	7	1	0.9716844	9.5829623	170.8963245
12	No	12	H	10	7	1	0.9701623	93.4118652	-27.0721677

Transition state for CH2ClCOO-HOradical with 2 explicit water molecules

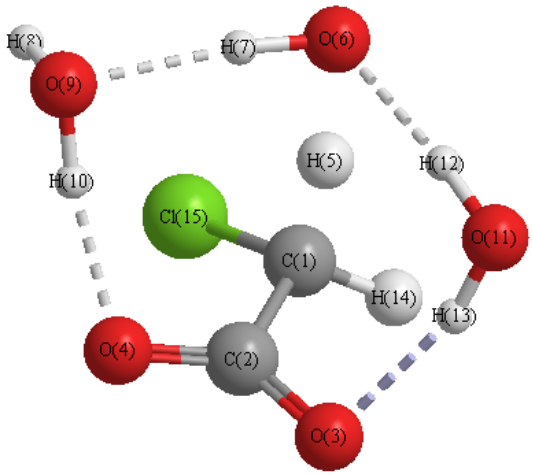

Row	Highlight	Tag	Symbol	NA	NB	NC	Bond	Angle	Dihedral
1	No	1	C						
2	No	2	C	1			1.5431174		
3	No	3	O	2	1		1.2545728	113.6957610	
4	No	4	O	2	1	3	1.2538842	118.9394254	177.7933590
5	No	5	H	1	2	4	1.1524552	107.1376471	83.3813474
6	No	6	O	1	2	4	2.6548727	100.3213252	80.5135740
7	No	7	H	6	1	2	0.9957262	87.5926404	-53.6196694
8	No	8	H	6	1	2	3.0651281	78.4519054	-73.9292695
9	No	9	O	4	2	1	2.7315796	107.6708334	-51.0914087
10	No	10	H	9	4	2	0.9859053	6.6337085	147.5762467
11	No	11	O	6	1	2	2.8853341	78.4472080	56.5033793
12	No	12	H	11	6	1	0.9733942	8.0624259	-165.4614784
13	No	13	H	11	6	1	0.9714420	95.1167892	-16.0726108
14	No	14	H	1	2	4	1.0890134	112.7321151	-159.6152916
15	No	15	Cl	1	2	4	1.7915725	115.3583410	-34.4580431

Transition state for CH2ClCOO-HOradical with 3 explicit water molecules

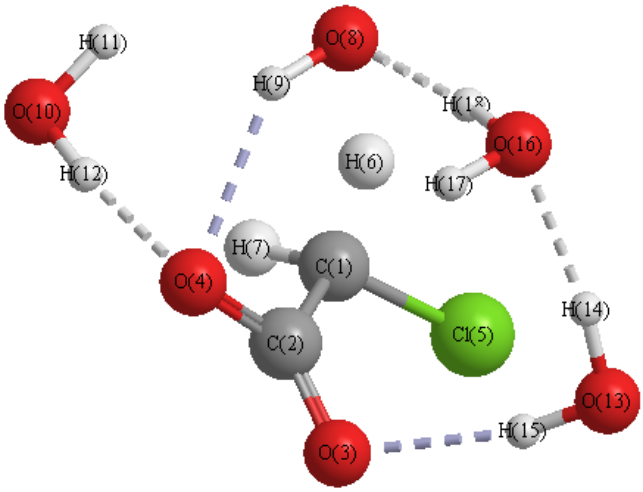

Row	Highlight	Tag	Symbol	NA	NB	NC	Bond	Angle	Dihedral
1	No	1	C						
2	No	2	C	1			1.5449020		
3	No	3	O	2	1		1.2439792	120.1254384	
4	No	4	O	2	1	3	1.2628756	112.3381453	-179.8768752
5	No	5	Cl	1	2	3	1.7798296	117.3730401	-4.6037156
6	No	6	H	1	2	3	1.1591788	105.0775918	-123.6898857
7	No	7	H	1	2	3	1.0899456	111.8064441	122.0475681
8	No	8	O	1	2	3	2.5854855	93.3665001	-134.4981319
9	No	9	H	8	1	2	0.9798887	78.6598616	-30.5491489
10	No	10	O	4	2	1	2.8080671	114.9290378	26.6788105
11	No	11	H	10	4	2	0.9643821	97.7773265	-71.8390731
12	No	12	H	10	4	2	0.9783154	4.6231257	123.5951555
13	No	13	O	3	2	1	2.8673937	107.4156771	68.5398483
14	No	14	H	13	3	2	0.9755688	92.5186934	26.2400772
15	No	15	H	13	3	2	0.9716397	10.0847775	-133.6542284
16	No	16	O	13	3	2	2.8371127	87.4936723	29.2757016
17	No	17	H	16	13	3	0.9652152	92.1113935	54.9109796
18	No	18	H	16	13	3	0.9775703	107.2860361	-49.5519409

Transition state for CHCl2COO-HOradical with 1 explicit water molecule

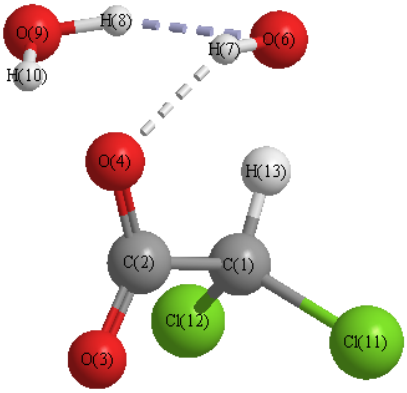

Row	Highlight	Tag	Symbol	NA	NB	NC	Bond	Angle	Dihedral
1	No	1	C						
2	No	2	C	1			1.5778446		
3	No	3	O	2	1		1.2368740	115.7229793	
4	No	4	O	2	1	3	1.2559985	114.3480667	179.7971522
5	No	5	H	1	2	3	1.1532287	109.0948716	179.0356074
6	No	6	O	1	2	3	2.5871818	96.3054493	-179.1674712
7	No	7	H	6	1	2	0.9843426	77.7144933	8.6117623
8	No	8	H	6	1	2	2.0679367	87.1118236	-70.6989463
9	No	9	O	6	1	2	2.9274237	81.9189974	-61.5557399
10	No	10	H	9	6	1	0.9688124	77.5773102	56.7346468
11	No	11	Cl	1	2	3	1.7867251	111.4879259	-64.3203511
12	No	12	Cl	1	2	3	1.7841096	112.0373487	61.4215128

Transition state for CHCl2COO-HOradical with 2 explicit water molecules

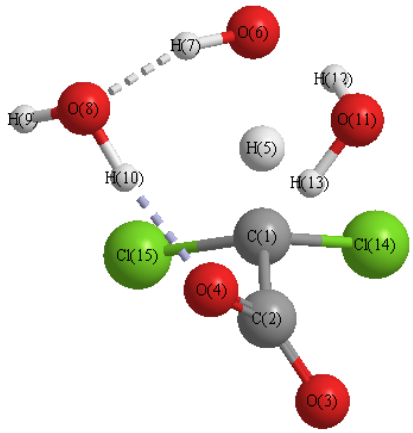

Row	Highlight	Tag	Symbol	NA	NB	NC	Bond	Angle	Dihedral
1	No	1	C						
2	No	2	C	1			1.5738602		
3	No	3	O	2	1		1.2329102	117.1487275	
4	No	4	O	2	1	3	1.2600957	113.8965177	-179.1689350
5	No	5	H	1	2	3	1.1487936	110.3835453	-142.0806251
6	No	6	O	1	2	3	2.6537247	111.2951866	-144.5410454
7	No	7	H	6	1	2	0.9961434	92.5053179	-57.3418795
8	No	8	O	4	2	1	2.7298588	125.6262031	2.2703621
9	No	9	H	8	4	2	0.9649886	107.1595916	67.6322492
10	No	10	H	8	4	2	0.9858250	4.7085723	119.9403429
11	No	11	O	6	1	2	2.8876757	83.3684880	24.9659891
12	No	12	H	11	6	1	0.9728529	12.4124435	132.5613274
13	No	13	H	11	6	1	0.9691733	88.8649283	-40.3722801
14	No	14	Cl	1	2	3	1.7816885	114.4083845	-24.0154672
15	No	15	Cl	1	2	3	1.7932952	109.5669877	101.1823870

Transition state for CHCl2COO-HOradical with 3 explicit water molecules

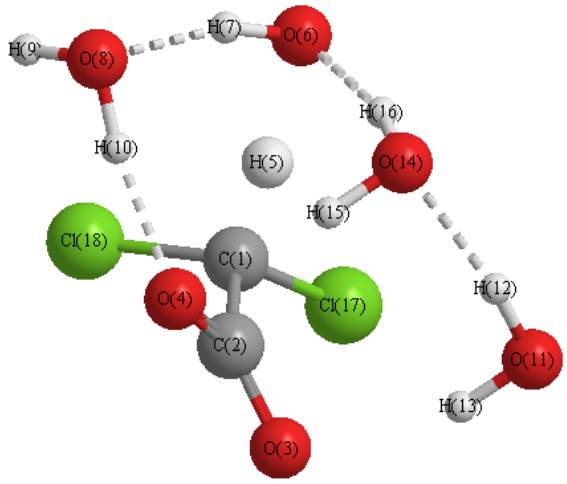

Row	Highlight	Tag	Symbol	NA	NB	NC	Bond	Angle	Dihedral
1	No	1	C						
2	No	2	C	1			1.5731013		
3	No	3	O	2	1		1.2383605	117.3508589	
4	No	4	O	2	1	3	1.2554791	113.9350651	179.6875104
5	No	5	H	1	2	3	1.1489391	109.0382926	-131.7298881
6	No	6	O	1	2	3	2.6611261	107.4467944	-133.7474532
7	No	7	H	6	1	2	0.9977313	92.1919301	-62.7147047
8	No	8	O	6	1	2	2.7226833	83.0631728	-57.3534654
9	No	9	H	8	6	1	0.9649813	106.7744196	-73.5501696
10	No	10	H	8	6	1	0.9848259	83.9238555	29.6389243
11	No	11	O	3	2	1	2.9727289	95.4986465	84.1578736
12	No	12	H	11	3	2	0.9767790	88.9042957	22.9532031
13	No	13	H	11	3	2	0.9678479	13.8467215	-172.7558987
14	No	14	O	11	3	2	2.8399185	83.3112259	22.9639824
15	No	15	H	14	11	3	0.9695051	91.9107575	23.1818126

16	No	16	H	14	11	3	0.9775488	100.8903790	-79.0176867
17	No	17	Cl	1	2	3	1.7800488	114.8915409	-14.0969196
18	No	18	Cl	1	2	3	1.7919684	110.2009991	111.8913762

Transition state for CHF2COO-HOradical with 1 explicit water molecule

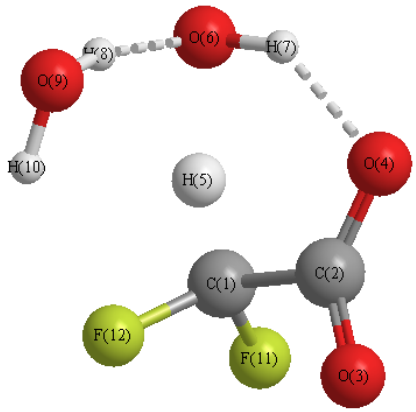

Row	Highlight	Tag	Symbol	NA	NB	NC	Bond	Angle	Dihedral
1	No	1	C						
2	No	2	C	1			1.5747367		
3	No	3	O	2	1		1.2422178	113.7182906	
4	No	4	O	2	1	3	1.2503275	115.6354314	179.3803041
5	No	5	H	1	2	3	1.1687238	108.2939558	172.9371418
6	No	6	O	1	2	3	2.5934733	94.3684393	170.0871065
7	No	7	H	6	1	2	0.9855825	76.5007111	9.9111207
8	No	8	H	6	1	2	1.8966327	80.4913833	-82.5103351
9	No	9	O	6	1	2	2.8589773	76.6183043	-81.5944698
10	No	10	H	9	6	1	0.9637594	96.8679876	-28.8170879
11	No	11	F	1	2	3	1.3456627	111.2090519	-66.6942064
12	No	12	F	1	2	3	1.3511914	111.5150581	53.2864004

Transition state for CHF2COO-HOradical with 2 explicit water molecules

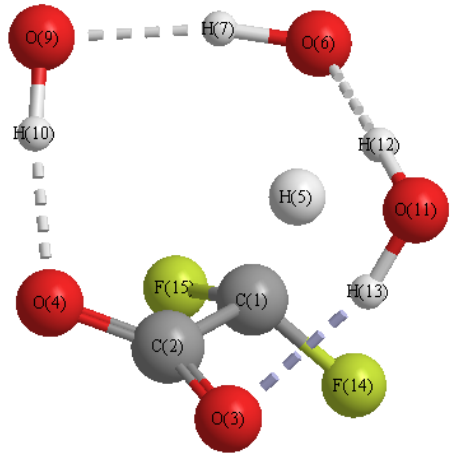

Row	Highlight	Tag	Symbol	NA	NB	NC	Bond	Angle	Dihedral
1	No	1	C						
2	No	2	C	1			1.5612198		
3	No	3	O	2	1		1.2466275	115.7176389	
4	No	4	O	2	1	3	1.2525004	115.2452876	177.6479777
5	No	5	H	1	2	3	1.1367334	108.7897784	-93.4811400
6	No	6	O	1	2	3	2.7373946	100.7442720	-99.7541008
7	No	7	H	6	1	2	0.9958710	84.1434394	-61.7353933
8	No	8	H	6	1	2	3.0147671	71.4629824	-83.4016880
9	No	9	O	4	2	1	2.7433336	110.5473579	-40.8114210
10	No	10	H	9	4	2	0.9849122	6.0823042	150.1164122
11	No	11	O	6	1	2	2.9041219	76.2295846	55.5933924
12	No	12	H	11	6	1	0.9728007	8.5086469	-141.2840269
13	No	13	H	11	6	1	0.9701696	97.5131631	-14.6318128
14	No	14	F	1	2	3	1.3487551	112.1093574	26.0413859

15	No	15	F	1	2	3	1.3528506	111.7997300	147.3858421

Transition state for CHF2COO-HOradical with 3 explicit water molecules

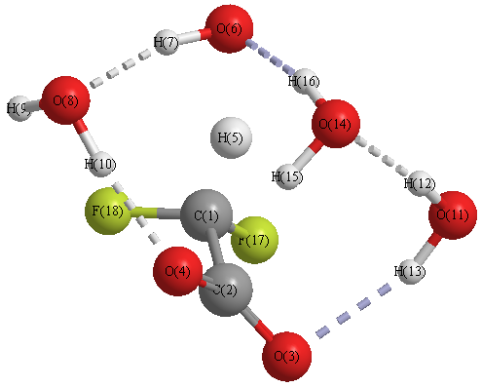

Row	Highlight	Tag	Symbol	NA	NB	NC	Bond	Angle	Dihedral
1	No	1	C						
2	No	2	C	1			1.5631222		
3	No	3	O	2	1		1.2414680	116.7225608	
4	No	4	O	2	1	3	1.2576920	114.3235709	178.3798520
5	No	5	H	1	2	3	1.1450822	109.0116741	-116.1533087
6	No	6	O	1	2	3	2.6943677	109.0879312	-127.4852595
7	No	7	H	6	1	2	0.9949167	84.2659838	-70.4643380
8	No	8	O	4	2	1	2.7584686	117.4998830	-4.8304468
9	No	9	H	8	4	2	0.9651446	104.1711535	59.3810378
10	No	10	H	8	4	2	0.9850926	5.0996531	140.9260889
11	No	11	O	3	2	1	2.9430135	92.0528949	69.8290427
12	No	12	H	11	3	2	0.9764795	86.2271512	41.1623826
13	No	13	H	11	3	2	0.9683257	16.3873027	-150.9591316
14	No	14	O	6	1	2	2.8328006	83.2897238	19.4075055
15	No	15	H	14	6	1	0.9695544	93.3014242	-42.5857146
16	No	16	H	14	6	1	0.9787395	9.1832195	160.5383025
17	No	17	F	1	2	3	1.3433604	112.9296389	4.8957580
18	No	18	F	1	2	3	1.3555387	110.3598389	125.6196862

Transition state for CHBr2COO-HOradical with 1 explicit water molecule

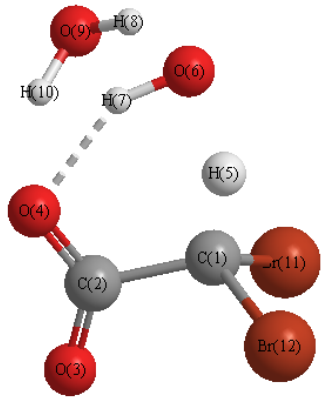

Row	Highlight	Tag	Symbol	NA	NB	NC	Bond	Angle	Dihedral
1	No	1	C						
2	No	2	C	1			1.5727336		
3	No	3	O	2	1		1.2350559	116.4739877	
4	No	4	O	2	1	3	1.2590939	113.8904788	179.6842941
5	No	5	H	1	2	3	1.1475834	109.8037050	176.3439783
6	No	6	O	1	2	3	2.5952437	96.0168232	178.9171038
7	No	7	H	6	1	2	0.9856147	76.8247624	9.7324199
8	No	8	H	6	1	2	2.0689591	89.3520420	-68.3455155
9	No	9	O	6	1	2	2.9278877	83.9461170	-59.3448486
10	No	10	H	9	6	1	0.9685690	77.7243760	54.3024822
11	No	11	Br	1	2	3	1.9433830	112.4934915	58.9508453
12	No	12	Br	1	2	3	1.9501061	111.2999380	-68.2490656

Transition state for CHBr2COO-HOradical with 2 explicit water molecules

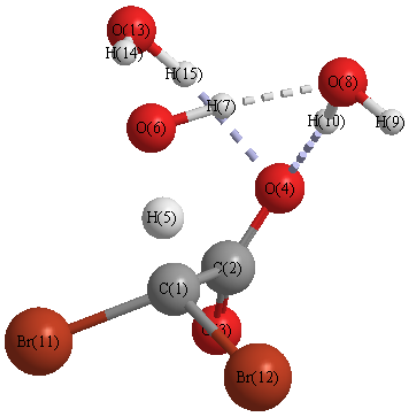

Row	Highlight	Tag	Symbol	NA	NB	NC	Bond	Angle	Dihedral
1	No	1	C						
2	No	2	C	1			1.5676855		
3	No	3	O	2	1		1.2328917	116.8259793	
4	No	4	O	2	1	3	1.2619394	114.5948417	-178.9275149
5	No	5	H	1	2	3	1.1502382	112.7342725	-158.8391709
6	No	6	O	1	2	3	2.6530793	113.7769692	-160.2686938
7	No	7	H	6	1	2	0.9952563	94.4678075	-48.4277862
8	No	8	O	4	2	1	2.7237660	126.4701656	16.6763389
9	No	9	H	8	4	2	0.9645526	108.1884450	68.0574228
10	No	10	H	8	4	2	0.9850763	5.2155320	118.7692401
11	No	11	Br	1	2	3	1.9445629	113.7508683	-41.1284608
12	No	12	Br	1	2	3	1.9552528	109.2011230	84.8753175
13	No	13	O	6	1	2	2.8930357	82.1617630	33.5188541
14	No	14	H	13	6	1	0.9722288	13.9727013	137.6925370
15	No	15	H	13	6	1	0.9702470	87.0363322	-39.6242768

Transition state1 for CH3CH2COO-HOradical with 1 explicit water molecule

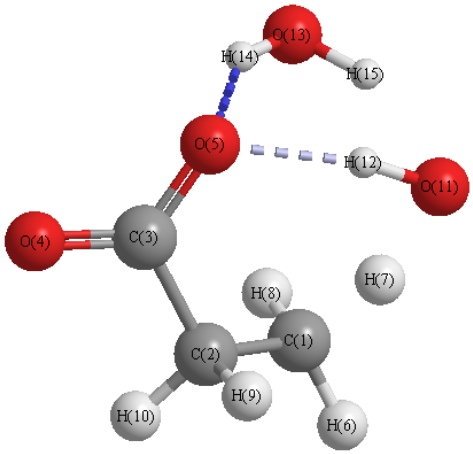

Row	Highlight	Tag	Symbol	NA	NB	NC	Bond	Angle	Dihedral
1	No	1	C						
2	No	2	C	1			1.5161956		
3	No	3	C	2	1		1.5419552	116.0113458	
4	No	4	O	3	2	1	1.2484262	117.7894069	140.5228400
5	No	5	O	3	2	1	1.2776584	117.7025702	-41.3875402
6	No	6	H	1	2	3	1.0936057	113.4007946	177.7418255
7	No	7	H	1	2	3	1.1998513	109.5744643	62.6034603
8	No	8	H	1	2	3	1.0924220	114.2015281	-53.4069699
9	No	9	H	2	1	3	1.0980921	109.5845201	-121.7679093
10	No	10	H	2	1	3	1.0966319	109.3829709	122.1008843
11	No	11	O	1	2	3	2.5367571	101.7824641	54.9953543
12	No	12	H	11	1	2	0.9959291	79.8752313	-29.6919381
13	No	13	O	5	3	2	2.8523876	116.1159227	72.3321718
14	No	14	H	13	5	3	0.9726836	19.1138954	81.1067351
15	No	15	H	13	5	3	0.9704643	80.4939451	-104.1723589

Transition state1 for CH3CH2COO-HOradical with 2 explicit water molecules

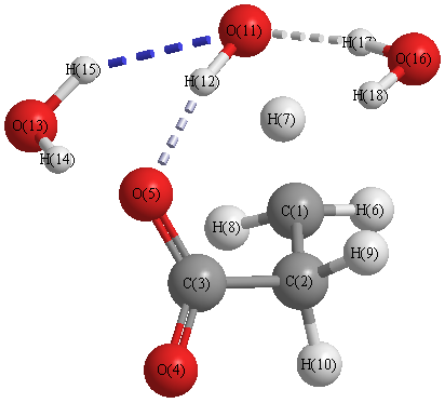

Row	Highlight	Tag	Symbol	NA	NB	NC	Bond	Angle	Dihedral
1	No	1	C						
2	No	2	C	1			1.5154993		
3	No	3	C	2	1		1.5401776	115.9378143	
4	No	4	O	3	2	1	1.2463967	117.9760965	142.1826350
5	No	5	O	3	2	1	1.2817228	117.7755810	-39.7765113
6	No	6	H	1	2	3	1.0934895	113.4071773	177.8494823
7	No	7	H	1	2	3	1.1932854	109.3636180	62.7501031
8	No	8	H	1	2	3	1.0923646	114.3571952	-53.0211468
9	No	9	H	2	1	3	1.0974344	109.1239824	-121.0831645
10	No	10	H	2	1	3	1.0963796	109.5674754	122.3802148
11	No	11	O	1	2	3	2.5482114	99.9989250	56.0806240
12	No	12	H	11	1	2	1.0025914	78.8122006	-36.5122571
13	No	13	O	5	3	2	2.8316905	113.9992677	73.4832523
14	No	14	H	13	5	3	0.9750654	11.9857719	80.1568161
15	No	15	H	13	5	3	0.9658696	88.9577453	-107.1123328
16	No	16	O	11	1	2	2.8355541	88.9127911	49.5874091
17	No	17	H	16	11	1	0.9775986	6.4925148	115.3823540
18	No	18	H	16	11	1	0.9642810	96.6744665	-90.9545877

Transition state1 for CH3CH2COO-HOradical with 3 explicit water molecules

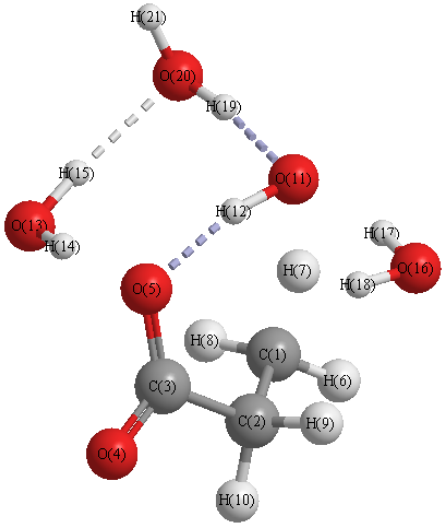

Row	Highlight	Tag	Symbol	NA	NB	NC	Bond	Angle	Dihedral
1	No	1	C						
2	No	2	C	1			1.5151388		
3	No	3	C	2	1		1.5397022	115.8953841	
4	No	4	O	3	2	1	1.2450139	117.9575284	147.4455633
5	No	5	O	3	2	1	1.2830629	117.8481454	-34.3273257
6	No	6	H	1	2	3	1.0935035	113.6171371	178.5837961
7	No	7	H	1	2	3	1.1867594	108.8789736	63.6902677
8	No	8	H	1	2	3	1.0922795	114.1235532	-52.0170520
9	No	9	H	2	1	3	1.0972606	109.4404077	-121.1904544

10	No	10	H	2	1	3	1.0964681	109.6582576	122.2139267
11	No	11	O	1	2	3	2.5550517	99.4902912	54.6033644
12	No	12	H	11	1	2	1.0117437	76.9629381	-40.8968101
13	No	13	O	5	3	2	2.8556698	107.0437002	82.1716198
14	No	14	H	13	5	3	0.9738328	6.5616991	108.8046512
15	No	15	H	13	5	3	0.9759794	98.5634578	-122.7997255
16	No	16	O	11	1	2	2.8596009	91.3530513	43.2598946
17	No	17	H	16	11	1	0.9751834	7.8079223	111.5192471
18	No	18	H	16	11	1	0.9643717	95.1242427	-88.9864337
19	No	19	H	11	1	2	1.8251415	95.2622905	-139.8458228
20	No	20	O	11	1	2	2.7987803	93.5145566	-137.3283753
21	No	21	H	20	11	1	0.9649038	104.5263213	152.9035296

Transition state2 for CH3CH2COO-HOradical with 1 explicit water molecule

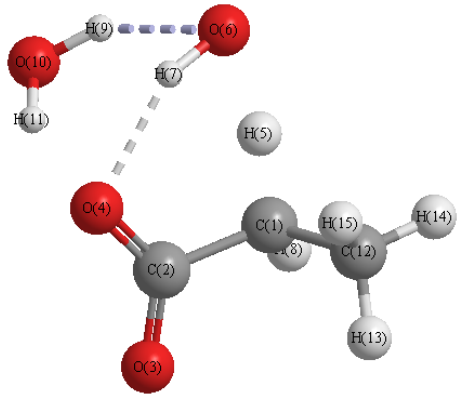

Row	Highlight	Tag	Symbol	NA	NB	NC	Bond	Angle	Dihedral
1	No	1	C						
2	No	2	C	1			1.5360063		
3	No	3	O	2	1		1.2507980	115.7236329	
4	No	4	O	2	1	3	1.2704258	118.1376642	178.2063005
5	No	5	H	1	2	3	1.1592884	106.1558848	162.3558136
6	No	6	O	1	2	3	2.5854317	95.3481837	174.1470925
7	No	7	H	6	1	2	0.9861328	73.6757158	14.4119272
8	No	8	H	1	2	3	1.0952489	110.9802732	47.6694472
9	No	9	H	6	1	2	2.0758527	92.0974285	-61.2083400
10	No	10	O	4	2	1	2.8901206	103.8995565	68.7445390
11	No	11	H	10	4	2	0.9717248	18.6363205	106.7567706
12	No	12	C	1	2	3	1.5228095	112.8785766	-78.5126554
13	No	13	H	12	1	2	1.0959715	110.0300786	62.1024359
14	No	14	H	12	1	2	1.0939352	111.3431520	-178.4074633
15	No	15	H	12	1	2	1.0944824	111.1120410	-57.4505512

Transition state2 for CH3CH2COO-HOradical with 2 explicit water molecules

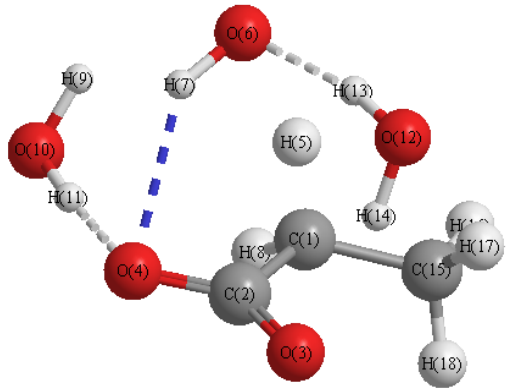

Row	Highlight	Tag	Symbol	NA	NB	NC	Bond	Angle	Dihedral
1	No	1	C						
2	No	2	C	1			1.5354100		
3	No	3	O	2	1		1.2557329	118.5497405	
4	No	4	O	2	1	3	1.2687708	116.3639639	177.2192739
5	No	5	H	1	2	3	1.1431905	103.2465191	-114.0921613
6	No	6	O	1	2	3	2.6906092	86.2509535	-116.5045670
7	No	7	H	6	1	2	0.9790764	76.9803817	-28.7825085

8	No	8	H	1	2	3	1.0946082	109.8635020	136.1495370
9	No	9	H	6	1	2	2.6561801	76.1739683	-93.8656420
10	No	10	O	4	2	1	2.7465573	117.1150079	6.3198230
11	No	11	H	10	4	2	0.9845257	2.9211698	103.7438848
12	No	12	O	3	2	1	2.9560306	89.8769034	71.5975066
13	No	13	H	12	3	2	0.9711740	90.7212322	5.4297266
14	No	14	H	12	3	2	0.9714687	11.6508992	178.6363737
15	No	15	C	1	2	3	1.5175608	117.0358267	5.4799765
16	No	16	H	15	1	2	1.0942844	110.9618346	-178.7923996
17	No	17	H	15	1	2	1.0929000	111.0263127	-57.9909450
18	No	18	H	15	1	2	1.0962590	110.5026579	61.7112233

Transition state2 for CH3CH2COO-HOradical with 3 explicit water molecules

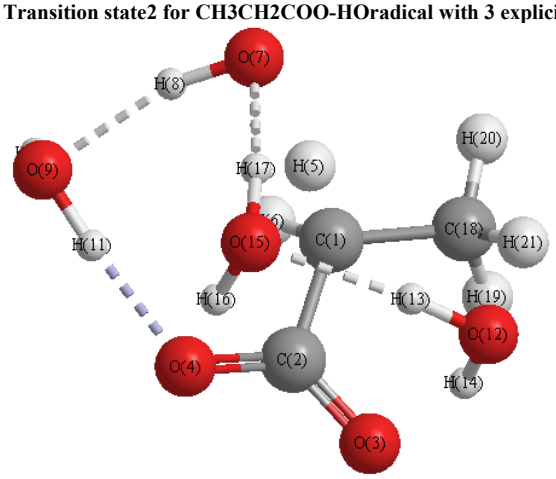

Row	Highlight	Tag	Symbol	NA	NB	NC	Bond	Angle	Dihedral
1	No	1	C						
2	No	2	C	1			1.5343462		
3	No	3	O	2	1		1.2530900	118.2602367	
4	No	4	O	2	1	3	1.2724199	117.2117626	179.5054190
5	No	5	H	1	2	3	1.1462174	105.3623284	-125.6694231
6	No	6	H	1	2	3	1.0956659	109.0447424	123.0547221
7	No	7	O	1	2	3	2.7094283	106.9919660	-133.6937350
8	No	8	H	7	1	2	0.9960068	85.2436440	-67.6624737
9	No	9	O	4	2	1	2.6866377	118.0111551	-1.2101089
10	No	10	H	9	4	2	0.9648969	106.8014570	60.7724196
11	No	11	H	9	4	2	0.9941746	4.0884612	108.5822093
12	No	12	O	3	2	1	2.9136887	92.8579024	79.8113703
13	No	13	H	12	3	2	0.9771523	89.8770876	30.2056087
14	No	14	H	12	3	2	0.9708366	12.9845529	-171.5157841
15	No	15	O	7	1	2	2.8376560	83.3472372	20.8335262
16	No	16	H	15	7	1	0.9730415	90.5461907	-41.7350974
17	No	17	H	15	7	1	0.9784949	10.6120701	146.3603513
18	No	18	C	1	2	3	1.5191149	116.7261927	-5.4207093
19	No	19	H	18	1	2	1.0954359	110.8904300	63.0550075
20	No	20	H	18	1	2	1.0943028	110.7166208	-177.3195043
21	No	21	H	18	1	2	1.0935090	110.8057937	-56.8534975

APPENDIX G: DEVELOPMENT OF ADOX2™ FOR OZONE AND OZONE/HYDRPGEN PEROXIDE ADVANCED OXIDATION PROCESS SIMULATION SOFTWARE

This appendix addresses the background knowledge and software manual for Adox2™ for ozone and ozone/hydrogen peroxide process simulation software. This software enables one to simulate reaction kinetics during ozonation and ozone/hydrogen peroxide processes. This also includes several options for mitigating bromate formation.

Introduction to Bromate and THMs Formation Software during Ozonation and O_3/H_2O_2 Advanced Oxidation Process.

Ozonation has been widely used as a disinfectant to inactivate microorganisms for potable water. Ozonation was in part replaced chlorine, chloramines or chlorine dioxide at the pre-oxidation and main-oxidation stages in many cities around the world, including Los Angeles, Barcelona, Singapore, Paris, and Zurich. Because a molecular ozone is such a strong oxidant in the aqueous phase (E^0 = 2.07 V), ozone has shown its superior ability against inactivate microorganisms (e.g. Cryptosporidium, Giardia lamblia cysts, E. Coli, Poliovirus and Rotavirus) to chlorine, chloramines and chlorine dioxide. In addition, ozonation does not form trihalomethanes (THMs) which is regulated under the current drinking water standard. It is well-known fact that ozonation produces biodegradable dissolved organic compounds (BDOC), and therefore, it is common practice to implement ozonation along with the subsequent biological treatment (e.g. GAC and BAC). When the aqueous ozone is degraded at higher pH (>7.5), more strong oxidant (HO radical) (i.e. E^0 = 2.59 V (aqueous)) is produced. The HO radical is also

formed by the reactions of ozone with natural organic matter (NOM). Therefore, ozonation works as one of Advanced Oxidation Processes (AOPs) and is expected to oxidize refractor trace organic compounds. Although ozonation hardly achieves a mineralization of toxic organic compounds, it is possible to degrade organic compounds into carbon dioxide, water, and minerals when used with hydrogen peroxide (H_2O_2) and ultraviolet (UV). As a consequent, ozonation and/or ozone based AOPs (i.e. O_3/H_2O_2, O_3/UV, O_3/UV/H_2O_2) are attractive and promising technologies.

When bromide ion (Br^-) is presented in the source waters, ozonation forms bromate ion (BrO_3^-) which is regulated under the current drinking water standard (U.S., Japan, and WHO, <10 μg/L). As a result, many studies have exploited the strategies to reduce formation of BrO_3^- kinetically (e.g. pH depression, NH_3 addition, Cl_2-NH_3 process) or remove BrO_3^- physically after ozonation (e.g. BAC, GAC, membrane-filtration). In engineering point of view, it would be ideal to control the formation of BrO_3^- kinetically without installing an additional treatment process. Designing inexpensive ozonation and/or O_3/H_2O_2 processes to control the BrO_3^- formation for commercial applications requires the determination of important design and operational variables. Carefully controlled laboratory and/or pilot plant studies can be used to design bromate mitigation processes. However, these studies can be time consuming and expensive if they are not properly planned. A complementary approach is taking advantage of the predictive capabilities of mathematical models that can effectively simulate the dynamics of ozonation and O_3/H_2O_2 system.

According to Peyton (1990), AOPs can be mathematically modeled at several different levels, depending on the amount of known kinetic information, computer

resources available and motivation for the application. Compared to other types of mathematical models, a kinetic model gives the most information and provides the best check of the model against actual laboratory data, because all defined or proposed reactions in the system are considered and the rate equations are written for all the main species in solution.

In the last decades, several models are developed to describe the kinetics of O_3 degrdation and O_3/H_2O_2 AOP combined with a bromate formation model. These kinetic modes were able to predict concentration of some contaminants as a function of time in different strategies of bromate mitigation. Although most of models that have been developed can be applied to laboratory scale reactors with different levels of success, their widespread application is limited for one or more of the following reasons: i) invoking pseudo-steady state assumption to simplify the governmental equations with the expense of losing accuracy and ii) constant pH though several important equilibrium reactions (e.g. OBr-/HOBr, HO_2^-/H_2O_2) significantly affect the bromate formation.

AdOx^{TM} was developed to aid design engineers in the design of AOPs. Compared to most of the previous models, AdOx^{TM} does not invoke the pseudo-steady-state and constant pH assumptions and thus provides a more accurate simulation of real systems. AdOx^{TM} includes the following capabilities:

(1) AdOx^{TM} provides a comprehensive understanding of the impact of key design and operational variables on process performance.

(2) AdOx^{TM} can dynamically simulate parent organic compound destruction and O_3 (and/or H_2O_2) consumption in both completely mixed batch reactors, completely

mixed flow reactors in series and plug flow reactors. (Steady state solutions are also provided.)

(3) AdOx™ can analyze dye study results to determine the number of tanks that are required in the tanks in series model to simulate non-ideal mixing in the photochemical reactor.

(4) AdOx™ includes all identified and reasonably proposed chemical reactions with regard to the degradation of parent organic compounds so it is the most comprehensive model to date.

(5) AdOx™ can simulate the destruction of all of the target compounds whose reaction mechanism and corresponding rate constants are known.

The AdOx™ software is designed for the Microsoft Windows™ environment with a graphical user interface (GUI) in order to maximize user-friendliness. Making use of the Microsoft Windows interface, with its built-in file and hardware control features, frees the engineer from concerns over printer drivers and other "machine" issues and allows you to give more attention to the computational algorithms. The GUI consists of a front-end shell written in Visual Basic™ that calls FORTRAN subroutines to perform the calculations.

This manual presents a description of the AdOx™ software capabilities including theoretical development, model descriptions and sample calculations where applicable. The manual also presents a description of the windows in the software and an example problem in order to aid the user.

References to specific commercial product, processes, or services by trademark, manufacturer, or otherwise does not necessarily constitute or imply

endorsement/recommendation by the authors or the respective organizations under which the software was developed.

Description of the Models

Ozonation and O_3/H_2O_2 Model Combined with Bromate Formation Model (Background)

An original kinetic model of bromate formation was developed by von Gunten and Hoigné (1994) using a non-linear differential equation solver, LARKIN, based on the experimental studies (Haag and Hoigné, 1983). Since then, a von Gunten's group has developed a kinetic model of bromate formation using ACUCHEM software by including different reaction mechanisms, such as bromate formation in ozone-based AOPs (von Gunten and Oliveras, 1998), bromate minimization using pH depression and NH_3 addition (Pinkernell and von Gunten, 2001), bromate control with the chlorine-ammonia process (2004). Other kinetic model combining ozone decomposition with bromate formation was developed by Westerhoff (1998; 1994).

Although most of models that have been developed can be applied to laboratory scale reactors with different levels of success, their widespread application is limited for one or more of the following reasons: i) invoking pseudo-steady state assumption to simplify the governmental equations with the expense of losing accuracy and ii) constant pH though several important equilibrium reactions (e.g. OBr-/HOBr, HO_2^-/H_2O_2) significantly affect the bromate formation. For example, Mariñas's group has developed a software with which cryptosporidium parvum oocyst inactivation and bromate formation are simultaneously predicted (Kim et al., 2007). This software includes the hydrodynamics in each chamber of the ozone contactor and implements the steady-state

governing equations for the concentrations of dissolved ozone, fast ozone demand (i.e. a portion of water constituents that consume dissolved ozone at a relatively fast rate during the initial phase of ozonation), gas-phase ozone, viable microorganisms, and bromate. However, this software does not invoke either i) or ii).

Elementary Reactions

Table A-G1 summarizes all elementary reactions implemented in this model with the reaction rate constants reported in the literature.

Table A-G1: Elementary reactions

	Elementary reaction	Rate constant	References
1	$O_3 + OH^- \rightarrow HO_2\bullet + \bullet O_2^-$	$k_1 = 70\, M^{-1}s^{-1}$	Staehelin and Hoigné, 1982
2	$O_3 + \bullet O_2^- \rightarrow \bullet O_3^- + O_2$	$k_2 = 1.6\times10^9\, M^{-1}s^{-1}$	Bühler *et al.*, 1984
3	$HO_3\bullet \rightarrow HO\bullet + O_2$	$k_3 = 1.1\times10^5\, s^{-1}$	Bühler *et al.*, 1984
4	$O_3 + HO_2^- \rightarrow HO\bullet + \bullet O_2^-$	$k_4 = 2.2\times10^6\, M^{-1}s^{-1}$	Staehelin and Hoigné, 1982
5	$HO\bullet + HO\bullet \rightarrow H_2O_2$	$k_5 = 5.0\times10^9\, M^{-1}s^{-1}$	Staehelin *et al.*, 1984
6	$HO\bullet + \bullet O_2^- \rightarrow OH^- + O_2$	$k_6 = 1.0\times10^{10}\, M^{-1}s^{-1}$	Staehelin *et al.*, 1984
7	$HO\bullet + HO_3\bullet \rightarrow H_2O_2 + O_2$	$k_7 = 5.0\times10^9\, M^{-1}s^{-1}$	Staehelin *et al.*, 1984
8	$HO_3\bullet + HO_3\bullet \rightarrow H_2O_2 + 2O_2$	$k_8 = 5.0\times10^9\, M^{-1}s^{-1}$	Staehelin *et al.*, 1984
9	$HO_3\bullet + \bullet O_2^- \rightarrow OH^- + 2O_2$	$k_9 = 1.0\times10^{10}\, M^{-1}s^{-1}$	Staehelin *et al.*, 1984
10	$O_3 + HO\bullet \rightarrow HO_2\bullet + O_2$	$k_{10} = 2.6\times10^8\, M^{-1}s^{-1}$	Staehelin *et al.*, 1984
11	$HO\bullet + H_2O_2 \rightarrow HO_2\bullet + H_2O$	$k_{11} = 2.7\times10^7\, M^{-1}s^{-1}$	Buxton *et al.*, 1988
12	$HO\bullet + HO_2^- \rightarrow \bullet O_2^- + H_2O$	$k_{12} = 7.5\times10^9\, M^{-1}s^{-1}$	Christensen *et al.*, 1982
13	$HO_2\bullet + H_2O_2 \rightarrow HO\bullet + H_2O + O_2$	$k_{13} = 3\, M^{-1}s^{-1}$	Koppenol *et al.*, 1978
14	$\bullet O_2^- + H_2O_2 \rightarrow HO_2\bullet + O_2 + OH^-$	$k_{14} = 0.13\, M^{-1}s^{-1}$	Judith *et al.*, 1979
15	$HO\bullet + HO_2\bullet \rightarrow H_2O + O_2$	$k_{15} = 6.6\times10^9\, M^{-1}s^{-1}$	Sehested *et al.*, 1968
16	$HO_2\bullet + HO_2\bullet \rightarrow H_2O_2 + O_2$	$k_{16} = 8.3\times10^5\, M^{-1}s^{-1}$	Bielski *et al.*, 1985
17	$HO_2\bullet + \bullet O_2^- \rightarrow HO_2^- + O_2$	$k_{17} = 9.7\times10^7\, M^{-1}s^{-1}$	Bielski *et al.*, 1985
18	$H_2O_2 + O_3 \rightarrow H_2O + O_2$	$k_{18} = 0.0065\, M^{-1}s^{-1}$	Neta *et al.*, 1988

19	$HO\bullet + HCO_3^- \rightarrow CO_3\bullet^- + H_2O$	$k_{19} = 8.5\times10^6\ M^{-1}s^{-1}$	Buxton *et al.*, 1988
20	$HO\bullet + CO_3^{2-} \rightarrow CO_3\bullet^- + OH^-$	$k_{20} = 3.9\times10^8\ M^{-1}s^{-1}$	Buxton *et al.*, 1988
21	$HO\bullet + NOM \rightarrow$	$k_{21} = 1.9\times10^4\ (mg/L)^{-1}s^{-1}$	Westerhoff *et al.*, 2007
22	$CO_3\bullet^- + CO_3\bullet^- \rightarrow CO_2 + CO_4^{2-}$	$k_{22} = 2.0\times10^7\ M^{-1}s^{-1}$	Westerhoff *et al.*, 1997
23	$CO_3\bullet^- + \bullet O_2^- \rightarrow CO_3^{2-} + O_2$	$k_{23} = 6.5\times10^8\ M^{-1}s^{-1}$	Holcman *et al.*, 1982
24	$CO_3\bullet^- + \bullet O_3^- \rightarrow CO_3^{2-} + O_3$	$k_{24} = 6.0\times10^7\ M^{-1}s^{-1}$	Buxton and Elliot, 1986
25	$CO_3\bullet^- + HO\bullet \rightarrow CO_2 + HO_2^-$	$k_{25} = 3.0\times10^9\ M^{-1}s^{-1}$	Westerhoff *et al.*, 1997
26	$CO_3\bullet^- + HO_2^- \rightarrow CO_3^{2-} + HO_2\bullet$	$k_{26} = 5.6\times10^7\ M^{-1}s^{-1}$	Crapski *et al.*, 1999
27	$CO_3\bullet^- + H_2O_2 \rightarrow HCO_3^- + HO_2\bullet$	$k_{27} = 8.0\times10^5\ M^{-1}s^{-1}$	Crapski *et al.*, 1999
28	$O_3\bullet^- + H_2PO_4^- \rightarrow HPO_4^{2-} + HO_3\bullet$	$k_{28} = 2.1\times10^8\ M^{-1}s^{-1}$	Bühler *et al.*, 1984
29	$HPO_4^{2-} + HO_3\bullet \rightarrow O_3\bullet^- + H_2PO_4^-$	$k_{29} = 2.0\times10^7\ M^{-1}s^{-1}$	Bühler *et al.*, 1984
30	$HPO_4^{2-} + HO\bullet \rightarrow OH^- + H_2PO_4\bullet^-$	$k_{30} = 1.5\times10^5\ M^{-1}s^{-1}$	Maruhamuthu and Neta, 1978
31	$H_2PO_4^- + HO\bullet \rightarrow H_2O + H_2PO_4\bullet^-$	$k_{31} = 2.0\times10^4\ M^{-1}s^{-1}$	Maruhamuthu and Neta, 1978
32	$O_3 + Br^- \rightarrow OBr^- + O_2$	$k_{32} = 160\ M^{-1}s^{-1}$	Sehested *et al.*, 1984
33	$O_3 + OBr^- \rightarrow Br^- + 2O_2$	$k_{33} = 330\ M^{-1}s^{-1}$	Sehested *et al.*, 1984
34	$O_3 + OBr^- \rightarrow BrO_2^- + O_2$	$k_{34} = 100\ M^{-1}s^{-1}$	Sehested *et al.*, 1984
35	$O_3 + HOBr \rightarrow BrO_2^- + O_2 + H^+$	$k_{35} = 0.013\ M^{-1}s^{-1}$	Haag and Hoigné, 1983
36	$O_3 + BrO_2^- \rightarrow BrO_3^- + O_2$	$k_{36} = 5.7\times10^4\ M^{-1}s^{-1}$	Sehested *et al.*, 1984
37	$O_3 + Br\bullet \rightarrow BrO\bullet + O_2$	$k_{37} = 1.5\times10^8\ M^{-1}s^{-1}$	von Gunten and Oliveras, 1998
38	$HO\bullet + HOBr \rightarrow BrO\bullet + H_2O$	$k_{38} = 2.0\times10^9\ M^{-1}s^{-1}$	Nicoson *et al.*, 2002
39	$HO\bullet + OBr^- \rightarrow BrO\bullet + OH^-$	$k_{39} = 4.2\times10^9\ M^{-1}s^{-1}$	Sidgwick, 1952
40	$BrO\bullet + BrO\bullet + H_2O \rightarrow BrO_2^- + OBr^- + 2H^+$	$k_{40} = 5.0\times10^9\ M^{-1}s^{-1}$	Sidgwick, 1952
41	$Br_3^- \rightarrow Br_2 + Br^-$	$k_{41} = 8.3\times10^8\ s^{-1}$	Mamou *et al.*, 1977
42	$Br_2 + Br^- \rightarrow Br_3^-$	$k_{42} = 1.0\times10^{10}\ M^{-1}s^{-1}$	Mamou *et al.*, 1977
43	$Br_2^{\bullet-} + Br_2^{\bullet-} \rightarrow Br_3^- + Br^-$	$k_{43} = 2.0\times10^9\ M^{-1}s^{-1}$	Kläning and Wolff, 1985
44	$OBr^- + Br\bullet \rightarrow BrO\bullet + Br^-$	$k_{44} = 4.1\times10^9\ M^{-1}s^{-1}$	Nicoson *et al.*, 2002
45	$BrO_2^- + HO\bullet \rightarrow BrO_2\bullet + OH^-$	$k_{45} = 1.9\times10^9\ M^{-1}s^{-1}$	von Gunten and Oliveras, 1997
46	$BrO_2\bullet + BrO_2\bullet \rightarrow Br_2O_4$	$k_{46} = 1.4\times10^9\ M^{-1}s^{-1}$	Amichai and Treinin, 1970

47	$Br_2O_4 \rightarrow BrO_2\bullet + BrO_2\bullet$	$k_{47} = 7.0\times10^{7}\,s^{-1}$	Amichai and Treinin, 1970
48	$Br_2O_4 + OH^- \rightarrow BrO_2^- + BrO_3^- + H^+$	$k_{48} = 7.0\times10^{8}\,M^{-1}s^{-1}$	Sidwick, 1952
49	$BrO_2\bullet + HO\bullet \rightarrow BrO_3^- + H^+$	$k_{49} = 2.0\times10^{9}\,M^{-1}s^{-1}$	Amichai and Treinin, 1970
50	$BrO\bullet + BrO_2^- \rightarrow OBr^- + BrO_2\bullet$	$k_{50} = 4.0\times10^{8}\,M^{-1}s^{-1}$	Schwarz and Bielski, 1986
51	$Br_2^{\bullet-} + BrO_2^- \rightarrow OBr^- + BrO\bullet + Br^-$	$k_{51} = 8.7\times10^{7}\,M^{-1}s^{-1}$	Sidwick, 1952
52	$Br\bullet + Br^- \rightarrow Br_2^{\bullet-}$	$k_{52} = 1.0\times10^{10}\,M^{-1}s^{-1}$	Haag and Hoigné, 1983
53	$Br_2^{\bullet-} \rightarrow Br\bullet + Br^-$	$k_{53} = 1.0\times10^{5}\,s^{-1}$	Haag and Hoigné, 1983
54	$HO\bullet + Br^- \rightarrow BrOH^{\bullet-}$	$k_{54} = 1.1\times10^{10}\,M^{-1}s^{-1}$	Haag and Hoigné, 1983
55	$BrOH^{\bullet-} \rightarrow HO\bullet + Br^-$	$k_{55} = 3.3\times10^{7}\,M^{-1}s^{-1}$	Haag and Hoigné, 1983
56	$OBr^- + CO_3\bullet^- \rightarrow BrO\bullet + CO_3^{2-}$	$k_{56} = 4.3\times10^{7}\,M^{-1}s^{-1}$	Sidwick, 1952
57	$BrO_2^- + CO_3\bullet^- \rightarrow BrO_2\bullet + CO_3^{2-}$	$k_{57} = 1.1\times10^{8}\,M^{-1}s^{-1}$	Sidwick, 1952
58	$HOBr + H_2O_2 \rightarrow Br^- + H_2O + O_2 + H^+$	$k_{58} = 7.0\times10^{4}\,M^{-1}s^{-1}$	von Gunten and Oliveras, 1997
59	$OBr^- + H_2O_2 \rightarrow Br^- + H_2O + O_2$	$k_{59} = 1.2\times10^{6}\,M^{-1}s^{-1}$	von Gunten and Oliveras, 1997
60	$HOBr + HO_2^- \rightarrow Br^- + H_2O + O_2$	$k_{60} = 7.6\times10^{8}\,M^{-1}s^{-1}$	Buxton and Dainton, 1968
61	$HO_2\bullet + Br_3^- \rightarrow Br_2^- + H^+ + Br^- + O_2$	$k_{61} = 10^{7}\,M^{-1}s^{-1}$	Bielski *et al*., 1985
62	$\bullet O_2^- + Br_3^- \rightarrow Br_2^- + Br^- + O_2$	$k_{62} = 3.8\times10^{9}\,M^{-1}s^{-1}$	Bielski *et al*., 1985
63	$BrOH^{\bullet-} + H^+ \rightarrow Br\bullet + H_2O$	$k_{63} = 4.4\times10^{10}\,M^{-1}s^{-1}$	Haag and Hoigné, 1983
64	$HO_2\bullet + Br_2 \rightarrow Br + Br^- + O_2 + H^+$	$k_{64} = 1.1\times10^{8}\,M^{-1}s^{-1}$	Bielski *et al*., 1985
65	$\bullet O_2^- + HOBr \rightarrow Br\bullet + OH^- + O_2$	$k_{65} = 3.5\times10^{9}\,M^{-1}s^{-1}$	Beckwith *et al*., 1996
66	$BrOH^{\bullet-} \rightarrow Br\bullet + OH^-$	$k_{66} = 4.2\times10^{6}\,M^{-1}s^{-1}$	Haag and Hoigné, 1983
67	$Br_2 + H_2O \rightarrow HOBr + H^+ + Br^-$	$k_{67} = 97\,s^{-1}$	Neta *et al*., 1988
68	$HOBr + H^+ + Br^- \rightarrow Br_2 + H_2O$	$k_{68} = 1.6\times10^{10}\,M^{-1}s^{-1}$	Neta *et al*., 1988
69	$BrOH^{\bullet-} + Br^- \rightarrow Br_2^{\bullet-} + OH^-$	$k_{69} = 2.0\times10^{8}\,M^{-1}s^{-1}$	Zahavi and Rabani, 1972
70	$HOBr + NH_3 \rightarrow NH_2Br + H_2O$	$k_{70} = 7.5\times10^{7}\,M^{-1}s^{-1}$	Wajon and Morris, 1982
71	$OBr^- + NH_3 \rightarrow NH_2Br + OH^-$	$k_{71} = 7.6\times10^{4}\,M^{-1}s^{-1}$	Wajon and Morris, 1982
72	$OH^- + NH_2Br \rightarrow NH_3 + OBr^-$	$k_{72} = 7.5\times10^{6}\,M^{-1}s^{-1}$	Pinkernell and von Gunten, 2001
73	$2NH_2Br \rightarrow NHBr_2 + NH_3$	$k_{73} = 250\,s^{-1}$	Pinkernell and von Gunten, 2001
74	$NHBr_2 + NH_3 \rightarrow 2NH_2Br$	$k_{74} = 100\,M^{-1}s^{-1}$	Pinkernell and von Gunten, 2001
75	$HOCl + Br^- \rightarrow HOBr + Cl^-$	$k_{75} = 1550\,M^{-1}s^{-1}$	Kumar and Margerum, 1987
76	$OCl^- + Br^- \rightarrow OBr^- + Cl^-$	$k_{76} = 0.001\,M^{-1}s^{-1}$	Kumar and Margerum, 1987
77	$NH_2Br + 3O_3 \rightarrow NO_3^- + Br^- + 3O_2 + 2H^+$	$k_{77} = 40\,M^{-1}s^{-1}$	Haag *et al*., 1984

78	$HOCl + NH_3 \rightarrow NH_2Cl + H_2O$	$k_{78} = 4.2 \times 10^6\ M^{-1}s^{-1}$	Morris and Issac, 1983
79	$NH_2Cl + Br^- \rightarrow NH_2Br + Cl^-$	$k_{79} = 0.014\ M^{-1}s^{-1}$	Trofe *et al*., 1980
80	$Br\bullet + OH^- \rightarrow BrOH^{\bullet -}$	$k_{80} = 1.3 \times 10^{10}\ M^{-1}s^{-1}$	Nicoson *et al*., 2002
81	$Br\bullet + NOM \rightarrow Br^-$	$k_{81} = 8.3 \times 10^4\ M^{-1}s^{-1}$	Pinkernell and von Gunten, 2001
82	$NH_2Br + NOM \rightarrow$	$k_{82} = 0.0017\ M^{-1}s^{-1}$	Assumed
83	$HOCl + NOM \rightarrow$	$k_{83} = 0.0004\ M^{-1}s^{-1}$	Westerhoff *et al*., 2004
84	$HOBr + NOM \rightarrow$	$k_{84} = 0.011\ M^{-1}s^{-1}$	Westerhoff *et al*., 2004
85	$HO\bullet + NH_2Cl \rightarrow$	$k_{85} = 5.0 \times 10^8\ M^{-1}s^{-1}$	Johnson *et al*., 2002
	$HO_2\bullet \leftrightarrow O_2\bullet^- + H^+$	$pK_a = 4.8$	Staehelin and Hoigné, 1982
	$HO_3\bullet \leftrightarrow \bullet O_3^- + H^+$	$pK_a = 8.2$	Bühler *et al*., 1984
	$H_2O_2 \leftrightarrow HO_2^- + H^+$	$pK_a = 11.6$	Staehelin and Hoigné, 1982
	$H_2CO_3 \leftrightarrow HCO_3^- + H^+$	$pK_a = 6.38$	Stumm and Morgan, 1996.
	$HCO_3^- \leftrightarrow H^+ + CO_3^{2-}$	$pK_a = 10.3$	Stumm and Morgan, 1996.
	$H_3PO_4 \leftrightarrow H_2PO_4^- + H^+$	$pK_a = 2.1$	Stumm and Morgan, 1996.
	$H_2PO_4^- \leftrightarrow HPO_4^{2-} + H^+$	$pK_a = 7.2$	Stumm and Morgan, 1996.
	$NH_4^+ \leftrightarrow NH_3 + H^+$	$pK_a = 9.3$	
	$HOCl \leftrightarrow OCl^- + H^+$	$pK_a = 7.5$	
	$HOBr \leftrightarrow OBr^- + H^+$	$pK_a = 8.8$	Haag and Hoigné, 1983; von Gunten and Hoigné, 1994
86	$[TTHMs] = [Cl_2]\{A_{TTHM}(1-\exp(-kt)\}$	see Equation.XX	Sohn et al., 2004

The Mechanisms of Aqueous Ozone Decomposition and O_3/H_2O_2 Process for Bromate Formation

Chemical reactions for mechanistic representation of ozone decomposition and bromate formation consist of four categories of reactions: i) reactions responsible for ozone self-decomposition and corresponding production of secondary oxidants such as HO radical, ii) O_3/H_2O_2 process as one of AOPs, iii) reactions leading to the formation of bromate from bromide, and iv) reactions involving carbonate and phosphate species. In the presence of natural organic matter (NOM), additional reactions involving NOM need to be considered in each category.

Ozone Self-Decomposition

The elementary reactions of ozone decomposition were extensively studied in 1970s and 1980s using the technique of pulse radiolysis (one group Hert & one group from Steahelin Buhler Hoigne). There are mainly two representative models to formulate the ozone decomposition, such as SBH model (Staehelin and Hoigné) and TFG model (Tomiyasu et al., 1985). The SBH model is established based on the experiments conducted in the solutions from weak acid to weak base, whereas the TFG model was from the experiments in the base solutions.

Figures A-G1 and A-G2 show the overview of SBH and TFG model. Figures include the elementary reactions used in each SBH and TFG model. In the both model, ozone initially reacts with hydroxyl ion, producing either hydroxyl peroxyl radical or hydrogen peroxide ion, respectively. Hydrogen peroxide ion is in equilibrium with super oxide anion at $pK_a = 4.8$. In the solutions from neutral to base, the superoxide anion is dominant, which produces an ozonide radical in both the SBH and the TFG model. The ozonide radical further produces HO radical. In the SBH model, an O_3OH radical is produced by the reaction of ozone with hydroxyl radical. The O_3OH radical reacts with hydroxyl proxyl radical, reproducing ozone. In the TFG model, the ozonide radical reacts with hydroxyl radical, reproducing ozone. In both the SBH and the TFG model, as a total, three moles of ozone produce two moles of hydroxyl radical through the radical chain reactions ($3O_3 + OH^- + H^+ \rightarrow 2HO\bullet + 4O_2$).

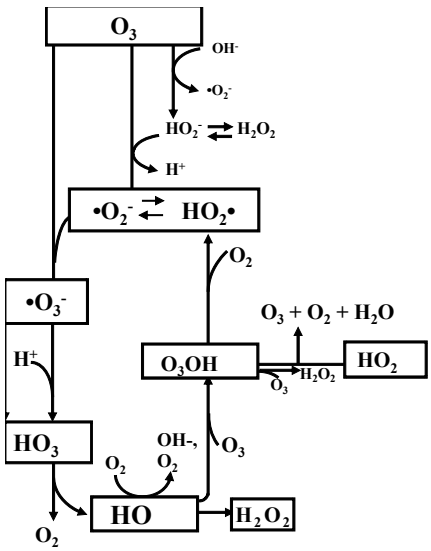

$O_3 + OH^- \rightarrow HO_2\cdot + \cdot O_2^-$	70	k_1	Staehelin and Hoigné, 1982
$HO_2\cdot \leftrightarrow \cdot O_2^- + H^+$	$pK_a = 4.8$		Staehelin and Hoigné, 1982
$HO_2^- + O_3 \rightarrow HO\bullet + O_2 \cdot^- + O_2$	2.2×10^6	k_2	Staehelin and Hoigné, 1982
$O_3 + \cdot O_2^- \rightarrow \cdot O_3^- + O_2$	1.6×10^9	k_3	Bühler et al., 1984
$\cdot O_3^- + H^+ \leftrightarrow HO_3\cdot$	$pK_a = 8.2$		Bühler et al., 1984
$HO_3\cdot \rightarrow HO\cdot + O_2$	1.1×10^5	k_4	Bühler et al., 1984
$\cdot OH + O_3 \rightarrow O_3OH\cdot$	2.0×10^9	k_5	Staehelin et al., 1984
$\cdot OH + \cdot OH \rightarrow H_2O_2$	5.0×10^9	k_6	Staehelin et al., 1984
$\cdot OH + \cdot O_2^- \rightarrow OH^- + O_2$	1×10^{10}	k_7	Staehelin et al., 1984
$\cdot OH + HO_3\cdot \rightarrow H_2O_2 + O_2$	5.0×10^9	k_8	Staehelin et al., 1984
$HO_3\cdot + HO_3\cdot \rightarrow H_2O_2 + 2O_2$	5.0×10^9	k_9	Staehelin et al., 1984
$HO_3\cdot + \cdot O_2^- \rightarrow OH^- + 2O_2$	1×10^{10}	k_{10}	Staehelin et al., 1984
$O_3OH\cdot \rightarrow HO_2\cdot + O_2$	2.8×10^4	k_{11}	Staehelin et al., 1984
$O_3OH\cdot + O_3OH\cdot \rightarrow H_2O_2 + 2O_3$	5.0×10^9	k_{12}	Staehelin et al., 1984
$O_3OH\cdot + HO_3\cdot \rightarrow H_2O_2 + O_3 + O_2$	5.0×10^9	k_{13}	Staehelin et al., 1984
$O_3OH\cdot + HO\cdot \rightarrow H_2O_2 + O_3$	5.0×10^9	k_{14}	Staehelin et al., 1984
$O_3OH\cdot + HO_2\cdot \rightarrow O_3 + O_2 + H_2O$	1×10^{10}	k_{15}	Staehelin et al., 1984
$O_3OH\cdot + \cdot O_2^- \rightarrow OH^- + O_3 + O_2$	1×10^{10}	k_{16}	Staehelin et al., 1984
$H_2O_2 = HO_2^- + H^+$	$pK_a = 11.65$		Staehelin and Hoigné, 1982

Figure A-G1: Ozone decomposition reaction scheme and elementary reactions of SBH model

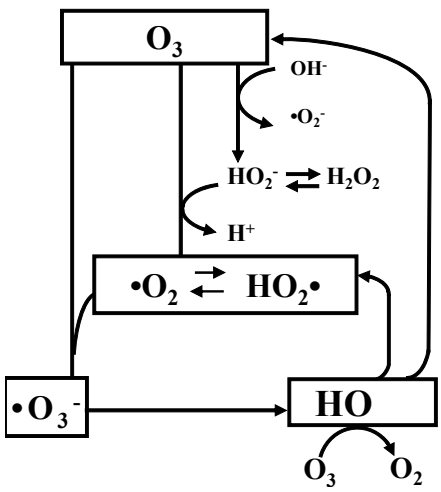

$O_3 + OH^- \rightarrow HO_2^- + O_2$	40	k_1	Tomiyasu et al., 1985
$HO_2^- + O_3 \rightarrow O_3^-\cdot + HO_2\cdot$	2.2×10^6	$k2$	Tomiyasu et al., 1985
$HO_2\cdot = \cdot O_2^- + H^+$	$pK = 4.8$		Tomiyasu et al., 1985
$O_3 + \cdot O_2^- = \cdot O_3^- + O_2$	1.6×10^9	$k3$	Tomiyasu et al., 1985
$\cdot O_3^- + H_2O \rightarrow HO\cdot + O_2 + OH^-$	20-30	$k4$	Tomiyasu et al., 1985
$\cdot O_3^- + HO\bullet \rightarrow \cdot O_2^- + HO_2\cdot$	6.0×10^9	$k5$	Tomiyasu et al., 1985
$\cdot O_3^- + HO\bullet \rightarrow O_3 + OH-$	2.5×10^9	$k6$	Tomiyasu et al., 1985
$O_3 + HO\bullet \rightarrow HO_2\bullet + O_2$	3.0×10^9	$k7$	Tomiyasu et al., 1985
$H_2O_2 = HO_2^- + H^+$	$pK = 11.65$		Tomiyasu et al., 1985

Figure A-G2: Ozone decomposition scheme and elementary reactions of TFG model.

Figure A-G3 demonstrates the scheme of ozone decomposition in this model. Figure A-G3 also includes the scheme of species that are involved in O_3/H_2O_2 process (detailed explanation of O_3/H_2O_2 AOP will be given in the subsequent session).

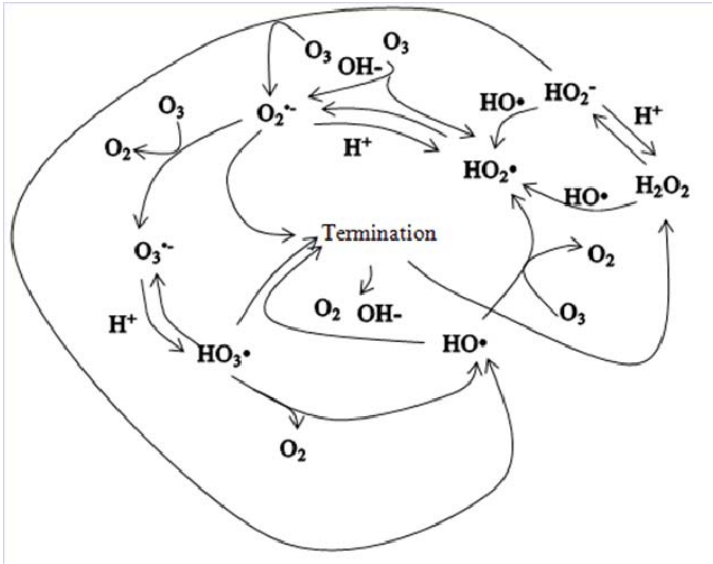

Figure A-G3: Ozone decomposition scheme

In the presence of NOM, O_3 directly reacts with NOM to produce low levels of HO radical (initiation reaction) via the following reaction:

O3 + NOM → HO• + byproducts

The HO radical that may be produced from the reaction above may also be quenched by the reaction with NOM as shown below:

HO• + NOM → byproducts

The quenching of HO radical with NOM is usually more important than quenching by bicarbonate and carbonate (discussed later) or metal species. Therefore, in this model, only quenching reaction is implemented (21). In fact, moieties of NOM react with HO• to form carbon centered radical which subsequently reacts with aqueous oxygen to produce peroxyl radical. The peroxyl radical eventually end up with super oxide anion radical $•O_2^-$ or hydroperoxyl radical $HO_2•$ by uni- or bi-molecular reactions. This process is called "promotion reaction" (Staehelin and Hoigné, 1985). The detailed reaction scheme is demonstrated in Figure A-G4. The extent of initiation, promotion, and

scavenging reactions depends on the types of NOM. Due to the complex and ambiguity of NOM structure, this model only consider the scavenging reaction of HO• with NOM.

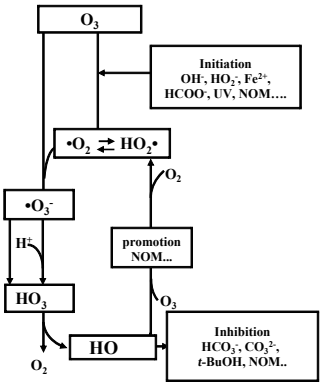

Figure A-G4: Ozone decomposition reaction scheme in the presence of initiators, promoters, and scavengers.

O_3/H_2O_2 model

In the presence of hydrogen peroxide (H_2O_2), hydroperoxide ion (HO_2^-), a disprotonated form of H_2O_2, reacts with O_3 to produce HO• (i.e. initiation reaction) (Staehelin and Hoigné, 1982). The pKa of hydrogen peroxide is 11.65. Consequently, hydroperoxide ion is dominant at around neutral pH, which produces HO radical in the reaction with ozone (4). However, it should be noted that hydrogen peroxide or hydrogen peroxide ion also reacts with HO radical, producing hydrogen peroxide radical (11 and 12). Therefore, excess dose of hydrogen peroxide is detrimental to production of HO radical.

Bromate Formation Mechanisms

When ozone is used as an oxidant, bromate ion (BrO_3^-) is formed from the oxidation of bromide ion (Br^-) through a combination of ozone and HO radical reactions. Because bromine (Br) is transformed into 6 oxidation states (Br^-(oxidation state; -I), Br•

(0), HOBr (+I), OBr^- (+I), BrO• (+II), BrO_2^- (+III), BrO_3^- (+V)), the whole reaction contributing to the formation of bromate ion is extremely complicated. The past extensive studies have revealed the general reaction pathway for the formation of bromate ion (shown in Figure A-G5).

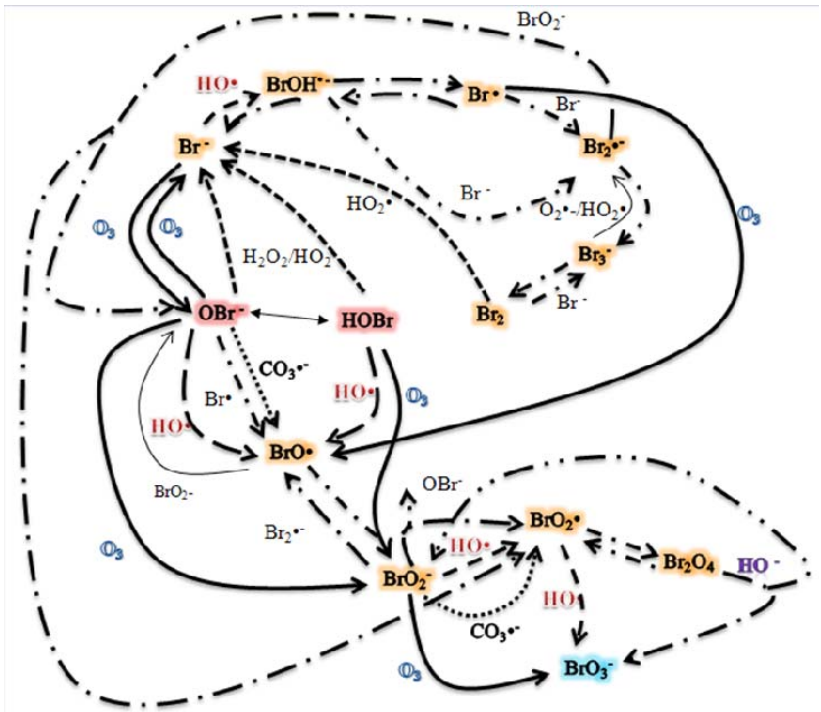

Figure A-G5. Bromate formation scheme via ozone and HO radical

Three major pathways have been identified for the formation of bromate ion, including

i) $Br^- \xrightarrow{O_3} OBr^-/HOBr \xrightarrow{O_3} BrO_3^-$

ii) $OBr^-/HOBr \xrightarrow{HO\bullet} BrO\bullet \xrightarrow{O_3} BrO_2^- \xrightarrow{O_3} BrO_3^-$

iii) $Br^- \xrightarrow{HO\bullet} Br\bullet \xrightarrow{O_3} BrO\bullet \xrightarrow{O_3} BrO_2^- \xrightarrow{O_3} BrO_3^-$

Because the equilibrium constant between hypobromite (OBr^-) and hypobromous acid (HOBr) is 8.8, HOBr is dominant for the typical drinking water treatment conditions (i.e.

pH = 6.5-8.0). OBr^- undergoes two reactions with O_3: i) attack of O_3 on the oxygen atom to produce $OOBr^-$ and eventually Br^- (33) and ii) attack of O_3 on the bromine atom to produce BrO_2^- (34). The reported reaction rate constants of (33) and (34) indicate that one-fourth of OBr^- is oxidized by O_3 leading to BrO_2^- and eventually BrO_3^- (von Gunten, 2003) (pathway i). Although HOBr undergoes the oxidation by O_3, the reaction rate constant for HOBr is approximately 5 magnitudes of order smaller than that for OBr^-. As a result, lowering pH is one of the strategies to reduce the BrO_3^-. The detailed discussion on the bromate mitigation will be given in the subsequent session. The OBr^-/HOBr is oxidized by HO radical to produce BrO• (38 and 39). The BrO• disproportionates to bromite ion (BrO_2^-) and eventually to BrO_3^- (pathway ii). The Br- is oxidized by HO radical to produce a bromine radical (Br•), which subsequently reacts with O_3 to produce BrO• (pathway iii). The Br• also undergoes the several reactions that radical species involved and eventually produces OBr^-/HOBr (41, 42, 52, 53, 64, 65, 67).

It is important to notice that BrO_3^- is not produced without O3. This is ensured by the fact that the BrO• is only formed from Br• in the presence of O_3. Furthermore, the BrO_2- is only oxidized by O_3 to produce BrO_3^-. As a consequent, where HO radical is the only oxidant (e.g. UV/H_2O_2 process, gamma-irradiation), the BrO• does not play any roles. In this manner, the Br• only reacts with Br- to produce OBr^-/HOBr, which is the decisive intermediate, BrO•.

Because the reaction pathway of the formation of BrO_3^- is not linear, it is not intuitive to predict the formation of BrO_3^-. Nevertheless, the known elementary reactions enable us to estimate the fraction of Br^- and OBr^-/HOBr oxidized by O_3 and HO radical, respectively, with use of the ratio of HO radical to O_3. It is straight-forward to examine

the fraction for the pH-independent Br-. The equation for the oxidation of Br^- can be expressed as below:

$$\frac{d\left[\mathrm{Br}^-\right]}{dt} = -k_{32}[\mathrm{O}_3][\mathrm{Br}^-] - k_{54}\left[\mathrm{HO}\bullet\right]\left[\mathrm{Br}^-\right]$$

By using the ratio, R_c = [HO•]/[O_3], the fraction of Br^- reacting with O_3 and HO•, $f_{\mathrm{HO}\bullet\ \mathrm{of\ Br}^-}$ and $f_{\mathrm{O}_3\ \mathrm{of\ Br}^-}$, can be written as below, respectively,:

$$f_{\mathrm{HO}\bullet\ \mathrm{of\ Br}^-} = \frac{k_{54}\,R_c}{k_{32} + k_{54}\,R_c}$$

$$f_{\mathrm{O}_3\ \mathrm{of\ Br}^-} = \frac{k_{32}}{k_{32} + k_{54}\,R_c}$$

Figure A-G6 represents the fraction of Br^- reaction with O_3 and HO• as a function of Rc (= [HO•]/[O_3]), respectively, calculated from the equations above. It is observed that only for higher Rc > 10^{-7}, a relatively larger amount of HO• oxidizes Br^-. In the range of typical drinking water treatment (i.e. Rc ≈ 10^{-8}), most part of Br- is oxidized by O_3.

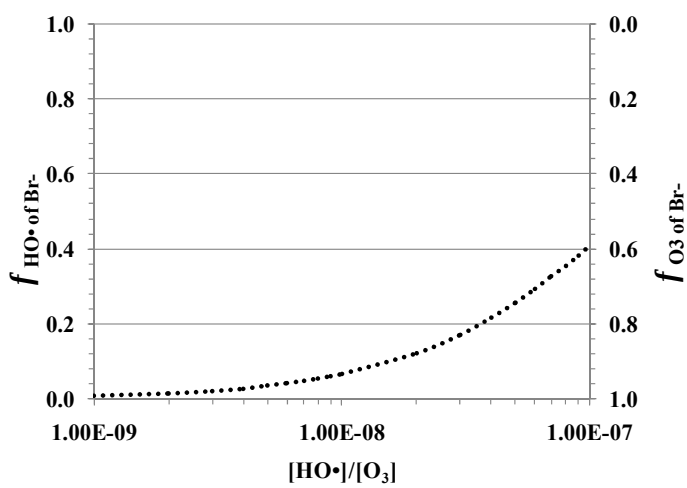

Figure A-G6: Fraction of Br- reaction with O3 and HO• as a function of Rc (= [HO•]/[O3])

For the case of the pH-dependent OBr^-/HOBr species (pKa = 8.8), the fraction of OBr-/HOBr reacting with O_3 and HO• dramatically changes with pH and the Rc (Figure 7). At lower pH (<7.0), almost entire oxidation of OBr^-/HOBr takes place by HO radical (i.e. HOBr is major oxidized species). At the neutral pH, approximately 80% of OBr^-/HOBr is oxidized by HO radical when the typical drinking water treatment Rc value is applied. As increase of pH (i.e. increase the fraction OBr-), O_3 contributes more to the oxidation of OBr^-/HOBr at the lower Rc. Although there is significant difference in reactivity of O_3 and HO radical with OBr^-/HOBr (i.e. magnitude of 7 for OBr^- (33 and 39) and of 11 for HOBr (35 and 38)), increase of pH considerably leads to the larger fraction of O_3 reacting with OBr^-/HOBr. Equation below represents the fraction of HO radical reacting with OBr^-/HOBr as an example.

$$f_{\mathrm{HO\bullet}\,of\,\mathrm{OBr\text{-}/HOBr}} = \frac{(k_{\mathrm{HOBr/HO\bullet}}\,[\mathrm{HO\bullet}][\mathrm{HOBr}]+k_{\mathrm{OBr\text{-}/HO\bullet}}[\mathrm{HO\bullet}][\mathrm{OBr^-}])}{(k_{\mathrm{HOBr/HO\bullet}}\,[\mathrm{HO\bullet}][\mathrm{HOBr}]+k_{\mathrm{OBr\text{-}/HO\bullet}}[\mathrm{HO\bullet}][\mathrm{OBr^-}])+(k_{\mathrm{HOBr/HO\bullet}}\,[\mathrm{O_3}][\mathrm{HOBr}]+k_{\mathrm{OBr\text{-}/HO\bullet}}[\mathrm{O_3}][\mathrm{OBr^-}])}$$

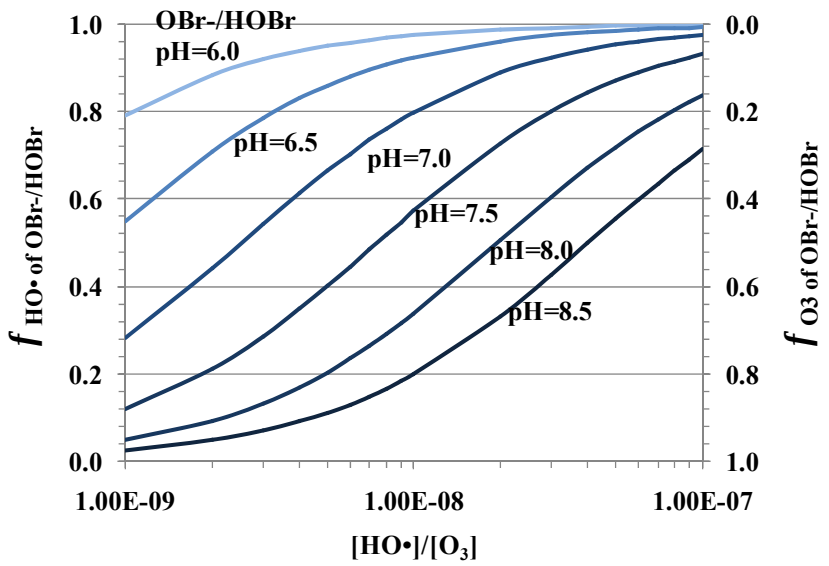

Figure A-G7: Fraction of HO radical and O_3 reacting with OBr^-/HOBr as a function of Rc (=[HO•]/[O_3])

The investigations in the fraction of HO• and O_3 reacting with OBr^-/HOBr reveals that those ratios significantly depend on the Rc ratios. In the initial reaction phase of ozonation (i.e. higher Rc ≈ 10^{-7}), Br^- is oxidized by HO radical to produce Br•. At around neutral pH, OBr^-/HOBr undergoes further oxidation from HO radical to produce BrO• and eventually to BrO_3^-. At the secondary phase of ozonation (Rc ≈ 10^{-8}-10^{-9}), Br^- is significantly oxidized by O_3 to produce OBr^-/HOBr. The HO radical oxidizes OBr-/HOBr to produce BrO•. The disproportionation of BrO• occurs and BrO_2^- produced is further oxidized by O_3 to produce BrO_3^-.

In the presence of NOM, Br• reacts with NOM to produce Br^- or bromo-organic compounds (81). Thus, the reactions of Br• with NOM fall into the same order of magnitude as those of Br• with bromide or ozone (e.g. 52 and 37). OBr^-/HOBr also interfere with NOM (84). Little is known about the quantitative formation mechanisms

of bromo-organic compounds. As a result, products are not considered in the kinetic model.

In Advanced Oxidation Processes (AOPs) where HO radical is a main oxidant, bromate formation is dominated by the HO radical induced in the pathway ii) and iii). When hydrogen peroxide (H_2O_2) is used as an oxidant, the reactions of OBr^-/HOBr with HO_2^- (H_2O_2) leading to Br- are important reactions (von Gunten, 2003).

Effect of Carbonate and Phosphate

The mechanism of carbonate species scavenging HO radical has been investigated by several researchers (Glaze *et al.*, 1988, 1989, Peyton *et al.*, 1988). Carbonate and bicarbonate ions (CO_3^{2-}/HCO_3^-) react with HO radical to produce carbonate radicals, $CO_3\bullet^-$ and $HCO_3\bullet$, respectively. In this model, these two reactions are reported to be similarly active (Chen *et al.*, 1975; Larson *et al.*, 1988), and therefore, can be referred to as one term, $CO_3\bullet^-$ (19, 20). The $CO_3\bullet^-$ reacts itself, superoxide anion radical, $\bullet O_2$-, ozonide ion radical, $\bullet O_3$-, and HO radical, respectively, at the comparable reaction rates to other radial involving reactions (22-25). In the O_3/H_2O_2 AOP, the reaction of $CO_3\bullet^-$ with H_2O_2 to form superoxide radical, $HO_2\bullet$, is significant (27). Since $CO_3\bullet^-$ is a weak oxidant, it may react with some target organic compounds. But for the treatment of most organic pollutants, these reactions are ignored because this reaction is insignificant.

The role of phosphate ions is similar to that of carbonate ions. Hydrogen phosphate ion, HPO_4^{2-}, reacts with $HO_3\bullet$ and HO• (29, 30), whereas dihydrogen phosphate ion, $H_2PO_4^-$, reacts with $\bullet O_3^-$ and HO• (28, 31) to form phosphate radical ions and reactive oxygenated species (ROS) further. In general, the reactions of phosphate ions do not significantly affect ozone-self decomposition.

The $CO_3\bullet^-$ also reacts with OBr^- (56) and BrO_2^- (57) at the comparable rate to the other ions which are produced from ozone self-decomposition.

Although the typical reaction rates that are induced from carbonate/bicarbonate ion or carbonate radicals are one or two magnitude of order smaller than those of HO•, the relatively higher concentrations of carbonate/bicarbonate present in the environmental waters make the scavenging reaction of carbonate/bicarbonate ions with HO• significant.

Bromate Mitigation Strategies

pH depression

Lowering pH shifts OBr-/HOBr equilibrium towards HOBr, and therefore, BrO_3-precursor, BrO_2-, is less produced by the reactions of O_3 with HOBr (35) as compared to those with OBr- (34). In addition, as was observed in Figure X, OBr-/HOBr oxidation is dominated by HO radical. As a consequence, lowering pH leads to the smaller fraction of O_3 reacting with OBr-/HOBr and reduces the formation of BrO_3-.

In addition to shifting the OBr-/HOBr equilibrium by lowering pH, it slows the O_3 degradation because of (1). As a result, integral of O_3 concentration as a function of time (i.e. $\int[O_3]dt$, ozone exposure) will be larger, whereas $\int[HO\bullet]dt$, HO radical exposure, will be constant. Accordingly, a ratio of $\int[HO\bullet]dt$ and $\int[O_3]dt$ (i.e. R_{ct} (von Gunten and reference)) will be smaller. Pinkernell and von Gunten (2001) observed a reduced bromate formation at lower R_{ct} values. Although the R_{ct} values do not have linear relationship with the bromate formation, the R_{ct} would be one of the important factors to assess the bromate formation.

Because the initial fast transformation of O_3 into HO radical is almost independent of pH, lowering pH does not lead to the significant decrease of the initial BrO_3^- formation. Accordingly, the effect of pH depression is expected to be small.

Ammonia addition

The addition of ammonia (NH_3) only interferes with OBr^-/HOBr producing monobromamine (NH_2Br) (70 and 71) (Figure A-G8). As was discussed, Br^- is dominantly oxidized by HO radical in the initial phase at the neutral pH. The Br• undergoes the oxidation by O_3 to produce BrO• and eventually to BrO_3^-. In this process, the NH_3 addition is not effective to reduce BrO_3^-. As a result, the NH_3 addition is only effective to the secondary phase of ozonation. Because the reaction of NH_3 with OBr^- is a base-catalyzed equilibrium reaction (72), it is not effective if source waters already have high levels of NH_3.

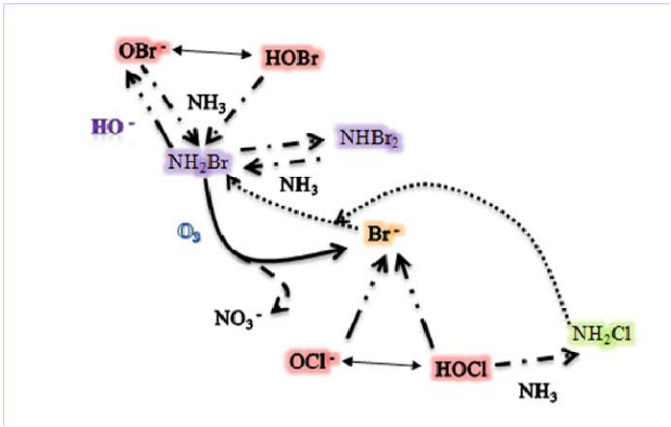

Figure A-G8: Bromate mitigation by adding ammonia and/or hypochlorous acid

Cl_2-NH_3 process

A Cl_2-NH_3 process is comprised of three major steps: i) pre-chlorination, ii) ammonia addition, and iii) mono-bromamine oxidation. With the condition that [NH_3] >

[HOCl] > [Br^-], Br^- is initially oxidized by hypochlorous acid (HOCl) to HOBr (75 and 76). The HOBr is masked by the addition of NH_3 to form NH_2Br (70 and 71). The NH_3 added in this step also reacts with the excess HOCl to produce monochloramine (NH_2Cl) (78). The reaction of NH_3 with HOCl does not compete with those of NH_3 with HOBr due to the 20 times smaller reaction rate constants. The NH_2Br undergoes the oxidation by O_3 to form nitrate (NO_3-) and Br- (77). An advantage of the Cl_2-NH_3 process over the single NH_3 addition is a hindrance of the reaction of HO radical with Br^- producing Br• during the initial phase.

It should be noted that the presence of NH_3 in the source waters significantly affect the efficacy of the Cl_2-NH_3 process. The NH_3 reacts with HOCl to produce NH_2Cl before reacting with Br^- according to (75) and (78). The NH_2Cl further reacts with Br^- to produce monobromamine, which is negligible due to the smaller reaction rate constant (79).

In addition to the hindrance of HO radical pathway for the BrO_3^- formation, the presence of NOM significantly contributes to the reduction of BrO_3^- by hindering HO radical. According to Buffle et al., (2004), two NOM-involving mechanisms could explain a decrease of HO radical by adding HOCl in the NH_3-containing source waters: i) HOCl and/or NH_2Cl oxidizes specific and reactive moieties of NOM toward O_3 and ii) HOCl or its oxidation or substitution products scavenge HO radical. NOM undergoes the oxidation by HOCl (83) and HOBr (84). The latter reaction producing total organic brominated compounds (TOBr) also contributes to minimize the BrO_3^- formation. However, products resulting from these reactions are not included in the model due to the

complex reactions of NOM. For the reaction mechanism ii), the HO radical scavenge reaction by NH_2Cl is represented (85).

Formation of TTHMs and TOX

The addition of HOCl and the presence of HOBr lead to the formation of halogenated organic compounds (TOX or THMs) by reacting with NOM (Figure A-G9).

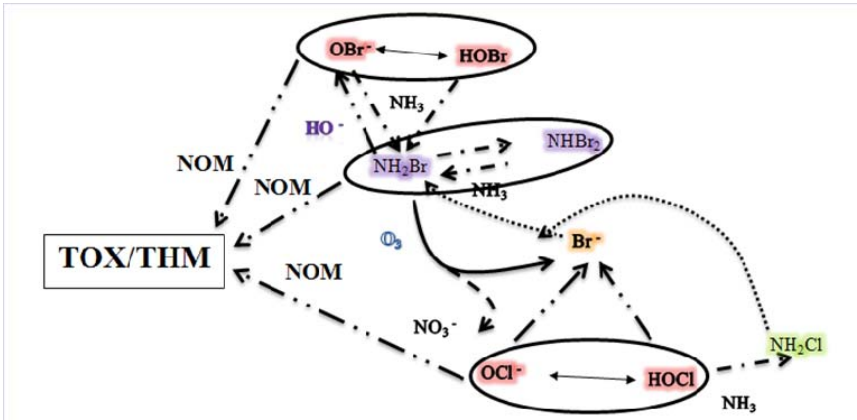

Figure A-G9: TOX and TTHMs formation scheme in the presence of NOM

Several empirical power function models are available for predicting total-trihalomethanes (TTHMs). Amy et al. developed models implemented in EPA 1998 models that were based on lower chlorine doses applied to either raw/untreated waters or chemically coagulated (conventionally treated) waters (Amy et al., 1998). This software implemented the improved EPA 1998 model developed by Sohn et al. (2004). In this improved model, chlorine consumption is splited into two phases, including i) fast initial phase of chlorine consumption (< 5h) and ii) the following second phase of slow chlorine consumption (5 h <).

The TTHMs predicting model in the initial phase is used. The empirical parameters were determined using the EPA 1998 database.

$$[TTHMs] = [Cl_2]\{A_{TTHM}(1-\exp(-kt)\}$$

where,

$$\ln(k) = 5.41 - 0.38 \ln\left(\frac{[Cl_2]}{[DOC]}\right) + 0.27 \ln([NH_3\text{-}N]) - 1.12 \ln(Temp) + 0.05 \ln([Br\text{-}]) - 0.854 \ln(pH)$$

$$\ln(A_{TTHM}) = -2.11 - 0.87 \ln\left(\frac{[Cl_2]}{[DOC]}\right) - 0.41 \ln([NH_3\text{-}N]) + 0.21 \ln([Cl_2]) + 1.98 \ln(pH)$$

[TTHM]=predicted trihalomethane conc. in initial phase (~5h), µg/L

$[Cl_2]$=applied chlorine dose, mg/L

[DOC] = dissolved organic carbon, mgC/L

$[NH_3\text{-}N]$ = ammonia-nitrogen conc., mg/L as N

[Br-]= bromide concentration, µg/L

Temp = temperature, °C

t = reaction time, h

The reactions of HOCl, HOBr, and NH_2Br with NOM to form the total organic halides (TOX) are complex due to the ambiguity of NOM properties. There are little studies attempted in the quantitative formation analysis of TOX. Therefore, in this model, the products from these reactions are not considered (82-84). Although the TOX is not currently regulated under the drinking water standard, the toxicity of TOX was reported much higher than bromate ion.

Modeling Equations

Kinetic Rate Expressions

Based on the elementary reactions in Table X, the overall kinetic rate expressions can be written as below. These species include: O_3, $HO_3\bullet/\bullet O_3^-$, $\bullet O_2^-/HO_2\bullet$, HO•,

H_2O_2/HO_2^-, $HPO_4\bullet^-$, $H_2PO_4^-/HPO_4^{2-}$, Br^-, $OBr^-/HOBr$, BrO_2^-, BrO_3^-, $Br\bullet$, $BrO\bullet$, Br_2^-, Br_3^-, $Br_2\bullet^-$, $BrOH\bullet$-, Br_2O_4, NH_2Br, $NHBr_2$, OCl-/HOCl, NH_4^+/NH_3, NH_2Cl, and NOM.

$$\frac{d[O_3]}{dt} = -k_1[O_3][HO^-] - k_2[\bullet O_2^-][O_3] - k_4[HO_2^-][O_3] - k_{10}[HO\bullet][O_3] - k_{18}[H_2O_2][O_3]$$
$$+k_{24}[CO_3\bullet^-][\bullet O_3^-] - k_{32}[O_3][Br^-] - k_{33}[O_3][OBr^-] - k_{34}[O_3][OBr^-] - k_{35}[O_3][HOBr]$$
$$-k_{36}[O_3][BrO_2^-] - k_{37}[O_3][Br\bullet] - 3k_{77}[O_3][NHBr_2]$$

$$\frac{d[HO_3\bullet]}{dt} = -k_3[HO_3\bullet] - k_7[HO\bullet][HO_3\bullet] - k_8[HO_3\bullet][HO_3\bullet] - k_9[HO_3\bullet][\bullet O_2^-]$$
$$+k_{28}[\bullet O_3^-][H_2PO_4^-] - k_{29}[HO_3\bullet][HPO_4^{2-}]$$

$$\frac{d[\bullet O_3^-]}{dt} = k_2[\bullet O_2^-][O_3] - k_{24}[CO_3\bullet^-][\bullet O_3^-] - k_{28}[\bullet O_3^-][H_2PO_4^-] + k_{29}[HO_3\bullet][HPO_4^{2-}]$$

$$\frac{d[\bullet O_2^-]}{dt} = k_1[O_3][HO^-] - k_2[O_3][\bullet O_2^-] + k_4[O_3][HO_2^-] - k_6[HO\bullet][\bullet O_2^-]$$
$$-k_9[HO_3\bullet][\bullet O_2^-] + k_{12}[HO\bullet][HO_2^-] - k_{14}[\bullet O_2^-][H_2O_2] - k_{17}[HO_2\bullet][\bullet O_2^-]$$
$$-k_{23}[CO_3\bullet^-][\bullet O_2^-] - k_{62}[\bullet O_2^-][Br_3^-] - k_{65}[\bullet O_2^-][HOBr]$$

$$\frac{d[HO_2\bullet]}{dt} = k_1[O_3][HO\text{-}] + k_{10}[HO\bullet][O_3] + k_{11}[HO\bullet][H_2O_2] - k_{13}[HO_2\bullet][H_2O_2]$$
$$+k_{14}[\bullet O_2^-][H_2O_2] - k_{15}[HO\bullet][HO_2\bullet] - k_{16}[HO_2\bullet][HO_2\bullet] - k_{17}[HO_2\bullet][\bullet O_2^-]$$
$$+k_{26}[CO_3\bullet^-][HO_2^-] + k_{27}[CO_3\bullet^-][H_2O_2] - k_{61}[HO_2\bullet][Br_3^-] - k_{64}[HO_2\bullet][Br_2]$$

$$\frac{d[HO\bullet]}{dt} = k_3[HO_3\bullet] + k_4[O_3][HO_2^-] - k_5[HO\bullet][HO\bullet] - k_6[HO\bullet][\bullet O_2^-]$$
$$-k_7[HO\bullet][HO_3\bullet] - k_{10}[HO\bullet][O_3] - k_{11}[HO\bullet][H_2O_2] - k_{12}[HO\bullet][HO_2^-]$$
$$+k_{13}[HO_2\bullet][H_2O_2] - k_{15}[HO\bullet][HO_2\bullet] - k_{19}[HO\bullet][HCO_3^-] - k_{20}[HO\bullet][CO_3^{2-}]$$
$$-k_{21}[NOM][HO\bullet] - k_{25}[CO_3\bullet^-][HO\bullet]$$
$$-k_{30}[HO\bullet][HPO_4^{2-}] - k_{31}[HO\bullet][H_2PO_4^-] - k_{38}[HO\bullet][HOBr] - k_{39}[HO\bullet][OBr^-]$$
$$-k_{45}[HO\bullet][BrO_2^-] - k_{49}[BrO_2\bullet][OH\bullet] - k_{54}[Br^-][HO\bullet] + k_{55}[BrOH\bullet^-]$$
$$-k_{85}[NH_2Cl][HO\bullet]$$

$$\frac{d\left[HO_2^-\right]}{dt} = -k_4[O_3][HO_2^-] - k_{12}[HO\bullet][HO_2^-] + k_{17}[HO_2\bullet][\bullet O_2^-] + k_{25}[CO_3\bullet^-][HO\bullet]$$
$$-k_{26}[CO_3\bullet^-][HO_2^-] - k_{60}[HO_2^-][HOBr]$$

$$\frac{d\left[H_2O_2\right]}{dt} = k_5[HO\bullet][HO\bullet] + k_7[HO\bullet][HO_3\bullet] + k_8[HO_3\bullet][HO_3\bullet] - k_{11}[HO\bullet][H_2O_2]$$
$$-k_{13}[HO_2\bullet][H_2O_2] - k_{14}[\bullet O_2^-][H_2O_2] + k_{16}[HO_2\bullet][HO_2\bullet] - k_{18}[H_2O_2][O_3]$$
$$-k_{27}[CO_3\bullet^-][H_2O_2] - k_{58}[H_2O_2][HOBr] - k_{59}[H_2O_2][OBr^-]$$

$$\frac{d\left[O_2\right]}{dt} = k_2[\bullet O_2^-][O_3] + k_3[HO_3\bullet] + k_6[HO\bullet][\bullet O_2^-] + k_7[HO\bullet][HO_3\bullet] + 2k_8[HO_3\bullet][HO_3\bullet]$$
$$+2k_9[HO_3\bullet][\bullet O_2^-] + k_{10}[HO\bullet][O_3] + k_{13}[HO_2\bullet][H_2O_2] + k_{14}[\bullet O_2^-][H_2O_2] + k_{15}[HO\bullet][HO_2\bullet]$$
$$+k_{16}[HO_2\bullet][HO_2\bullet] + k_{17}[HO_2\bullet][\bullet O_2^-] + k_{18}[H_2O_2][O_3] + k_{23}[CO_3\bullet^-][\bullet O_2^-]$$
$$+k_{32}[O_3][Br^-] + 2k_{33}[O_3][OBr^-] + k_{34}[O_3][OBr^-] + k_{35}[O_3][HOBr] + k_{36}[O_3][BrO_2^-]$$
$$+k_{37}[O_3][Br\bullet] + k_{58}[H_2O_2][HOBr] + k_{59}[H_2O_2][OBr^-] + k_{60}[HO_2^-][HOBr]$$
$$+k_{61}[HO_2\bullet][Br_3^-] + k_{62}[\bullet O_2^-][Br_3^-] + k_{64}[HO_2\bullet][Br_2] + k_{65}[\bullet O_2^-][HOBr] + 3k_{77}[NHBr_2]3[O_3]$$

$$\frac{d\left[HCO_3^-\right]}{dt} = -k_{19}[HO\bullet][HCO_3^-] + k_{27}[CO_3\bullet^-][H_2O_2]$$

$$\frac{d\left[CO_3^{2-}\right]}{dt} = -k_{20}[HO\bullet][CO_3^{2-}] + k_{23}[CO_3\bullet^-][\bullet O_2^-] + k_{24}[CO_3\bullet^-][\bullet O_3^-] + k_{26}[CO_3\bullet^-][HO_2^-]$$
$$+k_{56}[CO_3\bullet^-][OBr^-] + k_{57}[CO_3\bullet^-][BrO_2^-]$$

$$\frac{d\left[CO_3\bullet^-\right]}{dt} = k_{19}[HO\bullet][HCO_3^-] + k_{20}[HO\bullet][CO_3^{2-}] - k_{22}[CO_3\bullet^-][CO_3\bullet^-] - k_{23}[CO_3\bullet^-][\bullet O_2^-]$$
$$-k_{24}[CO_3\bullet^-][\bullet O_3^-] - k_{25}[CO_3\bullet^-][HO\bullet] - k_{26}[CO_3\bullet^-][HO_2^-] - k_{27}[CO_3\bullet^-][H_2O_2]$$
$$-k_{56}[CO_3\bullet^-][OBr^-] - k_{57}[CO_3\bullet^-][BrO_2^-]$$

$$\frac{d\left[CO_4^{2-}\right]}{dt} = k_{22}[CO_3\bullet^-][CO_3\bullet^-]$$

$$\frac{d[CO_2]}{dt} = k_{22}[CO_3\bullet^-][CO_3\bullet^-] + k_{25}[CO_3\bullet^-][HO\bullet]$$

$$\frac{d[H_2PO_4^-]}{dt} = -k_{28}[\bullet O_3^-][H_2PO_4^-] + k_{29}[HO_3\bullet][HPO_4^{2-}] - k_{31}[HO\bullet][H_2PO_4^-]$$

$$\frac{d[HPO_4^{2-}]}{dt} = k_{28}[\bullet O_3^-][H_2PO_4^-] - k_{29}[HO_3\bullet][HPO_4^{2-}] - k_{30}[HO\bullet][HPO_4^{2-}]$$

$$\frac{d[HPO_4^{\bullet-}]}{dt} = k_{30}[HO\bullet][HPO_4^{2-}] + k_{31}[HO\bullet][H_2PO_4^-]$$

$$\frac{d[OBr^-]}{dt} = k_{32}[O_3][Br^-] - k_{33}[O_3][OBr^-] - k_{34}[O_3][OBr^-] - k_{39}[HO\bullet][OBr^-]$$
$$+ k_{40}[BrO\bullet][BrO\bullet] - k_{44}[OBr^-][Br\bullet] + k_{50}[BrO\bullet][BrO_2^-] + k_{51}[Br_2^{\bullet-}][BrO_2^-]$$
$$- k_{56}[OBr^-][CO_3^{\bullet-}] - k_{59}[OBr^-][H_2O_2] - k_{71}[OBr^-][NH_3] + k_{72}[OH^-][NH_2Br]$$
$$+ k_{76}[OCl^-][Br^-]$$

$$\frac{d[HOBr]}{dt} = -k_{35}[O_3][HOBr] - k_{38}[HO\bullet][HOBr] - k_{58}[H_2O_2][HOBr] - k_{60}[HO_2^-][HOBr]$$
$$- k_{65}[\bullet O_2^-][HOBr] + k_{67}[Br_2][H_2O] - k_{68}[HOBr][H^+][Br^-] - k_{70}[NH_3][HOBr]$$
$$+ k_{75}[Br^-][HOCl] - k_{84}[HOBr][NOM]$$

$$\frac{d[BrO_2^-]}{dt} = k_{34}[O_3][OBr^-] + k_{35}[O_3][HOBr] - k_{36}[O_3][BrO_2^-] + k_{40}[BrO\bullet][BrO\bullet]$$
$$- k_{45}[HO\bullet][BrO_2^-] + k_{48}[Br_2O_4][OH^-] - k_{50}[BrO\bullet][BrO_2^-] - k_{51}[Br_2^{\bullet-}][BrO_2^-]$$
$$- k_{57}[CO_3^{\bullet-}][BrO_2^-]$$

$$\frac{d[BrO_3^-]}{dt} = k_{36}[O_3][BrO_2^-] + k_{48}[Br_2O_4][OH^-] + k_{49}[BrO_2\bullet][OH\bullet]$$

$$\frac{d[Br\bullet]}{dt} = -k_{37}[O_3][Br\bullet] - k_{44}[Br\bullet][OBr^-] - k_{52}[Br\bullet][Br^-] + k_{53}[Br_2^{\bullet-}]$$
$$+ k_{63}[BrOH\bullet^-][H^+] + k_{65}[HOBr][\bullet O_2^-] - k_{66}[BrOH^{\bullet-}] - k_{80}[Br\bullet][OH^-]$$
$$- k_{81}[Br\bullet][NOM]$$

$$\frac{d\left[\mathrm{BrO}\bullet\right]}{dt}=k_{37}[\mathrm{O_3}][\mathrm{Br}\bullet]+k_{38}[\mathrm{HO}\bullet][\mathrm{HOBr}]+k_{39}[\mathrm{HO}\bullet][\mathrm{OBr^-}]-k_{40}[\mathrm{BrO}\bullet][\mathrm{BrO}\bullet]$$
$$+k_{44}\left[\mathrm{Br}\bullet\right]\left[\mathrm{OBr^-}\right]-k_{50}[\mathrm{BrO}\bullet][\mathrm{BrO_2^-}]+k_{51}[\mathrm{Br_2^{\bullet-}}][\mathrm{BrO_2^-}]+k_{56}[\mathrm{CO_3^{\bullet-}}][\mathrm{OBr^-}]$$

$$\frac{d\left[\mathrm{Br_3^-}\right]}{dt}=-k_{41}\left[\mathrm{Br_3^-}\right]+k_{42}[\mathrm{Br_2}]\left[\mathrm{Br^-}\right]+k_{43}[\mathrm{Br_2^{\bullet-}}][\mathrm{Br_2^{\bullet-}}]-k_{61}[\mathrm{HO_2}\bullet][\mathrm{Br_3^-}]-k_{62}[\bullet\mathrm{O_2^-}][\mathrm{Br_3^-}]$$

$$\frac{d\left[\mathrm{Br_2^{\bullet-}}\right]}{dt}=-k_{43}\left[\mathrm{Br_2^{\bullet-}}\right]\left[\mathrm{Br_2^{\bullet-}}\right]-k_{51}[\mathrm{Br_2^{\bullet-}}][\mathrm{BrO_2^-}]+k_{52}\left[\mathrm{Br}\bullet\right]\left[\mathrm{Br^-}\right]-k_{53}\left[\mathrm{Br_2^{\bullet-}}\right]$$
$$+k_{69}[\mathrm{BrOH^{\bullet-}}]\left[\mathrm{Br^-}\right]$$

$$\frac{d\left[\mathrm{Br_2}\right]}{dt}=k_{41}\left[\mathrm{Br_3^-}\right]-k_{42}[\mathrm{Br_2}]\left[\mathrm{Br^-}\right]-k_{64}[\mathrm{HO_2}\bullet][\mathrm{Br_2}]-k_{67}\left[\mathrm{Br_2}\right]\left[\mathrm{H_2O}\right]$$
$$+k_{68}\left[\mathrm{HOBr}\right]\left[\mathrm{H^+}\right]\left[\mathrm{Br^-}\right]$$

$$\frac{d\left[\mathrm{Br_2^-}\right]}{dt}=k_{61}[\mathrm{HO_2}\bullet][\mathrm{Br_3^-}]+k_{62}[\bullet\mathrm{O_2^-}][\mathrm{Br_3^-}]$$

$$\frac{d\left[\mathrm{BrO_2}\bullet\right]}{dt}=k_{45}[\mathrm{HO}\bullet][\mathrm{BrO_2^-}]-k_{46}[\mathrm{BrO_2}\bullet][\mathrm{BrO_2}\bullet]+k_{47}[\mathrm{Br_2O_4}]-k_{49}[\mathrm{BrO_2}\bullet][\mathrm{OH}\bullet]$$
$$+k_{50}[\mathrm{BrO}\bullet][\mathrm{BrO_2^-}]+k_{57}\left[\mathrm{BrO_2^-}\right]\left[\mathrm{CO_3^{\bullet-}}\right]$$

$$\frac{d\left[\mathrm{Br_2O_4}\right]}{dt}=k_{46}[\mathrm{BrO_2}\bullet][\mathrm{BrO_2}\bullet]-k_{47}[\mathrm{Br_2O_4}]-k_{48}[\mathrm{Br_2O_4}][\mathrm{OH^-}]$$

$$\frac{d\left[\mathrm{BrOH^{\bullet-}}\right]}{dt}=k_{54}\left[\mathrm{HO}\bullet\right]\left[\mathrm{Br^-}\right]-k_{55}\left[\mathrm{BrOH}\bullet^-\right]-k_{63}[\mathrm{BrOH^{\bullet-}}][\mathrm{H^+}]-k_{66}\left[\mathrm{BrOH^{\bullet-}}\right]$$
$$-k_{69}\left[\mathrm{BrOH}\bullet^-\right]\left[\mathrm{Br^-}\right]+k_{80}\left[\mathrm{OH^-}\right]\left[\mathrm{Br}\bullet\right]$$

$$\frac{d\left[\mathrm{NH_2Br}\right]}{dt}=k_{70}\left[\mathrm{HOBr}\right]\left[\mathrm{NH_3}\right]+k_{71}\left[\mathrm{OBr^-}\right]\left[\mathrm{NH_3}\right]-k_{72}\left[\mathrm{OH^-}\right]\left[\mathrm{NH_2Br}\right]$$
$$-k_{73}\left[\mathrm{NH_2Br}\right]\left[\mathrm{NH_2Br}\right]+k_{74}\left[\mathrm{NHBr_2}\right]\left[\mathrm{NH_3}\right]-k_{77}\left[\mathrm{NHBr_2}\right]3\left[\mathrm{O_3}\right]+k_{79}\left[\mathrm{NH_2Cl}\right]\left[\mathrm{Br^-}\right]$$
$$-k_{82}\left[\mathrm{NH_2Br}\right]\left[\mathrm{NOM}\right]$$

$$\frac{d\left[\mathrm{NHBr_2}\right]}{dt}=k_{73}\left[\mathrm{NH_2Br}\right]\left[\mathrm{NH_2Br}\right]-k_{74}\left[\mathrm{NHBr_2}\right]\left[\mathrm{NH_3}\right]$$

$$\frac{d[\mathrm{HOCl}]}{dt} = -k_{75}[\mathrm{HOCl}][\mathrm{Br^-}] - k_{78}[\mathrm{HOCl}][\mathrm{NH_3}] - k_{83}[\mathrm{HOCl}][\mathrm{NOM}]$$

$$\frac{d[\mathrm{OCl^-}]}{dt} = -k_{76}[\mathrm{OCl^-}][\mathrm{Br^-}]$$

$$\frac{d[\mathrm{Cl^-}]}{dt} = k_{75}[\mathrm{HOCl}][\mathrm{Br^-}] + k_{76}[\mathrm{HOCl^-}][\mathrm{Br^-}] + k_{79}[\mathrm{NH_2Cl}][\mathrm{Br^-}]$$

$$\frac{d[\mathrm{NO_3^-}]}{dt} = k_{77}[\mathrm{NH_2Br}]3[\mathrm{O_3}]$$

$$\frac{d[\mathrm{NH_2Cl}]}{dt} = k_{78}[\mathrm{HOCl}][\mathrm{NH_3}] - k_{79}[\mathrm{NH_2Cl}][\mathrm{Br^-}] - k_{85}[\mathrm{NH_2Cl}][\mathrm{NOM}]$$

$$\frac{d[\mathrm{NOM}]}{dt} = -k_{21}[\mathrm{NOM}][\mathrm{HO}\bullet] - k_{81}[\mathrm{NOM}][\mathrm{Br}\bullet] - k_{82}[\mathrm{NOM}][\mathrm{NH_2Br}] - k_{83}[\mathrm{NOM}][\mathrm{HOCl}]$$
$$- k_{84}[\mathrm{NOM}][\mathrm{HOBr}]$$

The equlibrium relationships implemented in this model are as follows:

$$[\mathrm{HO_2^-}] = \frac{\mathrm{K_1}[\mathrm{H_2O_2}]}{[\mathrm{H^+}]}$$

$$[\bullet\mathrm{O_3^-}] = \frac{\mathrm{K_3}[\mathrm{HO_3}\bullet]}{[\mathrm{H^+}]}$$

$$[\mathrm{OBr^-}] = \frac{\mathrm{K_{18}}[\mathrm{HOBr}]}{[\mathrm{H^+}]}$$

$$[\mathrm{NH_3}] = \frac{\mathrm{K_{22}}[\mathrm{NH4^+}]}{[\mathrm{H^+}]}$$

$$[\mathrm{OCl^-}] = \frac{\mathrm{K_{25}}[\mathrm{HOCl}]}{[\mathrm{H^+}]}$$

$$[\bullet O_2^-] = \frac{K_{59}[HO_2\bullet]}{[H^+]}$$

$$[CO_3^{2-}] = \frac{K_{60}[HCO_3^-]}{[H^+]}$$

$$[HPO_4^{2-}] = \frac{K_{61}[H_2PO_4^-]}{[H^+]}$$

$$[HCO_3^-] = \frac{K_{62}[H_2CO_3]}{[H^+]}$$

$$[H_2PO_4^-] = \frac{K_{63}[H_3PO_4]}{[H^+]}$$

The ordinary differential equations resulting from the substitution of above rate expressions into the mass balances are solved using a backward differentiation formula method (Gear's method) called DGEAR. DGEAR and the associated nuclei are adaptations of a package designed by A.C.Hindmarsh based on C.W.Gear's subroutine DIFSUB (Hindmarsh, 1974).

Reactor Specific Equations

The mass balance for a species, "A", in a completely mixed batch reactor (CMBR) or a completely mixed flow reactor (CMFR) yields following two ordinary differential equations:

$$\frac{dC_a}{dt} = r_a \qquad \text{(CMBR)}$$

$$\frac{dC_a}{dt} = \frac{1}{\tau}(C_{ao} - C_a) + r_a \qquad \text{(CMFR)}$$

Where C_{ao} is the influent concentration of species A, C_a is the concentration of A at time t, τ is the hydraulic retention time of the reactor, and r_a is the overall kinetic rate expression of the species A in the reaction system.

Model equations for a plug flow reactor (PFR) and a real flow reactor (RFR) which has mixing characteristics somewhere between CMFR and PFR, can also be solved using the DGEAR algorithm using a Tanks-in-Series model. The same rate expressions describing the kinetics of the H_2O_2/UV process can also be used for modeling a PFR or RFR. The program can determine how many tanks are needed for modeling PFR or RFR according to dye study data provided by you.

Kinetic Parameters

The use of the AdOx software requires kinetic information and physicochemical properties of the target compounds. AdOx™ contains a database in which you can get information for more than 600 types of compounds. Kinetics parameters needed for the modeling are listed below.

- Dissociation constant(s) of the compound if dissociation(s) of that compound exists.
- Rate constants of the reaction between target compounds with $OH^{\cdot}$, $HO_2^{\cdot}$, $O_2^{\cdot}$, radicals.
- Rate constants of the reaction between the dissociated formats of target compound with $OH^{\cdot}$, $HO_2^{\cdot}$, $O_2^{\cdot}$ radicals (default as 0 if not applicable).

References

Amichai, O.; Treinin, A. *J.Phy.Chem*. On the oxybromine radicals. 1970, *74*, 3670-3674.

Amy, G.; Siddiqui, M.; Ozekin, K.; Zhu, H.W.; Wang, C. Empirically based models for predicting chlorination and ozonation by-products: Trihalomethanes, haloacetic acids, chloral hydrate, and bromated. EPA-815-R-98-005. 1998.

Beckwith, R.C.; Wang, T.X.; Margerum, D.W. Equilibrium and Kinetics of Bromine Hydrolysis. *Inorg. Chem*, 1996, *35*, 995-1000.

Bielski,B.H.J.; Cabelli,D.E.;Arudi,R.L.; Ross, A.B. Reactivity of perhyroxyl/superoxide radicals in aqueous solution. *J.Phys.Chem. Ref. Data*, 1985, *14*(4), 1041-100.

Bühler, R.E.; Staehelin, J.; Hoigné, J. Ozone decomposition in water studied by pulse radiolysis. 1. HO_2/O_2- and HO_3/O_3- as intermediates. *J. Phys. Chem*. 1984, *88*, 2560-2564.

Buffle, M-O.; Galli, S.; von Gunten, U. Enhanced bromated control during ozonation: The chlorine-ammonia process. *Environ. Sci. & Technol*. 2004, *38*, 5187-5195.

Buxton, G.V.; Greenstock, C.L.; Helman W.P.; Ross, A.B. Critical review of rate constants for reactions of hydrated electrons, hydrogen atoms and hydroxy radical (•HO/•O-) in aqueous solution. J.*Phys.Chem. Ref. Data*. 1988, *17*(2), 513-886.

Buxton, G.V.; Dainton, F.S. The radiolysis of aqueous solutions of oxybromine compounds; the spectra and reactions of BrO and BrO_2. *Proc. R. Soc. London A*, 1968, *304*, 427-439.

Buxton, G.V.; Elliot, A. J. Rate constant for reaction of hydroxyl radicals with bicarbonate ions. *Radiat.Phys.Chem*. 1986, *27*, 241-243.

Christensen, H.S.; Sehested, K.; Corftizan, H. Reaction of hydroxyl radicals with hydrogen peroxide at ambient temperatures. *J.Phys.Chem*. 1982, *86*, 15-88.

Crapski, G.; Lymar, S.V.; Schwarz, H.A. Acidity of the carbonate radical. *J.Phy.Chem A*, 1999, *103*, 3447-3450.

Gear, C.W. The automatic integration of ordinary differential equations. *Comm. ACM*. 1971, *14*(3), 176-179.

Haag. W. R.; Hoigné, J. Ozonation of bormide-containing waters: Kinetics of formation of hypobromous acid and bromate. *Environ. Sci. & Technol*. 1983, *17*, 261-267.

Haag. W. R.; Hoigné, J.; Bader, H. Improved ammonia oxidation by ozone in the reference of bromide ion during water treatment. *Wat. Res*. 1984, *18*, 1125-1128.

Hindmarsh, A.C. (1974)*, GEAR: Ordinary Differential Equation System Solver*, Lawrence Livermore National Laboratory Report UCID-30001, Revision 3, Lawrence Livermore National Laboratory, Livermore, Calif.

Holcman, J.; Sehested, K.; Bjergbakke, E.; Hart, E.J. Formation of ozone in the reaction between the ozonide radical ion, O3-, and the carbonate radical ion, CO3-, in aqueous alkaline solutions. *J. Phys. Chem*. 1982, *86*, 2069-2072.

Johnson, H.D.; Cooper, W.J.; Mezyk, S.P.; Bartels, D.M. Free radical reactions of monochloramine and hydroxylamine in aqueous solution. *Radiat.Phys.Chem*. 2002, *65*, 317-326.

Judith,W.; Bielski, B.H.J. Kinetics of the interaction of HO2 and O2- radicals with hydrogen peroxide. *J.Am.Chem. Soc*. 1979, *101*, 58-62.

Kläning, U.K.; Wolff,T. Laser flash photolysis of HCIO, CIO-, HBrO, and BrO in aqueous solution. Reactions of Cl- and Br atoms. *Ber.Bunsen-Ges. Phy.Chem*, 1985, *89*, 243-245.

Koppenol, W.H.; Butler, J.; Leeuwen, V.; Johan, W.L. The Harber-Weiss cycle. *Photochem.Photobiol*. 1978, 655-660.

Kumar, K.; Margerum, D.W. Kinetics and mechanism of general-acid-assisted oxidation of bromide by hypochlorite and hypochlorous acid. *Inorg.Chem*. 1987, *26*, 2706-2711.

Mamou, A.; Rabani,J.; Behar, D. On the oxidation of aqueous Br- by OH radicals, studied by pulse radiolysis. *J. Phy. Chem*, 1977, *81*, 1447-1448.

Maruthamuthu, P.; Neta, P. Phosphate radicals. Spectra, acid-base equilibria, and reactions with inorganic compounds. *J. Phy.Chem*. 1978, *82*(6), 710-713.

Morris, J.C.; Isaac, R.A. In Water Chlorination: Environmental Impact and Health Effects; Jolly, R.L., Brungs,W.A., Cotruvo, J.A., Cumming, R.B., Mattice, J.S., Jacobs V. A., Eds; Ann Arbor Science: Ann Arbor, MI, 1983; Vol. 4, pp 49-62.

Neta, P.; Huie, R.E.; Ross, A.B. Rate constants for reactions of inorganic radicals in aqueous solutions. *J.Phy.Chem. Ref. Data*, 1988, *17*, 1027-1284.

Nicoson, J.S.; Wang,L.; Becker, R.H.; Huff Hartz, K.E.; Muller, C.E.; Margerum, D.W. Kinetics and mechanisms of the ozone/bromide and ozone/chlorite reactions. *Inorg.Chem*. 2002, *41*, 2975-2980.

Peyton, G.R. Guidelines for the Selection of a Chemical Model for Advanced Oxidation Processes. *A symposium on advanced oxidation processes for the treatment of contaminated water and air (proceedings)* June 4&5, 1990, Toronto.

Pinkernell, U.; von Gunten, U. Bromate minimization during ozonation: Mechanistic considerations. *Environ.Sci. & Technol*. 2001, *35*, 2525-2531.

Schwarz, H.A.; Bielski, B.H. Reactions of HO_2 and O_2- with iodine and bromine and the I_2- and I atom reduction potentials. *J.Phy.Chem*. 1986, *90*, 1445-1448.

Sehested, K.; Holcman, J.; Bjergbakke, E.; Hart, E.J. A pulse radiolytic study of the reaction OH+O_3 in aqueous medium. *J.Phy.Chem*, 1984, *88*, 4144-4147.

Sehested, K.; Rasmussen, O.L.; Fricke,H. Rate constants of OH with HO_2, O_2- and H_2O_2+ from hydrogen peroxide formation in pulse-irradiated oxygenated water. *J.Phys.Chem*. 1968, *72*, 626-631.

Sidgwick, N.V. The Chemical Elements and Their Compounds: Vol. II; Oxford Press: Oxford, 1952.

Sohn, J.; Amy, G.; Cho, J.; Lee, Y.; Yoon, Y. Disinfectant decay and disinfection by-products formation model development: chlorination and ozonation by-products. *Wat.Res*. 2004, *38*, 2461-2478.

Staehelin, J.; Hoigné, J. Decomposition of ozone in water: rate of initiation by hydroxide ions and hydrogen peroxide. *Environ. Sci. &Technol*. 1982, *16*, 676-681.

Stumm, W.; Morgan, J.J. Aquatic Chemistry. John Wiley & Sons, Inc.3rd ed. 1996, New York.

Trofe, T.W.; Inman, G.W.,Jr.; Johnson, J.D. Kinetics of monochloramine decomposition in the presence of bromide. *Environ.Sci.& Technol*. 1980, *14*, 544-549.

von Gunten, U.; Oliveras, Y. Advanced oxidation of bromide-containing waters: Bromate formation mechanisms. *Environ.Sci. & Technol*. 1998, *32*, 63-70.

von Gunten, U.; Oliveras, Y. Kinetics of the reaction between hydrogen peroxide and hypobromous acid: implication on water treatment and natural systems. *Wat. Res*. 1997, *31*(4), 900-906.

von Gunten, U.; Hoigné, J. Bromate formation during ozonation of bromide-containing waters: interaction of ozone and hydroxyl radical reactions. *Environ.Sci. & Technol*. 1994, *28*, 1234-42.

Wajon, J.E.; Morris, J.C. Rates of formation of N-bromo amines in aqueous solution. *Inorg.Chem.* 1982, *21*, 4258-4263.

Westerhoff, P.; Chao,P.; Mash, H. Reactivity of natural organic matter with aqueous chlorine and bromine. *Wat.Res*. 2004, *38*, 1502-1513.

Westerhoff, P.; Mezyk, S.P.; Cooper, W,J.; Minakata, D. Electron pulse radiolysis determination of hydroxyl radical rate constants with suwanee river fulvic acid and other dissolved organic matter isolates. *Environ. Sci. & Technol*, 2007, *41*, 4640-4646.

Westerhoff, P.; Song, R.; Amy, G.; Minear, R. Application of ozone decomposition models. *Ozone Sci & Eng*. 1997, *19*, 55-73.

Zehavi, D.; Rabani,J. The oxidation of aqueous bromide ions by hydroxyl radicals. A pulse radiolytic investigation. *J.Phy.Chem*. 1972, *76*, 312-319.

Haag, W.R.; Hoigné, J. Ozonation of bromide-containing waters: Kinetics of formation of hypobrmous acid and bromated. *Environ. Sci. & Technol*. 1983, *17*, 261-267.

von Gunten, U.; Hoigné, J. Bromate formation during ozonation of bromide-containing waters: interaction of ozone and hydroxyl radical reactions. *Environ. Sci. & Technol*. 1994, *28*, 1234-1242.

von Gunten, U.; Oliveras, Y. Advanced oxidation of bromide-containing waters: Bromate formation mechanisms. *Environ. Sci. & Technol*. 1998, *32*, 63-70.

Pinkernell, U.; von Gunten, U. Bromate minimization during ozonation: Mechanistic consideration. *Environ. Sci. & Technol*. 2001, *35*, 2525-2531.

Westerhoff, P.; Song, R.; Amy, G.; Minear, R. Numerical kinetic models for bromide oxidation to bromine and bromated. *Wat.Res*. 1998, *32*(5), 1687-1699.

Westerhoff, P.; Ozekin, K.; Siddiqui, M.; Amy, G. Kinetics modeling of bromated formation in ozonated waters: Molecular ozone versus HO• radical pathways. J.AWWA. 1994, 901-920.

VITA

Daisuke Minakata

Daisuke Minakata was born in Wakayama, Japan. He attended School of Global Enginnering and received a B.A., and Environmental Engineering, Graduate School of Engineering and received a M.A. from Kyoto University, Japan. He began with his Ph.D. program at the Department of Civil and Environmental Engineering, Arizona State University in Fall, 2005. He transferred to the Department of Civil and Environmental Engineering, Georgia Institute of Technology in Spring, 2009. He loves swimming, biking and running. He enjoys playing with a dog, Kuro.